NASA TECHNICAL MEMORANDUM

July 1974

NASA TM X-64817

MSFC SKYLAB ATTITUDE AND POINTING CONTROL SYSTEM MISSION EVALUATION

Skylab Program Office

NASA

George C. Marshall Space Flight Center
Marshall Space Flight Center, Alabama

TECHNICAL REPORT STANDARD TITLE PAGE

1. REPORT NO.	2. GOVERNMENT ACCESSION NO.	3. RECIPIENT'S CATALOG NO.
TMX-64817		

4. TITLE AND SUBTITLE	5. REPORT DATE
MSFC Skylab APCS Mission Evaluation	July 1974
	6. PERFORMING ORGANIZATION CODE

7. AUTHOR(S)	8. PERFORMING ORGANIZATION REPORT #
W. B. Chubb	

9. PERFORMING ORGANIZATION NAME AND ADDRESS	10. WORK UNIT NO.
George C. Marshall Space Flight Center Marshall Space Flight Center, Alabama 35812	11. CONTRACT OR GRANT NO.
	13. TYPE OF REPORT & PERIOD COVERED

12. SPONSORING AGENCY NAME AND ADDRESS	
National Aeronautics and Space Administration Washington, D.C. 20546	Technical Memorandum
	14. SPONSORING AGENCY CODE

15. SUPPLEMENTARY NOTES

Prepared by Astrionics Laboratory, Systems/Projects Office, Guidance and Control Branch, System Design Section.

16. ABSTRACT

This report offers the results of detailed performance analyses for all Attitude and Pointing Control System in-orbit hardware and software. Performance is compared with requirements, test results, and prelaunch predictions.

A brief history of the Attitude and Pointing Control System evolution leading to the launch configuration is presented. This historical information, as well as a brief physical description of the launch configuration, is included as an aid to a clear understanding of mission performance.

In conclusion, the report asserts that the Attitude Pointing and Control System satisfied all imposed requirements. Conclusions based upon flight data analysis offer insights which may be beneficial during early concept and design requirement stages of future spacecraft systems.

Editor's Note

Use of trade names or names of manufacturers in this report does not constitute an official endorsement of such products or manufacturers, either expressed or implied, by the National Aeronautics and Space Administration or any agency of the United States Government.

17. KEY WORDS	18. DISTRIBUTION STATEMENT
Skylab. Control & Display Panel. Mission Description. Rate Gyro Processor. Design Evolution. Thruster Attitude Control Testing. Attitude Control System. Attitude & Pointing Control System.	Unclassified-Unlimited William B. Chubb

19. SECURITY CLASSIF. (of this report)	20. SECURITY CLASSIF. (of this page)	21. NO. OF PAGES	22 PRICE
Unclassified	Unclassified	441	NTIS

ACKNOWLEDGEMENT

This report was prepared from information, analyses and reports provided by numerous government and industry sources. Significant contributions were made by Astrionics Laboratory, Aero-Astrodynamics Laboratory and Astronautics Laboratory, all of George C. Marshall Space Flight Center; and by IBM Corporation, Martin Marietta Corporation, The Bendix Corporation and Sperry Space Support Services. The author would like to thank the APCS Report Team; Norman Vost, John Broom, Albert Chanasyk, Harold Brasher, Eric Hahn, Hayden Glenn and Michael Fague, for their dedicated assistance in preparing this report.

TABLE OF CONTENTS

LIST OF ILLUSTRATIONS

LIST OF ILLUSTRATIONS (continued)

LIST OF ILLUSTRATIONS (continued)

LIST OF ILLUSTRATIONS (concluded)

LIST OF TABLES

LIST OF TABLES (CONTINUED)

Non-Standard Abbreviations

A	Aft
AC	Alternating Current
ACE	Automatic Checkout Equipment
Acq. SS	Acquisition Sun Sensor
ACS	Attitude Control System
A/D	Analog to Digital
ADDT	All Digital Data Tape
AM	Airlock Module
AMPL	Amplifier
AOS	Acquisition of Signal
AOSO	Advanced Orbiting Solar Observatory
APCS	Attitude and Pointing Control System
APS	Auxiliary Power System
AR	Action Request
ASAP	Auxiliary Storage and Playback Unit
ASCO	ATMDC Software Control Officer
ASRM	Analog Signal Redundancy Management
ASSY	Assembly
AST	All Systems Test
ATM	Apollo Telescope Mount
ATMDC	Apollo Telescope Mount Digital Computer
AU	Astronomical Unit
BMF	Bending Mode Filter
BRG	Bearing
BRL	Bendix Research Laboratories
CAL	Calibration
CAP	Critical Angle Prism
CC	Cluster Configuration
CDT	Converted Data Tape
CE	Control Electronics
CMG	Control Moment Gyro
CMGEA	Control Moment Gyro Electronics Assembly
CMGIA	Control Moment Gyro Inverter Assembly
CO_2	Carbon Dioxide
CPU	Central Processing Unit
CSM	Command Service Module
C&D	Control and Display
C&W	Caution and Warning
C/O	Checkout

Abbreviations (Continued)

DAS	Digital Address System
DC	Direct Current
DCR	Digital Command Receiver
DCS	Digital Command System
DEMOD	Demodulator
DESAT	Desaturation
DET	Detection
DN	Down
DRC	Derived Rate Conditioner
D/TV	Data to Television
EA	Electronics Assembly
EMI	Electro Magnetic Interference
EPS	Experiment Pointing System
EPC	Experiment Pointing Control
EPCS	Experiment Pointing Control System
EPEA	Experiment Pointing Electronics Assembly
EPM	Experiment Pointing Mode
EPEA	Experiment Pointing Electronics Assembly
EREP	Earth Resources Experiment Package
ESR	Effective Sun Rise
EUC	Engineering Units Conversion
EVA	Extravehicular Activity
F	Forward
FCC	Flight Control Computer
FOD	Flight Operations Directorate
FOMR	Flight Operations Management Room
FSS	Fine Sun Sensor
GG	Gravity Gradient
GMT	Greenwich Mean Time
GNS	SWS Guidance, Navigation and Control System Engineer
GN_2	Gaseous Nitrogen
GSE	Ground Support Equipment
GSFC	Goddard Space Flight Center
G&C	Guidance and Control
H	Momentum
HCO	Harvard College Observatory
HOSC	Huntsville Operations Support Center
HRC	Honeywell Research Center
HSL	Hardware Simulation Laboratory
H/A	Habitation Area

Abbreviations (Continued)

IBM	International Business Machines
ICA	Information Correlator Assembly
IG	Inner Gimbal
IOA	Input/Output Assembly
IU	Instrument Unit
I&C	Instrumentation and Communications
JOP	Joint Operations Procedure
JSC	Johnson Space Center
KSC	Kennedy Space Center
L	Left
LBNP	Lower Body Negative Pressure
LM	Lunar Module
LOS	Line-of-sight
LOS	Loss of signal
LSB	Least Significant Bit
LVDC	Launch Vehicle Digital Computer
MAR	Mission Action Request
MMC	Mission Control Center
MDA	Multiple Docking Adapter
MDAC	McDonnell Douglas Astronautics Corporation
MDRS	Mission Control Center Data Retrieval System
MIB	Minimum Impulse Bit
MLU	Memory Load Unit
MMC	Martin Marietta Corporation
MMP	Momentum Management Program
MOCR	Mission Operations Control Room
MON	Monitor
MOPS	Mission Operations Planning System
MPC	Manual Pointing Controller
MSFC	Marshall Space Flight Center
MSG	Mission Support Group
NASA	National Aeronautics and Space Administration
NR	Non-conformance Report
O_2	Oxygen
OA	Orbital Assembly
OA	Optical Assembly
OD	Operations Director

Abbreviations (Continued)

OG	Outer Gimbal
OGDL	Outer Gimbal Drive Logic
OMA	Optical-Mechanical Assembly
OMSF	Office of Manned Space Flight
OSH	Off Scale High
OSL	Off Scale Low
OWS	Orbital Workshop
PE	Preamplifier Electronics
PCM	Pulse Code Modulation
PCS	Pointing Control System
PCSA	Power Control Switching Assembly
PDD	Program Definition Document
PI	Principal Investigator
PMC	Post-Manufacturing Checkout
PS	Payload Shroud
PSA	Power Supply Assembly
PTR	Program Trouble Report
R	Right
RAPS	Real-Time Astrionics Problem Solving
RCI	Rate Command Integral
RCS	Reaction Control System
RG	Rate Gyro
RGP	Rate Gyro Processor
RGRM	Rate Gyro Redundancy Management
RM	Redundancy Management
RPM	Roll Position Mechanism
RTC	Real Time Clock
SAL	Scientific Airlock
SAS	Solar Array System
SC	Signal Conditioner
SCCM	Standard Cubic Centimeters per Minute
SCIM	Standard Cubic Inches per Minute
SEC	Secondary
SHS	Skylab Hybrid Simulator
SI	Solar Inertial
S-1B	Saturn I-B
S-IC	Saturn I-C
S-II	Saturn II
S-IVB	Saturn IVB
SL-1	Skylab-1

Abbreviations (Concluded)

SL-2	Skylab-2
SL-3	Skylab-3
SL-4	Skylab-4
SPS	Samples per Second
SRB	Software Review Board
SS	Switch Selector
ST	Star Tracker
STAC	Support Team for Attitude Control
STE	Star Tracker Electronics
SUS	Suit Umbilical System
SWCR	Software Change Request
SWS	Saturn Workshop
SVWS	Saturn V Workshop
SWS	Saturn Workshop
TACS	Thruster Attitude Control System
TCS	Thermal Control System
TGMT	Greenwich Mean Time (Software Parameter)
TM	Telemetry
TMR	Triple Modular Redundancy
TR	Tape Recorder
T/V	Thermal-Vacuum
WACS	Workshop Attitude Control System
WCIU	Workshop Computer Interface Unit
WPS	Workshop Propulsion System
WT	Waste Tank
X-POP	X Axis Perpendicular to Orbit Plane
X-LV	X-Local Vertical
Z-LV	Z-Local Vertical

SECTION I. INTRODUCTION

A. Purpose

This report concludes the analysis of the Skylab Attitude and Pointing Control System in-orbit performance. The results are presented in discipline language and are intended for discipline use. Conclusions and recommendations are presented which could be useful during the establishment of design concepts, requirements and constraints for future spacecraft.

B. Scope

The APCS is considered as an integral system composed of a number of subsystems. In the interest of emphasizing specific performance characteristics, system performance is discussed at the system, subsystem, hardware, and software levels.

Significant concept and requirement evolution, testing, and modifications resulting from tests are briefly summarized to aid in understanding the in-orbit configuration description procedures, and performance.

Only in-orbit hardware, operational interfaces, repairs, work arounds, unscheduled and scheduled activities are included under mission performance. Anomalous performance is treated separately for emphasis and visibility.

Manned operations covered 174 of the total 272 mission days which began May 14, 1973 and ended on February 8, 1974. The three 3-man missions were for 29, 60 and 85 days respectively. The primary time references used throughout this report are DAY and Greenwich Mean Time (GMT).

Table 1 contains a list of DAYs, Dates and Mission Days. This report uses DAY 1 through DAY 272 to designate dates.

Detailed event times may be found in the Skylab Mission Events List, 25M00700, available in the MSFC Documentation Repository. Additional Skylab systems evaluation details may be found in the following NASA Technical Memoranda.

TMX-64808 MSFC Skylab Final Program Report

TMX-64809 MSFC Skylab Corollary Experiments Final Technical Report

TMX-64810	MSFC Skylab Airlock Module Final Technical Report
TMX-64811	MSFC Skylab Apollo Telescope Mount Final Technical Report
TMX-64812	MSFC Skylab Multiple Docking Adapter Final Technical Report
TMX-64813	MSFC Skylab Orbital Workshop Final Technical Report
TMX-64814	MSFC Skylab Mission Report-Saturn Workshop
TMX-64815	MSFC Skylab Apollo Telescope Mount Summary Mission Report
TMX-64818	MSFC Skylab Electrical Power System Mission Evaluation Report
TMX-64819	MSFC Skylab Instrumentation and Communication System Mission Evaluation Report
TMX-64820	MSFC Skylab Corollary Experiments Systems Mission Evaluation Report
TMX-64821	MSFC Skylab Apollo Telescope Mount Experiment Systems Mission Evaluation Report
TMX-64822	MSFC Skylab Thermal & Environmental Control System Mission Evaluation Report
TMX-64823	MSFC Skylab Apollo Telescope Mount Thermal Control System Mission Evaluation Report
TMX-64824	MSFC Skylab Structures and Mechanical Systems Mission Evaluation Report
TMX-64825	MSFC Skylab Crew Systems Mission Evaluation Report
TMX-64826	MSFC Skylab Contamination Control Systems Mission Evaluation Report
TMX-64852	Skylab Thruster Attitude Control System

Table 1. Mission Day Time Reference

DAY	DATE (1973)	DAY OF YEAR	MISSION PERIODS
1	5-14	134	UNMANNED PERIOD (FIRST)
2	5-15	135	
3	5-16	136	
4	5-17	137	
5	5-18	138	
6	5-19	139	
7	5-20	140	
8	5-21	141	
9	5-22	142	
10	5-23	143	
11	5-24	144	
12	5-25	145	1
13	5-26	146	2
14	5-27	147	3
15	5-28	148	4
16	5-29	149	5
17	5-30	150	6
18	5-31	151	7
19	6-1	152	8
20	6-2	153	9
21	6-3	154	10
22	6-4	155	11
23	6-5	156	12
24	6-6	157	13
25	6-7	158	14
26	6-8	159	15
27	6-9	160	16
28	6-10	161	17
29	6-11	162	18
30	6-12	163	19
31	6-13	164	20
32	6-14	165	21
33	6-15	166	22
34	6-16	167	23
35	6-17	168	24
36	6-18	169	25
37	6-19	170	26
38	6-20	171	27
39	6-21	172	28
40	6-22	173	29
41	6-23	174	FIRST MANNED PERIOD MISSION DAYS
42	6-24	175	
43	6-25	176	
44	6-26	177	
45	6-27	178	
46	6-28	179	
47	6-29	180	
48	6-30	181	
49	7-1	182	
50	7-2	183	
51	7-3	184	
52	7-4	185	
53	7-5	186	
54	7-6	187	
55	7-7	188	
56	7-8	189	
57	7-9	190	
58	7-10	191	
59	7-11	192	
60	7-12	193	
61	7-13	194	
62	7-14	195	
63	7-15	196	
64	7-16	197	
65	7-17	198	
66	7-18	199	
67	7-19	200	
68	7-20	201	
69	7-21	202	(SECOND UNMANNED PERIOD)
70	7-22	203	
71	7-23	204	
72	7-24	205	
73	7-25	206	
74	7-26	207	
75	7-27	208	
76	7-28	209	1
77	7-29	210	2
78	7-30	211	3
79	7-31	212	4
80	8-1	213	5
81	8-2	214	6
82	8-3	215	7
83	8-4	216	8
84	8-5	217	9
85	8-6	218	10
86	8-7	219	11
87	8-8	220	12
88	8-9	221	13
89	8-10	222	14
90	8-11	223	15
91	8-12	224	16
92	8-13	225	17
93	8-14	226	18
94	8-15	227	19
95	8-16	228	20
96	8-17	229	21
97	8-18	230	22
98	8-19	231	23
99	8-20	232	24
100	8-21	233	25
101	8-22	234	26
102	8-23	235	27
103	8-24	236	28
104	8-25	237	29
105	8-26	238	30
106	8-27	239	31
107	8-28	240	32
108	8-29	241	33
109	8-30	242	34
110	8-31	243	35
111	9-1	244	36
112	9-2	245	37
113	9-3	246	38
114	9-4	247	39
115	9-5	248	40
116	9-6	249	41
117	9-7	250	42
118	9-8	251	43
119	9-9	252	44
120	9-10	253	45
121	9-11	254	46
122	9-12	255	47
123	9-13	256	48
124	9-14	257	49
125	9-15	258	50
126	9-16	259	51
127	9-17	260	52
128	9-18	261	53
129	9-19	262	54
130	9-20	263	55
131	9-21	264	56
132	9-22	265	57
133	9-23	266	58
134	9-24	267	59
135	9-25	268	60
136	9-26	269	SECOND MANNED PERIOD MISSION DAYS
137	9-27	270	
138	9-28	271	
139	9-29	272	
140	9-30	273	
141	10-1	274	
142	10-2	275	
143	10-3	276	
144	10-4	277	
145	10-5	278	
146	10-6	279	
147	10-7	280	
148	10-8	281	
149	10-9	282	
150	10-10	283	
151	10-11	284	
152	10-12	285	
153	10-13	286	
154	10-14	287	
155	10-15	288	
156	10-16	289	
157	10-17	290	
158	10-18	291	
159	10-19	292	
160	10-20	293	
161	10-21	294	
162	10-22	295	
163	10-23	296	
164	10-24	297	
165	10-25	298	
166	10-26	299	
167	10-27	300	
168	10-28	301	
169	10-29	302	
170	10-30	303	
171	10-31	304	
172	11-1	305	
173	11-2	306	
174	11-3	307	
175	11-4	308	
176	11-5	309	
177	11-6	310	
178	11-7	311	
179	11-8	312	
180	11-9	313	
181	11-10	314	
182	11-11	315	
183	11-12	316	
184	11-13	317	
185	11-14	318	
186	11-15	319	
187	11-16	320	1
188	11-17	321	2
189	11-18	322	3
190	11-19	323	4
191	11-20	324	5
192	11-21	325	6
193	11-22	326	7
194	11-23	327	8
195	11-24	328	9
196	11-25	329	10
197	11-26	330	11
198	11-27	331	12
199	11-28	332	13
200	11-29	333	14
201	11-30	334	15
202	12-1	335	16
203	12-2	336	17
204	12-3	337	18
205	12-4	338	19
206	12-5	339	20
207	12-6	340	21
208	12-7	341	22
209	12-8	342	23
210	12-9	343	24
211	12-10	344	25
212	12-11	345	26
213	12-12	346	27
214	12-13	347	28
215	12-14	348	29
216	12-15	349	30
217	12-16	350	31
218	12-17	351	32
219	12-18	352	33
220	12-19	353	34
221	12-20	354	35
222	12-21	355	36
223	12-22	356	37
224	12-23	357	38
225	12-24	358	39
226	12-25	359	40
227	12-26	360	41
228	12-27	361	42
229	12-28	362	43
230	12-29	363	44
231	12-30	364	45
232	12-31	365	46
233	1-1	1	47
234	1-2	2	48
235	1-3	3	49
236	1-4	4	50
237	1-5	5	51
238	1-6	6	52
239	1-7	7	53
240	1-8	8	54
241	1-9	9	55
242	1-10	10	56
243	1-11	11	57
244	1-12	12	58
245	1-13	13	59
246	1-14	14	60
247	1-15	15	61
248	1-16	16	62
249	1-17	17	63
250	1-18	18	64
251	1-19	19	65
252	1-20	20	66
253	1-21	21	67
254	1-22	22	68
255	1-23	23	69
256	1-24	24	70
257	1-25	25	71
258	1-26	26	72
259	1-27	27	73
260	1-28	28	74
261	1-29	29	75
262	1-30	30	76
263	1-31	31	77
264	2-1	32	78
265	2-2	33	79
266	2-3	34	80
267	2-4	35	81
268	2-5	36	82
269	2-6	37	83
270	2-7	38	84
271	2-8	39	85
TESTS & ORBITAL STORAGE			THIRD MANNED PERIOD MISSION DAYS (CONTINUED)
272	2-9	40	

SECTION II. SUMMARY AND CONCLUSIONS

A. Summary

The Skylab Attitude and Pointing Control System (APCS) provided three axis attitude stabilization and maneuvering capability for the Orbital Assembly (OA) and provided pointing control of the Apollo Telescope Mount (ATM) experiment canister for observing targets of opportunity on the sun. A number of new concepts evolved into the design of the Skylab APCS. Skylab was the first manned spacecraft to utilize large Control Moment Gyros (CMG) for momentum storage and attitude control, the first to utilize vehicle maneuvers for CMG momentum desaturation, the first to utilize a fully digital control system with in-orbit reprogramming capability and extensive automatic redundancy management, and the first to utilize an attitude reference system based on a four parameter strapdown computation.

The APCS was the culmination of a prolonged evolutionary process. This evolution was prompted by major changes in mission objectives, design requirements, state-of-the-art advances, test results and crew requirements.

Pre-mission design verification was conducted at the component, black box, software subsystem and system level. On the system level, extensive computer simulation and software verification was performed. Unexpected anomalies during the mission required additional ground testing and simulation studies to verify analytical conclusions and new hardware developed for crew installation.

During the mission, two of nine APCS Rate Gyro Processors, the Star Tracker, one Control Moment Gyro, and one EPCS Rate Gyro Processor failed. Three additional APCS Rate Gyros were seriously degraded. However, sufficient built-in redundancy was available to accomodate all these failures, and pointing and maneuver requirements were satisfied. Six additional Rate Gyros were taken into orbit and installed in the system by the SL-3 crew. This was done to provide additional capability in the event of more Rate Gyro failures.

The APCS performed a central role in the survival of Skylab after loss of the Meteoroid Shield and one Orbital Workshop (OWS) Solar Array Wing during launch. The built-in flexibility allowed off-nominal vehicle attitude maneuvers to be performed for vehicle

thermal control until a sunshade could be deployed by the SL-2 crew. Although these maneuvers consumed considerable Thruster Attitude Control System (TACS) gas, it was possible to complete the expanded 272 day mission, and also meet the additional maneuver requirements imposed by experiments to study the Comet Kohoutek and perform Stellar X-Ray photography during the SL-4 mission.

The simulations developed during design verification proved to be invaluable for evaluating and optimizing the mission flight plans and contributed directly to the success of the mission. The integrity of the simulation techniques was verified by extensive mission and post-mission comparisons of flight and predicted performance.

Analysis of the data retrieved from the mission resulted in valuable APCS engineering knowledge, useable for establishing effective design concepts and requirements for future spacecraft.

B. Conclusions

1. General. Based on analysis of flight data, it can be concluded that the Skylab Attitude and Pointing Control System successfully performed within design specification and met or exceeded all imposed requirements. Problems and hardware failures were dealt with primarily by means of built-in system flexibility and hardware redundancy. Some problems were resolved through crew participation in unusual contingency procedures, such as installation of the Rate Gyro Six-Pack.

As the first mission of its kind, Skylab provided experience with long term operation of manned spacecraft control system concepts and hardware, many of which had never been flown before. This experience provided a valuable base for the design and planning of future long duration missions.

2. Specific Conclusions. Conclusions for particular APCS subsystems and hardware components are presented in their respective section. However, to provide an overview, this summary is presented.

a. Test and Verification Program. The Skylab APCS was composed of components and subsystems of which most had not been qualified for orbital space flight. A thorough hardware, software and systems test program was developed to verify proper design and operation of the APCS. Many significant problems were found and corrected as a result of the test program. In addition, the experience gained in the program aided immeasurably in the operation of Skylab.

b. Telemetry Instrumentation. Additional or expanded telemetry instrumentation would have been highly desirable for APCS analysis and evaluation. This became evident as a result of the APCS problems and anomalies encountered during the mission. In particular, additional measurements of system parameters and command functions, greater resolution of sensor outputs and increased data recording capability would have been useful.

c. Attitude Control Systems.

(1) Navigation and Attitude Reference. The digitally implemented, four parameter strapdown calculation, used to maintain vehicle attitude reference for attitude control and maneuvering, worked as designed and demonstrated the value of a strapdown system for long term orbital operations. Use of an onboard navigation and timing scheme utilizing a closed form solution for a circular orbit proved to be satisfactory for all system requirements when coupled with the capability for periodic updates to navigation parameters by ground support.

Degraded knowledge of vehicle roll reference resulted from the problems and ultimate failure of the Star Tracker. In view of the importance of accurate roll reference information for momentum management and ATM experiments, a redundant system for obtaining roll attitude updates would have been very useful.

(2) Attitude Control. Based on analysis of the flight data and in-orbit tests, the compensation filters performed as predicted and the pointing accuracy requirements were met. The CMG and TACS Control Law, under both two and three CMG control, performed as predicted. Expanded ATMDC memory allotment would have allowed expansion of the Flight Program for improved control of the momentum states. Consideration should be given to removing the CMG gimbal stops from future CMGs. This would greatly simplify the CMG Control Law and eliminate Gimbal Stop encounters.

The designed flexibility of the maneuver scheme contributed to the survival of the Skylab after loss of the Meteoroid Shield and OWS Solar Array Wing and allowed the off-nominal vehicle attitude maneuvers imposed for thermal control.

(3) Momentum Management. The success in bounding the CMG momentum by the momentum management scheme verified the desirability of using a momentum exchange system as the primary attitude control system for long term earth orbiting space flight.

(4) ATMDC Software Program. The flexibility of a digitally implemented APCS was verified by Skylab. The ability

to modify or patch the existing Flight Program proved to be highly advantageous. This capability enhanced survival of the Skylab and made it possible to support the new program objectives related to Kohoutek. Many of the routines were imperative for a successful mission.

(5) Redundancy Management. Automatic Redundancy Management was instrumental in the rapid identification of the Rate Gyro problems and provided the essential short response time required to recognize and correct any failure in mission critical components which could have jeopardized the mission or endangered the crews. Manual Redundancy Management performed as designed, but an added capability to select the back-up 800 Hz power source and/or EPC Roll resolver would have been desirable.

d. APCS Hardware.

(1) Rate Gyro Processors. The Rate Gyro Processors (RGP) experienced serious problems and failures as a consequence of two design deficiencies. The RGP anomalies and failures together with the installation of the Rate Gyro Six-Pack demonstrated that in future long-duration manned missions, consideration should be given to replacement or maintenance of mission-critical components, such as the Rate Gyro Processors, during the mission.

(2) Star Tracker. It should be recognized in the future that a Star Tracker flown on any manned space station similar to Skylab will most likely be exposed to frequent drifting bright contaminant particles. This appears to be unavoidable in the vicinity of such a station due to life system vents, large area paint surface deterioration, etc. Thus every attempt should be made to design a Star Tracker, or other roll attitude reference system, to recognize and avoid tracking such particles.

(3) Control Moment Gyros. The CMGs demonstrated the desirability and effectiveness of a momentum exchange system for attitude control. The failure of CMG No. 1 and the threatened failure of CMG No. 2 demonstrated the need for continued analysis on wheel bearing design in a zero gravity environment. In addition, it would be advantageous to eliminate gimbal stops and provide increased momentum storage capability.

(4) TACS Hardware. The TACS hardware performed as designed.

(5) ATMDC/WCIU and MLU. The ATM Digital Computer, Workshop Computer Interface Unit and Memory Load Unit successfully performed their designed functions. The capability to completely

load a computer memory by means of RF uplink was demonstrated for the first time on Skylab.

(6) Acquisition Sun Sensor. The Acquisition Sun Sensor (Acq. SS) performed as designed throughout the mission. Due to potential problems with detector deterioration or contamination, future long duration missions should include a sun sensor design which would be insensitive to solar intensity.

e. Experiment Pointing Control System.

(1) Subsystems. The Experiment Pointing Control (EPC) subsystems exceed all imposed design requirements. Indications from the crews and the Experiment Principal Investigators indicate that the stability and pointing accuracy were excellent and well within specifications.

The concept of a separate, gimbaled Experiment Pointing and Control System to isolate transient disturbances and provide greater pointing accuracy and stability was proven.

(2) Hardware. Performance of the EPC was as designed. On two occasions the UP/DN orbital locks did not uncage on command but they later recovered.

Although the Fine Sun Sensor (FSS) performed as designed, the crew had difficulty in zeroing the wedge counters and the wedge incrementing problem demonstrated the need for consideration of alternative designs which would eliminate those problems.

SECTION III. GENERAL

This section includes a description of the Attitude and Pointing Control System (APCS), a History of APCS development and the APCS Test Program.

A. System Description

1. Introduction. The Skylab Orbital Assembly (OA) and its associated control axes are shown in figure 1. The APCS provided three-axis attitude stabilization and maneuvering capability for the vehicle throughout the mission and pointing control of the Skylab experiment package during experimentation periods.

The APCS was comprised of two separate control systems. The Attitude Control System (ACS) provided the attitude stabilization and maneuvering capability for the vehicle. The Experiment Pointing and Control System (EPCS) provided pointing control of the ATM Experiment Canister and allowed offset pointing to targets of opportunity on or near the solar disk.

The major sections of the APCS, shown in figure 2, are:

ATM Rate Gyro Processors (RGP)

ATM Acquisition Sun Sensor (Acq. SS)

Star Tracker (ST)

ATM Digital Computer (ATMDC)

Workshop Computer Interface Unit (WCIU)

Control Moment Gyros (CMG)

Thruster Attitude Control System (TACS)

Experiment Pointing Control System (EPCS)

Control and Display (C & D) Panel.

Six control modes were addressable by CM Console switches and Digital Address System/Digital Command System (DAS/DCS) for APCS operation. These are briefly described as follows:

a. Standby. This mode was used when no attitude control was required of the APCS. While in the standby mode, the

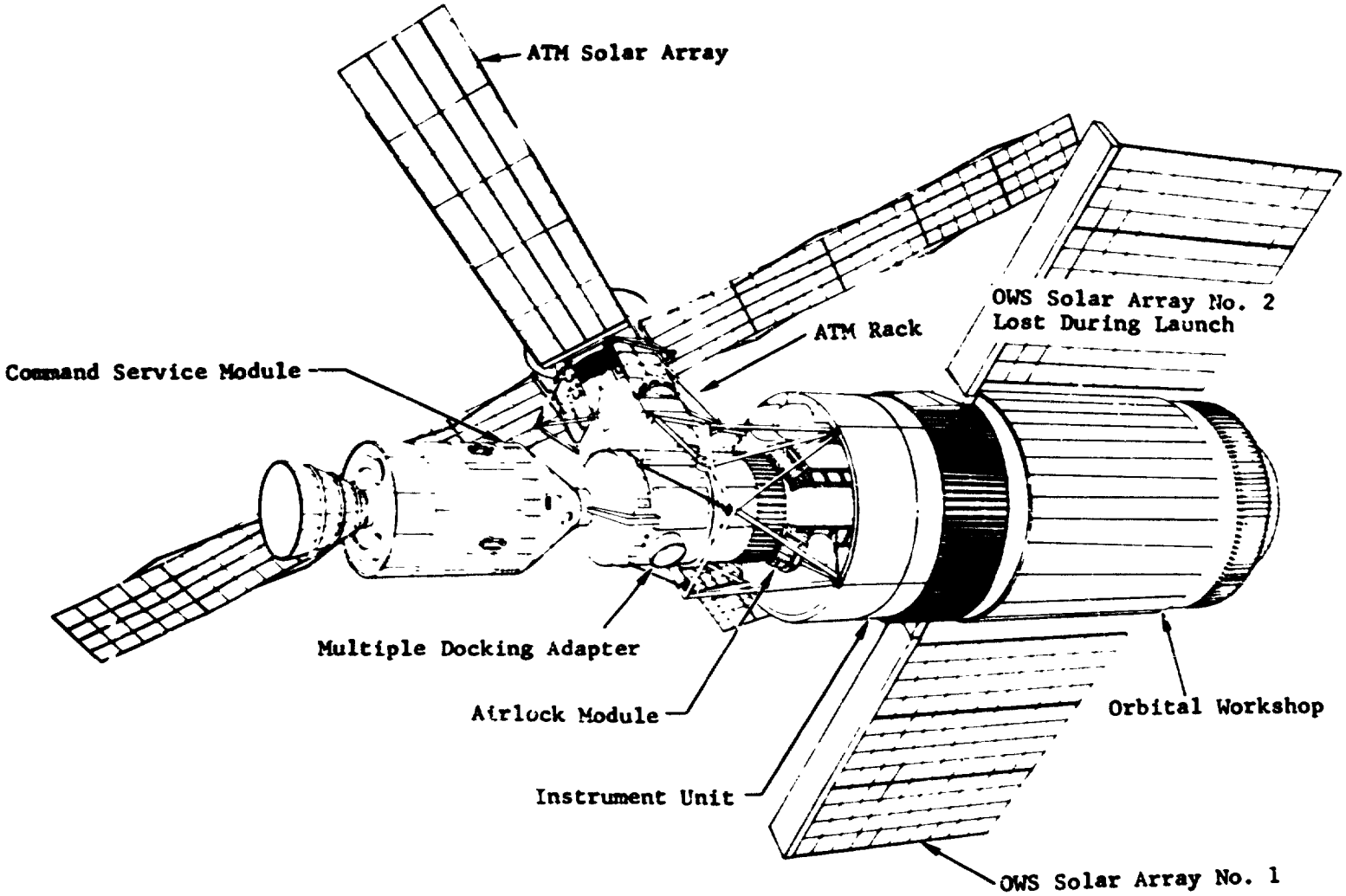

Figure 1. Skylab Orbital Assembly

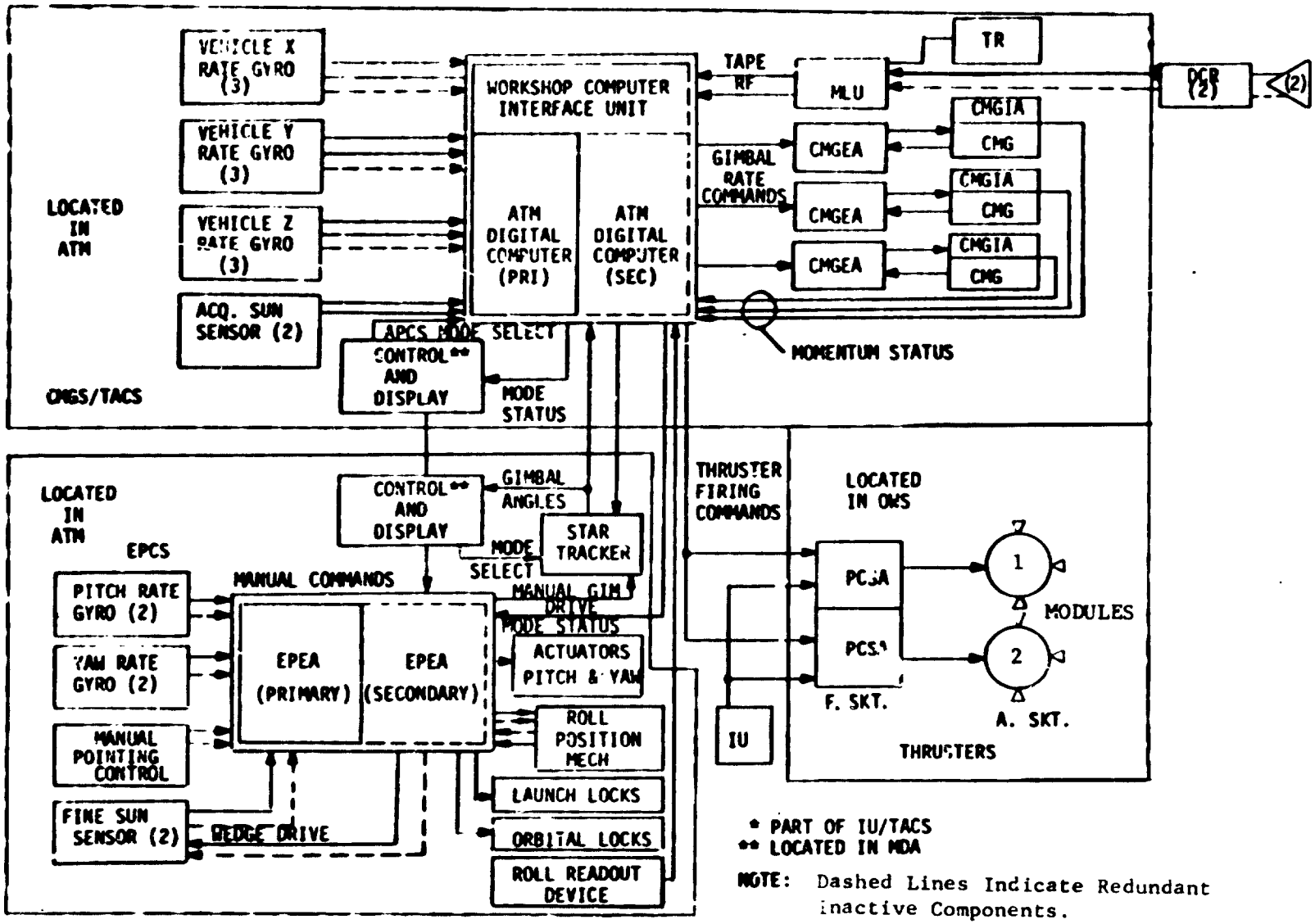

Figure 2 APCS Functional Block Diagram

CMG gimbal rate commands for attitude control were zeroed and no firing commands were issued to the TACS.

b. Solar Inertial (SI) This mode was used during periods of solar experiment operation and for momentum dumping. The vehicle attitude during orbital day was the OA + Z-axis pointing toward the sun and the X-axis close to the orbital plane. Vehicle control was maintained through the CMG/TACS control systems. The EPCS was not active in this mode.

c. Experiment Pointing. This mode was identical to the day portion of the SI mode with respect to vehicle control. In this mode, however, the EPCS was activated.

d. Attitude Hold (CMG). This mode required that the vehicle be held inertially fixed and/or maneuvered to any desired attitude, with control torques furnished by the CMG/TACS system.

e. Attitude Hold (TACS). This mode required that the vehicle be held inertially fixed and/or maneuvered to any desired attitude with control torques furnished by the TACS.

f. Local Vertical (Z-LV). This mode was entered during the rendezvous phases of the mission or when Earth Pointing was required for experimentation periods. The Z-LV (Rendezvous) attitude was defined as the -Z-axis pointing toward the earth along the local vertical (nadir), with the +X-axis in the orbital plane and opposite the velocity vector. The Z-LV (Earth Resources) attitude was defined as the -Z control axis pointing toward the earth along the local vertical (nadir), with the +X control axis in the orbital plane and pointing in the direction of the velocity vector.

System redundancy was provided to ensure crew safety and preclude degradation of system performance.

2. Attitude Control System (ACS). The ACS was a digitally implemented combination CMG momentum exchange and reaction jet control system. The system was designed to operate in unison with the TACS providing assistance if the CMGs were unable to control the vehicle. The TACS could also operate as the primary control system. Attitude error and rate sensing was provided by two Acquisition Sun Sensors nine Rate Gyros (three per axis), and a Star Tracker (ST).

a. Thruster Attitude Control System. The TACS was composed of six cold gas thrusters and the necessary logic to select and fire the proper thruster. The ATMDC used the TACS Control Law to provide thruster firing commands to null out attitude and rate errors when control deadbands were exceeded, and to assist the CMGs when system momentum approached saturation. The thrusters were mounted on the OWS as shown in figure 3. Two thrusters provided uncoupled Y-axis

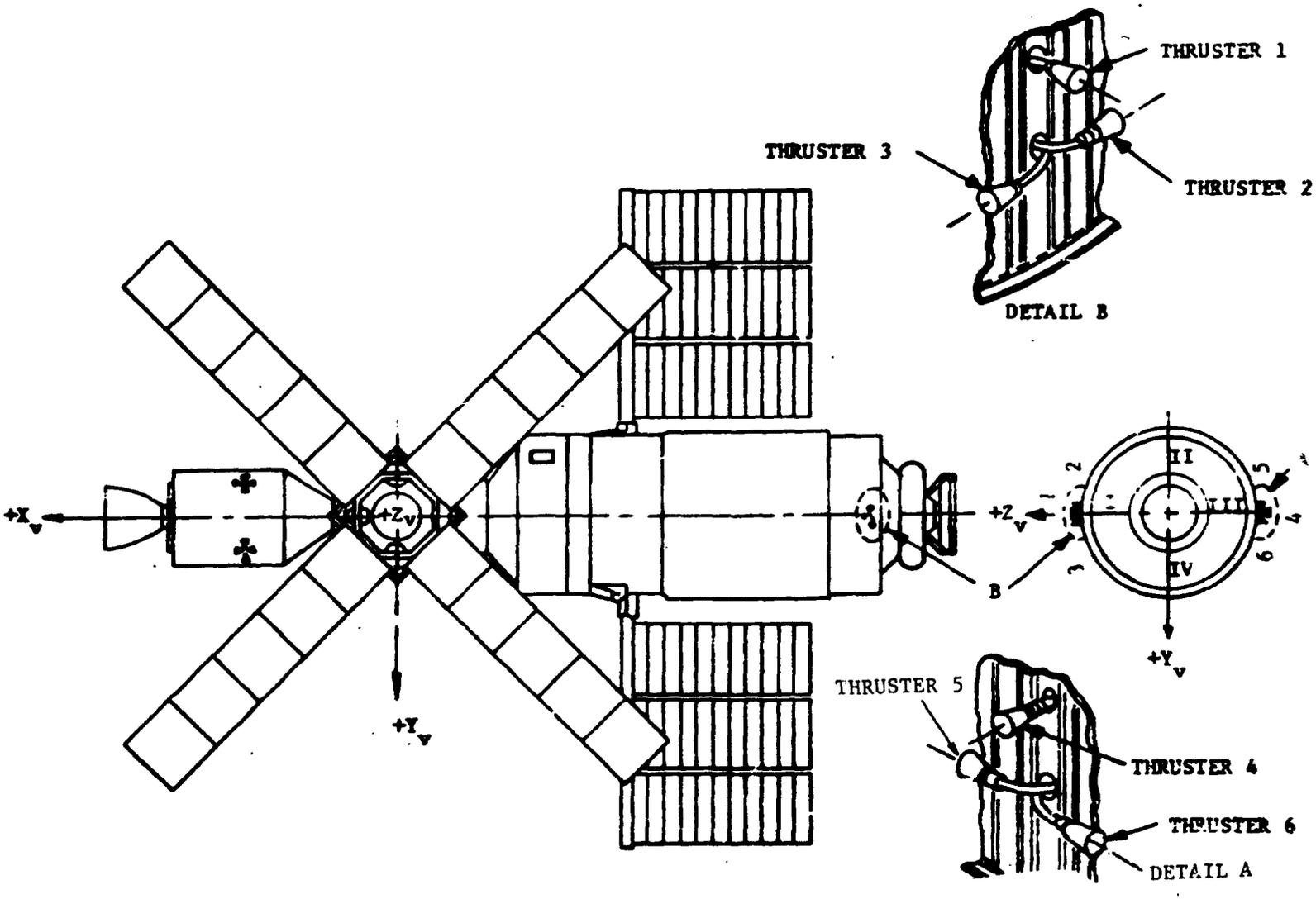

Figure 3. TACS Thruster Configuration

control and four thrusters provided coupled X and Z-axis control. Two types of thruster firings were commanded, Full-On and Minimum Impulse Bit (MIB) firing time. For Full-On firings the selected thruster was fired continuously for one second. The MIB firing time was selectable from 40 to 400 milliseconds to compensate for pressure decrease in the TACS cold gas supply tanks. At the beginning of the mission a thruster produced 463 Newtons of thrust. This decreased to approximately 82 Newtons at the end of the mission, as the TACS gas was depleted.

b. CMG Control System. The CMG System was composed of three orthogonally mounted, double-gimbaled CMGs with a stored momentum capability of approximately 3000 N.m.s. per CMG. When all gimbals were at their zero position the spin axes were parallel to the vehicle coordinates. This configuration is shown in figure 4.

The CMG Control Law in the ATMDC utilized three normalized torque commands and the CMG momentum status to generate proper CMG gimbal rate commands. The Control Law consisted of three parts: the Steering Law, the Rotation Law and a Gimbal Stop Avoidance Law. Additional routines were included for specialized situations.

The Steering Law provided torques on the vehicle either for attitude maneuvers or to oppose torques from gravity gradient, vehicle vents, or crew disturbances. Gimbal rate commands were generated in such a way that the torques resulting on the vehicle were identical to the desired torques in direction and magnitude.

The Rotation Law attempted to minimize the probability of contact with the gimbal stops by reducing the largest gimbal angles. This was accomplished by rotation about the vector sums only. The total angular momentum was unaffected and no torque was exerted on the vehicle.

The last portion of the CMG Control Law utilized a mathematically defined pseudo gimbal boundary to prevent driving the CMG gimbals into the gimbal stops (shown in figure 5).

A reset routine was incorporated into the CMG Control Law to allow the CMG system to recover from undesirable gimbal angle positions and/or momentum configuration.

Outer gimbal drive logic was provided during maneuvers in order to force a desirable gimbal angle position. If it was sensed that a gimbal was moving in a direction which would bring it in contact with a stop, a momentary attitude perturbation was allowed and an open loop drive was executed to force the gimbal to the proper side of the stop.

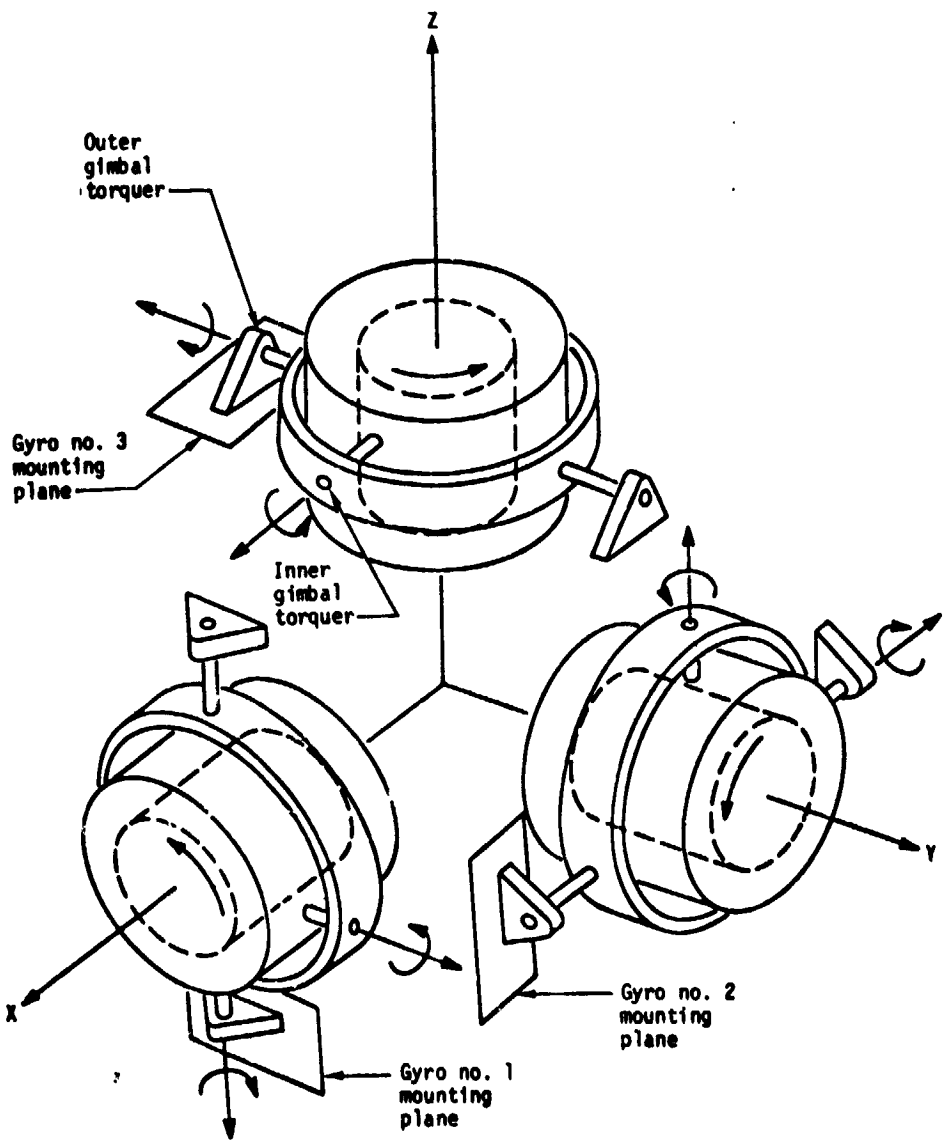

Figure 4. CMG Mounting Configuration

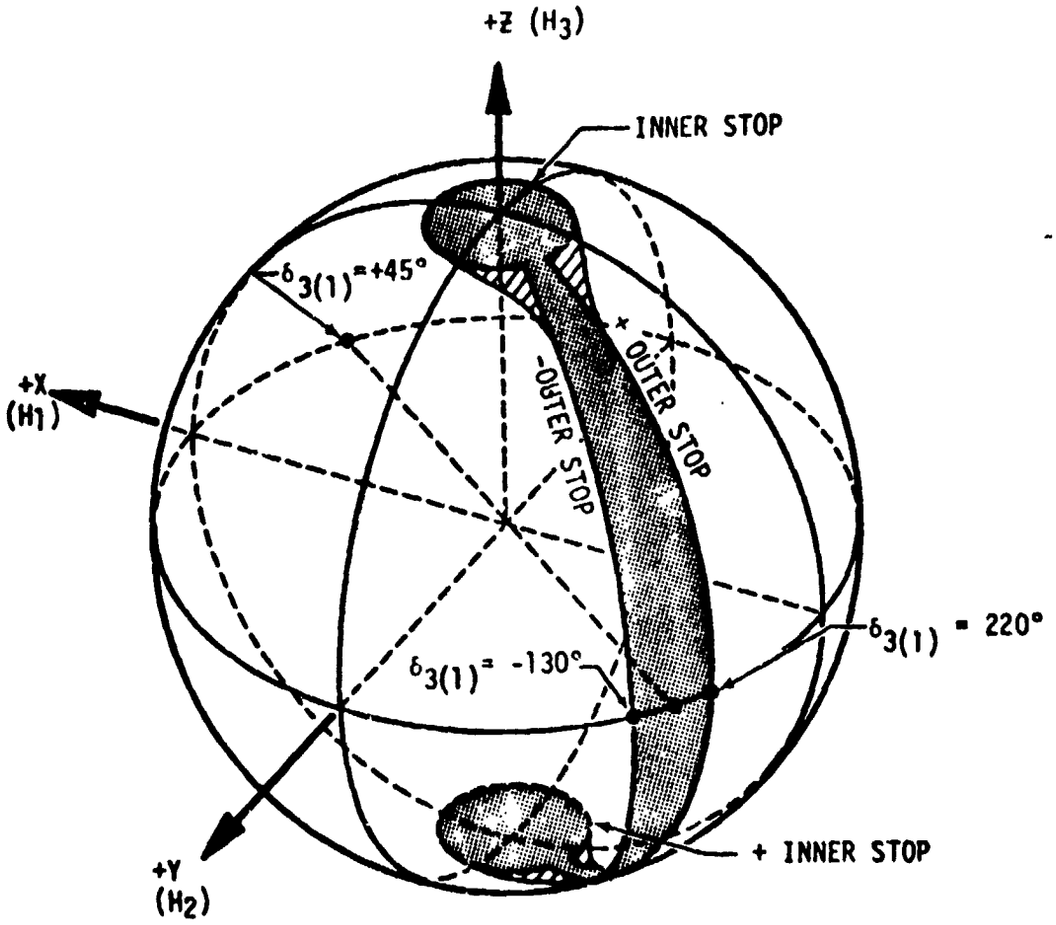

(a) H_1, H_2, H_3 INDICATE SPIN VECTOR POSITION TO $IG_S = 0°$ & $OG_S = 0°$

(b) CROSSHATCHED AREA SHOWS THE ADDITION GIMBAL BOUNDARY AREA USED IN THE CONTROL LAW

Figure 5. Gimbal Stops of CMG (H_1)

c. Attitude Control System Operation. When the TACS and CMG systems were operated in the augmented configuration, all control was delegated to the CMG system as long as it was capable of maintaining the attitude error within 20 degrees. If CMG momentum approached saturation, TACS would fire to assist the CMGs. The system would switch to Auto TACS Only control, with deadbands of (3°, 2°, 2°) in X, Y, and Z, respectively, whenever the attitude error exceeded 20 degrees on any axis.

The Skylab used a 4-parameter strapdown attitude reference system consisting of Rate Gyros as inertial sensors and the ATMDC to calculate the strapdown algorithm. A two-axis Sun Sensor, a Star Tracker and onboard analysis of the Attitude Control System response provided information to update the strapdown system. When an attitude error occurred, the CMG control Law and/or the TACS Control Law determined the proper CMG gimbal rate commands and/or thruster firing commands. The CMG momentum status was monitored by the Flight Program through the CMG direction cosine resolvers.

A filter was incorporated in the CMG Control Law for each control axis. The purpose of filters was to remove undesirable flexible body effects, disturbances and provide adequate stabilization and pointing of the flexible vehicle. The control loop gains and filter coefficients were different for each axis.

There were two classes of vehicle maneuvers: Solar Inertial offset pointing and general purpose. Solar Inertial offset pointing was limited to small angles ($\pm$ 4 degrees) about the X and Y-vehicle axes and was accomplished by biasing the attitude error signal with the desired offset angle. The general purpose maneuvers required maneuvering the vehicle to arbitrary time variant or inertial attitudes and was accomplished via strapdown commands. Large momentum changes in the CMG system were generally required to provide the desired maneuver rates.

d. Digital Implementation. Digital implementation was accomplished using an ATMDC and WCIU. The Flight Program was responsible for:

Operating modes

Skylab attitude reference

Navigation and timing

CMG Control Law

TACS Control Law

Maneuvering

Automatic Redundancy Management

Function command, data display, telemetry, and experiment support.

The ATMDC Flight Program was modular in design, and consisted of two basic software subsystems: the Executive or Control Program and the Application Subsystem. The Control Program controlled the sequence of the program execution and provided a software priority on executable functions in order to achieve a multi-task keying capability. The application subsystem consisted of all the application program modules which when executed by the control subsystem performed all required Flight Program functions. From a timing standpoint the Flight Program consisted of two loops. A slow loop completed approximately once per second and an intermediate loop completed five times per second. The attitude control functions were performed at the rate of five times per second. Following the execution of the slow loop the ATMDC entered a wait state.

e. CMG Momentum Management. Any noncyclic disturbance-torque acting on the vehicle would result in a net CMG momentum buildup. Because of finite storage capacity of the CMG cluster this momentum accumulation would eventually cause CMG saturation. After complete saturation the CMG cluster could not compensate for disturbance torques about the axis of saturation.

To preclude CMG saturation and minimize the effects of noncyclic gravity gradient torques, the vehicle X-principal axis was maintained close to the orbital plane and CMG momentum desaturation maneuvers were performed periodically during the night portion of the orbit. The magnitude of the desaturation maneuvers was based on factors obtained by sampling normalized components of the total momentum four times during the day portion of the orbit.

3. Experiment Pointing Control System. The Experiment Pointing Control (EPC) Subsystem was used for pointing control of the ATM experiment package. The experiment package (canister) was mounted within a three-degree-of-freedom gimbal mechanism. Open loop positioning was provided for the roll Z-axis and the EPCS provided automatic stabilization of the canister about the X and Y-axes. This allowed the EPCS to isolate the canister from most perturbations due to vehicle and crew motion disturbance torques.

The Fine Sun Sensor (FSS) and Rate Gyro (RG) sensors mounted on the canister supplied position and rate feedback to the Experiment

Pointing Electronics Assembly (EPEA). The EPEA contained the electronic functions to command the gimbal actuators, closing the control loop. The Z-axis stabilization was provided by the ACS.

Manual positioning about all three axes was provided for offset/roll pointing of the experiment canister. X and Y-axis offset pointing were achieved by means of rotating optical wedge mechanisms within the FSS. Offset commands could be issued from the Manual Pointing Controller (MPC) or from the ATMDC. The Roll Position Mechanism (RPM) was activated by command switches located on the Control and Display Panel and on the ATM EVA Rotation Control Panel. All offset/roll commands were processed by the EPEA. A line-of-sight pointing capability during roll operations was provided by the ATMDC, utilizing the ATMDC wedge drive capability.

The EPEA also provided an interface between the Star Tracker and the MPC for manual positioning of the Star Tracker gimbals.

Other EPCS related functions were canister caging control, experiment alignment calibration, and experiment and FSS door control.

Figure 6 is a block diagram of the EPCS, showing interfaces with the APCS. The gimbal and roll mechanisms are shown in figure 7. Descriptions of the EPCS and hardware components are presented in Section VIII and IX.

4. Redundancy Management. Reliability considerations for long missions required component redundancy. All mission-critical single point failures were made redundant by switchover capability and redundant components. System redundancy was provided to the point that any component failure that could cause the mission to be aborted or preclude mission objectives was provided with a backup unit or with an alternate subsystem configuration that could be selected with minimum performance degradation.

Hardware redundancy included the following items:

Nine Rack Rate Gyro Processors (3 per axis)

Two Acquisition Sun Sensors (2 channels per axis)

Three CMGs (two required for control)

Two ATMDC/WCIU Units

Two TACS Power Control Switching Assemblies (PCSAs) and quad-redundant solenoid valves for each thruster

Two Fine Sun Sensors (two channels per axis)

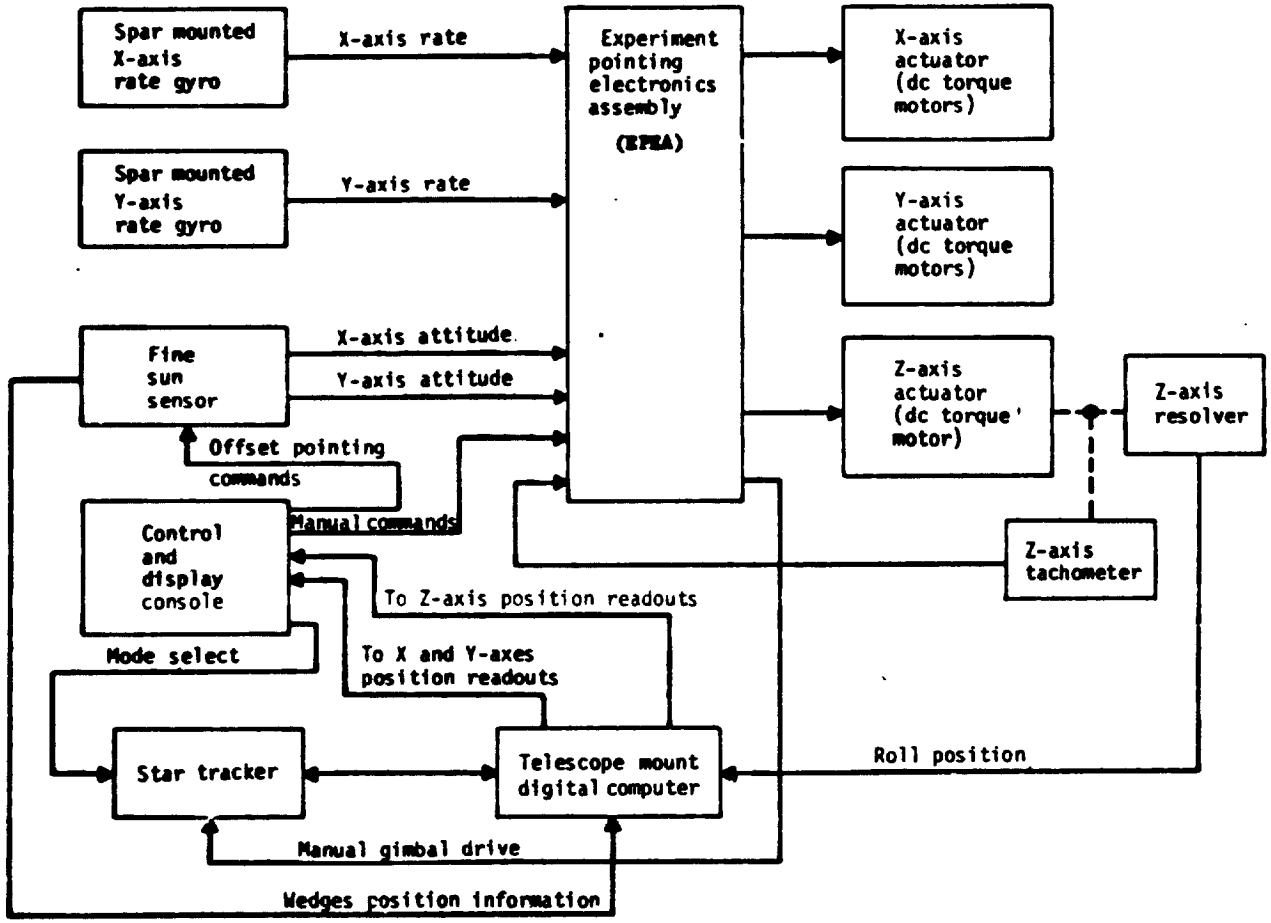

Figure 6. EPCS Block Diagram

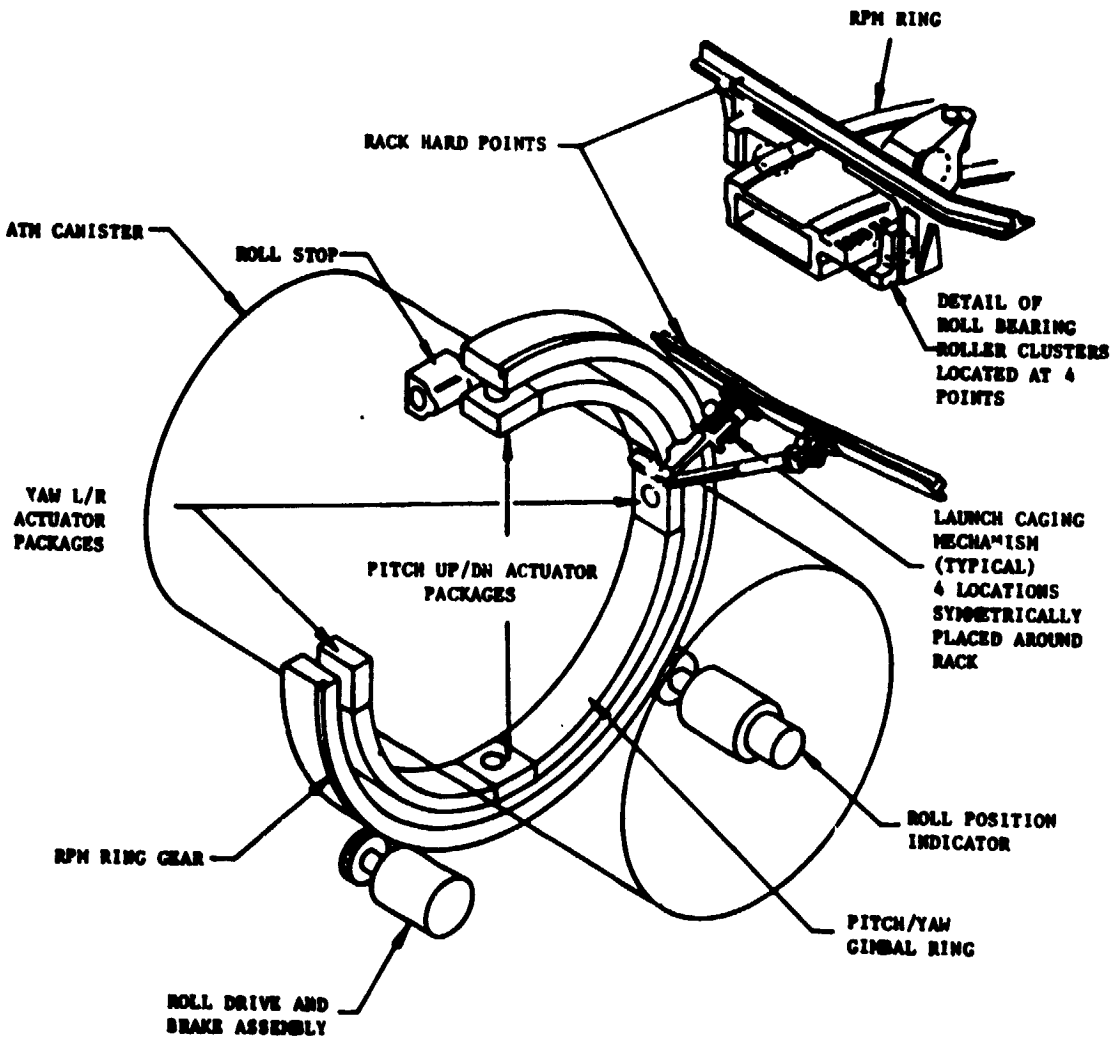

Figure 7. ATM Solar Experiment Package Pointing Mechanism

Two Control Moment Gyro Inverter Assemblies

Four EPCS Rate Gyro Processors (2 per axis)

EPEA with five redundant channels individually selected.

Four canister torque motors (2 per axis)

Redundant power sources.

The Redundancy Management philosophy was that primary APCS mission critical systems, those related to system performance or crew safety, would be monitored and managed automatically, utilizing the Flight Program and backed by a manual switching capability. Capability existed to inhibit all or portions of the automatic redundancy program. The less critical systems were monitored manually by the astronauts using the C&D Panel and by ground support using the telemetry link. Manual Redundancy Management switching capability existed via a switch selector and were commanded using the DAS/DCS, or by C&D Panel switches.

To ensure the integrity of the Flight Program, an ATMDC self-check capability was included. To increase the reliability of the computer system, capability was included to reload the ATMDC from a Memory Load Unit with onboard magnetic tape or by RF uplink via the DAS/DCS.

A skeleton program capable of fitting an 8K Memory was provided to maintain limited use of the ATMDC during flight should a memory failure occur which precluded the use of the 16K Program.

B. System History

The APCS described previously was the final result of many changes in design that reflected the evolution of Skylab configuration as the mission developed. This section presents a brief outline of those design changes and some of the reasons for them.

The development of the Skylab Attitude and Pointing Control System (APCS) was based on evolving ground rules and directives for the Apollo Telescope Mount (ATM) Pointing Control System (PCS) dating from June 1966. Prior to that time, various concepts, proposals and control moment gyro systems were studied. The design ground rules were established in response to directives from the Office of Manned Space Flight (OMSF) and were included in the July 1966 Preliminary Design Review.

1. Free Flying ATM. The PCS ground rules provided for a design using the Langley CMG, LM/Rack in free flight, a 28-day maximum life, no redundancy and a 1968 launch.

The extended ATM orbital mission required that the ATM vehicle roll axis be colinear with the solar vector. The requirement for extremely precise attitude control during long duration missions eliminated consideration of conventional reaction jet control systems for attitude control. The practical limitation on minimum impulse vehicle control obtainable with reaction jet control systems was inconsistent with precision control in the arc-sec range. Also, fuel consumption with the associated weight penalty precluded the use of reaction jet control systems for long-term missions. The Control Moment Gyro (CMG), which is a momentum exchange device, was therefore chosen as the controlling device for the ATM vehicle, since it offered the advantages of precision attitude control, extended mission capability, avoided optics contamination, and provided a weight savings over a reaction control system since no fuel would be required in normal operation.

Based on these ground rules, design of a PCS was begun and procurement action for long lead time components was initiated. The PCS design (1966) consisted of fine and coarse sun sensors, a single analog control computer with switching and logic, three CMGs, CMG electronics and inverters, three rate gyros, a hand controller and analog meters. This system depended on a Reaction Control System (RCS) for manual dumping of CMG bias momentum and visual pointing of the experiments. All telemetry was conditioned external to the PCS. Ground commands were decoded in the control computer.

2. Workshop Attitude Control System (WACS) Development. The first major design change occurred when the primary ATM vehicle was clustered. This assembly was referred to as the cluster configuration.

The necessity for a major new operational capability, unmanned rendezvous and docking and provision for attitude stabilization during the manned and storage periods prior to the ATM docking required the development of the Workshop Attitude Control System (WACS).

The WACS was a hot gas reaction control system using nitrogen tetroxide (N_2O_4) as the oxidizer and monomethyl-hydrazine (MMH) (pressurized by nitrogen) as the fuel.

The WACS was to be activated following S-IVB stage passivation and commanded to assume control of the cluster configuration. Astronaut commands or ground commands selected the WACS control modes and the necessary control phases. After PCS activation the WACS would be placed in a minimum power consumption condition and could be re-energized as required. The CSM RCS would be turned on to maneuver the cluster configuration to the ATM acquisition attitude. Control would then be assumed by the PCS.

3. Wet Workshop. By June 1969, the WACS had evolved to the system shown in figures 8 and 9 and consisted of the following basic hardware:

Rate Gyros

Discrete Horizon Sensors, Conical Scan Horizon Sensors and Processing Electronics

Sun Sensors

Control Computer

Control Switching Assemblies

WACS Propulsion Module

Control and Display (C&D) Panel.

Redundant components and circuitry were provided to meet crew safety and mission success criteria. With the aforementioned equipment, the WACS provided the following operational modes which would maintain the reference attitudes in addition to maneuvering through the transitional phases:

Gravity Gradient

Storage

X-POP (Perpendicular to Orbital Plane) Acquisition

X-POP

X-POP/Z-LV

Inertial Hold and Maneuver

Standby.

During the manned missions the Orbital Assembly (OA), originally the cluster configuration, would have most often been maintained in the X-POP reference attitude.

The WACS used rate sensors in its inertial reference systems. To compensate for gyro and integrator drifts and orbital regression effects, the X-POP attitude was to be updated regularly. Updates were determined using the Horizon Sensor System and the Sun Sensor. During the storage mode the OA would be placed in the Gravity Gradient Attitude and all WACS components would be turned off except the

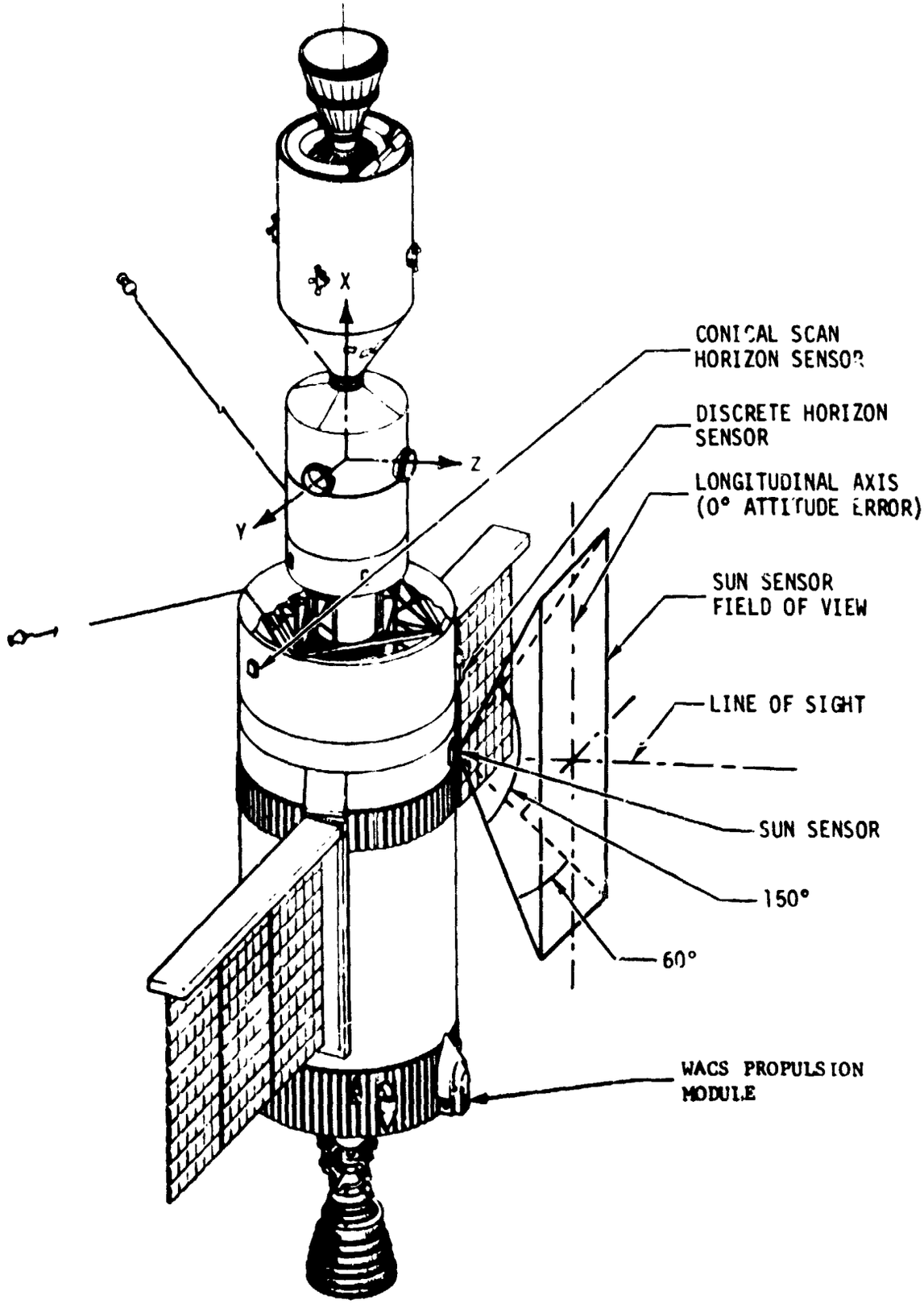

Figure 8. Workshop Attitude Control System

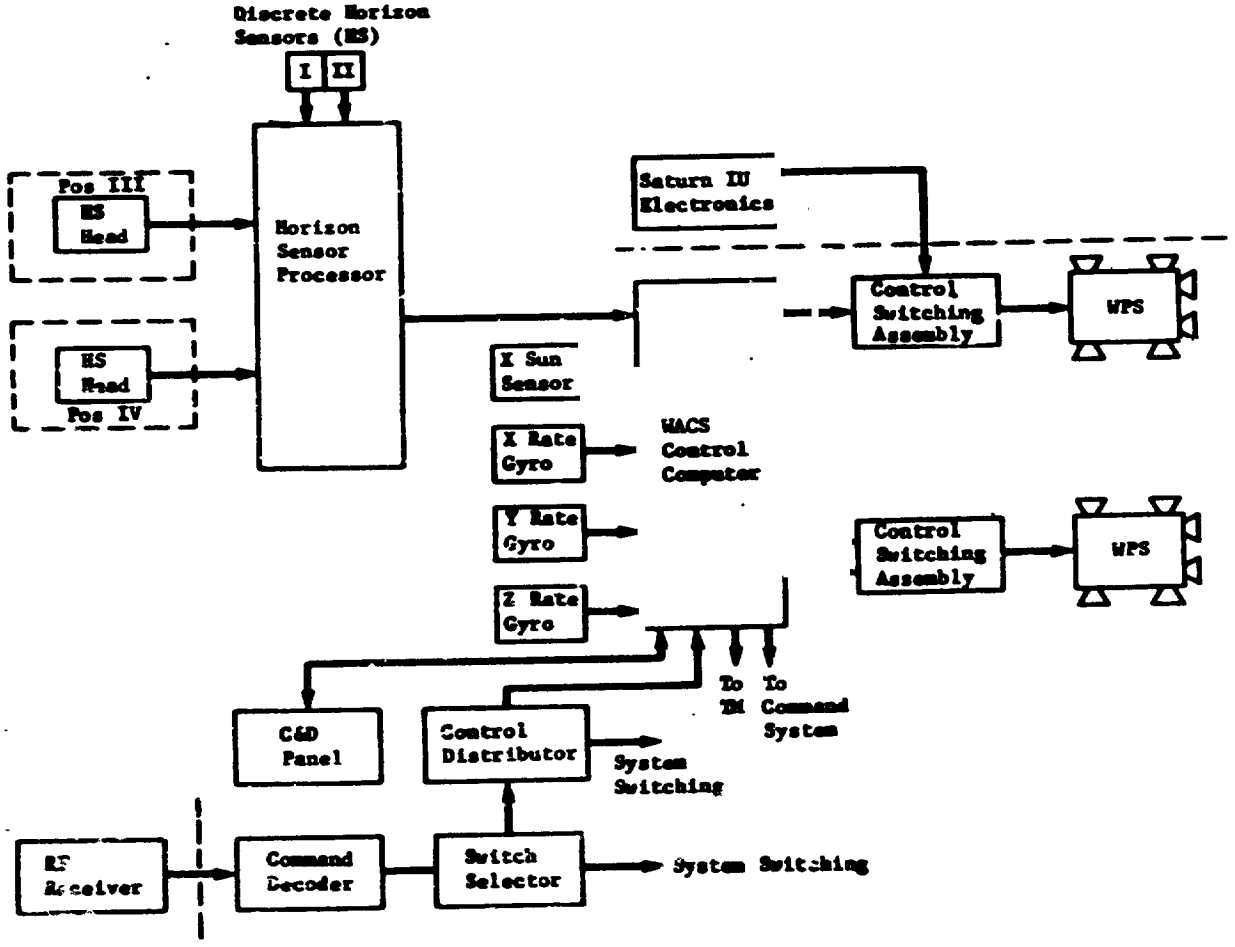

Figure 9 WACS Block Diagram

Discrete Horizon Sensors and the thermal control system for the electronics. With no active control, OA oscillations due to aerodynamic and gravity gradient torques would build up attitude errors. When a 20 degree attitude error was reached, the Discrete Horizon Sensors would issue a telemetry signal and a power-up command. At power-up a CG orientation was commanded and then the system reverted to a power-down state.

The Control and Display Panel provided onboard monitoring and manual control capability. Rate and attitude biases, mode commands, and computer channel selection were available to the astronaut.

4. Pointing Control System. The primary configuration for the ATM became the cluster configuration, with a free flying and tethered concept being considered as backup configuration. Clustering the ATM imposed additional requirements on the PCS. Increased CMG momentum was required due to increased vehicle moments-of-inertia. To significantly reduce constant gravity gradient bias torques the vehicle's principal axis of minimum moment-of-inertia had to be constrained to lie as closely as possible to the orbital plane while the ATM experiment canister was pointed toward the sun. Since this constrained the vehicle attitude about the solar line-of-sight, a roll positioning capability was added to the experiment canister. To preclude CMG saturation, the Lunar Module (LM) and Command Service Module (CSM) reaction control systems would be used to dump excess momentum. About the same time, experiment demands and crew motion combined to require a decoupled experiment canister mounting with separate controls. It was realized that man-motion disturbances would tax the capability of the CMG subsystem to maintain the experiment pointing stability requirements. These impacts along with increased readout needs and the addition of a Star Tracker reference, added to the complexity of the analog control computer such that a separate electronics box, called the Information Correlator Assembly (ICA), was proposed.

By August 1967, the PCS had evolved to the system shown in figure 10. During the daylight portion of the orbit the cluster X and Y-attitude errors were sensed by the Acquisition Sun Sensor (Acq. SS). Differentiating the Acq. SS outputs provided the necessary rate damping. During the night when the experiment pointing canister was caged, the integrated EPC Rate Gyro outputs were used to obtain attitude error information. Due to $\pm$ 95 degree EPC roll capability, resolvers were provided to transform the gyro rates to the CMG control system coordinate system. Roll attitude errors for the cluster were obtained by integrating the Rack-mounted Roll Rate Gyro output.

Attitude error signals for the EPCS were derived from the Fine Sun Sensors (FSS) and rate damping was provided by the Canister-mounted Rate Gyros. The experiment canister offset capability for each axis was developed by controlling the FSS optical wedges.

Isolation between the rack and canister was provided by a three degree-of-freedom gimbal system using frictionless compensated

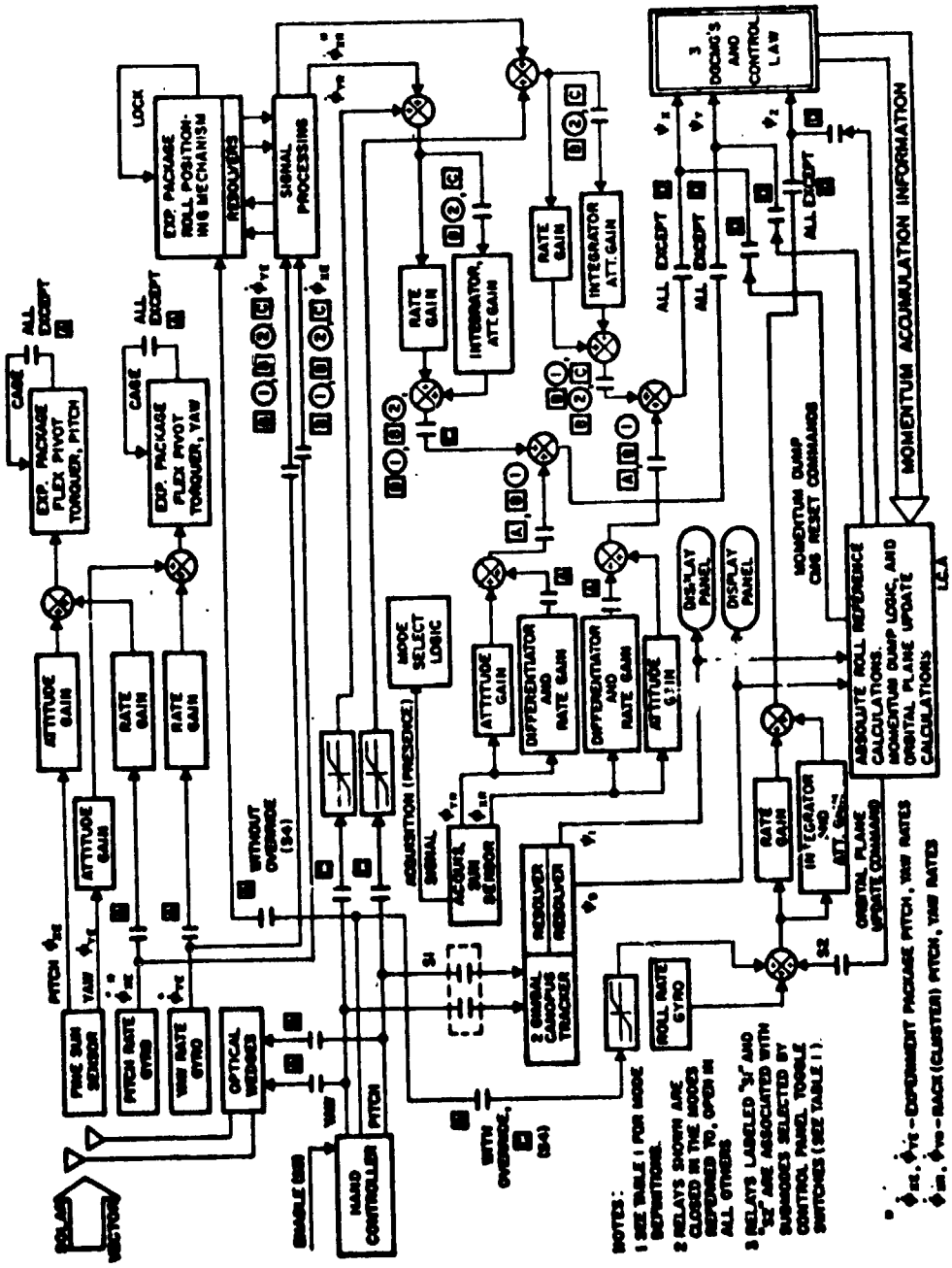

Figure 10. Pointing Control System

flexpivots. The canister attitude was controlled by two redundant torque motors per axis. A ± 95 degree roll position mechanism provided roll attitude positioning of the experiment canister. A Star Tracker was used to provide an attitude reference. An analog computer was used to implement the CMG H-vector Control Law, the CMG Steering Law and the EPC and CMG error processing. The device is not specifically labeled in figure 10 but was an integral part of the CMG, EPCS and RPM systems.

Reliability considerations for long-range mission times forced a new look at redundancy. All mission-critical single-point failures were made redundant by introducing switchover capability to added duplex components. To accomplish this, additional Rate Gyros were added to the ATM rack. This eliminated the need for the coordinate transformation resolver. Sensor averaging was implemented later. The flexpivots were designed to allow ± 2 degrees of rotation about the EPC X and Y-axes. Rotation about the Z-axis was extended first to +95, -120 degrees, then to ± 120 degrees by moving the roll ring gear stops. A study of the ICA design revealed that the minimum complexity was close to that of a small digital computer. After extensive investigation a digital computer (ATMDC) and an input/output assembly were added to interface with the PCS. By August 1969, the PCS had evolved to the system shown in figure 11. To minimize the CSM and TACS fuel requirements, a CMG momentum desaturation scheme utilizing vehicle maneuvers during night portion of the orbit was instituted.

5. Wet-to-Dry Workshop Transition. It was recognized that if the launch stack could accommodate the ATM, it would greatly simplify the program by eliminating extensive program and technical requirements. The capability to reduce program cost and complexity by eliminating ATM as a free-flying module, the ability to rapidly activate the Workshop by pre-installation and checkout prior to launch and the capability to significantly expand the mission potential with the weight margins offered by a Saturn V launch vehicle supplied the rationale for conversion from a Wet-to-Dry Workshop.

The PCS and WACS were designed to operate individually during separate mission phases; however, the Wet-to-Dry conversion made a marriage of the two systems desirable. This new system was renamed and called the Attitude and Pointing Control System (APCS). Due to more ample weight margins and lower impulse requirements the WACS was replaced by a blowdown cold-gas (nitrogen) Thruster Attitude Control System (TACS). TACS was a simpler and more reliable system than WACS. The use of nitrogen gas eliminated the risk of experiment contamination by control system exhaust gasses that existed with WACS.

The role of the digital computer was increased and the ATM control computer was eliminated. The CMG Control Law, error processing, and the bending mode filtering was performed in a digital fashion. The EPC analog portion of the control computer was retained and

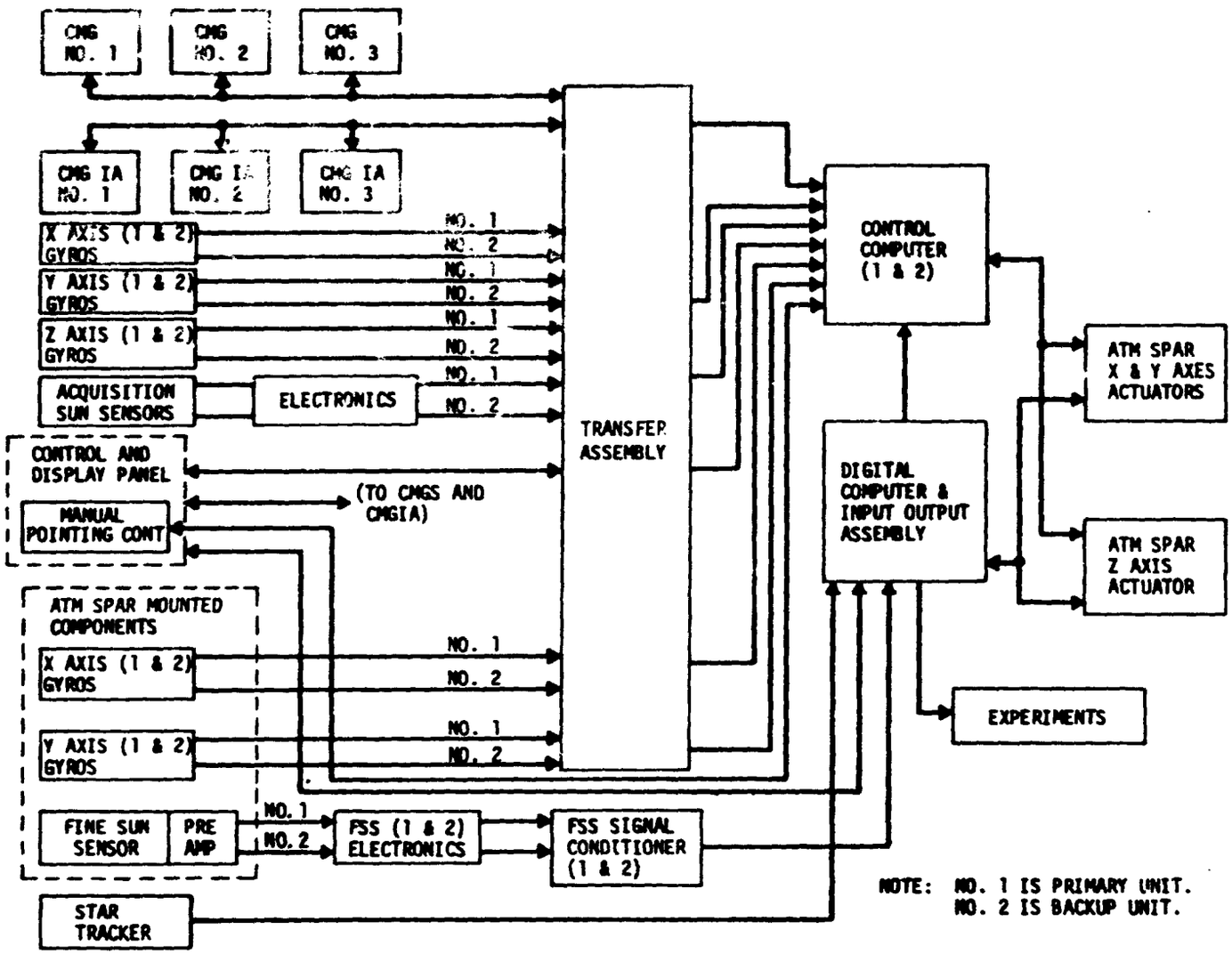

Figure 11. Early ATM Pointing Control Subsystem

assembled in a new unit called the Experiment Pointing Electronic Assembly (EPEA). The new mission requirements eliminated the need for a Lunar Module.

The concept of automatic redundancy management was developed for the ACS. This was accomplished by the ATMDC Flight Program which monitored behavior of the various redundant components, and switched to different combinations as required to ensure proper system operation.

The requirement for long-term operation of the ATMDC without failure forced a change in concept from a single ATMDC to two ATMDCs and a redundant WCIU operating in a 1 + 1 configuration. In this configuration one ATMDC was on, one ATMDC was off, the WCIU common section and one-half of the input/output section were on, the other half of the WCIU input/output section was off. The ATMDC program performed selfchecks and maintained the capability to switch to the redundant ATMDC/WCIU if a failure was detected.

An expansion in the experiment program imposed a major new operational capability on the APCS. The experiment program was refined and required an earth pointing capability with negative Z-vehicle axis colinear with the local vertical and +X-principal axis in the orbital plane. Initially, all these attitude maneuvers were to be handled exclusively by the TACS and the remainder of the mission was to be controlled by the CMGs.

As impacts of the new Skylab mission were determined, the inadequacies of both the TACS and the CMGs became apparent. The TACS did not have sufficient propellant to perform the total number of maneuvers being planned. Also, the longer mission time, increased vehicle inertias, and a more thorough accounting of external disturbances made the design of the CMG system marginal. A solution to this problem was sought by combining the operation of the two systems. Thus, the CMGs would provide assistance in making maneuvers and the TACS would be available if the CMGs were unable to control the Skylab. From this the "nested" attitude control concept was derived. As studies progressed on the "nested" system, several problem areas arose which necessitated changes in both the CMG and the TACS Control Laws.

Vehicle inertia increased to the point where performance in the two CMG case became marginal. The CMG wheel speed was increased approximately fourteen percent to increase performance and momentum storage capability. This required changes in the CMG inverters, and the Star Tracker and Fine Sun Sensor which obtained power from the inverters.

The ability to offset command the EPC system via the ATMDC was added. Automatic control of the Star Tracker with the ATMDC was considered, but this redesign was not made because of the magnitude of changes to the ST mode logic electronics.

To increase the probability of the ATMDC successfully completing the Skylab mission the Memory Load Unit (MLU) was developed

to provide inflight computer reloading. A skeleton program capable of filling one of the two 8K ATMDC Memory Modules was provided to maintain limited use of the ATMDC during flight should a failure occur in one of the memory modules.

When the EPC was in the offset position and a roll command was initiated, the solar image, as viewed from the crew's display screen, underwent an apparent roll about the sun center. For some experiments this would have required a reposition of the line-of-sight after roll adjustments. To correct this procedural inconvenience and decrease the response time for experiment set-up, a roll about line-of-sight capability was added to the ATMDC Flight Program.

C. Test Program

The Skylab APCS was composed of components and subsystems most of which had not been previously qualified for orbital flight. Therefore each component and subsystem required extensive testing and qualification. The integrated APCS, including software, also required extensive simulation and verification. Figure 12 shows the overall APCS test program and the relationships between the hardware, software and systems tests.

1. Hardware Component Design Verification Testing. The APCS hardware design verification test program consisted of developmental tests and qualification tests.

Developmental tests were performed to select parts and components, investigate the adequacy and optimization of the preliminary design, determine significant failure modes and effects, evaluate effects of varied stress levels, and select materials or determine compatibility.

Qualification tests were conducted as formal demonstrations of the design and performance adequacy of the production flight hardware.

Development test hardware was representative of the flight hardware insofar as possible. Qualification test hardware was flight-type, and was identical in performance, configuration, and fabrication to the flight hardware.

2. Flight Hardware Verification. Flight APCS verification testing was performed at the module level on the prototype and flight ATMs. Testing included in-process tests (performed during final assembly of the ATM), post-manufacturing checkout (performed to verify that the overall system functioned per design), vibration tests (performed to verify the effects of the launch vibration environment on the system), and thermal-vacuum tests (performed to verify proper APCS operation in the space environment). These tests were all performed using a special pre-flight ATMDC test program.

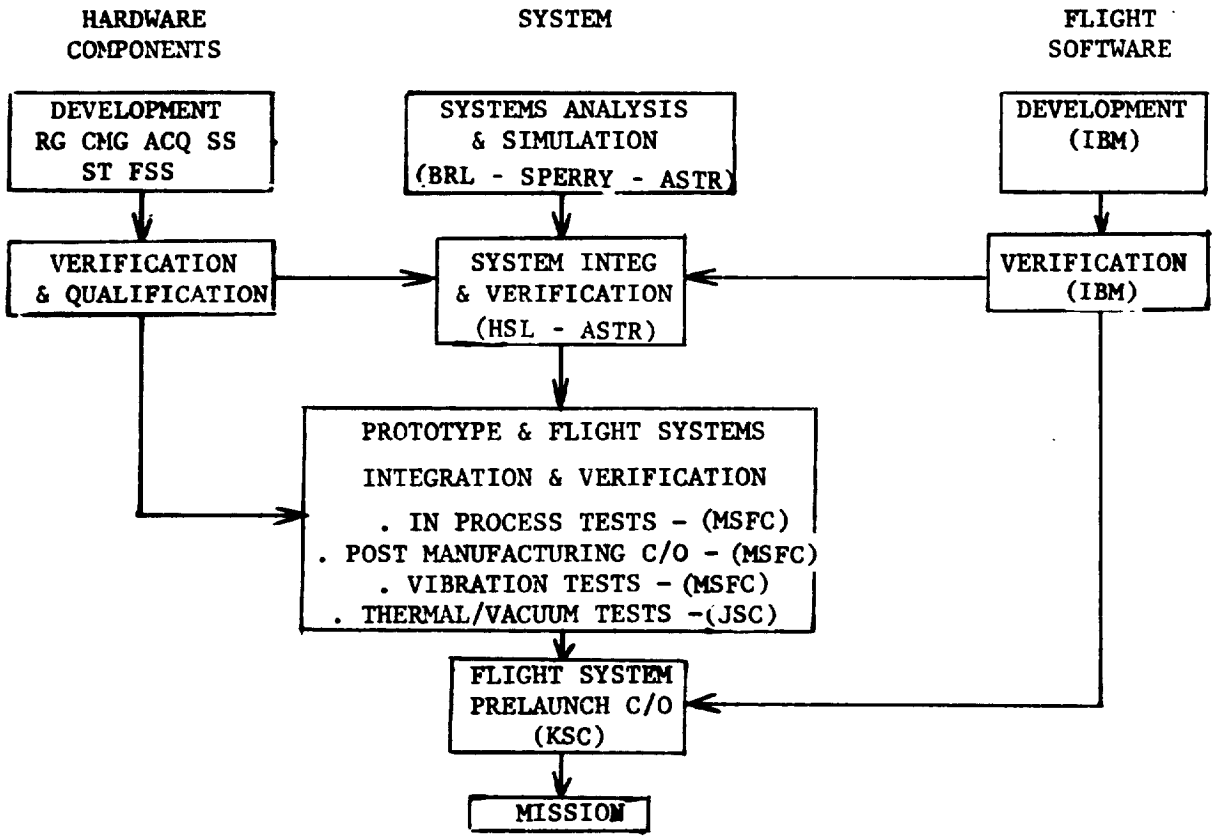

Figure 12. APCS Test Program

TACS subsystem level testing was performed during similar module level testing of the OWS. This testing was performed using simulated ATMDC thruster firing commands.

Additional tests were performed at the multi-module and cluster levels at Kennedy Space Center. Multi-module level testing validated the interface between the ATM and the Airlock Module (AM) (primarily the C&D Panel). The cluster level systems test verified overall operation of the APCS including TACS, and was the only flight APCS test performed before launch using the flight ATMDC program.

3. Software Development and Verification Tests. The following paragraphs describe the simulations that were used in the design and analysis of the ATMDC software. These are listed in Table 2.

The System/360-75 AS-II Simulator evolved from a general purpose system analysis simulator of an orbiting vehicle in the Wet Workshop era. This exceptionally fast simulator was used for many of the initial studies of control law selection and maneuver concept design.

The Skylab Workshop Simulator was built because of the necessity for a high fidelity simulator to evaluate the APCS pointing requirements using fixed point implementation of critical Flight Program modules, such as CMG control and strapdown reference.

The IBM 1800 Skylab Hybrid Simulator was developed to validate the redundancy management system under perturbations in a full fixed-point environment.

The Workshop Interpretive ATMDC Simulator provided unique facilities for debugging and assuring proper Flight Program operation. The simulator was designed to give repeatable results for runs with identical setups or with changes which did not alter timing.

The System/360 Model 75 was an all-software simulation which modeled both the vehicle and the ATMDC. It provided capability for faster than real-time operation with the Flight Program.

The System/360 Model 44 Simulator incorporated a flight-type ATMDC with software models of the WCIU and the vehicle. It provided a tool for real-time operation to permit a realistic run ratio, as well as for real-time follow-up on suspected program problems.

The Skylab ATMDC Mission Support Simulator was built to provide additional capability to verify long term performance of the final Flight Program utilizing two Flight-type ATMDCs in a computer switch-over test environment and a WCIU operating in real-time.

Table 2. APCS Simulators and Location

Astrionics Hardware Simulation Laboratory (HSL)/MSFC-ASTR
Astrionics Simulation Laboratory (Non-Linear CMG Model Simulation)/MSFC-ASTR
Astrionics Simulation Laboratory (Skylab Simulation)/MSFC-ASTR
Astrionics Simulation Laboratory (ATM/EPCS Analog Simulation)/MSFC-ASTR
Control System Design Simulation/MSFC-COMP/ASTR
TACS System and Venting Simulation/MSFC-COMP/AERO
System/360-75 Fortran Flight Program Simulator/IBM-Huntsville
System/360-75 AS-II Simulator/IBM-Huntsville
Skylab Hybrid Simulation/MMC-D
QD212, Digital Simulation Model for Skylab Control and Momentum Management/MMC-D
Skylab APCS Verification and Evaluation Model/MMC-D
Skylab Simplified APCS Verification and Evaluation Model/MMC-D
Skylab Rendezvous and Docking Analysis Simulator/MDAC-W
Skylab Attitude Control System Simulator/MDAC-W
CMG/TACS Control System Model/BRL
CMG Control Subsystem Model/BRL
CMG/EPC Control System Model/BRL

The Hardware Simulation Laboratory (HSL) was an all-flight hardware (ATMDC/WCIU, CMGs, RGPs, Acq. SS, and ST) simulation located at Marshall Space Flight Center. Software equations were used to simulate vehicle dynamics, and the APCS environment. This simulation permitted long-term evaluation of the Flight Program and its interfaces with the flight hardware.

A formal verification program was performed for each development phase of the 16K and 8K Flight Programs. This verification effort was directed toward verifying the accuracy and adequacy of the Flight Program to guarantee that it met mission requirements and conformed to program specification. Both logic tests and performance tests were made to accomplish that goal. Each program for each phase, was subjected to a rigorous set of logic cases to check every logic path through the program, every data constant specified, and the accuracy of each calculation. The System/360-75 Simulator was utilized extensively for this effort, with a more limited use of the System/360-44 Simulator and the HSL.

The performance testing was accomplished primarily on the final program with subsets run on earlier programs. The performance tests were divided into two categories, general performance and mission requirements. The HSL and, to a lesser extent, the System/360-44 Simulator were used for these tests. The general performance cases were used to demonstrate that the Flight Program was capable of proper functioning in the environment it would experience during the actual Skylab mission. The philosophy used in the design of this verification was to simulate as many variations of program input perturbations and off nominal situations as could be conceived and classified as realistic possibilities. The ultimate purpose of this effort was to simulate, detect, and isolate at system level (all functions in operation) the following types of problem areas:

Unusual program execution sequences.

Function interference due to unexpected timing situations.

Parameter scaling overflows associated with equation input extremes.

The mission requirements performance cases were used to demonstrate that the ATMDC Flight Program was capable of meeting all of its function requirements with respect to the planned overall mission objectives and activities for the entire mission duration.

4. APCS Simulations. A list of simulations used in APCS development is given in Table 2. Due to the length of the planned mission, it was not feasible to simulate the entire mission. Therefore, the various simulators verified concepts and software at the normal and extreme limits. In addition, contingencies such as 2-CMG operation were studied extensively. The speed range of these simulators varied from real-time to 100 times real-time depending on the speed of the computer and the complexity of the models. In general, those simulations concentrating on dynamic response utilized greater hardware detail models and operated more slowly but did not require as long an examination period. The most complex and demanding areas simulated were of TACS budgeting, momentum management and maneuvering. The type of parameters that were varied included solar elevation, CMG configuration and maneuver profiles. These studies had to be repeated many times in the development history as simulations were updated to reflect changes in control concepts. After the Momentum Management Laws had been finalized, computer outputs showing expected maneuver profiles were generated. While those curves were not explicitly utilized during the mission, the experience gained in generating those curves was very useful during the mission. The same techniques of examining maneuver profiles, CMG gimbal angles and TACS usage that were utilized by the various simulations during system verification proved invaluable in evaluating and optimizing the daily flight plan during the mission.

5. APCS Verification. In addition to the simulations using representative versions of the Flight Program, the actual ATMDC was used for system verification. The various phases of the Flight Program were used either with hardware, such as Rate Gyros and CMGs or with their math model equivalents.

Due to the physical size of the Skylab, no complete dynamic simulation using actual inertias was feasible. Instead the APCS components whose orientation was important, such as Acquisition Sun Sensor, were mounted on a three axis dynamic platform which was slaved to a support computer so that the position of the inner platform followed that of an ideal vehicle. Due to the much smaller inertia of the experiment canister, a spar, which was a physical representation of experiment canister inertias and was suspended by mercury bearings, was developed. All experiment canister components were mounted on this spar which tracked a simulated sun and was perturbed by external torquing devices. This simulation was known as the Hardware Simulation Laboratory (HSL), located in the Astrionics Laboratory at MSFC. The HSL simulations were used to verify proper system operation using flight-type hardware and software.

SECTION IV. MISSION OPERATIONS

This section provides a summary of the significant APCS mission events, a detailed summary of the anomalies and discrepancies that occurred during the mission and a description of the mission support team and its activities during the mission.

A. Mission Description

Following is a brief description of the Skylab mission from SL-1 lift-off through post SL-4. Table 3 identifies the significant APCS related mission events and gives the sequence in which they occurred.

1. Skylab 1. The Saturn Workshop (SWS) was launched, unmanned, at 17:30 GMT on May 14, 1973 (DAY 1), from Launch Complex 39A at Kennedy Space Center (KSC), Florida. The SWS launch vehicle was the first two stages of the Saturn V launch vehicle. At approximately 63 seconds following the SWS launch, the Orbital Workshop (OWS) meteoroid shield was severed from the SWS. This event also damaged the OWS Solar Array Wing 2 fairing tiedown which allowed the assembly to deploy prematurely. At approximately 590 seconds from the SWS launch, the ignition of the second stage retrorockets was accomplished from the SWS vehicle. At this time the Solar Array Wing 2 was lost. The SWS was then separated from the Saturn V second stage, and the Skylab Thruster Attitude Control System (TACS) was activated across the separation interface via wire disconnects. The TACS thrusters, in conjunction with the Launch Vehicle Digital Computer (LVDC), provided the SWS attitude control required from S-II separation until transfer of control to the Skylab APCS.

Approximately eight seconds following S-II separation, the SWS was inserted in a near-circular orbit of 434 kilometers above the earth's surface with an orbital inclination of 49.84 degrees and orbital period of near 93 minutes. Vehicle rates shortly after S-II engine cutoff and before orbital insertion were X = -0.8 deg/sec.

Shortly after achieving orbit, the SWS was maneuvered into a gravity-gradient attitude with the forward end pointed toward the center of the earth, and payload shroud was jettisoned in four sections. Following the payload shroud jettison, deployment of the ATM, the ATM Solar Arrays, the remaining OWS Solar Array Wing, and release of the ATM Canister launch locks, was initiated. A signal indicating release of Wing 1 was received, but there was no indication that the wing reached the fully deployed position.

Table 3. APCS Events/Anomalies

Time DAY:HR:MIN	Title	Description
1:17:39	Insertion	Launch phase essentially nominal but micrometeoroid shield was torn away and OWS Solar Panel did not deploy.
1:17:39	IU/TACS Control	Nominal
1:17:45	Shroud Jettison	Nominal
1:17:48	ATM Deployed and Locked	Nominal
1:17:54	Release ATM Canister Launch Locks	Nominal
1:19:07	Activate APCS	Nominal
1:20:12	First RGRM Integral Test discompare	Discompare of integrals of the two RG in control. Integral test discompare occurred frequently until Six-Pack installation. Probable cause was bubbles in RG fluid causing RG drift.
1:20:34	Z1 RG Temp Off-Scale High	Data indicates transducers were working properly and RG temp was above transducer limit. Problem probably caused by thermal runaway of transister in RG heater control circuit.
1:22:20	TACS IU/ATM Control Transfer	Nominal
1:22:20	CMG Control Enable	Nominal

Table 3. APCS Events/Anomalies (continued)

Time DAY:HR:MIN	Title	Description
1:22:23	Z2 RG Temp Off Scale High	Data indicates transducers were working properly and RG temp was above transducer limit. Problem probably caused by thermal runaway of transistor in RG heater control circuit.
1:22:23	Engage Canister Orbital Locks	Worked nominally.
2:05:17	Y2 RG Temp Off Scale High	Data indicates transducers were working properly and RG temp was above transducer limit. Problem probably caused by thermal runaway of transistor in RG heater control circuit.
2:06:30	First Thermal Maneuver	Skylab was maneuvered to X=0, Y=-90, Z=0 due to OWS overheating. Shortly afterwards vehicle was maneuvered to X=0, Y=-45, Z=0 and this attitude was utilized through parasol deployment (DAY-14).
2:12:16	End of IU Lifetime	
2:13:58	First Rate Gyro Drift Compensation Commanded	The drift of each Rate Gyro was computed and commands uplinked to ATMDC for compensation. The drift values changed requiring continuous updating.
2:15:14	Y3 RG Temp Off Scale High	Data indicates transducers were working properly and RG temp was above transducer limit. Problem probably caused by thermal runaway of transistor in RG heater control circuit.
2:20:22	First CMG Momentum Dump	This occurred during a temporary return to SI and worked nominally.

Table 3. APCS Events/Anomalies (continued)

Time DAY:HR:MIN	Title	Description
12:09:56	CMG No. 3 Wheel Speed Transducer Failure	Wheel speed went from nominal to 0 within 1 sec. Phase currents and bearing temps remained normal indicating failure of the speed measurement.
13:00:39	First SL-2 Unsuccessful Docking Attempt	After normal soft dock on DAY 12, 21:15:00 there were two unsuccessful attempts at hard docking before hard docking occurred on DAY 13, 03:53:00.
13:21:30	Parasol Deployment Begun	Parasol deployment through Scientific Airlock (SAL) started.
14:01:45	Parasol Deployment Complete	Parasol deployed and OWS temperature started to fall immediately. Return maneuver to SI required crew intervention to point Z-axis at sun and left X-principal 60° out of orbit plane.
16:13:40	Unable to Drive EPC/ Canister Oscillation	FSS turned off then back on. Wedges were not rezeroed. Drove to back of FSS Wedges. During malfunction procedure Secondary. RG switched into loop before being spun-up thus causing oscillation.
16:17:56	First FSS Wedge Count Increment	Due to navigation errors and Acq. SS sun presence not occurring at t_{SR} as expected, the FSS door was not fully open when the ATMDC released the FSS Wedge Counter. Changes in light intensity as the FSS door opened were seen as a change in wedge position. The problem continued throughout the mission.

Table 3. APCS Events/Anomalies (continued)

Time DAY:HR:MIN	Title	Description
17:20:21	First EREP	Worked nominally.
18:01:26	Pri UP/DN RG Temp Off High Scale High	Data Indicates transducers were working properly and RG temp was above transducer limit. Problem probably caused by thermal runaway of transistor in RG heater control circuit.
19:19:11	Crew ran around the water Rockers	Caused vehicle transients.
24:02:27	X2 RG Temp Off Scale High	Data indicates transducers were working properly and RG temp was above transducer limit. Problem probably caused by thermal runaway of transistor in RG heater control circuit.
25:15:15	SL-2 EVA No. 1	Solar Array successfully freed but still not deployed due to frozen lubricant.
25:18:11	Attempt to Free Solar Array	Thermal soak maneuver started.
26:03:05	Solar Array Deployed	Thermal soak maneuver complete with OWS Panel deployed.
27:16:38	Computer Switchover	Commanded switch from Pri to Sec Computer. Worked nominally.
37:10:45	SL-2 EVA No. 2	Film retrieval.
53:16:29	Dump Half Angle Changed	Changed from 63 deg to 51 deg to improve ATM unattended operations.

Table 3. APCS Events/Anomalies (continued)

Time DAY:HR:MIN	Title	Description
59:20:14	Z1 RG Failure	Full scale oscillations.
64:01:40	Pri UP/DN Failure	RG temp went from off scale high to off scale low indicating a RG power supply failure or blown input fuse. Output was zero and not responsive to input. Canister became unstable causing overheating of UP/DN actuator.
74:23:47	Dump Half Angle Changed	Changed back to 63 deg from 51 deg.
76:19:39	SL-3 Hard Docking	
79:00:36	First ST Shutter Fail to Close	Shutter failed to close as momentum dump started. The shutter closed 1.5 hours later. Probable cause was binding of the shutter mechanism. Similar occurrences continued throughout the mission.
85:15:00	SL-3 EVA No. 1	Twin-pole sun shield deployed. Temperatures at AFT end started falling.
86:14:14	Single RG Control	Y1 RG selected for control due to numerous RG integral test failures.
91:17:00	Dump Problem	Insufficient momentum available in X, resulting in vehicle rates, attitude error, went to TACS only.
91:17:00	C&D Panel Meter Indicates Incorrect CMG OG Angles	C&D Panel meter indicated CMG No. 1 and No. 3 angles - 100% (-135 deg) when actual angles were 55 deg. Probable cause was failure of relay which switches inputs to C&D panel meter.

Table 3. APCS Events/Anomalies (continued)

Time DAY:HR:MIN	Title	Description
99:12:13	LOS Roll Problem	EPC drove off the sun during a line-of-sight roll. Probable cause was FSS Wedge counter incrementing (see 16:17:56). As wedge is driven through 0, with 1 or more bit error on wedge counter, ATMDC loads all 1's in register but does not get sign bit from FSS zero pulse. This is seen as large positive error and ATMDC issues maximum negative drive command.
103:16:15	SL-3 EVA No. 2	Primarily for rewiring Rate Gyro connectors such that Six-Pack RGP replaced Rack RGP to ATMDC. Probably due to crew motion in MDA.
104:00:22	Six-Pack Rate Gyro Scale Changes	
106:15:20	Six-Pack Alignment Test	Maneuvers performed to determine Six-Pack misalignment which turned out to be sufficiently small that no coordinate transformation patch was required in ATMDC.
119:23:28	Stability Test	Used S052 data with canister caged to obtain SWS stability in attitude hold mode.
132:10:36	SL-3 EVA No. 3	Primarily for film retrieval.
177:03:19	TV Bus 2 Failure	500 AMP short for 3 seconds. Caused FSS wedge count to be zeroed.
185:17:48	Orbital Lock Anomaly	Mechanical binding of Pri UP/DN orbital lock. Drew stall currents. Temp rise of 0.695°C/Min. ΔT=3.7°C.

Table 3. APCS Events/Anomalies (continued)

Time DAY:HR:MIN	Title	Description
187:21:41	SL-4 Docking	
190:06:35	LBNP Vent Modification	LBNP vents made non-propulsive by routing through waste tank.
193:17:44	SL-4 EVA No. 1	Camera and antenna repair.
194:08:15	CMG No. 1 High Temp and Failure	BRG No. 1 went to 82°C. A current went to 2.3 AMPS. Wheel speed indication went to 0. Probable cause was failure of BRG No. 1. Momentum wheel current indicated wheel was spinning at approximately 4000 RPM when CMG brake was applied 35 minutes after failure.
195:17:54	Orbital Lock Problem	Mechanical binding of Sec UP/DN orbital lock. Freed 1 hour later with no further problems.
196:22:01	First Kohoutek Maneuver	Worked nominally.
201:20:12	Klunk-Klunk Sound	Transient disturbances on Rate Gyro outputs occurred concurrently with klunk-klunk sound. Cause was unknown.
226:21:04	SL-4 EVA No. 2	S201 Kohoutek experiment required sun shading maneuver.
228:14:13	Star Tracker Failure	ST OG drove to stop. OG tachometer indicated 1.24 volts. Problem was duplicated in lab test failing the OG encoder.
230:17:30	SL-4 EVA No. 3	S201 Kohoutek experiment required sun shading maneuver
266:14:00	SL-4 EVA No. 4	Film retrieval.

Table 3. APCS Events/Anomalies (concluded)

Time DAY:HR:MIN	Title	Description
271:12:09	Gravity Gradient Maneuver	Vehicle was maneuvered in TACS Only for passivation such that +X was pointed away from the earth and orbital rate was put into Y-axis.
271:12:12	Final Testing	Unsuccessful attempt to spin-up CMG No. 1, "Failed Rate" Gyros spun-up and outputs were still erratic. MLU successfully utilized.
271:20:00	APCS Powered Down	

During this sequence the Instrument Unit (IU), using the TACS thrusters, maneuvered the SWS into a Solar Inertial attitude, with its longitudinal axis in the orbital plane and the solar arrays perpendicular to the incident sunlight.

On DAY 1, 19:07:00, the ATM portion of APCS was activated. The CMG wheels were spun up and the ATMDC entered a standby mode until control could be switched from the IU. Telemetry data on Rate Gyro Z-1 temperature indicated that the temperature was increasing and on DAY 1, 20:34:00, the temperature went off-scale high. At Acquisition of Signal (AOS) on DAY 1, 20:12:00, Y and Z-axes Rate Gyro integral test discompares occurred. These Gyros remained in isolation for approximately 1-1/2 hours before r configuration. Occurrence of these test discompares was to continue until the Rate Gyro Six-Pack was installed. The SWS Attitude Control was transferred from the Instrument Unit (IU) to the APCS on DAY 1, at approximately 22:20:00. At this same time the CMG/TACS control was enabled. Three minutes later the Z-2 Rate Gyro temperature went off-scale high. Excessive RG drift rates soon became evident. Drift rates as high as 18 degrees/hour were noted. The Spec Values were two orders of magnitude less.

On DAY 1, at approximately 22:23 the EPEA was powered-up to activate the spar caging logic and engage the orbital locks.

On DAY 2, at 05:17 the third Rate Gyro Processor (RGP) (Y2) temperature went off-scale high. Eventually, three more RGPs, making a total of six, were to experience similar temperature problems. Normally, the SWS would have remained in Solar Inertial attitude, however, the OWS temperatures began to increase due to the loss of the meteoroid shield.

A procedure was developed to maintain the internal temperatures of the SWS within critical limits. This was accomplished by maneuvering the SWS so the sunshine was not perpendicular to the longitudinal axis of the SWS for long periods of time. This solution of simply maneuvering away from the sun was compounded by the loss of the SWS Solar Panels which restricted the time and distance the SWS could be maneuvered from the sun, the occurrence of RGP anomalies which caused inaccuracies in maneuvering, and CMG momentum management while in a non-Solar Inertial attitude.

After experimenting with a few maneuver attitudes and sequences such as alternating orbits of Solar Inertial and Z-LV attitudes during orbital daylight, a thermally stable attitude which satisfied power requirements and reduced the complications caused by the RGP anomalies and CMG momentum management considerations was decided upon. The chosen thermal attitude was such that the sun-line was at an incident angle of

45 deg (±10) with the SWS longitudinal axis (X-axis) and the vehicle X-principal (Xp) axis of inertia in the orbital plane. The 45 degree solar incident angle satisfied the thermal and power constraints, reduced the effects of the Rate Gyro anomalies, and the X-axis constraint helped simplify the CMG momentum management problems. Near the end of the initial 10 days when the Suit Umbilical System (SUS) began to freeze, a third constraint on attitude was imposed. This required maneuvers to a bias attitude of at least 50 degrees to allow sunlight to enter the region of the SUS and warm it.

The high RG drift rates were compensated for by changes in the ATMDC software. The frequent and sudden changes in the drift rates were a nuisance because of the time and effort required to measure and recompensate the new drift rates.

Within the first 24 hours after APCS power on, eight rate gyro integral test discompares had been detected: two in the X-axis, five in the Y-axis, and one in the Z-axis. All Rate Gyros except Z3 had been placed in vehicle control during that 24-hour period. More failures would have been logged except that redundancy management was inhibited for extended periods of time, and Gyros were allowed to remain in redundancy management isolation routines for hours. The first Y-axis failure occurred approximately one hour after APCS power on. The second discompare occurred one hour later and remained in isolation one hour. Ten minutes elapsed before a third discompare occurred, which remained in isolation 1-1/2 hours. The fourth discompare occurred 15 minutes later. Thus, in a period of slightly more than six hours, four Y-axis discompares occurred. During approximately four of these six hours, the Y-axis failure isolation logic was being executed. The rate integral test is not performed on an axis in failure isolation. Following the fourth Y-axis discompare, approximately four hours elapsed before a reconfiguration was commanded. With that reconfiguration, redundancy management was inhibited for nearly 10 hours. Less than 30 minutes after re-enabling redundancy management, the fifth Y-axis discompare was detected. Only the extended periods of failure isolation and the long period of inhibited redundancy management held the total number of discompares detected to a relatively low level.

The launch of the first crew was delayed from a planned DAY 2 launch to twelve days following the Skylab 1 launch. This delay was for the purpose of assessing the situation that existed in the SWS and to make the necessary plans to alleviate the problem and to accomplish an overall successful Skylab mission. During this period, studies and tests on the ground resulted in three devices for shielding the Workshop from the sun; a parasol, to be deployed through the Solar Scientific Airlock; a sail, to be deployed from a Command Module; and a twin-boom sunshade, to be deployed from the workstation on the telescope mount. Each of these was built and delivered in time for the launch of the first crew. At the same time, the crew was being trained in procedures

for installing the sunshades and releasing the remaining solar wing. Besides the sunshades, replacements for a number of items which might have been damaged by high temperatures in the Workshop were delivered and stowed in the Command Module.

Throughout this period, a program of careful management of attitude had been instituted to keep temperatures within the Workshop as low as possible while providing enough power to keep the SWS operational. Available power was strictly allocated, and as far as possible, systems using power were turned off or operated intermittently. Other effects required consideration. Reducing the heating rates in the Workshop caused some other parts of the Workshop to become too cold, but electric heaters could not be used because of the power shortage. The maneuvers themselves introduced another problem: excessive use of TACS propellant. Each maneuver had to be planned carefully to minimize use of the thrusters.

Since the momentum management scheme was designed to operate only in Solar Inertial attitude, it could not be used. On one occasion during a temporary return to the Solar Inertial attitude, the momentum dump scheme was used and worked nominally. This occurred on DAY 2, 20:22:00.

The large Rate Gyro drift present in the Rack Rate Gyros presented serious difficulties in maintaining attitude and attitude reference. By causing movement of the X-principal axis out of the orbital plane, the Rate Gyro drift caused frequent CMG momentum saturations and subsequent resets.

In an attempt to utilize the dump scheme in non-Solar Inertial attitudes, consideration was given to implementation of an ATMDC patch. The patch, however, could not be developed in the time available.

The means used to desaturate the CMGs was the reset routine. As the reset routine caged momentum to the nominal value for Solar Inertial attitude, effective resets could only be commanded at orbital points where the Solar Inertial and thermal attitude nominal momentum curves intersected. In addition, adequate station coverage was required for these points. The large and changing Rate Gyro drift present in the original Rack Rate Gyros presented serious difficulties in maintaining attitude and attitude reference. Due to the length of time in maintaining the thermal attitude without a position update the strapdown reference became greatly degraded. The strapdown was occasionally reinitialized to the present attitude so that in the event of a computer switchover the Flight Program reinitialization would have automatically commanded the vehicle to an erroneous Solar Inertial attitude. Since the ATMDC had no information on vehicle attitude, it was necessary to maintain attitude reference on the ground.

Approximately one hour prior to the launch of the first crew on DAY 12, 09:56:00, the CMG No. 3 wheel speed transducer failed.

2. Skylab 2. The CSM carrying the first crew was launched at 13:00 GMT on DAY 12 from Launch Complex 39B at Kennedy Space Center, Florida. This crew consisted of Captain Charles Conrad, Jr., Commander; Commander Joseph P. Kerwin, Science Pilot; and Commander Paul J. Weitz, Pilot.

After the Skylab 2 CSM reached orbit it was maneuvered during the following six hour period to achieve an orbit which coincided with the orbiting Workshop.

The crew made a flyaround inspection of the SWS, while maintaining communication with the ground. During this inspection the crew described the condition of the SWS, photographed it, and transmitted live television views of its exterior. The crew confirmed that the meteoroid shield was mission, that Workshop Solar Array Wing 2 was missing, and that Solar Array Wing 1 was partially deployed and restrained by a piece of the meteoroid shield. After the flyaround inspection, the CSM was soft-docked.

After a rest period the crew undocked and performed a stand-up EVA to free the partially deployed Solar Array Wing. This attempt at freeing the Solar Array Wing was unsuccessful and resulted in considerable TACS usage. TACS usage was due to CSM RCS impingement on the vehicle and the reaction to the crewman pulling on the Solar Array Wing.

The stand-up EVA and the subsequent docking attempts were performed with the APCS in the Attitude Hold TACS mode.

Following several CSM docking attempts a hard dock was attained on DAY 13, 03:53:00. The activities of the Skylab 2 crew were many, including the deployment of the parasol. Following this deployment the Workshop temperature began to decrease and by DAY 21 had stabilized to an acceptable level where activation of the Workshop continued and the Workshop was habitable.

The Skylab 2 operations were initially limited by availability of power, but this restriction was removed when Solar Array Wing 1 was deployed during estravehicular activity on DAY 25. When the Solar Array was initially freed it did not deploy because of frozen dampers. The SWS was maneuvered using the attitude hold CMG mode and a thermal soak was performed on the dampers to free them.

On DAY 16 the crew experienced considerable difficulty with EPC offset pointing. The FSS wedge counter did not track the wedges

over the entire range and meaningless readouts were encountered. After consultation with ground support, the situation was corrected by re-zoning of the wedges.

On DAY 16, 17:56:00, the first FSS count increment was noted. The wedge reading changed by one count even though there was no actual change in wedge displacement. This phenomenon was to recur through the mission primarily at sunrise. On DAY 17, 20:21:00 the first EREP was performed and it worked nominally.

Following the Solar Array Wing 1 deployment, the Skylab 2 activities were placed on a near-nominal type mission plan. As a result of the early mission problems and the thermal extremes experienced by the vehicle, it was decided to perform a manual switchover to the secondary computer system on DAY 27. This was a test to verify that the redundant capability of the computer subsystem was functional. At 16:38:00 on DAY 27, the crew selected the secondary computer and enabled auto switchover using the C&D panel computer select switch. The secondary computer system powered on, initialized, and began operating properly. During the next two days, the program was updated to the FF70 level (same as the primary) by uplinking three program patches necessary to compensate for the continuing Rate Gyro anomalies and vehicle inertia changes due to loss of SAS Wing 2 and meteoroid shield.

On several occasions during SL-2 the Star Tracker erroneously locked on to objects other than the required star. As a contamination particle with reflected light brighter than the star being tracked came into the Star Tracker field-of-view the Star Tracker would track the particle. In order to avoid these situations a procedure was formulated. Effective utilization of this procedure alleviated the problem. On DAY 37, the SL-2 crew performed their second EVA primarily for the purpose of film retrieval. On DAY 40 the SL-2 undocked for their return to earth. This represented at that time, Man's longest space flight.

During the unmanned period problems with an experiment door led to a desire to avoid desaturation maneuvers continuing into the daylight portion of the orbit. The half-angle of the dump maneuver was decreased from 63 degrees to 51 degrees. Prior to SL-3 the dump half-angle was changed back to 63 degrees and was retained at that value for the remainder of the mission.

On DAY 59 the Z1 Rate Gyro began to oscillate full scale and was declared failed.

The Rate Gyros continued to exhibit high drift rates. The initially observed drifts were successfully compensated via biases uplinked to the ATM Digital Computer. As time passed in the mission, the magnitudes of required bias corrections decreased.

Efforts were undertaken to determine the cause. Areas of investigation focused on component failures, Electromagnetic Interference (EMI) and design deficiencies. During this period a crash program was initiated to prepare a package of ATM Rate Gyro Processors that could be interfaced into the APCS system should additional Rack Rate Gyro failures threaten mission termination.

On DAY 64 the primary UP/DN EPC Rate Gyro became very noisy and ultimately failed. Loss of rate damping in the EPC loop resulted in canister oscillations which caused eventual overheating of the canister actuators. The overheating caused the actuator rotor and stator to eventually bind.

It was believed that a significant possibility existed that the secondary UP/DN Gyro could fail. The EPCS was equipped with two Gyros per axis, so a second UP/DN Gyro failure would have terminated use of the EPCS. Replacement or supplementing of the EPC Gyro system, such as had been done in the CMG/TACS system, was not considered feasible. Subsequentially, a device, the EPC Derived Rate Control Assembly, was designed to be inserted in series with the FSS output for the purpose of producing a pseudo rate signal to stabilize the EPC system in lieu of Spar Rate Gyros. This device was to be carried into orbit by the SL-3 crew. To preclude irreversible damage to the EPCS actuators, if a similar failure occurred, a constraint was added that continuous active and unattended EPCS operation should not exeed fifty minutes without station coverage.

3. Skylab 3. Skylab 3 was launched at 11:10:50 GMT on DAY 76 from Kennedy Space Center, Florida. The Skylab 3 crew consisted of Captain Allen L. Bean, Commander; Dr. Owen K. Garriott, Science Pilot and Major Jack R. Lousma, Pilot.

After Skylab 3 attained a nominal orbit and rendezvoused with the SWS a flyaround was performed to inspect the parasol installed by the Skylab 2 crew. The flyaround was terminated earlier than planned due to RCS inpingement on the parasol. The impingement forces resulted in increased TACS usage. With the APCS in the attitude hold TACS mode hard dock was completed on DAY 76, 19:39:00.

On DAY 79 the Star Tracker shutter failed to close at momentum dump commence when commanded by the ATMDC. Attempts by the crew to close the shutter manually using the C&D Panel were also unsuccessful. On later occasions the same shutter problem was to occur. In all cases the failure would recover after several hours. A protective procedure was developed to prevent permanent damage to the Star Tracker photo multiplier by exposure to the earth's albedo or the sun while the shutter was open. This procedure included positioning the Star Tracker so that it looked at the dark surface in the back of the ATM Solar Arrays.

On DAY 86 single Rate Gyro control was selected in the Y-axis because of the numerous redundancy management integral test discompares.

On DAY 91 during a nominal GG dump maneuver certain events occurred that resulted in loss of attitude control. Following a Z-axis redundancy management discompare an additional 0.3H of momentum was required to bring the controlling gyro rate to the gyro rate to the required rate. The additional momentum requirement forced the CMG into saturation and siphoned momentum from the X-axis at the same time. The X-axis momentum change produced an uncontrolled rate and resulted in a 20 degree attitude build-up in the X-axis requiring an automatic switch to TACS only control. In the process of stabilizing the system the crew observed that the C&D Panel analog meters were incorrectly indicating that CMG No. 1 and CMG No. 3 were on a stop. The gimbals were actually caged This malfunction resulted in an incorrect assessment of the CMG status, leading to excessive TACS usage. During a later test the problem was observed only on the CMG No. 1 measurement.

On DAY 99 at 12:13:00 the EPCS drove off the sun during a line-of-sight roll. The EPCS worked nominally after the occurrence.

Because of the continuing Rate Gyro problems one of the foremost concerns of the crew was the installation of the Six-Pack. The Six-Pack was mounted in the Multiple Docking Adapter (MDA) and powered from an existing utility outlet of AM Bus No. 2. A new unit, Rate Gyro Control and Distributor was installed in the MDA; its function was to provide overcurrent protection in the input power lines and to serve as a junction box for input power, gyro outputs, and RGP coarse/fine gain commands. An existing cable was disconnected from the C&D Panel and a new T cable installed to permit routing of RGP outputs and gain commands through existing spare wires to the ATM.

The Six-Pack RGPs were then briefly powered up, polarities and temperatures verified and then powered down. Six-Pack installation was then completed by an EVA performed on DAY 103. Extensive wiring changes were required. The existing cable which routed the Rack Rate Gyro outputs to the WCIU was disconnected at the WCIU. The ATM end of the cable used for routing Six-Pack functions was disconnected at the ATM Trunion Plate. Two T cables which were an integral part of the Rate Gyro Select Box were connected to the WCIU, ATM Trunion Plate, and the two disconnected cables. Through these cables and the Rate Gyro Select Box. Six-Pack outputs were connected to pins on the WCIU where Rack Rate Gyros No. 1 and No. 2 had previously been connected. Rack Rate Gyro outputs were routed to the Rate Gyro Select Box where one of the three outputs in each axis could be selected as Gyro No. 3 for redundancy management purposes in the ATMDC. Plans were to use the two Six-Pack

Rate Gyros in each axis for control with the selected Rack Rate Gyro as a spare, but due to a single failure point which existed in the Six-Pack Power source, the remainder of the mission was flown with one six-Pack RGP and the selected Rack RGP for each axis in control.

As Rate Gyros are essential to APCS control, both with TACS and CMGs, no control of the OWS with APCS was possible during the period of Six-Pack Installation. Since the CSM for SL-3 had thruster problems, it was decided not to utilize CSM control. Instead a procedure was developed to allow the vehicle to drift. The procedure was:

> Go to TACS only, Nominal Momentum Cage (Allowed vehicle momentum and nominal momentum to be as close as possible prior to Standby period of control).
>
> Go to CMG Control. This allowed Attitude Errors in the TACS Deadband (3 degrees, 2 degrees, 2 degrees) to be brought to zero prior to going to Standby.
>
> Go to Standby, Nominal Momentum Cage. The vehicle was now in free drift with oper loop compensation for gravity gradient torques.
>
> Performed Six-Pack Wiring change.
>
> Enabled CMG control and reacquired Solar Inertial.

After the installation of the Six-Pack, calibration maneuvers were performed on DAY 106, 15:20:00 to establish the alignment. The maneuvers were performed in the attitude hold mode using CMG control. A three-minute settling time was allowed for each maneuver and a two-minute se tling time was allowed for each maneuver requiring a total of 5 minutes per maneuver. The maneuver sequence consisting of 8 maneuvers initiated shortly after orbital sunrise.

After analysis of the data by the mission support team the misalignment of the Six-Pack was determined to be small and no compensation in the Flight Program was required.

On DAY 119, a test was performed to verify vehicle stability in the Attitude Hold mode. The purpose was to plan SL-4 Kohoutek Maneuvers. S052 solar data was utilized for this purpose. The results of this test indicated that stability was within acceptable bounds for future viewing of Kohoutek.

On DAY 1[illegible] the first JOP-13 maneuver, pointing ATM at a star for X-ray photogra[illegible], was performed. This maneuver was successfully completed using 47 MIBs. The technique of maneuvering the workshop to point the ATM at a non-solar target was later extensively used in the Kohoutek studies.

On DAY 132, the SL-3 crew performed an EVA for the purpose of film retrieval using a total of 1470 n.s. of TACS propellent.

During the unmanned phase on DAY 177, 03:19:00, a 500 ampere short developed on Television Bus 2 for 3 seconds. This had a minor impact on the APCS; the power transient caused the FSS wedge counter to be zeroed. Driving the FSS wedges through zero was required to correct the problem.

The SL-3 manned period ended with the CSM undocking on DAY 135, 19:53:00.

The UP/DN Orbital Lock failed to uncage on DAY 185 at 17:48:00 GMT. A temperature rise of 3.7 degrees C was observed on the lock housing. Tests run on the motor in thermal vacuum at stall currents produced a temperature rise similar to that seen during the anomaly. The EPEA was switched to secondary for the purpose of using the secondary caging loop. On DAY 195 the UP/DN lock again failed to uncage while using the secondary caging loop. Without any configuration changes, the lock successfully uncaged when tested about an hour after the second anomaly.

4. Skylab 4. The third three man crew was launched from Kennedy Space Center on DAY 187 at 14:03 GMT. The crew consisted of Lt. Col. Gerald P. Carr, Commander; Dr. Edward G. Gibson, Science Pilot; and Lt. Col. William R. Pogue, Pilot. Docking of the Command Service Module to the Skylab cluster occurred on DAY 187, 21:41:00.

On DAY 190 the crew modified the M092 vent so it vented into the OWS waste tank instead of directly overboard. This was done to eliminate the disturbance torques which the vent caused.

Failure of CMG No. 1 occurred between tracking stations on DAY 194 at approximately 08:15. At the preceding tracking station, Honeysuckle, CMG No. 1 phase A current increased 65 ma, bearing No. 1 temperature increased 5 degrees C, and wheel speed decreased 120 RPM. At AOS Bermuda (08:42 GMT) the phase A current was 2.06 amps, bearing No. 1 temperature was 82 degrees C, and wheel speed was indicating zero RPM. A speed of approximately 4000 RPM was inferred from the wheel currents. Beginning at 08:50:00 the CMG No. 1 brake was applied for seven minutes and control was switched to the two CMG mode.

The Comet Kohoutek was studied extensively during Skylab. In order to verify instrument capability and maneuver accuracy a maneuver to point the ATM at Mercury was performed. The APCS supported Kohoutek observations by performing three types of maneuvers. One was a roll maneuver about the X-principal axis for the purpose of viewing Kohoutek with an articulated mirror system. The second type maneuver involved pointing the ATM experiment at Kohoutek. The third type maneuver was one which would shade the astronaut held S201 camera and was performed

in conjunction with an EVA. Two EVAs were performed for S201 photography of Kohoutek.

On DAY 228 at 14:13:00 the Star Tracker failed. Analysis of telemetry data was made and laboratory tests were performed to simulate the failure mode. The failure was duplicated by interrupting the outer gimbal encoder output. Operation of the Star Tracker was terminated and backup techniques were implemented to calculate the vehicle roll reference on the ground.

Skylab 4 undocking occurred at DAY 271 at 10:34:00. After crew departure, several engineering tests were performed in the APCS area. These tests consisted of:

CMG No. 1 spinup - Power was applied to the wheel for 8.5 hours without response

RG power up - All RGs were powered up and those which had exhibited erratic outputs on off-scale temperature indications were observed. Operation was not significantly different than had been previously observed.

ATMDC reprogram - The ATMDC was successfully reprogrammed via RF uplink and via the MLU.

On DAY 271, 12:09:00, a maneuver was performed to place the Skylab cluster in the Gravity Gradient Attitude such that the +X-axis was pointed away from the earth. The APCS was powered down on DAY 271, 20:00:00.

B. Mission Anomalies and Discrepancies

1. Anomalies.

a. Rate Gyro Failures

(1) Rate Gyro Drift Anomaly.

(a) Description. The Rack Rate Gyro Processors (RGPs) were powered up on DAY 1, 19:07.00. At 20:12:00 a RGP redundancy management discompare in the Y-axis was noted. Additional failures were noted over the next several hours. Eventually it was determined that five Rack RGPs (X_1, X_2, X_3, Y_1, and Y_3,) had out-of-specification drift rates. These drift rates were sometimes quite high and changed suddenly in random fashion. The drift rates of the RGPs gradually decreased as the mission progressed. By DAY 78, all except X_3 had stabilized at low rates.

Extensive analysis was performed to determine the cause of the Rate Gyro drift anomalies. The high drift rates were attributed to gas bubbles in the Gyro flotation fluid which formed when the float chamber bellows was exposed to the hard vacuum of space. This problem had been seen during ATM Thermal-Vacuum Testing and was judged an acceptable risk because the high drift rates could be compensated in the ATMDC software.

(b) Impact. The large erratic drifts present in the Rack Rate Gyros caused serious difficulty in maintaining attitude and attitude reference. The drift changes caused movement of the X-principal axis of the vehicle out of the orbital plane, which caused CMG momentum saturation and frequent resets. During the time when it was necessary to maintain thermal attitude, the strapdown attitude reference became greatly degraded due to erratic RGP dirft.

(c) Corrective Action. The large RGP drifts noted during the SL-1/SL-2 mission were compensated in the ATMDC software by commands uplinked to the ATMDC. The capability to compensate for RGP drift was designed into the ATMDC software.

During the SL-2 mission, a crash program was begun to prepare a package of the six RGPs (2 per axis) that could be installed in the MDA and interfaced into the APCS, if necessary. The RG Six-Pack was carried to the SWS by the SL-3 crew. On DAY 103 the Six-Pack was installed in the system. Three Six-Pack RGPs were paired with the remaining Rack RGPs (X_1, Y_1, Z_3). No further RGP problems were encountered. The Six-Pack Rate Gyros were modified to protect the float chamber bellows from the vacuum of space. This modification was also incorporated on the backup ATM RGPs.

(2) Rate Gyro Overheating Anomaly.

(a) Description. The APCS Rate Gyro Processors (RGPs) were powered up on DAY 1, 19:07:00. At 20:34:00 the Z_1 RGP temperature went off-scale high. At 22:23:00 the Z_2 RGP temperature went off-scale high. Eventually, a total of six RGPs showed off-scale high temperatures. These were X_2, Y_2, , Z_1, Z_2 and Primary UP/DN. Eventually, the Primary UP/DN RGP failed completely with zero output.

The RGP overheat problem was traced to a fiber washer used in mounting the RGP heater power switching transistor on its heat sink. The washer shrank in the space environment, which allowed the transistor mounting to loosen. This caused the transistor to thermally saturate and leak excessive current to the RGP heating blanket, which caused the RGP to overheat. This problem had not been seen during ground testing.

(b) Impact. There was concern that as the RGPs grew hotter and the float fluid viscosity decreased, they would become unstable. This apparently occurred with the Z_1 and Y_3 RGPs. In addition, the hot Rate Gyros showed a change in scale factor, which caused redundancy management discompares during maneuvers.

The primary concern was, however, that if three RGPs failed in any one vehicle axis, it would be impossible to continue the mission. Also, if two RGPs failed in either EPC axis it would be impossible to perform ATM experiments.

(c) Corrective Action. The scale factor errors noted in the Y-axis RGPs were compensated in the ATMDC software. The scale factor errors in the X and Z-axis RGPs could not be compensated because of software limitations.

The RGP Six-Pack successfully eliminated the possibility of terminating the mission due to failure of all three RGPs in any one axis. At the time of SL-3 launch, the cause of the RGP overheat problem had not been determined. When the cause of the failure was determined, a quick fix for use by the crew was devised which would have allowed the crew to repair overheating Six-Pack RGPs. Overheating did not occur and the fix was not used.

A Derived Rate Conditioner Assembly (DRC) was developed to provide rate inputs to the EPC system if the secondary EPC UP/DN RGP failed. This device conditioned the FSS output to provide EPC rate information. The DRC was carried into orbit with the SL-3 crew. The secondary EPC UP/DN RGP performed satisfactorily through the rest of the mission and the DRC was not used.

b. CMG No. 1 Failure.

(1) Description. The CMGs performed nominally during the Skylab mission until DAY 194, 08:03:00, when CMG No. 1 failed. The failure was characterized by a rise in the No. 1 wheel spin bearing temperature from a normal 21 degrees C to a point just under the auto shutdown temperature of 90 degrees C, a gradual decrease in wheel speed accompanied by an increase in wheel spin motor current, and failure of the wheel speed pickoff. The failure occurred between tracking stations and was first observed by the Bermuda tracking station forty-seven minutes later. The No. 1 wheel spin bearing temperature at that time was 83.2 degrees C and decreasing. The wheel speed was estimated from spin motor current to be about 3800 rpm, down from 9060 rpm before the failure. The failure was not detected by the Redundancy Management Scheme, since the bearing temperature did not exceed the auto-shutdown temperature of 90 degrees C. The spin bearing temperature did exceed the caution level

of 74 degrees C and the caution was set. The caution indication was not seen by the crew, who were asleep. Shortly after detecting the failure over Bermuda, the Flight Director directed that power be removed from the wheel spin motor and applied the brake for seven minutes. This probably did not slow the wheel appreciably. At that time, the ATMDC switched to 2-CMG control, and the mission continued normally.

Considerable analysis was performed to determine the mode of failure of CMG No. 1. Preliminary analyses indicate the failure mode was failure of the No. 1 wheel spin bearing due to insufficient lubrication. The failure appeared to be progressive, with indications of bearing distress as early as DAY 174. At the time, these indications were not considered to be significant. Unfortunately, the telemetered data were not sufficient to show all symptoms of bearing distress.

(2) System Impact. The APCS was programmed to provide normal control of the SWS with two CMGs operating. The system performed satisfactorily after the CMG No. 1 failure. However, failure of CMG No. 1 reduced the total CMG momentum transfer capability from approximately 9000 N.m.s. to approximately 6000 N.m.s. TACS usage increased accordingly. CMG gimbal stop encounters became more frequent.

(3) Corrective Action. The mission continued in 2-CMG operation. Ground support simulations were used to optimize vehicle control for EREP passes and JOP experiment passes to reduce TACS usage. CMG momentum biases were used to minimize the CMG gimbal stop encounters. These measures enabled completion of the SL-4 mission essentially as planned.

c. Star Tracker Anomalies.

(1) Description. Four major problems were encountered with the Star Tracker (ST): tracking contaminants, shutter sticking, photomultiplier tube degradation and outer gimbal encoder failure. Work-arounds were developed for the first three problems, but the encoder failure terminated use of the ST.

(a) Contaminant Particle Problem. The ST was activated at the beginning of SL-2 and operated satisfactorily except for frequent disturbances when star acquisition was lost due to contaminants entering the field of view. If a particle reflects light of intensity above the photomultiplier tube threshold and enters the field-of-view, the particle will be tracked as a target star. This type of disturbance was noted thirty-five times during

SL-2 and 4 times during SL-3. Typical particles were generated by dust, outgassing, sloughing of paint, and venting from the vehicle.

(b) Shutter Anomaly. Five times during SL-2 the ST shutter stuck in the open position. On the first occasion, on DAY 79 at 00:31:00 just prior to the momentum dump, the ATMDC issued a ST Hold discrete. The ST exited Auto Mode, but ST Hold and Shutter Close discretes were not issued by the ST, and the Star Presence discrete stayed on until the vehicle maneuvered away from the star. The crew tried to close the shutter by a C&D Panel command, but without response. The ST was then manually positioned to point at the backside of a Solar Array, to prevent damage to the photomultiplier tube. About 1.5 hours later, the shutter was observed to be closed when telemetry was acquired at a ground station. The ST was powered down. On DAY 79, 02:26:00, the shutter operated normally. Similar events were noted on the other occasions.

Possible explanations were examined, and intermittent binding at some point in the shutter mechanism was found to be the most likely problem. All the events and symptoms can be explained if it is assumed the Star Tracker Shutter hung up due to binding in a position where it was not fully open or closed but it was still possible to obtain a star presence.

(c) Photomultiplier Tube Degradation. On DAY 101, the ST failed to acquire the target star, Alpha Crux. It was believed that bright light, presumably from the earth's albedo, impinged on the photomultiplier tube during a shutter anomaly. Light as bright as the earth's albedo would permanently degrade the ST sensitivity by 50% if exposed for twenty minutes.

In order to determine if photomultiplier tube degradation had occurred, and to determine the level of any degradation, a number of stars of different magnitude were selected and attempts to acquire each were made. It was found that the stars of magnitude 0.56 and brighter could be acquired and tracked. Stars of magnitude 0.66 and below could not be acquired. Comparison with ground test results indicate a sensitivity degradation of 30 - 50%.

(d) ST Encoder Failure. On DAY 228, a failure was noted when the outer gimbal position indication went to zero and the outer gimbal rate signal recorded a constant output. An analysis of telemetry data was made and laboratory tests were performed to simulate the failure mode. The failure was exactly duplicated by interrupting the outer gimbal encoder output or the encoder lamp excitation. It was therefore concluded that the outer gimbal encoder had failed and in all probability would not recover. This failure mode rendered the Star Tracker useless and its operation was terminated

(2) Impact. On several occasions during SL-2, the Star Tracker erroneously locked on to objects other than the required

star. This caused the outer gimbal angle input to the roll reference calculations to be inaccurate. On one occasion the erroneous inputs were received just prior to calculation of the momentum desaturation maneuvers. This resulted in degraded momentum management performance and in less than optimum momentum states.

The Star Tracker Shutter anomaly resulted in temporary degradation in roll position information, but since the shutter problems cleared themselves after a few hours, the data loss was considered minimal. Work-around procedures required somewhat longer operating time by the crew.

The photomultiplier tube degradation resulted in the loss of all stars of magnitude 0.66 or less as potential target stars. Alpha Crux was among the stars which could no longer be acquired. Since there were periods when both Achenar and Canopus, the prime target stars, were occulted, another star of sufficient magnitude was found (Rigil Kent).

Failure of the ST Outer Gimbal Encoder terminated use of the unit, and backup roll update techniques had to be implemented.

(3) Corrective Action. To preclude occurence of the dump scheme interface problem and minimize tracking of stray contaminants, use of the ST was restricted. A procedure was developed where the ST was utilized only during discrete periods. This procedure impacted the experiments area since the ATMDC provided roll information based on ST information.

Work-around techniques were developed to deal with the shutter anomalies and photomultiplier tube problem. If a stuck shutter condition arose, the ST was immediately powered down, then powered up during orbital night and repositioned to parking angles looking at the dark surface of a blocking plate. The unit would then be powered down again.

There were two reasons for keeping the ST powered down anytime a shutter anomaly was present. First, the photomultiplier tube was not as sensitive to light damage with the power off. Second, internal logic in the ST maintained power to the shutter motor if the shutter was not in the required logic state. This could result in permanent damage to the shutter motor.

As a consequence of photomultiplier tube degradation, the star Alpha Crux had to be deleted as a target star. Studies were made to find suitable substitute stars. Ultimately, the star Rigil Kent, magnitude +0.06, was selected.

Since the ST was a simplex device, failure of the gimbal encoder terminated use of the Star Tracker. After the failure, on DAY 228, outer gimbal backups were computed by ground support personnel using vehicle inertia and solar elevation. This method was later improved by having the crew periodically measure star positions with a sextant.

2. Discrepancies.

a. Excitation of ATM Spar Bending Modes.

(1) Description. Dynamic coupling between the vehicle ACS and the EPC was a major source of transient disturbances to the ACS. Two predominant bending modes were excited. These frequencies were approximately 0.81 Hz on the vehicle X and Z-axis and 1.48 Hz on the Y-axis. Rolling the EPC canister caused X and Z-axes Rack Rate Gyro oscillations. Peak amplitudes of approximately 0.02 degrees/second occurred at the start of the roll and 0.09 degrees/second occurred when the roll command terminated. Caging the canister at sunset also excited the same frequencies.

(2) Impact. The transients associated with the EPC roll activity caused momentary degradation of spar pointing stability. There was concern that the structural ringing due to spar roll might reach sufficient magnitude to cause Rack Rate Gyro gain changes. The caging transient was not detrimental since experiment pointing was terminated.

(3) Corrective Action. The crews were requested not to use the 7 deg/sec roll rate or pulse the spar at the 3.5 deg/sec rate.

b. Sun Presence Timing Errors.

(1) Description. During early SL-2, the ATMDC Effective Sun Rise (ESR) flag occurred in an irregular manner with respect to the Acquisition Sun Sensor sun presence discrete. For the solar elevation at the time, the ESR should have occurred 15.5 seconds after the sun presence discrete. However, ESR was observed occurring within 2-3 seconds of sun presence, and sometimes came prior to sun presence. There was some irregularity at sunset, but the irregularity was not as great as at sunrise. The state vector indicated that the on board navigator was within 2.5 seconds of being correct.

(2) Impact. The timing problem had direct impact on the Fine Sun Sensor (FSS), and was a potential problem for Rate

Gyro Redundancy Management (RGRM). Because actual sun presence came somewhat later than planned, the FSS wedges were often released before the aperture door was fully open. This resulted in an incorrect change in wedge count (this problem is discussed below).

If RGRM was performing a Rate Gyro isolation at an orbital sunrise and the Acquisition Sun Sensor sun presence discrete came after ESR, RGRM would have interpreted the disparity as being the result of drift in the primary strapdown calculations, and secondary strapdown would have been selected. Although this situation did not occur, the Rate Gyro difficulties being experienced at the time made it an important area of concern.

(3) Corrective Action. Several possible causes for the timing error was investigated:

Possible error in earth radius to orbital radius ratio.

The ATMDC had an 11 second error in (TGMT), which was being compensated in navigation updates.

Possibility that sunlight was being refracted through the atmosphere differently than anticipated.

Correlation with solar elevation angle.

Acquisition Sun Sensor hardware problem.

No specific error source could be found. It was felt that small errors in navigation parameters were having a detrimental, cumulative effect on the navigation calculations. By DAY 24, however, the time between sun presence and ESR had increased to 8-9 seconds. This time was considered adequate to preclude RGRM problems. The rate of navigation updates increased after DAT 27, and the sunrise timing was kept within acceptable bounds.

c. Fine Sun Sensor Wedge Count Error.

(1) Description. Disparities arose between the actual FSS Wedge position and the wedge position readout as a result of the wedges being released (enabled) by the ATMDC prior to the FSS Aperture Door being fully open. Transit of the door shadow across the encoder detectors produced an output which the FSS Signal Conditioner interpreted as wedge rotation. This disparity could only be removed by driving the wedges through the actual zero position, where the encoder zero pulse would reset the counter to zero.

Allowance for the FSS aperture door opening time was incorporated in the ATMDC Flight Program when the experiment pointing mode was automatically entered at sunrise. Navigation and timing errors at times made these allowances inadequate. In addition, no provisions were made in the Flight Program for the aperture door opening time when the Experiment Pointing mode was entered manually during the day period.

(2) Impact. Under most conditions, the error was not significant. During ATMDC controlled pointing, however, erratic spar behavior could result as the wedges were driven through zero. the wedge counter would overflow when the count reached zero, but the sign bit for the counter was tied to the encoder zero pulse. In the absence of the zero pulse, the counter would reset to its maximum value. The ATMDC would interpret this condition as a large error and issue saturated wedge rate commands, causing unusual spar motions.

The effect of the error was particularly evident if the disparity occurred during line-of-sight (LOS) roll (see Section VIII). This problem was the cause of several LOS roll anomalies.

(3) Corrective Action. A corrective procedure of rezeroing the wedges at the beginning of orbital day was established.

d. EPC UP/DN Orbital Lock Discrepancies.

(1) Description. On DAY 185, the UP/DN Orbital Lock failed to uncage at orbital sunrise. As a result, the lock motor and UP/DN actuators drew maximum current for about eight minutes. The EPEA was switched to secondary and the spar uncaged successfully when tested a few hours later. Normal ATM experiment operation was not resumed until DAY 191, however. The UP/DN lock again failed to uncage on DAY 201, but operated normally when tested about an hour later.

It was concluded that an intermittent mechanical binding had occurred, possibly due to contamination from wiring insulation in the vicinity of the lock.

The uncage failure was not observed again, and the secondary orbital lock motor was used for the remainder of the Skylab mission.

(2) Impact. Primary impact of the lock problem was the temporary halting of Experiment Pointing Mode operations. There was concern that a hard failure might occur between tracking stations which would seriously limit ATM experiment operations.

(3) Corrective Action. Studies were made to develop contingency plans. Following the second lock problem, however, it was concluded that there was no need to limit or inhibit EPC operations.

e. TACS Only Control on DAY 91.

(1) Description. On DAY 91, EREP and EREP Calibration Maneuvers were performed during two consecutive orbits, during which momentum dumps were inhibited. As a result, the vehicle entered a single-sample dump maneuver with a total momentum of 2.5 H. This did not leave sufficient momentum to maneuver the vehicle in all three axes. Momentum was prorated on each axis according to the control gains, the X-axis gain being about 1/6th of the Y and Z-axis gains. A rate buildup resulted on the X-axis, and the X-axis attitude error eventually exceeded 20 degrees. This caused an automatic switch to TACS Only Control.

The Auto TACS Only Mode terminated the dump maneuver, caged the CMGs to nominal momentum and initiated a return to Solar Inertial attitude at maximum rate. The crew responded to the CMG Saturation and Vehicle Over-Rate Alerts and attempted to determine the cause of the alerts and state of the control system.

An involved and unusual sequence of events followed during which a large amount of TACS fuel was consumed. The fact that the CMGs were inhibited was not obvious and the situation was clouded by Rate Gyro integral test failures and the faulty CMG gimbal angle readouts (discussed below). In addition, the vehicle was outside station coverage at the time, so that ground support was not available.

(2) Impact. During the time that the vehicle was in TACS Only Control, there was 11,454 N.sec of TACS impulse expended.

(3) Corrective Action. A software patch was studied which would prevent recurrence of the problem. However, because the probability of a recurrence of the extreme TACS expenditure was very small, the patch was never implemented. It was recommended that if the X-axis momentum ever exceeded 2000 N.m.s. and the attitude error exceeded 10 degrees during dump, the maneuver would be inhibited. This would allow Z-axis attitude to be updated. The momentum cross coupling in X would produce a better momentum state for the next dump.

f. Faulty CMG Gimbal Angle Readout.

(1) Description. During the sequence of events on DAY 91, the crew selected the CMG gimbal angles for display on the C&D Monitor Panel. This was done by setting two rotary switches, one which determined the measurement and another which determined the hardware source (e.g., CMG No. 1). The selected signal was displayed on a meter readout.

In this case, the outer gimbal angles of CMG No. 1 and CMG No. 3 read off-scale-low. The crew interpreted the reading as gimbals on the stops. At the time, the CMGs were actually caged to nominal momentum, and the two gimbals were not near the stops.

(2) Impact. Since the problem occurred at a time when the crew was attempting to determine the system status, the erroneous reading implied that CMG control was active when, in fact, it was inhibited. It thereby materially added to the problem of restoring the vehicle to CMG control.

(3) Corrective Action. The crew was instructed to move the Rotary Select Switch to the next position and back any time a reading of -100% occurred.

g. CMG No. 3 Wheel Speed Transducer Failure.

(1) Description. On DAY 12, 09:56:00, the CMG No. 3 wheel speed indication on telemetry went to zero. All other data from CMG No. 3 remained nominal, which indicated that the wheel speed transducer had failed.

(2) Impact. Failure of the CMG No. 3 wheel speed transducer on DAY 12 had no impact on the mission. CMG motor currents were an adequate indication of wheel speed.

(3) Corrective Action. None.

C. APCS Mission Support Team

1. Purpose. The Mission Support Team for the Attitude and Pointing Control System was organized to provide real time support for Johnson Space Center (JSC). This support was to provide direction, answer questions and analyze and solve problems that occurred. The STAC (Support Team for Attitude Control) would receive problems or questions from the OD (Operations Director) in HOSC (Huntsville Operations Support Center). The STAC would then obtain answers from the proper support group or groups, coordinate the answers and furnish a reply to FOMR (Flight Operations Management Room) at JSC through the OD at HOSC. After some mission time had passed, a rapport was established with ASCO (ATMDC Software Control Officer

and GNS (SWS Guidance Navigation and Control Systems Engineer) Flight Controllers at JSC allowing direct communications with these personnel.

2. Organization.

a. Personnel. The original plan was to have two complete APCS Teams (Red and Blue). Each team consisted of a specialist in his field--such as TACS, Test, Software, Stability, Simulators and each of the hardware components--plus additional personnel to cover other contingencies. Each team was to work or be on-call for 24 hours allowing the other team time to relax or perform other tasks.

After the meteoroid shield was torn away, APCS support was changed to provide continuous coverage of 24 hours per day. Many members worked seven days per week for three weeks until the APCS teams were changed. Five teams were then formed so that full-time coverage would be available in each of the SPCS disciplines and yet allow some much-needed time off for the members. The MSFC-COMP/AERO and IBM simulator also provided this same coverage while the coverage of the other areas varied depending on the situation. This type support continued until the end of the mission, although the coverage was somewhat reduced during the unmanned portions.

b. Data Source. A prime factor in providing support for the APCS team was adequate data. The six different data sources providing data for the support teams were Real Time Console, Data to Television (D/TV) Formats, Houston D/TV Formats, IBM Data Conversion, MOPS (Mission Operation Planning System) and Data Books.

A description of each source follows:

(1) Real Time Console (Attitude Console). The Attitude Console was set up to display the telemetered data received from JSC. Any of 265 APCS measurements or events could be displayed. Meters were used to display items such as CMG wheel speeds, bearing temperature and TACS pressure. Lights were used to indicate events or to indicate when a measurement may be nearing its limits. The console also contained two D/TV monitors. The formats were changed at the console by notifying a teletype operator of the desired change.

Two eight channel recorders were used to record items such as gimbal angles, commands and Rate Gyro performance. Later in the mission, another recorder was utilized to record the various CMG parameters to maintain a close watch on the CMG performance.

Prior to launch of SL-2, mission support programs were developed for use on a Hewlett-Packard desk type programmable calculator to be located behind the Attitude Console. New programs were developed during the mission, as the need arose.

(2) D/TV Formats. Data TV formats were displayed on monitors. Any of 39 APCS formats could be called up on a monitor by the operator of the Attitude Console. The formats displayed the telemetered data plus some calculated parameters. The formats were limited to 25 items of data.

(3) Houston D/TV Formats. Houston D/TV formats could also be viewed on the monitor through special arrangements with JSC. These formats contained much more information and were updated more often than MSFC formats.

(4) IBM Data Conversion. Originally, the IBM data reduction programs were written to convert only the 131 ATMDC parameters. The program would take as an input a data tape produced by HOSC at MSFC and convert it to a Converted Data Tape (CDT). When the IBM data reduction role was increased to include the capability to process all PCM data, the programs had to be significantly modified. This was true of both the real time conversion programs as well as the All Digital Data Tape (ADDT) user tape conversion programs. Later when the capability was required to process Engineering Units Conversion (EUC) tapes, the ADDT user tape conversion programs were again modified; however, these modifications were minimal.

(5) MOPS. Other data was obtained from the Mission Operations Planning System (MOPS), which was a JSC system. This system was a storage system in which real time or tape dump data could be recalled for periods of up to 48 hours. This allowed data parameters to be obtained to analyze problems or various occurrences. Data could be obtained at the regular sample rate or as in some cases as much as 12 samples per second.

(6) Data Books. All Digital Data Books were published containing specific APCS parameters. These were issued several days after data was received and were useful in analyzing major problems.

c. Facilities. The APCS Team was assigned a work room in Huntsville Operations Support Center (HOSC). This room contained a data TV, and communication lines consisting of a direct line to JSC in addition to normal telephone communications. Several remote sites having various capabilities were also utilized. These areas are listed below:

IBM Support Room at IBM, Huntsville

RAPS Room (Real Time Astrionics Problem Solving)

HSL (Hardware Simulation Laboratory) in Astrionics Building

MSFC-COMP/AERO Simulation in Computation Laboratory

TACS Support Room in HOSC

Denver Support Room, Martin Marietta, Denver, Colorado

Bendix Research Laboratories, Detroit, Michigan

A brief description of each remote site is contained in the following paragraphs.

(1) IBM Mission Support. The primary role of IBM was to provide support in the areas of ATMDC software and hardware. As the mission progressed their role was greatly expanded to include Data Reduction, Problem Tracking and Anomaly Analysis.

The IBM support team was comprised of specialists in the following areas:

ATMDC Software System Analysis

Flight Programming

Simulation

CMG Control and Momentum Management

ATMDC/WCIU/MLU Hardware System Engineering

Data Reduction.

The personnel identified in these areas were the people who played a significant part in the design, development, and verification of the ATMDC Flight Program. In addition, hardware adn systems engineers familiar with the flight hardware and system interfaces in both the hardware and software area were assigned as team members.

The computers used in the mission support role were the same as those used in the design, development and verification

of the ATMDC Flight Program. These computers were utilized as Skylab simulators, for telemetry data reduction, maintaining ATMDC memory images, and for development and verification of Flight Program patches.

A room at IBM, Huntsville was dedicated to the mission support activity and contained communication lines, a D/TV monitor and a telecopier.

More details concerning IBM participation in the mission are contained in Reference 12.

(2) RAPS Support. The primary role of the RAPS support was to provide an area in which the hardware designers could monitor systems and hardware and provide real-time problem solving. The personnel manning the room consisted of the hardware personnel who designed and built the various items of hardware. They monitored hardware performance daily to determine trends that might have developed. They also provided information about limits, proper usage of hardware, analyzed problems and furnished answers to problems and questions that arose.

The RAPS Room was located in Astrionics Laboratory. It contained a D/TV monitor, a hard copy machine and communication lines.

(3) Hardware Simulation Laboratory. The primary objective of the Hardware Simulation Laboratory was to verify the Flight Programs. In addition the HSL was called upon to develop procedures and examine various hardware problems.

Two support teams were established for the HSL. Each consisted of a RAPS Room Engineer, two systems engineers, a simulation engineer, a programmer and two technicians.

The HSL consisted of a Control Moment Gyro Subsystem installation, an Experiment Pointing Control Subsystem installation, a Control and Display Cockpit Unit, the Flight and Support Computers, and the necessary control and monitoring consoles. The selection and placement of these test configurations was planned to facilitate testing the system to simulated orbital conditions within the bounds of practical methodology.

(4) MSFC-COMP/AERO Simulator. The MSFC-COMP/AERO simulation was used to optimize the daily flight plan in order to minimize TACS usage and gimbal stop problems during maneuvers. The studies became critical after the failure of CMG No. 1 and the resulting switch to 2-CMG control.

The MSFC-COMP/AERO simulator had several teams consisting of a systems engineer, a simulator engineer, a computer programmer and computer technicians. The simulator had been planned to be dedicated to Skylab only during critical phases. However, the anamolous configuration of the vehicle caused the simulator to be dedicated to Skylab for the entire mission.

The analog models included rigid and flexible body dynamics, limited CMG dynamics and TACS. Digital models included CMG control, momentum management, disturbance torques, maneuvering logic and orbital ephemeris.

(5) TACS Mission Support. The primary roles of the TACS Mission Support were observation of TACS performance and fuel usage, monitoring for trends, real-time problem solving, and special studies.

The TACS Mission Support Room was located in the main conference room of the HOSC. Additional MDAC personnel were located at the MDAC-W facility.

(6) Bendix Research Laboratories (BRL). The primary function of BRL was to provide assistance in solving long range problems and simulations.

A support group consisting of separate teams of four analysts, three hybrid programmers, two digital programmers, two computer technicians and a supervisory engineer was formed at Bendix Research Laboratories. This group worked together in the prelaunch period in preparing the four hybrid simulation models of Skylab Control Systems as well as during the course of the mission to provide technical support.

Four simulation models of Skylab Control Systems were used for mission technical support. The four model simulated the CMG Control System but differed in their emphasis on details. The four models were:

CMG/TACS Control System Model

CMG Control Subsystem Model

CMG/EPC Control System Model

Six-Mass CMG Servo Model.

(7) Martin Marietta, Denver, Colorado. The primary function of Martin Marietta, Denver was to provide a simulations and assistance in long range solutions of problems. The personnel involved were those who programmed and ran the simulations prior to the mission.

Several simulators were available for long-range problem analysis and solving.

One was an all-digital simulation programmed in Fortran IV. During a typical Skylab orbit, which included a momentum desaturation maneuver but no TACS firing, the simulation ran approximately 80 times faster than real time. Two other simulations, an all digital and a hybrid simulator, were used to obtain attitude reference calculations, vehicle Control Law calculations, and CMG Control Law calculations.

3. Preparation. Several months were spent in practicing mission support by the STAC. The first practices were used to acquaint the team personnel with communications, procedures, reference documents and the coordination aspects of problems. Problems or contingency situations requiring solutions were used in the final practices. These practices involved the full team including various simulators to arrive at a solution to the problem.

4. Activities. Following the launch of SL-1, the problems which occurred significantly changed the level of support planned for the Skylab mission. The thermal problems and maneuvers of the first 12 days and Rate Gyro scale factor and drift anomalies required constant monitoring and corrective action. The tempo of the problems, action items and short response times during this phase of the mission support effort taxed the team close to the limit of capacity.

A few normal activities are listed below:

Daily reports

Daily tracking of system and hardware

Maneuver planning

Anomaly analysis

Inflight data analysis

Generation of Memory patches

Provide data to JSC

Provide answers to JSC

Answer all Action Requests (ARs) and Mission Action Requests (MARs)

Information came from a coordinated effort of all remote locations. Maneuver planning heavily involved the MSFC-COMP/AERO Simulator and IBM. IBM was also directly responsible for providing daily status reports, daily Rate Gyro drift plots, Rate Gyro noise plots, and generating, verifying and delivering memory load patches. The other support activities were involved in the detailed analysis and long-range solutions of mission problems.

STAC effectiveness in solving mission problems was greatly enhanced by the presence of many of the key personnel responsible for the design, development, analyses and verification of the APCS. No group of purely mission support personnel, regradless of their training, could have provided the depth of system knowledge required to determine solutions to the many problems. Had these design personnel not been dedicated to Skylab during the mission, an inevitable dilution of their APCS knowledge would have occurred.

5. Conclusions and Recommendations. The entire operation performed admirably considering that no one was prepared for continuous mission support. However, improvements are in order and should be implemented if MSFC is to undertake any programs similar to Skylab in the future.

MSFC should not be dependent on JSC for data flow. MSFC should have direct access to the tracking network through GSFC. Furthermore, the backup command center should have been MSFC, not GSFC, since the system specialists were at MSFC.

The HOSC Data System was inadequate for the support required. The following improvements are suggested:

More than 25 parameters per D/TV format.

More capability to display computer parameters.

Display update rate of once per second.

Real time programming capability on console and D/TV

Better format call-up capability, i.e., eliminate the teletype and institute a system similar to JSC's.

Long-term D/TV plot capability. Fifteen minute maximum is not adequate to detect trends.

Stripchart range should be variable.

Increase system redundancy.

Improvements could be made in the areas of facilities and communication and should include:

Better display capability to remote support areas. These areas should have their own display select capability.

Better communication to remote areas (internal conference loops).

More full-period voice lines between MSFC and JSC, e.g., one for APCS, one for EPS, etc.

At least one handset at each console.

A call director in each support room. This would eliminate the need for four phones in each room.

Larger facilities for support teams should be provided to accomodate the large numbers of people required during emergency operation.

SECTION V. APCS Interfaces

A. Control and Display Panel

1. Description. The C&D Panel provided crew interface for controlling and monitoring the APCS. APCS related C&D Panel functions were as follows:

a. Switching.

Redundancy management of the ATMDC, EPEA, SPAR RG, FSS, ROLL RSLVR, & 800 Hz power

APCS mode selection

ST power, mode, and shutter control

EPC roll enable/inhibit, rate, & direction control

FSS door control

MPC enable/inhibit

CMG control

TACS enable/inhibit

Momentum dump enable/inhibit and caging control

Timing selection

Rate gyro monitor control

b. Analog Meters. Two meters provided capability for crew monitoring of:

Momentum

CMG wheel speed, phase currents, bearing temperatures and gimbal angles

Acq. SS angles

TACS pressure

c. Digital counters. The following ATMDC data could be selected for display on three C&D Panel counters:

Vehicle rates

Attitude errors

Caution and warning conditions

Alert conditions

ATMDC status words

ATMDC single memory data

Acq. SS angles

Roll reference and roll position

ST gimbal angles

FSS wedge position

Navigation parameters

d. Alerts. Five alerts were displayed on the C&D Panel:

CMG malfunction

CMG bearing overtemperature

Attitude control system malfunction

Computer reject of DAS/DCS command

FSS or experiment door open

e. APCS System Status Flags. Provided the crew with indications of hardware configurations selected, modes selected, sun and star presence, momentum dump status, and TACS firings.

f. Manual Pointing Controller. Provided the crew with the capability of manually pointing the ATM Canister and for positioning the Star Tracker.

g. Digital Address System. Provided astronaut command capability to the ATMDC and to other APCS hardware through a Switch Selector.

2. Mission Operation. Operation of the APCS portion of the C&D Panel was nominal with one exception. On DAY 217, ATMDC software recognized that the ATMDC had received excessive interrupts at the ATMDC/DAS interface. This resulted when three or more interrupts were received in

180 milliseconds or less and caused the ATMDC software to lock out the interrupt. The probable cause of the problem was that cycling of the DAS-ORBIT PHASE Switch on the C&D Panel upset the logic state of the DAS Electronics. When a command was then keyed in to this undefined state, the ATMDC enable bit was pulsed several times with no data bits. The problem was transient and did not cause any major impact on the mission. The DCS was used to uplink a patch which re-enabled the masked interrupt.

3. Conclusions. The C&D Panel layout, control capability, and parameter display was adequate to support crew efforts in APCS trouble-shooting. No major problems were encountered in activation or deactivation.

The DAS provided the crew with command capability which would have been impossible to implement with switches because of space limitations. Ground command interferred with the use of the DAS at times. Automatic lockout of the DAS or DCS as a command was entered from the other would have been a desirable design feature. The SL-4 crew reported that the use of octal for commanding maneuver angles was awkward since the feedback provided was in decimals. In addition, they reported the DAS to be time consuming for making small trial and error cluster maneuvers and would have preferred to have had a control stick similar to the MPC for this purpose.

The alert system functioned as desigred and contained an adequate number of parameters to alert the crew of APCS system anomalies. One problem with the system was that the alert lights occasionally went unnoticed for long periods of time. An audible alarm would have been desirable in the alert system.

B. Caution and Warning System

1. Description. The Caution and Warning (C&W) System provided the crew with indications of major problem existence. In the APCS area there were three types of C&W alerts.

a. Computer C&W. Activated by computer switchover or a computer self-test failure.

b. ACS Malfunction C&W. Activated by CMG saturation, switch to TACS only, or a second Rate Gyro or Acq. SS failure in any axis.

c. Cluster Attitude C&W. Activated by vehicle rates greater then 0.3 deg/sec or by a stuck thruster which was determined from momentum.

When a Computer or ACS Malfunction C&W occurred the crew was alerted by a 1 KHz continuous tone. When a cluster attitude C&W occurred, the crew was alerted with 1 KHz tone frequency modulated at 1.4 KHz and a red master alarm lamp.

The C&W condition which existed was stored in the C&W system memory and the major type condition could be recalled by a switch on the C&W Panel. In addition, the specific C&W condition could be displayed on the C&D Panel by keying a code into the DAS. The capability existed for individually inhibiting each C&W condition.

2. Mission Operation. Performance of the C&W system was as intended. Crewmen reported that the inhibit switches were difficult to locate at times (even though the layout corresponded to the display) and that checkout procedures were too extensive and not easy to understand.

C. EVA Rotation Control Panel

1. Description. When enabled from the C&D Panel, the EVA Rotation Control Panel gave the crew the capability of rolling the Experiment Canister to the proper position for film removal and installation during an EVA. Canister rates of 0.35/0.7 and 3.5/7.0 degrees per second could be commanded from the EVA Panel. Selection rate gain (X1 or X2) was determined by C&D Panel switch status. Controls for opening and closing the S082A and S082B doors were also provided on the EVA Panel since these doors had to be opened for film removal/replacement.

2. Mission Operation. No problems were encountered with the EVA Panel; it performed as designed. One APCS system problem resulted from rolling the canister at high rates, this being coupling of Canister motion into the Rack Rate Gyros. As a result of this, Canister roll rates were limited to 3.5 deg/sec from both the EVA Panel and the C&D Panel.

D. Electrical Power System

1. Description. The Electrical Power System converted solar power to 28 Vdc electrical power. The 28 Vdc power was supplied to the APCS from redundant, diode isolated buses. The APCS used part of the power in the 28 Vdc form and converted part to different voltages and frequencies. All APCS power was supplied from the ATM power system except for the TACS and the Rate Gyro Six-Pack which were powered by the AM power system.

The CMGIA used the 28 Vdc power for circuitry within the CMGIA and also generated 130 Volt - 455 Hz, 28 Volt - 800 Hz, and 10 Volt - 4.8 Khz, from the 28 Vdc power for distribution to other hardware. The following is a description of the uses of the power generated in the CMGIA:

a. 455 Hz. 130 volt, 455 Hz power was supplied to the CMG spin motor, to the FSS and to the ST.

b. 800 Hz. 28 volt, 800 Hz power was supplied to the MPC, to the MPC channel of the EPEA for reference in demodulating the MPC signal, to the EPC UP/DN, L/R, and Roll Resolvers, and to the WCIU for demodulation of the EPC resolvers.

c. 4.8 KHz. 10 volt, 4.8 Khz power was supplied to the excitation coils of the linear and desaturation resolvers in the CMG and to the WCIU for reference in demodulating the CMG desaturation resolver outputs. In addition, 4.8 KHz power was supplied to the CMG Servo Amplifiers.

2. Mission Operation. Due to the loss of one OWS Solar Wing and the failure of the second Wing to deploy, some APCS hardware was initially powered down to conserve power. One Rack Rate Gyro in each axis was powered down. The Star Tracker, Spar Rate Gyros, Fine Sun Sensor, and Experiment Pointing Electronics Assembly were off-loaded when not required for a maneuver. After the remaining OWS Solar Wing was successfully deployed, power off-loading of APCS hardware was not required. The APCS power off-loading did not interfere with the operation of the APCS.

One anomaly occurred in the Electrical Power System which impacted the APCS. On DAY 177 a short developed on TV Bus 2. This caused a transient on the APCS power buses which caused the FSS wedge counter to be zeroed. There were other occasions when the FSS wedges were zeroed; however, due to insufficient data the occurrencies could not be attributed to power transients. This had a minor impact on the APCS; driving the FSS wedges through zero, so that the wedge counter indicated true wedge position, was required to correct the problem.

3. Conclusions. Other than the TV Bus 2 anomaly and the minor inconvenience, caused by power off-loading, the EPS/APCS interface functioned as intended.

E. Networks

1. Description. Networks provided the relay logic for power control, redundancy switching, and controlling the state of APCS hardware. In addition, Networks provided the interconnect cabling for routing signals between various pieces of APCS hardware and interfacing the APCS with other systems. Functions provided by Networks were as follows:

Control and distribution of power to the CMGIA, ST. Acq. SS, RG, EPEA, FSS, ATMDC, WCIU, and MLU

CMG wheel control

RG wheel control

CMG desaturation resolver source and reference switching

800 Hz redundancy switching

FSS door control

ATMDC, CMGIA, and CMG bearing heater enable/ inhibit

Interconnection between APCS hardware and interfacing the APCS with other systems

2. Mission Operation. Because of the problems encountered with the rack RGPs early in the mission, a major design change was implemented during SL-3. This involved installation of the six Rate Gyros (Six-Pack) and associated cabling and control boxes to replace six of the Rack Rate Gyros. The RGP Six-Pack was mounted in the MDA and powered from an existing utility outlet off AM Bus No. 2. A new unit, Rate Gyro Control and Distributor, was installed in the MDA. The function of the Distributor was to provide overcurrent protection in the input power lines and to serve as a junction box for input power, gyro outputs, and gyro coarse/ fine gain commands. An existing cable was disconnected from the C&D Panel and a new "T" cable installed to permit routing of Gyro outputs and gain commands through existing spare wires to the ATM. An EVA was performed to install another new unit, the Rate Gyro Select Box, and to attach break-in cables. The existing cable which routed the Rack Rate Gyro outputs to the WCIU was disconnected at the WCIU and the cable used for routing Six-Pack functions was disconnected at the ATM Trunion Plate. Two "T" cables which were an integral part of the Rate Gyro Select Box were connected to the WCIU, ATM Trunion Plate, and the two disconnected cables. Through these cables and the Rate Gyro Select Box, Six-Pack outputs were connected to pins on the WCIU where Rack Rate Gyros No. 1 and No. 2 had previously been connected. Rack Rate Gyro outputs were routed to the Rate Gyro Select Box where one of the three outputs in each axis could be selected as Gyro No. 3 for redundancy management purposes in the ATMDC. Plans were to use the two Six-Pack Rate Gyros in each axis for control with the selected Rack Rate Gyro as a spare, but due to a single failure point which existed in the Six-Pack power source, the remainder of the mission was flown with one Six-Pack Rate Gyro and the selected Rack Rate Gyro for each axis in control.

After Six-Pack installation, Rate Gyros were no longer a problem but system analysis did suffer from loss of high speed telemetry (12 samples/sec) of the Six-Pack outputs although the outputs were available on ATMDC telemetry at 1 sample every 2.5 seconds. Also, the Six-Pack RG temperature measurements were not available on telemetry. As a result, the crew was required to monitor Six-Pack RG temperatures periodically.

Only one anomaly occurred in Electrical Networks which was related to the APCS. On DAY 91, following an EREP calibration maneuver, a control system deviation occurred because of an extremely bad momentum state. Due to insufficient momentum in the X-axis, there was a buildup of vehicle

rates and attitude error resulting in a switch to auto TACS only. In the process of stabilizing the system the crew observed that one of the C&D Panel analog meters was indicating CMG No. 1 and CMG No. 2 outer gimbals were on a stop when actually they were caged. This caused the crew to command a nominal H cage but had no effect on the CMGs since the CMGs were already caged. In a later test, the problem was observed only on the CMG No. 1 measurement. The cause of the problem was determined to be intermittent operation of a relay in the Networks.

Loading of CMG wheel speed and Phase A current telemetry measurements by the C&D Panel analog meter was recognized during SL-4 as a system design problem. When the crew selected one of these measurements on the C&D meter a decrease in the telemetry measurements occurred instanteously. Since the C&D meter and the telemetry measurement were paralleled in Networks without any isolation, current drawn by the meter caused a voltage drop across a resistor common to both measurements in the CMGIA. The measurement should have been taken off the CMGIA Signal Conditioners through separate resistors.

3. Conclusions. Except for the relay failure discussed under Mission Operation above, the Electrical Networks/APCS interface functioned as designed. Installation of the Rate Gyro Six-Pack demonstrates that design changes/hardware replacement can be accomplished in space and that future spacecraft should be designed with repair/replacement in mind.

F. Thermal Control System

1. Description. The Thermal Control System (TCS) provided thermal protection to APCS hardware. This was accomplished by passive methods on rack mounted hardware. In addition to passive thermal control, temperatures of equipment mounted within the ATM Experiment Canister were controlled by an active fluid thermal control system. All APCS hardware was rack-mounted except for the Spar Rate Gyros and the Fine Sun Sensor Opto-Mechanical Assembly, Preamplifier Electronics, and Control Electronics.

The Canister active thermal control system, which could supply heat as well as radiate heat, maintained the Canister temperature at 10 $\pm$ .5°C. The Canister wall contained cold plates through which fluid was circulated to absorb the heat. The heat absorbed was then transported to radiators where it was radiated to space.

Passive methods used for APCS hardware thermal control were as follows:

Surface coatings - White paint was used on all externally exposed surfaces

Solar shield - The sun end of the ATM contained a shield to prevent direct sunlight impingement on rack hardware

Thermal shields - Heat losses of components with low power density were reduced by using thermal shields which were covered with insulation.

Insulation - Mounting panels were covered with insulation

Thermal isolation - Various components were conductively isolated from the rack structure

Thermostatically controlled heaters were used on some APCS hardware to supplement the TCS. CMG bearings were maintained within a + 15 to + 26°C range by heaters internal to the CMG. Rate Gyros contained heaters for maintaining their fluid temperature at 67.8 ± 1°C. The ATMDC, CMGIA and ST OMA had heaters for regulating the temperature of the entire units.

2. Mission Operation. Due to the loss of the OWS meteoroid shield during Skylab launch, the vehicle was flown in a thermal attitude (X = 0, Y = -45, Z = 0) for the first 13 days of the mission to regulate OWS temperatures. This created a thermal environment for some APCS hardware which was different than anticipated. Although APCS hardware temperatures were different than expected while in the thermal attitude, they were maintained within design limits and there was no adverse effect on the equipment operation. While in the thermal attitude, temperature measurements on the Solar Arrays and the OWS skin were used to roughly determine attitude. This was necessary since the sun was out of the Acq. SS field-of-view.

There were thermal fluctuations in the APCS hardware which were caused by changes in solar elevation and maneuvering. Temperatures changed gradually with solar elevation for all hardware except for the Acq. SS which had a change of 15°C for each day/night cycle. The effects of solar elevation are tabulated in Table 4. Increases in solar elevation increased the cycle time for the CMG bearing heaters and at large solar elevation the bearings were maintained in the range where heater turn-on was not required. The only unit which had a large thermal fluctuation due to normal operation was the Roll Actuator. Temperature changes of 13°C were observed when the Roll Actuator was activated.

3. Conclusions. Thermal control of APCS hardware was satisfactory. Even during the period that Skylab was in the thermal attitude, temperatures of APCS hardware were maintained within design limits.

C-7

Table 4. Hardware Temperatures (°C) vs. Solar Elevation

SOLAR INTENSITY	100	70	63	61	62	64	72	100	79	68	63	61	100	
Solar Elevation	-70	-50	-30	-10	10	30	50	70	-62	49	-27	0	70	T
DAY	42	48	52	57	175	179	184	190	100	130	220	230	249	
HARDWARE														
CMG IA No. 1	8	3	2	3	5	6	6	20	12	15	16*	16*	28*	18
CMG No. 1 Frame	-4	-6	-6	-6	-6	-6	-6	2	0	-1	-2	-11	-5	8
CMGIA No. 2	6	2	1	0	-1	-1	-1	11	11	4	7	6	12	13
CMG No. 2 Frame	-5	-7	-8	-8	-9	-10	-10	-3	-4	-7	-6	-5	0	10
CMGIA No. 3	5	0	-1	0	1	2	3	16	8	10	7	8	20	21
CMG No. 3 Frame	2	-1	-1	-1	-2	-1	-1	4	3	3	0	0	6	8
ATMDC	43	35	33	32	33	35	37	46	37	36	34	34	48	16
WCIU	18	8	5	4	2	2	5	15	11	5	4	3	19	17
Acq. SS (AUG)	31	12	7	7	10	15	16	42	25	18	15	17	48	41
FSS OMA	18	17	16	16	16	17	17	17	19	17	18	17	21	5
EPEA	3	N/A	-10	-12	-15	-14	-12	2	-2	-10	-8	-10	9	24
UP/DN ACT #1	2	3	-3	-3	-6	-5	-7	2	3	-1	0	-3	5	12
4 R ACT No. 2	-1	-4	-6	-6	-6	-5	-5	2	2	-1	-5	-2	7	13
UP/DN ORB. LOCK	-5	-9	-11	-11	-18	-17	-17	-9	-4	-1	-15	-15	-10	17
ROLL ACT	N/A	N/A	N/A	N/A	-24	-23	-23	-12	-12	-12	-15	-19	-24	12

*After CMG No. 1 failure

G. Instrumentation and Communication

1. Description. The Instrumentation and Communication (I&C) System provided the ground capability for control and monitoring of the APCS. This allowed the ground to perform routine monitoring and control which would have required considerable crew time, provided backup for onboard controls, and gave ground operation control of the APCS during unmanned flight.

The Telemetry System took raw analog data from the APCS and signal conditioned the data into amplitude limits compatible with the system. This data was then fed into multiplexers. Other data which was conditioned within the APCS hardware and APCS digital data were fed directly into multiplexers. The multiplexed data was then fed to the PCM telemetry system where it was converted to a 10-bit digital word and formated for real time transmission to the ground or recording when not over a ground station. APCS real time data was available at sample rates of up to 24 samples/sec. While not over a ground station, the Auxiliary Storage and Playback Unit (ASAP) extracted preselected portions of the data and recorded it for playback later. This data was available at a rate of one sample per second for PCM data and one sample per 15 seconds for ATMDC digital data.

The Digital Command System provided the ground with the same capability of commanding the APCS that the Digital Address System gave the crew. The DCS could address one of four Switch Selectors or the ATMDC which in turn executed the command.

2. Mission Operation. Performance of the I&C/APCS interface was as designed. Although noise on APCS measurements met design requirements, some measurements, for example the FSS errors, contained noise which degraded the usefulness of the measurement. Only one APCS measurement was lost during the mission, that being CMG No. 3 wheel speed which was caused by a transducer failure.

3. Conclusions. ATMDC telemetry and PCM telemetry were difficult to correlate due to the different cycle times of the two systems. Cycle times that were a multiple of each other would have aided data analysis. Some additional measurements, especially on the Star Tracker, would have been helpful in solving problems. There was some difficulty in determining what the crew was commanding; a telemetry measurement on each command function would have been desirable. An increased recording capability for ASAP data would have been highly desirable.

H. Space Environment

Several Star Tracker problems resulted from the environment in which it operated. Contamination produced by the sloughing of paint and dust, outgassing, and venting caused Star Tracker loss of star numerous times. As a contamination particle with reflected light brighter than the star being tracked came into the ST field-of-view, the ST would track the particles. False ST lock-on also occurred, due to reflected light from the vehicle surfaces. See Section VII.B.

SECTION VI. ATTITUDE CONTROL SYSTEM

A. Navigation and Attitude Reference

1. Attitude Reference.

a. Description and Design Goals. The SWS attitude reference was maintained for attitude control and display purposes. The four-parameter strapdown method, based on Euler's theorem, provided an SWS attitude reference relative to a desired reference. Vehicle rates were sensed by triple redundant Rate Gyros. The Rate Gyro outputs were sampled by double redundant multiplexed Analog-to-Digital (A/D) Converters. The outputs of the A/D Converters were used as the primary input to the strapdown reference calculations. The dynamic range of the Gyros and the A/D Converters was extended by operating the Rate Gyros with selectable gains. The two gain ranges were $\pm$ 1.0 and $\pm$ 0.1 degrees per second full scale. The scale change was commanded by the digital computer at about 0.09 degrees per second. The ATMDC made a conversion calculation of the information received from the A/D Converters. The A/D Converters operated with 10 bits plus sign. During orbital daylight in the Solar Inertial attitude, attitude error data from Acquisition Sun Sensors (Acq. SS) was used to update the strapdown reference in the X and Y-axes. The Star Tracker, ground updates, and the momentum management scheme were used to update and stabilize the Z-axis reference. Figure 13 shows the role of the strapdown in the APCS.

The attitude reference design goals consisted of a computational accuracy requirement and an updating or compensation capability. The computational accuracy requirement was a portion of the total Skylab system pointing requirements and the compensation capability provided the means for compensation of system anomalies.

(1) Accuracy. The error sources were categorized according to the factors on which they were primarily dependent. These were initialization, time-dependent, and maneuver-dependent errors.

The initialization errors included the accuracy of the Sun Sensor and its misalignment, and errors in computing the location of the orbital plane.

The significant time-dependent errors were caused by the Rate Gyro drift, drift in the digital computation, and the A/D Converter scale factor error. The maneuver magnitude-dependent errors were caused by Rate Gyro scale factor errors, and Rate Gyro misalignment.

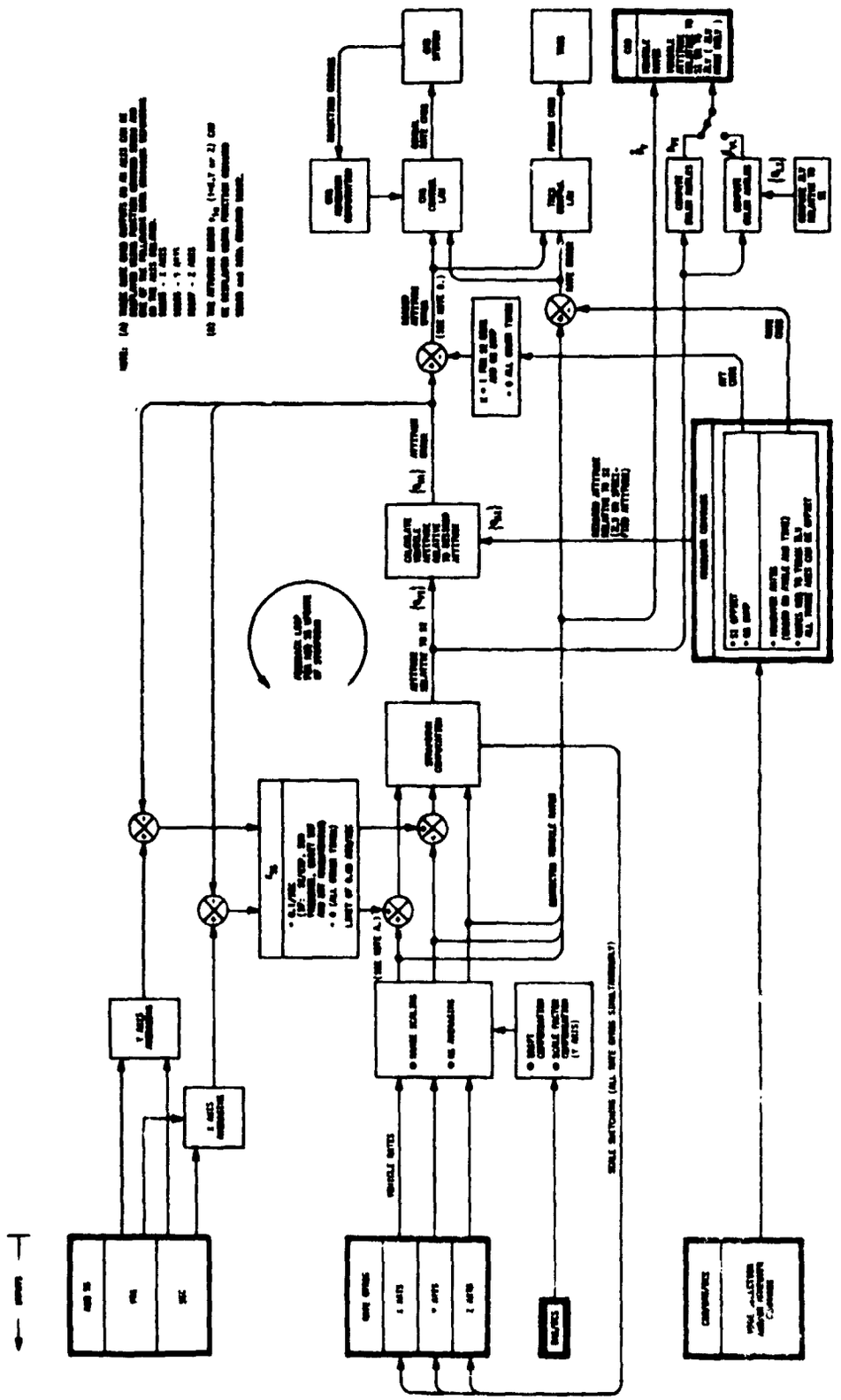

Figure 13. ATM ACS Control Loop

The attitude reference computational accuracy requirement was that the eigen-axis rotation represented by the attitude reference quaternion must not drift, due to software implementation of the attitude reference equations, more than 0.15 degrees per hour when operating with fine scale Rate Gyro readings, or 1.5 degrees per hour when operating with coarse scale Rate Gyro readings.

The most stringent requirements occurred when the system was operating in the Z-LV rotating reference frame. Table 5 gives the accuracy requirements for the APCS operating in Z-LV.

Table 5. Pointing Accuracy Requirements and Budget

Operational Attitude	Requirement and Purpose (deg)	Attitude Navigation (deg)	Structural Misalignments (deg)	Position Navigation and Control Error (deg)
Z-LV	2.5 Each Axis Earth Resources	1.5	0.5	0.5

In the Solar Inertial and Experiment Pointing modes, strapdown calculations were performed double-precision. These calculations were performed single-precision while in all other modes. As an example, the strapdown calculations X-axis jitter was about 0.6 arc minutes using double-precision compared with 1.7 arc minutes using single-precision.

(2) Rate Gyro Scale Factor and Drift. Due to the physical characteristics of the Rate Gyros on the Skylab vehicle, the ATMDC software was designed and programmed to compensate for possible errors. These errors were of two distinct types: Rate Gyro scale factor errors and Rate Gyro drift errors. Scale factor error is one in which the amount of error is directly proportional to the sensed rate. Drift is a constant error or bias. Software capability was provided to change the Y-axis Rate Gyro scale factor compensation. The scale factor compensation had a range from 0.0 to 2.0 and could be entered as an ATMDC memory load via the DAS/DCS. The Rate Gyro drift compensation could be applied to any Rate Gyro in any axis and could be entered as an ATMDC memory load. The range of the drift compensation was approximately $\pm$ 22.7 degrees per hour.

(3) Attitude Updates. Since the attitude reference did drift during test and flight, it had to be updated periodically. The system was designed so that the attitude reference would be

updated while in the Solar Inertial attitude and allowed to drift while in other attitudes (Z-LV, etc.). This was acceptable since no long periods of non-Solar Inertial attitude were planned. The X and Y-axes attitudes were updated continuously while in the Solar Inertial orbital daylight. The Z-axis attitude was updated once per orbit using the Star Tracker data.

b. History. The attitude navigation system for Skylab uses components originally designed for the earlier Wet Workshop ATM. A much more demanding mission requirement was imposed in the Dry Workshop than in the earlier Wet Workshop and yet the hardware components were basically unchanged. The design of the new system was constrained to utilize existing hardware if at all possible. The upgrading of the system, using the same hardware was accomplished in three ways:

By tightening component specifications where conservative design would permit without hardware impact.

By using onboard compensation for some of the deterministic errors.

By selecting the most accurate instruments to fill critical positions.

c. Design, Test, and Verification. A number of digital simulations were built to study the effects of sampling noisy Rate Gyro signals, the roundoff error on the A/D Converter, and the truncation and roundoff error of the strapdown algorithm. The fixed-point arithmetic of the ATM Digital Computer and the computation cycle time were also simulated. Typical maneuver profiles were chosen to study the combination of these effects. Table 6 lists the results of an error source study.

The computational drift was tested prior to delivery of the final Flight Program using both the actual Flight Program and an IBM System/360 Flight Program Model. Tests were run at high and low rates during Z-LV and Attitude Hold maneuvers, and while maintaining an intertial attitude. The results showed that the attitude reference drift was less than 0.15 degrees per hour for all tests with the majority being less than 0.1 degrees per hour.

d. System Performance.

(1) Accuracy. Loss of the meteoroid shield and resulting thermal and solar power requirements shortly after orbital insertion required maintenance of an attitude where the Z-axis was not pointing at the sun. This was accomplished using the Attitude Hold Mode. The large and changing Rate Gyro drift present in the

Table 6. Strapdown Inertial Reference Error Sources Study

Error Source	Specification	Results		
		X	Y	Z
Gyro Drift (deg/hr)	0.1	0.06	0.03	0.01
Scale Factor Nonlinearity (percent)				
Fine Scale	1.0	0.18	0.14	0.40
Coarse Scale	1.0	0.74	0.42	0.52
Gyro Misalignment (arc min)	30	10	10	10
A/D Converter (percent full scale)	0.1	0.1	0.1	0.1
Computation (deg/hr)				
Fine Scale	NA	0.15	0.15	0.15
Coarse Scale	NA	1.0	1.0	1.0
Initialization (deg)				
Star Tracker	NA	0.1	0.1	0.1
Momentum Management	NA	0.1	0.1	3.54

original Rack Rate Gyros presented serious difficulties in maintaining attitude and attitude reference. Due to the length of time in maintaining the thermal attitude without a position update the strapdown reference became greatly degraded. The strapdown was continuously reinitialized to the present attitude because in the event of a computer switchover the Flight Program reinitialization would have automatically commanded the vehicle to an erroneous Solar Inertial attitude. Since the ATMDC had no information on vehicle attitude, it was necessary to maintain attitude reference on the ground. It became apparent that Rate Gyro drift made it impossible to determine attitude from a reconstruction of the command history. Therefore, an improved method of attitude determination was required. Solar panel power was proportional to the cosine of the sun angle (i.e. between the Z-axis and the sun line) and this data could be utilized. However the power indication alone left two degrees of freedom of uncertainty. These were the Z-axis in a cone about the sun line and the vehicle rotation about the sun line. To resolve these additional degrees of freedom, thermal measurements, shadow patterns and momentum sample data were used. The temperatures of

certain ATM components indicated the angle of the sun line to the vehicle Y-Z plane. The momentum samples provided the angle of the vehicle X-principal axis relative to the orbit plane.

Despite inaccuracies, the results were sufficient to provide information on vehicle attitude accurate to a few degrees.

After installation of the solar umbrella the vehicle was returned to Solar Inertial attitude. The Gyro drifts were compensated and strapdown attitude reference was updated using the Acquisition Sun Sensor and Star Tracker.

After installation of the Six-Pack Gyro Package, Six-Pack calibration maneuvers were performed to determine the Gyro misalignment. The misalignment was determined to be 0.1 degree $\pm$0.1 degree about the X-axis, -0.24 degrees $\pm$ 0.1 degree about the Y-axis and 0.30 degrees $\pm$ 0.2 degrees about the Z-axis. The misalignment angles were quoted with tolerances because they were so small they stretched the accuracy of the alignment determination method. A Six-Pack misalignment patch for the Flight Program was developed but was not loaded because the misalignment was so small that compensation was not required.

As the mission progressed, the Star Tracker deteriorated. Backup methods of updating the Z-axis attitude reference were developed. These are discussed in Section VI. A. 3.

(2) Rate Gyro Scale Factor and Drift Compensation. A limitation on the amount of scale factor correction and drift compensation was imposed by the fact that scale switching relays for the Rate Gyros were activated by the flight software when the compensated rate (sensed rate plus any compensation) exceeded a certain limit (initially 0.095 deg/sec for a switch to coarse scale and 0.085 deg/sec for a switch to fine scale). In order to maintain the integrity of this program, no scale factor corrections smaller than 0.95 could be entered, and no drift compensation greater than 0.005 degrees per second could be used. The switching limit was changed on DAY 39 (from 0.095 to 0.088 and from 0.085 to 0.078) to allow greater scale factor error compensation and larger drift compensation values to be used.

The scale factor correction capability was exercised four times during the Skylab mission and the resulting corrections applied to the Y2 and Y3 Rate Gyros. The Y3 Rate Gyro scale factor in the primary ATMDC program was changed from 1.000000 to 0.9942383 on DAY 22. On DAY 28 the same change was implemented in the secondary ATMDC software. The Y2 Rate Gyro scale factor was changed from 1.000000 to 0.938967 in the secondary ATMDC software on DAY 39.

After installation of the Six-Pack Rate Gyro package on DAY 103 the scale factors for both Y2 and Y3 were restored to a value of 1.000000 in the secondary ATMDC software. The Rate Gyro drift compensation capability in the ATMDC Flight Program was exercised considerably more than the scale factor capability. Between DAY 1 and DAY 103 the Rate Gyro drift compensation DCS/DAS command input was utilized over 280 times to change the drift compensation for the nine Rate Gyros. After the Six-Pack Rate Gyro package was installed, only two drift compensation changes were entered.

(3) JOP 13 Maneuvers. A procedure was developed during the mission to utilize the high resolution Solar Inertial computation accuracy for JOP-13 and JOP-18D (Kohoutek). The secondary Acquisition Sun Sensor was selected for control and Acquisition Sun Sensor Redundancy Management was inhibited. The secondary Acquisition Sun Sensor was then powered down. This insured zero error signal from the Acquisition Sun Sensor to the strapdown update. After the maneuver to point at the target was completed in the Attitude Hold Mode, the strapdown calculation was reinitialized. The Solar Inertial Mode was then selected for the experiment. After completion of the experiment, Attitude Hold was selected and the maneuvers for an approximate return to Solar Inertial were commanded. After the return maneuver was completed, the repowering of the Acquisition Sun Sensor and the selection of Solar Inertial caused the Acquisition Sun Sensor to update the strapdown in X and Y and converge the vehicle Z-axis to the sun. The maneuver had put the X-principal axis approximately in the orbit plane and the next desaturation maneuver converged the X-principal axis into the orbital plane.

2. Navigation and Timing.

a. Description. The ATMDC Flight Program was configured to provide navigation and timing information for the SWS. The navigation scheme was designed to maintain knowledge of SWS position in orbit relative to orbital midnight. Significant orbital event times were calculated and, along with SWS position in orbit, were used to determine day/night phase of orbit and time remaining in the prevailing orbital phase. This information along with several intermediate parameter calculations, were used to support other functional areas of the program such as maneuvering, momentum management, orbital plane error, roll reference, etc., as well as for display purposes.

The navigation equations were derived to relate the orientation of the orbital plane in inertial space to the equatorial plane and the orientation of the sun vector relative to the orbital plane. In deriving equations for the necessary parameters, significant

simplification was achieved by assuming a circular orbit. The assumption was made that between orbital midnights the movement of the earth about the sun and the regression of longitude of the orbital ascending node could be ignored. To facilitate periodic compensation for navigation drift due to these assumptions and anticipated off-nominal orbits, sufficient navigation parameters were made updatable to reinitialize the scheme per ground calculations.

Other navigation scheme functional requirements included maintenance of mission time from one of two available timers and execution of a partial navigation scheme following switchover. The partial scheme was a subset of the primary navigation equations designated to be executed following switchover until a navigation update was issued. The partial scheme was demonstrated as properly implemented following the switchover on DAY 27.

Eleven navigation parameters were made updatable via the DAS/DCS command system in order to adjust the navigation scheme to off-nominal orbits. The 11 parameters are:

Longitude of orbital ascending node

Period between ascending nodal crossings

Orbital plane inclination

Ratio of earth to orbital radius

Change to previous orbital midnight time

Orbital rate

Mean anomaly of earth in solar orbit referenced to perihelion

Solar Elevation Angle

Geographic longitude of orbital ascending node

Orbital plane nodal regression rate

Orbital midnight period change

The value of each update parameter, with the exception of Solar Elevation Angle, was valid at the actual time of the update. The Solar Elevation Angle was updated to the value for the previous orbital midnight.

One of the most important navigation parameters was the Solar Elevation Angle, which was defined as the angle that a line from the center of the earth to the sun makes with the orbital plane. The Solar Elevation varied between plus and minus 73 degrees and its time history during the mission is shown in figure 14.

b. Development. The original Wet Workshop navigation and timing requirements consisted of maintaining the orbital plane, sun and SWS orientations to provide navigation and timing information for the SWS.

The first Dry Workshop program replaced the computation and display of earth-referenced latitude and longitude data with earth-referenced ascending node and time from nodal crossing computation and display. This simplified the computation and still provided the necessary crew display data. Later programs had four major changes:

Computed t_{GMT} from the real time clock as opposed to the A and B mission timers.

Deleted the testing and automatic selection of the A and B mission timers.

Deleted the backup navigation scheme which derived its information from the Acq. SS. A simplified navigation was still provided for use following an ATMDC switchover to maintain a navigation reference until DAS/DCS updates could be transmitted.

Based the navigation and timing reference on orbital midnight crossing instead of ascending node crossing.

All of these changes were primarily for memory savings and reduced the complexity of the program without sacrificing any capabilities.

Aside from several navigation data changes, there were no other major navigation and timing design changes.

c. Mission Operations. The original Skylab launch achieved a near-circular orbit with an initial apogee of 441 Km and a perigee of 437 Km. During the course of the mission, several trim burns were executed to adjust the Skylab orbit to provide repeatable ground tracks for Earth Resources Experiment passes. These trim

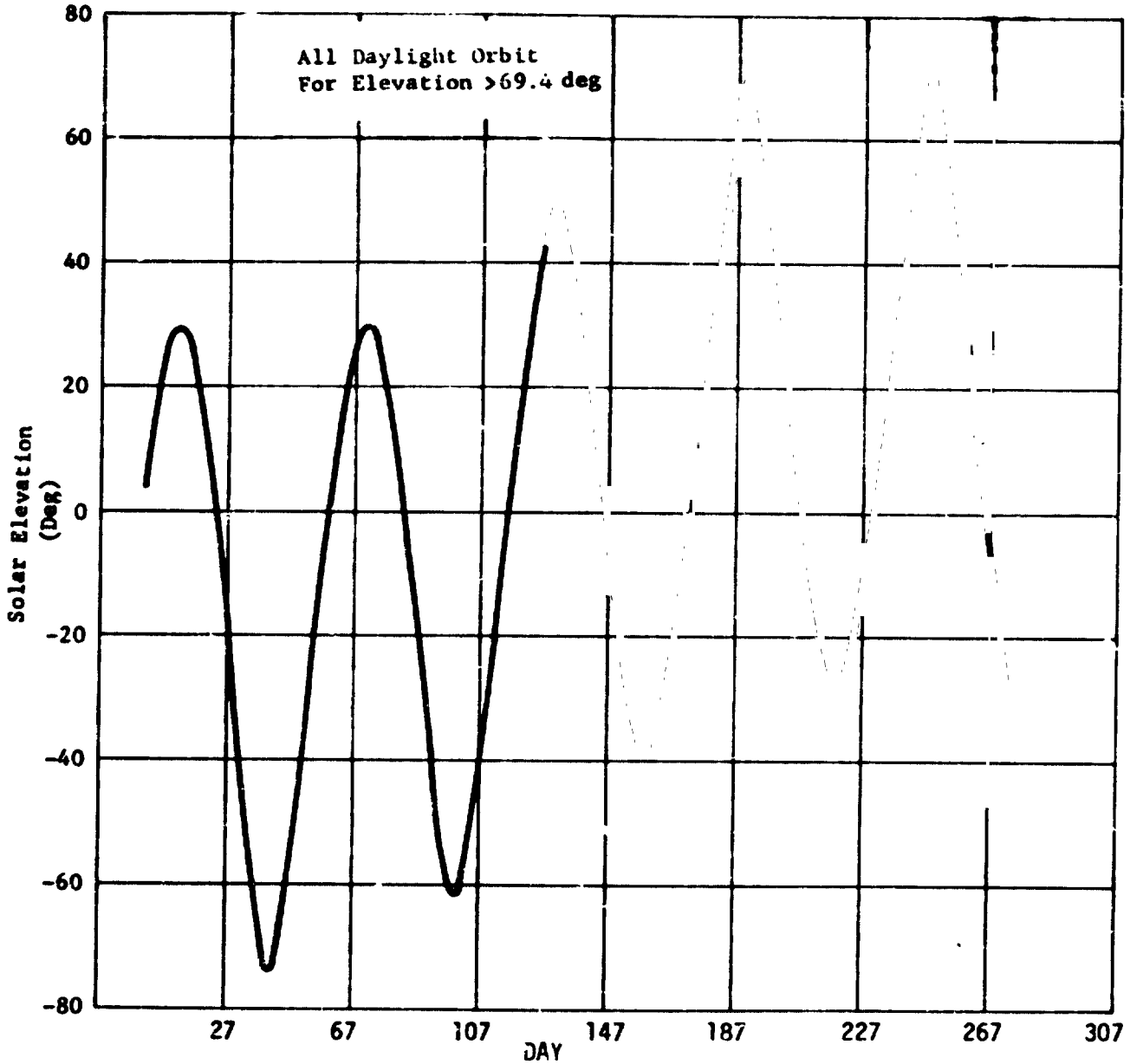

Figure 14. Variation Of Solar Elevation

burns combined with normal orbit degradation resulted in the apogee ranging from 441 Km to 456 Km and the perigee ranging from 421 Km to 437 Km.

The navigation update capability was used extensively during the course of the mission. During the 271 days of Skylab, there were 152 navigation updates issued. Six of these occurred during primary computer operation in the first 26 days of the mission and the remaining 146 were issued during secondary computer operation following switchover on DAY 27. The criteria used for determining the requirement to update the navigation scheme involved a comparison of the actual time of orbital midnight to the Flight Program calculated value was in error by five or more seconds, then a navigation update would be formulated and uplinked. Navigation updates were also used to help control navigation day/night conflicts with sun presence indications from the Acquisition Sun Sensors (see Section VII.D). Several of the updated parameters involved angle variables cycled 0 - 360 degrees each earth orbit and as expected exhibited a cyclic update value history. Others, such as the time parameters, exhibited non-cyclic update histories.

In summary, all the parameters which were critical to the integrity of the navigation scheme were updated successfully in order to adapt the navigation scheme to the changes in orbit as the SWS orbit degraded between trim burns. This success was indicative of not only sound design and critical parameter designation, but also good performance of the software designed to process updates to the navigation scheme.

Mission time for display was maintained from one of two available mission timers. The redundant mission timers were 29 bit registers that stored time in terms of days, hours, minutes, and seconds. These timers utilized basic oscillators separate from those used to provide ATMDC software timing. Mission time data was obtained from either Timer A located in the ATMDC or Timer B located in the WCIU. Either timer could be selected for use via switch selector command and timer drift could be compensated via a DCS command to the ATMDC.

During the first 26 days of the Skylab mission, the two timers were alternately used in an effort to determine which timer was most stable. The first timer update occurred on DAY 11 when Timer B was updated by (-11) seconds. The next update was to Timer A on DAY 21 and was an amount of (-4) seconds. The last update to Timer B was on DAY 24 by a delta of (-18) seconds. After the switchover to the secondary computer, on DAY 27, Timer A was used for the remainder of the mission. During this time, Timer A exhibited a positive drift of approximately 0.3 seconds per day which was well

within the specification tolerance. Following switchover, the timer was held within an accuracy of 3 seconds requiring an update every 11 to 13 days. This resulted in a total of 21 updates to the secondary computer Timer A.

The navigation scheme interfaced with various program functional areas including both Rate Gyro and Acquisition Sun Sensor Redundancy Management. The navigation logic determined whether the vehicle was in the "day" or "night" portion of the orbit. This day/night indication affected dual Rate Gyro post failure detection processing, single Rate Gyro failure detection processing, and Acquisition Sun Sensor failure detection processing. These Redundancy Management functions, if required, were performed if all the following conditions were satisfied.

> The APCS was in the Solar Inertial or Experiment Pointing Mode.
>
> A Solar Inertial Acquisition maneuver was not in progress.
>
> The SWS was in the "day" portion of the orbit.
>
> The Sun Presence Indicator was set to light.

However, these Redundancy Management functions would also be executed if only the first three of the four conditions above were satisfied and the prime strapdown indicated that the SWS was within 3.25 degrees of the Solar Inertial attitude. The day/night indication was a function of true sun time or effective sun time depending upon whether the sun timing option or the computer timing option, respectively, was selected. The integrity of the redundancy management interface required that the Sun Presence Indicator, which was set in reaction to the status of the Sun Presence discrete inputs, must be set to "light" at all points in the navigation determined "day" portion of the SWS orbit. This was required because a Rate Gyro failure would be declared if the conditions discussed above indicated that a "light" indication was expected (i.e., navigation indicated "day" portion of orbit), but the Sun Presence Indicator was set to "dark". Also, if this integrity was not preserved, then Acquisition Sun Sensor Redundancy Management logic would be executed during a portion of orbit not considered by the original design, possibly introducing problems.

A potential problem existed during the course of the mission relative to the navigation/sun presence indication interface. The Sun Presence discretes appeared to indicate "light" approximately 5 seconds after computed true sunrise and disappeared

to indicate "dark" approximately 5 seconds prior to computed true sunset. This left a 5 second window at sunrise/sunset in which the vehicle would be in the "day" portion of the orbit with the sun presence indication set to "dark" if the sun timing option was selected.

Another program area affected by navigation was program control of the Fine Sun Sensor (FSS) aperture door OPEN/CLOSE and wedge HOLD/RELEASE functions. The FSS aperture door was opened at sunrise when the Sun Presence discretes were activated. The FSS wedges were released at the start of the navigation "day" portion of orbit. Due to the navigation timing situation introduced by the Sun Presence sensitivity, with computer timing selected, the FSS wedges were, on some occasions, released approximately 3 - 5 seconds prior to completion of the aperture door open operation. Since FSS wedge position readouts were sensitive to changes in light exposure, the wedge readings sometimes changed by one count at sunrise even though there was no actual change in displacement. (See Section VIII. B).

A similar discrepancy involving experiment interface was attributed to navigation timing properties during periods of all daylight orbit (absolute value of solar elevation greater than 69.4 degrees) processing. It was possible during periods of an all daylight orbit that the time remaining in orbital phase calculation might result in a negative value at orbital midnight. This possibility had been documented prior to the mission in an ATMDC software program note (PN6-057). When this happened during the mission, it caused some concern because as a consequence of time remaining being negative, the navigation logic determined "night" phase of orbit and disabled the EPEA, closing various experiment doors. This happened only once during the mission and was at a time when the experiments were not actively being used. Also, the situation was in effect a maximum of two slow loops before the time remaining value corrected itself and the experiment doors were reopened.

Related also to the navigation Sun Timing/Sun Presence interactions was the up-linking of a program patch prior to the planned switchover on DAY 160. Since Sun Timing was automatically selected by the software following switchover and the Rate Gyros were behaving so erratically, there was considerable concern about what might happen following the switchover. This concern resulted in a Flight Program patch (S3030) to alter the initial value which the ratio of earth radius to Orbital Radius would have following the switchover. The ratio was changed so as to effect a true sunrise value not to precede the Sun Presence indication at sunrise

value not to occur subsequent to loss of Sun Presence, thus avoiding any potential Redundancy Management interface problems.

Since the effective sunrise define a significantly longer "night" phase of orbit, the computer timing option was not affected by the Sun Presence indicator sensitivity characteristics as far as Redundancy Management interface was concerned. Hence, computer timing was the option selected for the greater part of the mission. Occasionally, Sun Timing was selected to extend the viewing time during various experimental observation periods. This advantage of Sun Timing was due to the fact that the true sunrise and sunset times define the longer navigation "day" phase and this is required to activate the Experiment Electronics Assembly. During periods of Sun Timing Operation, the Rate Gyro and Acquisition Sun Sensor Redundancy Management performance was monitored very closely to insure that the potential problems never materialized. Consequently, the unexpected Sun Presence indication sensitivity characteristics were never allowed to be a deterrent to performing any planned experiment activities and at the same time any potential Redundancy Management interface problems were avoided.

3. Roll Reference.

a. Description. The Star Tracker acquired one of three reference stars to provide an orbital plane error angle and a solar reference angle, called the roll reference angle. The primary reference star, Canopus, and the secondary reference stars, Achenar and Alpha Crux, were selected on the basis of their magnitudes and locations.

The orbital plane error angle was defined to be the angle between the orbital plane and the X-vehicle axis about the vehicle-to-sun line. It was a function of Star Tracker gimbal angles, relative positions of the earth, sun and reference star, and orientation and position of the vehicle in its orbit. It primarily supported momentum maneuvers and maneuvering to Z-Local Vertical attitudes.

The roll reference angle was defined to be the angle between the projection of both the solar north and the experiment pointing systems Y-axis into the plane of the solar disc. It was a function of Star Tracker inputs, relative positions between the earth, sun and reference star, and the orientation of the Canister relative to the experiment pointing system's axes. This angle primarily supported experiment film recordings.

b. Development. To support the SWS attitude reference maintenance, a stellar reference was provided for display, telemetry,

orbital plane error, and roll reference information. The star occultation intervals were computed and used to control the Star Tracker track and search functions. The Star Tracker position data was used in computing the orbital plane error (vehicle attitude reference) and roll (EPC) reference information.

Additional requirements after change to the Dry Workshop are listed below:

Deletion of an arbitrary star selection capability.

Star Tracker control function ENABLE/INHIBIT capability.

DAS/DCS Star Tracker outer gimbal backup capability for use in the event of Star Tracker failure.

EPC line-of-sight roll capability was added. The FSS was positioned according to EPC roll changes to allow EPC roll about the ATM experiment line-of-sight.

The next level of changes included:

EPC line-of-sight roll filter was bypassed for FSS fixed positioned pointing.

HCO door opening delay capability was added.

Protection for erroneous FSS position input data was provided.

Subsequent changes:

Star Tracker data was compensated for known Solar Inertial attitude offsets prior to use in orbital plane error and roll reference computations.

Protection for erroneous Star Tracker input data was provided.

An ENABLE/INHIBIT Star Tracker data use capability was provided to prevent erroneous tracking data from contaminating attitude reference.

EPEA activation logic was modified to account for Solar Inertial offset pointing.

An EPC roll change threshold for EPC line-of-sight roll activation was added to prevent erroneous activation.

c. Mission Operations.

(1) General. During the SL-2 mission, the Star Tracker performed normally at most times. However, on several occasions, the Star Tracker either acquired contaminant particles as false stars, or failed to acquire the reference star because the vehicle was not closely aligned to the vehicle-to-sun line when acquisition of a star was commanded by the ATMDC. When these discrepancies occurred, they were corrected according to procedures developed at Johnson Space Center. To reacquire a star after the Star Tracker failed to acquire either because the star was not in the field-of-view of the Star Tracker or the Tracker locked on a contaminant was a task that the SL-2 crew characterized as one of the biggest attitude control problems. A procedure was developed in the SL-3 manned spacecraft-experiment management criteria which minimized the impact on the crew timeline, but which could not prevent the Star Tracker from losing star presence for the above reasons.

The criteria permitted the Star Tracker to track a star while the crew was awake. However, it selectively permitted the ATMDC to correct the orbital plane error angle and roll reference angle. According to the criteria, in those cases where the Star Tracker did not acquire a star, the discrepancy was to be corrected by the crew at their convenience, but within four revolutions. In those cases where the Star Tracker failed or its data was invalid, the orbital plane error angle was to be updated when its ATMDC computed value differed by a specified amount from a JSC computed value.

The Star Tracker could not be controlled from the ground during the unmanned phases of the Skylab mission. An abbreviated criteria was developed to be used during the unmanned phases of the mission. According to this criteria, the orbital plane error angle was to be updated when the ATMDC computed value differed by a specified amount from a JSC computed value, but subject to restrictions related to TACS firing, vents, ATM data availability, and momentum buildup.

During SL-3, the performance of the Star Tracker began to deteriorate. On several occasions, the shutter failed to respond to ATMDC commands. Investigation indicated an apparent intermittent problem with the shutter mechanism, its associated switch, or a circuit relay that commanded the shutter flag. The

simplex shutter system and minimal telemetry data precluded isolating the failure to a specific relay, logic module, or to the shutter mechanism.

Procedures for limited utilization of the Star Tracker were developed and transmitted to the crew. Under these procedures, whenever the problem occurred, the crew cycled both the Star Tracker power switch and the shutter switch at the Control and Display Panel. When this was unsuccessful, the Tracker was placed in a parking position away from light sources. The Star Tracker was used only at discrete times specified in the daily flight plan.

Also, during SL-3, Alpha Crux, or a star dimmer than Alpha Crux could not be successfully tracked because the sensitivity of the star phototube degraded faster than was expected. The ATMDC Flight Program was modified to substitute Rigil Kent for Alpha Crux as a secondary reference star.

The SL-4 manned spacecraft/experiment management criteria was developed with emphasis upon minimizing the number of cycles of the shutter and to preclude the unwanted effects of the Star Tracker locking on a foreign object. According to the criteria, the automatic operation of the Star Tracker was replaced by positive manual control of the Tracker. On DAY 228 the Star Tracker failed and its use was discontinued. For more information see Section VII.B.

The SL-4 manned spacecraft/experiment management criteria was changed to reflect the loss of the Star Tracker. According to the criteria, the crew performed sextant sightings using the sextant/scanning telescope in the Command and Service Module. Each sighting was performed to establish a baseline for the orbital plane error angle. The ground support team, using DCS commands to the ATMDC would then continue to update the orbital plane error angle with a computed value until the sextant data differed from the computed value by a specified amount. When this occurred, the procedure was repeated using the most recent sextant measurement.

(2) Impact of Degraded Performance of Star Tracker. Maneuvering accuracies and experiment data were characterized as doubtful whenever the Star Tracker failed to provide valid inputs to the ATMDC.

Errors in the orbital plane error angle led to automatic resets of the CMG gimbal angles, a procedure which allowed the CMG system to recover from undesirable momentum configurations. The TACS was fired to assist the CMGs in recovering

to a desirable momentum state. Under certain conditions, relatively large quantities of TACS fuel was expended because erroneous orbital plane error angles were used by the CMG momentum management system.

Errors in the orbital plane error angle also affected maneuvers to support selected experiments. For example, a JOP 18D maneuver on DAY 215 with an orbital plane error of one degree created an error in the X-vehicle axis equal to 0.37 degrees against a desired total error of less than $\pm$ 0.04 degrees for the experiment.

The ATM experiments relied on the Star Tracker for accurate roll reference information during solar observations. Losing the Star Tracker did not prevent Solar Pointing activities. However, it did result in losing an accurate solar north reference. Experience with the results obtained while the Star Tracker was degraded has shown that large errors in the experiment roll accumulated when the vehicle attitude was not frequently updated with Star Tracker data. This uncertainty in experiment roll caused serious data evaluation problems for the various ATM principal investigators.

(3) Corrective Actions. As a result of the Star Tracker problems, STAC developed a means to calculate the orbital plane error from telemetered data. A program was written for a programmable calculator to model the equations specified in the ATMDC Program Definition Document. Data reduced from telemetry tapes were used as the source for inputs into the program. The program was verified by using data reduced from DAY 20 real time telemetry tapes as inputs into the program. Two comparisons were made between the calculated value and the telemetered value of the orbital plane error. The maximum difference between the two values was less than one least significant bit of the telemetered value.

STAC also developed an analysis of the SL-2 and SL-3 data to demonstrate the drift of the telemetered experiment roll reference angle with respect to its probable true value. First, the sources which contributed to errors in calculating the value of the roll reference angle were identified and analyzed. Analysis showed that the requirements for accuracy of the roll reference angle could be met only during the period when the Star Tracker was actively tracking a star. Second, an algorithm was developed which expressed the change to the roll reference angle between successive Star Tracker updates as a function of those sources and time. Third, telemetry data from the time interval DAY 114 through DAY 125 was reduced. Two techniques for reconstructing the roll reference angle were used in conjunction with the telemetered data and were validated for automated processing of telemetry tapes. Fourth, costs were estimated for designing computer programs and for processing Skylab mission telemetry tapes to satisfy the requirement.

As a result of the analysis to identify sources of error in the roll reference angle calculations, STAC developed a modification to the Flight Program that would update both orbital plane error angle and roll reference angle with the effects of orbital procession and momentum desaturation. This modification increased the crew's capability to point to the same solar positions on successive orbits.

4. Random Reacquisition.

a. Description. A Random Reacquisition maneuver capability was provided in the ATMDC software. This capability permitted reacquisition of the sunline by the Acquisition Sun Sensor from any random vehicle attitude.

b. Mission Operations. The Random Reacquisition maneuver was not used during the mission. Acquisition of the sun by Attitude Hold Maneuver was accomplished from random vehicle attitudes during SL-1. Thermal and solar panel data were used to find the approximate vehicle attitude.

c. Conclusions and Recommendations. The random reacquisition capability was not needed. This provision is not required on future long-duration spacecraft. Simple sensors located stragegically would provide all the needed vehicle attitude information.

B. Attitude Control

After orbital insertion the TACS under Saturn V Instrument Unit (IU) control maintained attitude control. IU/TACS was used during the following events:

Separation of the S-II stage from the SWS

Maneuver to gravity gradient attitude for Payload Shroud jettison

Payload Shroud jettison

ATM deployment

Maneuver to and hold Solar Inertial attitude prior to CMG spin-up

ATM and OWS Solar Array deployment

CMG spin-up

During CMG spin-up, control was switched to the ATMDC and attitude control and maneuver capability was provided by the ACS for the duration of the mission.

The ACS operated in two control modes: CMG/TACS and TACS only. Selection of the controlling mode was determined by the status of the CMG and TACS ENABLE/INHIBIT switches, DAS/DCS commands and the active APCS functional mode. CMG/TACS was the primary control mode, in which the CMGs actively controlled the vehicle and TACS provided assistance only in the event of CMG saturation. Automatic selection of TACS only from CMG/TACS would occur if the attitude error about any axis exceeded 20 degrees.

1. Control Moment Gyro Control.

a. Description. Three vehicle mounted doubled gimballed CMGs were used as momentum exchange devices for maintaining vehicle attitude. The underlying principle of momentum exchange is the conservation of momentum. The total Skylab system momentum was made up of vehicle momentum plus CMG momentum and constrained such that the change in vehicle momentum was equal to zero. Any transient change in vehicle momentum due to external torques (i.e., gravity gradient or venting torques) was compensated for by an equal and opposite change in CMG momentum.

To compensate for an external torque, a restoring torque was generated by the CMG system. This was accomplished by rate commanding a change in direction of the three CMG spin vectors. The rate commands to the CMG gimbals were computed in the ATMDC as part of the CMG Control Law.

As long as the CMGs were capable of maintaining the attitude error within specific limits, all control was delegated to the CMG system. If the attitude error exceeded the limits, the CMGs were caged to a nominal momentum profile and the TACS was placed in complete control of the vehicle. Normally, while under CMG control TACS would also assist the CMGs when the system momentum approached saturation. The CMG momentum status was monitored by the flight program through the CMG direction cosines resolvers and was utilized with the vehicle rates to calculate system momentum. When a vehicle maneuver was required the CMG gimbals were rate commanded, changing the CMG momentum. This caused the vehicle to maneuver in keeping with the conservation of momentum.

A simplified functional diagram of the CMG Control Subsystem is shown in figure 15.

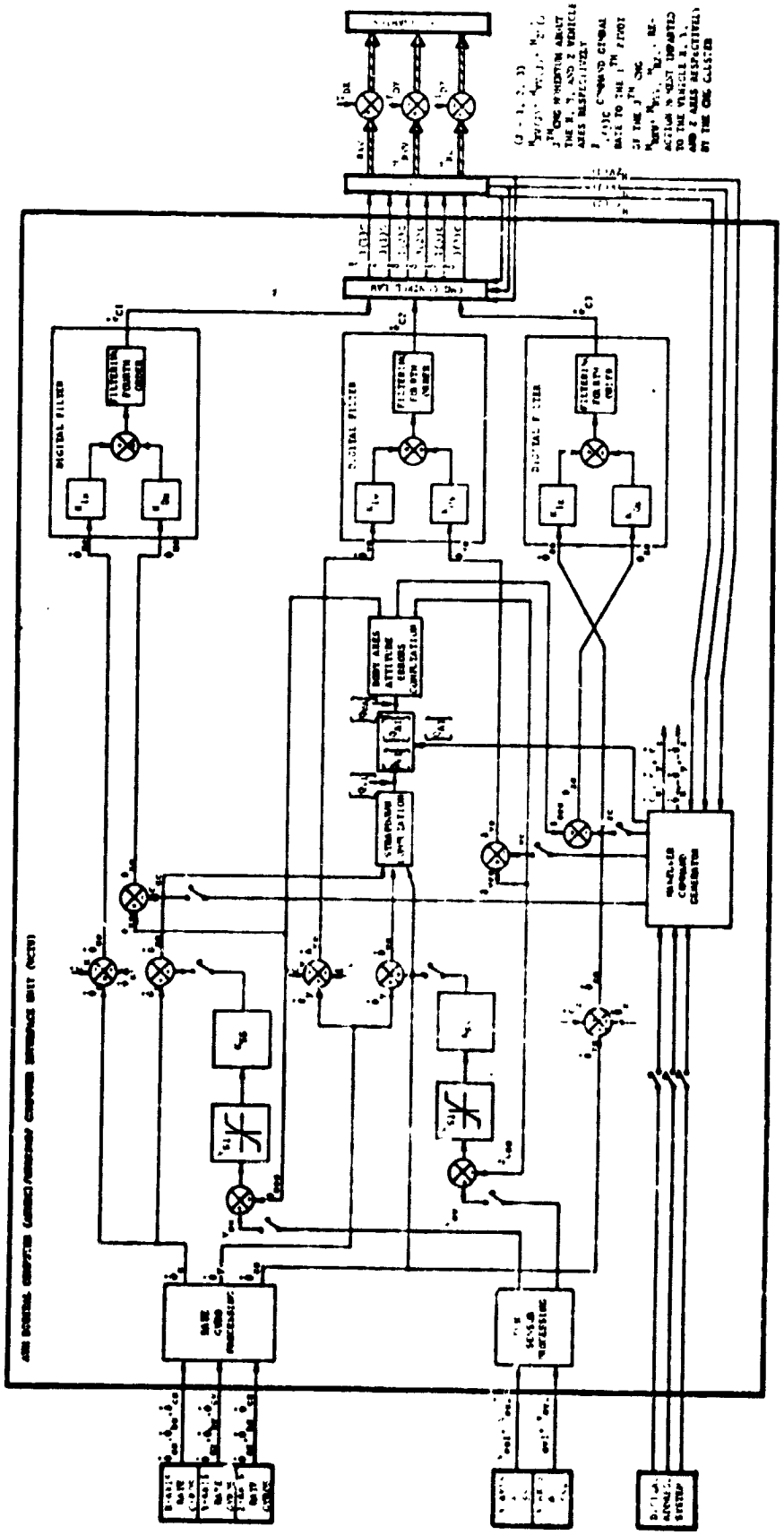

Figure 15. CMG Control Subsystem Functional Block Diagram

The attitude errors for the CMG Control Law were derived from the strapdown reference. The attitude rate errors were determined from the difference in the actual measured vehicle rates and the commanded rates. The error commands for the Control Law were obtained by combining the attitude errors and the attitude rate errors, and modifying them with appropriate gains. The X, Y, and Z-axis attitude errors were magnitude limited. The error commands were also limited and scaled to insure the commanded torque direction was maintained if the maximum CMG gimbal rate capabilities were exceeded.

(1) Digital Bending Filters. The bending filters for the CMG vehicle loop were used to damp bending modes that are inherent in the vehicle and to provide adequate stabilization and pointing. These bending modes, which are due to structural flexibility of the vehicle, may interact with the vehicle control system to produce instability. The dominant flexible body modes resulted from the ATM deployment arm mechanization.

The design approach was to stabilize all bending by attenuation, but with a sufficient high control gain to meet pointing requirements. The filtering of the flexible body effects allowed only the rigid motion of the vehicle as in input into the CMG Control Law. The bending filters were instrumented in the ATMDC and were composed, for each axis, of three cascaded second order linear difference equations. The numerical values for the coefficients gain and scale factors are given in Reference 1. Different scaling coefficients were used for the CSM docked and undocked cases.

(2) Pointing Accuracy. While in the Solar Inertial attitude, the CMG/TACS was required to provide a pointing accuracy of $\pm$ 6 arc-minutes about the X and Y-axis and $\pm$ 10 arc-minutes about the Z-axis. The pointing stability requirements were $\pm$ 9 arc-minutes for 15 minutes of time about the X and Y-axis and 7.5 arc-minutes per 15 minutes of time about the Z-axis.

(3) CMG Control Law. The CMG Control Law used three normalized commands (derived from the strapdown computation) and the present orientation of the CMG spin Vectors (from the gimbal mounted resolvers) to generate six gimbal rate commands. The CMG Control Law solutions were computed five times per second. The law took advantage of the six degrees of freedom of the CMG system to generate gimbal rate commands that caused uncoupled torques to be imparted on the vehicle when required. Thus the gimbal commands were steered in such a way that (assuming that the actual gimbal rates are equal to the commanded gimbal rates) the torques resulting

on the vehicle were identical to the desired torques in direction and magnitude. Only when the maximum gimbal rate capability was exceeded, would the magnitude of the resulting torque be less, but the direction would still be that of the command.

The Steering Law drove the spin vectors to provide the desired torques in direction and magnitude. The CMGs participated in pairs: pair A was composed of CMGs 1 and 2; pair B was composed of CMGs 2 and 3; and CMGs 3 and 1 formed pair C. Each CMG was therefore participating in two pairs, and the resulting angular velocity commands were combined. Each vector pair generated a control torque, and the demand on each pair was scaled according to the individual torquing capability of each pair, while maintaining the desired total control torque. Each vector pair handled its share of the command by splitting it into two components: one, along their sum; and, another, perpendicular to their sum. The first component was adjusted by a scissoring action of the two CMG vectors with respect to each other; the second component was adjusted by a rotation of the pair as a unit.

The Rotation Law attempted to minimize the probability of contact with the gimbal stops by reducing the largest gimbal angles. This was accomplished by rotations about the vector sums only, and thus the total angular momentum was unaffected, i.e., there was no torque exerted on the vehicle from the Rotation Law.

The last portion of the CMG Control Laws made use of an equation that generally described the inner and outer gimbal boundaries. By proper scaling, a pseudo gimbal boundary could be mathematically implemented such that the intersection point of the inner and outer gimbal boundaries was rounded. If a spin vector approached the pseudo boundary, the law would deflect it away without it ricocheting against gimbal stops, as it would were the law not a part of the CMG Control Law and the actual hard stops were impacted.

The gimbal rate commands generated by each law were derived from the angular velocity commands and adjustments were calculated to drive the outer gimbal of each CMG away from its stops whenever both gimbals for that CMG were near their gimbal stops. All of the gimbal rate commands were checked, and if any command exceeded current limits, all of the commands were reduced proportionally to assure that all of the commands were within the limits. This was necessary to maintain the desired torque direction and avoid cross-coupling.

If one of the CMGs failed, the APCS was required to maintain attitude control using two CMGs. This situation

modified the Control Law in that the momentum of each of the remaining CMGs would then operate about some momentum bias value (as seen in vehicle axis momentum profiles), whereas with three CMG operation, each CMG operated without bias. This bias momentum varied with; solar elevation; CMG configuration; proposed minimum TACS usage, etc., and was updatable by DAS/DCS.

A reset routine was incorporated into the CMG Control Law to allow the CMG system to recover from undesirable gimbal angle positions and/or momentum configurations. This routine was primarily added to aid a two CMG operational situation, though it will function with three CMGs when the appropriate conditions exist. A reset was to be executed if the vehicle was in either the SI mode or the EXP PTG mode and one of the following conditions was satisfied: requested via a DAS/DCS command; total attitude error greater than 5.7 degrees with a CMG gimbal on a mechanical stop.

At the initiation of the reset routine, TACS was inhibited and the CMG would be commanded to the spin up configuration, i.e., inner gimbals at 0 degrees and outer gimbals at 45 degrees. At 60 seconds after initiation, the CMGs were commanded to a nominal momentum value for the orbital position. At 100 seconds after initiation, TACS would be enabled to reduce the attitude rate error to less than 0.01 degrees per second in the Y-axis and less than 0.02 degrees per second in the X and Z-axes, while the CMGs were held at the nominal momentum value. At 160 seconds, the CMG/TACS operating configuration was enabled to reduce any accumulated attitude error to zero.

The ATMDC monitored the performance of the CMG outer gimbal movements with respect to the desired torque vector and the attitude error and drove the gimbals to more desirable positions when necessary to complete SWS maneuvers. This is called the Outer Gimbal Drive. While the details of the logic utilizing the Outer Gimbal Drive were complicated, three conditions must always be present. These were:

Outer gimbal within 90 degrees of its stop

Torque command driving gimbal into stop

Be within first or last 60 seconds of a maneuver

Outer Gimbal Drive was available under a modified set of logic conditions while the vehicle was in Z-LV attitude. See Reference A.1., for complete details.

The rate commands to that CMG were then issued to drive the CMG to the opposite side of the outer gimbal stop where it could again generate a useful control torque. During this period of open loop commands, attitude errors were allowed to build up.

b. Design and Verification History.

(1) Bending Mode Filters. The compensation filters for the Wet Workshop configuration were designed and implemented as analog filters. After conversion to the Dry Workshop concept the filters were implemented digitally in the ATMDC.

The structural dynamic characteristics of the Skylab vehicle were simulated by a mathematical structural model from which the flexible body mode, slopes, deflections, and frequencies were generated. Also included in the model was the weight and mass distributions for both the SWS with and without the docked CSM. As the evolution of the Skylab vehicle changed, so did the structural dynamics. Each of the configurations and mass distribution changes, required generating a complete new set of structural data and updating the structural model. Because of uncertainties in the mathematical model and structural testing, tolerances were then specified for each of the flexible body modes.

The structural dynamic characteristics dictated the design of the digital compensation filters. The frequency range of modes considered for the design of the digital filters was from 0.188 to 1.6 Hz.

The CMG/TACS control system consisted of both a rate and altitude feedback loop the sum of which was used as input into the compensation filters. To insure rigid body stability in terms of phase and gain margins, a gain had to be determined for each of the rate and attitude loops. These gains established the rigid body control system bandwidth. Also included in the control loop were configuration compensation gains which were required to compensate for the change in the Skylab configurations from docked to undocked CSM. The change in the compensation gains are approximately the ratio of the inertia of each axis for the undocked CSM configuration to that of the docked.

With the control system gains determined and the structural modes defined, compensation filters were designed. The design of the filters was such that the rigid body phase and gain margins and control system frequency were maintained but at the same time attenuated the dominant flexible body modes. The digital compensation filter design was then verified, using the tolerance structural data for each configuration with its respective configuration compensation gain. The compensation filter design

underwent extensive analysis and simulation verification. In the process of designing the filters, and in conjunction with the structural data, it was determined that the dominant flexible body modes for either configuration consisted of an 0.8 Hz for the X and Z-axes, and a 1.5 Hz for the Y-axis. These frequencies were to be seen corrupting the ATM Rack Rate Gyro signals during the entire mission.

The simulation verifications were conducted in the HSL using both software and/or hardware in the control loops. (References 2, 3, 4, and 5 are summaries of the design and analysis verifications). These simulations consisted of system-level verification in the area of dynamics and control. Dynamics verification of the various phases of the Flight Program included Nyquist stability checks and studying the effects of disturbances and parameter variations. The purpose of the verification activities was to verify that the control system would perform satisfactorily with the flight hardware and models of the flight vehicle. Anomalies attributable to the Flight Programs, found during the dynamics verification, were corrected, or program notes were written. The dynamics verification on the Final Flight Program deemed it flight-worthy in the area of dynamics and control.

(2) CMG Control Law. The first Control Law under investigation converted moment commands to CMG gimbal rate commands. The law was deficient in that for some regions of CMG gimbal angles, the primary axes moments were reduced but the cross-coupling moments were increased significantly. One of these regions was when all inner gimbals were zero and all outer gimbals are minus 45 degrees.

The Cross-Product Steering Law was an alternate Control Law. To nullify a disturbance torque, the H-vector of each CMG was commanded to move into the direction of the disturbance torque. While both of these laws basically were designed to do this, the Cross-Product Law included the sine functions of the inner gimbal angles to reduce the cross-coupling effects. If used directly to control the CMG cluster, the Steering Law would still fall short of the control goals; an invariant forward gain with a minimization of cross-coupling torques.

The H-vector Control Law which was developed was a closed loop controller. This law, when used with the Cross-Product Steering Law, provides an almost optimal CMG cluster control law. The ideal control law implies that the torque obtained from the CMG cluster must be identical with the commanded torque to the CMG cluster. The H-vector Control Law scales a vector to be a commanded torque. This vector is based on vehicle body sensor information and

thus indicates the direction of the disturbance moment. The commanded torque vector is then electronically integrated and compared to the angular momentum of the CMG cluster. The error momentum vector is then nulled by driving the six CMG gimbal angles with the aid of the Steering Law.

Using the H-vector Control Law and its associated Cross-Product Steering Law, the CMG gimbal angles required to produce a given total momentum vector were not uniquely defined. A highly undesirable momentum distribution could develop where two of the three individual angular momentum vectors are parallel and the third is antiparallel, or 1H. For this antiparallel orientation, the CMG cluster exhibits zero gain along the axis of colinearity. Thus, even though the CMGs were not saturated they would not be able to compensate for a disturbance along that axis. Studies were then started on the development of an Isogonal Distribution and Rotation Law.

It had been shown that for any given total angular momentum vector, it is desirable to place the three individual spin vectors into an orientation in which each contributes an equal component along the total vector. This constraint results in equal angles between the actual vectors and the total, i.e., an isogonal distribution. The H-vector Control Law utilized only three of the available six degrees of freedom; the isogonal distribution used two of the remaining three degrees of freedom. Rotation of the individual angular momentum vectors about the total angular momentum used the remaining degree of freedom. This Rotation Law minimized impact of the CMGs inner gimbal stops. The Isogonal Distribution and Rotation Law not only eliminated any antiparallel condition, but also extended the bandwidth of the direct gain and reduced the cross-coupling torque.

At the time of the change from the Wet to Dry Workshop concept, it was apparent that the avoidance of outer gimbal stops and the switch to 2-CMG control in the case of a failure required too much logic for an analog computer and CMG control was inserted into the ATMDC.

The original requirements for CMG control definition for the Dry Workshop ATMDC indicated that the commands to the CMGs were to come from one of two sources: the first being the output of a digital filter whose input was composed of a proportional attitude plus rate feedback parameter (CMG control enabled), the second being the scaled difference between the CMG momentum state and a calculated desired momentum state (caged operation). Regardless of the command source, control logic was then entered to prevent gimbal rate limit cycling when a saturated momentum state

was reached. The function of the CMG Control Law was to take the torque command vector and produce CMG gimbal rate commands. The initial form of the Control Law was conceptually broken down into the following five portions:

Steering Law. Using vector pairing exclusively (three pairing combinations from the three CMGs), the Steering Law equations defined the individual momentum vector rotational rates that would produce an exact torque on the vehicle equal to the commanded torque.

Distribution Law. The Distribution Law attempted to equally distribute the CMG momentum vectors along the orbit nominal. The effect was to reduce the angular velocity required of the momentum vectors to meet the needed momentum change.

Rotation Law. The Rotation Law utilized rotations about CMG pair sums so that the total angular momentum was not disturbed. The purpose was to generate the angular rotations such that the largest gimbal angles are reduced.

CMG Re-distribution Maneuver. Used in conjunction with the Distribution Law, this logic would force a right or left-handed distribution depending on which was preferred.

Gimbal Angle Rate Commands and Limiting. This function provided the transformation of angular rate vectors into gimbal rate commands and provided a proportional scale if the capability of the CMG servo loops was exceeded. In addition, logic for generating outer gimbal rate commands for avoiding the position stops, if both inner and outer were sufficiently close to the stops, was present.

Subsequently the CMG Control Law was subjected to extensive analysis. Two points were key to the investigation: 1) requirements were exceeding computer core capacity, and 2) performance of system with a CMG gimbal on a position stop was marginal. Therefore, the following changes were made:

Saturation control logic, distribution law and CMG redistribution maneuver were deleted as analysis showed small performance gain, core usage was large.

New logic was developed for computing gimbal rate commands when the gimbal was on a stop. Function of logic was to provide a smooth transition of gimbal around stop without significant attitude perturbation.

Upon recognition of the severity of the control problems that could ensue if gimbal stops were encountered, the CMG Reset Routine was developed.

TACS definition allowed firing the TACS thrusters based on vehicle state information and at the same time firing a thruster based on CMG momentum. Regions of incompatibility between TACS and CMG control phase planes were identified and adjustments were made to prohibit the CMG system from attempting to develop torques in opposition to those developed by the TACS.

The desire to cut core requirements and lessen the impact of gimbal stop encounters, was still most important. Numerous memory saving changes were made which were shown to have little or no effect on system performance. The Reset Routine was further refined in order to make it more generally applicable. However, deficiencies in maneuvering and the TACS desaturation firing scheme instigated major changes. These were:

The CMG/TACS incompatibility logic was removed. This was possible due to the decision to eliminate having both TACS and CMG control active at the same time. This eliminated the concept of nested control and was a key factor in designing a maneuver scheme that made efficient use of TACS.

The Outer Gimbal Drive Logic (OGDL) for CMG gimbal angle management during maneuvers was added. With the new CMG/TACS utilization philosophy and the concept of a closed loop maneuver scheme (continuous checking of present position versus desired position), it became feasible to allow a momentary attitude perturbation in order to force a desirable gimbal angle position. Therefore, logic was added that predicted the polarity of outer gimbal angle required in order to allow the momentum swing required during maneuvers. If it was

sensed that the gimbal was moving in a direction opposite to the desired one, an open loop drive was executed to force the proper polarity.

The generation of control torque commands during maneuvers was made to be a function of rate error only. This change provided a significant performance improvement. By utilizing rate only control, the momentum vector would always attempt to align along the maneuver eigen-axis. This resulted in a clear decision as to where the OGDL should place the outer gimbal and in addition would result in constant maneuver rates. Constant maneuver rates were preferred by the crew.

There were basically no conceptual changes in CMG control in the final ATMDC Program. The design activity concentrated on optimizing the existing system and insuring that all nominal and reasonable off-nominal conditions could be handled efficiently. The following changes resulted from the activity and represented the last major updates to CMG control:

The rate ledges were given dual values. One set for when GG dump was in progress and the other for all other times. This was done in order to lower the rate ledge for nominal use. Analysis of design verification simulations indicated that if attitude transients did occur (such as the completion of a maneuver) the probability of hitting a stop in recovery was proportional to the amount of momentum change that occurred in the CMGs. Lowering the rate ledges was a technique that limited the momentum change allowed. Higher rate ledges were required during GG dump because of the manner in which the dump maneuver was executed. As the maneuvers were commanded as an attitude ramp, a rate ledge lower than the ramp slope would have interfaced with the execution of the maneuver. Therefore, the rate ledges during dump had to be set higher than the expected worse case rates during dump maneuvers.

The modified outer Gimbal Drive Logic was added. This logic was similar to the previously mentioned OGDL and was operational during the Z-LV Mode. This resulted from

certain 2-CMG rendezvous Z-LV simulations in which the required two orbits of Z-LV could not be maintained without gimbal stop encounters.

The CMG Control Law underwent extensive analysis and simulation under varied conditions. The actual ATMDC Flight Program version of the Control Law then was verified, also, under varied conditions. For a summary of design analysis and verification, see Reference 2.

c. Mission Operations

(1) Bending Mode Filters. During the mission, the ACS met the necessary stability and pointing accuracy. Extensive analyses were carried on to evaluate the system performance. Using telemetry data, various parameters were analyzed and, where possible, compared to premission simulation results. Also, certain mission time periods were run on simulators using actual telemetry data for initialization. References 6-10 include the results of the APCS data acquisition and evaluation studies for all Skylab missions.

The comparisons of flight data with preflight simulations demonstrated that the performance of the ACS was reasonably close to expectation. However, there were some deviations from predicted performance. These deviations resulted primarily from the difference in mass properties due to the missing solar panel and meteoroid shield, and the anomalous behavior of the Rate Gyros. The telemetry data exhibited structural dynamic characteristics somewhat different than preflight predictions. The premission structural data did not disclose some flexible body modes which were discovered in the early flight data analysis. The structural model program was subsequently reevaluated and modified. Once this was done the model reproduced the flight modes.

The unexpected bending modes were first observed on DAY 16 when the SPC spar was rolled at the high (7.5 deg/sec) rate. Frequencies of 0.8 Hz on the X and Z-axes and 1.5 Hz on the Y-axis were the dominant modes seen and were associated with the ATM supporting structure. The Z Rack Rate Gyros saw rates of about $\pm$ 0.1 degrees per second dur to the transients. This caused concern that gyro gain switching might occur as a result of the SPC roll operations. Subsequently, the crews were requested not to use the 7.5 degrees per second roll rate. The

0.8 and 1.5 Hz modes were observed throughout the mission, but at generally lower levels. EPC roll and spar caging operation were the primary means of exciting the bending modes. However, on DAY 237, a combination of roll and MPC operations excited the 0.8 Hz frequency enough to cause gain switching of the Six-Pack Rate Gyros.

There were other occurrences of unexpected or high level bending mode excitation. On DAY 19, crew motion (foot race) around the water tanks set up low frequency (approximately 0.1 Hz) oscillations with peak rates of 0.025 to 0.035 degrees per second on the X and Y-axes. Z-axis amplitude was about $\pm$ 0.012 degrees per second. Other bending mode frequencies were seen riding on the 0.1 Hz oscillation. The low frequency oscillation, which was near the rigid body natural frequency, allowed large amplitude attitude excursions.

An oscillation seen only on the Y-axis was observed several times during the mission. The oscillation was not of sufficient magnitude to cause any difficulties. Studies indicated that the frequency of 0.5 Hz, beating with a rigid body oscillation of about 0.025 Hz, could be set up by ergometer operation, ATM operations and momentum dump maneuvers.

On DAYS 201 and 220, "klunk" sounds were heard in the CSM which seemed to have originated in the vicinity of the ATM and were transmitted through the structure. Data analysis indicated that a number of bending modes were set up on on both occasions. However, the magnitude of the Rack Rate Gyro responses were much lower for DAY 201 than DAY 220 and the DAY 220 disturbance was continuous while three distinct periodic disturbances were seen on DAY 201. Also, a 5 Hz oscillation seen on DAY 201 was not present on DAY 220. No causes could be determined.

Throughout these transient disturbances, and in normal operations, the Bending Mode Filters functioned as designed, removing almost all of the flexible body effects from the Rate Gyro outpups before the CMG gimbal rate commands were computed. This was demonstrated by the absence of oscillations of bending mode frequencies on the CMG gimbals.

(2) Pointing Accuracy. As a result of the DAY 19 crew motion around the water lockers, a low frequency oscillation was set up which allowed attitude excursions in excess of 10 arc-min on X and Z-axes. The excursions exceeded the X and Z-pointing requirements by 4.8 and 0.8 arc-min, respectively. Consequently, the crew was requested not to use this exercise mode.

On DAY 194, six days into the SL-4 mission, CMG No. 1 was declared failed and turned off. From this point the CMG control subsystem functioned with the two remaining CMGs. An analysis was performed to compare 2 CMG and 3 CMG control pointing accuracy. The pointing accuracy was found to be very much the same. The X-axis rates did appear to be slightly higher in the 2 CMG control case.

A procedure was developed to improve the pointing in a near-Solar Inertial Attitude by utilizing the Solar Inertial computation accuracy. This is summarized in Section VI.A.

As requirements for Kohoutek evolved, special interest focused on ACS pointing. To determine the pointing accuracy of the CMG control subsystem a test was performed on DAY 119. The test was performed by placing S052 experiment near the sun center, with the canister caged, using a Solar Inertial bias (X = 0, 4 = 0.1 deg, Z = 0) command. A star was acquired by the Star Tracker and the attitude hold mode was selected. The pointing accuracy data obtained from the test during a 25 minute period is summarized in Table 7. The numbers fall well within the pointing requirements for the CMG control subsystem.

Table 7. Measured Pointing Accuracy Data

Vehicle Axis	Total Excursions	Strapdown Drift	Worst-Case Limit Cycle
X	2.8 arc min p-p	1.8 arc min	1.2 arc min p-p
Y	0.9 arc min p-p	0.5 arc min	0.9 arc min p-p
Z	1.5 arc min p-p	0.5 arc min	1.0 arc min p-p

(3) CMG Control Law. During the mission the CMG Steering Law performed as designed including switching to 2-CMG operation after failure of CMG No. 1. However, the requirements of 2-CMG operation dictated that momentum bias values were continuously uplinked to the ATMDC as a function of solar elevation. This prevented gimbal stop encounters and antiparallel CMGs. Table 8 is a list of momentum bias values uplinked for normal 2-CMG control. Some special biases uplinked for maneuvers are not included.

The CMG Rotation Law worked as designed. However, a refinement involving rotation about the total momentum vector in the 3-CMG case, was omitted from the ATMDC in order to save memory. This rotation would have helped avoid gimbal stops. In the 2-CMG case, a gain change in the Rotation Law would also have helped avoid gimbal stops.

Table 8. CMG Momentum Bias History

DAY	TIME (H:M:S)	BIAS (%3H)		
		X	Y	Z
194	08:56:00	-13	20	0
194	18:19:29	-13	13	0
198	07:36:45	-11	8	0
201	19:43:06	-11	-4	-9
208	04:57:23	-17	0	-7
211	08:41:42	-15	2	-5
213	08:05:00	-13	4	-2
217	08:18:00	-16	4	-2
218	17:06:18	-11	6	0
219	13:15:00	-16	4	-2
220	12:31:23	-20	6	2
220	16:09:33	-16	4	-2
222	09:01:47	-20	6	-6
223	03:36:22	-16	4	-2
224	16:46:40	-20	6	-6
224	21:41:52	-16	4	-2
225	15:48:11	-20	6	-6
225	21:39:11	-15	2	-5
226	20:13:01	0	2	-5
227	00:52:16	-15	2	-5
234	12:32:07	-7	-13	-9
235	01:27:13	-11	-4	-9
235	23:06:06	-14	4	-4
243	00:45:05	-11	11	0
243	09:31:42	-17	7	0
243	18:36:20	-11	11	0
244	10:11:01	-17	7	0
244	17:53:22	-11	11	0
245	07:52:22	-17	7	0
246	18:34:45	-11	11	0
250	16:50:37	-17	7	0
250	23:56:14	-11	11	0
251	16:27:28	-11	7	0
251	23:06:29	-11	11	0
252	07:58:48	-17	7	0
253	06:16:00	-11	7	0
256	21:35:46	-11	1	-5
257	04:16:20	-4	-9	3
261	23:56:17	-11	54	4
262	01:23:46	-19	-4	-9
262	03:00:57	-15	-4	-9
262	04:49:08	-11	-4	-9
263	06:37:52	-11	2	-5

The outer gimbal drive and modified outer gimbal drive were designed to prevent a CMG from driving into an outer gimbal stop during maneuvers. They were primarily utilized in 2-CMG operation and functioned well. Additional availability of an outer gimbal drive logic at the end of maneuver in the presence of large attitude errors would also have been desirable several times in the mission in preventing a switch to "TACS Only" Mode.

The gimbal angle reset routine was developed specifically for the purpose of recovering from CMG gimbal-on-stop situations and was automatically initiated in the ATMDC Flight Program when this problem occurred. During the mission, this recovery capability was proven workable and essential to the control of the SWS by the CMG control subsystem. It was automatically initiated several times during the mission, during both tracking station acquisition and loss.

In addition to the automatic entry, the reset routine can be initiated by ground or crew command. This capability led to an extensive and varied use of the reset routine during the Skylab mission. Below is a description of three additional ways that the reset routine was used:

Dump CMG momentum while in thermal attitude. Thermal attitude refers to a variety of inertial attitudes that were maintained during the first 10 days of the mission to satisfy thermal and power requirements. These attitudes prevented normal gravity gradient desaturation of the CMGs. Therefore, the reset routine was used several times each mission day to desaturate the CMGs.

Force particular momentum profiles. This use was necessitated by the CMG No. 1 failure. Following the failure of CMG No. 1, gimbal stop encounters became more frequent during experiment maneuvers. It became essential to eliminate these encounters because entire experiments and data-taking passes were being cancelled due to attitude divergence from gimbal stop encounters. One method used to minimize these encounters was to force the momentum on to particular trajectories using the reset routine. These trajectories had been shown to be free of gimbal stop encounters by simulation.

Prevent thruster firing during JOP experiment. During some of the JOP experiments, extremely fine pointing of the SWS was desired. This made it mandatory that TACS desaturation firings not occur during the data take. To ensure that no desaturation firings would be needed, the reset routine was employed to initialize the CMG momentum to a desired level at the beginning of the data take.

The reset routine was also required to use a minimum amount of TACS fuel. It was designed to meet this requirement and the design performed well during the mission. However, the use of the reset routine to cage the CMGs to a nominal momentum had several minor problems which were:

Memory savings caused the removal of a more accurate momentum profile from the ATMDC

Removal of residual vehicle rates, following return to CMG control during reset, caused momentum bias

Removal of attitude error, following return to CMG control during reset, could represent a significant vehicle rotation. The subsequent transformation of CMG momentum would then represent a momentum bias.

d. Conclusions

(1) The Bending Mode Filters operated as designed throughout the Skylab missions and successfully removed most flexible body effects from the control loops.

(2) The Skylab ACS maintained the pointing accuracy and stability requirements, with minor exceptions, for the entire mission.

(3) Skylab proved the feasibility and desirability of CMG control. CMG control concepts worked as designed for both stabilization and maneuvering.

(4) The absence of CMG outer gimbal stops would have significantly simplified the control software and prevented many periods of attitude excursions.

(5) Greater CMG momentum would have reduced TACS propellant consumption, particularly during 2-CMG operation.

(6) Inclusions of a more accurate CMG momentum profile would have improved performance during CMG resets.

2. TACS Control

a. Description. The TACS was composed of six cold gas thrusters and the necessary logic to select and fire the proper thruster. The TACS Control Law provided thruster firing commands to null out attitude and rate errors when control dead-bands were exceeded. The thrusters were mounted on the OWS as shown in figure 3. Two thrusters provided uncoupled Y-axis control and four thrusters provided X and Z-axis control. Two types of thruster firings were commanded; full-on and minimum impulse bit (MIB). For full-on firings the selected thruster was fired continuously for one second. The MIB firing time was selectable from 40 to 400 milliseconds to compensate for pressure decrease in the TACS cold gas supply tanks. At the beginning of the mission a thruster produced 463 Newtons of thrust. This decreased to approximately 42 Newtons at the end of the mission. The value of a MIB stayed approximately constant during the mission.

A TACS firing was capable of exciting structural frequencies. To remove the corrupting flexible body effects on the rate signals and to minimize TACS usage bending mode filters were used. The filters for each control axis were composed of a second order linear difference equation. The numerical values for the coefficient gains and scale factors are given in Reference 1.

After initial transfer to ATMDC control, TACS was used for three functions during the mission.

(1) TACS Only Control. TACS Only attitude control could be initiated in two ways. These were:

Commanded

Absolute actitude error greater than 20 degrees in any axis.

MIB and full-on firings in TACS only were generated by a weighted sum of position and rate errors. If this sum exceeded the control law modulation region, a full-on of one second is commanded. A rate ledge to limit the turning rate of the vehicle is implemented by limiting the attitude error used in the control equations. In TACS only mode, the position deadband was 3 degrees,

2 degrees, 2 degrees for X, Y, Z, respectively. Shown in figure 16 is an uncoupled phase plane representation of the TACS Only control Law.

(2) System Momentum Desaturation. The TACS was used to desaturate the CMGs when the system momentum exceeded 0.96 of CMG system capability. A single thruster was fired to reduce the momentum about the axis of maximum accumulation. Single or multiple MIBs were fired depending upon the level of saturation.

(3) CMG Reset Routine. During the CMG reset routine the TACS was used to reduce the rate error generated in initializing and caging the CMGs. (See Section VI.B). The CMG/TACS control mode was then reentered to reduce any accumulated attitude error. During a CMG reset, TACS Only was selected if the absolute attitude error was greater than 60 degrees in any axis.

b. History. In the original Orbital Workshop (OWS) control system the Workshop Attitude Control System (WACS) was the primary controller except during that portion of the mission when the ATM was docked to the OWS radial port. The WACS consisted of six (22 pound) redundant hot gas engines, spatial amplifiers, horizon sensors, sun sensors, rate gyros and control logic. This control system was active also during launch and orbital insertion as well as during the OWS mission.

When the OWS was replaced by the Saturn Workshop (SWS) several major changes were made to the attitude control system. The rack mounted CMGs became the primary controller operating with the Thruster Attitude Control System (TACS) configures in a nested system. The six redundant hot gas engines were replaced with six cold-gas thrusters with redundant valves operating from a non-regulated gas supply.

The TACS control requirements were composed of the necessary logic to select and fire the proper thruster. The firing logic could either be triggered from an input based on vehicle state (deadband operation) or from an excessive momentum state magnitude. The logic for thruster selection in either of those two modes remained basically constant throughout the software evolutionary progress. However, the operational aspects of when to use which set of logic was totally changed and these changes were the key to efficient use of TACS impulse.

The early definition stated that the TACS operated in the following manner:

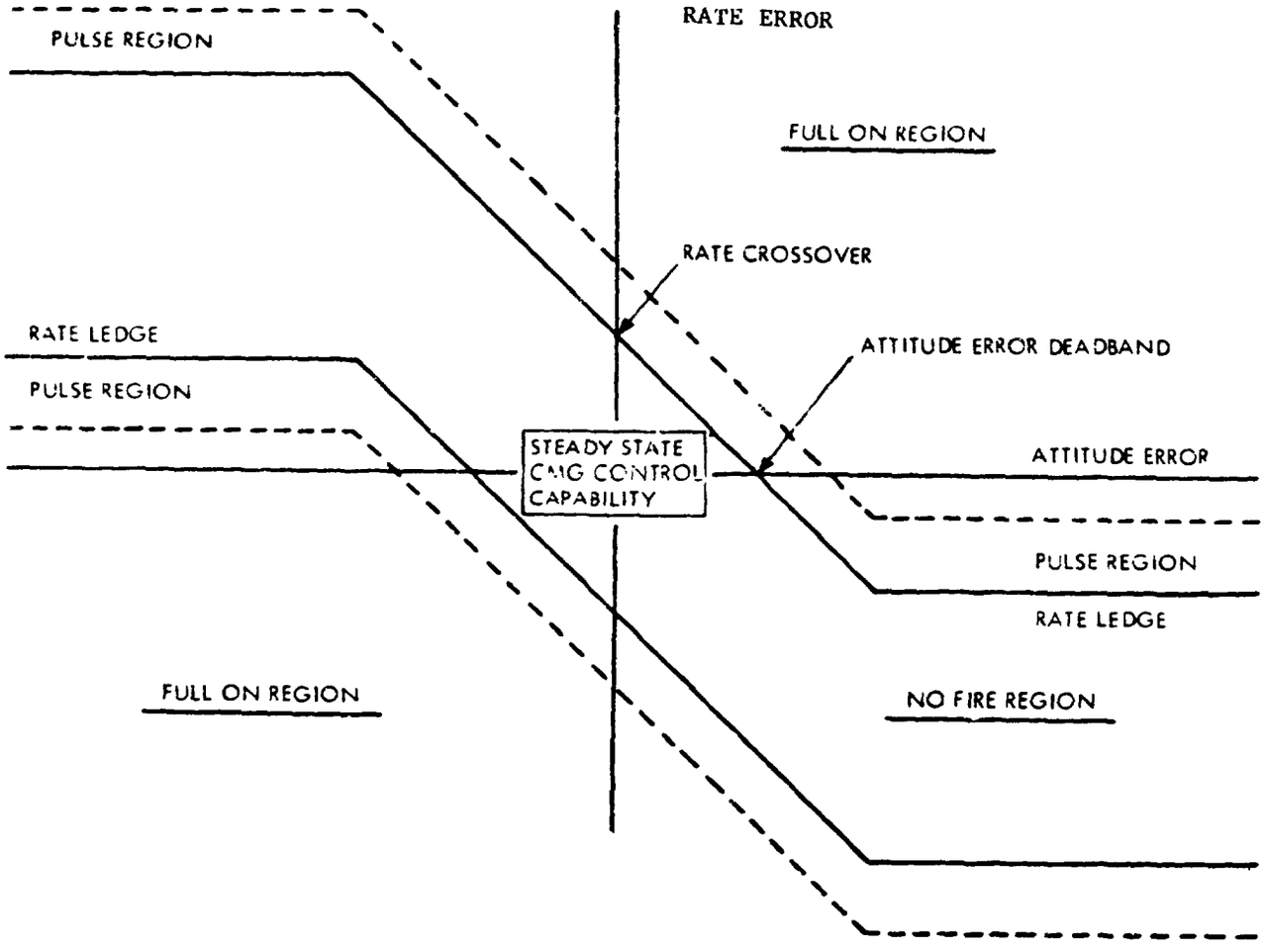

Figure 16. Uncoupled Phase Plane Diagram

Provided attitude control any time the deadbands were exceeded: one degree deadbands if CMG Control was enabled, and five degree deadbands if TACS Only.

Continuously monitored CMG momentum buildup and actuated a thruster when the momentum had reached a preset level. The selected thruster reduced the magnitude of the maximum momentum component.

This was the nested system operation whereby the CMGs were to provide the fine control and the TACS, if needed, would supply coarse control.

Problems with the nested concept began to manifest themselves. Steps were taken to try to alleviate some of these problems. The deadband was set at 20 deg for CMG/TACS control and the TACS desaturation firings were based on saturation of system momentum as opposed to CMG momentum. Moving of the TACS deadband, however, did not solve the real problem of allowing more than one source of error signal to fire the TACS at one time. This was not completely understood until later. The move to command the desaturation firings from system momentum, however, was of paramount significance. This allowed any small attitude disturbance to be removed with no TACS impulse, insured that GG dump would not fire TACS, and provided a means of immediately firing the proper amount of TACS at the initiation of any general purpose maneuver.

Later development led to one important change - that of making the TACS desaturation firing time a function of the system momentum deficiency. By increasing the thruster on time by the time equivalent of one minimum impulse firing for each one-half H of system momentum deficiency, it was guaranteed that, while maneuvering, the vehicle could always keep up with the commanded rate.

Later the nested concept was eliminated. Vehicle attitude was monitored and if it exceeded 20 deg, TACS Only Control with 3, 2, 2 deg deadbands was selected. Under this condition, CMG control was inhibited. This change removed the possibility the CMGs and TACS ever fighting one another. Another change made for the Final Program was the development of a TACS Only Maneuvering Control Mode. This allowed the TACS to execute maneuvers in a rate only mode similar to the CMGs except the TACS operated within a rate threshold. The magnitude of the threshold was set so that the vehicle would be within the normal attitude deadband upon time out of the maneuver. This change was made to eliminate the computation of a commanded attitude parameter used in conjunction with the vehicle-Solar Inertial quaternion for attitude error data.

c. Design Analysis and Verification. Analyses were performed to determine the effects of the flexible body rates on TACS propellant usage and to determine the digital filters which would decrease TACS firing. Simulation verifications were conducted at HSL and are summarized in References 5.

The TACS Control Law underwent extensive analysis and simulation under varied conditions. The actual ATMDC Flight Program version of the Control Law then was verified, also under varied conditions. For a summary of design analysis and verification, see Reference A.2.

d. Mission Operations. The TACS Only Attitude Control worked as designed. Due to the relatively large TACS rate ledge which was designed to protect against a stuck thruster, the automatic switch to TACS Only proved expensive in terms of fuel usage.

e. Conclusions. The TACS control system worked as designed. It demonstrated capability both for stabilization and maneuvering of the vehicle. No significant coupling problems were encountered in those cases where TACS was required only to augment CMG control.

3. Maneuvers.

a. Description. The maneuvering requirements for Skylab dictated two classes of maneuvers, SI offset pointing and general purpose. The general purpose maneuvering scheme was used for Attitude Hold, Z-LV and momentum desaturation maneuvers. The distinguishing factor between these two maneuver classes was the manner in which the control error signal was generated. SI offset pointing was limited to small angles ($\pm$ 4 degrees) about the X and Y-vehicle axes and was accomplished by biasing the attitude error signal with the designed offset angle. The control system command was derived by comparing the desired bias to the strapdown output. This automatically resulted in a rate ledge type closing response and allowed sun sensor update of the strapdown while offset pointing was in progress.

The general purpose maneuver class required maneuvering the vehicle to arbitrary time variant or inertial attitudes and was accomplished via strapdown commands. It can be characterized as a closed-loop maneuver scheme with a constant maneuver rate, the magnitude of which is dependent upon the desired maneuver angle and a predicted time to complete the maneuver. An eigenaxis maneuver was effected by configuring the CMG Control Law in a rate only mode which forced the vehicle angular rate vector to conincide with the maneuver eigenaxis.

As opposed to offset maneuvers large momentum changes in the CMG system was generally required to provide the desired maneuver rates.

The maneuvering scheme generated a desired attitude reference quaternion with respect to SI from the maneuver commands. This quaternion was continuously compared to the vehicle to Solar Inertial quaternion to generate an instantaneous attitude error between present position and desired position. A maneuver time was always specified and decremented as the maneuver progressed. Rate commands were computed by dividing the body axes attitude errors by the maneuver time-to-go parameter. When time-to-go reached 60 sec it was frozen to keep the rate commands orderly.

This type of maneuver scheme was advantageous for CMG gimbal management. With the CMGs operating on rate error alone a constant eigen-axis maneuver rate was generated. This allowed identification of the location of the final CMG momentum vector upon initiation of the maneuver. The final CMG momentum vector would attempt to align along the maneuver eigen-axis. It was therefore possible to design special logic for CMG control for insuring that gimbal stops were missed in achieving that final momentum state. The CMG outer gimbal drive logic for avoiding the stops during maneuvers was an open loop function that could momentarily perturb vehicle attitude. This closed loop scheme made allowances and a higher or lower maneuver rate would appropriately be commanded.

Skylab was required to maneuver as a result of a mode change or in response to an attitude maneuver command in a given mode.

The primary maneuver modes were:

Z-Local Vertical (Z-LV) Mode - The Z-LV attitude is defined as the Z-(geometric) axis pointing along the Local Vertical (positive away from the earth's physical geocenter) and the positive X-(geometric) axis in the orbit plane (in the direction of the velocity vector). The Attitude Pointing and Control System (APCS) was required to hold this attitude within $\pm$ 2 degrees during each Z-LV pass. Skylab was also capable of performing a Z-LV rendezvous maneuver with the negative X-axis in the direction of the velocity vector. In either case, attitude could be maintained for a maximum of two orbits.

Solar Inertial Mode - The Solar Inertial attitude was defined as the X (principal) axis in the orbit plane with the +Z (geometric) axis pointing toward the center of the sun. The +X-axis was in the direction of the velocity vector at orbital noon. Skylab was capable of maneuvering from Z-LV attitude to the Solar Inertial attitude. This would be required following each docking rendezvous and each EREP pass. The capability to bias the Solar Inertial attitude was also required for the purpose of Experiment Pointing.

Attitude Hold Mode - The capability to inertially point Skylab to any desired attitude was available. This, in turn, required a maneuver capability to reach the desired attitude. This capability was necessary because of the probability of experiments regarding stellar pointing and the possibility of emergency maneuvering.

b. History - Following the conversion to Dry Workshop acceptable maneuver concepts underwent major changes. The initial offset pointing maneuver was to be performed by summing a bias with the output of the acquisition sun sensor and an attitude error limit was placed in the summation in order to allow the CMGs to perform the maneuver within the TACS deadband. No update of the strapdown was to be performed if offset pointing was active. This was soon changed to the final scheme described above.

The initial general purpose maneuver scheme, upon initiation of the maneuver, formed an open loop rate profile, drove a maneuver quaternion with the computed rates, and derived attitude errors by comparing the maneuver quaternion with a quaternion representing the current vehicle position. This procedure assumed a level of acceleration capability and ramp up and ramp down times were allotted in the profiles.

It was soon recognized that a new approach to general purpose maneuvering must be found. As these maneuvers would require large CMG momentum swings, gimbal stop encounters were frequent. The result was the vehicle would deviate from the commanded attitude profile and subsequently broach the TACS attitude deadband. This was very costly in TACS impulse as the TACS system often would have to return the vehicle to the commanded attitude via rate ledge operation.

A scheme had to be developed that would allow attitude perturbations while CMG control straightened out the stop problems. A totally new and final maneuvering scheme was therefore devised. This change in conjunction with the changed TACS desaturation firing scheme provided for significant improvements in TACS impulse utilization and CMG system performance. In addition, the new maneuvering scheme required less operational constraints, was easier to command, offered greater flexibility and required less core storage than the previous maneuvering scheme.

c. Mission Operation

(1) Z-LV Mode. The Z-LV mode and, thus, maneuvers to Z-LV attitude were used extensively throughout the Skylab mission. During SL-1, a modified Z-LV attitude was experimented with in an attempt to cool the SWS and meet power requirements. However, use of Attitude Hold maneuvers were used extensively instead. Tables 24, 25, and 26 summarize the EREP passes performed during the mission.

The EREP pass maneuvers, as designed and performed, were based upon many different requirements (TACS fuel, CMG momentum, thermal, power, etc.), the major of which was the experiment data requirement. The most common EREP pass during the Skylab mission was to enter Z-LV attitude just prior to the data take period and return to Solar Inertial attitude at the end of the data take. This was the original maneuver profile design for an EREP pass.

Another EREP maneuver profile that was utilized during SL-4 was called a noon-to-noon pass. The Z-LV mode was entered near orbital noon and exited near the next orbital noon. To avoid momentum accumulation in the Y-axis due to gravity gradient torques, a Z-LV offset attitude was maintained while not in the data take period. This offset attitude was such that the X (principal) axis in the orbit plane and perpendicular to the radius vector to the center of the Earth. This type of pass was used because it minimized TACS fuel usage and CMG gimbal stop encounters.

A Z-LV rendezvous maneuver was never performed during the three rendezvous and docking phases of the Skylab mission. Due to rate gyro, thermal, and power problems, rendezvous and docking, during SL-1, were performed in the thermal attitude. For the remainder of the mission, rendezvous and docking were performed in Solar Inertial attitude.

(2) Solar Inertial Mode. The offset pointing capabilities in the Solar Inertial mode permitted accurate experiment pointing. One design change was uplinked to the ATMDC to meet Kohoutek pointing requirements. This change increased the Solar Inertial

offset command resolution to 0.01 degree and the offset limit from 4 degrees to 5.2 degrees. Previous to this change, the smallest offset that could be commanded was 0.1 degree. Kohoutek pointing requirements, which were defined w ll into the mission, necessitated this change. This design change contributed to the success of the Kohoutek pointing experiments.

The Solar Inertial acquisition maneuver capability functioned properly throughout the mission.

(3) Attitude Hold Mode. Before the mission, the Attitude Hold maneuver capabilities were required, but little use was outlined for them. However, during the mission, these capabilities were used extensively. During SL-1, the continuation of the mission was dependent upon the emergency Attitude Hold mode maneuvering done to cool the SWS. Approximately 55 Attitude Hold maneuvers were performed during SL-1 due to thermal, power, and rate gyro problems.

The number of Attitude Hold Mode maneuvers required to support experiments also increased significantly during the mission. The primary contributor to this was the Kohoutek comet activities defined for SL-4. Approximately 30 Kohoutek comet maneuvers were performed during SL-4 using two CMGs. During the entire mission, approximately 40 other Attitude Hold maneuvers were performed to support various other scientific activities.

d. Conclusions. The maneuvering capabilities of Skylab operated as designed. The ability to maneuver the vehicle in a number of modes allowed great flexibility for both planned experiment operations and observation of targets of opportunity such as Comet Kohoutek. The use of Attitude Hold maneuvers to obtain desirable thermal and power attitudes aided materially in avoiding serious damage to the vehicle during SL-1.

C. Momentum Management

Any noncyclic disturbance torques acting on the vehicle will result in a net momentum buildup of the CMG cluster. Because of the finite storage capacity of the CMG cluster this momentum accumulation will eventually cause CMG saturation and inability to compensate for a disturbance torque about the axis of saturation. Although it is not possible to eliminate the noncyclic torques, techniques are available that can be utilized to minimize them.

Three techniques utilized on Skylab are:

To minimize the noncyclic gravity gradient torques by maintaining the axis of minimum moment of inertia (X-axis) in or near the orbital plane

To minimize the vehicle vent torques by the design of non-propulsive vent hardware

To nullify the saturation effects of the remaining noncyclic disturbance torques by periodically during the night portion of the orbit producing controlled bias torques which tended to desaturate the CMG cluster.

1. Disturbances. Disturbance torque profiles resulting from Skylab vents during the mission were derived from TM data and compared with the predicted preflight vent torque profiles. The four types of vent disturbances primarily considered were:

Experiment M092 - Lower Body Negative Pressure (LBNP)

Airlock depressurization prior to Extra-Vehicular Activities (EVA) including astronaut suit venting during these EVAs

Habitation Area (H/A) Blowndown following the storage periods

Command and Service Module (CSM) vent.

The Waste Tank (W/T) vent was also observed but the largest pressure profile analyzed produced negligible disturbances on the APCS. For additional details on vent torques during the mission, see Reference 9.

a. Lower Body Negative Pressure Experiment Vent.

(1) Experiment Description. The M092 Inflight LBNP experiment is designed to determine the time course of cardiovascular deconditioning during space flight and to provide data for predicting the degree of orthostatic intolerance and impairment of physical capability expected following return to earth's environment. The experiment is conducted by two astronauts; a subject and observer. The subject's lower body is encased in the LBNP device and measurements of the cardiovascular system are recorded while the ambient atmosphere of the LBNP device is vented overboard.

The primary method of identifying the time at which the LBNP vent occurred was to correlate the vent with the Experiment M092 ambient temperature measurement number C7311M092 and the experiment M092 chamber temperature, temperature number C3730M092. These measurements are activated when the astronauts are preparing for the LBNP experiment. The first noticed event is when the data recorder is turned on which also automatically activates the temperature sensors. Part of the sequence in performing the experiment requires calibration of the sensors just prior to and immediately after the experiment.

The LBNP experiment vents that were analyzed and the actual duration of the event is presented in Table 9.

Table 9. Experiment Vents Analyzed

LBNP NO.	MISSION	TIME (DAY:HR:MIN)	DURATION (Sec)	ORBITAL POSITION * (Deg)
4	SL-2	18:21:15	1350	123
17	SL-2	33:16:04	975	246
24	SL-3	81:15:48	910	190
**27	SL-3	86:17:08	UD	232
33	SL-3	94:14:37	1100	206
36	SL-3	98:15:39	970	004
48	SL-3	110:21:16	1100	292
49	SL-3	111:19:17	1120	000
50	SL-3	113:22:30	1090	347
53	SL-3	116:16:05	1170	063
77	SL-4	191:15:40	1190	132
79	SL-4	196:20:40	960	264
85	SL-4	208:21:27	960	211

UD - Undetermined
* - Orbital position in degrees past orbital midnight
** - Not completely analyzed due to lack to TM data.

(2) Predicted Torque Profiles. The predicted torque profiles for this vent were essentially a rectangular pulse with a duration of 600 seconds. Due to the nature of the experiment being performed, this particular vent deviated from the predicted. The extracted torque profiles are compared with the predicted profiles in figure 17. The two curves on each axis represent the maximum and minimum torques imparted to the vehicle for the experiment vents analyzed. It is readily apparent that the loss of the micrometeroid shield changed these profiles considerably from the predicted. Also, the actual vent period was much longer than predicted.

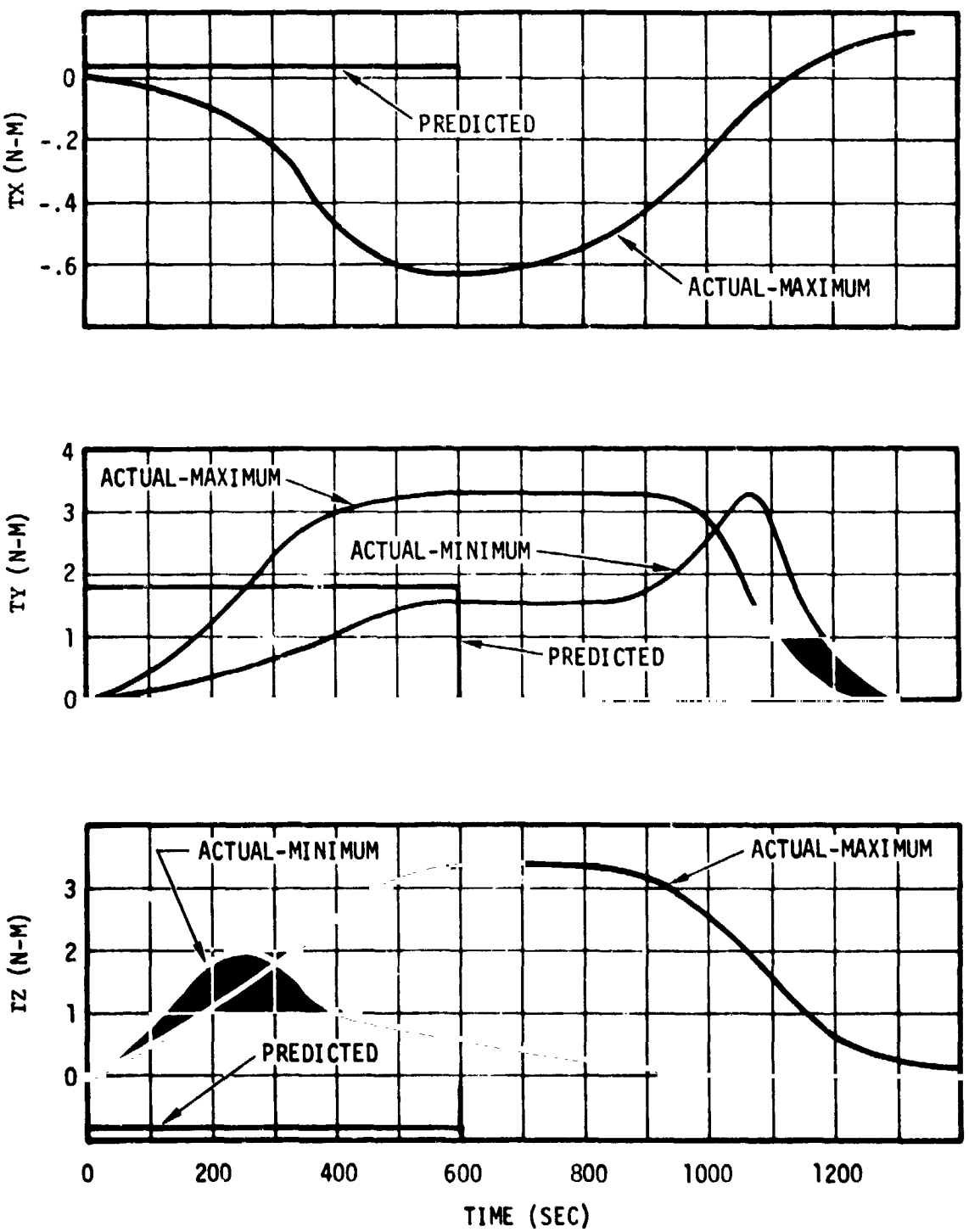

Figure 17. Predicted And Actual LBNP Vent Torque Profiles

(3) Extracted Torque Profiles. The extracted torque profiles vary considerably from each other as well as from the predicted. The individual variations were mainly due to the differences in the time history in which the experiment was performed. Since each time the experiment was performed, the amount of negative pressure applied to the LBNP device was controlled manually by the astronaut, it is unlikely that any two experiments would have the same venting time history. The sign reversal on the X and Z-axis torques from the predicted are apparently due to uncertainties in the impingement coefficients and to the change in mass properties when the micro-meteoroid shield and one solar wing was lost. A composite plot of the extracted torque profile is presented in figure 17.

At the beginning of the SL-4 mission, the astronauts modified the M092 Inflight LBNP experiment vent to be vented into the Orbital Workshop (OWS) waste tank instead of directly overboard. This was done in order to eliminate the disturbance torques acting on the vehicle due to this vent and to preclude the possibility of having any TACS thruster firings. The effect of this modification is that the magnitudes of the LBNP vent torques during these experiments were very low compared with vent torques which occurred before the modification. Hence the modification was successful. As a result, the modification eliminated M092 experiment scheduling constraints imposed by the APCS.

The results of the disturbance torque extraction task as applied to LBNP experiment vents is summarized in Table 10.

b. Extra-Vehicular Activity Vent.

(1) Vent Description. The Airlock Module (AM) lock depressurization vent is located at station number 3295.5, eight degrees from the +Z-axis toward the -Y-axis. This vent is manually controlled by the LOCK DEPRESS VALVE, located in the AM lock. It is operated by an astronaut just prior to opening the EVA hatch. Nominally, 1.45 Kg of oxygen and 0.45 Kg of nitrogen is vented overboard as the internal pressure in the lock is decreased from the nominal 35,800 N/m^2 down to approximately zero. Predicted EVA torques are shown in figure 18 while typical torques are shown in figures 19 and 20. The change in signs on the torque profiles are apparently due to uncertainties in the impingement co-efficients and to a shift in the center of mass because of loss of one solar array and the micro-meteoroid shield. Table 11 shows the depressurization vents investigated.

(2) Extracted Torque Profiles. The extracted disturbance momentum and torque profiles are summarized in Table 12.

Table 10. Disturbance Torque Results

MOMENTUM IMPARTED (N.m.s)				AVERAGE TORQUE (N.m)		
LBNP	X	Y	Z	X	Y	Z
4	-188	2800	630	-0.4	2.07	0.48
17	-180	1400	1280	-0.19	1.44	1.32
24	-130	2250	2000	-0.15	2.50	2.22
**27	-37	780	595	-0.10	2.10	1.58
33	-50	1720	2450	-0.05	1.56	2.23
36	*	2800	2700	*	2.89	2.78
48	-450	2500	2150	-0.41	2.27	1.95
49	*	1410	1050	*	1.56	1.17
50	-70	2020	1800	-0.64	1.85	1.65
53	*	2650	2050	*	2.67	1.75
77	16	200	-55	*	*	*
79	-310	300	490	*	*	*
85	-13	185	-100	*	*	*

NOTES: (1) The disturbance torque was obtained from an extracted disturbance momentum which had been averaged over the past six data points. This derived torque was then averaged over the past six data points.

(2) The extracted disturbance momentum was computer from TM data samples taken every 14.75 seconds. The torque was obtained from a filtered momentum profile and then filtered again. The filters used were 0.7 damped quadratic lags with a break frequency of 0.5 radians/second.

*Not discernable.
**Not completely analyzed due to lack of TM data.

Table 11. EVA Vents Investigated

IDENTIFICATION	START DEPRESSURIZATION TGMT (DAY:HR:MIN)	DURATION (Sec)	POSITION* (Deg)
SL-2 EVA 1	15:15:18	591	216
SL-2 EVA 2	37:10:45	480	150
SL-3 EVA 1	85:17:21	690	115
SL-3 EVA 2	103:16:15	540	183
SL-3 EVA 3	132:11:10	540	90
SL-4 EVA 1	193:17:36	480	170
SL-4 EVA 3	230:17:21	510	238

*Orbital position in degrees past orbital midnight.

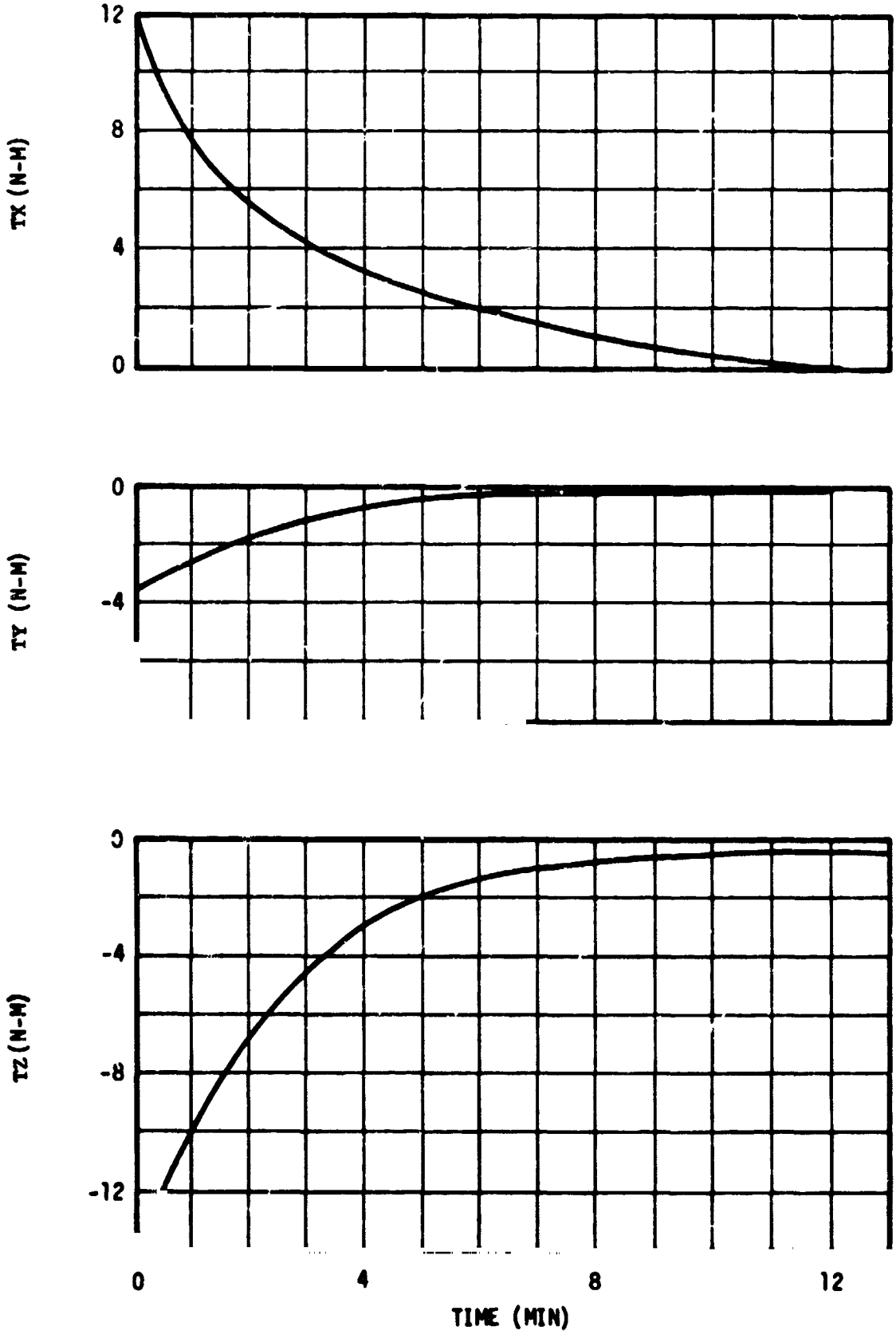

Figure 18. Predicted EVA Depressurization Vent Profiles

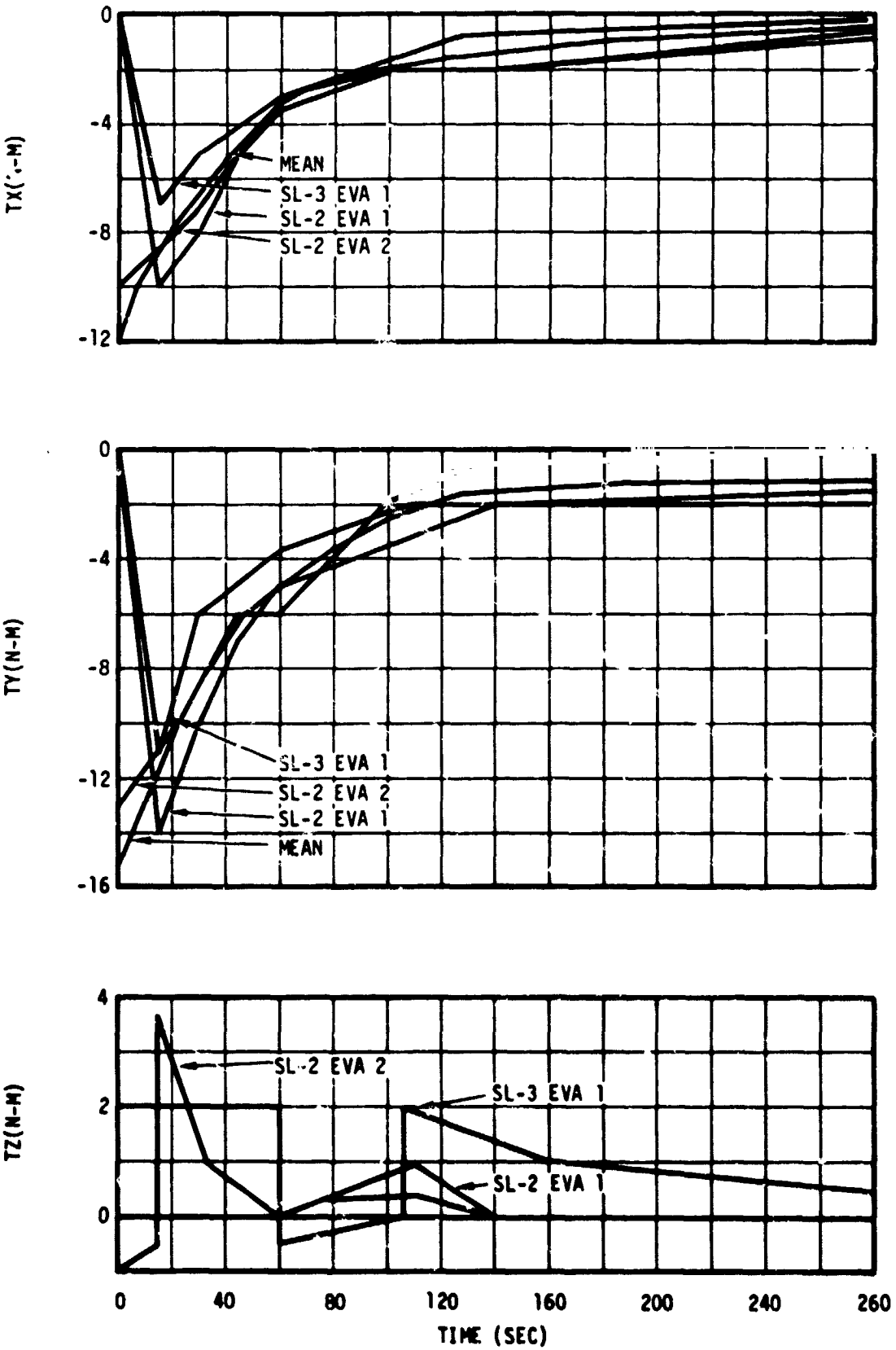

Figure 19. EVA Depressurization Torque

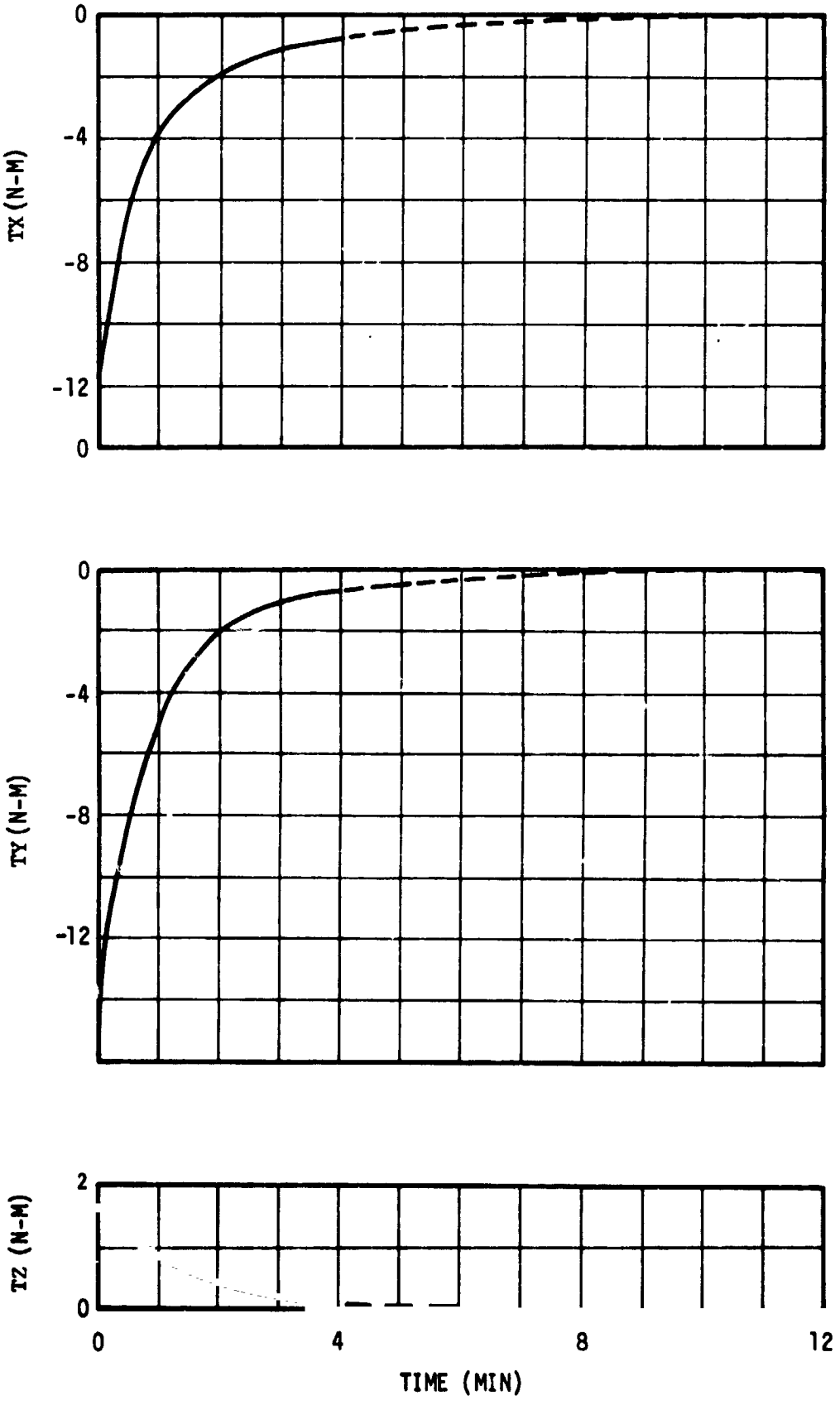

Figure 20. Typical EVA Depressurization Vent Torque

A composite of the "straight line" version is shown in Figure 19, while a typical vent profile is shown in Figure 20. These torques were those used in performing the evaluation of the APCS in response to the depressurization torques for the EVAs.

Table 12. EVA Vent Results

IDENTIFICATION	MOMENTUM IMPARTED X	Y	Z	AVERAGE TORQUE (NM) X	Y	Z
SL-2 EVA 1	-600	-750	+100	-1.0	-1.3	+002
SL-2 EVA 2				(1)		
SL-3 EVA 1	-700	-735	410	-1.0	-1.1	0.6
SL-3 EVA 2	-850	-800	+600	(3) -1.6	-1.5	111
SL-3 EVA 3				(1)		
SL-4 EVA 1	-900	-1050	450	-1.0	-2.2	0.9
SL-4 EVA 3				(2)		

(1) Not analyzed due to telemetry data gap.
(2) Not analyzed because CMG control was inhibited just prior to the vent.
(3) Insufficient data.

c. Extra-Vehicular Activity Torques.

(1) Description. During normal EVA, 3.59 Kg to 4.09 Kg/hour of Extra-Vehicular Mobility Unit (EMU) gases are vented overboard. This flow comes from the suit's Pressure Control Unit (PCU) which is mounted around the astronaut's waist. The vent is located near the small of the back.

While the astronaut is outside the vehicle moving around on the cluster, this vent is functioning and producing disturbance torques on the vehicle. It was the purpose of this portion of the study to extract these torque profiles from the telemetry data and attempt to determine magnitude of the suit vent forces. For this purpose, three of the EVAs were investigated as noted in Table 13.

Table 13. EVAs Investigated for Suit Vents

EVA NO.	DAY	DURATION	APCS MODE*
SL-3 EVA 3	132	2 Hrs 41 Min	SI
SL-4 EVA 1	193	6 Hrs 18 Min	SI
SL-4 EVA 3	230	3 Hrs 23 Min	SI

*During the first two EVAs investigated, the APCS was in SI mode under 3-CMG/TACS control. On DAY 327, one CMG failed and was secured. Therefore, SL-4 EVA 3 utilized only 2 CMGs. Also during portions of the EVA, the APCS was in the Attitude Hold (A/H) mode under CMG/TACS control.

Tables 14, 15 and 16 present the EVA torques for the three EVAs shown in Table 13. The torques were generated by differentiation of the momentum profile for these time periods.

It was not possible to extract the suit vent forces from the telemetry data. Several unknowns effected the analysis. These were astronaut station and attitude, and reflected force which occurred when the astronaut was in a semi-constrained space, such as the area near the EVA hatch.

d. Habitation Area Blowndown Vent.

(1) Approximately two days prior to docking, during the storage period, the Habitation Area (H/A) of the OWS was depressurized from the storage pressure down to approximately 3440 N/m^2 (see Table 17). This is accomplished by opening the OWS solenoid vent valves by DCS/DAS commands from the ground.

The vent is designed to be non-propulsive and is located at station 3165.0, 25 degrees from the -Z-axis toward the -Y-axis and 25 degrees from the +Z-axis toward the +Y-axis. The vent duration is nominally 6 to 8 hours.

Figure 21 shows the H/A pressure profile. This figure is the pressure profile as seen in measurement number D7111-436 of the AM telemetry system. In figure 22 the solid line shows the torque profile, etc. while the dashed line shows the extrapolated predicted profile.

e. Command and Service Module Vent.

(1) Vent Description. The vent is located on the CSM and was used to vent steam from the primary and/or secondary glycol evaporator as part of the CSM Environment Control System (ECS) function.

Due to the oxidizer leak problem with the SL-3 (CSM) during preparation for SL-3 undocking, the CSM ECS checkout procedures were modified to be in compliance with the procedures used during deactivation. The revised procedures resulted in operation of the Secondary Glycol Evaporator which produced steam which is vented directly overboard. A momentum build-up was observed which resulted in the CMG reset prior to securing the evaporator.

Upon observing the momentum build-up, a possible leak on the +Z-Scientific Airlock (SAL) vacuum source quick disconnect (QD) was suspect. This QD, which incorporates a shut-off valve,

Table 14. SL-3 EVA 3 Vent Torques

TIME* (Sec)	TDX (N.m)	TDY (N.m)	TDZ (N.m)
0	-0.84	-0.57	0.20
400	1.34	0.76	-1.55
2000	0.80	**	-0.85
3200	-0.90	1.64	0.85
4800	0.40	2.70	-0.50
5850	-1.10	1.64	0.65
6400	0.38	1.64	0.00
7600	-0.38	0.00	0.00
8350	-0.69	-1.00	0.50
9000	0.00	0.00	0.00

*Time is from T_{ref}. T_{ref} = 132:11:22:43.0
**Undetermined.
NOTE: Hatch open at -249 (132:11:18:34), close at 9411 (132:13:59:27).

Table 15. SL-4 EVA 1 Vent Torques

TIME* (Sec)	TDX (N.m)	TDY (N.m)	TDZ (N.m)
0	-0.05	0.15	-0.20
5010	0.00	0.04	0.26
5790	-0.97	-1.10	0.88
6270	-0.53	-0.65	0.26
6810	-0.37	-0.33	0.12
8760	-0.22	-0.35	0.44
9192	-0.13	0.66	-0.15
12700	-0.12	0.39	-0.79
12920	-0.46	-0.35	0.33
16740	-0.06	-1.03	-0.65
28480	**	**	**
29850	**	**	**

*Time is from T_{ref}. T_{ref} = 193:16:00
**Undetermined --- TACS firings.
NOTE: Hatch open at 6810 Sec (193:17:53:30), close at approximately 29490 (194:00:11:30).

Table 16. SL-4 EVA 3 Vent Torques

TIME* (Sec)	TDX (N.m)	TDY (N.m)	TDZ (N.m)
0	(TACS FIRINGS)		
850	-0.01	0.00	0.01
1030	(TACS FIRINGS)		
1470	0.00	0.00	-0.01
1860	(TACS FIRINGS)		
2030	0.00	0.00	-0.01
2280	(TACS FIRINGS)		
2300	-0.51	2.06	0.33
2600	(TACS FIRINGS)		
2610	-0.84	-0.52	0.92
2670	(TACS FIRINGS)		
2690	-0.28	-0.08	0.02
2870	(TACS FIRINGS)		
2900	-0.46	-0.52	0.38
3030	(TACS FIRINGS)		
3040	-0.31	-0.19	0.25
5980	(KOHOUTEK MANEUVER)		
13455	0.00	0.00	0.00

* Time is from $T_{ref.}$ $T_{ref.}$ = 230:17:14:45:184

NOTE: Hatch open at approximately 1095 (230:17:33)
close at approximately 13275 (230:20:59).

Table 17. Habitation Area Pressure

DAY	INITIAL N/m^2	FINAL N/m^2	DURATION (Hrs)	APCS MODE
74	12600	3940	7.9	SI
185	26000	*	*	SI

* No data.

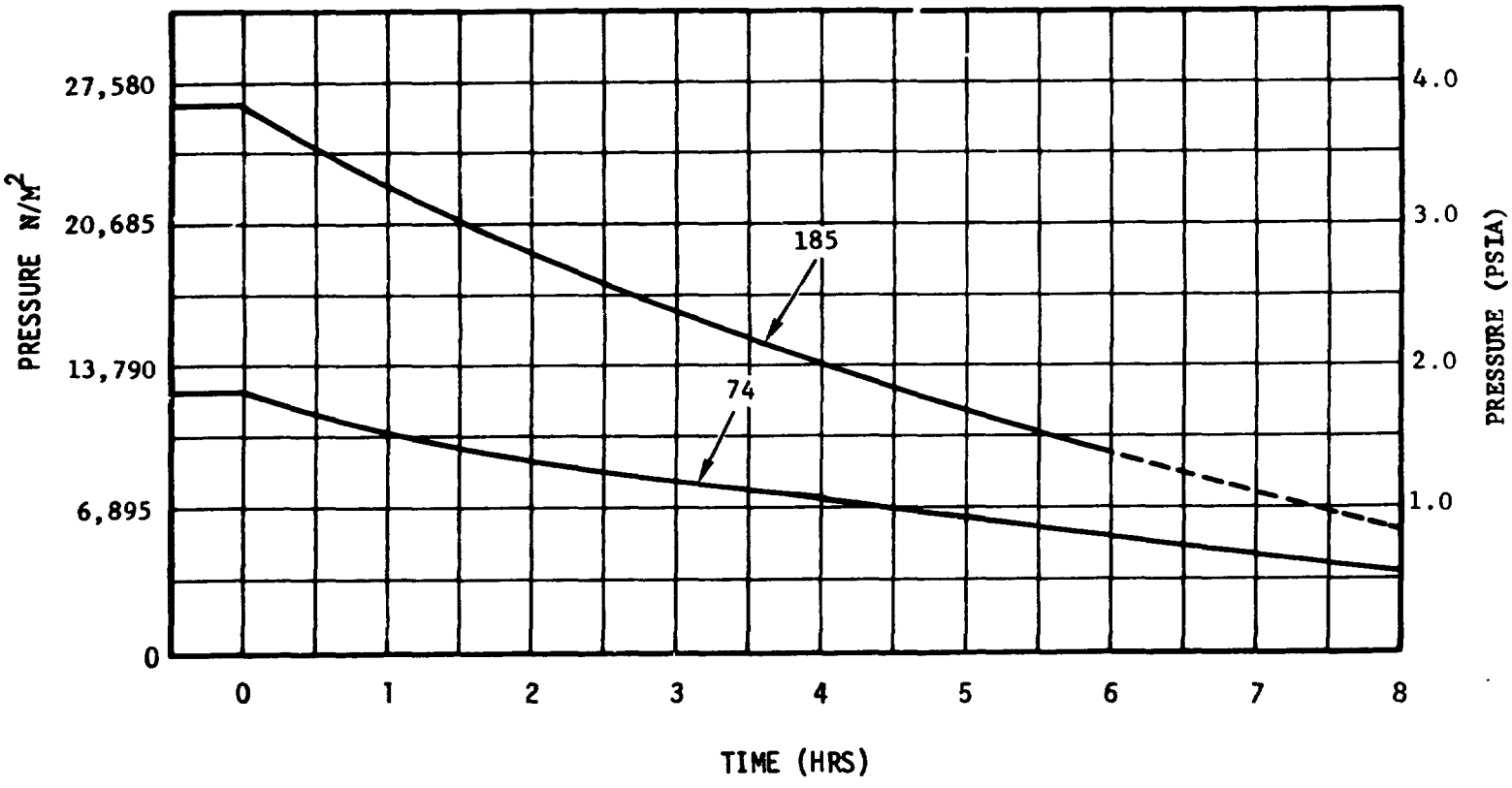

Figure 21. Habitation Area Pressure Profiles

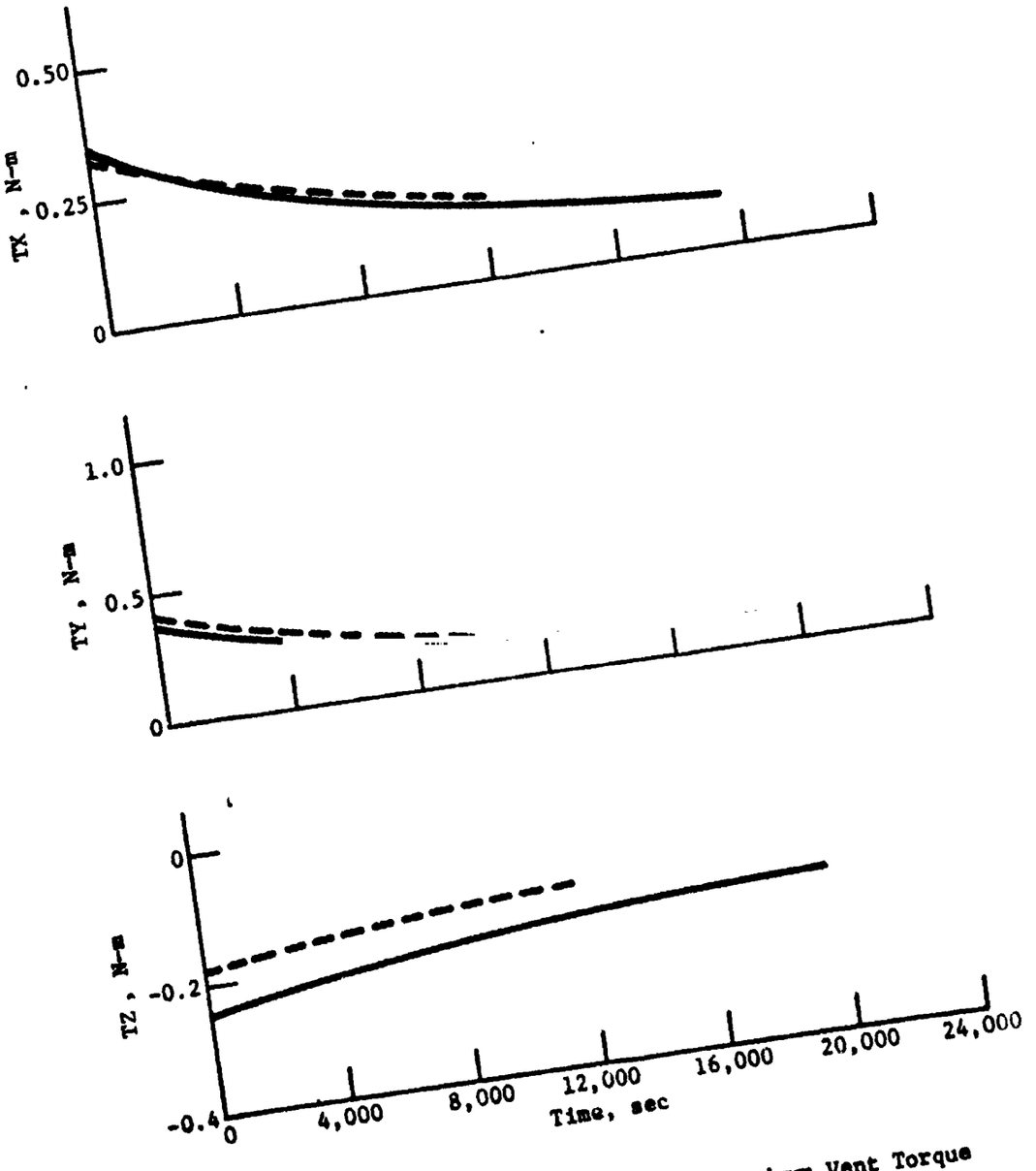

Figure 22. Typical Habitation Area Blowdown Vent Torque

was capped. The SAL valve was set to VENT. The cap was first replaced with a 183 cap and finally a hose was attached to the QD, neither of which seemed to halt the momentum build-up. The build-up was finally attributed to the CSM water boiler.

(2) Extracted torque profiles. At Greenwich Mean Time (GMT) on DAY 135, at approximately 13:06:28, the Secondary Glycol Evaporator Vent was initiated on the CSM. This vent occurred during preparation and checkout for the SL-3 undocking sequence which occurred at approximately 135:19:52:53. The vent lasted for 3901 seconds until approximately 135:14:11:29. The resulting momementum build-up on the CMGs forced a CMG reset which started at approximately 135:14:02:17. The vehicle was at an orbital position of approximately 243 orbital degrees with a solar elevation of approximately minus 44.7 degrees. The APCS was in the SI mode with the CMG-TACS in control. The events are summarized in Table 18.

Table 18. Sequence of Events

TIME (DAY:HR:MIN:SEC)	(SEC)	EVENT
135:12:00:23	23198423.	TGMT
135:13:06:28	23202388.	START VENT
135:13:55:04	23205304.	START CMG RESET
135:14:02:17	23206289.	END CMG RESET
135:14:11:19	23206289.	END VENT

The extracted disturbance torque profile is presented in figure 23.

2. Momentum Desaturation.

a. Description. Angular momentum desaturation was accomplished by performing three successive eigen-axis maneuvers during the night portion of the orbit. The first maneuver utilized 25% of the dump interval, the second 50% and the third 25%. The maneuver interval is symetric about the position in orbit where the x-principal axis is perpendicular to the gravity vector (defined as dump midnight).

A delta Z-axis rotation was included in the third maneuver. This correction minimized momentum accumulation during the next orbit.

The maneuvers were implemented utilizing attitude commands and based on navigation parameters and the desaturation momentum commands.

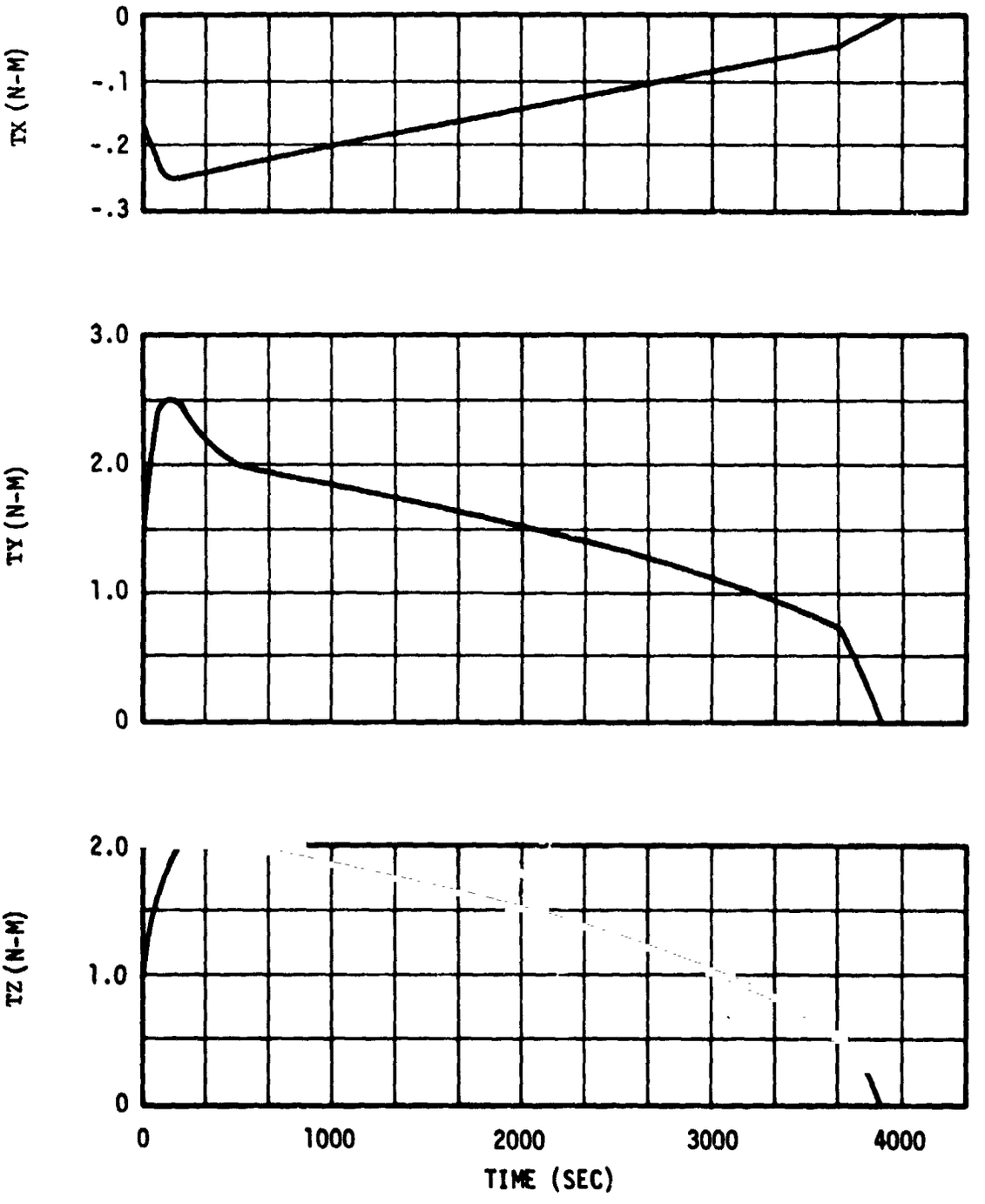

Figure 23. CSM Water Vent Torque Profiles

Information about the accumulated momentum was obtained by sampling the normalized components of the CMG momentum four times an orbit. The information contained in the momentum samples were used to establish a momentum bias, a momentum drift and a change in momentum drift. A weighted summation was then utilized to form body axis momentum commands.

Provision was included for the commands to be based on a single contingency sample if any of the normal samples were invalid.

To preclude CMG saturation during the momentum dump maneuvers momentum dump state prediction logic was included. If the logic predicted CMG saturation the original maneuvers were scaled down.

b. History. The original concept of Skylab was to desaturate the CMGs by means of TACS, but an energy-conservative approach was the one finally employed. In this method the vehicle was maneuvered, during the night portions of the orbit, to an orientation which caused momentum to accumulate in a direction which reduced the total momentum stored in the CMGs. Then, before the day portion of the orbit, the vehicle returned to Solar Inertial except for an offset about the sunline used for desaturating and minimizing momentum accumulation during the ensuing day.

The basic problems to be solved in developing a practical dump scheme included:

Sampling a momentum to be dumped

Generating a maneuver command profile

The sampling scheme changed from looking for maximum and minimum momentum accumulation along each axis to sampling at those points in orbits where the cyclic component of gravity gradient momentum were expected to be either zero or maximum. Therefore, bias and cyclic momentum can be extracted. The maneuver scheme underwent a major change in that the angle profile was changed from a trapezoid to a triangle allowing more desaturation over the desaturation period. Desaturation commands were computed in principal axis coordinates and then transformed into vehicle coordinates. Due to the similarity of vehicle Y and Z-inertias and their being much greater than the X-axis inertia, only Y and Z-axis principal axis maneuvers were computed. Therefore, by the time the change from the Wet to the Dry Workshop configuration had been made, the basic ground-rules for dump maneuvers had been developed.

In the development of the Dry Workshop ATMDC program, the momentum sampling was changed from five to four samples as the extra sample was not providing unique data. In addition, a major increase in performance was achieved with the addition of momentum state prediction logic. This was a set of logic used to ascertain whether the CMGs had the capability to execute the computed dump maneuvers. If the CMG momentum state was determined to be incompatible with the computed maneuver, the maneuver angles would be scaled down until an acceptable level was reached.

The next changes were basically clerical. For example, primarily for convenience, the alternate sample was specified to be taken at dump commence time. In addition, a list of specific criteria for determining the validity of the momentum samples was incorporated. This was necessitated by the various options that were emerging in CMG control (primarily the reset routine) and Redundancy Management. However, there was one performance related change, the incorporation of SI offset commands into the generation of the maneuver attitude profile. This provided the capability to dump from an SI offset attitude and to return automatically to that offset upon completion of the dump. This was initiated as an operational concern by the crew. They did not want to have to remove and re-enter the offset commands every orbit just before and after dump. A complete investigation was made as to the effects of dumping from an offset. The results indicated no performance problems.

The final version contained two significant changes. One was the removal of the rate commands in the execution of the maneuvers. This was done as a memory saving after extensive simulation work had shown that the steady state attitude offset that resulted from having only a ramp attitude command had insignificant effect on the dump scheme capability. The other change was the inclusion of the SI off-set commands in dump prediction and scale-down logic to make this logic compatible with the change made earlier of dump from the SI offset angle.

c. Analysis and Verification. The momentum management scheme underwent extensive analysis and simulation under varied conditions. The actual ATMDC Flight Program version of the Control Law then was verified, also, under varied conditions. For a summary of design analysis and verification, see Reference 5.

d. Mission Performance. Skylab was the first space vehicle to utilize vehicle maneuvers for desaturation and it worked extremely well. The desaturation scheme allowed Skylab to go two

entire unmanned missions without any TACS usage and allowed considerable TACS saving during the manned phases.

One problem arose from the interface of the dump scheme and the Star Tracker. The Star Tracker gave a direct independent indication of the angle between the vehicle X-axis and the orbit plane. During normal performance of the Tracker, this angle provided useful information to the momentum management scheme as to where momentum samples should be taken. However, the Star Tracker on several occasions during the SL-2 erroneously locked on to objects other than the required star. This caused the outer gimbal angle input to be inaccurate. On one occasion the erroneous inputs were received just prior to calculation of the momentum desaturation maneuvers. This resulted in a degraded performance by the momentum management scheme, resulting in less than optimum momentum states. In order to avoid these situations, a procedure was formulated wherein Star Tracker control and outer gimbal use were inhibited, the desired Star Tracker gimbal angles were calculated by ground support software, the Star Tracker was manually positioned on the star by the crew via the C&D Panel, and Star Tracker control and outer gimbal use were enabled. This allowed a valid outer gimbal reading to be obtained, after which Star Tracker control and outer gimbal use were inhibited again. Effective utilization of this procedure alleviated this problem with the Star Tracker readings.

This procedure to protect against Star Tracker false lock-on could have been avoided by having attitude about the sunline determined from momentum samples. While this information was not as accurate as that obtained from the Star Tracker, it was sufficiently accurate for momentum management and is independent of star availability or crew presence.

During the first unmanned period, the half-angle of the dump maneuver was decreased from 63 degrees to 51 degrees to ensure that for a solar elevation whose absolute value was less than 35 degrees, the dump maneuvers would be at night. This was done to protect an experiment with a failed door. Momentum management functioned well even though this smaller interval caused larger maneuver angles. The dump half-angle was changed back to 63 degrees at the start of SL-3 and retained at that value for the remainder of the mission.

Despite the generally nominal behavior of the dump scheme, on two occasions, certain events occurred during or just prior to initiation of the GG dump that resulted in loss of attitude control. Since the loss of control occurred during the active portion of the GG maneuvers, they were referred to as GG dump problems. The first loss of control occurred after a Z-axis Rate Gyro failure was

detected during the dump maneuver. The second event resulted from action taken because of unexpected vent torques during an EVA.

One important condition of the CMG control system existed during both instances of loss of control, i.e., CMG saturation. Once the CMG control system became saturated, it took on the following properties:

> Control Law attempted to align the total momentum vector along the torque command vector.
>
> Due to proportional scaling, any additional torque requirement in the axis of the largest command reduced the commands in the other axes (thus, altering the direction of the torque command vector).
>
> Momentum, therefore, changed in all axes (due to momentum vector swinging to realign with torque command).
>
> X-axis was the most sensitive axis to this phenomena because of:
>
> - Lower control gains
> - Small moment of inertia
> - Less momentum equivalency of X-axis rate ledge caused by desire to keep rate below Rate Gyro scale switching.

Historically, the above described phenomena was referred to as the X-axis momentum siphon effect. The relative difference in the momentum change among the three axes was small, but because of the small moment of inertia in the X-axis, the vehicle rate change was an order of magnitude greater than the Y and Z-axes.

TACS desaturation firings normally prevented CMG saturation, thus, not allowing the above described condition to exist. However, the GG dump maneuvers were designed so as to prevent needless desaturation firings. As the result of implementing the maneuvers by commanding a strapdown offset with a zero attitude rate command, system momentum saturation did not occur.

Special scaledown logic in the momentum management routine controlled the extent of CMG saturation during GG dump maneuvers to maximize dump capability. The logic proportionally scaled the maneuvers considering:

Momentum bias

Momentum ramp

Average cyclic momentum over dump interval

Commanded bias

Amount of momentum already dumped.

Additionally, the scaledown logic assumed that without maneuvers, the system would not saturate.

(1) Z-axis Rate Gyro Scale Factor Error. On DAY 91, at 17:03:00, a nominal GG dump maneuver commenced. At 17:03:32, the two controlling Rate Gyros in the Z-axis failed the integral test criteria because of a difference in rate readings. Prior to the integral test failure, the CMG control system was controlling, using the average of Gyros Z2 and Z3. After the failure detection, Gyro Z2 was arbitrarily chosen for control. Since the reading on Z2 was lower than required, an additional 0.3 H was required to bring the reading of Z2 up to the required rate. The additional momentum requirement forced the CMGs into saturation and siphoned momentum from the X-axis at the same time. The X-axis momentum change produced an uncontrolled rate and resulted in a 20 degree attitude buildup in the X-axis requiring an automatic switch to TACS only control.

A simulator was initialized with data taken prior to dump commence (17:02:30) with the following verifying results:

Computed same GG dump profile as ATMDC

With normal Gyros, no switch to TACS Only

With 0.01 degree/second difference in Z2 and Z3, switched to TACS Only within 15 seconds of flight and all control parameters tracked closely with flight.

(2) Control Problems During EVA Vent. The second incident, in which loss of control occurred during a GG dump,

took place on DAY 103, at 19:00 hours. The approximate timeline of events was as follows:

17:10:00 - EVA started to install Six-Pack Gyros

17:50:00 - Installation complete

17:53:00 - Solar Inertial mode selected to remove attitude errors

19:42:00 - By ground command, a single sample dump was forced

(Desaturation firings had occurred since 18:00 hours due to momentum ramp resulting from crew suit vents.)

19:53:00 - CMG saturation

19:52:00 - Siphoning of X-axis momentum followed by divergence of attitude error

19:57:00 - Attitude Hold mode commanded

The CMG saturation occurred as a result of the GG maneuver plus the crew suit vent. Since a single sample dump (versus the complete four-sample) cannot detect the presence of a momentum ramp component, the scaledown logic could not predict the CMG saturation and, therefore, did not reduce the magnitude f the maneuvers. A more sophisticated sample scheme could have detected a momentum ramp component with as little as five minutes Solar Inertial attitude. However, the lack of additional available memory in the ATMDC made this not feasible.

D. TACS Budget

1. Mission Usage. At launch, the Skylab vehicle was loaded with 376, 996 N.s. of TACS impulse capability. The predicted usage for the life of Skylab was 110, 102 N.s. The total TACS used during the entire Skylab mission was an impulse of approximately 340,311 N.s. The usable TACS impulse remaining at the end of the mission was approximately 36, 585 N.s., assuming minimum usable thrust of 44.5 Newtons. However, additional impulse could have been generat- by allowing TACS pressure to drop to zero. This usage is sum -ized in Table 19, according to five time periods:

Table 19. TACS Usage Summarized by Missions

TIME PERIOD (DAY:HR:MIN)	EVENT	TOTAL TACS USED (N.s)
1:17:30 to 13:18:00	SL-1 Launch to Acquisition of True SI.	190,895
13:18:00 to 40:09:24	Skylab-2	13,656
76:19:38 to 135:19:53	Skylab-3	27, 263
187:21:00 to 271:10:32	Skylab-4	
	3-CMG Operation	7,046
	2-CMG Operation	93,101
	Total	100,147
271:10:32 to 272:18:17	Deactivation & Storage	11,081

Table 20. Summary of TACS Used Prior to Acquisition of True Solar Inertial Attitude

EVENTS	TACS USAGE (N.s)
IU Control Period	36,716
APCS Activation Period*	29,807
Thermal Maneuvers	12,072
Resets	44,812
Destination Firings**	1,779
Rendezvous and Docking	48,566
Maneuver to SI	17,143
Total	190,895

*Includes three thermal maneuvers and TACS only period.

**Only those not associated with specific event.

Table 21. Summary of TACS Used During Skylab-2 Mission

EVENT	TACS USAGE (N.s.)
EREPs	2509
Trim Burn	2580
Rate Gyro Anomaly	142
Rate Gyro Calibration	267
Thermal Maneuver	3852
LBNP	142
Refrigeration Maneuver	3074
Resets	1090
Total	13,656

Table 22. Summary of TACS Used During Skylab-3 Mission

EVENT	TACS USAGE (N.s.)
Docking	3634
EREPs	1210
DAY 91 Anomaly	11,450
LBNP	360
EVAs	4146
Desaturation Firings	289
Resets	2180
Undocking	
Resets	1873
Attitude Hold	2032
Calibration Maneuver	89
Total	27,263

Skylab-1 launch to true Solar Inertial

Skylab-2 mission

Skylab-3 mission

Skylab-4 mission

Post Skylab-4 deactivation and storage.

Additional breakdowns are in terms of mission events such as maneuvers and EVAs.

A summary of TACS used during period of SL-1 launch to acquisition of true Solar Inertial attitude is shown in Table 20.

It should be noted that the impulse used during the mission subtracted from the initial stored impulse is not exactly equal to the final measured stored impulse. This was caused by Skylab being deactivated before TACS pressure had stabilized and approximations made in calculating TACS usage. See Section VI.E for additional details on problems associated with TACS pressure measurements.

a. Skylab-1 Launch to Solar Inertial. Essentially, all the TACS usage during this period can be classified as being used during the thermal attitude. Due to the loss of the micro-meteoroid shield and the non-deployment of the Solar Panel (Section IV), many maneuvers and attitudes other than SI attitude were required for extended periods. While in these extended non-SI attitudes, gravity gradient torques caused momentum buildup. Since momentum desaturation maneuvers were not possible, TACS was used for CMG desaturation purposes, as well as aiding with maneuvers.

b. Skylab-2 Mission. The Skylab-2 mission is considered to start when the Solar Inertial attitude was acquired on DAY 14, 18:00:00. TACS usage from the acquisition of Solar Inertial to the undocking of SL-2 are given in Table 21.

c. Skylab-3 Mission. The Skylab-3 mission began with SL-3 docking on DAY 76, 19:38:50, and ended with SL-3 undocking on DAY 135, 19:52:53. TACS usage for the mission is summarized in Table 22.

d. Skylab-4 Mission. The Skylab-4 mission began with SL-4 docking DAY 187, 22:00:00, and ended with SL-4 undocking DAY 273, 15:00:00. The first part of the mission was under 3-CMG control. However, on DAY 194, the number 1 CMG failed and the rest

of the SL-4 mission was under 2-CMG operation. Two CMG operation generally required more TACS usage than 3-CMG operation. Table 23 gives a summary of TACS usage for the SL-4 mission.

e. Post SL-4 Deactivation and Storage. After the CSM undocked, DAY 271, 17:15:00, ending the SL-4 mission, the SWS OA was maneuvered to an X-LV attitude under TACS only control. TACS used during the period SL-4 undocking to powering down of vehicle was 11,081 N.s.

2. Event Usage.

a. Thermal Attitude Maneuvers. Shortly after orbital insertion, the workshop began to overheat, due to loss of the micrometeoroid shield. To protect the contents of the Workshop from excessive heat, it was necessary to maneuver the vehicle to attitudes where the Z-axis did not point directly at the sun. The most acceptable compromise between thermal and electrical power constraints proved to be an attitude with the vehicle Z-axis point 40 degrees away from the sun line. Problems associated with maintaining the thermal attitude resulted in a TACS usage amounting to a large portion of the total Skylab impulse expenditure.

The large Rate Gyro drift present in the Rack Rate Gyros presented serious difficulties in maintaining attitude and attitude reference. By causing movement of the X-principal axis out of the orbital plane, the gyro drift caused frequent CMG momentum saturations and subsequent resets.

Since the momentum desaturation scheme was designed to function in Solar Inertial mode and would not operate at the thermal attitude, consideration was given to implementation of an ATMDC patch to provide momentum desaturation capability. The patch, however, could not be developed in the time available.

The only means used to desaturate the CMGs was the reset routine. As the reset routine caged momentum to the nominal value for Solar Inertial attitude, resets could only be commanded at orbital points where the Solar Inertial and thermal attitude nominal momentum curves intersected. In addition, adequate station coverage was required for these points.

b. Attitude Hold Maneuvers. Before the mission the Attitude Hold maneuver capabilities were required but little use was outlined for them. However, during the mission these capabilities were used extensively.

Table 23. Summary of TACS Used During Skylab-4 Mission

EVENT		TACS USAGE (N.s)
3-CMG	Docking	4608
Operation	Desaturation Firings	67
	EVA No. 1	2349
	CMG No. 1 Deactivation	22
2-CMG	EVA 2, 3 and 4	37,525
Operation	Trim Burn	22
	TACS Only (High X Rate)	2691
	Resets	2126
	Desaturation Firings*	3168
	EREPs	28,090
	EREP Cal	2865
	C Motion	22
	Maneuvers	
	S232	111
	S183	249
	JOP13	3582
	S063	765
	S019	226
	JOP18	3974
	Undocking Period	7784
	Total	100,147

*Many desaturation firings could be attributed to experiment-caused dump inhibits or maneuvers.

The first week of Skylab involving almost constant maneuvering in the thermal attitude gave the crew and the mission support team confidence in the vehicle maneuvering capability. After the installation of the thermal shield and the reacquisition of Solar Inertial, a wide variety of Attitude Hold maneuvers were performed. These maneuvers were for the following purposes:

Rate Gyro Calibration (Rack and Six-Pack)

Kohoutek Maneuvers

X-Ray Stellar Photography (JOP-13)

The first Rate Gyro calibration maneuvers were performed to check the scale factor of the Rack Gyros with respect to each other and with respect to the Acquisition Sun Sensor. After the installation of the Six-Pack Rate Gyros, a second set of maneuvers was performed to check their alignments to Workshop axis. The maneuvers showed this alignment to be sufficiently accurate that no additional ATMDC compensation was required.

The study of the Comet Kohoutek was an unplanned opportunity requiring the development of ground software and flight procedures. In order to verify instrument capability and the accuracy of maneuvering to a bright target, a maneuver to point the ATM at the planet Mercury was performed. The success of the maneuver led to the planning of a variety of maneuvers to investigate the Comet Kohoutek.

Three types of maneuvers were required for Kohoutek experiments. The first, consisting of a roll about the X-principal axis, was for the purpose of observing Kohoutek with experiments viewing through an articulated mirror system located in the Scientific Airlock (SAL). As these maneuvers were about X-principal, there were usually no problems with TACS usage or gimbal stop problems. The only problems occurred with gimbal stops in the 2-CMG case for some of the largest maneuvers. The second type of maneuver involved pointing ATM experiments at Kohoutek and maintained X-principal in the orbit plane. As these maneuvers required vehicle rates about both Y and Z-axis as well as the X-axis, they generally required extensive optimization in terms of maneuver rates, maneuver start and maneuver stop times and momentum biases in the 2-CMG case in order to minimize TACS usage. The third type of Kohoutek maneuver, used only during EVAs, involved a rotation about the X-principal axis in order to have the ATM Solar Panels shade the astronaut held S201 camera.

JOP-13 maneuvers, from the APCS point-of-view, were similar to Kohoutek maneuvers in that the ATM was pointed at a

celestial reference and X-principal was maintained in the orbital plane. As the X-ray experiment had no independent sensor to help determine whether the target was within the field-of-view, which was only six arc minutes, several JOP-13D maneuvers obtained no data. This was the only case of insufficient APCS maneuver accuracy and would have been avoided had the crew been provided with target detection capability. The maneuvering capability of the APCS would then have allowed target acquisition.

Table 24 is a summary of TACS usage in the Attitude Hold mode during SL-4.

c. Z-Local Vertical (Z-LV) Maneuvers. The Z-LV mode, utilized for Earth Resources Experiment Package (EREP) passes, puts the vehicle -Z-axis towards the center of the earth, vehicle +Y-perpendicular to the orbital plane and vehicle +X in the direction of the velocity vector. Hence, while the vehicle is in the Z-LV mode, orbital rate of about 0.066 deg/sec is present on vehicle Y-axis. In addition, maneuver bias capability allowing the maintaining of an arbitrary vehicle axis perpendicular to the local vertical existed. This capability was designed primarily for rendezvous of the CSM with the Skylab, but as rendezvous in the Solar Inertial move proved feasible, it was not used in this capacity. It was utilized for Z-LV offset biasing in the two-CMG Z-LVs and for insertion into the gravity gradient attitude at the end of SL-4. EREPs were limited to absolute solar elevation of less than 60 degrees and to the daylight portion of the orbit.

During the missions, it became apparent that EREP data-take constraints could be met by a variety of maneuvers, thus allowing system optimization. The areas to be optimized included:

Total TACS usage

No attitude excursions during data-take time.

The parameters that could be varied included:

Orbital position for maneuver-in initiation

Maneuver-in rate

Orbital position for maneuvering-out initiation

Maneuver-out rate

Momentum bias

Enable or inhibit dump.

Table 24. SL-4 Attitude Hold Maneuvers

MANEUVER DESCRIPTION		MANEUVER START TIME	MANEUVER TIME (MINUTES)		ATTITUDE HOLD COMMAND				TACS IMPULSE (NEWTON-SECOND)	
					DURATION	ATTITUDE OFFSET				
NO.	TYPE	(DAY:HR:MIN)	IN	OUT	(MINUTES)	X(DEG)	Y(DEG)	Z(DEG)	ESTIMATED	USED
1	S019	196:22:01	20	20	30	N A	N A	N A	0	0
2	S201	197:22:50	20	60	35	N A	N A	N A	0	0
3	S232	198:14:41	30	30	12	N A	N A	N A	890	3225
4	S201	206:21:45	10	20	19	-65.4	- 6.9	-3.07	89	0
5	S063	207:02:23	20	20	11	-66	- 6.9	- .08	0	0
6	S183	208:01:38	15	20	19	-67.2	- 7.0	-2.96	22	49
7	JOP13	209:18:37	20	20	31	+32.8	-44.7	+2.37	214	93
8	S019	209:23:29	10	20	18	N A	N A	N A	71	0
9	S063	209:18:06	20	20	10	N A	N A	N A	0	0
10	S052	210:14:13	15	15	77	N A	N A	N A	0	22
11	S063	210:20:37	15	15	N A	N A	N A	N A	22	49
12	S052	210:14:13	15	15	77	+8.83	-12.7	-0.98	0	22
13	S063	211:16:49	15	15	09	-72.0	-16.6	-5.56	142	289
14	S201	213:01	18	18	17	-75.0	+ 0.0	-2.01	N A	N A
15	S201	213:05	18	18	37	+53.1	- 3.7	+2.8	N A	N A
16	S019K	214:14:42	10	18	17	-79.2	+10.0	+1.94	22	67

Table 24. (continued)

MANEUVER DESCRIPTION NO.	MANEUVER DESCRIPTION TYPE	MANEUVER START TIME (DAY:HR:MIN)	MANEUVER TIME (MINUTES) IN	MANEUVER TIME (MINUTES) OUT	ATTITUDE HOLD COMMAND DURATION (MINUTES)	ATTITUDE HOLD COMMAND ATTITUDE OFFSET X(DEG)	ATTITUDE HOLD COMMAND ATTITUDE OFFSET Y(DEG)	ATTITUDE HOLD COMMAND ATTITUDE OFFSET Z(DEG)	TACS IMPULSE (NEWTON-SECOND) ESTIMATED	TACS IMPULSE (NEWTON-SECOND) USED
17	S183K	215:00:02	10	19	17	-79.1	+10.0	+1.94	22	N A
18	S019K	216:15:34	10	15	17	-85.0	+3.63	+0.32	0-44	N A
19	S063K	216:14:53			CANCELLED					
20	S201K	217:17:11	23	15	13	-86.0	+1.75	+0.12	0	0
21	S019K	217:21:51	23	15	10	-86.0	+1.58	+0.10	0	0
22	S019K	218:02:31	23	15	10	-87.0	+1.4	+0.07	0	0
23	S063K	218:16:35	23	15	08	-87.5	+1.18	+0,05	0	0
24	S183K	220:21:37	23	15	36	-91.3	+0.54	-0.01	0	0
25	S201G	220:02:17	23	15	38	N A	N A	N A	0	0
26	S019	220:22:27	23	15	39	-93.0	+0.40	-0.02	0-289	N A
27	JOP18D	220:15:51	10	10	133	3.07	-17.8	-8.4	267-890	653
28	S019	220:22:27	23	15	39	-93	+.39	+0.02	0	0
29	S063K	222:01:23	23	15	09	-95	-.37	-0.03	0	44
30	JOP18D	222:15:24	25	14	141	-0.19	-15.5	-6.7	98	98
31	S063	222:23:10	23	15	08	-97.0	0.72	-.05	0	0
32	S063	223:16:17	23	15	07	-98.0	0.59	-.08	0	0

Table 24. (continued)

MANEUVER DESCRIPTION		MANEUVER START TIME	MANEUVER TIME (MINUTES)		ATTITUDE HOLD COMMAND				TACS IMPULSE (NEWTON-SECOND)	
					DURATION	ATTITUDE OFFSET				
NO.	TYPE	(DAY:HR:MIN)	IN	OUT	(MINUTES)	X(DEG)	Y(DEG)	Z(DEG)	ESTIMATED	USED
33	S201K	224:02:36				CANCELLED				
34	S201	224:15:02	23	15	42	-98.5	0.97	-.15	311-956	299
35	JOP18D	224:18:41	25	20	93	-2.19	-10.67	-3.96	311-956	299
36	S019	225:01:25	23	15	17	-98.5	1.24	-.19	N A	22
37	JOP18D	225:17:58	25	20	159	-2.54	-8.22	-2.68	0	
38	S201K	226:21:04	TBD	N A	N A	N A	N A	N A	0	0
39	S201	230:17:30	TBS	N A	N A	N A	N A	N A	N A	N A
40	JOP18D	231:01:56	05	05	60	+2.29	+7.28	+0.21	0	0
41	JOP18D	231:14:16	06	06	234	+3.80	+7.68	-0.05	0	0
42	JOP18D	231:22:16	06	06	147	+4.90	+8.06	-0.26	129	1566
43	JOP18D	232:15:07	07	07	236	+5.54	+9.69	-0.74	200	112
44	JOP18D	232:22:53	08	08	60	+6.07	+10.26	-1.03	N A	N A
45	JOP18D	233:22:18	07	07	135	+8.25	+11.54	-2.09	334	156
46	S063	234:14:26	20	10	13	-88.1	-15.5	-0.53	89	N A
47	S063	234:17:32	20	10	08	-88.1	-15.5	-0.53	89	N A
48	S201	234:21:56	36	36	39	-91.9	-18.5	+0.64	0	N A

Table 24. (continued)

MANEUVER DESCRIPTION		MANEUVER START TIME	MANEUVER TIME (MINUTES)		ATTITUDE HOLD COMMAND				TACS IMPULSE (NEWTON-SECOND)	
					DURATION	ATTITUDE OFFSET				
NO.	TYPE	(DAY:HR:MIN)	IN	OUT	(MINUTES)	X(DEG)	Y(DEG)	Z(DEG)	ESTIMATED	USED
49	S183	235:15:11	26	20	39	-86.0	-11.7	-0.81	0	89
50	JOP18	235:20:36	15	15	38	+11.3	+14.9	-5.2	890	463
51	S019	236:23:52	23	15	39	N A	N A	N A	N A	N A
52	JOP18D	237:14:37	18	18	60	+14.4	+18.3	-9.3	200	200
53	S063K	237:23:11	23	15	12	-82.6	-8.0	-1.1	111	0
54	S201K	238:13:10	23	15	22	-81.1	-7.3	-1.2	0	0
55	JOP18D	238:23:12	20	20	157	+16.6	+21.8	-13.8		311
56	S019K	239:23:26	20	15	21	-79.0	-6.3	-1.3	89	22
57	S019K	240:11:48	13	15	36	-78.1	-6.6	-1.4	0	0
58	S063	241:00:16	20	20	23	-77.0	-5.9	-1.4	0	0
59	S063K	241:20:28	23	15	18	-76.6	-5.6	-1.3	0	0
60	S183K	241:23:34	23	15	34	-77.1	-5.7	-1.3	0	93
61	S201K	242:16:44	20	15	19	-75.1	-5.3	-1.4	0	N A
61A	S183K	243:22:18	20	15	28	-74.6	-5.0	-1.4	22	67
62	S019K	244:01:25	20	15	27	-74.6	-5.0	-1.4	0	0
63	S063K	244:21:39	20	15	22	-75.1	-4.9	-1.3	0	0

Table 24. (continued)

MANEUVER DESCRIPTION		MANEUVER START TIME	MANEUVER TIME (MINUTES)		ATTITUDE HOLD COMMAND				NEWTON-SECOND	
					DURATION	ATTITUDE OFFSET				
NO.	TYPE	(DAY:HR:MIN)	IN	OUT	(MINUTES)	X(DEG)	Y(DEG)	Z(DEG)	ESTIMATED	USED
64	S201K	245:00:46	20	15	20	-75.1	-4.9	-1.3	0	0
65	S063K	245:21:00	20	15	20	-74.0	-4.7	-1.4	22	49
66	S019K	246:20:24	20	15	13	-78.0	-5.0	-1.1	0	44
67	S201	247:01:04	20	15	13	-78.0	-5.1	-1.0	0	0
68	S201K	257:23:54	15	15	36	38.2	-4.4	5.6	0	0
69	S201G	258:13:03	05	05	05	+6.0	0.0	0.0	0	0
70	S063K	260:00:13	05	05	08	+35.6	-2.4	3.4	0	0
71	JOP13	261:23:45	26	25	47	+15.1	-52.9	+17.7	2068	1788
72	S019K	262:23:38	09	09	38	+32.0	-1.51	+2.41	0	187
73	S201K	263:21:23				CANCELLED				
*74	JOP13	269:12:25	28	25	41	+16.4	-74.2	+9.7	1650	1699
75	S201	264:23:49	08	08	06	+30.5	-1.25	+3.1	0	0

*MANEUVER TO NEW ATTITUDE HOLD -157.0 Deg about X, -56.0 Deg about Y, and -17.7 Deg about Z.

EREP passes were performed for absolute solar elevations less than 60 degrees and for data-take during the daylight portion of the orbit. After the loss of CMG No. 1, the first EREPs under two-CMG control had high TACS usage. This led to the development of the technique of noon-to-noon EREPs, possible where data-take through orbital noon was not required. The advantage of noon-to-noon EREP passes is that large maneuvers about the vehicle Y-axis (large inertia axis) are not required during the maneuver to Z-LV when Z-LV entry was at orbital noon.

The maneuver about the X-axis to position the Z-axis in the orbital plane is much less demanding from the momentum saturation aspect as the X-axis inertia is much less than the Y or Z-axis inertias. It then became apparent that due to the misalignment of the X-principal from the X-vehicle axis, a Y-axis momentum bias was generated. This led to the technique of utilizing the biased Z-LV maneuver to maintain the X-principal axis perpendicular to the vertical for the non-data take portion of the noon-to-noon EREPs and maneuvering the Z-axis along the vertical for the data take. This tended to minimize momentum accumulation.

The pre-launch requirements had not allowed noon-to-noon EREPs. However, the temperatures of the OWS proved to be somewhat higher than anticipated requiring less power from the OWS duct heaters. Thus, despite the loss of the OWS solar panel, power proved adequate for noon-to-noon EREPs. In addition, since the failure of CMG number one occurred relatively late in the mission, the additional battery depth-of-discharge caused by noon-to-noon EREPs could not significantly reduce battery capability to sustain the remainder of the mission.

All EREPs performed during SL-2 and SL-3 were done using 3-CMG control while all those performed during SL-4 were under 2-CMG control. Excluding the three EREPs where procedural problems occurred, the following comparison can be made. Forty-eight EREPs were made under 3-CMG control using a total of 1548 Newton-seconds. Thirty-six EREPs were made under 2-CMG control using 12, 290 Newton-seconds. Therefore, EREPs performed under 3-CMG control used an average of approximately 31 Newton-seconds while those performed under 2-CMG control used an average of 338 Newton-seconds. Had the noon-to-noon maneuver not been used, the TACS usage under the 2-CMG case would have been much higher. Due to an unique set of initial conditions which must be associated with each EREP maneuver, predicted TACS usage must be studied for a given EREP. However, the greater the available CMG momentum for a given maneuver, the less the TACS usage should be.

There were a total of 102 EREP passes scheduled during the Skylab mission, of which 94 were flown. They are summarized in this section.

(1) EREPs SL-2. Eleven EREP passes were made during the SL-2 mission. Table 25 lists the eleven EREPs, giving maneuver-in time, duration time of the data-pass, maneuver-out time, and the predicted and used TACS impulse.

EREP number 7 was the only one of the eleven which required TACS usage significantly different from the predicted value. The larger usage was attributed to the maneuver not being executed as planned.

(2) EREPs SL-3. Forty-one EREPs were scheduled during the SL-3 mission. Table 26 lists the 41 EREP passes giving maneuver-in time, duration time of the data pass, maneuver-out time, and the TACS impulse predicted and used.

EREP number 12 was the only one of the 41 which required a TACS usage significantly different from the predicted value. The large usage was attributed to the maneuver not being executed as planned.

(3) EREPs SL-4. Fifty EREP passes were scheduled during the SL-4 mission. Table 27 lists the 50 scheduled passes giving maneuver-in time, duration time of the off-set attitude and data pass combined, maneuver-out time, and TACS usage predicted and used.

All EREP passes during SL-4 were performed under 2-CMG control. Therefore, in general, TACS usage was much higher than the values required during SL-2 and SL-3 EREPs, which were performed under 3-CMG control.

Beginning with EREP 12 (SL-4) the noon-to-noon type EREP maneuver was used when necessary. This type maneuver resulted in a great saving in TACS usage.

EREP number 13 was the only EREP pass during SL-4 which resulted in significantly more TACS usage than predicted. This maneuver was not executed as planned.

d. Kohoutek and Other Non-EREP Maneuvers. A description of the maneuvers made for experiment purposes are given in Table 24, along with the time of occurrence, maneuver times, duration time, attitude, and TACS usage information. All of these maneuvers were made with the vehicle under 2-CMG control. TACS usage, for the most part, agreed reasonably well with the predicted value.

Table 25. SL-2 EREP Maneuver Times, Duration Time, and TACS Usage

EREP PASS NUMBER	TIME PERIOD (DAY:HOUR:MINUTE)		MANEUVER SI TO Z-LV		DURATION OF PASS		MANEUVER Z-LV TO SI		TACS IMPULSE (NEWTON-SECONDS)	
			ANGLE	TIME	ANGLE	TIME	ANGLE	TIME		
	FROM	TO	(DEG)	(MIN)	(DEG)	(MIN)	(DEG)	(MIN)	USED	PRED
1	17:20:21	17:21:21	35	09	128	33	69	18	249	200
2	20:19:59	20:20:19	19	05	39	10	19	05	334	156
3	21:19:17	21:19:38	19	05	58	11	19	05	22	40
4	22:16:56	22:17:21	31	08	46	12	19	05	0	0
5	23:17:49	23:18:14	30	08	46	12	20	05	0	0-44
6	27:14:48	27:15:36	54	14	101	26	31	08	22	0-83
7	28:13:54	28:14:56	94	25	105	27	38	10	1548	0-156
8	29:14:55	29:15:51	58	15	116	30	42	11	89	22-133
9	30:12:38	30:13:28	62	16	108	26	30	08	133	89-133
10	31:13:26	31:14:24	77	20	108	28	39	10	111	67-111
11	32:14:25	32:15:21	58	15	112	29	46	12	0	0

Table 26. SL-3 EREP Maneuver Times, Duration Time, and TACS Usage

EREP PASS NUMBER	TIME PERIOD (DAY:HOUR:MINUTE)		MANEUVER SI TO Z-LV		DURATION OF PASS		MANEUVER Z-LV TO SI		TACS IMPULSE (NEWTON-SECONDS)	
	FROM	TO	ANGLE (DEG)	TIME (MIN)	ANGLE (DEG)	TIME MIN	ANGLE (DEG)	TIME (MIN)	USED	PRED
1	82:17:31	82:18:46	77	20	143	37	70	18	22	22
2	83:16.27	83:17:54	137	35	158	39	50	13	0	0- 44
3	84:14:23	84:15:19	116	30	62	16	39	10	49	0
4	84:16:07	84:17:15	86	22	124	32	54	14	0	44-133
5	87:15:24	87:16:38	96	25	143	37	46	12	0	0
6	88:13:07	88:14:31	124	32	139	36	62	16	0	0
7	90:14:50	90:15:56	127	33	97	25	30	08	0	0
8	91:02:07	91:03:19	58	15	112	29	108	28	22	133
9	91:04:07	91:15:24	134.1	35	112	29	50	13	44	0
10	111:14:33	111:15:53	120.1	31	135	35	54	14	116	0
11	112:14:07	112:15:11	70	18	135	35	43	11	156	133
12	112:17:46	112:18:05	23	06	27	07	63	06	673	0
13	113:14:57	113:16:09	85	22	135	35	58	15	67	0
14	114:14:16	114:15:32	89	23	121	31	85	22	0	0
15	114:17:55	114:18:25	19	05	39	10	58	15	0	0

Table 26. (continued)

EREP PASS NUMBER	TIME PERIOD (DAY:HOUR:MINUTE)		MANEUVER SI TO Z-LV		DURATION OF PASS		MANEUVER Z-LV TO SI		TACS IMPULSE (NEWTON-SECOND)	
	FROM	TO	ANGLE (DEG)	TIME (MIN)	ANGLE (DEG)	TIME (MIN)	ANGLE (DEG)	TIME (MIN)	USED	PRED
16	116:21:14	116:21:58	12	03	62	16	97	25	0	0
17	117:20:32	117:21:12	04	01	62	16	89	23	0	0
18	119:18:48	119:20:07	55	14	124	32	67	33	0	0
19	120:18:07	120:19:03	39	10	66	17	77	20	0	0
20	120:19:54	120:20:36	20	05	73	19	69	18	0	0
21	121:12:58	121:13:32	24	06	60	15	52	13	0	0
22			CANCELLED							
23	121:20:49	121:21:25		08		11		17	0	0
24	122:12:16	122:12:51	27	07	47	22	62	16	0	0
25	122:16:35	122:17:28	65	17	97	25	50	13	0	0
26	122:20:02	122:20:45	27	07	62	16	78	20	0	0
27	123:17:42	123:18:30	35	09	85	22	65	17	0	0
28	123:19:17	123:20:24	31	08	108	28	120	31	22	0
29	124:16:48	124:17:41	74	19	104	27	46	12	0	0
30			CANCELLED							

Table 26. (concluded)

EREP PASS NUMBER	TIME PERIOD (DAY:HOUR:MINUTE)		MANEUVER SI TO Z-LV		DURATION OF PASS		MANEUVER Z-LV TO SI		TACS IMPULSE (NEWTON-SECOND)	
	FROM	TO	ANGLE (DEG)	TIME (MIN)	ANGLE (DEG)	TIME (MIN)	ANGLE (DEG)	TIME (MIN)	USED	PRED
31	125:16:20	125:17:03	65	17	120	31	54	14	0	0
32	125:17:36	125:18:38	93	24	88	22	64	16	22	0
33	126:15:20	126:16:21	66	17	99	31	51	13	22	22
34	126:16:40	126:17:41	131	34	48	15	47	12	0	22
35	127:14:29	127:15:44	97	25	128	33	65	17	0	0
36	128:00:07	128:00:39	50	13	35	09	39	10	0	0
37	128:15:39	128:16:14	54	14	35	09	46	12	0	0
38	129:13:38	129:14:40	50	13	54	14	76	35	0	0
39	129:19:47	129:20:40	46	12	85	22	109	28	0	0
40	130:20:40	130:21:37	52	13	56	14	120	30	0	0
41	130:13:23	131:14:36	73	19	147	38	62	16	22	44

Table 27. SL-4 EREP Maneuver Times, Duration Time, and TACS Usage

EREP PASS NUMBER	TIME PERIOD (DAY:HOUR:MINUTE) FROM	TO	MANEUVER SI TO Z-LV ANGLE (DEG)	TIME (MIN)	DURATION OF PASS ANGLE (DEG)	TIME (MIN)	MANEUVER Z-LV TO SI ANGLE (DEG)	TIME (MIN)	TACS IMPULSE (NEWTON-SECOND) USED	PRED
1			CANCELLED							
2			CANCELLED							
3			CANCELLED							
4	201:16:11	201:17:07	78	20	89	23	43	11	1218	890
5	202:17:10	202:18:05	58	15	87	23	59	15	985	800
6	203:16:26	203:17:03	58	15	43	11	35	9	0	0
7	203:17:59	203:18:37	58	15	50	13	31	8	0	0
8	204:15:47	204:16:21	46	12	46	12	31	8	3545	1308
9	204:17:20	204:17:51	46	12	35	9	30	8		1055
10	205:15:33	205:17:10	17	4	66	17	15	4	703	667
11	206:14:50	206:16:34	38	10*	58	15	20	5	191	111
12	208:13:27	208:15:11	20	5	151	39	19	5	360	445
13			UNSCHEDULED							
14	210:01:11	210:02:55	38	10*	73	19	18	5	2780	609
15	215:22:37	215:00:23	60	15*	73	19	40	10	165	133

*Z-LV OFFSET MANEUVER

Table 27. (continued)

EREP PASS NUMBER	TIME PERIOD (DAY:HOUR:MINUTE) FROM	TO	MANEUVER SI TO Z-LV ANGLE (DEG)	TIME (MIN)	DURATION OF PASS ANGLE (DEG)	TIME (MIN)	MANEUVER Z-LV TO SI ANGLE (DEG)	TIME (MIN)	TACS IMPULSE (NEWTON-SECOND) USED	PRED
16	219:01:15	219:02:51	39	10*	78	20	120	31	187	133
17	219:10:34	219:12:15	39	10*	81	21	66	21	93	222
18	233:11:50	233:14:03	39	10*	124	32	66	17	1014	889
19	235:10:27	235:12:05	19	5	47	12	33	10*	752	889
20	236:19:05	236:20:48	19	5	97	25	58	15*	378	272
21	238:17:42	238:19:20	20	5	101	22	59	15*	307	178
22	239:17:00	239 [illegible]:43	20	5	93	24	57	15*	3794	178
23	240:16:13	240:18:04	39	10	96	24	68	17*	271	111
24	241:15:30	241:17:26	38	10	85	22	157	15*	440	222
25	243:00:11	243:02:25	59	15*	102	26	78	20	640	475
26	243:17:15	243:19:10	38	10	97	25	58	15*	467	445
27	244:16:31	244:18:30	50	13	371	100	38	10	364	182
28			CANCELLED							
29	246:15:10	246:17:13	52	13	385	100	39	10	249	298
30									196	222
31			CANCELLED							

* Z-LV OFFSET MANEUVER

Table 27. (continued)

EREP PASS NUMBER	TIME PERIOD (DAY:HOUR:MINUTE) FROM	TO	MANEUVER SI TO Z-LV ANGLE (DEG)	TIME (MIN)	DURATION OF PASS ANGLE (DEG)	TIME (MIN)	MANEUVER Z-LV TO SI ANGLE (DEG)	TIME (MIN)	TACS IMPULSE (NEWTON-SECONDS) USED	PRED
32	252:18:49	252:19:32	62	16	65	17	39	10	387	445
33			CANCELLED							
34			CANCELLED							
35	253:19:46	253:20:52	50	13	112	29	93	24	943	920
36			CANCELLED							
37	254:17:47	254:19:45	38	10	371	96	47	12	93	0
38			CANCELLED							
39			CANCELLED							
40	256:17:40	256:18:27	19	5	224	58	55	14	44	N A
41	257:15:44	257:17:47	43	11	378	98	55	14	156	22
42	258:18:12	258:20:29	35	09	417	108	77	20	333	467
43			WAS NOT SCHEDULED							
44	259:11:17	259:13:07	34	09	356	92	35	09	280	253
45	259:17:30	259:19:45	35	09	409	106	77	20	329	200
46	260:17:56	266:18:58	58	15	120	31	61	16	1214	1245

* Z-LV OFFSET MANEUVER

Table 27. (concluded)

EREP PASS NUMBER	TIME PERIOD (DAY:HOUR:MINUTE)		MANEUVER SI TO Z-LV		DURATION OF PASS		MANEUVER Z-LV TO SI		TACS IMPULSE (NEWTON-SECOND)	
	FROM	TO	ANGLE (DEG)	TIME (MIN)	ANGLE (DEG)	TIME (MIN)	ANGLE (DEG)	TIME (MIN)	USED	PRED
47	261:16:07	261:18:13	35	09	394	102	58	15	151	89
48	262:15:26	262:17:30	34	09	388	100	58	15	124	22
49	263:14:42	263:16:40	35	09	388	100	34	09	502	533
50	269:15:39	264:17:22	19	05	360	93	19	05	0	0

e. Docking-Undocking. The docking and undocking TACS usage, are given in Table 28.

f. EVAs. TACs usage during EVAs is given in Table 29. For an analysis of some EVAs, see Section VI.C.

3. Conclusions. The actual TACS impulse used during Skylab was more than twice the anticipated amount. A large portion of the TACS fuel used during the mission can be identified as having been used under anomalous operation conditions. However, the TACS usage during nominal operation is consistent with preflight predictions. Most of the difference was due to the thermal attitude requirements which prevented the use of CMG momentum dump maneuvers. Nearly half of the loaded TACS impulse was expended during the thermal attitude phase. TACS usage during EVAs proved to be higher than expected as an apparent consequence of the astronaut suit vents.

During SL-4, TACS expenditures rose following the CMG No. 1 failure. Decreased CMG momentum capability coupled with increased maneuver requirements, especially for Kohoutek observation, placed an added burden on the TACS budget. Mission planners had to minimize TACS usage while allowing full experiment operation. The most significant conservation technique proved to be the noon-to-noon EREP.

Also, several simulators were used to determine TACS requirements during mission planning. The simulators were used to identify situations involving excessive TACS firings and to verify fuel saving alternatives. Because they provided accurate and realistic predictions, the simulations were an invaluable planning tool and were responsible for permitting mission objectives to be met and exceeded.

E. ATMDC Software Program

1. Description. The onboard computer subsystem for the Skylab vehicle consisted of two ATMDCs and a Workshop Computer Interface Unit (WCIU). Each ATMDC contained an input/output adapter 10A and a TC-1 (16K memory) Central Processing Unit (CPU). The 16K memory was configured in two 8K modules. The final 16K Flight Program fully utilized both 8K modules of memory. 16,329 ATMDC memory locations or 99.7 percent were used.

To increase the system reliability a skeleton 8K software system was developed which would provide limited capabilities and occupy only one 8K memory module.

Table 28. Skylab Docking and Undocking

DOCKING	TIME PERIOD (DAY:HR:MIN) FROM TO	TACS (N.Sec.) PREDICTED	USED
SL-2	012:20:24-146:03:58	N A	48,565
SL-3	076:19:09-209:20:07	2624	3634
SL-4	187:21:60-320:22:05	2535	4608
UN-DOCKING			
SL-2	040:06:45-173:08:19	3113	3074
SL-3	135:13:04-268:19:52	0	3905*
SL-4	271:08:30-039:17:15	N A	7784

Table 29. Summary of Total TACS Used During EVA's

EVENT	TIME PERIOD (DAY:HR:MIN) FROM TO	TACS (N.Sec) PREDICTED	USED
EVA NO. 1 SL-2	015:15:24-158:18:47	1334	0
EVA NO. 2 SL-2	037:10:53-170:12:30	0	1090
EVA NO. 1 SL-3	085:15:00- TBS	0	0
EVA NO. 2 SL-3	103:17:13-236:21:20	2980	3718
EVA NO. 3 SL-3	132:13:00-265:14:33	556	427
EVA NO. 1 S1-4	193:21:13-327:03:02	1112	2349
EVA NO. 2 SL-4	226:17:29-360:02:03	3336	17,210
EVA NO. 3 SL-4	239:17:21-363:21:00	8452	16,022
EVA NO. 4 SL-4	266:14:50-034:20:47	6552	4292

*Unscheduled CSM vent

In the event of an address failure where only one module of core memory was affected, the 8K Flight Program could be loaded into the operable module. The 8K Flight Program was resident on the on-board Memory Load Unit (MLU) and thus provided a means of prolonging the useful life of the computer if a failure occurred which incapacitated one of the ATMDCs such that there remained an operable Central Processing Unit and one memory module. The program could then be loaded into the operable memory module via the MLU and exercised normally.

a. 16K Flight Program. The 16K Flight Program's objectives were to provide the following capabilities:

Subsystem Mode Control

Command Processing

Subsystem Redundancy Management

Mission Navigation and Timing

Momentum Management

Attitude Reference Processing

Attitude Control

ATM Experiment Support

Information Display and Telemetry.

The Flight Program, which was modular in design, consisted of two basic software subsystems: the Executive or Control Program and the application subsystems. The Control Program, as the name implies, controlled the sequence of program execution and provided a software priority on executable functions in order to achieve a multitask keying capability. The application subsystems consisted of all application program modules which, when executed by the control subsystem, would perform all required Flight Program functions.

Each Program had an initialization that was executed when power was applied to the computer. This portion of the program initialized the interrupt processing logic, discrete output registers, and data quantities. When initialization was completed, control was given to the executive where tasks were performed based upon relative importance.

Time dependent functions such as slow loop, intermediate loop, and switchover processor were first scheduled by initialization, then rescheduled themselves by telling the executive when they would like to have control. The slow loop started every second, the intermediate loop started every 200 milliseconds, and the switchover processor every 500 milliseconds.

The externally controlled functions, such as telemetry outputs and command system inputs, were processed upon request by interrupting the currently cycling program. The Executive Control Program recorded the location and status of the current program before passing control to the requested function. When the interrupting program was completed, the executive restored the status and returned control to the interrupted program.

(1) Executive Control Subsystem. The Executive Control System consisted of the Executive Program and a common communications areas which allowed for centralization of inter-module communications, common data, and mission dependent parameters. The Executive Program, composed of sub-programs and tables, controlled the executive of application modules, serviced interrupts and routed control to the appropriate application module on a priority basis, and provided utility operations.

The ATMDC Flight Program Executive provided the following capabilities:

Priority multitask support

Interrupt Processing

Interval Timer Support

Time Keeping Support.

Each of these areas will be discussed in detail in the following paragraphs.

(2) Priority Multitask Support. Each application module had an assigned priority level denoting its relative importance with respect to the other application tasks. The execution of a task was keyed (requested) through any of the following means:

The occurrence of a particular interrupt signal

The occurrence of a particular discrete signal

Elapsed Time

Direct request of another application task.

Every application task was executed with the interrupts enabled in order to allow the executive to perform the functions of task keying and task switching. Any task, regardless of its associated priority level, was interrupted when a new task was requested. The executive then entered the requested task into the priority level control tables. If the new task was of a higher priority, it was completed prior to return of control to the interrupted task.

From the individual task point of view, the overall result of the multitask executive capability is as described below:

> Precise task initiation occurs with only the limitation that higher priority processing will be accomplished first.
>
> Task may be interrupted for short durations to accomodate task keying. These interrupts are transparent to the interrupted task in that all information required for restoration is automatically provided.
>
> Temporary suspension of a task can occur in order to accomplish a higher priority task.

(3) Interrupt Processor. The Executive Program provided the capability to process the following interrupts defined for the ATMDC Flight Program:

Interval Timer

24 PPS Telemetry

Command Enable

Command Execute

24 PPS Telemetry Backup

1 PPS Telemetry

Command Enable Backup.

Upon occurrence of any of the interrupts, program control was passed automatically by the ATMDC hardware to the program's interrupt processor. The interrupt processor determined the interrupt source and performed the following functions:

Obtained the tasks to be executed from the Interrupt Control Table entries.

Provided for simpler maintenance or alteration as requirements were changed.

Provided a framework for progressive levels of testing.

Permitted addition of new modules as new requirements were defined.

Allowed control to lowest level during program development.

(4) Application Subsystem. An application module is defined as a program unit exclusively designed to perform one or more associated functions. Module execution is governed by the Executive Control Program either directly (the module is called by the executive) or indirectly (the module is called as a subroutine by a module which was called by executive). When entered, each module will perform its function and return control to the executive or to the calling module. Through the use of macros, an application module may request re-execution at some future time or may request execution of another module.

For a more complete description of these subsystems, this area has been further sub-divided into the following categories:

Time Dependent Sequence Functions

Asynchronous Functions

Utility Functions

(5) Time Dependent Sequenced Functions. These applications modules, (i.e., program units specifically designed to perform one or more associated functions), fell in the category that utilized system task queue capability of the Executive or Control Program. Those functions that were time dependent and sequence oriented were included in four categories:

Slow Loop - involved the execution of all functional requirements which must be performed at a cyclic rate of approximately once per second.

Intermediate Loop - involved the execution of all functional requirements which must be performed at a cyclic rate of approximately five times per second.

Output Write - during each intermediate loop, attitude control signals were calculated which must be issued at a rapid rate. Due to hardware limitations, these outputs were spaced between intermediate loops to effectively utilize the input/output converters.

Switchover Controller - to insure the TMR timer in the WCIU did not count to zero, and thus initiate computer switchover, the switchover control maintained the TMR timer approximately once per second. If no self-test computer errors occurred, the timer was loaded to full value so that automatic switchover did not occur.

(6) Asynchronous Functions. All areas of the Flight Program which responded to or were entered on the receipt of an external signal were called asynchronous functions. The following modules were classified as asynchronous functions:

Telemetry Processor - the Flight Program output fifty bits of digital data from the ATMDC to the telemetry system 24 times per second. To synchronize this operation, two external signals from the telemetry system generated interrupts to the ATMDC. Recognition and receipt of the interrupts caused the Flight Program to execute the Telemetry Processor which output the data.

Command System - the Command System provided a communication link between the ground station and the Flight Program and also provided an astronaut interface through the Digital Address System (DAS).

(7) Utility Functions. Various common functions to be executed as subroutines from the various application modules were known as utility functions. The following is a list of utility functions utilized in the 16K Flight Program:

Square Root

Sine/Cosine

Arctangent

Matrix Multiply and Matrix Product

Vector Dot and Vector Cross Products

Scaled Divide

Quaternion Multiply

Alert Display Indicator Update

Gimbal Angle Computation

Double Precision Multiply

Limit Routine

Status Word Set/Reset

(8) Computation Cycle Profile. Figure 24 is a representation of a typical 16K Flight Program computation cycle.

Level 1. Experiment input data, CMG gimbal rates, WCIU wrap tests and Command System processing was done on this level.

Level 2. Telemetry outputs were issued on this level.

Level 3. Switchover timers were reset once per second and the 64 bit transfer register was loaded approximately every 17 seconds at this level.

Level 4. The intermediate loop which was made up of strap-down and CMG control was executed 5 times per second on this level. The once per second TACS module also ran on this level.

Level 5. The slow loop was cycled once per second on this level. Timing, navigation, mode logic, maneuvering, momentum

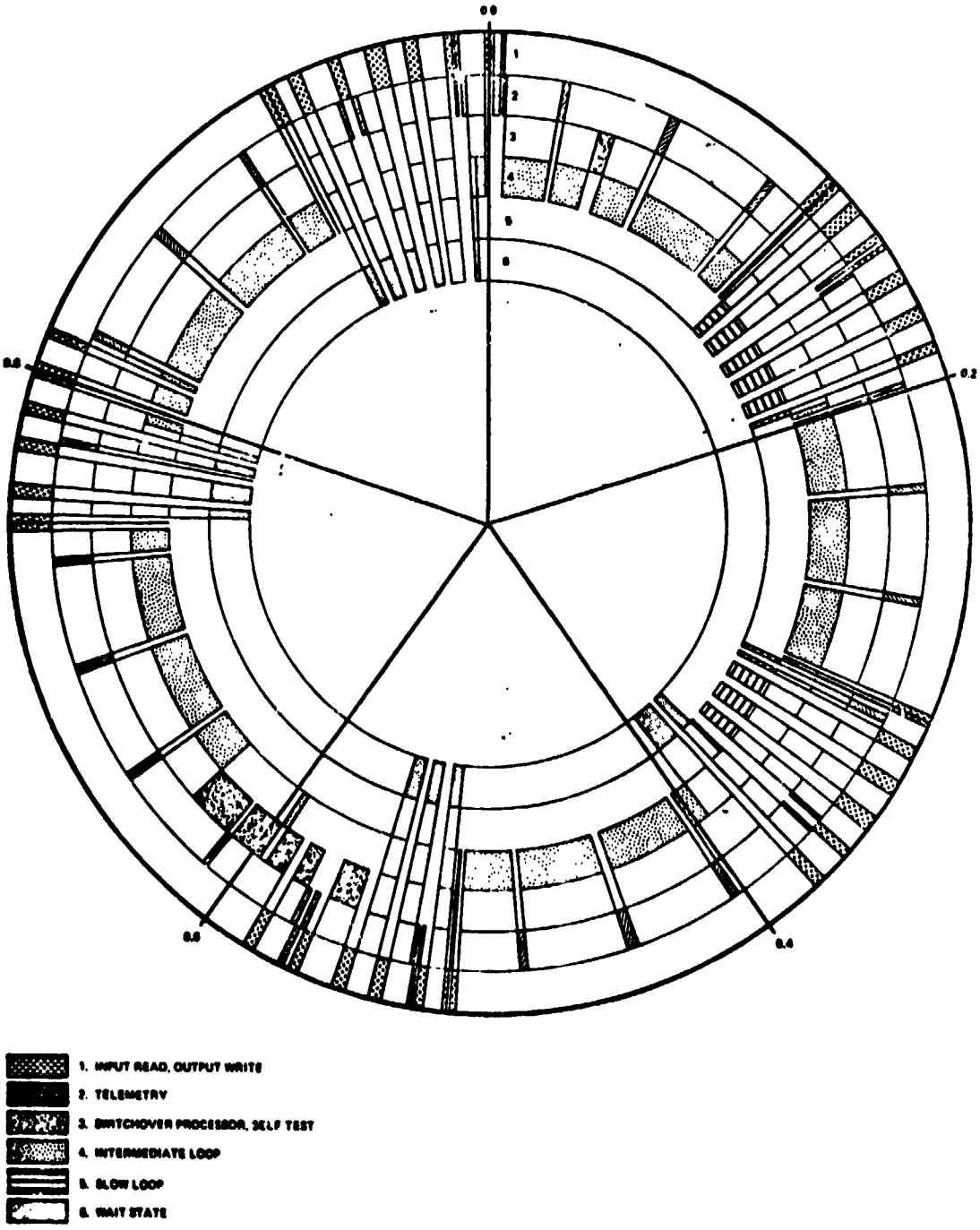

Figure 24. 16 K Flight Program Computation Cycle

management, display control, redundancy management, self test, and experiment support made up the slow loop modules.

Level 6. When all computations were finished, the Program entered the "WAIT" state from Level 6.

The final Program had an 85% duty cycle or 15% "WAIT" state. This meant that 15% of the time the Program had no tasks to perform and the ATMDC was in a "reduced power consumption" mode.

b. 8K Flight Program. The objectives of the 8K Flight Program were to provide the following functions for the Skylab mission:

Critical parameter monitoring

Attitude reference processing

Attitude control

Subsystem mode control

ATM experiment support

Mission navigation and timing

Information display and telemetry

Command processing.

The 8K Flight Program was modular in design and consisted of two basic software subsystems: the Executive, which was identical in operation to the 16K Flight Program, and the application subsystems. The Executive controlled the sequence of program execution and provided a software priority on executable functions in order to achieve a multitask keying capability. The application subsystem consisted of the applicable 16K Flight Program modules modified to meet the memory size constraints.

The operating characteristics and modes were in essence analogous to those discussed in the 16K Flight Program section. The 8K Flight Program had an Intermediate Loop and Slow Loop and handled Command System and Interrupt processing as required.

Most of the applicable 16K Flight Program routines used in the 8K Flight Program were modified in order to reduce their memory size to a level where the Program could meet the 8K memory requirements.

Figure 25 is a representation of a typical 8K Flight Program computation cycle.

2. Design Development. In order to allow an orderly build-up of the ATMDC software system a three phase Flight Program development schedule was established. These phases, namely Phase I, Phase II, and Final, were configured following the criterion that each phase would be baselined and developed on the preceding phase, thus providing the necessary documentation and testing on each segment. However, due to a significant amount of requirements changes/additions after the Phase I baseline, an additional phase (Phase IA) was scheduled to come between Phase I and Phase II, thus alleviating a portion of the problems encountered with the Phase I program schedule. Additionally, a requirement from the Johnson Spacecraft Center (JSC) was introduced which requested a "best available" Flight Program delivery between Phase I and Phase III for use in crew training procedures. The following paragraphs briefly describe each of the four phases with respect to:

General software requirements

Changes/additions to requirements

Sizing/timing estimates

Schedules

Impacts of requirements modifications.

a. Phase I Flight Program (16K). The baseline PDD for the Phase I 16K ATMDC Flight Program was released on November 4, 1970. The Phase I software was generated according to the specifications in this document, addended by subsequent changes in requirements which were approved by the Software Review Board (SRB). The Phase I program consisted of the following functional elements.

Discrete I/O and interrupt processing

Command system processing

Initialization

Redundancy management

Attitude reference determination

Attitude control

Mode Control

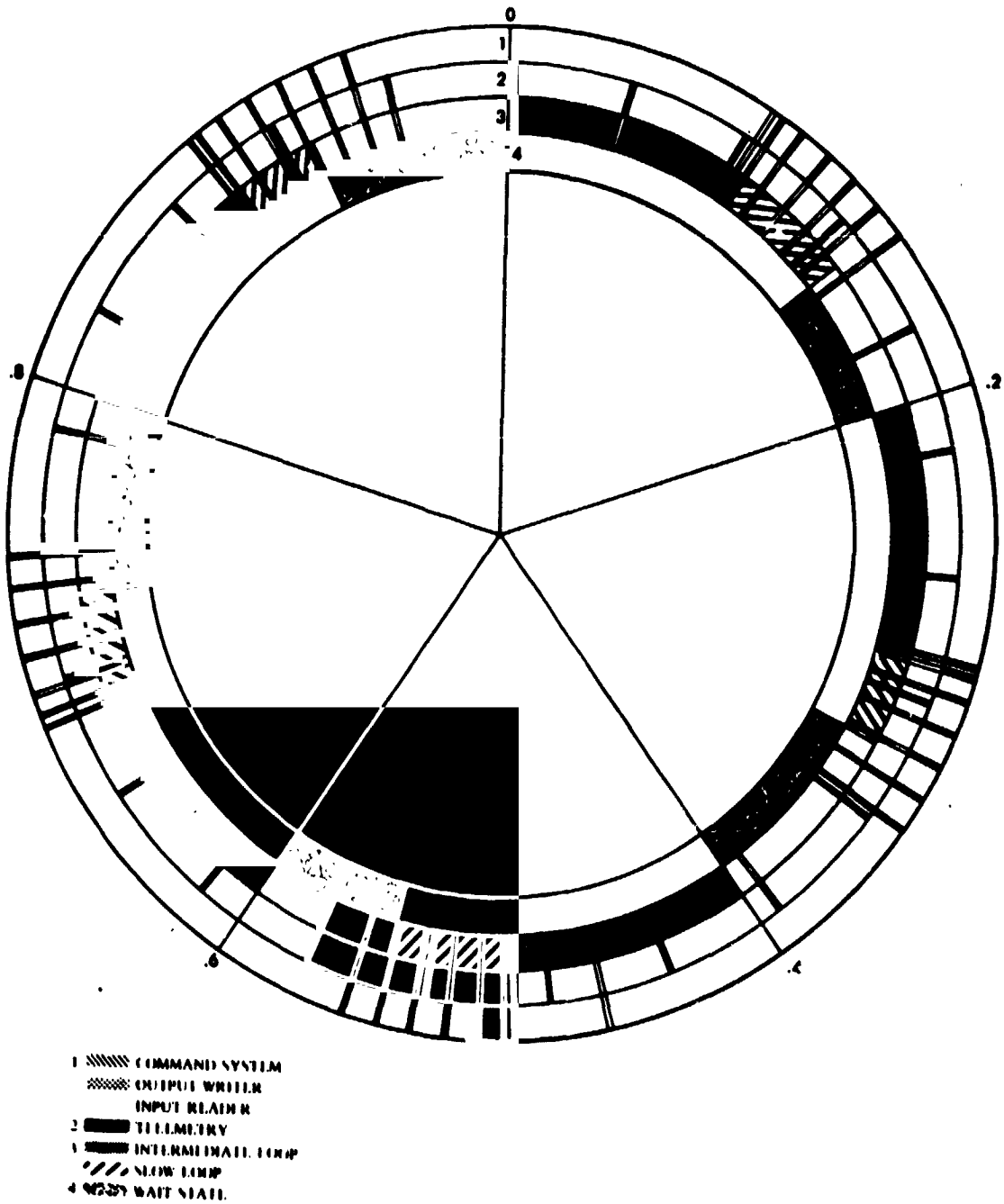

Figure 25. 8K Flight Program Computation Cycle

Momentum desaturation

Maneuvering

Navigation and timing

ATM experiment control

Display

Telemetry

Algorithms.

This version of the Flight Program occupied 16,224 memory locations in the ATMDC (or approximately 99%) and had a duty cycle of 73%. The Program was released for verification on June 23, 1971, with a projected delivery date (to NASA) of October 4, 1971. These Program milestones were based on a requirements change cutoff of April 23, 1971, with all subsequent changes to be incorporated in the Phase II Program. However, changes to the baseline requirements prior to the April 23 cutoff date had necessitated four revisions to the PDD, and six additions; PDD revisions had been released by the October 4 delivery date. Due to this large number of changes, and the prospect of significantly more changes before delivery of the Phase II Program, the decision was made to add an intermediate program release, called the Phase IA Program, to be delivered on February 9, 1972.

(1) Phase IA Flight Program (16K). The Phase IA ATMDC Flight Program development was begun on September 15, 1971, utilizing the Phase I Program scheduled for delivery on October 4, 1971 as a baseline, the forty-five (45) waivers which were written against the Phase I Program, as well as all requirements changes introduced through Revision 13 of the PDD. A requirements update on August 31, 1971 concluded the changes to be implemented on the Phase IA Program. A total of 105 Software Change Requests (SWCRs) were incorporated into this program. Major requirements changes in critical program areas such as strapdown reference, CMG control, mode logic, maneuvering, navigation and timing, TACS control, Star Tracker control, and Redundancy Management were implemented in this version. To summarize, approximately 40% of the Flight Program logic was modified as a result of requirements change and/or problem correction in the Phase IA release. Six separate internal deliveries were made for program verification activities during development of this program, and final delivery to NASA was made on February 9, 1972. This program occupied 16,111 locations in the ATMDC memory (approximately 98.3%), and had a duty cycle of 90%.

(2) Phase II Flight Program (16K). The original development schedule for the Phase II 16K ATMDC Flight Program assumed that the Phase I Program would be utilized as a baseline for the Phase II version. However, introduction of the Phase IA software necessitated a change in scheduling, and hence the Phase IA Program was used as a baseline in lieu of the Phase I version. The extended implementation period for the Phase II Program (beginning July 23, 1971 and ending June 19, 1972) was due to impacts from both the Phase IA development and the large number of requirement modifications. As a result, the Phase II baseline consisted of the Phase IA Program plus implementation of forty-nine (49) Software Change Requests, and thus included all requirements changes contained in Revision 14 of the PDD. The program was released for verification on June 19, 1972. Additional requirements contained in the delivered program included implementation of 102 additional SWCRs (through PDD Revision 19), all waivers written against the Phase IA Program, and thirty-eight (38) Program Trouble Reports (PTRs) written against the Phase IA Program. Major differences between the Phase IA and Phase II Programs were in the areas of command system processing, initialization, redundancy management, maneuvering, momentum management, CMG control, TACS control, experiment support, and displays. These changes resulted in a software system which occupied 16,338 locations of ATMDC memory (99.7%), had an 85% duty cycle, and required approximately 35% change in program code.

(3) Final Flight Program (16K). The Final 16K ATM Flight Program, as in the preceding programs, utilized the previously delivered version (Phase II, in this case) as a baseline and developed from there. Four distinct levels of the Final Program were released. The first, designated FF32, was released to NASA on December 4, 1972, for use in Software Integration Tests (SIT) and All-Systems Tests (AST) at KSC. The three subsequent releases, designated FF40, FF50, and FF60, were delivered to NASA on January 26, February 16, and March 20, 1973, respectively. The final delivery, FF60, was the version which was loaded into the ATMDC for the launch of the Skylab vehicle on May 14, 1973. This version was developed by utilization of the Phase II Program as baseline, implementation of seventeen (17) SWCRs, and implementation of twelve (12) PTRs. Major areas of the software which were modified between the Phase II and the Final Program included mode logic, experiment support, CMG control, Redundancy Management, navigation, self test, command system processing, and data modules. Requirements changes reflected in Revisions 20,21, and 22 of the PDD were included in the modifications. The Final Flight Program used 16,329 ATMDC memory locations (99.7%) and had a duty cycle of 85%.

b. 8K Flight Program. The onboard computer subsystem for the Skylab vehicle consisted of two (2) ATMDCs and a Workshop Computer Interface Unit (WCIU). Each ATMDC contained an Input/Output Adapter (IOA) and a TC-1 Central Processing Unit (CPU) with a 16K memory. The 16K memory was configured in two (2) 8K modules (module 0 and module 1), with both modules addressable by the CPU. Due to the length of the mission, the computing load, and other factors, the reliability of the computer subsystem was 0.87. To increase the reliability, a software system was conceived which would provide limited capabilities, occupy only one 8K memory module, and increase the reliability factor to 0.97. To implement the 8K software system, two modifications to the ATMDC were necessary:

The capability to force the ATMDC to address module 1 only

The addition of a Memory Load Unit (MLU) to enable loading of the ATMDCs without active participation by the resident computer program.

This software system was developed only as a contingency program, and was designed to provide stable attitude control, allow continuation of solar experiment activity and data collection, and other functions as allowed by memory constraints.

Althouth two versions of the 8K ATMDC Flight Program were released, they were both developed from the same baseline model. The requirements were generated, starting November 15, 1971, by modification of the Phase IA 16K Flight Program. Specifications in the form of a PDD were subsequently baselined on April 3, 1972. The programming effort was actually begun on December 1, 1971, with logic changes being terminated on April 25, 1972, and data changes being terminated on June 6, 1972. Interim versions of the 8K Program were delivered to JSC for testing on August 15, 1972 and September 22, 1972. The first official release to NASA was made on November 14, 1972, after ten (10) weeks of verification testing by IBM. This 8K Program release implemented requirements in the major functional areas of :

Discrete I/O and interrupt processing

Command system processing

Initialization

Attitude reference determination

Rate Gyro Redundancy Management

Attitude control

Mode control

Maneuvering

Navigation and timing

ATM experiment support

Displays

Telemetry

Algorithms.

Although the differences between the major functional areas of the 16K and 8K Programs are few, the 8K Program offered reduced capabilities in those common functions, when compared to the 16K Program. In addition to the baseline PDD, forty-six (46) SWCRs (reflecting requirements changes) were implemented in this version of the 8K Program. This program used 7,884 locations of ATMDC memory (96.2%) and had a duty cycle of 73%.

A subsequent contingency delivery was made February 15, 1973, which provided updated capabilities in Redundancy Management, maneuvering, display, experiment support, and command system processing. This version of the 8K Program occupied 8,001 ATMDC memory locations (97.7% of total available) and had a duty cycle of 73%. Requirements changes documented in nine (9) SWCRs were implemented in this program.

3. Software Verification.

a. Test Descriptions. Ten weeks prior to each scheduled delivery date, a formal verification phase was initiated. This verification effort was directed toward verifying the accuracy and adequacy of the Flight Program to guarantee that it meets mission requirements and conforms to program specification. Both logic tests and performance tests were made to accomplish that goal.

b. Logic Tests. Each program for each phase, 16K and 8K, was subjected to a rigorous set of logic cases to check every logic path through the program, every data constant specified, and the accuracy of each calculation. The System/360-75 Simulator was utilized extensively for this effort, with a more limited use of the System.360-44 Simulator and the HSL.

c. Performance Tests. The performance testing was accomplished primarily on the Final Program with subsets run on earlier programs. The performance tests were divided into two categories, general performance and mission requirements. The HSL and, to a lesser extent, the System/360-44 Simulator were used for these tests. The general performance cases were used to demonstrate that the Flight Program was capable of proper functioning under the adverse environments, for which it was designed to compensate, that it might experience during the actual Skylab mission. The philosophy used in the design of this verification was to simulate as many variations of program input perturbations and off-nominal situations as could be conceived and classified as realistic possibilities. The ultimate purpose of this effort was to create, detect, and isolate at system level (all functions in operation) the following types of problem areas:

Unusual program execution sequences

Function interference due to unexpected timing situations

Parameter scaling overflows associated with equation input extremes.

The mission requirements performance cases were to demonstrate that the ATMDC Flight Program was capable of meeting all of its function requirements with respect to the planned overall mission objectives and activities for the entire mission duration. The approach used in the design of the verification cases was to identify the mission time frames and vehicle configurations (nominal and perturbed) that would place the maximum stress on the ATMDC software system. One of the major areas of interest associated with execution of these performance studies was attainment of the knowledge that the Flight Program scaling was adequate for the computational loads that would be experienced during the various phases of the Skylab mission. This was accomplished through analysis of data on the yearly variation of Skylab navigation data and experiment reference angles and star availability data for the entire mission. Orbits containing worst case combinations of these parameters were "flown" in a simulated environment using an actual Flight Program in a real (as opposed to a simulated) ATMDC. Anticipated external torques that might be experienced by the Skylab vehicle during each phase of the mission were included if they were applicable to the flight segments simulated. The average duration of the cases defined for this phase of Flight Program verification was six orbits. This, in general, allowed for one or two orbits with the vehicle positioned in the

desired test configuration and four or five orbits in the normal Solar Inertial configuration for evaluation of control system transient recovery. The following types of cases were run and analyzed:

CSM/Skylab rendezvous and docking

Earth Resources Experiment Pointing (EREP)

All daylight orbits

CSM/Skylab undocking

Rescue mission

Maneuver effects of performance.

4. Software Operation. Prior to Skylab launch a number of "what if" situations were identified and 24 software patches were developed as solutions to these situations. Table 30 lists the routines developed during this period.

During the mission, as problem areas were identified, the procedures developed for prelaunch were utilized to develop solutions. Table 31 lists those SWCRs defined for delivery after the launch, including their disposition. There were fourteen canned routines implemented during the Skylab mission. Three routines were implemented for a second time after the commanded ATMDC switchover (DAY 27) from the primary computer to the secondary. Seventeen canned patches were implemented. In all cases, the DCS memory load was implemented with no problems.

A brief description of each implemented patch follows:

S3013 - Implemented into Secondary on 16 Dec. 73. The purpose of this patch to the Flight Program was to reset and re-enable all runaway interrupt protection tests and to re-enable the capability to use all external interrupts if the runaway interrupt condition could be fixed or if it was only transitory.

S3029 - Implemented in Primary on 8 June 1973. Implemented in Secondary on 11 June 1973. Purpose to provide new vehicle data to represent SAS position II deployed at 90 degrees, SAS position IV gone; solar shield deployed and SWS CSM docked (at port V) and SWS undocked.

Table 30. Prelaunch Canned Patches

SWCR #	DELIVERED DATE	TITLE	DISPOSITION PRIOR TO LAUNCH
S3001	4/26/73	Sumcheck Tests Disable	Available
S3002	4/26/73	Sumcheck Test Re-Enable	"
S3003	4/26/73	Re-Enable TACS Transfer Testing	"
S3004	4/26/73	DI709 Only for TACS Transfer Test	"
S3005	4/26/73	DI713 Only for TAC Transfer Test	"
S3006	4/26/73	Ripple Test Failure Identification	"
S3007	4/26/73	Complete DIR6 Mask	"
S3008	4/26/73	CSM Docking in Port 3, Vehicle Data	Disapproved
S3009	4/26/73	Select Primary DC Input Multiplexer	Available
S3010	4/26/73	Select Secondary DC Input Multiplexer	"
S3011		Select Primary AC Input Multiplexer	"
S3012		Select Secondary AC Input Multiplexer	"
S3013	4/26/73	Reset Runaway Interrupt Protection	Available
S3014	4/26/73	Reset Rate Gyro Scale Switch Inhibit	"
S3015	4/26/73	ATM Failure to Deply-TACS Only	"
S3016	4/26/73	Reset Canned Routine S3015	"
S3017	4/26/73	TACS Only Contingency Mode	"
S3018	4/26/73	Select Coarse Rate Gyro Gain	"
S3019	4/26/73	Select Fine Rate Gyro Gain	"

Table 30. (continued)

SWCR #	DELIVERED DATE	TITLE	DISPOSITION PRIOR TO LAUNCH
S3020	4/26/73	ATM Failure to Deploy-CMG/TACS	Available
S3021	4/26/73	Reset Canned Routine S3020	"
S3022	4/26/73	TACS Control Transfer Test Disable	"
S3023	(Prepared after Launch)		
S3024	4/26/73	Change FF50 to FF60 Status	Available

Table 31. Patches Developed During the Mission

SWCR #	DATE DELIVERED	TITLE	FINAL DISPOSITION
S3025		Allow SI Operations for Offset Attitudes	Verified but Cancelled
S3026		Restrict TACS to MIB Firing	Verified but Cancelled
S3027		Reset SWCR 3026	Verified but Cancelled
S3028		New Docked Vehicle	Verified but Cancelled
S3029	Day-24	New Vehicle Data - SASII Deployed	Implemented in Primary Day 26
S3029	Day-24	New Vehicle Data - SASII Deployed	Implemented in Secondary Day-29
S3030	Day-24	Strapdown Updating	Implemented in Primary Day-26
S3030	Day-24	Strapdown Updating	Implemented in Secondary Day-29
S3031		Rate Gyro Drift Compensation	Verified and Cancelled
S3032	Day-21	Y-3 Rate Gyro Scale Factor Compensation	Implemented in Primary Day-22
S3032	Day-21	Y-3 Rate Gyro Scale Factor Compensation	Implemented in Secondary Day-28
S3033	Day-38	Y-2 Rate Gyro Scale Factor (R.G. Scale Switch Limits)	Implemented in Secondary Day-39
S3034	Day-86	Reset Rate Gyro Scale Switch Inhibit	Implemented in Secondary Day-103

Table 31. (continued)

SWCR #	DATE DELIVERED	TITLE	FINAL DISPOSITION
S3035		Select Fine Rate Gyro Scale	Verified Day-86 Available
S3036	Day-86	Select Coarse Rate Gyro Scale	Implemented in Secondary Day-92
S3037	Day-100	Set all Y Rate Gyro Scale Factors to One (1)	Implemented in Secondary Day-103
S3038		X_1, Y_1, Z_2 with 6 Pack (Via J6)	Cancelled
S3039		X_1, Y_2, Z_2 with 6 Pack (Via J6)	Cancelled
S3040	3/15/73	Correction of Timing Accumulation	For Sim Use Only
S3041	4/30/73	1 PPS Backup for Memory Dump	For Sim Use Only
S3042	4/9/73	DI601/602 Reset Mask	
S3043		6 Pack Misalignment Quaternion (J3)	Verified Day-86 Available
S3044	5/12/73	Patch for Location $01FE_{16}$ Failure - Sim Use Only	
S3045		6 Pack Misalignment Quaternion (J6)	Cancelled
S3046		X and Z Rate Gyro Scale Factors	Verified Day-86 Available
S3047		Reset S3037/S3038/S3039	Cancelled
S3048		Use $_{ZE}$ for GG Dump and Nominal Cage	Verified Day-86 Available

Table 31. (continued)

SWCR #	DATE DELIVERED	TITLE	FINAL DISPOSITION
S3049		Inhibit J6/Software Interface	Cancelled
S3050		Reset S3049	Cancelled
S3051	Day 86	Y System Momentum Test Constant	Available
S3052	Day 86	Reset S3051	Available
S3053		Y Axis Control without Rate Gyros	Verified Day 138 Cancelled Day 189
S3054		Reset S3053	Cancelled
S3055		SWS Control with No Rate Gyros	Cancelled
S3056		Reset of S3055	Cancelled
S3057	Day 96	Y/Z System Momentum Test Constants	Available
S3058		Reset S3057	Prel.SWCR Only
S3059		X,Y,Z Rate Gyro Scale Factors	Verified Day 94 Available
S3060		Reset Rate Gyro Scale Switch Inhibit	Verified Day 94 Available
S3061	Day 96	Reset Rate Gyro Scale Switch Inhibit	Available
S3062		X-Axis Control without Rate Gyros	Verified Day 152 Cancelled Day 191
S3063		Reset of S3062	Cancelled
S3064		Rate Gyro Scale Switching Limits	Verified Day Cancelled Day 191
S3065	Day 106	Data for Star Rigil Kent	Implemented in Sec. Day 107
S3066	Day 108	X_3Rate Gyro Multiplexer Definition	Implemented in Sec. Day 109

Table 31. (continued)

SWCR #	DATE DELIVERED	TITLE	FINAL DISPOSITION
S3067		Primary ATMDC Updates	Verified Day 116 Cancelled Day 193
S3068		X1 Rate Gyro Multiplexer Definition	Verified Day 120 Available
S3069		Y1 Rate Gyro Multiplexer Definition	Verified Day 120 Available
S3070		Z_1 Rate Gyro Multiplexer Definition	Verified Day 120 Available
S3071		6 Pack Power Failure Detection X Axis	Verified Day 164 Cancelled Day 189
S3072		6 Pack Power Failure Detection Y Axis	Verified Day 138 Cancelled Day 189
S3073		6 Pack Power Failure Detection Z Axis	Defined Day 145 Further Scheduling Not Performed
S3074		Z Axis Control Without Rate Gyros	
S3075		Reset S3074 and S3073	
S3076	Day 136	Changes for Kohoutek Pointing	Implemented in Sec. Day 189
S3077		GG Dump for X-Axis Derived Rates	
S3078		GG Dump for Y-Axis Derived Rates	
S3079		Additional Kohoutek Pointing Changes	Delivered to MSFC Sim Use Only
S3080		Rate Gyro Drift Compensation	
S3081	Day 178	Roll Reference Update	Implemented in Sec. Day 189
S3082		Select Coarse Rate Gyro Scale	Verified Day 177 Cancelled Day 189

Table 31. (continued)

SWCR #	DATE DELIVERED	TITLE	FINAL DISPOSITION
S3083		Reset Rate Gyro Scale Switch	Verified Day 177 Cancelled Day 178
S3084	Day 193	Update Primary ATMDC	Available
S3085		Post SL-4 Navigation & Timing Changes	Verification Cancelled Day 249
S3086	Day 197	TACS Only Contingency Mode	Available
S3087	Day 197	Single CMG Control Law	Defined Only. Cancelled Day 213
S3088		Acceleration Limit for CMG Gimbals	Cancelled Day 213
S3089	Day 215	Revised TACS Only Selection Logic	Implemented in Sec. Day 218
S3090	Day 215	TACS Only Contingency Mode	Available
S3091	Day 220	Gimbal Rate Limits During GG Dump	Implemented Day 222
S3092	Day 220	TACS Only Contingency Mode	Available
S3093	Day 222	Update Primary ATMDC to FF80	Available

S3030 - Implemented in Primary on 8 June 1973. Implemented in Secondary on 11 June 1972. Patch updated R_{EV}, f_t and TACS MIB pulse width for initialization so as to reflect changes in these quantities since launch and to prevent undue errors in the event of computer switchback. Additionally, strapdown, primary and backup, references were to be updated with the Acq. SS during Rate Gyro failure isolation. This was to prevent destruction of the primary strapdown (due to current Acq.SS strapdown updates) while on the backup strapdown and to prevent loss of backup reference due to use of gyros with large drift rates.

S3032 - Implemented in Primary on 4 June 1973. Implemented in Secondary on 10 June 1973. Patch modified the No. 3 Y-axis Rate Gyro scale factor compensation. Flight data indicated approximately a 6% high scale factor error on the No. 3 Y-axis Rate Gyro. The compensation was to prevent Y-axis Rate Gyro failure during maneuvers.

S3033 - Implemented in Secondary on 21 June 1973. Patch modified No. 2 Y-axis Rate Gyro scale factor compensation for an approximately 6.9% high error and was for the purpose of preventing Y-axis Rate Gyro Failure during EREP maneuvers. This routine also changes Rate Gyro scale switching limits to 0.088 deg/sec for coarse scale selection and .078 deg/sec for fine scale selection in order to allow scale switching initiation by Rate Gyros which have been compensated for large scale factor (5.2%) and drift (18 deg/Hr.) errors.

S3036 - Implemented in Secondary on 13 August 1973. This patch modified the Flight Program to select coarse Rate Gyro scale, to inhibit further scale switching and scale switching verification and to limit control parameters accordingly. The patch was expected to be used in the event of a scale switching error.

S3034 - Implemented in Secondary on 24 August 1973. This patch was to re-enable previously inhibited scale switching logic and to restore control parameters to original values in the

event the scale switching failure condition could be fixed or if it was transitory. The patch was used, in this case, to reset S3036 implemented on 13 August 1973.

S3037 - Implemented in Secondary on 24 August 1973. This patch set all Y-axis Rate Gyro scale factor compensation terms (G_{1Y}, G_{2Y}, G_{3Y}) to unity. This patch was needed, at the time of the Rate Gyro Six-Pack installation, to facilitate calibration of the scale factor errors for the new Gyros.

S3065 - Implemented into Secondary on 28 August 1973. This change modified the Flight Program to replace the Alpha Crux star coordinates with those of Rigil Kent after the Star Tracker could no longer acquire Alpha Crux.

S3066 - Implemented into Secondary on 30 August 1973. This patch required the X_3 Rate Gyro input to be read using the backup input multiplexer. This change reconfigured the Rate Gyro/Input Multiplexer relationship to the initial one of Gyros 1 and 3 on the backup multiplexer and Gyro 2 on the primary multiplexer. With this change, Six-Pack Rack Gryo redundancy and multiplexer redundancy could be provided by selecting Gyros 2 and 3 in each axis. Also, the Gyro Multiplexer relationship was properly configured for 3 Gyro operation if the Six-Pack single point failure in the power input was solved on SL-4.

S3076 - Implemented in Secondary on 18 November 1973. This routine changed the DAS/DCS "Maneuver Bias" command to provide 0.01 degree Least Significant Bit (LSB) instead of 0.1 degree LSB. The routine also changed the Solar Inertial offset pointing limit from 4.0 degrees to 5.2 degrees. This was done to provide increased SI mode offset pointing resolution and range to provide pointing accuracy for observing the comet Kohoutek.

S3081 - Implemented in Secondary on 18 November 1973. This patch redefined the computation of parameters in the roll reference and orbital plane

error calculations so as to allow changes in the angle between the vehicle X-axis and the orbital plane due to GG dump maneuvers to update the value of roll reference and to allow changes due to orbital precession to be reflected in the roll reference.

S3089 - Implemented in Secondary on 17 December 1973. This routine changed the program I.D. to $FF80_{16}$. Functionally, the TACS Only control selection logic was redefined to effect TACS fuel savings if TACS conditions were met during the maneuvers by allowing the crew/ground to command a maneuver instead of having the system automatically select TACS Only. This change also relieved the crew monitoring requirements for APCS maneuvers.

S3091 - Implemented in Secondary on 21 December 1973. This routine modified the Flight Program to provide smaller CMG wheel bearings by limiting the rate of movement of the CMG spin axis during GG Dump. When the APCS was in the Solar Inertial or Experiment Pointing mode and a CMG reset was not in progress and GG Dump was active within the last 200 seconds, the rate of change of the momentum vector was limited to 2 deg/sec. At all other times, the limit was 4 deg/sec.

5. Conclusion. The ability to modify or patch the existing Flight Program proved to be highly advantageous. This capability enhanced survival of the Skylab and made it possible to support the new program objectives related to Kohoutek. Many of the routines were imperative for a successful mission.

F. Redundancy Management

Due to the length of the Skylab mission and because it was a manned mission, considerable emphasis was placed on reliability. A high level of confidence was obtained in the APCS by the use of high reliability components as demonstrated by previous use and/or qualification tests and by the use of redundancy. The design philosophy was that no single point failure would jeopardize mission success and no double failure would endanger the crew. Sneak circuit analysis of all circuitry was performed to insure that no circuit paths existed which caused an unwanted function or inhibited a wanted function.

The Redundancy Management philosophy was that primary APCS mission critical systems would be monitored and managed automatically, utilizing the Flight Program and backed by a manual switching capability. Failures which would cause loss of thruster fuel, loss of attitude reference, or loss of control were detected and eliminated by automatic Redundancy Management. Automatic Redundancy Management was required because of the rapid response time needed to recognize and correct a failure. Rapid response was necessary to prevent endangering the crew or jeopardizing the mission. Automatic response was necessary due to the possibility of a failure occurring during LOS while unmanned. Capability existed to inhibit all or portions of the automatic redundancy program. The less critical systems were monitored manually by the astronauts using the C&D Panel and by ground support using the telemetry link. Manual Redundancy Management switching capability existed via the C&D Panel and the DAS/DCS.

To insure the integrity of the Flight Program, an ATMDC self-check capability was included. To increase the reliability of the computer system the ability to reload the ATMDC from the memory load unit or via the RF link was included. A skeleton program capable of fitting in one 8K Memory Module was provided to maintain limited use of the ATMDC during flight should a failure occur which precluded the use of the 16k Program.

1. Automatic Redundancy Management.

a. Description. Automatic Redundancy Management of mission critical components consisted of the following:

(1) Rate Gyro Redundancy Management. The APCS contained nine vehicle Rate Gyros, three per axis, in a pair and a spare configuration. Two RGs were averaged for control and the third was powered up with the wheel not spinning. RG outputs were monitored by the ATMDC for failure detection, isolation, and RG reconfiguration. DAS/DCS commands were provided as a backup for controlling RG configuration.

All classes of Rate Gyro failures such as scale factor, drift, full-on, zero, etc., were detected by comparison of the rate integrals from the controlling Gyros in each axis. RGRM testing was performed once per second for all axes. The test constant developed included a constant noise factor of 0.5 degree, a drift factor of 0.005 deg/sec. and scale factor compensation of 2% of the "prime" gyro integral. This test was used in failure detection both for the three Gyro and two Gyro configurations. A momentum reasonableness test was used for single Gyro failure detection, along with reasonableness testing from Acquisition Sun Sensor and Star Tracker information.

Failure isolation in the three Gyro case involved spinning up the spare Gyro and using its output as a standard for comparison with the control Gyros. During two Gyro operation, post failure detection processing included additional logic for determining the adequacy of the controlling strapdown. For the Z-axis, this test involved a comparison of the actual vehicle X-axis to orbital plane displacement to a software calculated estimate. For the X and Y-axes, this involved a check to insure that the sun was being viewed by the Acq.SS during periods when it should have been as determined by software equations. This logic was also used for failure detection in a single Gyro configuration.

Logic was designed into RGRM to prevent a control catastrophe from occurring during RGRM post failure detection processing. This involved maintaining redundant strapdown references, each of which used one of the presently designated "control" Gyros for input data. A concurrent test was made to monitor measured system momentum change versus expected change over the test period. A test failure would result in switching control to the backup strapdown if available, or inhibiting control in the affected axis if a switch to backup strapdown had already occurred.

(2) CMG Redundancy Management. Three CMGs and CMGIAs were used for redundancy although only two were required for control. Determination of when a CMG was to be removed from control, CMG shutdown and Control Law reconfiguration were managed automatically by the ATMDC. Capability to power UP/DOWN the CMG and to control the CMG sheel was provided by C&D Panel switches and by Switch Selector commands. In addition, circuitry was provided in the CMGIA to automatically turn off wheel power and apply the brake when a bearing temperature exceeded 93.4 degrees C.

CMG desaturation resolver power (V_{ref}) could be supplied from either CMGIA No. 1 of CMGIA No. 2. Switchable reference lines off the V_{ref} bus were input to the WCIU for use in demodulating the resolver outputs. Both the source and reference lines were under the control of ATMDC automatic Redundancy Management but the capability of manually switching these functions by Switch Selector command existed.

To insure that an acceptable excitation voltage was constantly applied to the CMG resolvers, the reference voltage was compared to a standard value. If the difference was out of tolerance, then all possible redundancy combinations of multiplexer channels, WCIU input lines, and reference voltage sources were utilized in an effort to obtain an acceptable V_{ref}. This logic was also designed to detect and isolate a shorted CMG resolver and eliminate the failed CMG from control. The V_{ref} comparison test constant was conditioned to insure that in an over voltage or under voltage situation, the test tolerance would be exceeded once per second.

The Rate Command Integral (RCI) test was designed to monitor CMG unit performance by comparing the integrals of the commanded gimbal rates to measured changes in the gimbal positions over a test period. The test was made each 10 seconds and the integrals were accumulated over a 100 second period and then the test was reinitialized. Direction cosine data was used to calculate actual gimbal change and both inner and outer gimbals were tested. If gimbal response was found to be out of tolerance five times, not necessarily consecutive, before 20 consecutive acceptable tests on both gimbals were completed, then that CMG was declared failed and was removed from control. Dual multiplexers were incorporated for the direction cosine inputs during RCI test failure processing.

If a CMG gimbal was determined to be on its stop, the RCI test was bypassed for that unit. Two tests were designed to monitor CMG performance when a gimbal was on a stop. The first was the H-vector magnitude test which was used to determine whether a gimbal was actually on its stop or a gimbal resolver failure had resulted in an erroneous stop indication. The test involved a comparison of the sum of the squares of the non-normalized momentum components for the selected CMG to the square of the reference voltage. A difference in excess of 15% of the V_{ref} value resulted in a failure being determined. The second such test was executed if the H-vector test passed. This test monitored the gimbal rate commands to determine if they were of a convention to drive the gimbal off its stop. If so, and the gimbal remained on its stop for 15 degrees of rate integral, then the CMG was declared failed.

(3) Acq. SS Redundancy Management. Redundant Acq. SSs were provided in the X and Y-axes. Determination of the validity and use of Acq. SS errors for updating the strapdown was controlled by the ATMDC. The capability to select a single or dual Acq. SS configuration was provided by DAS/DCS commands.

Analog Signal Redundancy Management (ASRM), for a dual Sun Sensor system, consisted of a comparison test of the redundant signals in each axis and was performed each slow loop. If the difference was out of tolerance five consecutive passes, then a failure was determined. Redundant multiplexer channels for the analog signal inputs were exercised during failure processing. If the command system had selected either Sun Sensor as prime, the associated ASRM test consisted of minitoring the sun presence indication during periods of time when the "light" indication was expected. If the sun was not present for 30 consecutive passes, then the sensor being tested was failed.

(4) ATMDC Redundancy Management. The APCS contained redundant computers, one which was powered up and selected for control and the other powered down but loaded with the flight software and available for control if needed. Each ATMDC was supported by a section in the WCIU which expanded the computer INPUT/OUTPUT capability. Switchover from one computer system to the other could be accomplished manually or automatically. Automatic switchover, when enabled by a C&D Panel switch or the DAS/DCS, was controlled by a timer in the common section of the WCIU. The timer was reset each slow loop if a series of software self-tests were completed successfully. Otherwise, the timer timed out in 1.5 to 2.75 seconds and switchover occurred automatically. Approximately every 17 seconds, at the completion of a successful self-test cycle, a 64-bit transfer register in the WCIU common section was loaded with information necessary for initializing the off-line computer. Both the self-test timers and the transfer registers were made triple redundant.

A series of ATMDC/WCIU error detection tests were designed to support the automatic switchover capability. The basic test frequency was once per slow loop and test failures would have resulted in the computer entering the wait state until the self-test timers timed out and forced automatic switchover. These critical systems self-tests included the following:

ATMDC/WCIU Self Tests. These tests served to check the integrity of the computer memory circuitry and instruction execution. They included a check on fixed memory data by comparison of the sum of all fixed memory locations to a preset constant. This particular test required that a new comparison constant be calculated and uplinked with each real time software patch effected during the mission.

Instruction Counter Test. Verified the capability of the instruction counter to route program flow to the proper memory location.

Interval Timer Test. Designed to detect failures of the interval timer which was used by the software for scheduling all time-dependent functions.

Real Time Clock Test. Verified correct operation of the RTC which was the basic software timing source.

WCIU Analog Wrap Test. Designed to verify correct operation of the A/D and D/A converters used for INPUT/OUTPUT functions.

TACS Wrap Test. Served to check for proper implementation of the TACS thruster firing commands.

Slow Loop Completion Test. Designed to check for acceptable slow loop cycling characteristics.

The capability to troubleshoot an off-line computer by switchover to that computer and executing TSM routines designed to telemeter any portion of memory, execute the self-test error detection programs, and accept any required software modifications was designed into the ATMDC Flight Program.

b. History. The initial design of automatic Redundancy Management (RM) was developed without a set of groundrules. Each piece of hardware was studied to identify tests which would verify proper operation. As a result, memory required for Redundancy Management was excessive. Since the memory used was large and due to inconsistency in design of different routines, a set of groundrules was established in September, 1970. These groundrules and failures experienced in hardware testing resulted in the following changes to the initial Redundancy Management design.

(1) Rate Gyro Redundancy Management. The direct compare test and the integral divergence tests were deleted in a memory saving effort. The integral test was retained as the sole failure detection test. The test constant used with this test was simplified by deletion of cross axis rate terms.

A major change was made to the initial interim control strapdown verification test. A more simple test which counted TACS full-on and MIB firings until monitored rates began to decrease replaced the initial definition which was based on a requirement that rates sensed outside of a 1 degree attitude deadband should be approaching commanded rate as time progressed.

Single Rate Gyro failure detection was added. This was implemented in logic by executing the two good Gyro failure isolation logic and the interim control strapdown verification testing to indicate a failure of a single controlling Gyro.

A major improvement in the interim control strapdown verification test occurred with the definition of a "system momentum reasonableness test" to replace the previous tests based in MIB counts, decreasing rates, etc. This was the first time that gyro performance could be quickly and accurately evaluated as a single input to a controlling strapdown.

A WCIU Multiplexer failure test was designed that would establish and maintain an input multiplexer configuration for the Rate Gyros that would insure detection of a multiplexer failure. This logic was added to Rate Gyro Redundancy Management so that the WCIU Multiplexer failure rate could be assigned to specific Rate Gyros for management purposes and because multiplexer switching logic was already defined as part of the Rate Gyro Redundancy Management routine.

(2) CMG Redundancy Management. Problems experienced with the CMG tachometer during system testing resulted in exhaustive testing of CMG errors. Only the tachometer scale factor was determined to be a concern. Test results were utilized to expand the RCI test constant to compensate for tachometer scale factor errors.

The capability to remove CMG power from a CMG not available for control was added.

A "gimbal-on-a-stop" test was added. Since RCI testing must be bypassed near a mechanical stop, the possibility existed that a failure could have driven a gimbal to a stop and held it there. Since no RCI test was run, the failure could have gone undetected.

The capability to monitor ground or crew removal of CMG power was added. This was necessary so immediate action could be taken to reconfigure the Control Law.

Logic to detect a shorted CMG desaturation resolver, remove power from the resolver, and make the appropriate reconfiguration was added.

Logic which caused an ATMDC switch on certain CMG Redundancy Management failures was deleted.

Differences in MANNED/UNMANNED CMG RM were deleted. A major change in the application of the RCI test was incorporated. Previously, long term (100 sec.) and short term (10 sec.) tests were run on each CMG gimbal. This produced quick reaction to hard failures, and also provided sensitivity to subtle failures. This was replaced by an improved RCI test that was initially evaluated at 10 seconds, and incremented for an additional 10 second period if a "pass" occurred. Thus, for a "passing", gimbal test time increments of 10 seconds occurred until a 100 second test was completed. At this point reinitialization of the test occurred. The new test gave all of the advantages of the previous test with less memory and additional sensitivity to certain failure modes, such as open tachometer feedback loops.

(3) Acq. SS Redundancy Management. Automatic isolation of a failed analog signal was deleted. A degraded mode of no Sun Sensor update of strapdown was added. This resulted in a significant memory savings with no severe operational penalty.

Logic was added to permit single Sun Sensor Redundancy Management.

Sun presence Redundancy Management was deleted. This was permitted by use of computer timing for navigation in lieu of sun timing.

c. Mission Operations. In the course of the mission, the Redundancy Management scheme was very active in insuring the operational integrity of various hardware components, expecially the Rate Gyro subsystem. The RGRM integral test was failed many times during the early phase of the mission. It was during this phase that RGM proved so versatile in maintaining the best RG configuration. It not only responded to failures and reconfigured the subsystem automatically, but also recognized and effected commanded subsystem reconfigurations from the ground/crew.

CMG RM failed the RCI test one time for CMG No. 1, twelve times for CMG No. 2, and four times for CMG No. 3. RCI failures were widely intermittent and never threatened to eliminate one of the CMGs. All of these RCI failures occurred, as predicted pre-launch, during periods of maximum gimbal rates. Under certain conditions, high rates on the CMG outer gimbal would result in a back-torque on the inner gimbal which exceeded the controlling capability of the inner gimbal torquer. This brief period of torquer saturation would be incorrectly identified as an RCI failure, due to the sensitivity of the RCI test.

All the critical hardware components serviced by the ATMDC/WCIU detection program performed acceptably during the mission, hence ATMDC automatic switchover capability was not used. The manual switchover capability was exercised twice during the mission, once on DAY 27 to demonstrate the functional integrity of the secondary computer system and again on the last day of the mission as part of a test which loaded the ATMDC program via the MLU.

d. Conclusions. Automatic Redundancy Management performed as intended. Use of automatic RM proved essential to the accomplishment of a successful mission.

There was a design deficiency in the circuitry used for selection of which ATMDC was powered; a rapid switch from primary

to secondary and back to primary resulted in a relay race which could cause both computers to be powered up simultaneously. Crewmen were aware of the deficiency and no problem resulted from it during the mission.

2. Manual Redundancy Management.

a. Description. In addition to the manual switching used as a backup for automatic redundancy switching, the following manual Redundancy Management capability existed.

(1) 28 Vdc Power. 28 Vdc power was supplied to the APCS from redundant, diode isolated, overcurrent protected power buses. Either of these buses could be powered down via a C&D Panel switch or DAS/DCS command.

(2) 455 Hz Power. 130 volt, 455 Hz power was supplied to the ST from either CMGIA No. 1 or CMGIA No. 2 and to the FSS from either CMGIA No. 2 of CMGIA No. 3. Selection of the 455 Hz source was controlled by Switch Selector command.

(3) 800 Hz Power. 28 volt, 800 Hz power could be supplied to the EPC from either CMGIA No. 1 or CMGIA No. 2. Selection of the source of 800 Hz was controlled by a C&D Panel switch.

(4) EPEA. The EPEA contained five redundant channels: Roll, MPC, UP/CN, L/R, and Caging. Both a C&D Panel switch and Switch Selector commands were provided to switch all five channels from primary to secondary or vice versa. In addition, each channel could be switched to primary from secondary individually by Switch Selector commands.

(5) FSS. Two FSS opto-mechanical assemblies and associated electronics were provided in both the UP/DN and L/R axes. Switching could be accomplished via a C&D Panel switch and Switch Selector commands.

(6) EPC Rate Gyros. The EPC contained redundant RGPs in both the UP/DN and L/R axes. Selection of the RG in control could be accomplished by a C&D switch or by Switch Selector command.

(7) MPC. In order to provide redundancy for the MPC, a secondary MPC was stored in the MDA. In the event of a failure, the primary MPC could be removed from the C&D Console and the spare MPC mounted in its place. The two units were identical except for the electrical connectors at the base of the unit. Two connectors, one functional and one dummy, were present to interface with the primary and secondary MPC cables in the C&D Console.

(8) Roll Reslovers. Redundant Roll Resolvers were provided. Selection of the active Resolver could be accomplished only by a C&D Panel switch.

b. Mission Operation. Manual Redundancy Management was used extensively throughout the mission. Reconfiguration of vehicle Rate Gyros was required numerous times due to Redundancy Management integral test failures. CMG No. 1 wheel was powered down due to a bearing failure. A switch to secondary ATMDC was performed to verify that two operational computers existed. The primary Acq. SS was powered down in support of a Kohoutek experiment. The EPEA was switched to secondary in an attempt to isolate a caging anomaly (see Section VIII). The secondary EPC UP/DN RG was selected due to a failure of the primary and the secondary EPC L/R RG was selected in an engineering test. The FSS was switched during EPC troubleshooting. No problems were encountered in Manual Redundancy switching.

c. Conslusions. There was no capability of switching 800 Hz and Roll Resolver while unmanned. Loss of Resolver outputs due to failure of either the selected 800 Hz source or the selected Roll Resolver would have caused the ATMDC to drive the FSS wedges and thereby jeopardize experiment operations. Backup DAS/DCS commands for Redundancy Management of the 800 Hz power and the Roll Resolvers would have been desirable. Since there were no 800 Hz or Roll Resolver failures, there was no impact on the mission.

SECTION VII. ATTITUDE AND POINTING CONTROL SYSTEM HARDWARE

A. Rate Gyro Processor

1. Hardware Description.

a. General. The ATM Rate Gyro Processor (RGP) consisted of a single Kearfott series 2519 rate integrating gyroscope and the electronics necessary to operate it in the rate mode, and was contained in a rectangular enclosure 30.28 X 21.74 X 14.60 centimeters. The RGP weighed 5.58 kilograms. The RGP was attached to the spacecraft by four gusseted mounting feet with 1/4 X 28 screws on 20.32 X 20.32 centimeter centers. Thermal isolators were used on experiment package gyros. External connectors, a lapsed-time indicator and the vent port were located on one end of the enclosure. The external finish was a flat black high emissivity paint.

The RGP electrical components included:

Power supply

Heater control

4800 Hz generator

Three-phase inverter

AC amplifier

Demodulator

Torque driver.

b. Operation. A block diagram of the RGP is shown in figure 26. The commands and input voltages of the RGP are shown in Table 32. The commands and output voltages are shown in Table 33.

The RGP had two modes of operation. The fine mode gave a scale factor of 450 volts per degree per second for inputs up to $\pm$ 0.1 degree per second while the coarse mode gave a scale factor of 45 volts per degree per second for inputs up to $\pm$ 1.0 degree per second. The mode of operation was selected by gain control commands applied by the ATMDC to the ac amplifier (figure 26). This command then determined the mode by selecting appropriate gains for the ac amplifier, demodulator, and torquer driver. Except for different gains, both modes operated in the same manner. All Rack RGPs were commanded to change modes simultaneously.

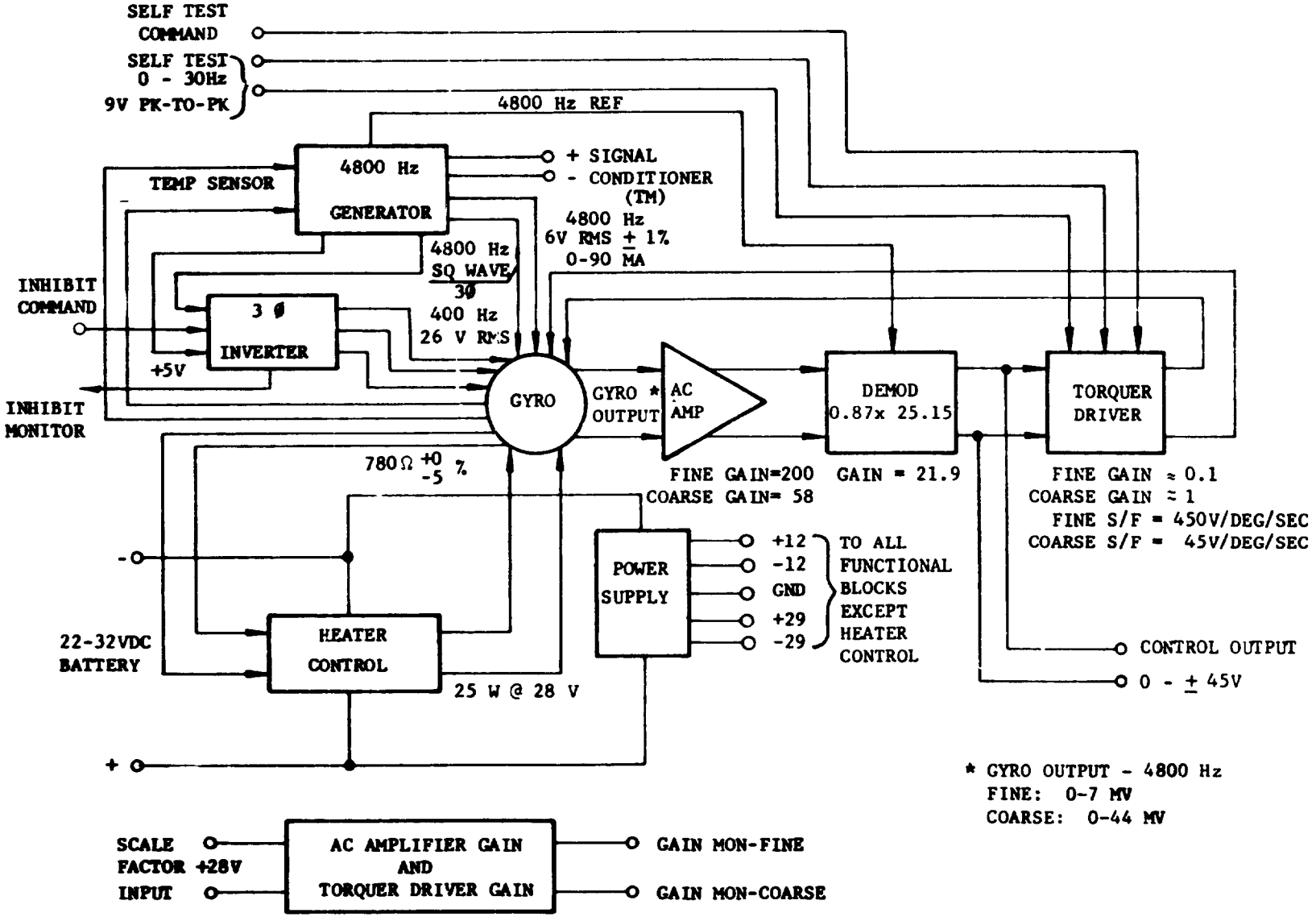

Figure 26. RGP Functional Block Diagram

Table 32. Rate Gyro Input

Inputs	Function
22 to 32 Vdc	Battery voltage to package.
28^{+4}_{-8} Vdc gain control No. 1 (fine)	Selects fine mode of operation.
28^{+4}_{-8} Vdc gain control No. 2 (coarse)	Selects coarse mode of operation.
28^{+4}_{-8} Vdc self test command	Energizes relay that applies test signal source to input of torquer driver.
28^{+4}_{-8} Vdc wheel inhibit command	De-energizes wheel excitation.
Torque test input	Applies test voltage to torquer driver.

Table 33. Rate Gyro Output

Outputs	Function
0 to $\pm$ 45 Vdc control output	Output proportional to rate input of gyro and used to correct attitude of ATM.
Gain Monitor (fine)	Discrete signal indicating RGP is in fine mode.
Gain monitor (coarse)	Discrete signal indicating RGP is in coarse mode.
Signal conditioner	0 to 5 Vdc indicating temperature of gyro.
Wheel inhibit monitor	28 Vdc indicating wheel inhibited.

The 3-phase, 400 Hz excitation to the gyro spin motor was provided by the 3-phase inverter assembly. The output of the inverter was phase locked to the output of the 4800 Hz generator assembly and was provided with an inhibit capability. The outputs of the inverter provided phases A, B, and C in the proper amplitude and phase separation to drive the gyro spin motor.

The 4800-Hz generator assembly provided a regulated, stable, low-distortion excitation to the gyro pickoff primary. In addition, a reference output to the demodulator, phase shifted to compensate for the gyro shift, was provided. There was also a 4800 Hz square wave clock and a regulated +5 Vdc output which were used by the inverter assembly.

In addition, a signal conditioning circuit produced an output proportional to the temperature of the gyro. A temperature sensor in the gyro provided the input signal to the telemetry signal conditioner. The output ranged between 0.0 and 5.0 volts and represented a temperature range from 62.2 degrees to 73.3 degrees C.

The secondary of the gyro pickoff produced an output which was proportional to the rate input to the gyro. This signal was applied to the ac amplifier where it was amplified by one of two precisely controlled gains. The gain used was selected by an external command signal and was a function of the operating mode selected.

The output of the ac amplifier was applied to the demodulator, which converted the ac output to a proportional dc voltage. The polarity of the dc voltage indicated the phase of the input signal relative to the reference signal from the pickoff driver.

The output of the demodulator provided an error signal to the vehicle control system, telemetry, and to the torquer driver which provided the gyro torquer feedback current. The torquer driver, like the ac amplifier, had two gain levels so that operation in two different modes was possible. The gain was switched by an external command signal. Auxiliary inputs to the torquer driver permitted preflight checkout as well as system bandpass measurements during manufacturing test.

A heater control circuit was provided to maintain the temperature of the gyro at 67.8 degrees $\pm$ 0.5 degrees C.

The power supply received a 22 to 32 Vdc battery voltage and produced +12, -12, and -29 Vdc for the RGP.

c. Applications. The RGPs performed the vehicle rate sensing function for the ATM Attitude and Pointing Control System.

Nine RGPs, mounted three per vehicle axis on the ATM Rack, were used in a pair and spare Redundancy Management scheme. Additionally, four identical RGPs, two per axis, were used in the coarse mode for rate feedback in the experiment pointing control system UP/DN and L/R control loops. The EPC RGP redundancy was manually managed via either the onboard Control and Display Panel or ground command. For a more detailed description of the RGP, see Reference 14.

2. Design History.

a. Design Goals. The RGP was designed to meet the following goals:

(1) The package was to have the ability to operate in both "fine" and "coarse" modes. The "fine" mode (±.1 deg/sec) was to be used for accurate control of the OWS. The "coarse" mode (± 1 deg./sec) was to be used for rapid maneuvering, and to allow for accidental vehicle over-rates. In addition, the EPC Rate Gyros (operated in the coarse mode) were used for EPC rate damping.

(2) The package was to operate over a temperature of -40 degrees C to +32 degrees C, and at altitudes from sea level to 200 nautical miles.

(3) All heat generated within the package was dissipated by surface radiation.

RGP design specifications may be found in Reference 15.

b. Design Growth. In July 1969, a decision was made to fly the AAP (Skylab) mission in a "Dry Workshop" configuration. Two design modifications were made to the RGP.

(1) An integral inverter was installed to eliminate the need for an external AC power source.

(2) A telemetry signal conditioner was added for the gyro temperature output.

3. Design Verification.

a. Hardware Qualification. Qualification testing of the RGPs was performed at the Martin Marietta Corporation, Orlando, Florida, facility and at MSFC during the period from December 1969 through January 1970. The Qualification Test Program was conducted as specified in Reference 16 and Reference 17.

The requirements of the Qualification Test Procedure were maintained during all phases of the test program except for the thermal vacuum test and the vibration test. During the thermal vacuum test the test temperature varied during the eight hour cold soak and the vibration test was entirely repeated due to the inadvertent application of gyro wheel power during the initial test.

Two component (piece part) failures occurred during the qualification program (both associated with the vibration test) and minor out of specification conditions were noted during the transient susceptibility and EMI tests. In each failure a defective component was found to have been the cause. In both instances the defective component was replaced and the test repeated. A waiver was granted to permit acceptance of the minor deviations noted during the transient susceptibility and EMI tests.

At completion of testing, the RGP was certified to have met all the performance specifications in Reference 14 with the exception of the one deviation concerning transient susceptibility and EMI.

It should be noted that Rate Gyro Processor Qualification Test Procedure, Reference 15 , does not require that RGP scale factor and drift be measured under thermal-vacuum conditions. As a result, RGP drift and scale factor changes under thermal-vacuum conditions were not measured until much later in the program.

For additional information see Reference 17.

In addition to the formal qualification tests, a life test was performed on the complete RGP assembly. The intent of this test was to test the RGP failure. At the time of SL-1 launch, the RGP had accumulated approximately 27,000 hours with no failures. This test was performed in ambient conditions rather than the expected flight environment.

b. Hardware Integration. The RGPs were first integrated into the closed loop Attitude and Pointing Control System during integration testing in the Hardware Simulation Laboratory (HSL) in Astrionics Laboratory, MSFC. This testing was performed in the summer and fall of 1971. Rate Gyro Processor performance was examined in closed loop operation with both the CMG/TACS system and the Experiment Pointing Control System. All testing was performed under ambient conditions with earth's rate biased out by use of the Rate Gyro Torquers. The Rate Gyro Processors performed satisfactorily. No problems were encountered.

For additional information, see Reference 18.

4. Hardware Verification. System-level tests were performed on the prototype and flight ATMs to verify system design and flight readiness. These tests included post-manufacturing checkout, vibration testing, thermal-vacuum testing, and pre-launch checkout. During these tests a number of Rate Gyro Processor problems occurred. These are listed in Table 34. Most of the confirmed failures were traced to solid-state devices and were closed. The problem involving bubbles in the gyro flotation fluid during systems-level thermal-vacuum tests were not closed at the time of SL-1 launch, but were regarded as an acceptable risk because the resulting gyro drift could be compensated in the ATMDC software.

For additional information, see Reference 19.

5. Mission Operations. The APCS Rate Gyro Processors were powered up on DAY 1, 19:07:00 GMT. Following switchover from launch vehicle IU control to OWS ATMDC control, it became apparent that some of the RGPs were behaving anomalously. First, ATMDC Redundancy Management rate integral discompares showed that several RGPs had out-of-spec drift. Second, telemetry showed that the Z_1 RGP was hotter than the telemetry temperature window of 62 degrees C to 73 degrees C. Eventually, six RGPs became hot, as shown in Table 35.

a. RGP Drift Anomaly. The excessive RGP drift rates first became evident shortly after switchover to ATMDC control, on DAY 1, 18:22:20 GMT. Drift rates as high as 18 degrees per hour were noted. Specification values were two orders of magnitude less. The high drift rates made it difficult to maintain the correct attitude for thermal control during the first ten days after SL-1 launch. The high drift rates were compensated for by changes in the ATMDC software uplinked from MCC, however, the drift rates often changed suddenly. This caused difficulty until the new rates could be measured and compensated. As time passed in the mission, the magnitude of the drift rate changes decreased. Eventually, the X_1, Y_1, and Z_3 RGPs became stable, and were used through the remainder of the mission. Table 36 is a history of Rate Gyro drift compensation during SL-1 and figure 27 is a typical plot of drift trends of the X_3 RGP during the SL-2 mission. Several abrupt drift level changes are shown, with a gradual decrease in drift beginning on DAY 30.

After considerable investigation, the cause of the high drift rates was shown to be gas bubbles in the Rate Gyro flotation fluid. The formation of bubbles in the fluid was apparently caused by a design deficiency which exposed the float chamber bellows to the hard vacuum of space, and by entrained gasses present in the flotation fluid. Figure 28 presents a section of the original Kearfott

Table 34. Rate Gyro Problem Summary

LOCATION/ITEM	S/N	PROBLEM	NR/IDR-OPEN/CLOSED	FINDINGS	COMMENTS
PROTOTYPE PMC					
RACK Y_1	111	TEMP 5°C ABOVE NOMINAL	09224-SYS./CLOSED 09225-COMP/CLOSED 09287-SYS./CLOSED 09289-COMP/CLOSED	FAILURE COULD NOT BE REPEATED IN LAB - CONNECTOR SUSPECTED	6/28/72
FLIGHT PMC					
1. CANISTER PRI YAW	127 111	HI READING AT NULL	15196-SYS./CLOSED	TRANSISTOR IN DEMODULATOR WAS FAILED - PROCEDURE POSSIBLY CAUSED FAILURE - PROCEDURE CHANGED.	3/28/72
2. RACK Z_3	120 127	WOULD NOT TURN ON	15494-SYS./CLOSED 15543-COMP/CLOSED	FAILURE ANALYSIS FOUND DIODE IMPROPERLY MOUNTED - NUT NOT TIGHT ON STUD MOUNTED DIODE-ALL UNITS TESTED TO VERIFY CORRECT MOUNTING.	5/01/72 DURING REACCEPTANCE, GYRO DRIFT RATE OUT OF SPEC. (NR 02723) - GYRO ASSY REPL, BUT DEMODULATOR NOISE NOW SLIGHTLY OUT OF SPEC. (OPEN)

Table 34. (continued)

LOCATION/ITEM	S/N	PROBLEM	NR/IDR-OPEN/CLOSED	FINDINGS	COMMENTS
FLIGHT PMC					
3. RGP	127	TEMP MONITOR OUTPUT FROM SIGNAL CONDITIONER WAS OUT OF SPEC. READ 0 Vdc	M013822/CLOSED	CR4 ON 48 kHz GENERATOR CHECK-OUT BOARD WAS SHORTED.	5/08/72 CR4 (S/N 752A) A ZENER DIODE WAS PROBABLY OVER-STRESSED BY AN EXTERNAL CURRENT SPIKE.
FLIGHT T/V					
1. RACK Z_1, Z_3, AND Y_2		HI OUTPUTS AT NULL IN VACUUM	198-S/C-96-SYSTEM/ CLOSED	N/A - SEE COMMENTS	7/25/72 Y_2 WAS WITHIN SPEC. Z_1 AND Z_3 ABOUT 2 V HI-Z_1 AND Z_3 SUBSEQUENTLY REPLACED.
2. CANISTER PRI PITCH	124 108	FAILED TO TURN ON - LATER OUTPUTS WERE RANDOM	123-S/C-SYS/CLOSED 128-COM-8 /CLOSED	3 TRANSISTOR IN PS FAILED - 2N190 AND SM-2880	7/27/72 FAILED ANALYSIS INCONCLUSIVE. FAILURE CAUSED BY REFLOW OF SOLDER TERMINATED WHILE ATTACHING TEST LEADS.
3. RACK Z_1	129	SPIKING OUTPUTS THEN GAIN DROPPED ABOUT 70%.	129-S/C-59/CLOSED 130-COM-9/CLOSED	OPERATIONAL AMPL FAILURE. SM107-G	8/01/72 PIN 4 WAS NOT BONDED, CAUSING LOW GAIN IN AMPLIFIER.

Table 34. (continued)

LOCATION/ITEM	S/N	PROBLEM	NR/IDR-OPEN/CLOSED	FINDINGS	COMMENTS
FLIGHT T/V					
4. RACK Z_3	127 106	HI OUTPUTS AT NULL DURING 2ND PUMPDOWN (SEE 1 ABOVE)	224-COM-28/OPEN	FAILURE ANALYSIS CONFIRMED BUBBLE IN THE GYRO FLUID BUT THE SOURCE WAS NOT IDENT-IFIED.	8/29/72 A MODIFICATION WAS DESIGNED AND TESTED WHICH SEALS THE END CAP OF THE GYRO (EFFECTIVE WITH 6-PACK)
5. RGP	129	A HI NULL OUTPUTS WAS MEASURED ON Z_1	M003914/OPEN	BUBBLES IN THE 2519 GYRO FLO-TATION FLUID	1/12/73 GYRO S/N 104 WAS REPLACED WITH S/N 105.
6. MOST GYROS	ALL	FAILED TO OPERATE WITHIN SPEC. AFTER 40 MINUTE WARM-UP	DR-MH-SC-609/ CLOSED	ENVIRONMENTAL CONDITIONS. CHANGE WARMUP TIME, GYROS WERE IN SPEC IN ABOUT 1 HOUR. NOT A PROBLEM - SPEC SHOULD BE CHANGED	SPEC WAS CHANGED.

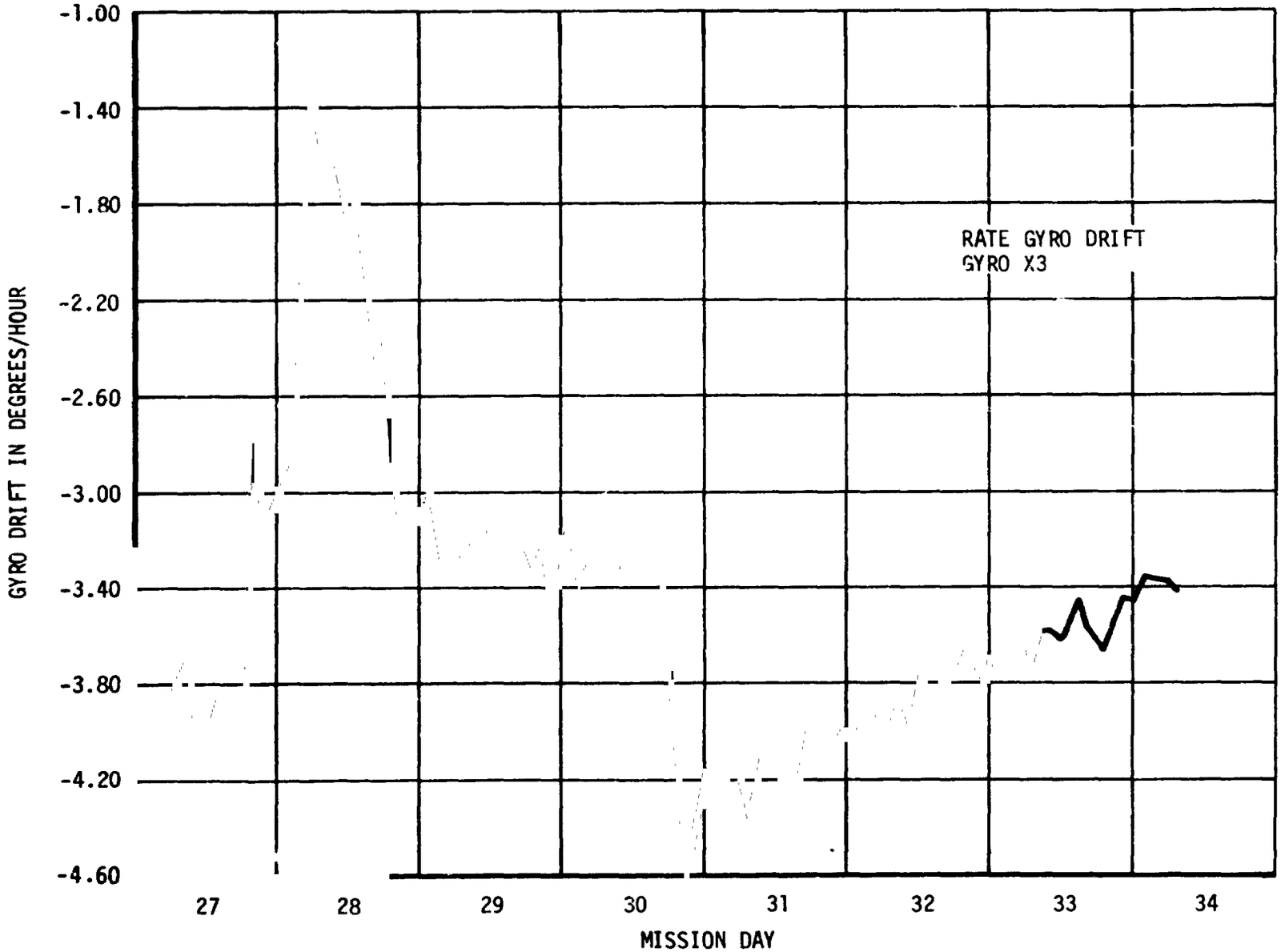

Figure 27. RGP X_3 Drift Trend

series 2519 Gyroscope. This section shows the float chamber and fluid, the float chamber bellows, and the vented end cap. The decrease in drift rates as the mission progressed were attributed to either reabsorption of the gas by the flotation fluid, or relocation of the bubbles in the float chamber due to float fluid agitation.

Table 35. Rate Gyro Temperature

RGP	Condition	Time of Thermal Rise After Power-Up (Hours)
X_1	Normal	----
X_2	Hot	271.0
X_3	Normal	----
Y_1	Normal	----
Y_2	Hot	10.5
Y_3	Hot	21.0
Z_1	Hot	1.5
Z_2	Hot	3.0
Up/Down Primary	Hot	82.0
Up/Down Secondary	Normal	----
L/R Primary	Normal	----
L/R Secondary	Off	----

Corrective action for the drift rate problem included tests to verify the theory of bubble formation, and a design modification which sealed the float cavity from the hard vacuum of space. The design modification consisted of replacing the vented bellows end up cap with an unvented end cap so that internal float pressure would remain near the original float fill pressure despite external pressure changes. The change was incorporated on six RGPs which were installed in the MDA on SL-3. None of the six replacement RGPs showed excessive drift similar to those experienced on SL-1.

It is believed that the RGP drift anomaly is the same as the RGP gas bubble anomaly encountered during ATM Thermal-Vacuum Testing (see Paragraph VII.A.4).

Table 36. Gyro Drift Compensation History

TIME DAY:HR:MIN	X_1 (Deg/Hr)	X_2 (Deg/Hr)	X_3 (Deg/Hr)	Y_1 (Deg/Hr)	Y_2 (Deg/Hr)	Y_3 (Deg/Hr)	Z_1 (Deg/Hr)	Z_2 (Deg/Hr)	Z_3 (Deg/Hr)
02:17:05	4.608	2.232	-3.744	11.95	0.0	-6.264	0.0	0.0	0.0
02:19:59						0.0			
03:30:49			8.244						
04:16:16							-.324	-.324	
05:00:26	3.679	3.161							
06:17:10		8.28	9.144						
08:07:26							.576		
09:07:45					-.702	.702			
09:08:32		13.356							
09:16:46			11.603						
10:00:00				3.960					
11:21:30	3.348	13.176	13.176	3.744	.576	.972	.591	1.944	-7.560
14:18:00		13.968	8.244	4.932					-5.724
14:21:20	.973	9.828		4.143		0.0			
15:05:44					-4.68				
15:15:03	.3515		2.813						
15:16:47			3.341		-4.327		.5760	.180	
78:17:50	.0	0.352	-0.703	0	11.65	OFF	OFF	0.352	0
TEMP STATUS	NORMAL	HOT	NORMAL	NORMAL	HOT	HOT	HOT	HOT	NORMAL

b. High Temperature Anomaly. Within the first 21 hours of APCS operation, failures of either telemetry measuring circuits or heater control circuits were evident on four Rack RGPs. Later in the mission, an additional Rack RGP and one EPC RGP showed identical symptoms. The EPC RGP (Primary UP/DN) eventually failed.

A detailed thermal analysis was performed, relating RGP base plate heat sink temperatures to RGP temperatures. It was determined that base plate temperatures of 14 degrees C corresponded to RGP temperatures of about 110 degrees C. Also, a hot RGP was powered down, allowed to cool, and then powered up. The RGP temperature was seen to increase and become off-scale high. It was concluded that the six RGPs in question had experienced heater control failures, and that the RGP temperatures were about 108 degrees C.

There was much concern that as the RGP temperatures increased, the RGPs would become unstable and cause loss of control. Test and analysis data indicated that the RGP stability margin expected at 67.8 degrees C would disappear at 110 degrees C because of the reduction in float damping fluid viscosity. It was expected that normal increases in solar elevation angle during the mission would cause increased RGP base plate temperatures, and higher RGP temperatures. The EPC pitch primary RGP continued to deteriorate and failed on DAY 64.

All the hot RGPs showed much noisier outputs than the normal RGPs. This can be seen in figure 29. Z_1 and Y_3 RGPs had extremely noisy outputs, suggesting that they were on the verge of instability. Analyses were performed which showed that the hot RGPs were more stable in the coarse mode than in the fine mode when temperatures approached 110 degrees C (base plate temperature near 14 degrees C). Therefore, it was decided to operate the RGPs in the coarse mode whenever the base plate temperature of any of the operating RGPs exceeded 14 degrees C. This action reduced the system maneuver accuracy slightly, but had no harmful effects.

To preserve the Y_3 and Z_1 RGPs for possible use later, these two RGPs were powered down and vehicle control was transferred to the remaining RGPs in the Y and Z area. The Y_3 and Z_1 RGPs were later powered up again to obtain diagnostic data.

Another problem noted with the hot RGPs was a change in scale factor. A comparison of ATMDC-computed rate integrals during a nominal momentum dump is shown in figure 30. RGP Z_2 was hot, while RGP Z_3 was normal. This problem caused Redundancy Management rate integral discompares during maneuvers. It was possible to compensate in the ATMDC software for scale factor errors in the Y-axis.

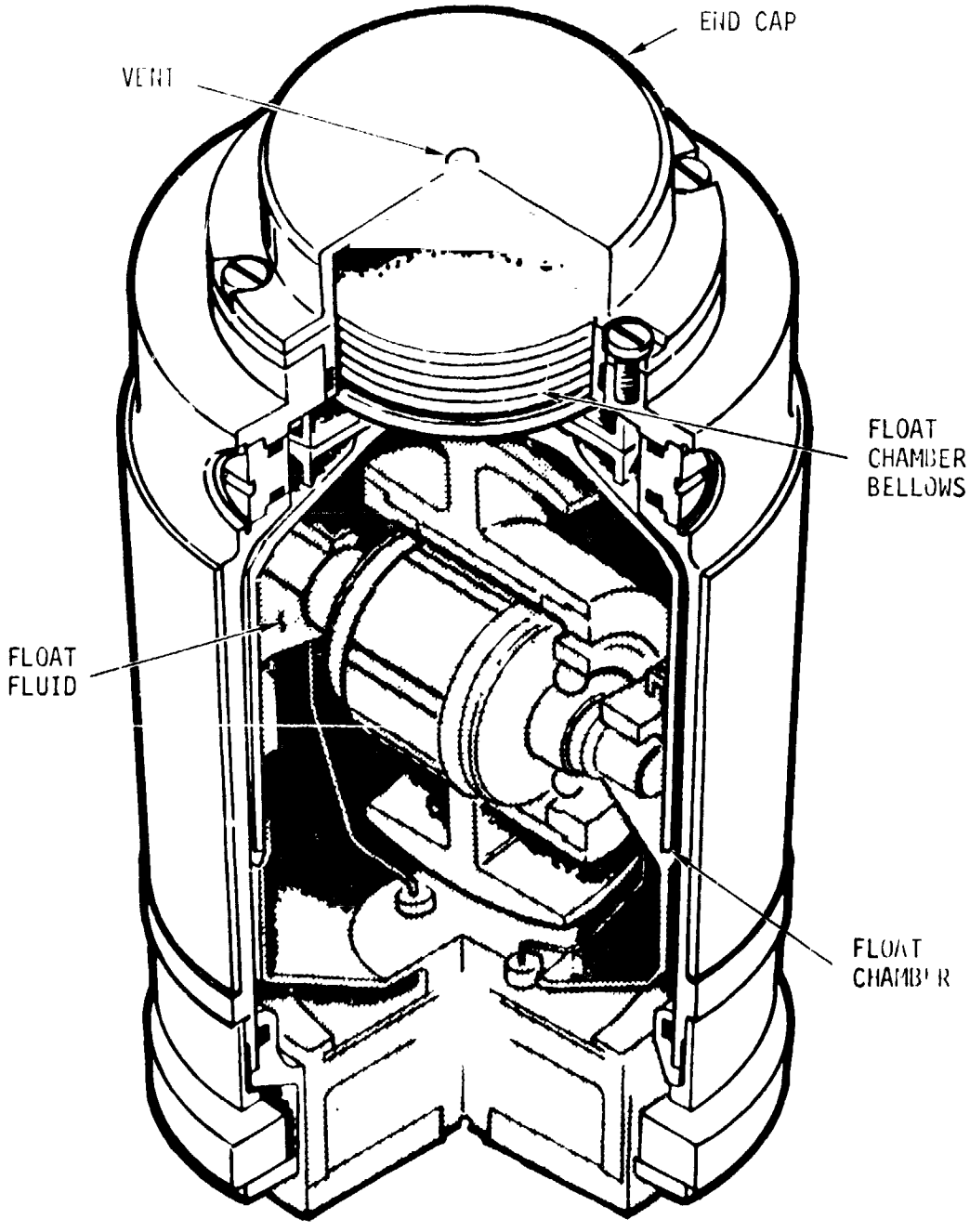

Figure 28. Typical Rate Gyro Mechanical Section

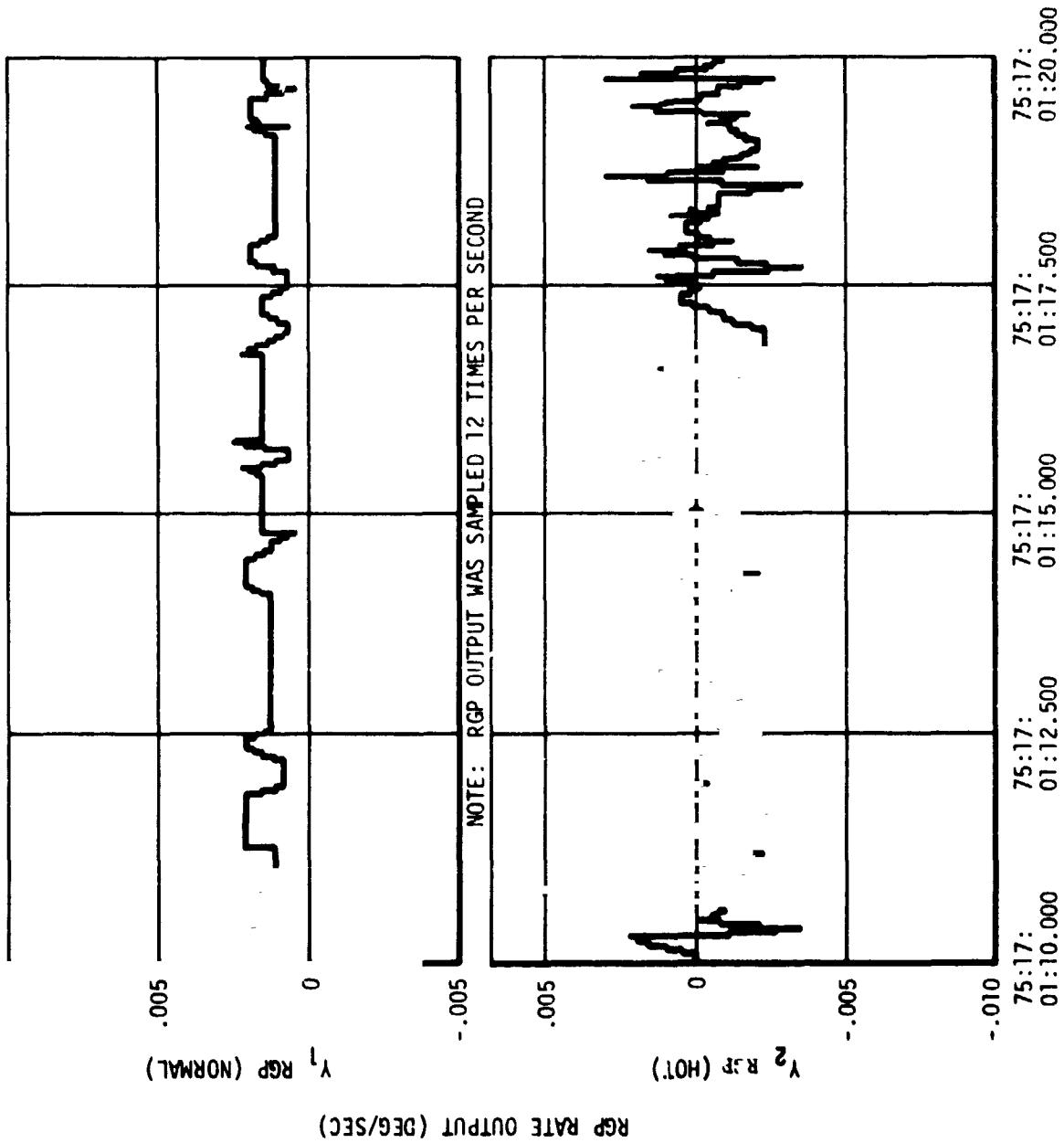

Figure 29. Comparison Of Cold & Hot RGP Outputs

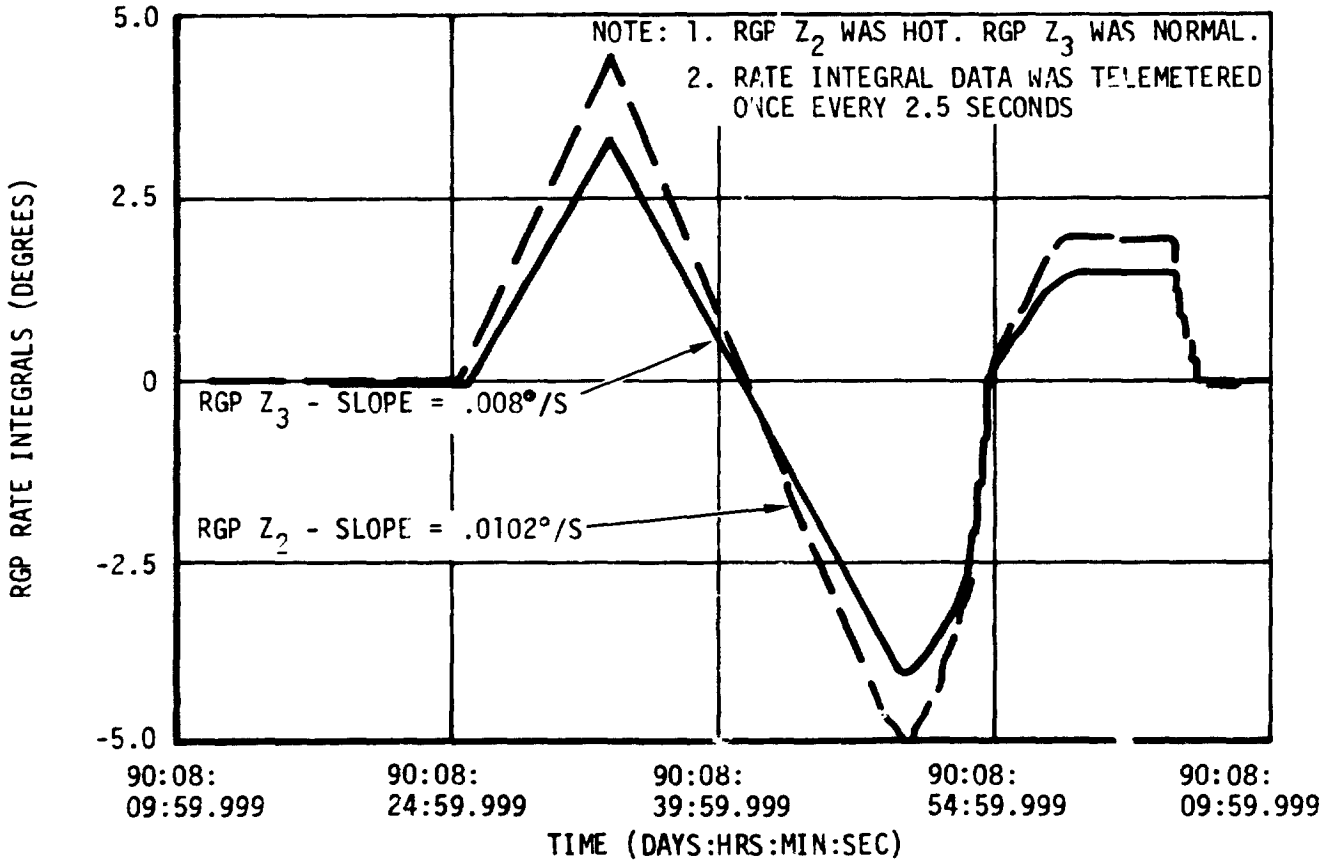

Figure 30. Comparison Of Normal & Hot RGP Scale Factors

Table 37 summarizes the status of the Rate Gyros midway through the SL-2 mission. No further significant RGP changes occurred until the Rate Gyro Six-Pack was installed.

Efforts to determine the cause of the temperature anomaly focused on component failures, electromagnetic interference (EMI), and design deficiencies. Ultimately, through extensive analyses and test, the cause was proved to be a design deficiency. Use of a fiber washer which shrunk in the space environment, allowed loosening of the power switching transistor mounting system. Loosening of the transistor heat sink allowed the transistor to thermally saturate. Under a condition of thermal saturation, the transistor leaked excessive current to the gyro heater blanket causing the gyro to overheat. The recommended fix was to replace the fiber washer with a spring steel washer to maintain tension in the mounting bolt. Figure 31 shows the original mounting and the recommended mounting of the power switching transistor.

Although it was determined that the RGP was susceptible to EMI, tests on the ATM ground backup unit were not able to demonstrate a sufficient level of EMI to cause the temperature anomaly as observed in flight.

The cause of the overheating anomaly was determined after the six replacement RGPs were installed in the MDA. Consequently, the power switching transistor mounting could not be modified. However, provisions were made prior to SL-4 to provide an easily implemented corrective action had any of the six RGPs exhibited high temperatures. The corrective action consisted of removing the covers of the RGP box and applying a thermally conductive silicone grease to the power switching transistor/heat sink junction. Tests had shown this to be a very effective way of preventing thermal saturation of the power switching transistor. A backup procedure was also developed to be used in case the silicone grease fix was unsuccessful. The procedure would have disabled the RG heater by cutting wiring to the heater. The RGPs on the backup unit were to be refurbished with a positive tension stud mounting system which would eliminate the possibility of breakdown of the heat condition path to the mounting plate. Because of the susceptibility of the RGP to EMI, the refurbished processors on the ATM backup unit were to have circuitry modified to reduce the susceptibility level. Because of the EMI susceptibility, future qualification test specifications will be more explicit in testing for EMI susceptibility at the black box level.

The overheating anomaly was not encountered at any time during ground test before SL-1 launch.

Table 37. Rate Gyro Performance Capability Status

Gyro	Temperature	Quality of Output	Usefulness
X_1	Normal	Good	In use, good for all conditions.
X_2	Hot	Fair	Use in coarse mode if base plate above 14°C.
X_3	Normal	Good	In use, good for all conditions.
Y_1	Normal	Good	In use, good for all conditions.
Y_2	Hot	Fair	Use in coarse mode if base plate above 14°C.
Y_3	Hot	Oscillating	Not useful except for diagnostic data.
Z_1	Hot	Oscillating	Not useful except for diagnostic data.
Z_2	Hot	Fair	In use, good for all conditions.
Z_3	Normal	Good	In use, good for all conditions.
PP	Hot	Not useful	Not useful.
PS	Normal	Good	In use, in all conditions.
YP	Normal	Good	In use, in all conditions.
YS	Not turned on	----	Never activated, assumed good.

Efforts to determine the cause of the temperature anomaly focused on component failures, electromagnetic interference (EMI), and design deficiencies. Ultimately, through extensive analyses and test, the cause was proved to be a design deficiency, use of a fiber washer which shrunk

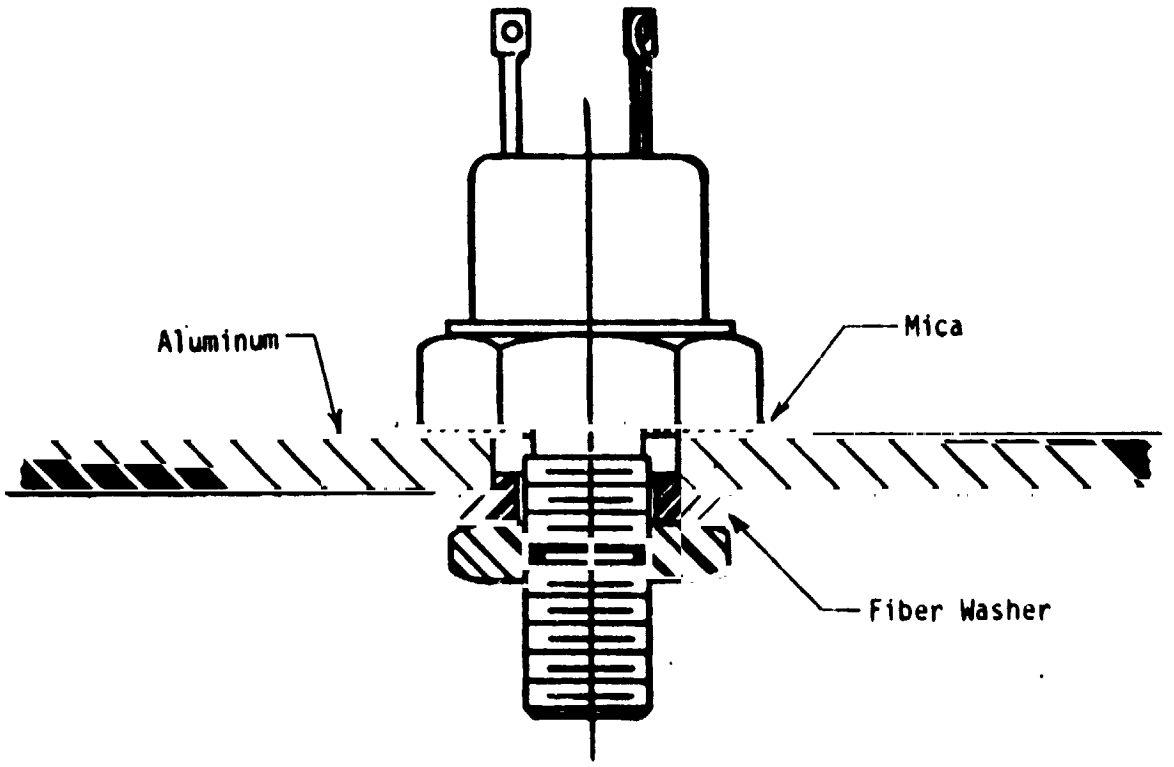

ORIGINAL MOUNTING

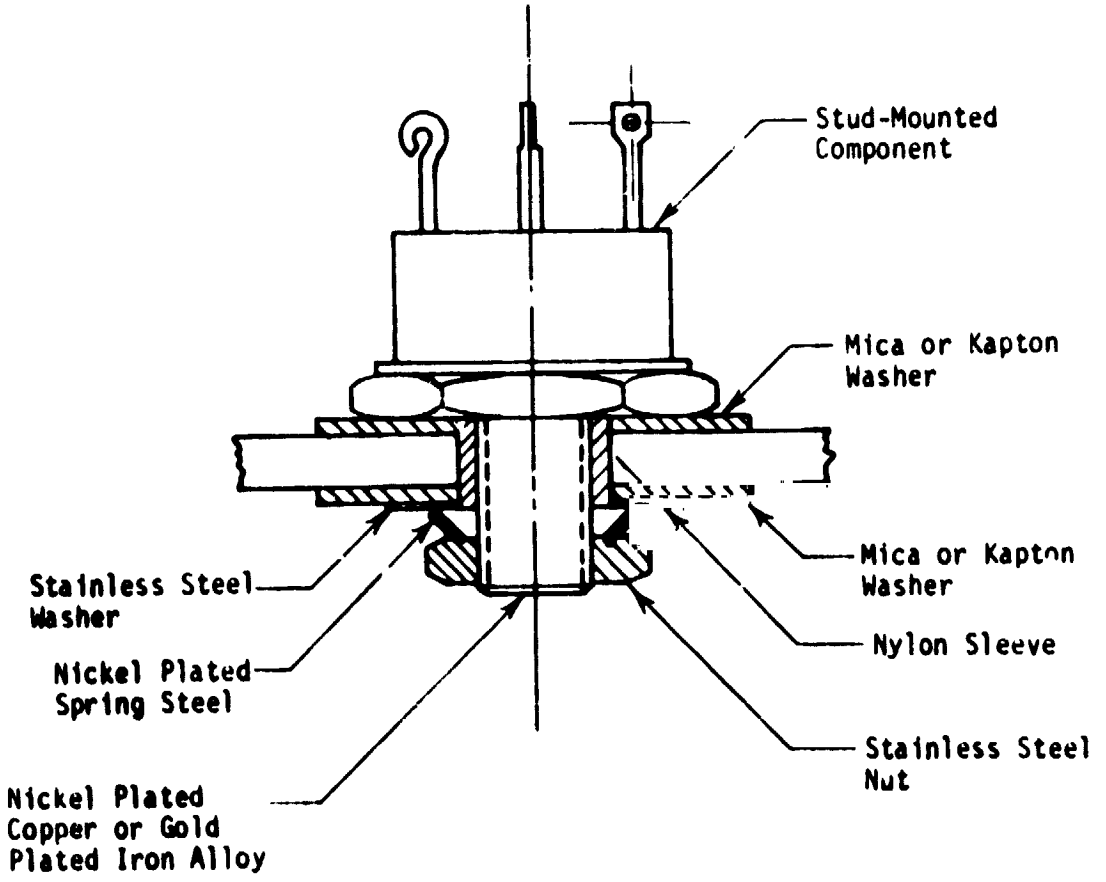

RECOMMENDED MOUNTING

Figure 31. RGP Power Switching Transistor Mounting

c. RG Six-Pack Development. During SL-2, a crash program began to prepare a package of ATM Rate Gyro Processors that could be interfaced into the APCS system should additional Rack RGP failures threaten mission termination. The Six-Pack containing six RGPs (two per axis) was designed, tested, integrated and weighed in the HSL, checked out on the flight backup vehicle and interfaced at the MDAC facility during SL-2 and was ready to be sent up on SL-3. Additionally, a Derived Rate Control Assembly was designed and built to replace the RGPs in the EPC loop (see Paragraph IX.F). These two subsystems were carried up on SL-3. The Six-Pack was installed in the MDA, powered up and checked out by the SL-3 crew (see figure 32). An EVA consisting of four electrical connections was required for installing the Six-Pack in the APCS systems. The greatest risk involved the disconnect and reconnect of the standard connector J3 at the WCIU. Failure to reconnect (or pin breakage) would most likely have meant mission termination since all RGP signals feed into the ATMDC through this connector.

On DAY 103, the Six-Pack was installed in the system. No problems were encountered. Three Six-Pack RGPs were paired with the remaining Rack RGPs (X_1, Y_1, Z_3) to avoid a potential single-point failure in the Six-Pack power source.

The Six-Pack and the selected Rack RGPs performed satisfactorily. Only one RGP (Y_5 of the Six-Pack) required drift compensation. No gross anomalies occurred subsequent to the Six-Pack installation; however, integral test failures occurred when the Six-Pack was inadvertently bumped by the crew and when the vehicle was maneuvering. This resulted from using for control purposes one Six-Pack and one Rack RGP on each vehicle axis; the different resonance modes of the locations contributed to integral test failures.

The cause of the excessive drift rates experienced on Rack RGPs was determined during the time the Six-Pack was being designed. A modification was made to the Six-Pack RGPs to preclude the drift problem. The cause of off-scale high temperature was not found until after SL-3 however, a quick fix was formulated and a procedure defined for implementing the fix with onboard materials and tools as noted in Paragraph VII.A.5.b. No further RGP problems were encountered.

6. Conclusions and Recommendations.

a. Conclusions.

(1) The cause of the Rate Gyro Processor drift anomaly was determined to be the presence of gas bubbles which formed in the

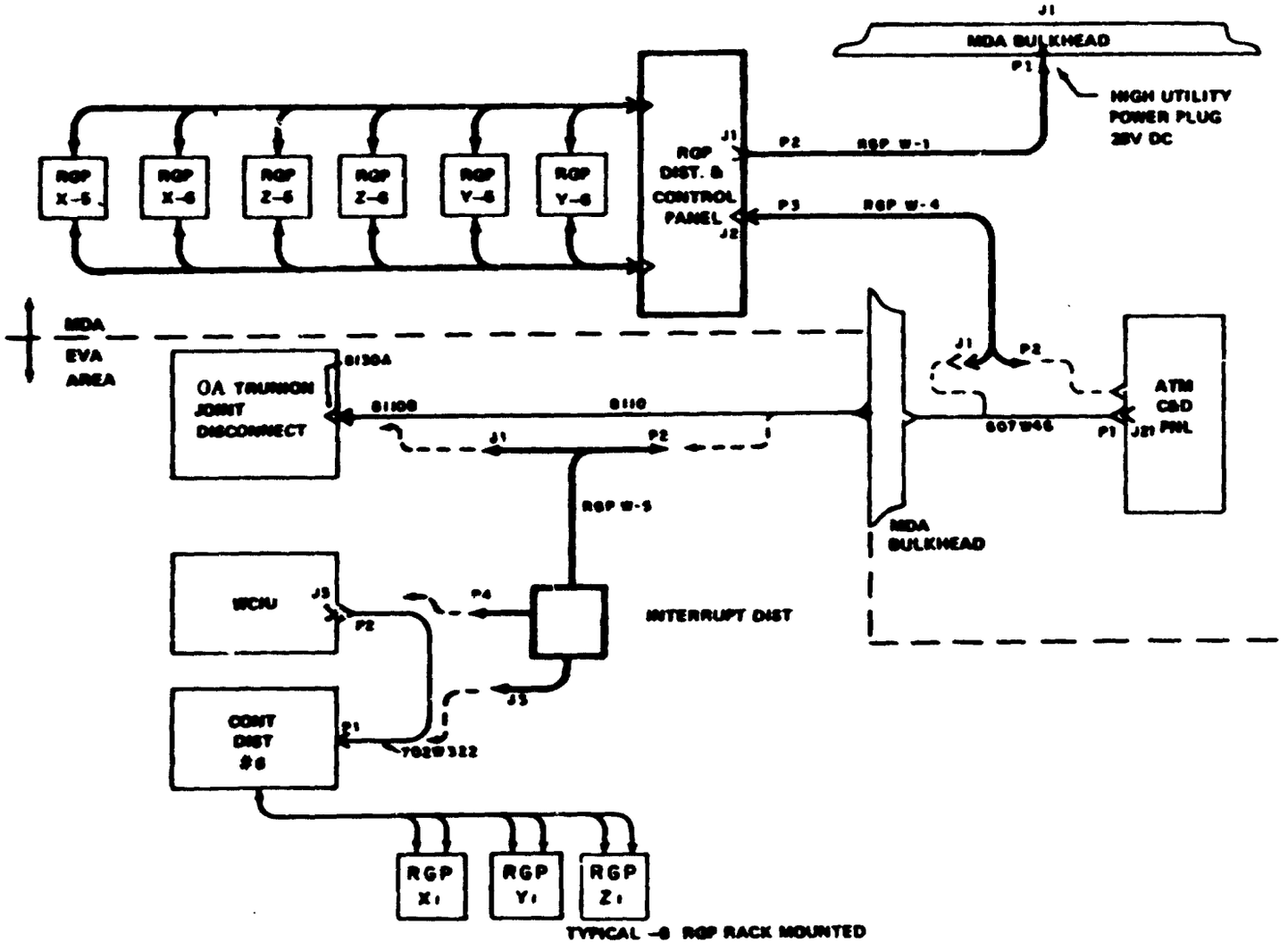

Figure 32. RGP Six-Pack Connection Schematic

gyro flotation fluid when the Rate Gyro Processors were exposed to the hard vacuum of space. This was caused by a design deficiency which exposed the float chamber bellows to the space environment.

(2) The cause of the RGP overheat anomaly was determined to be a design deficiency which allowed loosening of the power switching transistor mounting system, which caused the transistor to overheat.

(3) Neither of the two RGP problems were discovered during qualification testing, or life testing of the Rate Gyro Processor.

(4) Replacement of the failed Rack RGPs with the Six-Pack restored the system to a more normal configuration and permitted normal operations during the SL-3 and SL-4 missions.

b. Recommendations.

(1) Precision performance data should be monitored during hardware qualification and life tests when exposed to the operating environment.

(2) In future long-duration manned missions, consideration should be given to replacement or maintenance of mission-critical components such as Rate Gyro Processors during the mission.

B. Star Tracker

1. Hardware Description. The Star Tracker furnished star position inputs with respect to the spacecraft for calculation of the vehicle roll reference and EPC roll reference.

The Tracker system consisted of two subassemblies; the Optical Mechanical Assembly (OMA), and the Star Tracker Electronics (STE). The OMA consisted of a refractive telescope, photomultiplier tube detector, and telescope electronics with a high voltage power supply. This was contained and mounted on a double gimbal suspension. Gimbal freedom was $\pm$ 40 degrees on the inner gimbal and $\pm$ 87 degrees on the outer gimbal. See figure 33.

The STE contained servo control circuits, power supplies, digital logic unit, shutter drive amplifier, and auxiliary electronics. All input/output functions to other systems were interfaced in the STE.

Star light was detected through a baffled sunshade into the telescope lens, and into the photomultiplier tube aperture. The signal generated by the photomultiplier by light impingement was

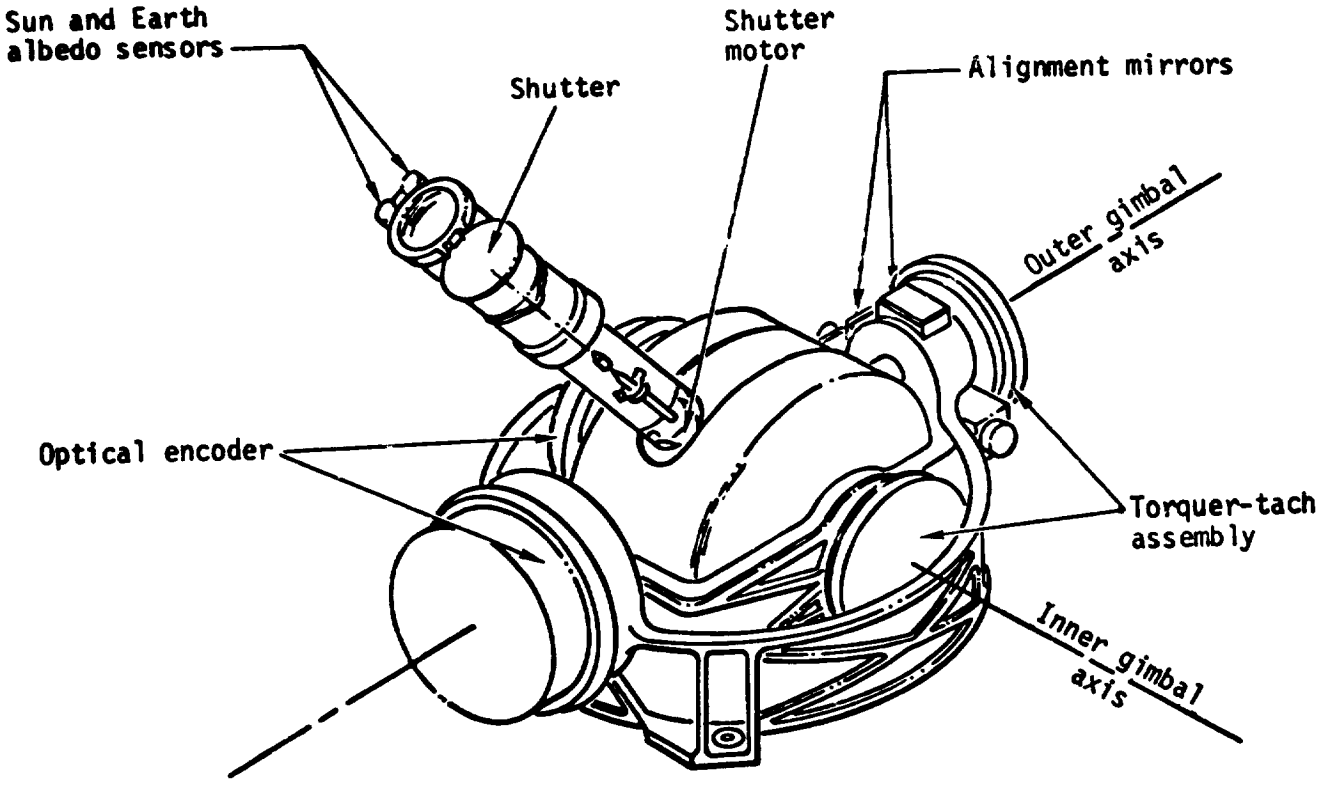

Figure 33. Star Tracker OMA

conditioned by a video amplifier, sweep generator, scan electronics, and a demodulator, and was used as an error signal to close a servo loop to the gimbal torquer amplifiers and the torquer motors. Gimbal position information was provided by an optical encoder mounted on each pivot which was fed through conditioned logic to the digital computer in a 15-bit serial binary word, and to telemetry using a parallel binary word.

The sunshade had a lid type shutter which was driven by a motor and worm gear actuating assembly. It could be activated by mode selection or by automatic closure from sensors which operated when the optical axis was within 45 degrees of the sun or within 5 degrees of the earth's albedo. This was done to protect the photomultiplier from light damage.

The Tracker operated in three modes: the first was "Hold" which maintained a digital position loop for each gimbal and closed the shutter; next was "Manual" mode which enabled the astronaut to drive each gimbal to a desired position with a MPC rate command from the Control and Display Panel, and also opened the shutter; the third was "Auto" mode which allowed the Tracker to search in a programmed pattern, acquire the target star, and track the star while providing gimbal position information to the digital computer and telemetry. Manual mode commands from the C&D Panel (manual, shutter Closed/Hold, and Auto) took precedence over commands issued from the ATMDC (Auto and Shutter Closed/Hold). The computer commands were effective only after the astronaut had issued an "Auto" command.

In the search submode the outer gimbal search motion was achieved by driving the outer gimbal rate loop at a constant speed. At the start of the search operation, the outer gimbal position was stored and thereafter the new outer gimbal position was subtracted from it. The results of the subtraction were examined by "Error Detectors" which disconnected the rate-loop drive signals when angles of $\pm$ 2 degrees were reached in the "Fine" mode, or $\pm$ 15 degrees in the "Coarse" mode.

The initial inner gimbals were stored and the actual gimbal position subtracted from it to provide an error to drive the position servos to null. The "initial position" register was incremented in 3/4 degree steps after each outer gimbal cycle. The search pattern is shown in figure 34.

Under ATMDC Star Tracker control, the coarse search pattern was not used. If the search submode was entered, and a star was not acquired within 25 seconds, the ATMDC would set the ACS alert condition 04 and issue a Star Tracker hold command. The 25 second limitation would allow the fine search to be completed. The coarse mode could be reached only by inhibiting ATMDC Star Tracker control. (Reference Table 38 for Performance Specification).

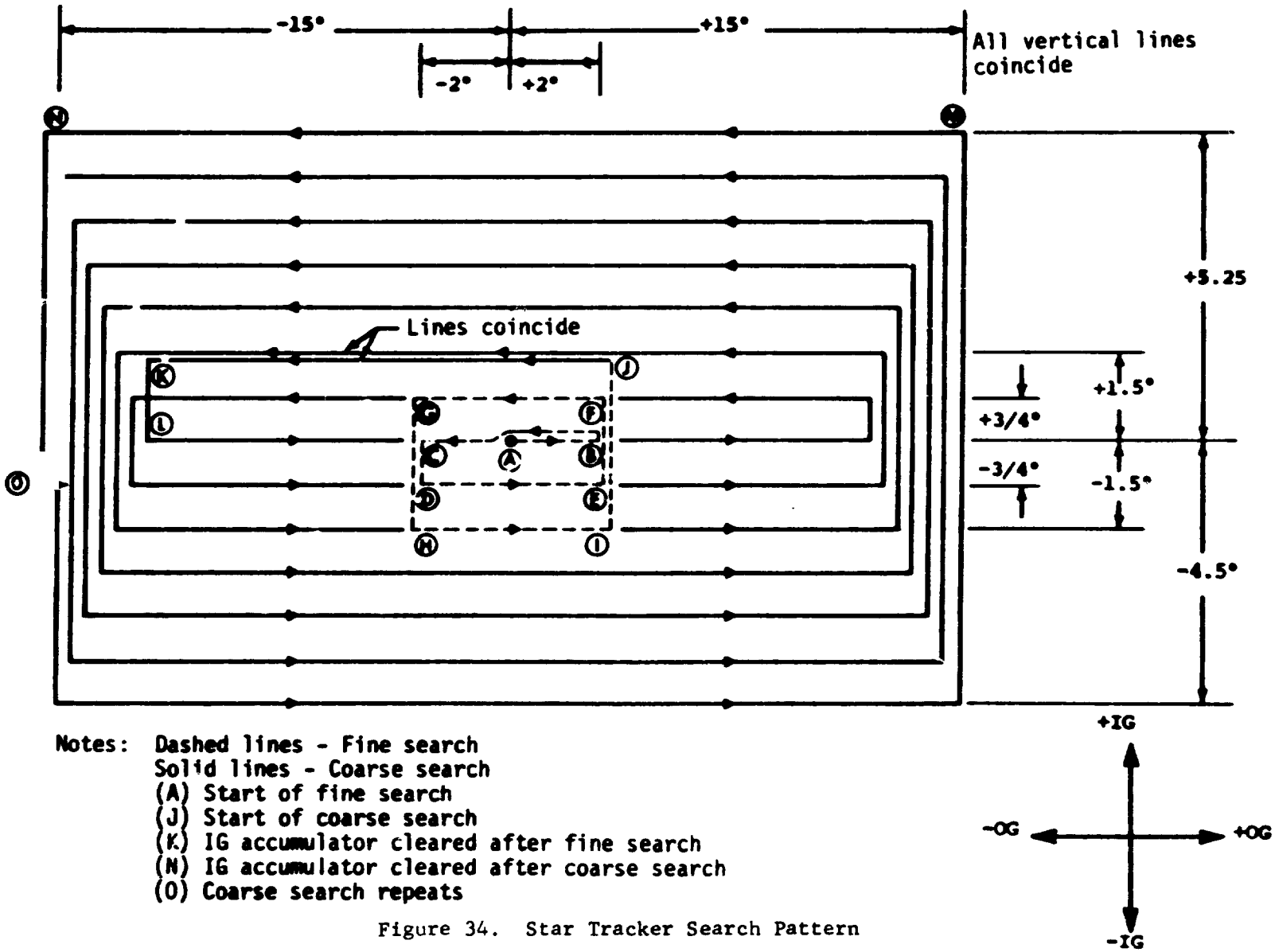

Notes: Dashed lines - Fine search
Solid lines - Coarse search
(A) Start of fine search
(J) Start of coarse search
(K) IG accumulator cleared after fine search
(N) IG accumulator cleared after coarse search
(O) Coarse search repeats

Figure 34. Star Tracker Search Pattern

Table 38. Star Tracker Performance Characteristics

Field-of-View	
Acquisition	1 arc degree (±8 arc minutes)
Track	10 arc minutes (+10, -1 arc minute)
Tracking Accuracy	±10 arc seconds
Capable of tracking to within 5 ± 3 degrees of Earth (0.35 albedo) and 45 ± 3 degrees of Sun, if not occulted by vehicle structure.	
Shutter fully opened or closed in less than one second.	
Search Angles	
Coarse - Inner Gimbal	-4.5 to +5.25 deg (+10,-0 arc min.)
Outer Gimbal	-15.0 to +15.0 deg (+10,-0 arc min.)
Fine - Inner Gimbal	-1.5 to +1.5 deg (+10,-0 arc min.)
Outer Gimbal	-2.0 to +2.0 deg (+10,-0 arc min.)
Gimbals	
Freedom	
Outer Gimbal	±87 degrees
Inner Gimbal	±40 degrees
Readout	Serial binary (ATMDC), parallel binary (telemetry)
Gimbal Position Resolution	40 arc seconds (serial binary and parallel binary)
Gimbal Position Accurary	±30 arc seconds (1 sigma)
Gimbal Rate	1.0 deg/sec. (max)
Capable of operating in automatic search/track, manual (from Manual Pointing Controller), and shutter closed/hold modes.	

2. Design History. Most changes to the original design of the Tracker resulted from deficiencies or problems uncovered during various levels of testing, covered below. Two significant design requirements changes were:

a. Modification of the initialization logic in the gimbal drive circuitry was done to assure that the Tracker, when powered up, would drive the gimbals to the zero or zenith angle position. The original design was such that the gimbals would usually drive to the limit stops when power was applied.

b. The Star Tracker Electronics Unit was modified to operate with an input of 130 volts at 455 Hz instead of the original 115 volts, 400 Hz power. This was done when the CMG inverters were changed from 400 Hz to 455 Hz in order to increase wheel speed. The Star Tracker, except for heaters, was powered from the CMG inverters.

3. Design Verification. During the hardware qualification thermal vacuum test a failure occurred when the photomultiplier tube assembly cracked at approximately -30 degrees C. The design specification was -50 degrees C. As a result, a thermostatically controlled 10 watt heater was mounted close to the photomultiplier tube assembly. The heater would turn on when the temperature of the assembly reached + 5 degrees C. Also, tube supports were modified slightly to relieve stress points encountered at low temperatures.

No problems were encountered during hardware integration tests.

4. Hardware Verification. The following problems were encountered during final acceptance tests and systems level testing.

a. The search pattern logic was redesigned after a vulnerable one-shot was found to be noise sensitive at certain positions in the search pattern. This problem was noted during final acceptance testing in Astrionics Laboratory, MSFC, when the Tracker would inadvertently stop in the middle of a search routine.

b. During thermal vacuum tests at JSC, the Star Tracker was noted to display false star presence signals. This problem was found to be an increase in the star threshold which was a result of resistor changes in the photomultiplier voltage divider circuit. This problem triggered the "Vamistor" investigation which resulted in some ATM subsystems being purged of the Vamistor film resistors.

c. During prelaunch tests at KSC, the Star Tracker gimbals were recording periods of oscillation when commanded in a "Hold" mode. The Star Tracker Electronics Unit was replaced with the flight spare. The problem was eventually traced to a faulty connection in a potted logic module (microstick) which occurred in manufacturing.

5. Mission Operations. The Star Tracker was activated at the beginning of SL-2 and operated satisfactorily except for frequent disturbances when star acquisition was lost due to contaminants entering the field of view. If a particle reflected light which had an intensity above the photomultiplier tube threshold and entered the field of view, the particle was tracked as a target star. This type of disturbance was noted thirty-five times during SL-2 and four times during SL-3. A large majority of these anomalies can be attributed to contaminant particles. Typical particles were generated by sloughing of paint, dust, outgassing, and venting from the vehicle.

Fewer problems were encountered on the SL-3 mission with tracking stray particles. This was attributed to a different operating procedure. During SL-2 the Tracker was placed in the "Auto" mode throughout each day part of the orbit and was automatically switched to "Shutter Close/Hold" during the night or a dump period. The Tracker was tracking continuously during the day and was susceptible to any bright particle that passed in the field of view. During SL-3 the Tracker was placed in "Shutter Close/Hold" as a normal mode and was switched to "Auto" by the crew only when it was used for an attitude update. These updates were accomplished in less than three minutes so that the possibility of a stray particle entering the field was reduced considerably.

During SL-3 there were five occasions when the shutter stuck in the open position. On each occasion the shutter would recover, usually within several hours. The system would be reactivated and normal operation would resume. Protective procedures were established after the first failures, to prevent damage to the photomultiplier tube due to the sun or reflections from the earth's surface and the vehicle. This procedure called for an immediate power down. Later, during the orbital night, the system was powered up and positioned to parking angles looking at the dark surface on a blocking plate.

The shutter failures were analyzed. All available data were evaluated, a sneak circuit analysis was performed, and the mechanical and electrical designs were reviewed. It was concluded that the most likely failure mode was a mechanical binding of the shutter drive mechanism.

One consequence of the shutter problem was that bright light from the earth's albedo apparently impinged the photomultiplier tube. This apparently degraded the tube response and lowered the sensitivity so that the target star, Alpha Crux, could not be acquired. A light as bright as the earth's albedo would degrade the tracker sensitivity arc 50% if it is exposed for twenty minutes. It was estimated that the tube was degraded 30% to 50% during SL-3 before protective procedures were established. The star Rigel Kent was selected as an alternate to Alpha Crux and was tracked successfully.

Satisfactory operation was recorded during SL-4 until DAY 228. At this time a failure was noted when the outer gimbal position indication went to zero and the outer gimbal rate signal recorded a constant output. An analysis of telemetry data was made and laboratory tests were performed to simulate the failure mode. The failure was exactly duplicated by interrupting the outer gimbal encoder output or the encoder lamp excitation. It was therefore concluded that the outer gimbal encoder had failed and in all probability would not recover. This failure mode rendered the Star Tracker useless and its operation was terminated. Backup techniques were implemented to calculate the vehicle roll reference. This was used in lieu of the Star Tracker for the remainder of SL-4 mission.

The Star Tracker was designed to provide both a fine and coarse search pattern; however, due to operational constraints implemented through the ATMDC, the coarse search was never used. All other features of the design operated normally (except for the aforementioned malfunctions).

Thermal conditions created no problems during system operation. The Tracker had internal heaters (30 watts) that maintained the temperature above a critical value of -18 degrees C. At first, it was felt that the shutter sticking problem was a result of low temperature, but when the problem occurred at times during the warmest part of the orbit this possibility was discounted. No electrical problems were encountered.

The interfaces with the ATMDC, EPEA, C&D Panel, and telemetry created no problems and it worked satisfactorily.

6. Conclusions and Recommendations. Test results with mission data and comparison with preflight analyses showed that the Star Tracker performed as designed except for the shutter failure, and the encoder failure.

Future Star Tracker systems should consider incorporating redundancy in optical encoders, e.g. lamps and power supplies. Also, alternate techniques in obtaining digital position data, e.g., multi-speed resolvers with resolver-to-digital converter electronics should be considered.

Problems with the shutter mechanism indicated a mechanical design deficiency and that a redesign should be considered.

Future designs should provide additional telemetry data to permit a more complete evaluation of problems and workaround techniques. It might also be desirable to provide for remote control operations during unmanned phases of the mission.

It should be recognized in the future that a Star Tracker flown on a large manned space station similar to Skylab would be exposed to drifting contaminant particles which, by reflecting sunlight, are brighter than target stars. The presence of such contaminant particles appears to be unavoidable because of life support systems vents and paint deterioration on large surface areas. Thus, every effort should be made to design a star tracking system which would be less susceptible to drifting contaminant particles. Concepts that should be considered are dual trackers, limiting tracking rate and limiting brightness and spectral characteristics of targets.

C. Control Moment Gyro

1. Hardware Description. The Control Moment Gyro (CMG) consisted of a motor driven rotor which was gimbaled to provide two-degrees-of-freedom within the limits of the electrical and mechanical stops. The instrument by utilizing its rotation momentum was capable of producing torques on a vehicle proportional to the angular rate of the gimbals. By controlling the CMG gimbal rates, attitude control of a vehicle was achieved. Figure 35 shows the assembled CMG.

a. Inner Gimbal (IG) and Rotor Assembly. The 21 inch diameter rotor rotated at a speed just under 9000 RPM and had an angular momentum of approximately 3000 N.m.s. The rotor was supported at each end by a single angular contact bearing and was constrained such that the correct bearing preload was maintained regardless of orientation during its operation within a wide environment range. A strut was inserted through the hollow rotor shaft and was rigidly attached to the gimbal at both bearing ends insuring a constant preload over the thermal operating range of the CMG. Lubricant was supplied to each bearing by means of a lubrication nut that also locked the bearing inner race to the shaft. The nut was hollow and was filled with sufficient lubricant to maintain the CMG through its operating life. The centrifugal force from the wheel rotation generated a pressure upon this volume of oil and forced oil through a metered portion on the lip of the nut. Centrifugal force carried the oil from the nut lip to the step in the bearing retainer. From this step in the retainer three holes carried the oil to the line contact of balls and races. The IG and rotor assembly was instrumented so that bearing temperature, rotor speed, and cavity pressure could be monitored (cavity pressure was monitored only during ground operations). Figure 36 shows a crosssection of the Inner Gimbal.

b. Motors. The rotor was rotated by two identical double squirrel cage induction motors. The motor rotors were an integral part of the rotor shaft. The stators were mounted in the gimbal. The two motors provided redundancy as well as a symmetrical design for balanced heat dissipation. A single motor was capable of maintaining sufficient RPM if a failure occurred.

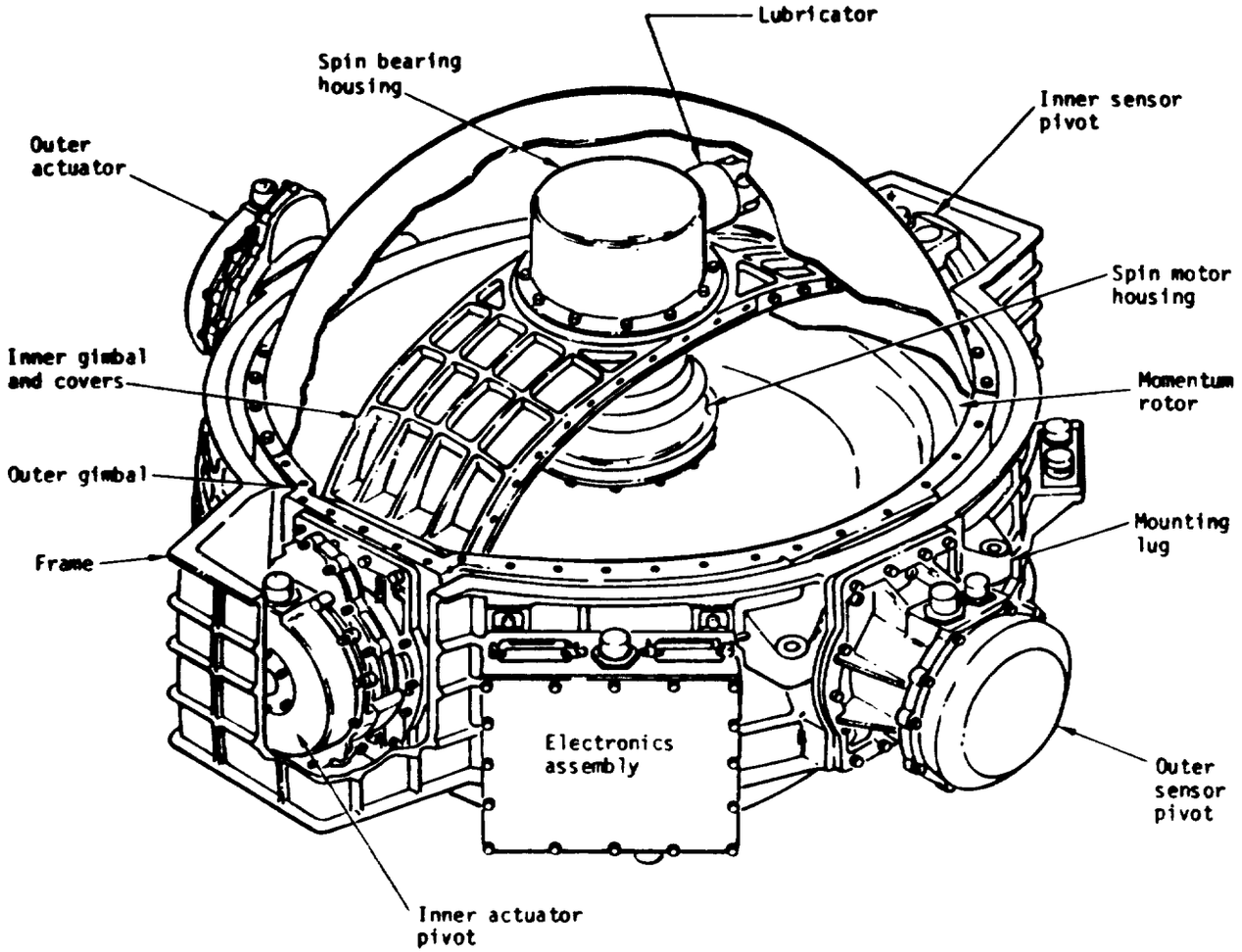

Figure 35. Control Moment Gyro (CMG)

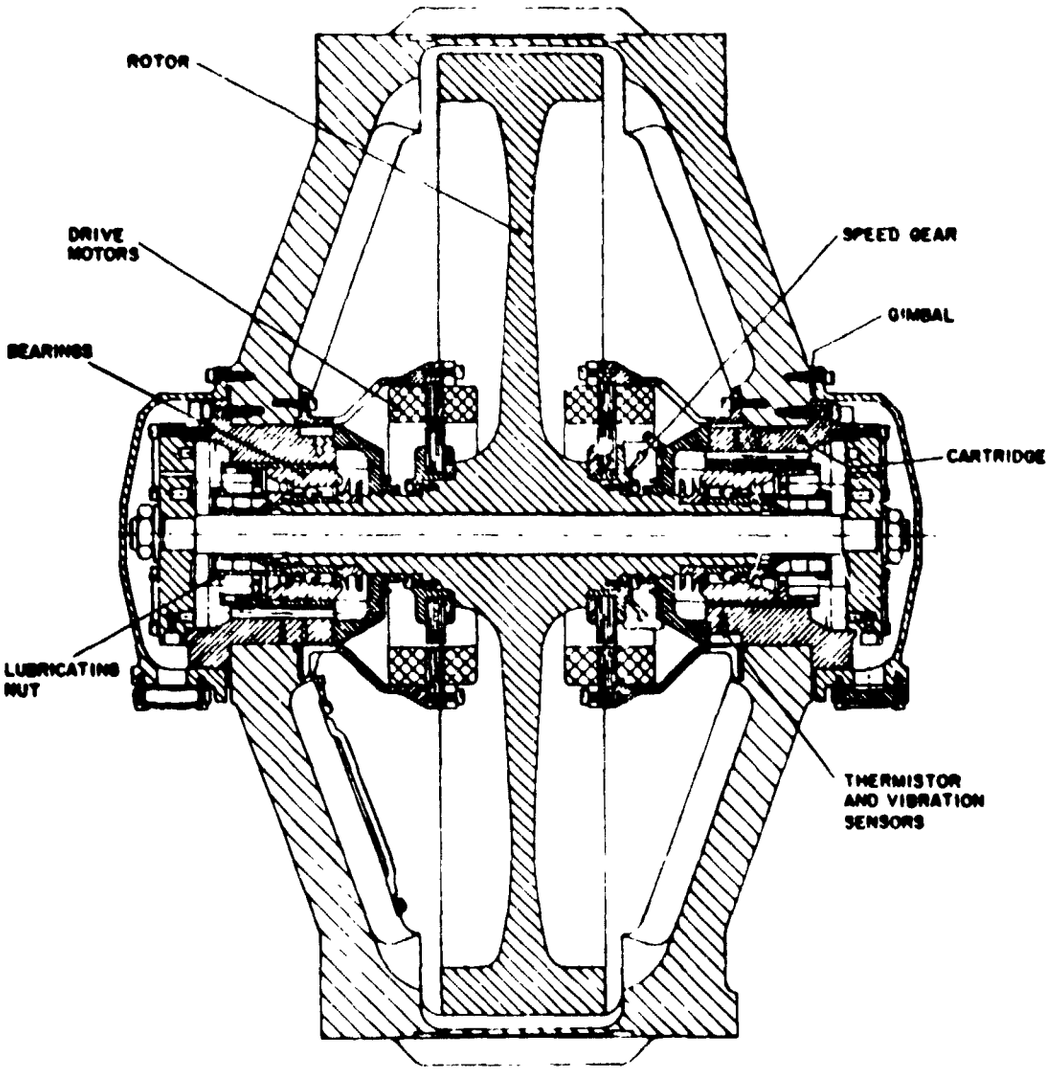

Figure 36. Cross-Section Of The CMG Inner Gimbal

The motors were driven at 8900 RPM by 130 V, 455 Hz three-phase electrical power supplied from a CMG Inverter Assembly (CMGIA). Synchronous speed for the six-pole motor was 9100 RPM. The motor efficiency under operational conditions was approximately 90 percent. The motors developed a relatively constant accelerating torque of 0.127 N.m. up to the region near synchronous speed. Just below synchronous speed, the motors provided a steep torque versus speed characteristic which made them behave as synchronous motors for good speed regulation with varying load. Input power was relatively constant during acceleration and dropped sharply near synchronous speed, resulting in high operating efficiency.

The double cage induction motor used two squirrel cage windings placed in slots one above the other. The outer cage winding had a high resistance and high leakage inductance, while the inner cage winding had low resistance and high leakage inductance. At stall, the frequency of the rotor current equaled the line frequency, allowing the outer cage to provide a high starting torque. As the motor accelerated, the rotor slip frequency decreased and the inner cage impedance approached the outer cage impedance. The combination tended to maintain a constant power transfer to the rotor and a relatively constant level of developed torque during acceleration. When the motor reached the normal operating speed, the reactances of the cage windings were small compared to the resistances. The currents in each cage were determined almost entirely by the resistances. The lower resistance inner cage then provided the major share of torque producing capability of the motor. The characteristics of a low resistance rotor at low slip are high efficiency and good speed regulation through a range of varying load torques. Figure 37 shows typical spinup and braking curves for CMG SN 10.

c. Motor Braking. The motor brake could be actuated by a crewman or by ground command to disconnect a CMG in case of a failure. The command (to the CMGIA) disconnected wheel excitation power and initiated the motor brake. Electrical means for providing braking torque to stop the CMG wheel consisted of applying a dc voltage (from the CMGIA) between two phases of the wye-connected motor stator; the third phase was left open. The dc current set up a field that caused the motor to behave as a short circuited ac generator to dissipate the energy stored in the rotating wheel.

d. Gimbal Seals and Covers. The rotor and inner gimbal assembly were sealed so that during earth testing, the gimbal cavity pressure could be maintained at a level of 100 microns of mercury or less. This was necessary to minimize windage friction losses on the high speed rotating wheel. During orbital operation, the evacuation valve was opened and the gimbal cavity vacuum was maintained by outer space.

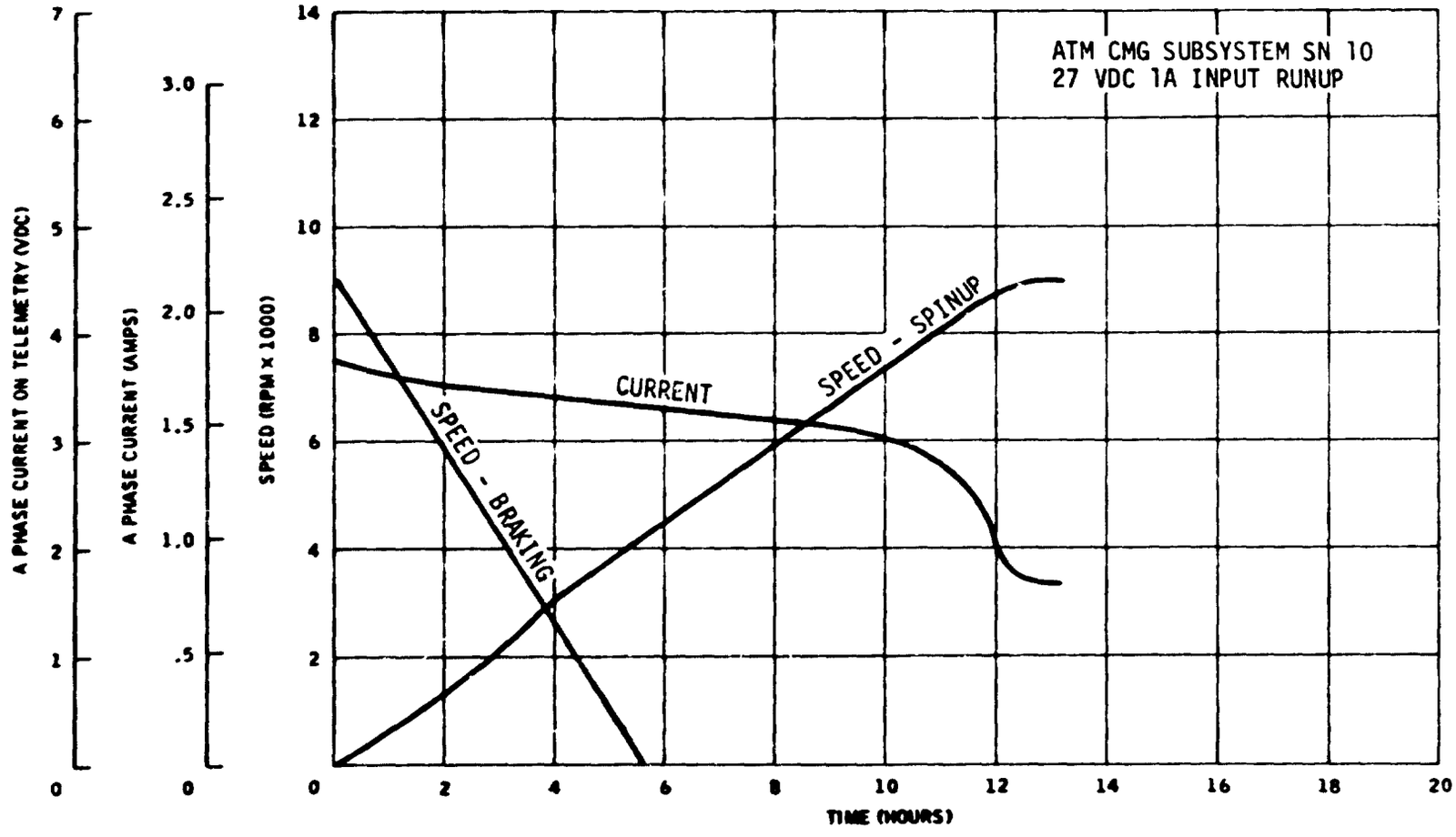

Figure 37. CMG Wheel Current Characteristics During Spin-up and Braking

External covers were provided and were attached to the upper and lower surfaces of the CMG frame. A thermal insulating blanket was attached to the CMG covers to assist in maintaining the proper thermal environment for the IG and rotor assembly.

e. Actuator Pivot Assembly. Both inner and outer gimbal rotation was accomplished by identical actuators. The actuator also served as a gimbal pivot. Each actuator consisted of a housing assembly, a dc torque motor, gear train, output shaft, and rate-feedback dc tachometer.

The actuator was capable of delivering 245 N.m. of torque. The tachometer operated at motor speed and provided an output of 1.0 volt/radian/second. The ratio of the two stage spur gear train was 56.55 to 1.

f. Sensor Pivots. The sensor assemblies served as gimbal pivots and provided electrical readouts that were used for gimbal position information. Each sensor consisted of a housing, ball bearing mounted pivot shaft, resolver assembly, cam-operated microswitches, and a flex lead assembly.

g. CMG Electronics Assembly (CMGEA). The CMG Electronics Assembly contained the rate servo electronics (amplifiers, modulator, detectors, etc.) to drive the CMG gimbals. The gimbal torquing rates were controlled by rate servo loops with a dc tachometer output for feedback. The rate servo amplifiers for either the inner or outer gimbal were functionally identical, differing only in servo characteristics.

h. CMG Inverter Assembly (CMGIA) - Each CMG derived its gyro wheel power from an individual solid state inverter. One CMGIA was also required to supply 455 Hz primary reference power to the Star Tracker and the Fine Sun Sensor CMGIA (No. 1). A second CMGIA (No. 2) supplied the same excitations as a secondary reference power source. The CMGIA also supplied 4.8 kHz, to the CMG resolver and 800 Hz power to the EPC resolvers and the MPC via the control distributor. The control distributor performed the switching operations between the primary and secondary reference power.

2. Design History.

a. Design Concept. The CMG was a spinning gyroscope mounted in two gimbals to provide two-degrees-of-freedom for the gyro spin vector. Driving the spin vector at some angular rate caused the gyro to produce a torque about an axis perpendicular to both the spin vector and the axis about which the spin vector was driven. The

torque was proportional to the angular rate and the angular momentum of the gyro. Three CMGs mounted orthogonally, were used on the ATM. For a description of the CMG subsystem, see Section III.A.2.b.

b. Design Goals. The CMG was originally designed in 1966 for an ATM mission period of 56 days. Momentum storage capability was 2700 N.m.s, and maximum gimbal rate was 4.5 deg/sec. Operating altitude was to be greater than 100 nautical miles. Performance and design data are presented in Table 39.

Table 39. CMG Perfo ance and Design Data

Angular Momentum Storage:	3115 N.m.s @ 9115 Rpm
Degrees of Freedom:	2
Output Torque·	
Range:	0 to 245 N.m
Threshold:	0.112 N.m
Gimbal Rates:	
Range:	0 to 7.0 degrees per second
Threshold:	0.0057 degrees per second
Gimbal Rate Servo:	
Bandwidth:	5 Hz
Phase Margin:	70 degrees
Gimbal Pivot:	
Actuator Motor Torque (Maximum):	9.52 N.m
Tachometer Gain	1 VDC/radian/second
Gear Ratio:	56.66 : 1
Resolvers Speed:	Single (4.8 khz excitation)
Gimbal Freedom:	
Inner:	±80 degrees (mechanical)
Outer:	+220 degrees (mechanical) -130 degrees (mechanical)

Table39. CMG Performance and Design Data(continued)

Wheel: Operating Speed:	8900 rpm
Electrical	
Power:	
Wheel Acceleration:	120 watts
Wheel at Operating Speed:	50 watts
Bearing Heater:	
15.6 degrees to 26.7 degrees C.	48 watts
Physical	
Size:	
CMG:	Within a 1.06 meters sphere
CMG Electronics Assembly (CMGEA):	0.249 by 0.218 by 0.0761 meters
Weight:	
CMG:	190 Kg
Wheel:	65.8 Kg
CMGEA:	3.7 Kg

c. Design Growth. In 1969, it was decided to fly Skylab in the "Dry Workshop" configuration. A number of design changes to the CMGS were required by this desicion. These included:

(1) Design life was increased to 10,000 hours (approximately 400 days).

(2) Momentum storage capability was increased to 3115 N.m.s at 9115 rpm.

(3) Maximum gimbal rate was increased to 7 deg/sec.

The CMG was originally designed to operate on a 400 Hz power source which caused the wheel to spin at 7900 rpm (sync speed was 8000 rpm). The angular momentum of the wheel at this speed was 2700 N.m.s. To increase the angular momentum of the wheel to 3000 N.m.s, it was necessary to increase the wheel speed to 8950 rpm. This was done by changing the CMG motor power supply frequency from 400 Hz to 455 Hz, which provided a synchronous speed of 9100 rpm. This required a major modification of the CMG inverter design, and retrofit of the 11 CMGs which had been delivered. Engineering studies were made to update the CMG stress and thermal analyses, and to determine the CMG safety margin at the higher rpm.

The increase in CMG design life forced a redesign of the gimbal actuators. For the 56 day mission, the actuators had used a simple spur gear design lubricated with a dry lubricant. For a 10,000 hour design life, it was necessary to redesign the gear train using hardened steel and a Bray grease lubricant. Other actuator changes included actuator pivot grease seals to avoid torque motor contamination, and redesign of the torque motor commutator and brushes.

The increase in gimbal rate limits was made by a scaling resistor change on the rate command input card in the CMGEA. All 12 delivered CMGs were retrofitted. ATMDC software was designed to command the maximum CMG torque output consistent with inner and outer gimbal torque motor capability for all cimbinations of rate commands and outer gimbals.

3. Design Verification.

a. Hardware Qualification. Qualification testing of the CMGs was completed March 15, 1973. The Qualification Test Program was conducted as specified in Reference 14. No significant problems were encountered. Minor out-of-specification conditions were noted during the EMI tests. A waiver was granted to accept these deviations. For additional information, see Reference 15.

In addition to the formal qualification test program, life tests were performed on the major CMG components. These tests were performed in a vacuum chamber at ambient temperatures. No significant problems were encountered.

b. Hardware Integration. Flight type CMGs were first integrated into the APCS during testing in the Hardware Simulation Laboratory (HSL) at MSFC. This testing was performed in the Summer and Fall of 1971. All testing was performed under ambient conditions with torques due to earth's rate and gravity biased out of the Torque Measuring Fixture output. The CMGs performed normally. No problems

were encountered. Since the CMGs were spinning continuously for months at a time, care was taken in the HSL to keep the spin axis of the No. 3 CMG horizontal when the simulation was not in use, to avoid excessive wear of the wheel spin bearings. By February 1974, these CMGs had accumulated over 27,000 hours with no problems.

For additional information see Reference 19.

4. Hardware Verification. System-level tests were performed on the prototype and flight ATMs to verify system design and flight readiness. These tests included post-manufacturing checkout, vibration testing, thermal-vacuum testing, and prelaunch checkout. During these tests several significant CMG problems were encountered. These are discussed below:

a. Belleville Washer Problem. The power transistors and diodes in the CMG Inverter Assembly (CMGIA) were mounted to the heat sink by a nut and a stud with a Belleville washer used to provide tension on the stud. This tension maintains firm contact between the transistors and the heat sink to provide for heat conduction from the transistor to the heat sink. During post-manufacturing checkout of the flight ATM CMG output became quite noisy. Investigation showed that this was caused by overheating of some transistors in the CMGIA. These transistors were found to be loose. The problem was traced to improper heat treat of the Belleville washers used in the transistor mounting. The washers deformed under stress, which allowed the transistor mounting to loosen. This caused a decrease in the heat flow from the transistors to the heat sink. The faulty washers were replaced.

b. Resolver Coupling. During post-manufacturing checkout it was noticed that the output of the CMG outer gimbal linear resolvers decreased when the outer gimbal approached the negative stop. This was caused by coupling between the linear and desaturation resolvers which were mounted side-by-side, but were excited by independent power sources which were not in synchronization. The systems networks and the CMGIAs were modified so that excitation voltages from a common source were applied to both resolvers. The resolver excitation in each CMG was fused so that a shorted resolver in one CMG would not affect the other CMGs.

c. Noisy Tachometer. During Thermal Vacuum (T/V) testing of the prototype ATM at JSC, it was noted that an excessive number of caging commands from the ATMDC (preflight program) were required to maintain the CMGs caged to any desired gimbal configuration. The problem was traced to a noisy output from the tachometer used to provide gimbal rate feedback in the CMG gimbal actuator control loop. The noisy output caused the control loop to drive the gimbals at a

rate greater than commanded by the ATMDC, which resulted in over-controlling the gimbals. The actuator tachometer brushes were made of a newly developed material designed for use in the vacuum of space. During T/V testing, the brush outputs became intermittent. This was caused by buildup of a non-conducting film layer on the surface of the brushes. The film layer was caused by a reaction between the brush material and outgassed products from the potting compound in an electrical connector in the actuator. The problem was corrected by changing the brush material to silver graphite and eliminating the potting compound from the connector.

d. Bearing Failure. During post-T/V testing of the flight ATM, a wheel bearing of the Z-axis CMG (S/N 11) failed. The spin axis of the Z-axis CMG was normally vertical when the ATM was mounted in the test fixture. The lower bearing failed. A detailed analysis of the failure was performed. It was concluded that the failure occurred because the oil flow rate in the bearing was insufficient to maintain an adequate lubrication film in one "g" spin axis vertical operation with the normal range of gimbal rates. The failure was believed to have occurred as follows:

(1) The lubrication make-up rate was insufficient to support unlimited operations in earth gravity. This was caused by a low flow rate from the lube nut combined with a relatively short time for the oil to accumulate in the bearing raceways.

(2) Marginal oil film thickness, caused by insufficient lubrication, led to breakdown of the elastohydrodynamic film which caused initial metal damage. In addition, sufficient oil was not available in the raceways and bearing pockets to dissipate local heat.

(3) Heating from metal damage caused the allowable temperature differential across the bearing to be exceeded causing loss of radial clearance and destructive failure of the bearing.

(4) Local heating was believed to have been caused by two factors, neither of which was sufficient to cause the failure:

Higher bearing loads because of the addition of wheel weight and radial loads caused by gimbal rates.

Flow of oil away from the bearing raceways for a vertical orientation in one "g".

Changes in wheel speed and bearing temperature had been noted on this CMG for about 35 hours before the failure.

It was noted that the failed bearing had had the lowest make-up lubrication rate of all CMG bearings, (0.026 mg/hr). Another bearing with low make-up lubrication rate was on CMG S/N 9, also on the flight ATM. This bearing also showed temperature abnormalities. Disassembly and analysis of this bearing showed early metal damage to the bearing raceways.

As a result of the failure investigation, three actions were taken:

> A visual and test screening program was conducted on all flight CMGs. This consisted of a visual screening for oil in the spin bearings, followed by a 270 hour screening test which operated the inner gimbal and rotor assembly in vertical and horizontal positions while monitoring cavity pressure, bearing temperature and vibration, wheel speed, spin motor currents, and bearing drag.
>
> The spin bearing lube nut flow rates were increased to a range of 0.05 to 0.12 mg/hr.
>
> The spin axes were maintained horizontal during ground testing.

No further difficulties were noted, and the CMGs were certified flight-worthy. For more information, see Reference 16.

5. Mission Operations. Spinup of the CMGs were begun on DAY 1 at 19:05:00. CMG control was enabled at 22:20:00. CMG No. 1 and CMG No. 2 reached nominal wheel speed on DAY 2, 06:30:00, a spinup time of 11 hours and 25 minutes. CMG No. 3 reached nominal wheel speed at 07:30:00 on DAY 2, a spinup time of about 12 hours and 25 minutes. These spinup times were nominal. CMG wheel speeds, spin motor currents, bearing temperatures, and general behavior were all nominal.

On DAY 12 at 09:56:00, the CMG No. 3 wheel speed indication on telemetry went to zero. All other data from the No. 3 CMG remained nominal, which indicated that the wheel speed transducer had failed.

The CMGs continued to perform nominally until DAY 194, 08:42:00 when CMG No. 1 wheel speed went to zero, accompanied by a rapid rise in spin motor currents and bearing temperatures. This indicated failure of CMC No. 1. The APCS was reconfigured for two-CMG operation on DAY 194, 08:57:35. CMGs No. 2 and No. 3 continued to run until conclusion of the SL-4 mission on DAY 271. After several post-mission tests, the CMGs were powered down on DAY 272, 13:25:06.

a. CMG No. 3. CMG No. 3 performed nominally throughout the entire mission except for the wheel speed transducer failure on DAY 12. On DAY 272 a wheel speed run down test was performed on No. 3 CMG. Using the CMG wheel speed/motor current curves, the initial wheel speed was calculated. Power to the wheel was turned off and the wheel was allowed to coast for 85 minutes. Wheel power was then turned on and the new wheel speed calculated from the speed/current curves. From this information, spin bearing torque was calculated to be 0.0205 N.m, which is nominal.

b. CMG No. 1. CMG No. 1 appeared to perform nominally until about DAY 194, 07:57:00. At that time, over the Honeysuckle tracking station, the No. 1 spin bearing temperature rose about 5 degrees C, the wheel spin motor current increased about 65 milliamps and the wheel speed decreased about 110 rpm.

On DAY 194, 08:42:00, the Bermuda tracking station acquired Skylab telemetry. The following anomalies were observed in CMC No. 1:

Wheel speed	-	zero rpm
Bearing No. 1 temp	-	83 degrees and decreasing
Bearing No. 2 temp	-	23 degrees and increasing
Phase A current	-	2.06 amps
Phase B current	-	2.01 amps
Phase C current	-	2.03 amps

The CMG was shut down by Mission Control Center (MCC). Since the failure occurred while the OA was not in range of a tracking station, no real time data were available. Playback recorder data for the time of the failure included:

Phase A spin motor current

Gimbal rates

DC bus voltage

ATMDC Rate Gyro rates

These data were reduced and tabulated in Table 40 together with bearing temperature data available from Honeysuckle and Bermuda. A plot of Y-axis rates, Phase A current, system momentum and gimbal rates are shown in figure 38.

Table 40. CMG No. 1 Failure Analysis

DATA POINT	TIME DAY:HR:MIN	A PHASE CURRENT RAW DATA	WHEEL SPEED RPM	GIMBAL RATE °/SEC	Y AXIS RGP °/SEC	BEARING #1 TEMP °/C	BEARING #2 TEMP °/C
1	194:06:08	1.003 amp	9060 (raw data)	Less than 0.1	-	21.8	18.55
2	194:08:00	1.018 amp	9060 " "	-.5IG +.50G	-0.025	24.69	19.14
2A	194:08:03	1.064 amp	9015 " "	-.5IG +.50G	-	26.22	19.22
3	194:08:15	1.076 amp	8980 inferred from current	+.5 IG -3.5 OG	-0.025 to +0.025		
4	194:08:17	1.415 amp	8341 "	Less than .1			
5	194:08:22	1.790 amp	7700 "	"			
5	194:08:23	1.760 amp	7831 "	"			
7	194:08:25	2.300 amp	stall "	"	Significant noise superimposed on normal rate		
8	194:08:30	1.960 amp	6100 "	+.5 IG 2.00G	+.025 to -.025		
9	194:08:40	2050 amp	4800 "	+1.0 IG +2.00G	-.025 to +0.000		
10	194:08:50 194:08:50:30	2.100 amp	3864 "			74.82	24.45
11	194:08:50:37	Brake on				74.0	24.77
12	194:08:57:35	Brake off				68.07	26.46

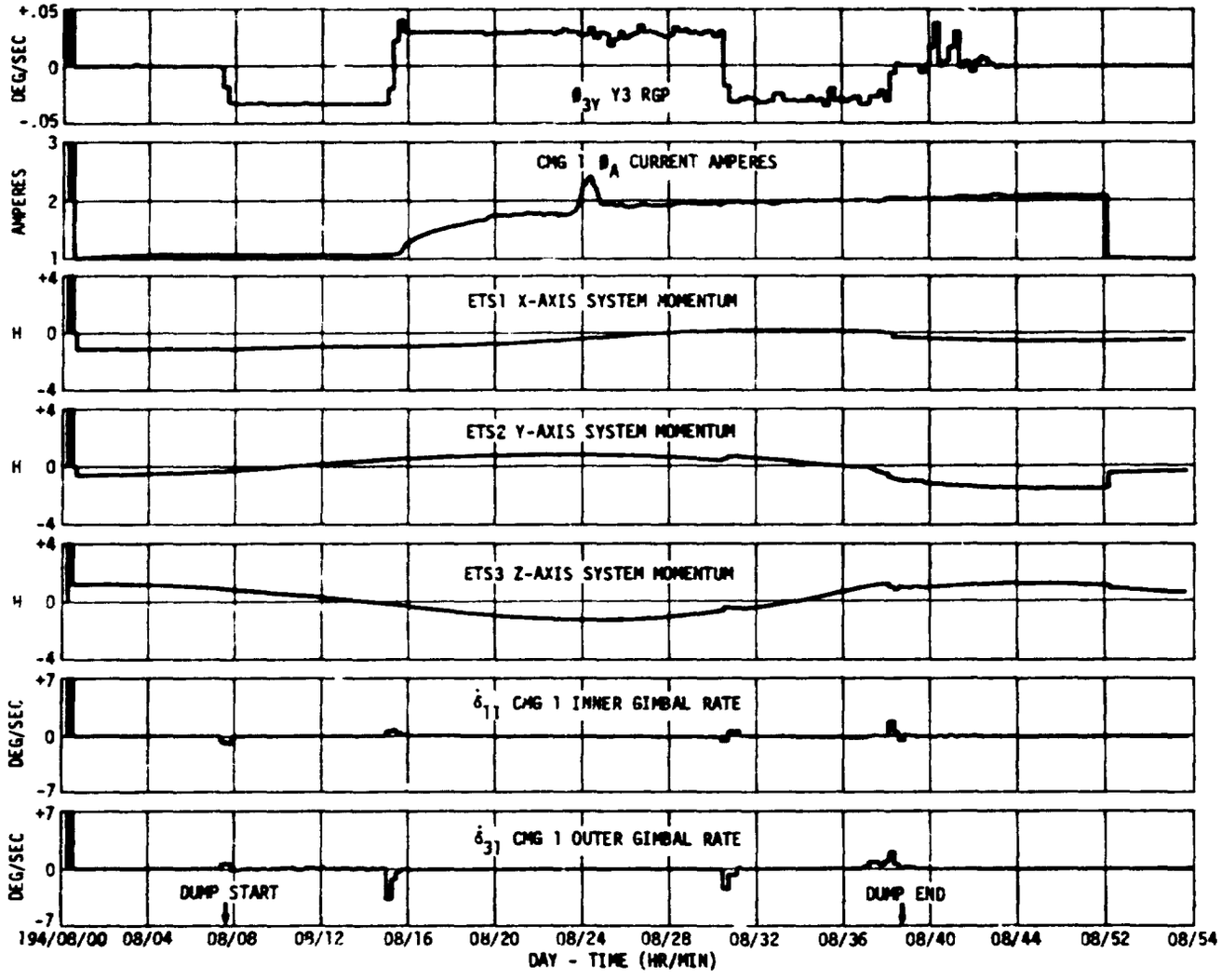

Figure 38. CMG No. 1 Failure

Analysis of Data Points 1 through 11 on Table 40 follows:

(1) This appeared to be the beginning of the final failure.

(2) This reflected a worsening condition as evidence in increasing bearing temperature and approximately a 15 milliamp increase in motor current. Suppose the distress is in bearing No. 1, causing it to heat up (21.8 degrees C to 24.69 degrees C to 26.22 degrees C) more than bearing No. 2 (18.55 degrees C to 19.14 degrees C). The heat flows from 1 to 2. Normally the temperature differences between temperature measurements does not change this much. The gimbal rate command coincidence with the increase in current (1.0A to 1.98A) is considered significant here even though it is considered negligible in a normal system.

(3) Analysis here is based on playback recorder A phase current, RGP, and gimbal rate commands. The situation is worsening as judged by a higher current value which implied a further decrease in wheel speed. A point of significance is that this worsening condition coincides with initiation of gimbal rate commands of +1/2 deg/sec IG -3.5 deg/sec OG. The Y rack RGP output appears normal.

(4) The rapid increase in current, (0.339A) over a two minute period, infers an increase in torque; tending to slow the wheel (646 rpm decrease).

(5) Although the overall condition appears to be worsening, the current decreased by 30 milliamps from item 5, and the inferred speed increased by 131 rpm. A motor of this torque capability (0.127 N.m peak) cannot accelerate the inertia of the CMG assembly this rapidly.

(6) The peak current indicated (2.3A) would infer a stall condition for a normal motor. However, approximately one minute after, the motor current inferred a rotor speed of approximately 7,000 rpm and it was physically impossible for this to occur. This current anomaly was not understood. At that time, the Rack Yaw RGP indicated considerable perturbations leading one to conclude initially that the CMG system was causing the rack to vibrate. However, subsequent data analysis disclosed other periods of similar Rack RGP indications leading to some doubt about the cause and effect relationship.

(7) The inferred wheel speed based on current indication is 6,100 rpm, at times followed by small intervals of increased speed.

(8) Current value was increasing and inferring a decrease in wheel speed to 4,800 rpm. At the same time, a gimbal rate command was initiated. The Rate Gyro indications showed increased vibration shortly after the gimbal rate command. This and the evidence of constant current just preceding, indicated a rise in current value. These conditions inferred that the CMG rotor was spinning. Momentum management calculations of rotor speed from 25% to 35% ± 1,000 rpm did not corroborate speed as inferred from current.

(9) Utilizing analysis based on realtime data at AOS Bermuda and inferred wheel speed (based on current) one would conclude that the rotation was 3,864 rpm. However, the real time wheel speed indication was zero. This loss of wheel speed data from real time data inferred the loss of the wheel speed pickoff. A composite of a real and recorded ASAP data for line currents were constant for 4 1/2 minutes and were balanced (A phase 2.01A, B phase 2.07A, C phase 2.07A). Bearing No. 1 temperature was 74.82 degrees C and decreased from a high at AOS of 82.3 degrees C. This value of temperature was considered valid because the caution light set at 74 degrees was initiated during LOS, however, auto shutdown at 90 degrees C wasn't initiated. Bearing No. 2 showed a value of 24.45 degrees C and increasing from an AOS value of 22.59 degrees C. The RGP inferred a quiet rack condition at this time.

(10) Because of evidence high bearing No. 1 temperature and loss of real time wheel indications, the CMG No. 1 system was shut down by applying the dynamic brake for seven minutes. The inverter was left operating. The bearing temperature showed that bearing No. 1 was decreasing and No. 2 was increasing as expected (short time after shutdown). Both bearings attained the same temperature of 28 degrees C in approximately four hours after shutdown.

The exact mode of failure of CMG No. 1 could not be determined because of insufficient data. Bearing failure, due to insufficient lubrication, appeared to be the most likely cause. Review of data recorded before the failure showed that four CMG No. 1 bearing anomalies had occurred, all of which had been thought to be insignificant. These anomalies were characterized by a change of differential temperatures between the bearings, a slight decrease in wheel speed, and a slight increase in spin motor current. The first occurred on DAY 174 and the last over Honeysuckle about one hour before the failure on DAY 194.

After completion of the SL-4 mission, CMG No. 1 was turned on to determine if it would run. The bearing heaters were turned on 24 hours before spinup was attempted. Initial spin motor

currents were 2.26 amperes. During the first 90 minutes, the phase currents decreased about 110 milliamps to about 2.15 amperes. At this point the currents leveled off and remained constant. Power was applied to the wheel for 8.5 hours. At the end of this time, the spin motor currents should have been 1.85 amps and the wheel speed should have been 6700 rpm. Bearing temperatures increased slowly during the test. The slight drop in spin motor current at the beginning of the test was attributed to an increase in spin motor winding impedance and a decrease in rotor gap caused by a rise in temperature resulting from current flow. It was concluded that the spin motor torque (about 0.127 N.m) did not overcome the bearing friction and the wheel did not turn.

c. CMG No. 2. CMG No. 2 performed nominally until DAY 190, when the first of a long line of CMG No. 2 bearing anomalies occurred. The anomaly was characterized by a change in differential temperature between the bearings, a slight decrease in wheel speed, and a slight increase in spin motor current. This anomaly went unnoticed at the time, but was discovered during data review after the CMG No. 1 failure. As a result, MCC and STAC were asked to monitor CMG No. 2 and CMG No. 3, 24 hours a day, until the end of the mission, and a committee was created to investigate the CMG anomalies and to determine how best to conserve CMGs No. 2 and No. 3. CMG No. 2 continued to exhibit periods of anomalous behavior of increasing frequency and duration until DAY 255 when an anomaly began which lasted until the end of the mission, except for brief periods of normal behavior. The anomaly gradually became more severe as time passed. A typical CMG No. 2 anomaly is shown in figure 39. In general, all the anomalies showed the characteristics presented here for varying periods of time.

A detailed review of all CMG bearing data was performed by the committee to investigate the CMG No. 2 anomalies. It was concluded that the CMG No. 2 anomalies were probably caused by insufficient lubrication in the proper locations in the bearings; i.e., in the ball track and the ball retainer. It was recommended that the bearing heaters be cycled manually to maintain the bearing temperature between 21.1 degrees C and 26.7 degrees C, and that the CMG gimbal rates be limited to 2 deg/sec during momentum dumps. These recommendations were implemented. The suggestion was also made to limit all gimbal rate commands to 2 deg/sec, and to ramp in rate commands, but it was decided that the software impact of these changes outweighed their value. It was felt that the increase in bearing temperature enhanced bearing lubrication by lowering the oil viscosity, increasing the oil flow from the lube nut, and promoting better oil distribution. Limiting the gimbal rates reduced the radial loads applied to the spin bearings.

CMG No. 2 was used for attitude control until the end of the SL-4 mission. On DAY 272 a wheel speed rundown test was performed

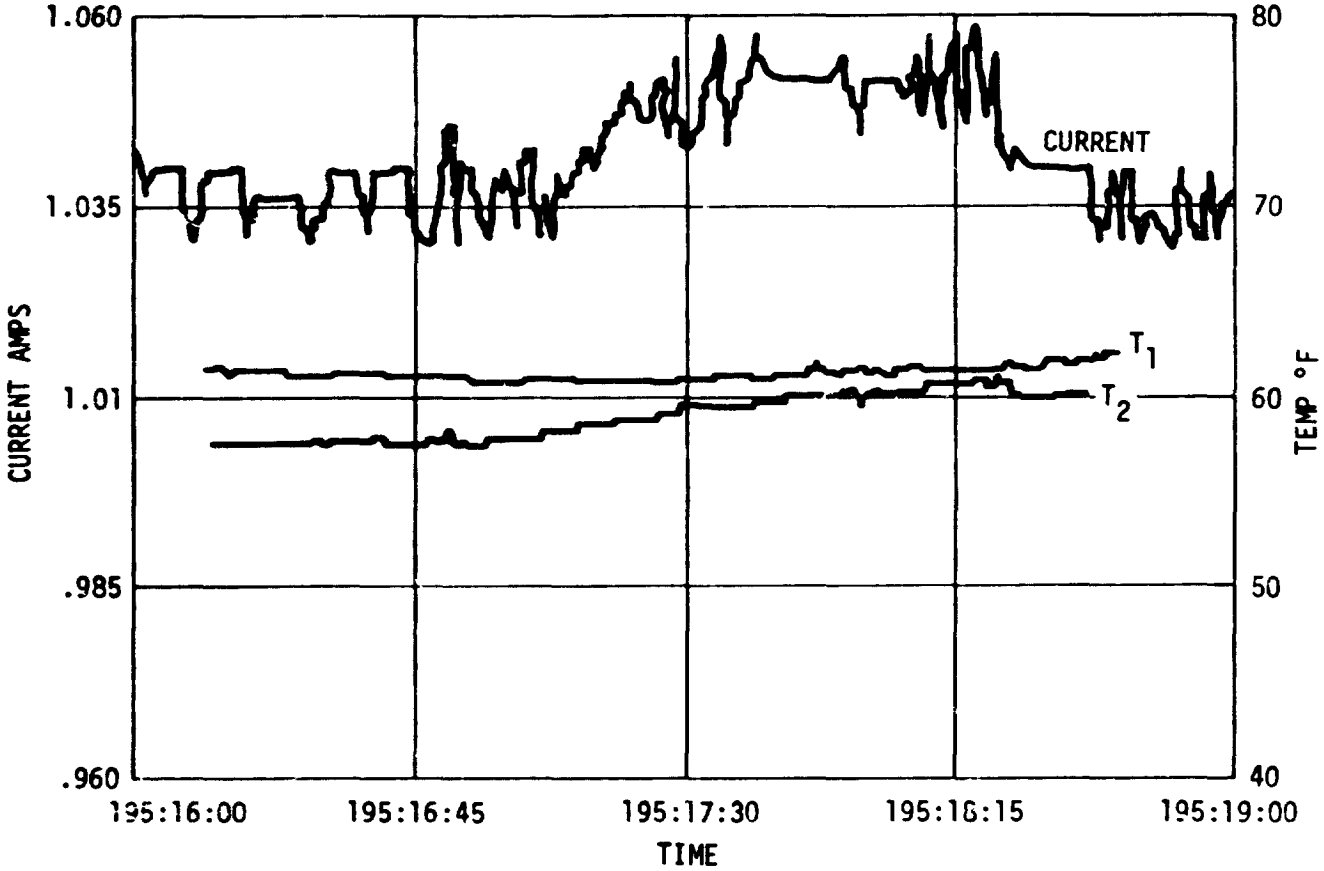

Figure 39. Typical CMG No. 2 Anomaly

on CMG No. 2. Power was removed from the wheel for 85 minutes. In that period, the wheel speed decreased 496 rpm. The bearing torque was calculated to be 0.034 N.m, which while greater than nominal is within the range of torque for normal bearings. This indicated that little permanent damage had been incurred by the bearings. It was felt that the results of this test support the theory of retainer ring instability due to insufficient lubricant in the bearing raceways and the retainer ring.

6. Conclusions and Recommendations.

a. Conclusions.

(1) The cause of the CMG No. 1 failure was not firmly established, but can be attributed to insufficient lubrication.

(2) The cause of the CMG No. 2 anomalies was not firmly established, but can be attributed to insufficient lubrication.

(3) Bearing and lubricant behavior in zero "g" is not well understood.

(4) The Control Moment Gyro (CMG) concept was thoroughly tested during Skylab and found to be very satisfactory for control of long-lived spacecraft in earth orbit.

(5) Data provided by the ATM PCM telemetry system were inadequate for real time analysis of CMG anomalies.

b. Recommendations.

(1) Tests of high speed bearings in zero "g" should be performed to further the state-of-the-art in bearing technology for future space application.

(2) In future long-duration manned missions, consideration should be given to replacement or maintenance of mission-critical components.

D. Acquisition Sun Sensor

1. Hardware Description. The Acquisition Sun Sensor consisted of two major subassemblies, the Optical Assembly (OA) and the Electronics Assembly (EA). The Optical Assembly used a family of five photovoltaic cells arranged in a geometric configuration to generate voltage analogs of the sun's angular position about two orthogonal axes, linear to $\pm$ 5 degrees, and a discrete signal any time the sun is within the field-of-view of the error detectors (9 $\pm$1 degrees

circular). The Electronics Assembly used conventional electronics to shape and scale the signals from the Optical Assembly and then transmits the angular error signal and the sun presence signal to the APCS digital computers for subsequent processing and use in the Attitude and Pointing Control. The Optical Assembly optical axis was aligned parallel to the Z-axis of the vehicle and measured angular errors about the X and Y-axes.

The Optical Assembly contained two pairs of fine-pointing detectors (one pair per axis) and a target detector. Each pair of detectors was connected so that the output currents were differenced and functioned as an energy balance null sensor. When the sensor was pointed directly at the sun both photocells received the same amount of energy and the electrical output was at a null. When not pointed directly at the sun, the optics (lenses and baffles) produced a difference in the solar energy reaching the two cells in the pair. The electrical output from the cells was proportional to the angle between the optical axis of the sensor and the sun line. The target cell drone level detecting electronics which triggered a discrete when the energy entering a 9 ± 1 degree circular field-of-view was equivalent to one-half solar constant.

The subsystem was completely redundant. There were two independent systems operating at all times. (See figure 40).

2. Design History. Although the original design requirements for the Sun Sensor were based on a 56-day mission, no significant design changes were made to adapt the sensor to the longer requirements of the mission as flown.

3. Design Verification. All qualification and integration testing was successfully completed with each flight type sensor meeting all specifications.

Integration testing pointed out that the sensor was sensitive to reductions in solar light intensity. The sensor was designed to operate at one solar constant. However, any degradation or contamination which would result in reduced light intensity at the detection cells also caused a reduction in the scale factor of the analog angular error signal. It was felt that this would not be a problem during the period of the Skylab mission.

4. Hardware Verification. All test requirements were met during the hardware verification testing.

5. Mission Operation. The Acquisition Sun Sensor performed throughout the mission without malfunction or failure. The sensor was in continuous operation from initial power-up to final power-

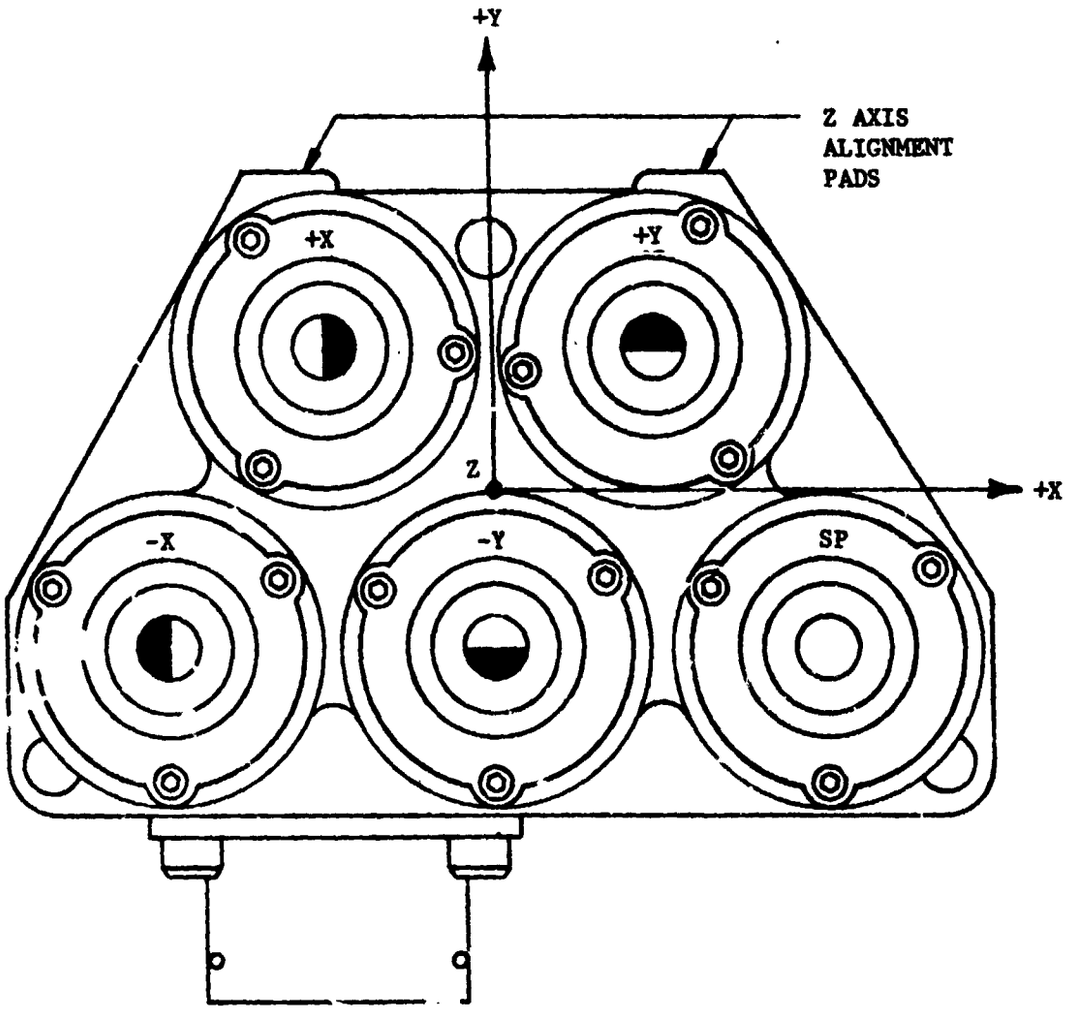

Figure 40. Acq. SS Detector Block Assembly

down. It operated within and fulfilled all design requirements. There were no problems with system interfaces.

Telemetered temperatures of the mounting plate ranged from -11 to +43.9 degrees C, well within the design operating range of -40 to +70 degrees C. There were no active heating elements in the Optical Assembly, so all heating was due to the sun and cooling due to conduction and radiation. Temperature rises of 15 degrees C in 10 minutes were observed during orbital sunrise.

6. Conclusions and Recommendations. The Acquisition Sun Sensor operated as desired and fulfilled all requirements. Analyses of flight data have shown that the sensor scale factors and operating characteristics were consistent with preflight test data. Based on the temperature data, it has been concluded that there was some deterioration of the S-13G paint on the Optical Assembly. The extent of the deterioration could not be determined.

There were no indications that any changes should be made to the sensor design. For long duration missions, a sun sensor design which is not sensitive to solar intensity should be considered.

E. TACS

1. Description.

a. Mechanical Components. A schematic representation of the Thruster Attitude Control System is presented in figure 41. The location of the system on the Skylab spacecraft and the mounting of key components are shown in figures 42, 43, 44, and 45.

The six thruster nozzles had 50:1 expansion ratios and bell-shaped expansion contours. These features were selected to maximize specific impulse while confining the exhaust plume to minimize impingement on the vehicle aft skirt. An impingement shield was provided to eliminate unbalanced forces on the vehicle due to plume impingement on aft skirt structural elements.

There were 24 propellent control valves (figure 45) in the system. The solenoid actuated, pneumatically operated, valve contained a small pilot poppet integral and coaxial with the main poppet. The pilot poppet controlled pressure forces that opened the main poppet. The pilot Poppet and main poppet were linked mechanically so that energizing the solenoid coil opened the valve against the springs at low supply pressures. When the solenoid was de-energized, both poppets were pressure-unbalanced closed to assure leaktight sealing.

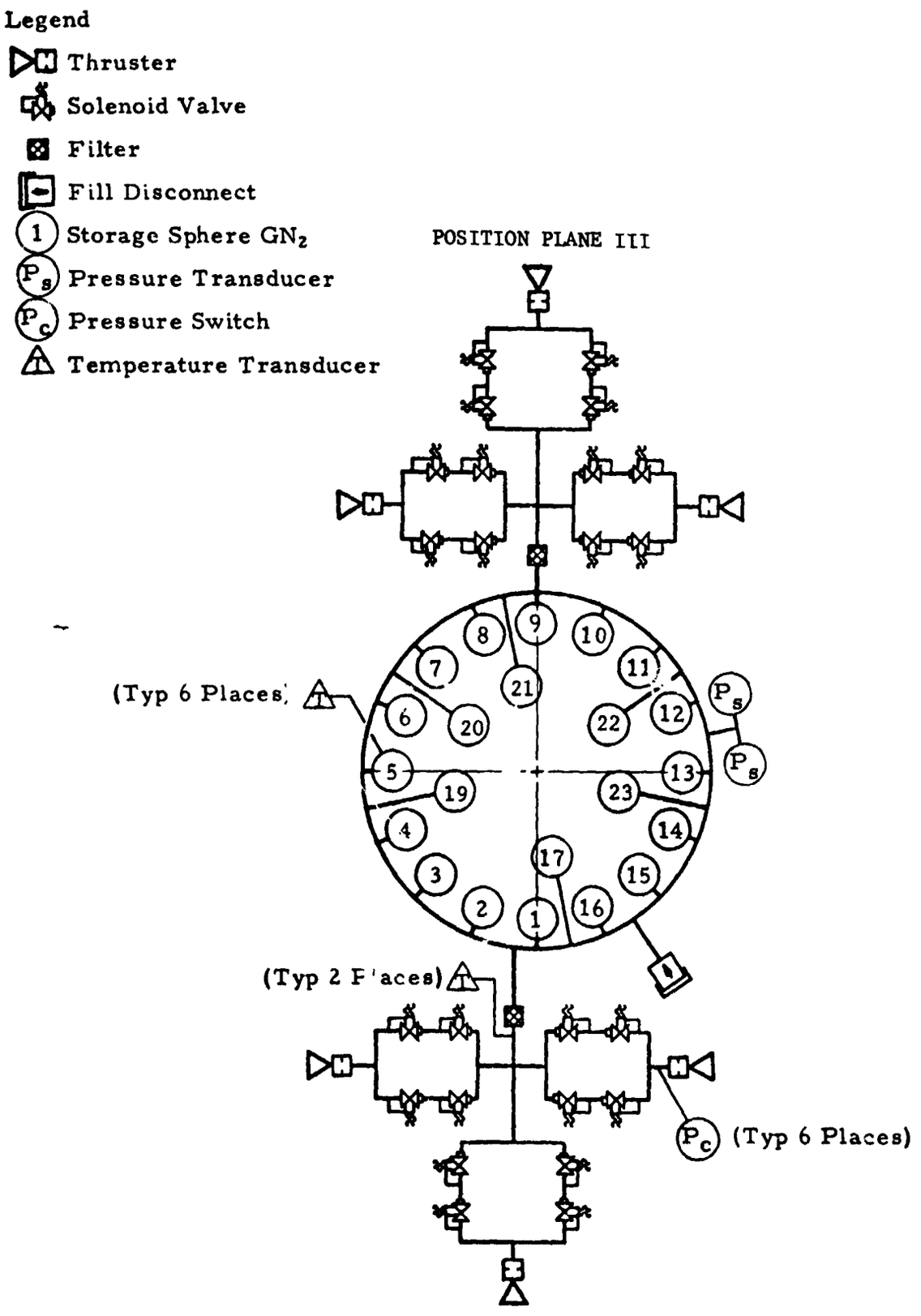

Figure 41. TACS Hardware Schematic

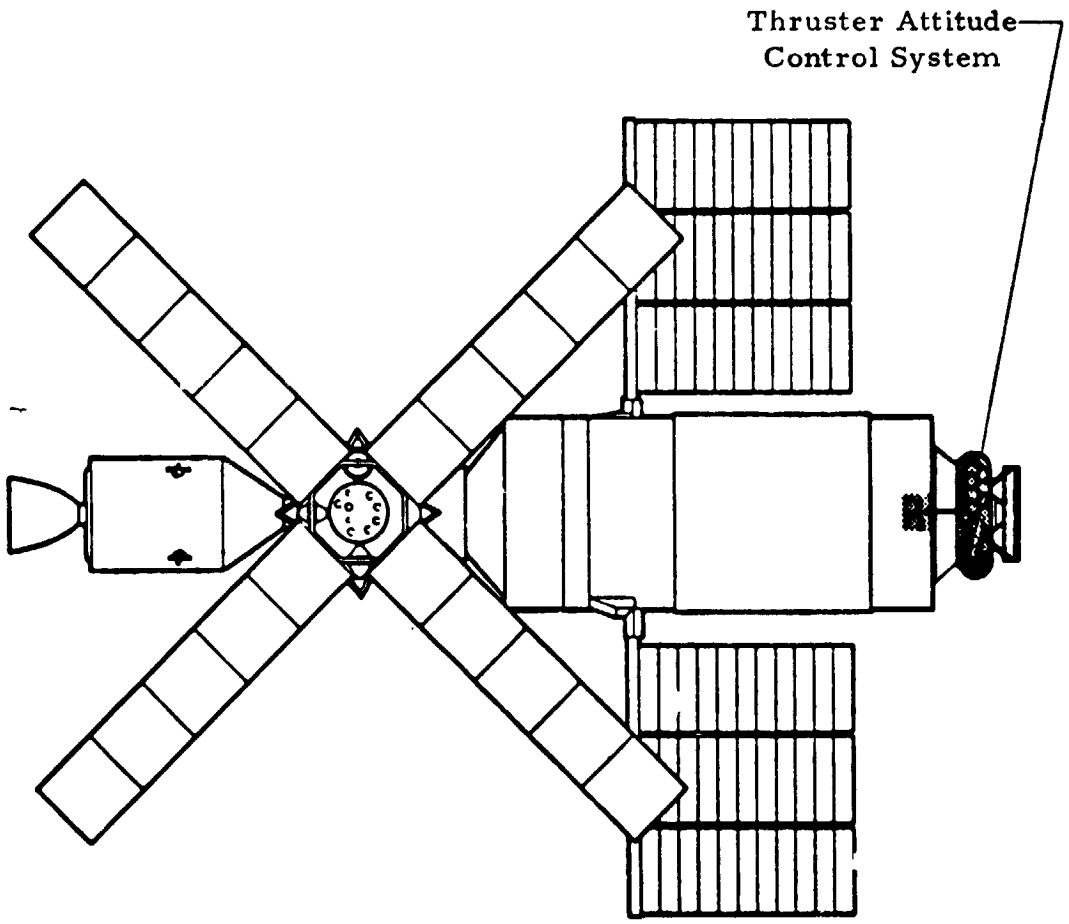

Figure 42. Skylab Cluster Configuration

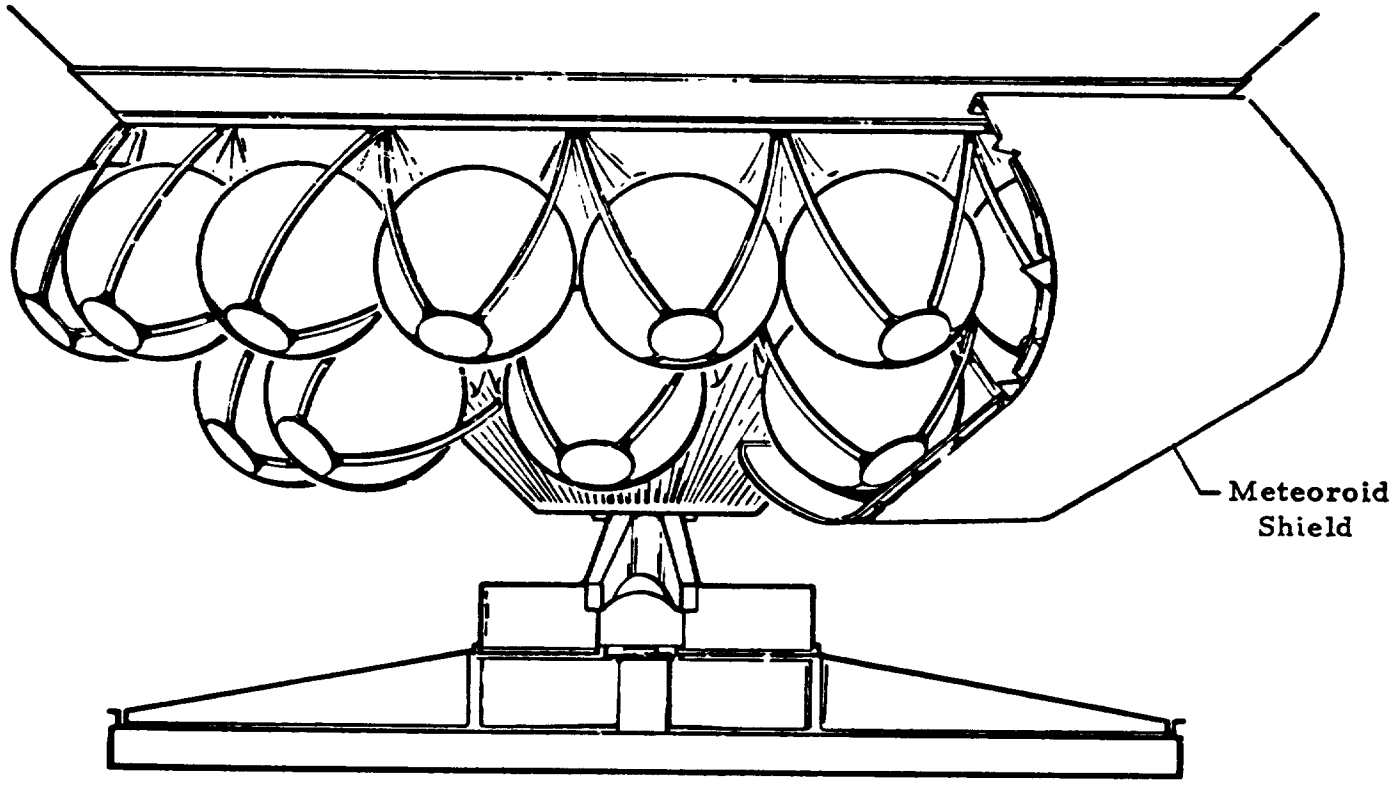

Figure 43. TACS GN_2 Storage Sphere Installation

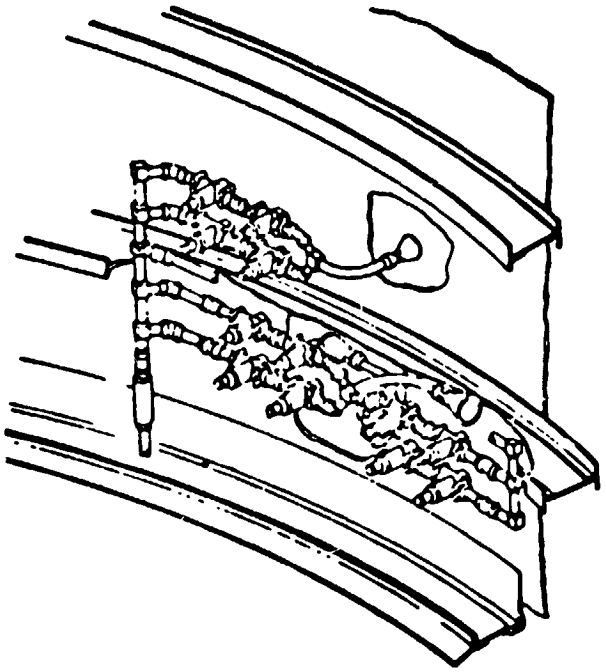

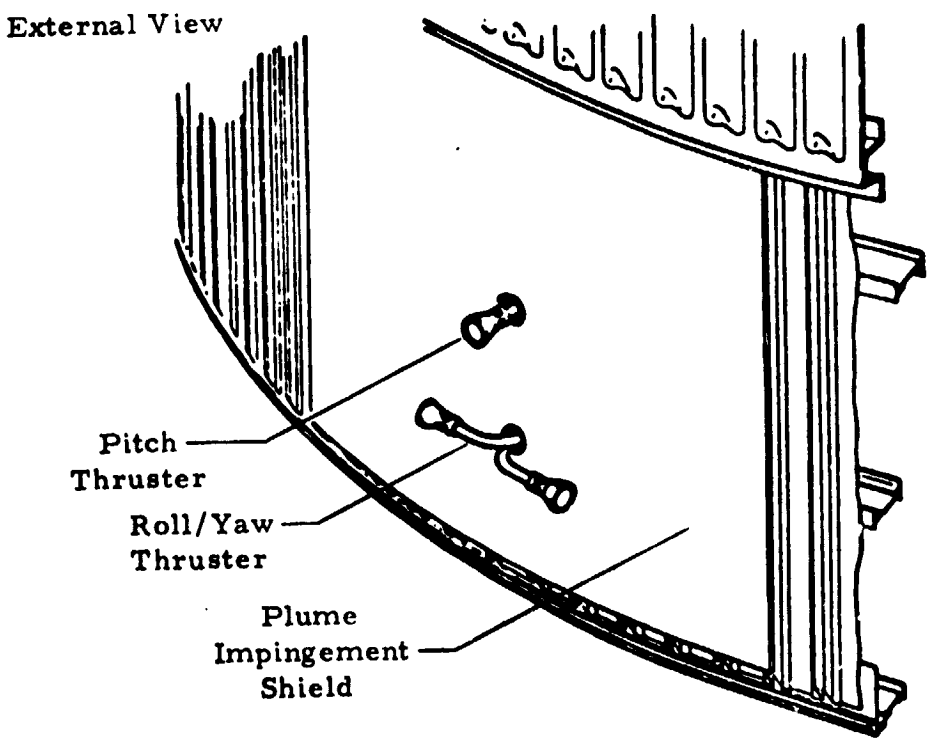

Figure 44. Thruster Module Installation

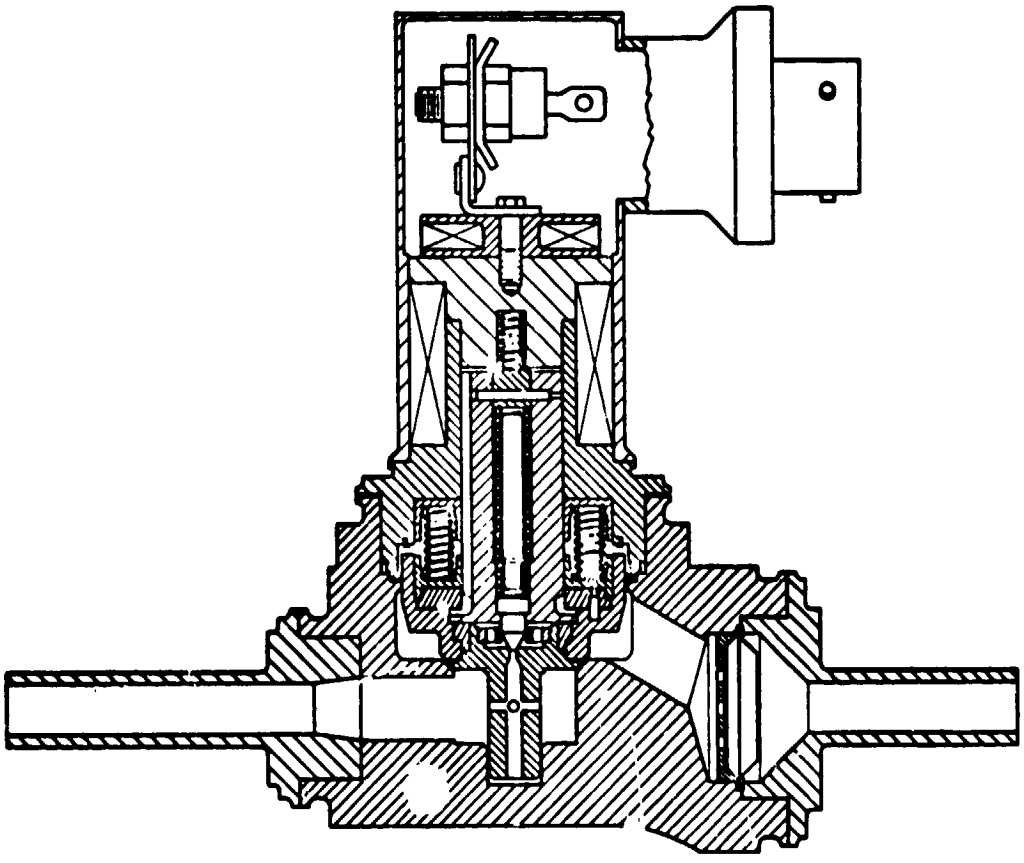

Figure 45. TACS Solenoid Control Valve

The 22 nitrogen supply storage spheres in the system were of the same design as those used in the S-IVB ambient helium repressurization system. They were constructed of welded titanium hemi-spheres, and were qualified for operating pressures up to 22 N/mm^2. The storage spheres were loaded through a self-sealing disconnect mounted at the vehicle skin. The disconnect was hard-capped prior to launch to provide redundant sealing protection against gas leakage.

The propellant supply and distribution system was induction brazed at all tubing connect points to minimize leakage. Fluxless induction brazing provided a lightweight leakproof joint. A modification to the inlet fitting of each sphere and the addition of a bi-metal joint provided the capability of "in-place" brazing of the supply feed line to the distribution manifold and the sphere temperature instrumentation. The propellant distribution system included 24 flexible metal tubing sections to provide for relative motion between the shock mounted thruster module panels and the hard mounted distribution manifold.

The two supply line filters utilized a multilayer etched-disk construction to provide 10 micron nominal filtering capability.

Instrumentation was provided for system loading, checkout and flight monitoring. Two pressure transducers located on the distribution manifold were provided to monitor system pressure. Six temperature transducers located in six storage spheres equally spaced on the aft vehicle support structure were provided to determine the average bulk gas temperature. Two temperature transducers were located at the inlet to each cluster of three modules at position plane I and III. Six pressure switches, one for each thruster, provide a positive indication of thruster firings.

b. Electrical Components. The TACS electrical subsystem was developed to (1) utilize Airlock Module (AM) power; (2) accomodate command or control signals from the Apollo Telescope Mount Digital Computer (ATMDC), the Instrument Unit (IU) Flight Control Computer, the AM Digital Command System and the OWS Switch Selector (depending on the mode of operation and the phase of the mission); and (3) provide instrumentation measurement capabilities for telemetry and Skylab panel display monitoring requirements.

The electrical system utilized separate redundant circuits and components to protect against single-point failures and employed high reliability in parts selection and design while insuring compatibility of command signals, control signals and power and measurement signals with the interfacing system and equipment.

Relay logic and control circuits, with solid-state time-delay circuits, were selected as the electrical configuration. Relays were chosen because of:

High reliability, based on past experience

Excellent isolation features for interface compatibility

Non-loading circuit features

No status change from loss of power

Compatibility with the installation environment and structural load conditions.

The Power and Control Switching Assembly (PCSA) contained the circuitry and relays necessary to command and control TACS. The PCSA translated commands from the OWS Switch Selector and/or the DCS to enable TACS, apply power to thruster buses, and transfer the control mode between the IU and the ATM. The PCSA transferred thruster commands from either the IU or ATM to energize the quad-redundant valve opening solenoids of the thruster selected to be fired. The relays within the PCSA changed state upon receiving commands of 28 Vdc with a minimum duration of 20 milliseconds.

Power for the PCSA was supplied by AM buses 1 and 2, utilizing each bus to power a different half of the TACS quad-redundant thruster units. Buses were kept separate within the PCSA.

Eighteen time delay modules were utilized in the TACS. Six modules, in conjunction with the pressure switches, were used for the on-board display of thruster firing events. The time delay module extended the duration of the pressure switch pulse from 40-400 to 500 milliseconds to drive the thruster indicator lights on the ATM Control and Display Panel in the MDA.

The remaining 12 time delay modules were used for re-application of thruster bus power after a manual inhibit command had been removed. Functionally, the time delay module was of capacitor discharge design. The application of the manual inhibit command charged the module. Removal of the inhibit command by placing the switch to ENABLE allowed the module to discharge. The power from the module closed the contacts of the enable relay and held the relay closed for approximately 500 milliseconds (minimum) and 18 to 33.5 Vdc.

Two voltage sensor modules were utilized with the TACS to monitor the 12 telemetered thruster bus voltages between 0 and 35 Vdc.

The output of the sensors was routed to low-level multiplexers of the instrumentation system. Each voltage sensor module contained six independent voltage sensor circuits (one for each thruster bus).

c. Design Data.

(1) N_2 Supply

Parameter	Value	
	1 Sphere	22 Spheres
Volume	.127 m^3	2.8 m^3
Nitrogen Capacity		
@ 10°C & 22 N/m^2	32.2Kg	706Kg
@ 24°C & 20 N/m^2	28.5Kg	627Kg
Residual Nitrogen *		
@-10.5°C & 2.4 N/m^2	3.98Kg	87.7Kg
@ 4.4°C & 2.2 N/m^2	3.46Kg	76.3Kg
Usable Nitrogen *		
With zero leakage (max.)	28.3Kg	623Kg
With max. leakage (min.)	24.1Kg	528Kg
Nitrogen Leakage		
TACS (max.)	N/A	9.53Kg
Leakage Rate	N/A	24 sccm

Sphere Operating Temperature * - 26° to +78°C

Spere Operating Pressure * - 0 to 2.1 $\pm$ .1 N/mm^2

Sphere Proof Pressure @ 99°C - 33 N/mm^2

Sphere Burst Pressure @ 99°C - 55 N/mm^2

* Based on TACS operating at thrust levels above 44.5N

(2) Control Valves

Parameter	Value
Operating Pressure Range	0 to 22 N/mm^2
Proof Pressure	33 N/mm^2

(2) Control Valves (Continued)

Parameter	Value
Burst Pressure	55 N/mm^2
Cperating Life	35,000 cycles
Nitrogen Temperature Range	-101°C to 74°C
Environmental Temperature Range	-101°C to 74°C
Valve Response	
Opening Time Maximum	42 msec
Closing Time	35 msec max.
Nitrogen flow rate with inlet conditions of 2 N/mm^2 & 21°C (3000 psig & 70°F)	.675Kg/sec
Pressure drop @ .675Kg/sec (1.5 lb/sec) of nitrogen, maximum	.12 N/mm^2
Valve Leakage Rates (using nitrogen)	
External maximum @ operating temperature and pressure	10^{-6} sccm
Internal (inlet to outlet) maximum @ operating temperature and pressure	2 sccm 100 sccm (with 10-12% of inlet pressure across valve)
Electrical	
Solenoid Voltage	24 to 30 Vdc
Solenoid Dropout Voltage	2 Vdc min.; 8 Vdc max.
Solenoid Pull-in Voltage	5 Vdc min.; 22 Vdc max.
Solenoid Current	3 amp max.

(3) Thruster

Parameter	Value
Throat Diameter	4.16 mm
Exit Diameter	29.5 mm
Throat Area, At	13.6 mm^2
Exit Area, Ae	682 mm^2

(3) Thruster (Continued)

Parameter	Value
Expansion Ratio, Ae/At	50
Length, Throat to Exit	3.68 cm

d. Performance Data.

(1) Total Impulse. The total TACS impulse available for attitude control was 377,000 N.s. This included both primary control requirements prior to CMG spin-up (first 6 orbits) and CMG backup requirements.

(2) Thrust Level Requirements. The pre-mission thrust level requirements for the Thruster Attitude Control System are presented in Table 41. The defined Minimum thrust, for vehicle control, of 44.5 N corresponded to a system pressure of 2.52 N/mm^2. The pressure included telemetry and instrumentation inaccuracies. This resulted in available impulse being defined as the initial loaded impulse minus the impulse remaining at a pressure of 2.52 N/mm^2.

Since the potential to gain additional impulse existed by lowering the rescue mission thrust level and therefore the system pressure, a review of rescue and other mission thrust level requirements was initiated during the second Skylab manned mission. An analysis was performed to evaluate thrust level requirements for various mission events utilizing available flight and design data. The results of the analysis shown in Table 42 indicated that a rescue mission CSM docking in the radial port would require 44.5 N which would not allow the pre-mission thrust level requirement to be lowered.

(3) Minimum Impulse Bit (MIB). During the period of IU control of the SWS, the TACS impulse provided by a MIB was 41.4 N.s. This was the result of a standard Launch Vehicle Digital Computer (LVDC) MIB pulse width of 65 milliseconds, and a thrust of 445 N.

During the mission period, the TACS thrust declined from about 445 N down to 82 N as a result of nitrogen pressure decay. The impulse of a MIB was controlled during this decay to about 22 N.s by increasing the duration of the MIB as commanded by the ATMDC. The impulse of the MIB declined between changes in MIB duration due to the thrust decay noted above. The MIB duration at the start of the mission was 50 milliseconds. The duration was increased in steps

Table 41. Thruster Attitude Control System

Pre-Mission Minimum Thrust Level Requirements	
Mission Events	Newtons
Booster Separation Transients	222
Each Manned Mission Command Service Module Docking	89.1
From Last Manned Mission Docking to End of Mission	44.5
Rescue Mission Command Service Module Docking *	44.5

* This requirement appended to original pre-mission thrust requirements.

Table 42. Thruster Attitude Control System

Minimum Thrust Level Requirements Analysis	
Mission Events	Newtons
Earth Resources Experiment Pointing *	8.91
Control Moment Gyro Reset Maneuver *	8.91
Momentum Desaturation Maneuver *	8.91
Trim Burn - Four Command Service Module Engines	89.1
Trim Burn - Two Command Service Module Engines	44.5
Rescue Mission - Nominal End Port Docking	22.2 - 44.5
Rescue Mission - "Worst Case" Radial Port Docking	44.5

* This thrust level is not optimum but is usable. Lower thrust levels might be acceptable but were not studied because it required rescaling of the simulation.

during the mission to a maximum of 200 milliseconds. For post-mission testing, the MIB duration was decreased to 50 milliseconds, which provided an impulse of about 6 N.s per MIB. A typical MIB thrust profile is shown in figure 46.

e. System Operation. Thruster control of TACS was provided by the PCSA. The PCSA received discrete commands for thruster operation, and routed these commands to the respective control relay or thruster control valve solenoid. Figure 47 is a simplified schematic showing the controls to a single thruster module.

Power for the PCSA was supplied by AM buses 1 and 2 through 20 circuit breakers on panel 202 in the AM Structural Transition Section. Power was supplied to the BUS ON/OFF logic and the thruster buses through 12 circuit breakers, THRUSTER 1 through 6 for both AM buses 1 and 2. Logic control power was provided to the command control buses 1 and 2 through four circuit breakers, TACS COMMAND CONTROL 1 PRIMARY and SECONDARY for AM bus 1 power and TACS COMMAND CONTROL 2 PRIMARY and SECONDARY for AM bus 2. Power to the manual inhibit controls was provided through the TACS MANUAL CONTROL circuit breakers (4) 1-INHBT-2, and 1 and 2.

All OWS Switch Selector DCS and GSE commands to the PCSA required an enable command before they could be implemented. The enable commands accomplished the connection of AM buses 1 and 2 to command control buses 1 and 2. To enable the TACS for operation, all circuit breakers, with the exception of the manual control circuit breakers, were closed before launch. TRANSFER ENABLE 1A-ON, 2A-ON, 2B-ON was sent either by the OWS Switch Selector or by DCS command to power up command control buses 1 and 2, respectively, prior to launch. Command control buses 1 and 2 supplied power to the thruster bus ON/OFF logic and the transfer command logic.

After the command control buses were enabled, and prior to lift-off, the GSE sent BUS 1-ON and BUS 2-ON commands. These commands could also be sent by DCS prior to launch. BUS 1-ON relays connected the command control bus 1 to six thruster bus-on relays. The six thruster bus-on relay contacts closed, allowing power to be supplied to thruster buses 1-3A, 1-1A, 1-2A, 2-2A, 2-1A, and 2-3A from AM bus 1.

Similarly, the BUS 2-ON command connected the command control bus 2 power to be supplied to thruster buses 1-3B, 1-1B, 1-2B, 2-2B, 2-1B, and 2-3B (Schematic not provided). With power on the 12 thruster buses, the TACS was configured to receive thruster commands from the Flight Control Computer (FCC) in the IU. TACS could be disabled by sending BUS OFF and BUS 2-OFF by DCS command, which removes power from the 12 thruster buses.

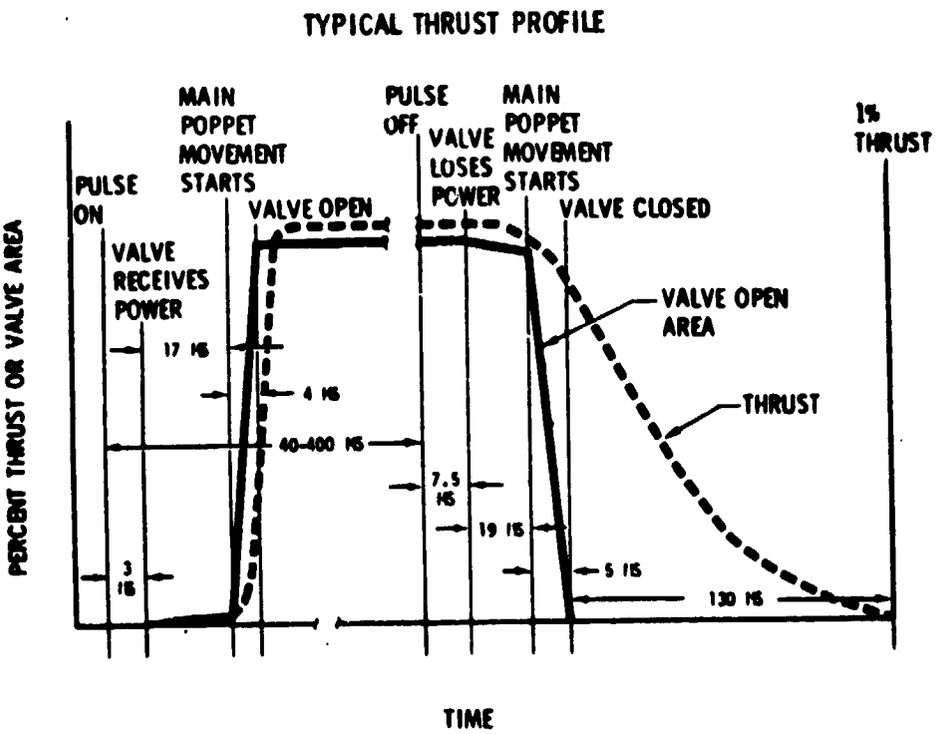

Figure 46. Typical Thrust Profile

C-4

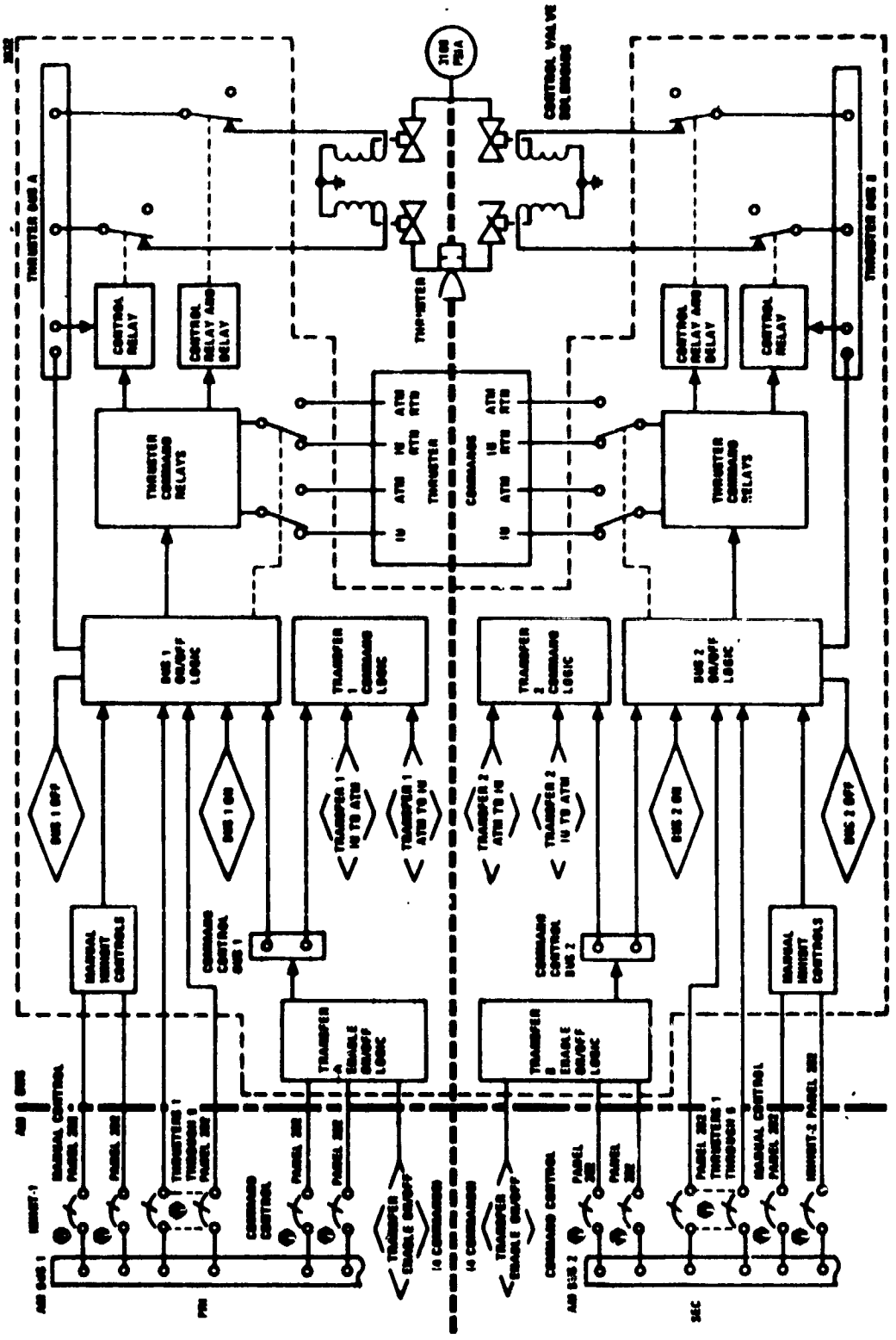

Figure 47. Single Thruster Control Schematic

With TACS configured in the IU mode, attitude control commands from the IU were initiated by grounding the return within the FCC. Power to the thruster command relay coils was provided by the IU (figure 48). A fire command was generated within the Flight Control Computer (FCC) by grounding the circuit. This simultaneously applied power to the thruster command relay coils. The command from the IU closed eight sets of relay contacts. Four sets of contacts provided a redundant path for supplying power from the thruster bus A, and four sets similarly provided power from the thruster bus B. Thruster bus A and B power energized the four control valve solenoids, which opened the control valves, allowing N_2 to flow through the thruster.

The IU thruster commands were in the form of electrical pulses of 65-millisecond duration or to Full-on. When the pulse was applied to the thruster fire relays, the thruster control valves opened. The valves closed upon termination of the pulse to the solenoids.

Transfer to the ATM mode was sent approximately 4 1/2 hours after launch of SL-1 by ground command. The TACS TRANSFER 1-IU to ATM and TACS TRANSFER 2-IU to ATM commands removed command control bus power from the IU mode buses and applied power to the ATM mode buses. Application of power to the ATM mode buses switched the transfer command relays to the ATM mode. Transfer back to the IU could be accomplished by sending both TACS TRANSFER 1-ATM and 2-ATM to the IU. In the ATM mode, the TACS augmented the CMGs of the ATM. Attitude control commands from the ATM passed through the same contacts of the thruster command relays and the thruster fire relays to energize the control valve solenoids as did the IU commands. Commands from the ATMDC were issued when the Workshop Computer Interface Unit TACS driver switches closed. This applied 28 Vdc to the thruster command relay coils (figure 49). The Thruster fire commands from the ATM APCS were in the form of 40 to 400 millisecond electrical pulses in contrast to the 65 millisecond IU command pulses. These pulses varied the on time to allow for the drop in thruster operating pressure with mission duration. As the N_2 storage pressure dropped, the thrust available at the thruster dropped. Lower thrust required that the thruster control valve stay open longer to obtain the same amount of impulse.

Upon entry into the SWS, the crew reconfigured TACS to provide manual inhibit control capability and disable the ground command capability. The crew opened the TACS COMMAND CONTROL 1 PRIMARY and SECONDARY and the TACS CONTROL 2 PRIMARY and SECONDARY circuit breakers, and closed the TACS MANUAL CONTROL 1 and 2 and 1-INHIBIT-2 circuit breakers.

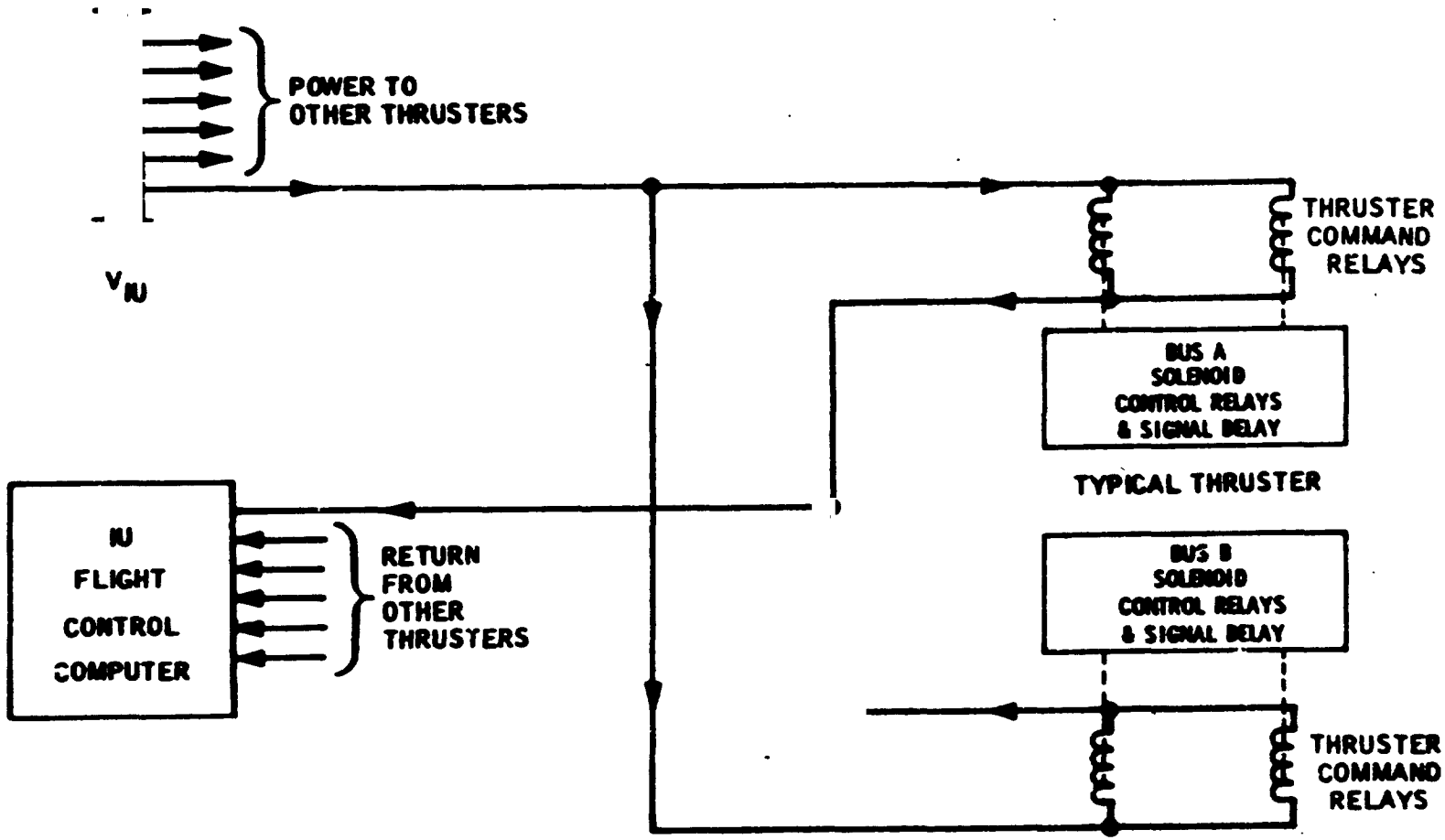

Figure 48. IU Command/Thruster Interface

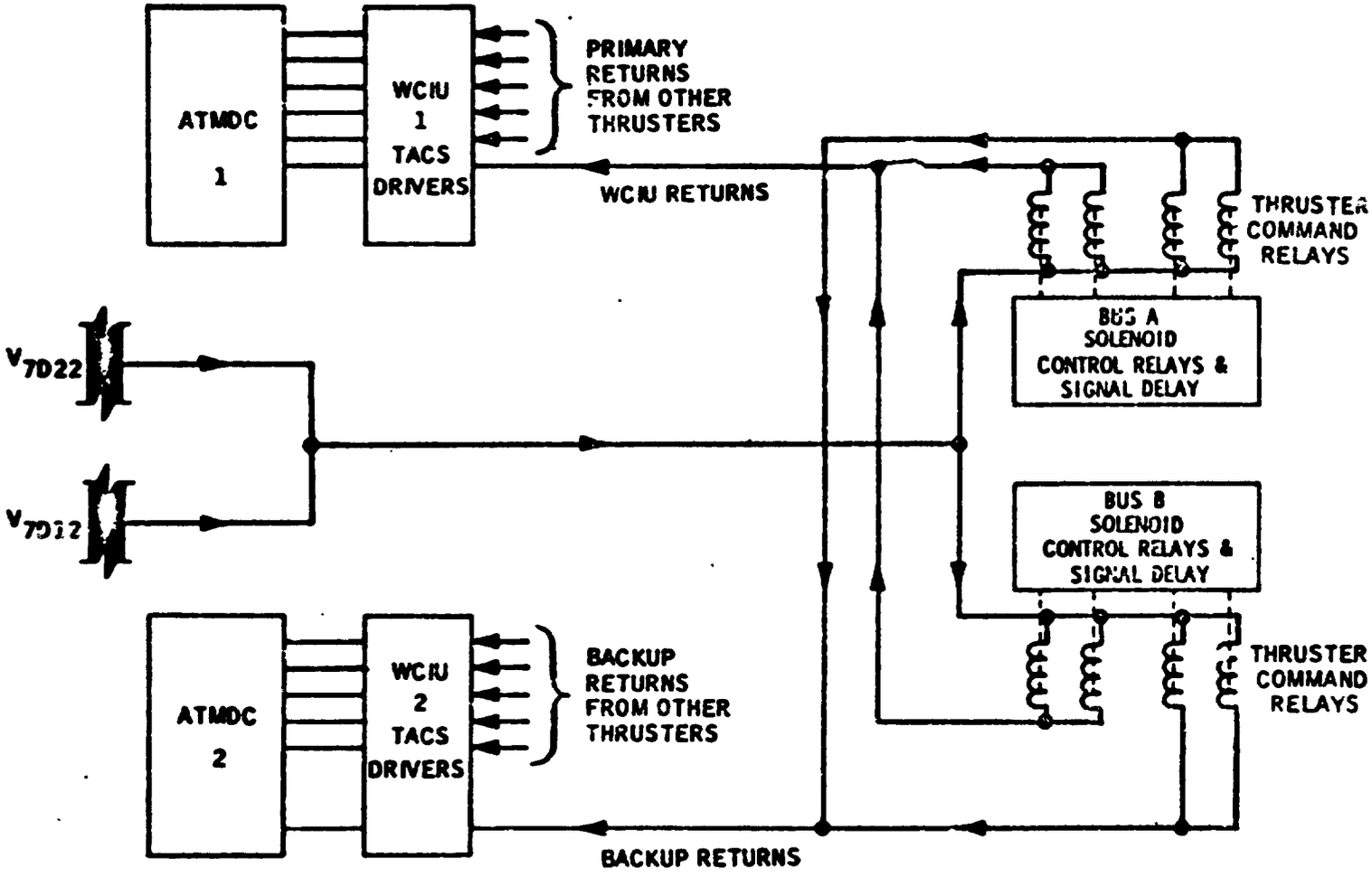

Figure 49. ATMDC/Thruster Interface

Power for any of the six thruster units could be manually inhibited by placing its TACS ENABLE-INHIBIT (panel 130) switch to INHIBIT. Power was then applied to the thruster bus 1 and thruster bus 2-OFF relays to open the supply from AM bus 1 and 2 to the thruster buses A and B of the selected thruster. Inhibit power was also provided to the 500 millisecond timer for charging. When the inhibit command was removed, the 500 millisecond timer caused a 500 millisecond reset signal to be generated. AM bus 1 and bus 2 power was then supplied through the enable relays to the thruster bus 1 and 2-ON relays to close the relays, which reapplied AM bus 1 and 2 power to the thruster buses A and B.

Positive indications of thruster firings were provided for each thruster on panel 130, ATM Control and Display, in the MDA. These indications were actuated by pressure switches monitoring chamber pressure. A 500 millisecond time delay module was used to lengthen the thruster-on indication from 40 milliseconds (minimum) to 500 milliseconds to accommodate the display by incandescent indicators. N2 supply pressure could be monitored on the ATM Control and Display Panel by placing the ACS monitor select switch to TACS P. The readout was in percent of full scale (i.e., 100 percent equals 24N/mm^2).

The TACS ONLY indication flagged the crewman that the APCS was operating on the TACS only. This indicated a possible large usage of TACS propellant. Additional failure checks were provided through the use of the Digital Address System (DAS).

2. Design Concept. For most of the eight-month long Skylab mission, the primary source of attitude control was the three Control Moment Gyros (CMGs) which provided the pointing accuracy and stability necessary for many Skylab astronomical and Earth Resources Experiments, and which maintained the Solar Inertial attitude necessary for the Skylab solar arrays. A propulsive Attitude Control System (ACS) was needed to provide control during CMG spinup (the first ten-hours of the mission), to handle docking transients and large maneuvers beyond the capability of the CMGs, to desaturate the CMGs when necessary, and to provide a contingency capability in case of a CMG failure. This system designated TACS (Thruster Attitude Control System), was required to provide a minimum of 272,000 N.s of impulse. A high thrust level of 222 N. was required at the start of the mission for separation transients, a 89 N. thrust minimum was required for each of the three dockings with Apollo command modules, and a 44.5 N. minimum was specified for the rest of the mission.

Because of the ample payload capability of the Saturn V Booster, the design was not subject to weight constraints normally imposed on such a system. This permitted selection of an ambient gas system to

minimize development costs and maximize reliability. Nitrogen was selected as the propellant to minimize contamination of Skylab external equipment and to avoid the complexity of preventing condensation in cold propellant lines that would have resulted from use of a heavier gas. The thrust requirement permitted deletion of system pressure regulators. Thrust level was allowed to decay with bottle pressure in a simple blowdown mode.

3. Design Verification.

a. Hardware Development and Qualification. The Thruster Attitude Control System was certified for flight after successful completion of development, qualification, and checkout test programs. This effort included development and qualifications tests of the solenoid control valve, the in-line gas filter, the fill-drain disconnect, the storage sphere, the bi-metal joint, the manifolding, the temperature transducer, the pressure transducer, and the pressure switch. The primary test objectives, major problem areas, and solutions are summarized in this section.

(1) Thruster Module Assembly.

(a) Development Test Program. The purpose of the development test program for the Thruster Module Assembly was to evaluate and establish a production configuration for the Thruster Attitude Control System solenoid valve. The development valves were tested at the valve, dual valve, and module levels to evaluate the valve's functional, performance and dynamic characteristics at various environmental and system operating conditions.

Several different main poppet seal materials and configurations were evaluated in the initial phase of testing. The configuration that demonstrated minimum leakage over the operating pressure range was a conical poppet with a conical sealing surface using "Vespel" as the seal material. In addition the preload on the main poppet springs was increased and all machined parts were chemically deburred to further enhance the leakage characteristics.

Testing of this configuration revealed that the upstream valves did not seal effectively with a high inlet pressure and low delta-pressure across the valve. All valves exhibited sufficient sealing characteristics at moderate or high delta-pressure with gas trapped downstream of the valves. The valves were leak tight at all inlet pressures with ambient downstream pressures. The solution to the problem consisted of maintaining the proper delta-pressure across each upstream valve during operation. This was accomplished by removal of the zener diode in the valve's voltage suppression circuit. This increased the closing time at the downstream valve, lowering the trapped pressure between the valves.

During high temperature testing, electrical shorts developed in the magnum solenoid coil wire. This was corrected by changing the coil wire to constantan and changing the insulation from teflon to polymide. In addition, this wire was wrapped on an aluminum spool and the entire assembly potted to provide greater heat dissipation.

A problem with bent plunger flanges was identified in the downstream valves. Analysis revealed that pressure surges from the upstream valves caused the plunger flange to impact the orifice plate thus yielding the plunger flange. This resulted in slow pneumatic response within the valve. A main poppet stop was incorporated in all production valves which precluded impact of the plunger flange with the orifice plate.

Testing also revealed the existence of a leak path behind the lip seal retainer, which tended to slow the valve's opening response. The cause of the problem was associated with gas leakage into the solenoid chamber. A "Vespel" static seal was added behind the lip seal retainer. In addition the plunger vent holes were increased from two to four and microlube lubricant was applied to the lip seal to further enhance the response characteristics of the valve.

Loss of voltage suppression was encountered during testing. The problem was associated with failure of the diodes in the voltage suppression circuit. This problem was solved by changing to high reliability diodes from a new supplier.

During vibration tests of a module assembly it was determined that the valve main poppets were experiencing high dynamic loads and were actually unsealing (chattering) at a frequency which might cause damage to the poppet seals and/or seats. To reduce the loads on the valve poppets during vibration, "shock" mounts were installed between the thruster panels and the vehicle aft skirt. Because the "shock" mounting introduced more degrees of freedom of movement between the valve panels and the distribution manifold, additional flexible metal tubes were required.

(b) Qualification Test Program. The purpose of the qualification test program for the Thruster Module Assembly was to establish the flight worthiness of the solenoid valve, module, and cluster (three modules). The pressure switches, temperature transducer, filter, flexible metal tubes, and manifold were included in the test specimen.

During pre-qualification production acceptance tests at the module level, an upstream valve developed a blowing leak.

Subsequent disassembly revealed that the main poppet seal was fragmented with large segments of it missing. Extensive tests at simulated production acceptance test conditions revealed that the valve failure was due to an incorrect test setup. The inlet manifold was improperly sized causing a high reverse delta-pressure condition to exist across the upstream valve thus failing the seal under very severe back-flow conditions. This sensitivity to back-flow was recognized and all subsequent test and operating procedures were reviewed and rewritten if required to insure that no valve was subjected to possible reverse flow conditions.

During vibration testing of the inlet manifold installation consisting of the filter and one flexible tube assembly mounted on a section of the aft skirt, the clamp mounting the filter to the skirt yielded. The clamps were redesigned and the test repeated. The specimen successfully met the qualification requirements with an additional tube clamp between the fill line and thruster manifold and the addition of doublers to the filter support bracket. In addition, post vibration tests revealed that the filter would not meet imposed cleanliness requirements. The cleanliness requirements were waived and no further action was taken primarily because the flight filters had been installed and each valve contained an integral filter capable of providing protection from the amound of contaminants that would be generated by the filter.

Qualification testing of the thruster module assembly (three modules) consisted of proof, leakage, functional, vibration, ordnance shock, duty cycling, continuous duty, thermal vacuum environment, electrical, and nozzle cover blow-off tests. The module inlet temperature transducer was found to be inoperative due to mishandling. This necessitated the qualification of the component under a separate test program. All pressure switches used in the test specimen failed at various times in the program. The cause of failure was determined to be diaphragm fatigue in all cases. Further qualification testing occurred in a separate test program. During high temperature functional testing and prior to vibration tests, a downstream valve developed a blowing leak. The cause of the severe leakage was determined to be a fragmented seal with similar characteristics to the earlier failure in the module production acceptance tests. Extensive testing and analytical investigation did not reveal the exact cause of failure. The most probable cause of the failure can be attributed to a reduction in impact and fatigue resistance of the seal material resulting from the assembly stress condition which varies randomly with material strength properties, manufacturing tolerances, and flow forces. The valve was replaced and all testing was successfully completed.

Concurrent with the thruster module assembly qualification tests additional test programs were performed to investigate inherent valve characteristics, to evaluate and identify environmental and operational conditions which might contribute to or cause the seal to fail, to establish confidence in the production seal configuration, and to develop and evaluate backup seal configurations for use if the production seal configuration had been assessed unsatisfactory for flight.

The extensive seal failure testing did not identify any specific factors which caused the seals to fail. Increased confidence was gained in the production seal configuration for flight from this test program. A back-up seal was developed and tested but was not implemented into the production valve program because it did not offer any known advantage over the production configuration seal used for flight.

Because of the difficulties experienced with qualifying the pressure switch and temperature transducer in the thruster module assembly qualification test program, these items were qualified at the component level in a separate test program. Both components were subjected to proof, leakage, functional, vibration, shock, burst, and cycle testing.

Prior to the qualification of the temperature transducer at the component level during checkout of the flight Thruster Attitude Control System, one of the module inlet temperature transducers was found to have an out of specification leak from a weld joint. The magnitude of the leak did not warrant removal of the transducer. A stainless steel "clam-shell" doubler was epoxy bonded over the body of the transducer. "Clam-shell" doublers were epoxy bonded to every temperature transducer in the system to preclude further leakage of this type. The temperature transducer with the "clam-shell" doubler attached to it completed all qualification testing with no anomalies or deviations from the requirements.

In the qualification test program the pressure switch failed to actuate during the post vibration life cycle test. The cause of failure was determined to be a fatigue rupture of the diaphragm. An evaluation test program was performed using a pressure switch with Kapton diaphragms and production flight pressure switches with stainless steel diaphragms. The results of this program indicate that the Kapton material is better suited to meet the cycle life requirements for this application than the stainless steel material. However, due to the cost and schedule impacts from changing the diaphragm material and more realistic cycle life requirements, the pressure switch was considered qualified at a reduced number of cycles. In addition, the pressure switch talkback parameters were not critical to mission success and the nominal mission cycle prediction for the pressure switch was less than the demonstrated cycle life of the production units.

(2) Pressure Sphere Assembly.

(a) Development Test Program. The bi-metal joint was the only component in the Pressure Sphere Assembly requiring development testing. The purpose of the development test program for the bi-metal joint was to evaluate the design configuration of the joint with respect to the Skylab mission environmental and operating requirements. Specific areas investigated were the redundancy of the joint, pressure and load capabilities, weld joint and sphere neck configuration, and tooling and welding procedures. Six test specimens were successfully tested to demonstrate the acceptability of the bi-metal joint configuration for production and flight usage.

(b) Qualification Test Program. The purpose of the pressure sphere assembly qualification program was to qualify the pressure sphere installation for Skylab usage. The test specimen included a pressure sphere assembly with temperature transducer, bi-metal joint and a segment of the thrust structure. The test specimen was qualified without any problems.

(3) No information was available on qualification of:

Power and Control Switching Assembly

Time Delay Module

Voltage Sensor Module

b. Hardware Integration. The Power and Control Switching Assembly (PCSA) was first integrated into the closed loop APCS during testing in the HSL in Astrionics Laboratory, MSFC, in the winter of 1971-1972. All testing was performed under ambient conditions. No problems were encountered. For additional information see Reference D.3

The complete TACS subsystem was integrated during OWS prototype In-Process Tests and Post-Manufacturing checkout in 1972. These tests verified the TACS from the PCSA downstream to the thruster.

The TACS was integrated with the ATMDC/WCIU during assembly and checlout at KSC. All interfaces were verified and the system performed satisfactorily. Two problems were noted:

(1) One of the sphere mounted temperature transducers leakage rate did not meet specification requirements when leak checked with a mass spectrometer operating in the vacuum mode. The magnitude of the leak did not warrant removal of the transducer from the system.

Extensive tests were performed to quantify the maximum leakage possible through the existing leak path to insure flight worthiness. The results of the tests and the magnitude of the leak indicated that the leak would not be detrimental to the mission and no further action was required.

(2) During component inspection, the back-up vehicle pressure switches were found to be contaminated with mercury. It was postulated that the flight vehicle pressure switches were also contaminated. Since mercury forms an amalgam with gold and gold is used in the braze alloy material, it was feared that the structural integrity of the system might be compromised. To preclude loss of structural strength, clam shell doubler assemblies were epoxy bonded over most of the brazed fittings in the areas adjacent to the pressure switches. One fitting at each thruster location was inaccessable for retrofit. In addition, extensive tests were performed to evaluate the effect mercury contamination has on the properties of the braze alloy used. The tests did not reveal any detrimental short term effect on the strength of the brazed fittings.

4. Mission Operations.

a. First Unmanned Orbital Storage Period, SL-1. The Thruster Attitude Control System was pressurized for flight to 20.8 newtons per square millimeter on April 30, 1972. Approximately 647 kilograms of ambient temperature nitrogen gas was loaded.

The Thruster Attitude Control System was activated at 17:39:52 at which time firing commands were received from the Launch Vehicle Digital Computer. It functioned as the primary attitude control system until control was switched to the ATMDC at 22:20:05, enabling CMG control. The CMGs had spun up to about 25% of full wheel speed at that time. The low momentum capability coupled with excessive Rate Gyro drifts caused TACS Only control to be automatically selected at 23:29:06. CMG control was not enabled again until DAY 2 at 05:33:00, when the CMGs were approaching 100% wheel speed.

At 06:24:29, Attitude Hold (TACS) mode was selected in order to perform a series of maneuvers. The maneuvers represented the first attempts to position the vehicle in a thermally acceptable attitude. CMG control was enabled again at 11:48:31.

The total impulse remaining for this initial unmanned period is presented in figure 50. Large gas consumption on DAY-1 and DAY-2 resulted from removal of orbit insertion transients and operation in TACS Only control until final transfer of control to the CMGs was affected. The total impulse usage rate remained high because the system was required to perform frequent CMG resets.

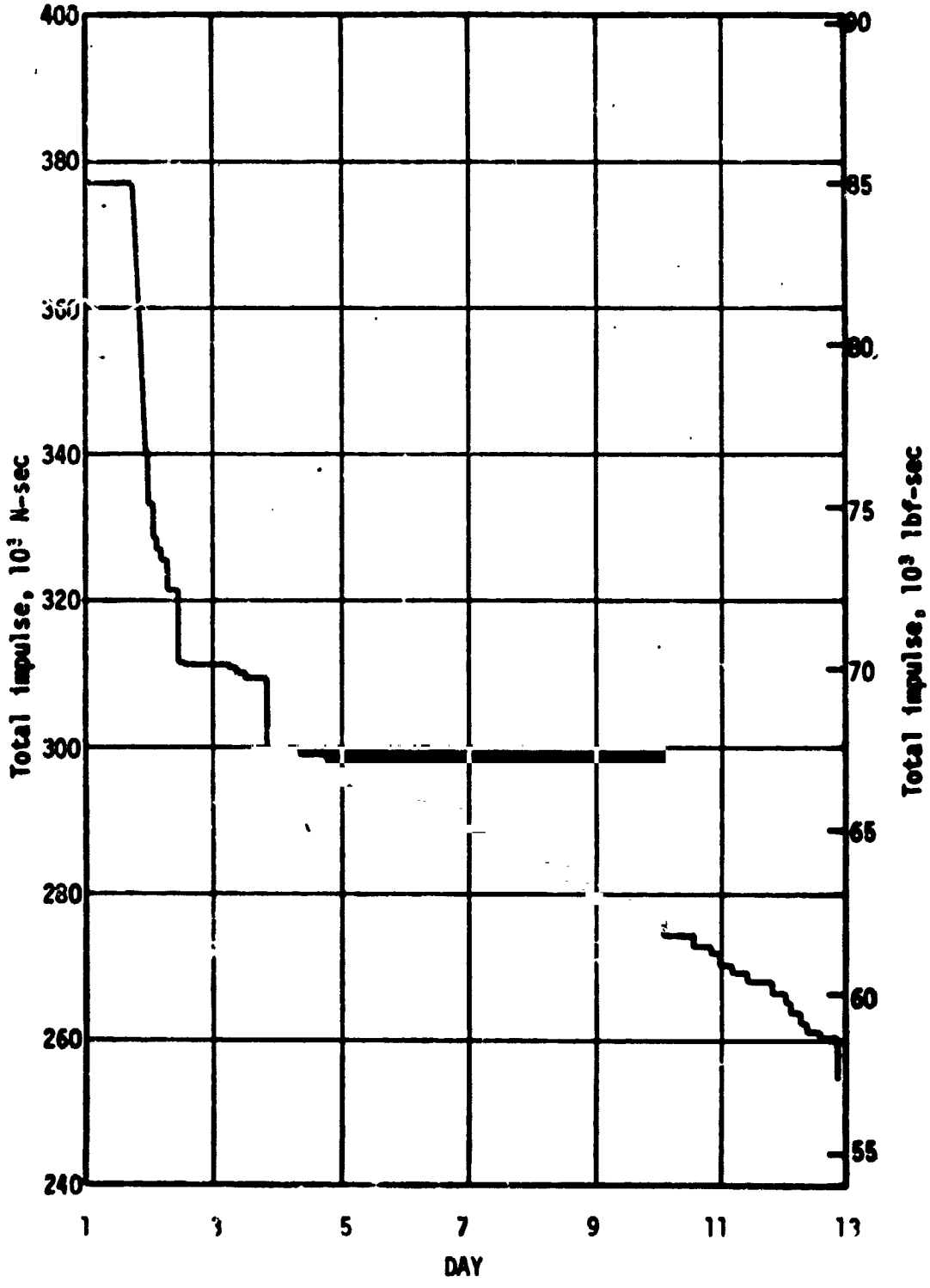

Figure 50. Usable Total Impulse Remaining, SL-1

The system pressure decay and gaseous nitrogen mass are shown in figures 51 and 52. Both parameters display blowdown characteristics similar to the total impulse remaining curve. The thrust level variation for this phase of the mission is shown in figure 53 and is compared to the thrust level stored in the ATMDC. The variation in Minimum Impulse Vit, figure 54, also shows the times at which the ATMDC command pulse width were updated. With the exception of a brief period during DAY-3 and early in the mission when the system pressure was high, the minimum impulse bit was maintained at about 27 N.s for vehicle control.

Figures 55 and 56 present thruster firing histories during ATMDC Control. The firing history while on Instrument Unit control was not recorded. The Minimum Impulse Bit (MIB) firings and the Full-On firings are shown separately. A Full-On firing is defined as a firing of one second command pulse width duration. Firings of longer duration are counted as individual one second Full-On firings equal to the number of seconds of the firing command.

The average bulk gas temperature is presented in figure 57. The average bulk gas temperature is the arithmetic average of the six temperature transducers located in equally spaced storage spheres on the aft structure. The solar elevation angle variation is shown in figure 58. Solar elevation angle describes the orientation of the orbital plane with respect to the sun vector. It should be noted that during most of this phase of the mission, the average bulk gas temperature does not increase as is expected with a increase in absolute solar elevation angle. The bulk gas temperature should increase with an increase in absolute solar elevation angle. The fact that it does not is attributable to cooling of the bulk gas after orbit insertion. Orbital thermal equilibrium was established at approximately DAY 9, thereafter the bulk gas temperature responded to the changes in solar elevation angle.

The module inlet gas temperatures and the average module inlet temperature are presented in figures 59 and 60. In Solar Inertial attitude, Module One is located on the hot side of the vehicle at Position Plane I and Module Two is located on the cold side of the vehicle at Position Plane III. Cooling of the hardware and gas occurred at these positions after orbital insertion until thermal equilibrium was established. The process was similar to that occurring in the storage spheres.

b. First Manned Mission, SL-2 (28 Days). The TACS was utilized extensively during the first five days of this initial manned phase. The total impulse remaining is presented in figure 61. It can be seen that the system usage was low after DAY 17.

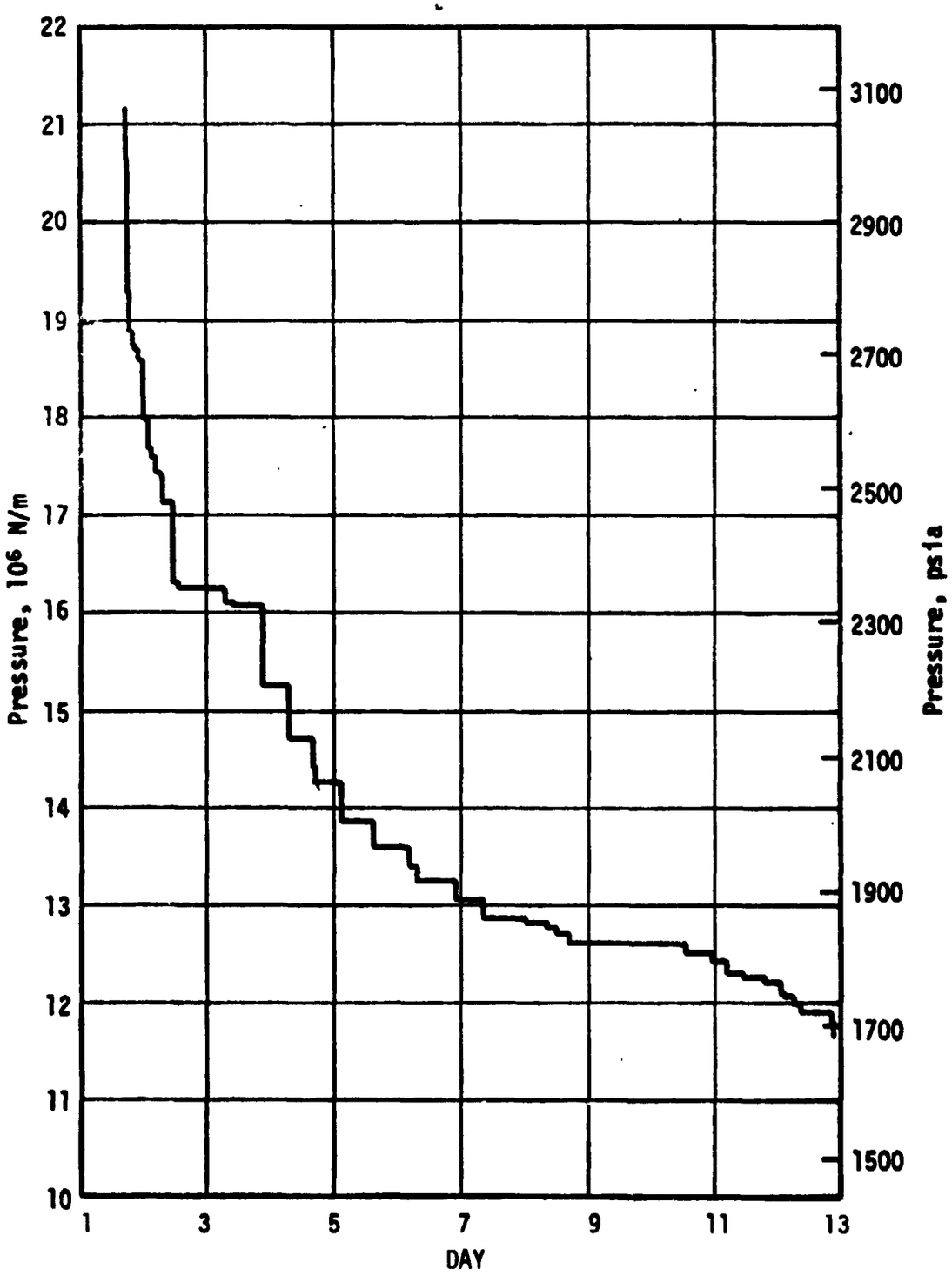

Figure 51. TACS GN_2 Pressure, SL-1

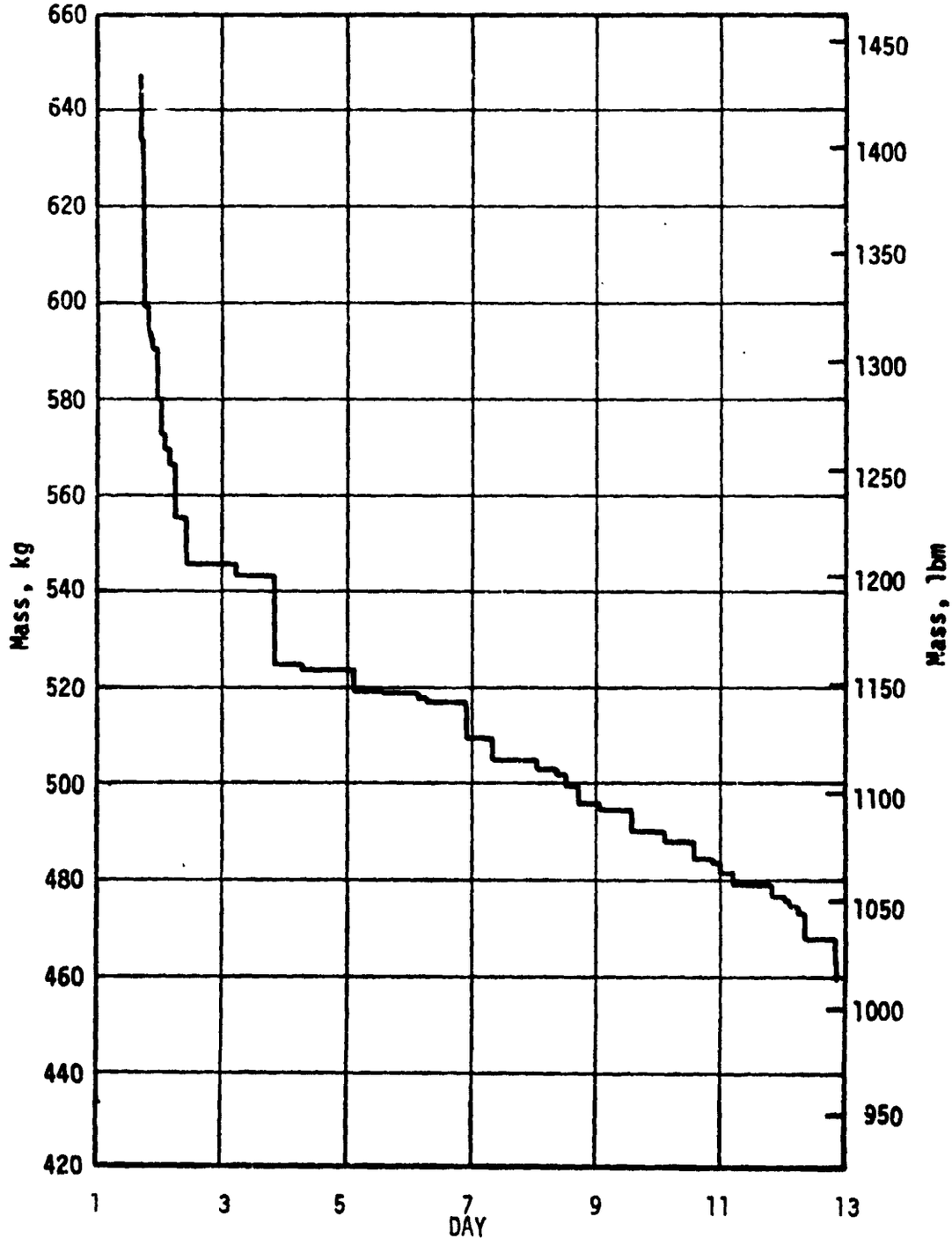

Figure 52. TACS GN_2 Mass Remaining, SL-1

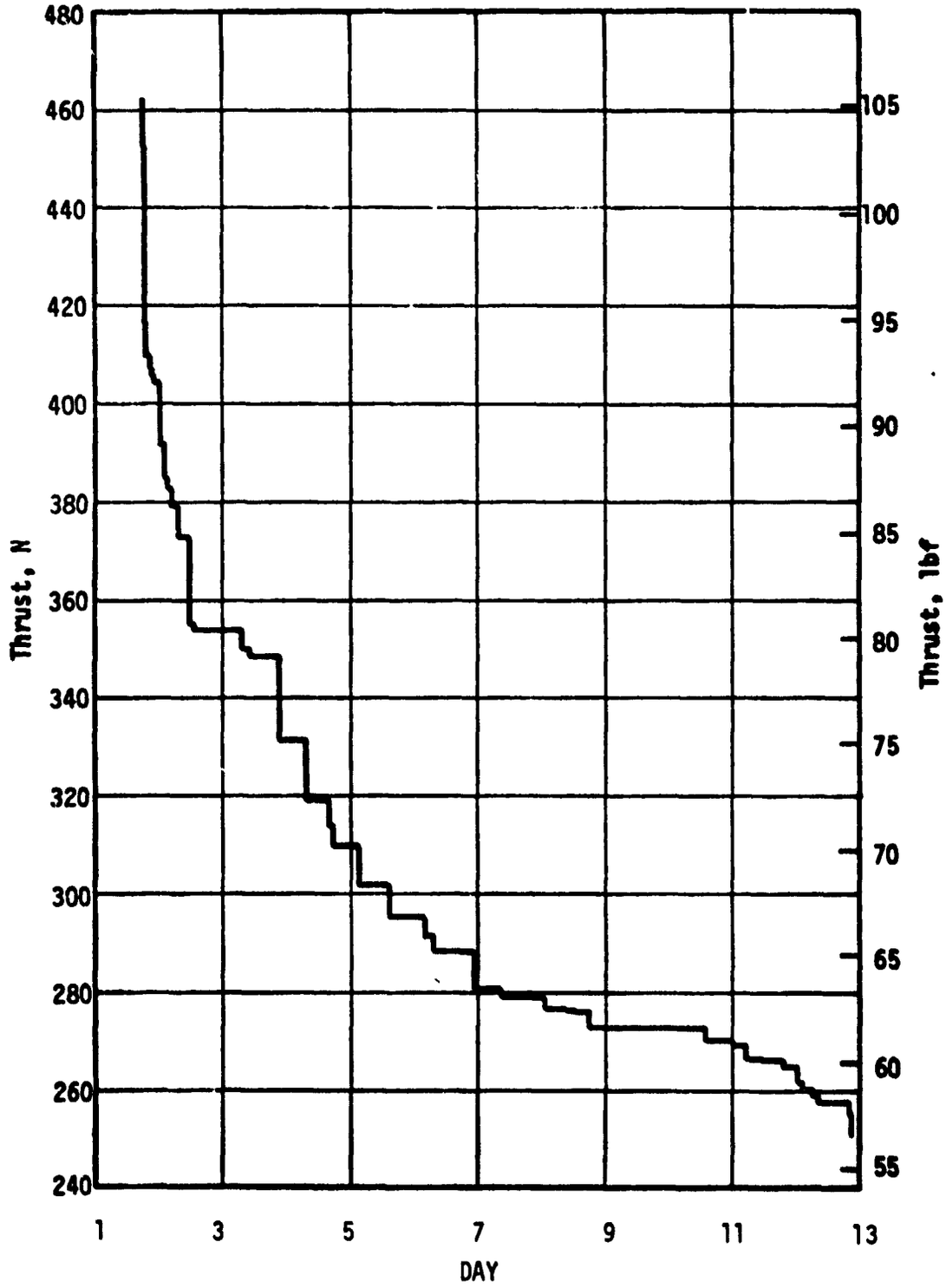

Figure 53. Thrust Levels, SL-1

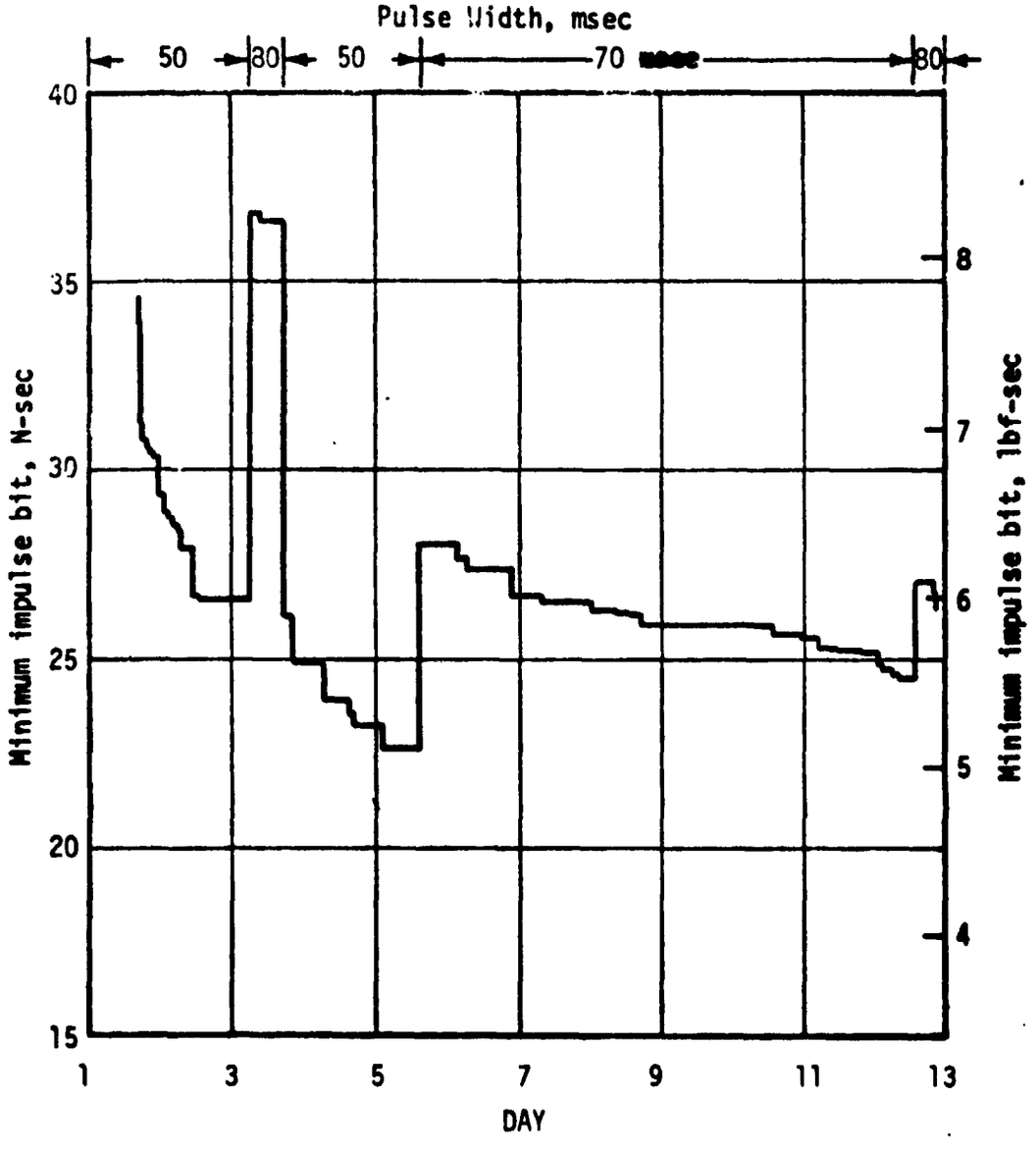

Figure 54. Nominal Minimum Impulse Bit, SL-1

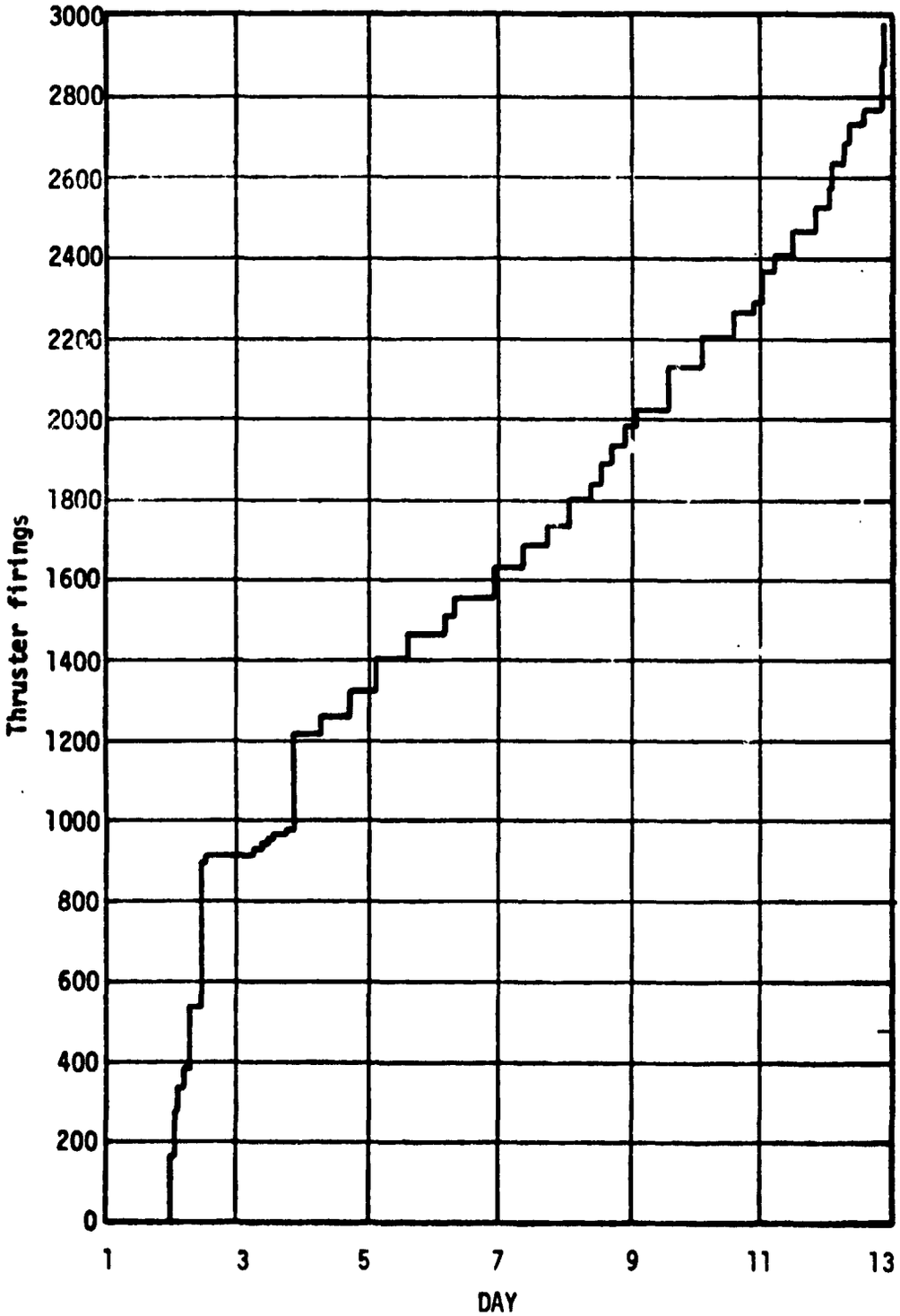

Figure 55. Accumulated Minimum Impulse Bit Firings, SL-1

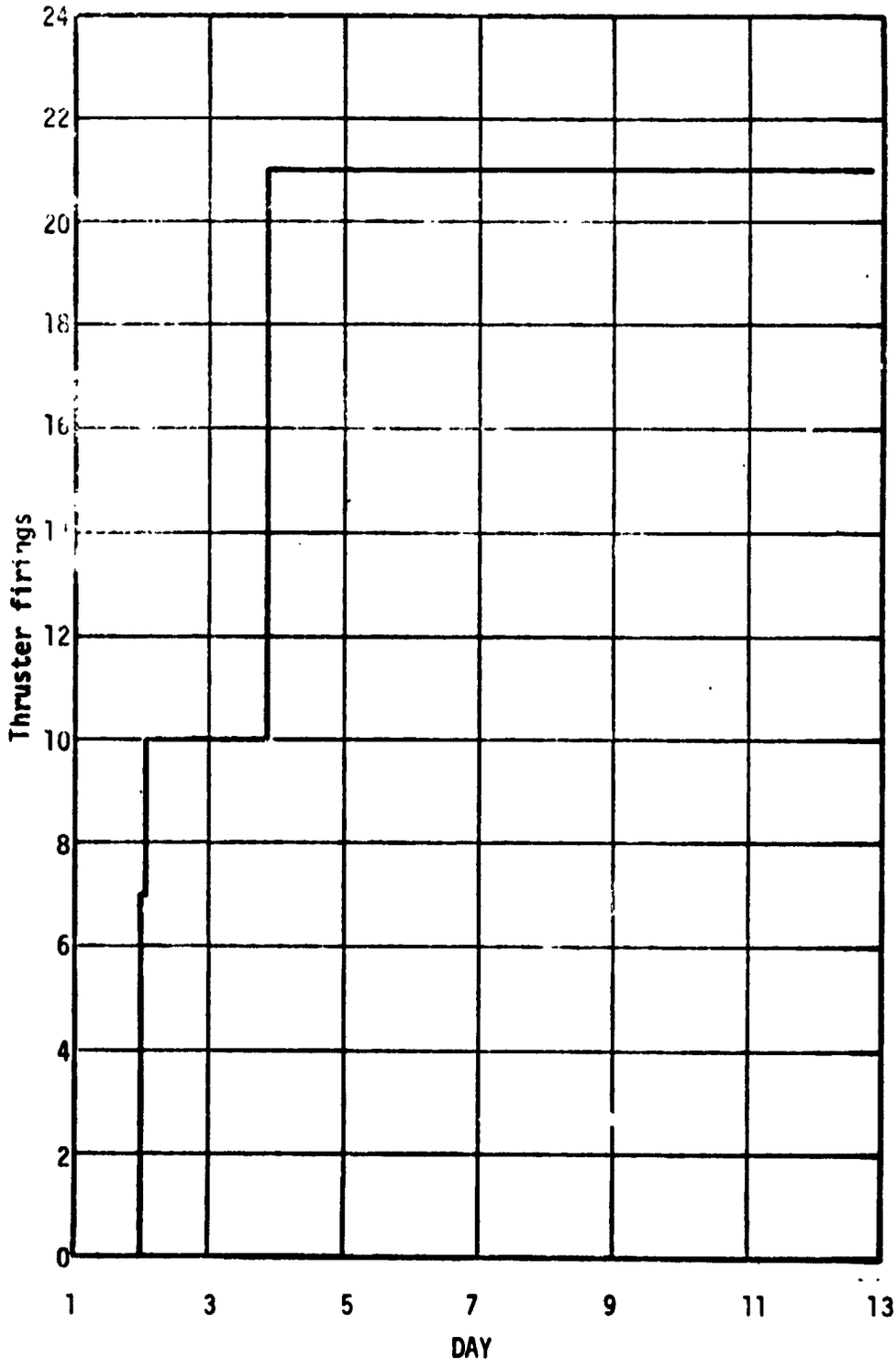

Figure 56. Accumulated Full-On Firings, SL-1

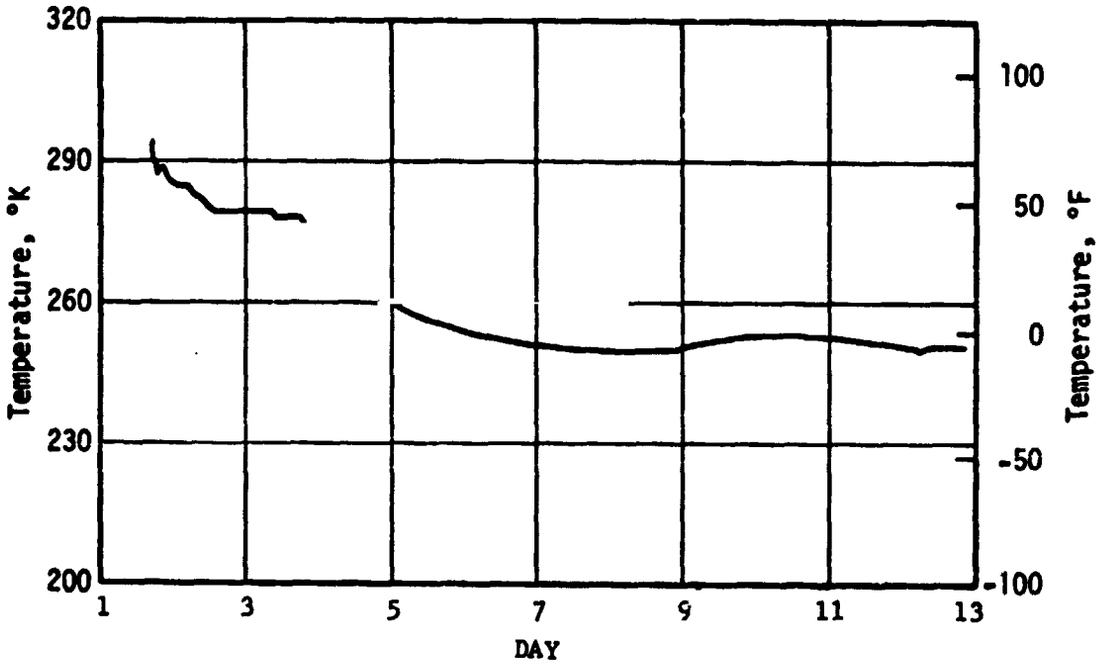

Figure 57. Average GN_2 Bulk Temperature, SL-1

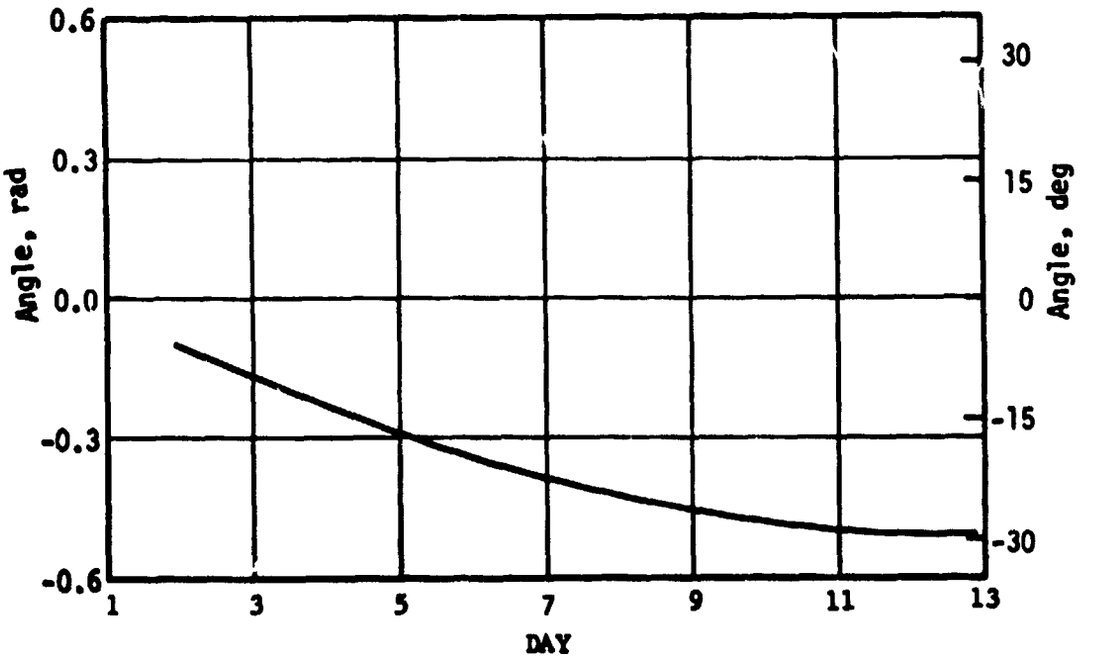

Figure 58. Solar Elevation, SL-1

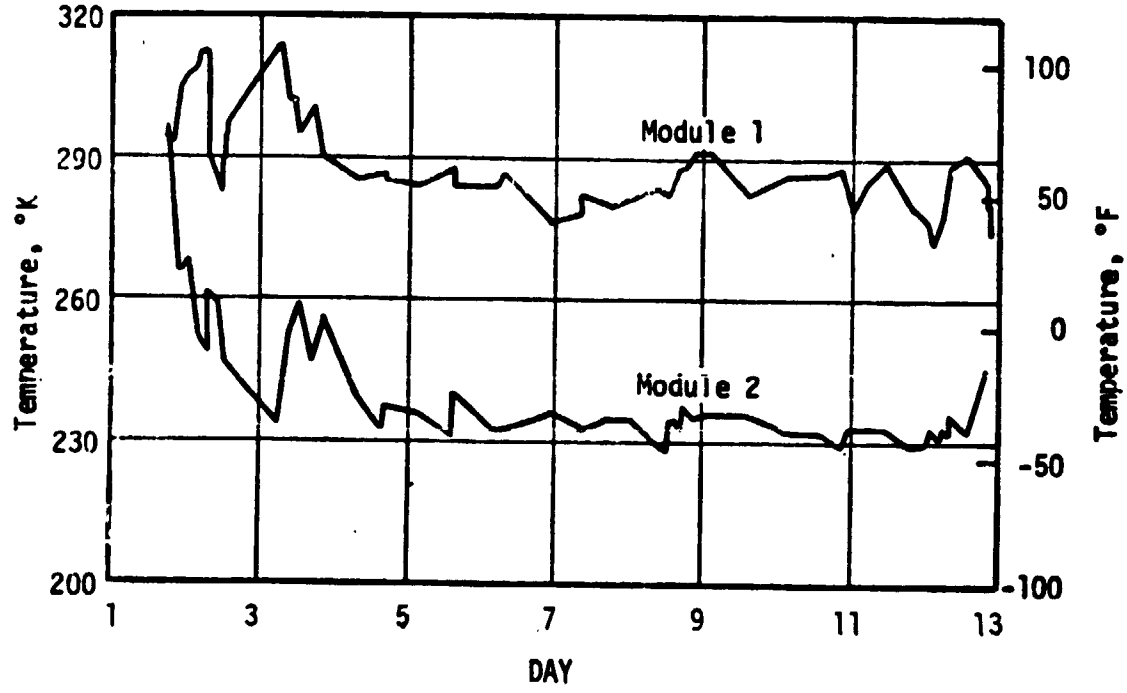

Figure 59. Thruster Module Inlet Temperatures, SL-1

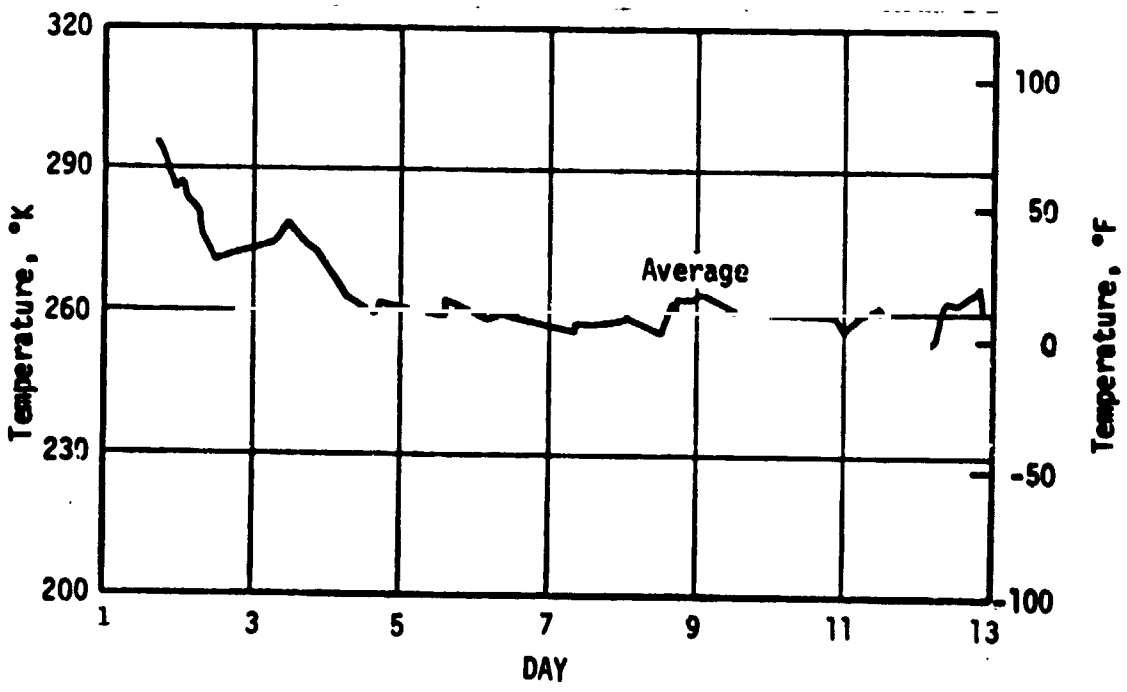

Figure 60. Average Thruster Module Inlet Temperature, SL-1

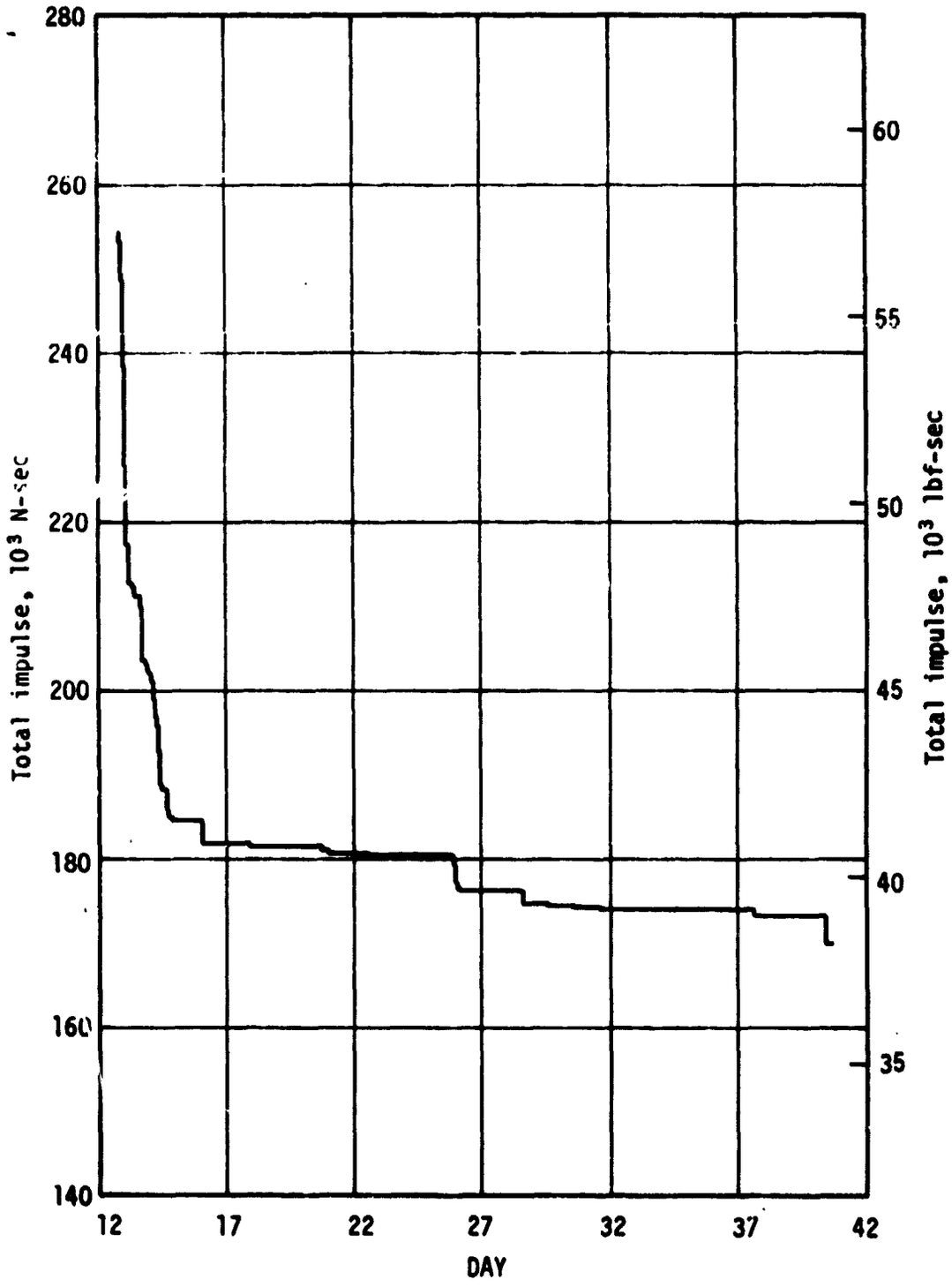

Figure 61. Usable Total Impulse Remaining, SL-2

The system pressure decay and GN_2 mass are shown in figures 62 and 63. The thrust level variation for this phase of the mission is shown in figure 64 and is compared to the thrust level stored in the ATMDC. The variation in Minimum Impulse Bit, figure 65, also shows the times at which the ATMDC command pulse width was updated. The Minimum Impulse Bit was maintained at about 22 N.s.

Figures 66 and 67 present thruster firing histories for this mission phase. The MIB firings and Full-On firings are shown separately. The large usages early in the mission are associated with the stand-up Extra Vehicular Activity (EVA) to free the partially deployed Solar Array and several docking attempts before final hard dock was achieved.

The average bulk gas temperature is presented in figure 68. The Solar Elevation Angle variation is shown in figure 69 for this mission phase. Note that the temperatures responded to the changes in solar elevation angle during this period of time because orbital thermal equilibrium conditions had been established.

The module inlet gas temperatures and the average module inlet temperature are presented in figures 70 and 71.

c. Second Unmanned Orbital Storage Period. The Thruster Attitude Control System was inactive throughout the orbital storage period from approximately DAY 40 to DAY 76. Consequently the total impulse remaining, the GN_2, the MIB firings, and the Full-On firings were constant. The variation in thrust and MIB reflected the changes in system pressure due to changes in bulk gas temperature.

d. Second Manned Mission, SL-3 (59 Days). The total impulse remaining for this second manned mission is presented in figure 72.

The system pressure decay and gaseous nitrogen mass are shown in figures 73 and 74. The thruster level variation for this phase of the mission is shown in figure 75 and is compared to the thrust level stored in the ATMDC. The variation in Minimum Impulse Bit, figure 76 also shows the times at which the ATMDC command pulse width was updated. The Minimum Impulse Bit was maintained at approximately 22 N.s.

The thruster firing histories are shown in figures 77 and 78.

The average bulk gas temperature and solar elevation angles are presented in figures 79 and 80.

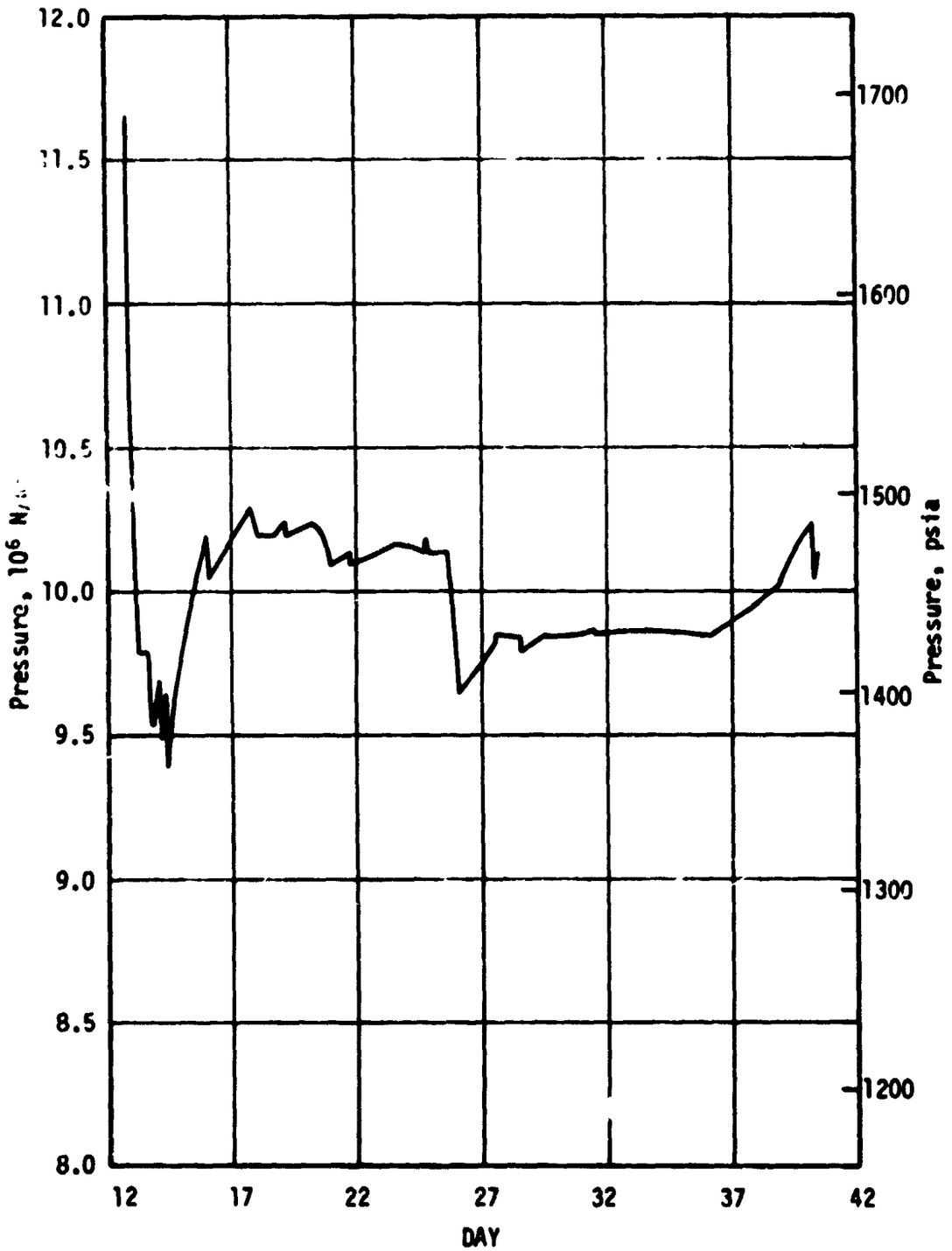

Figure 62. TACS GN_2 Pressure, SL-2

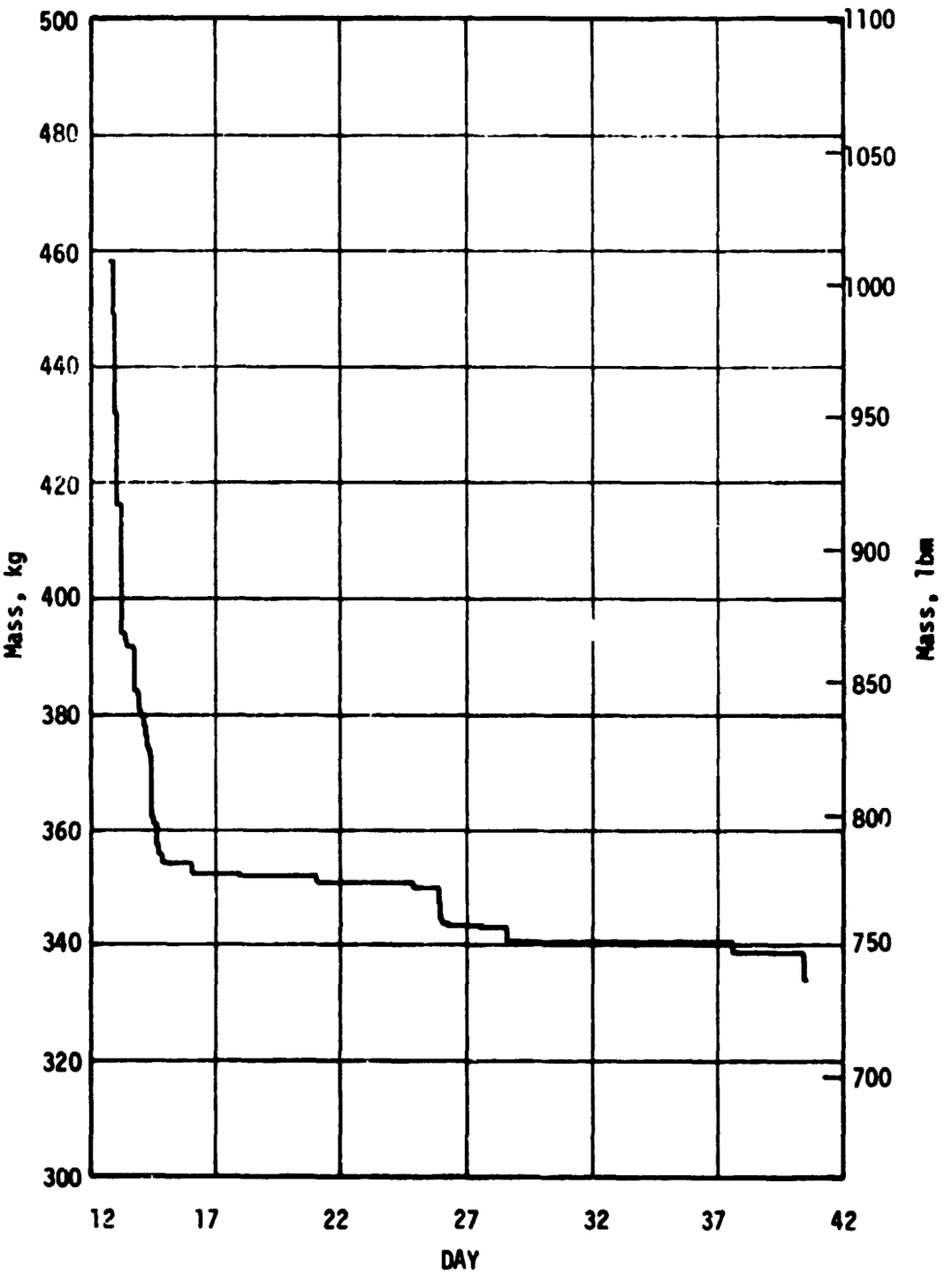

Figure 63. TACS GN_2 Mass Remaining, SL-2

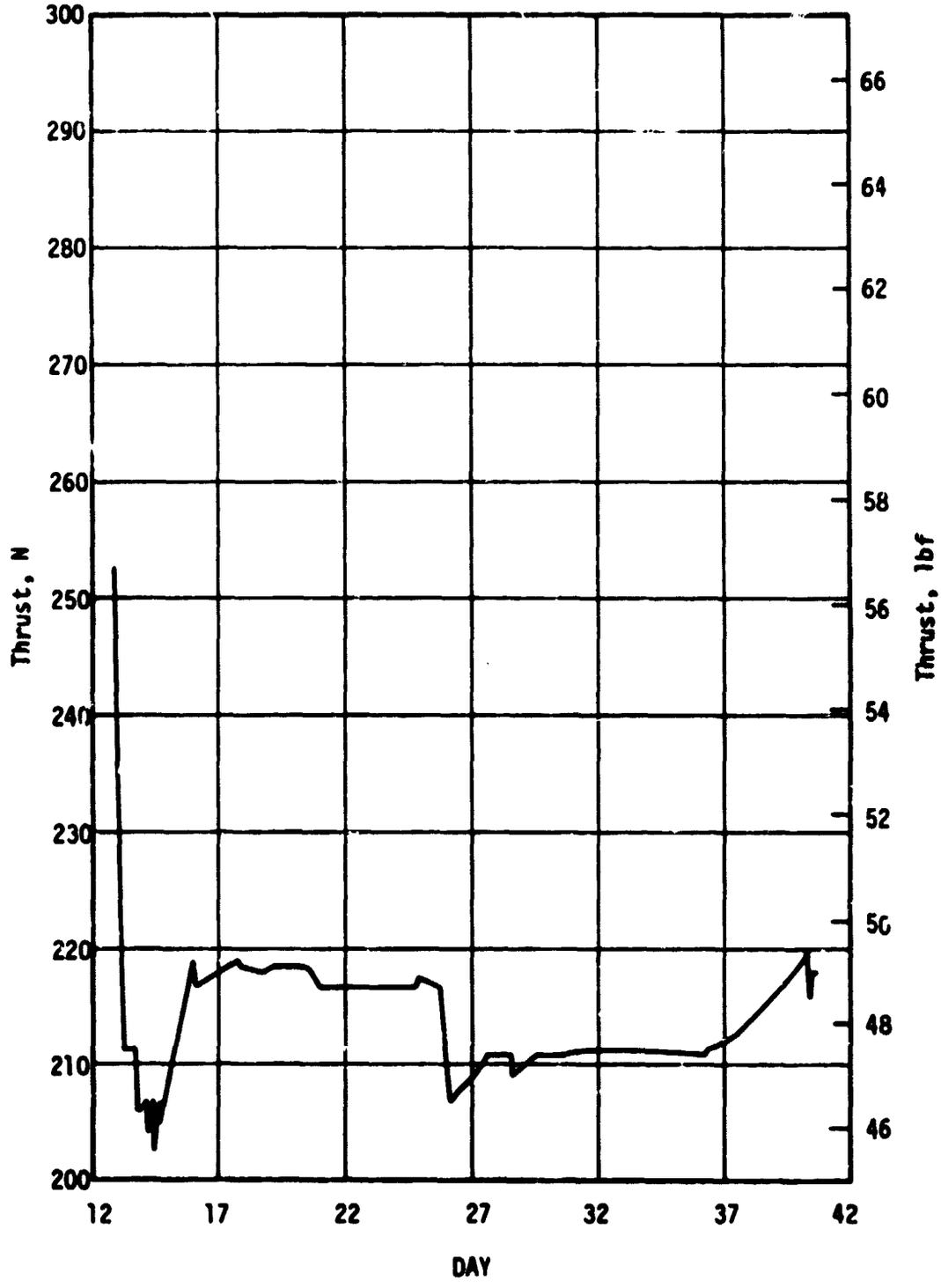

Figure 64. Thrust Levels, SL-2

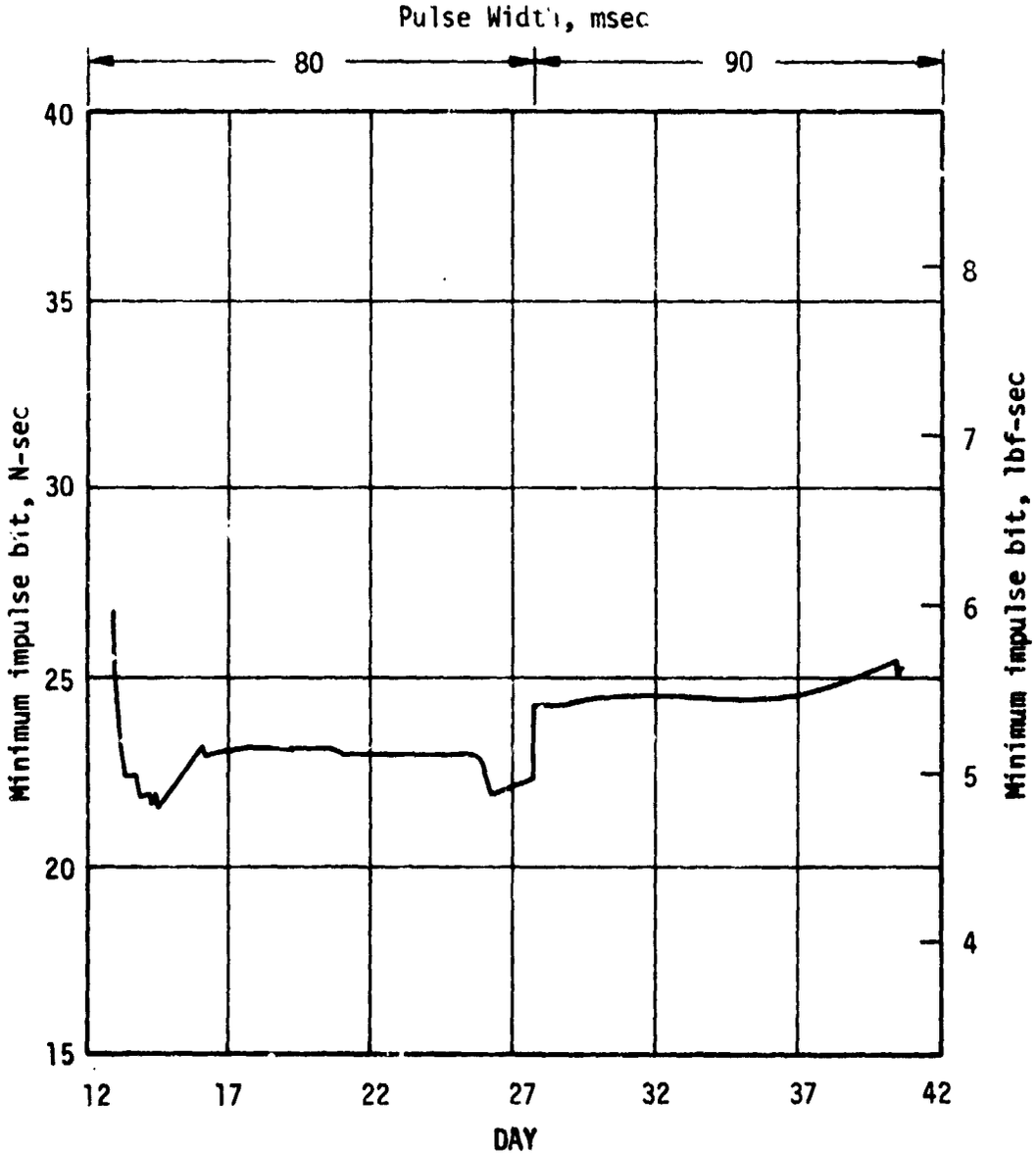

Figure 65. Nominal Minimum Impulse Bit, SL-2

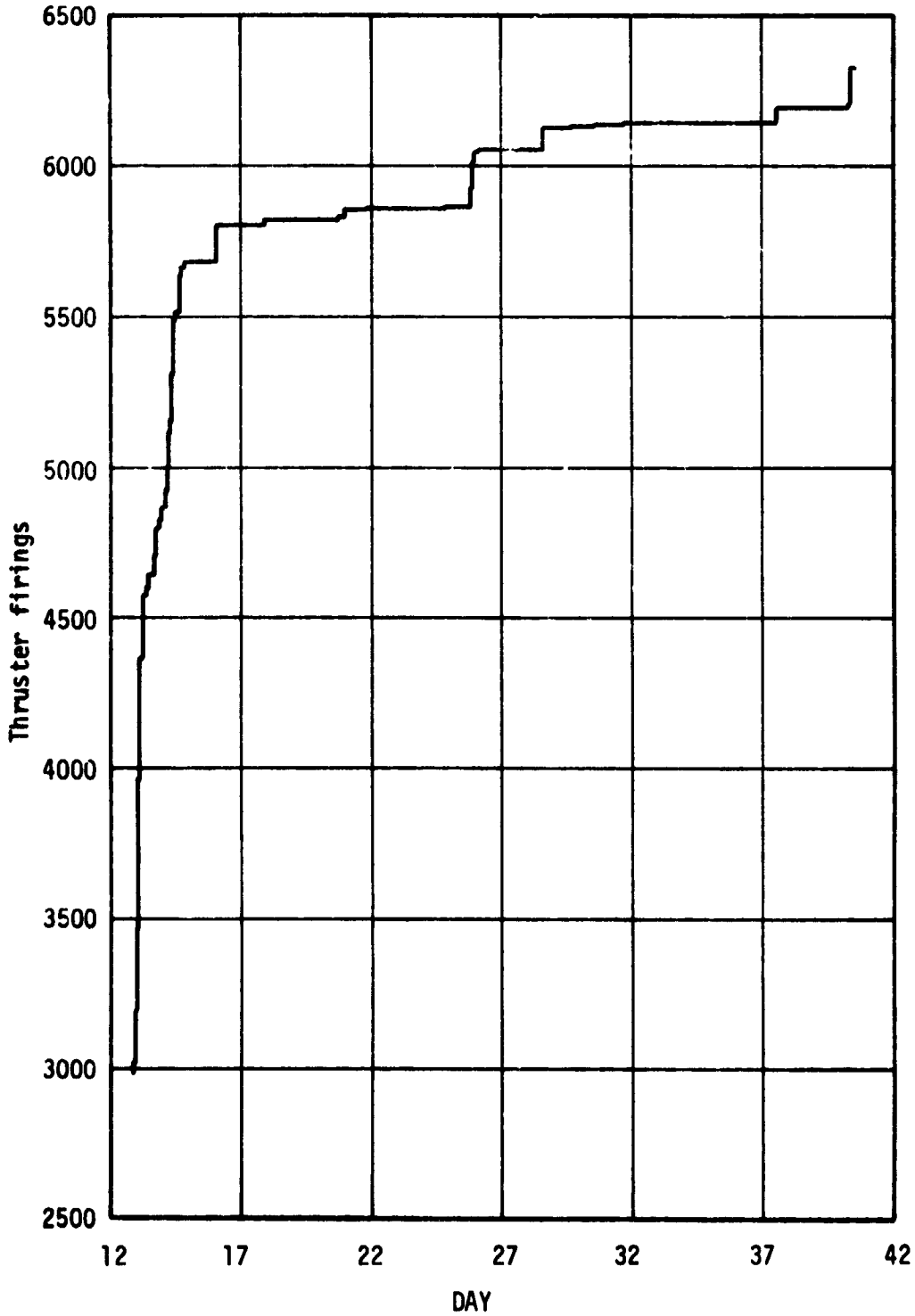

Figure 66. Accumulated MIB Firings, SL-2

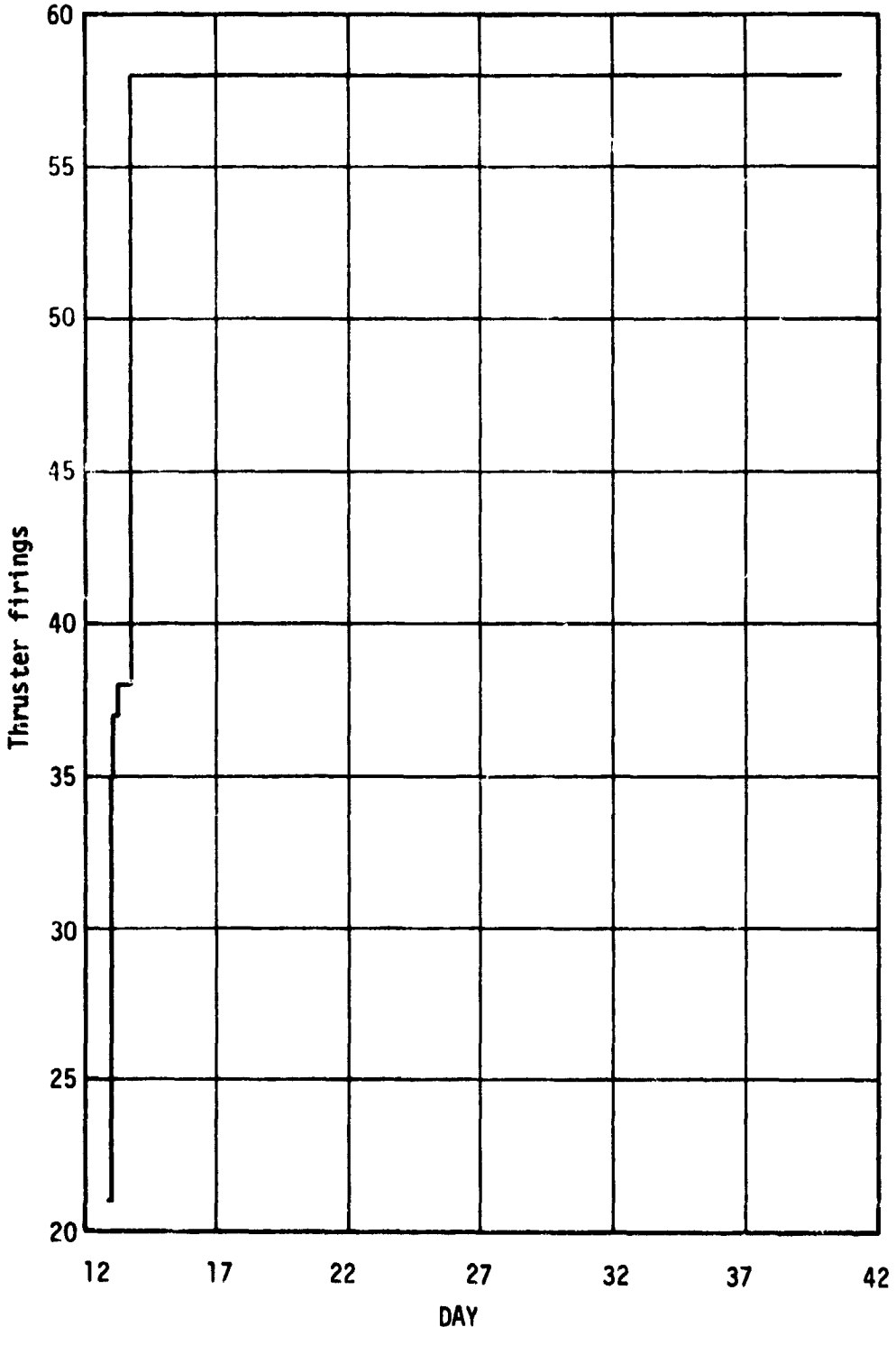

Figure 67. Accumulated Full-On Firings, SL-2

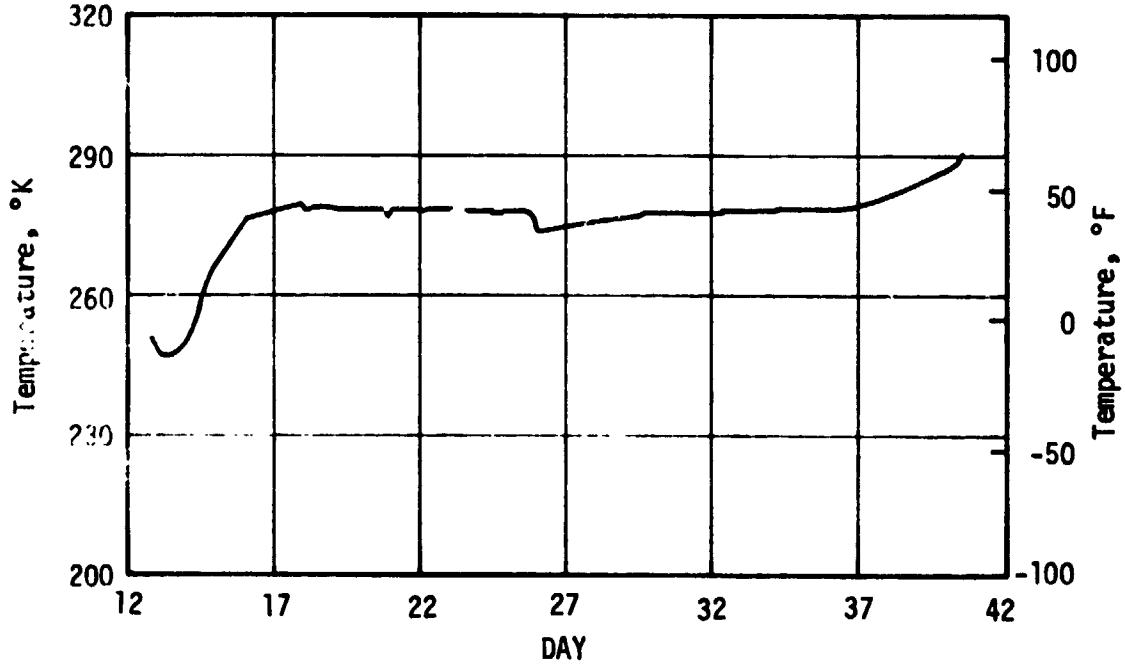

Figure 68. Average GN_2 Bulk Temperature, SL-2

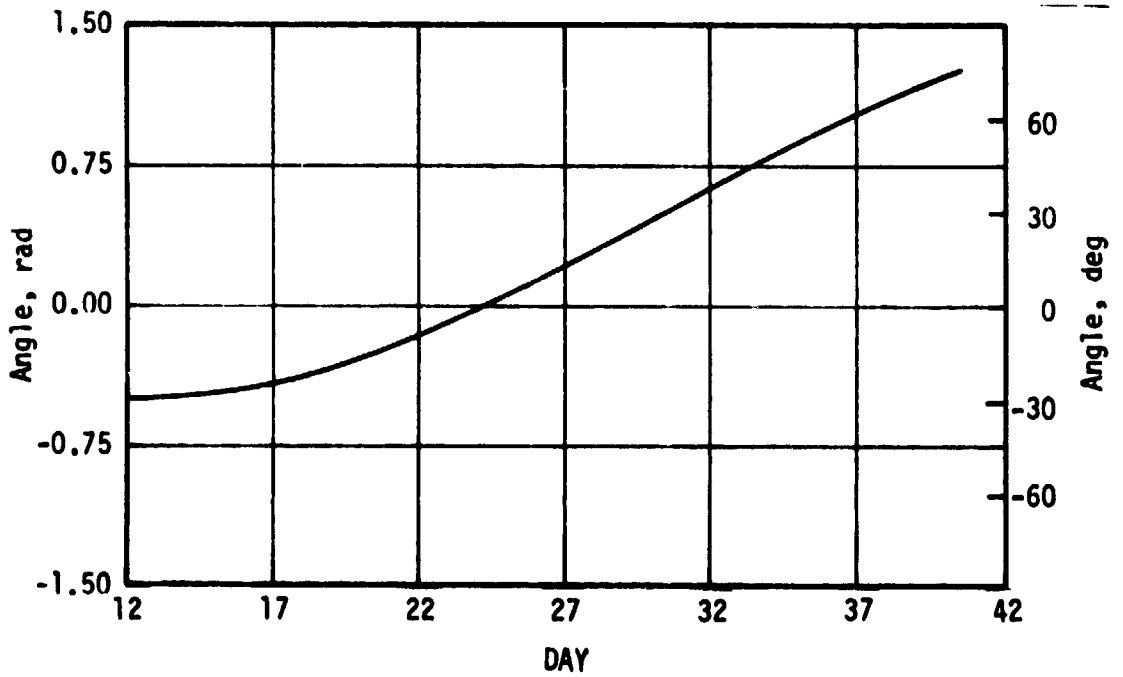

Figure 69. Solar Elevation Angle, SL-2

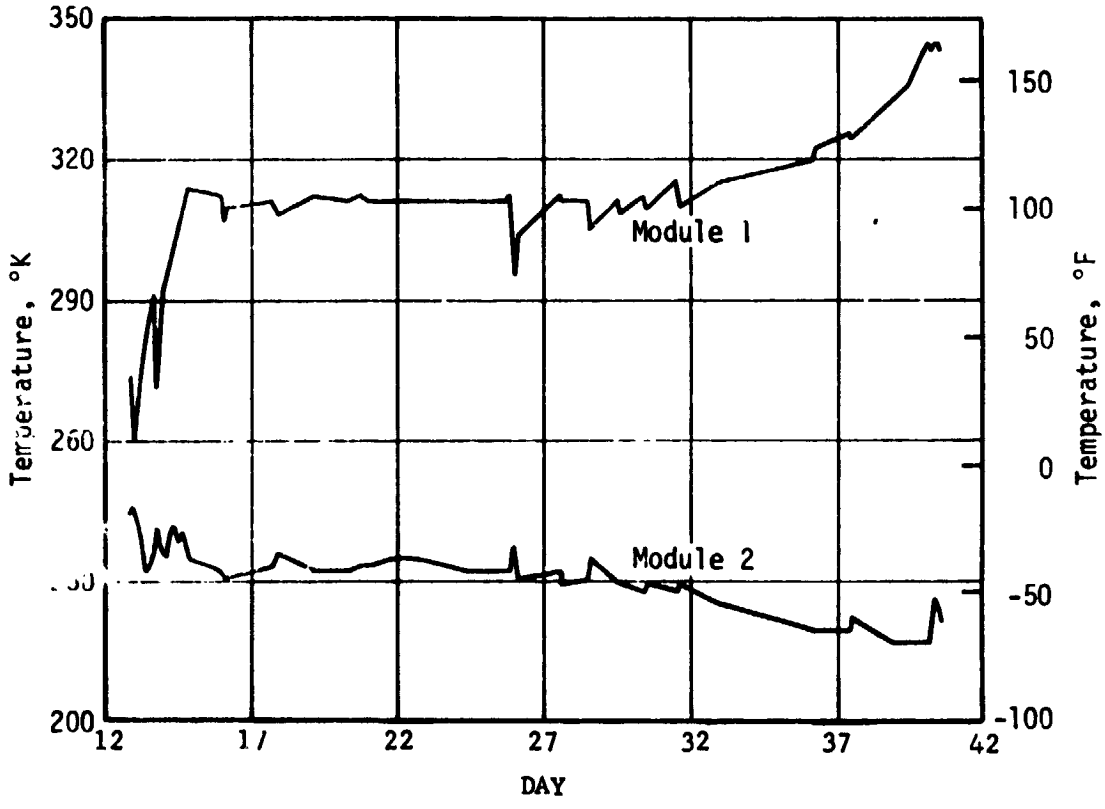

Figure 70. Thruster Module Inlet Temperatures, SL-2

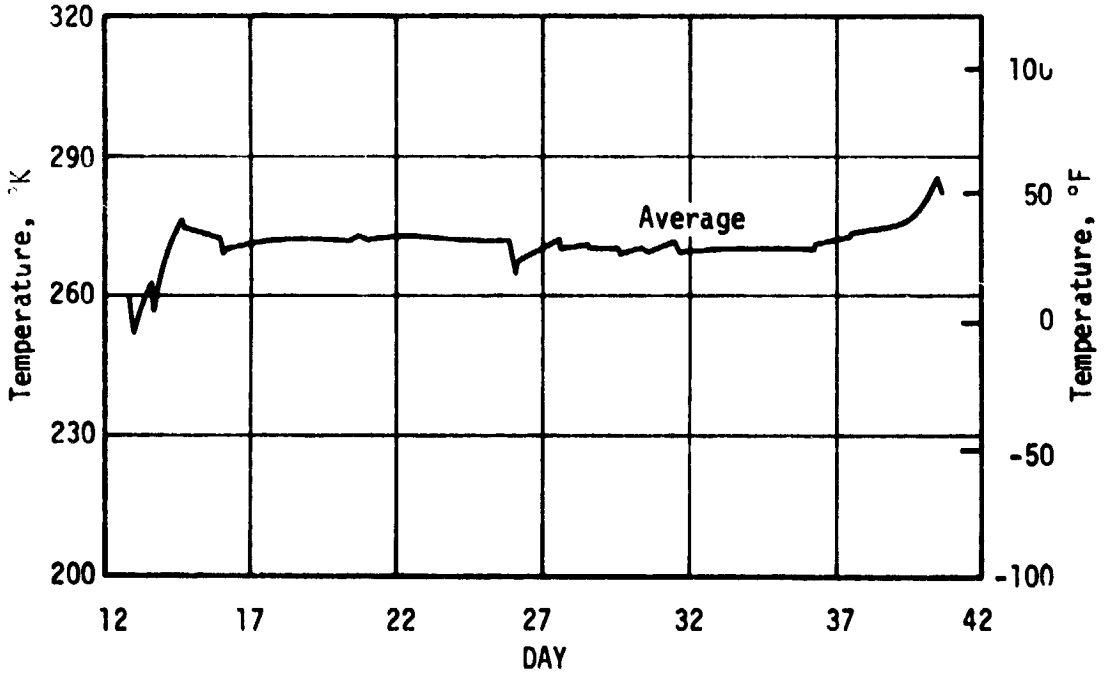

Figure 71. Average Thruster Module Inlet Temperature, SL-2

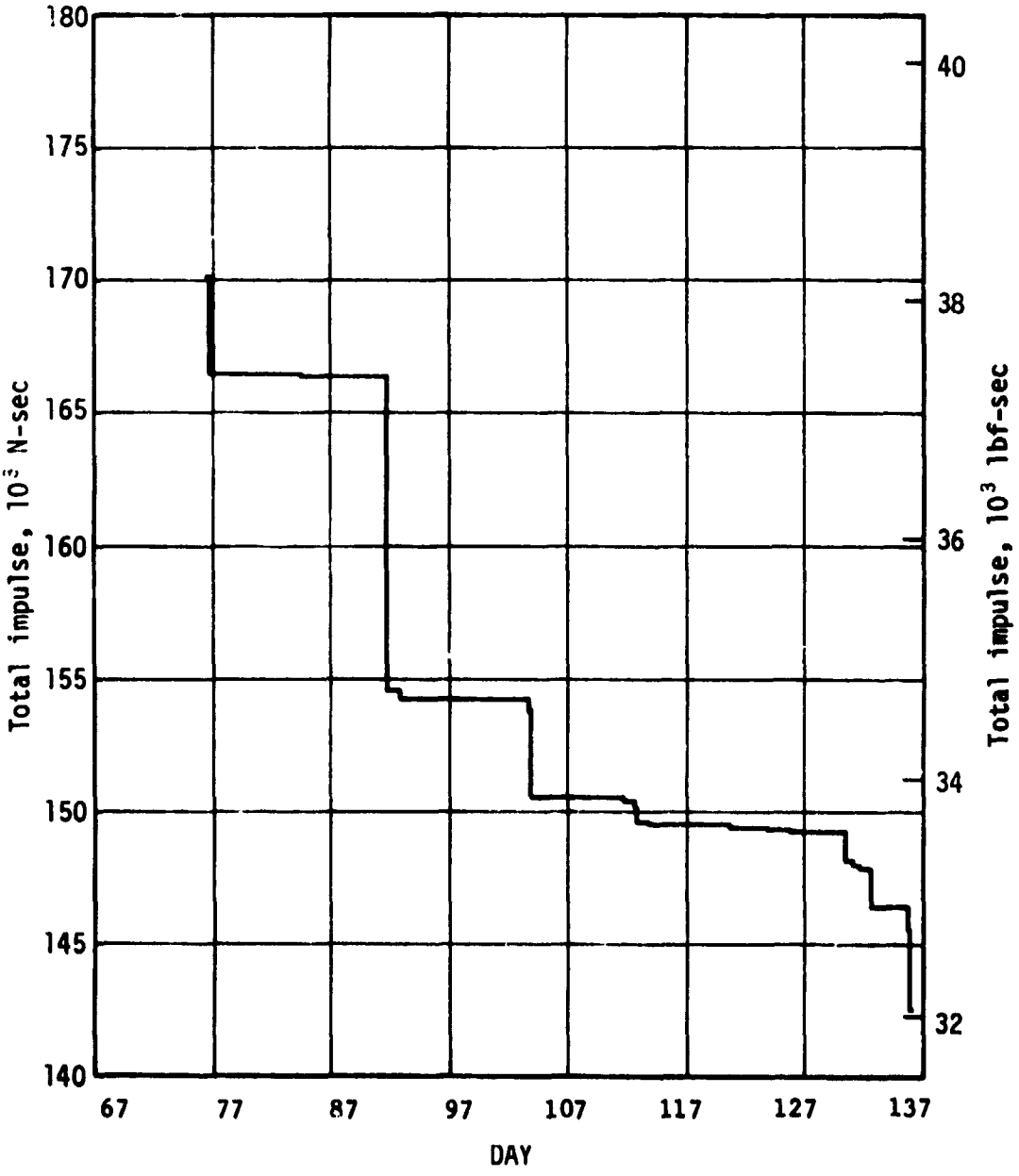

Figure 72. Usable Total Impulse Remaining, SL-3

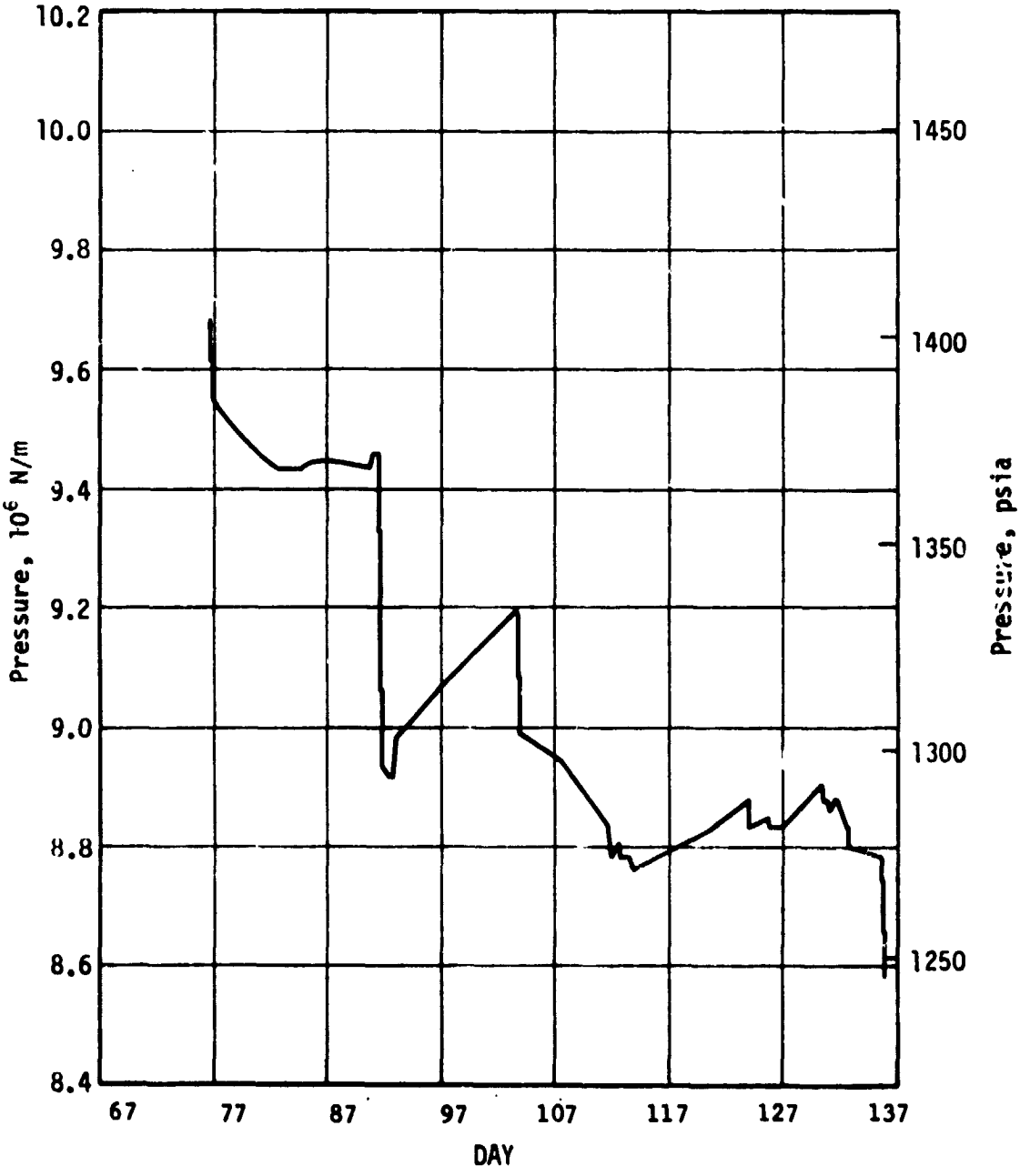

Figure 73. TACS GN_2 Pressure, SL-3

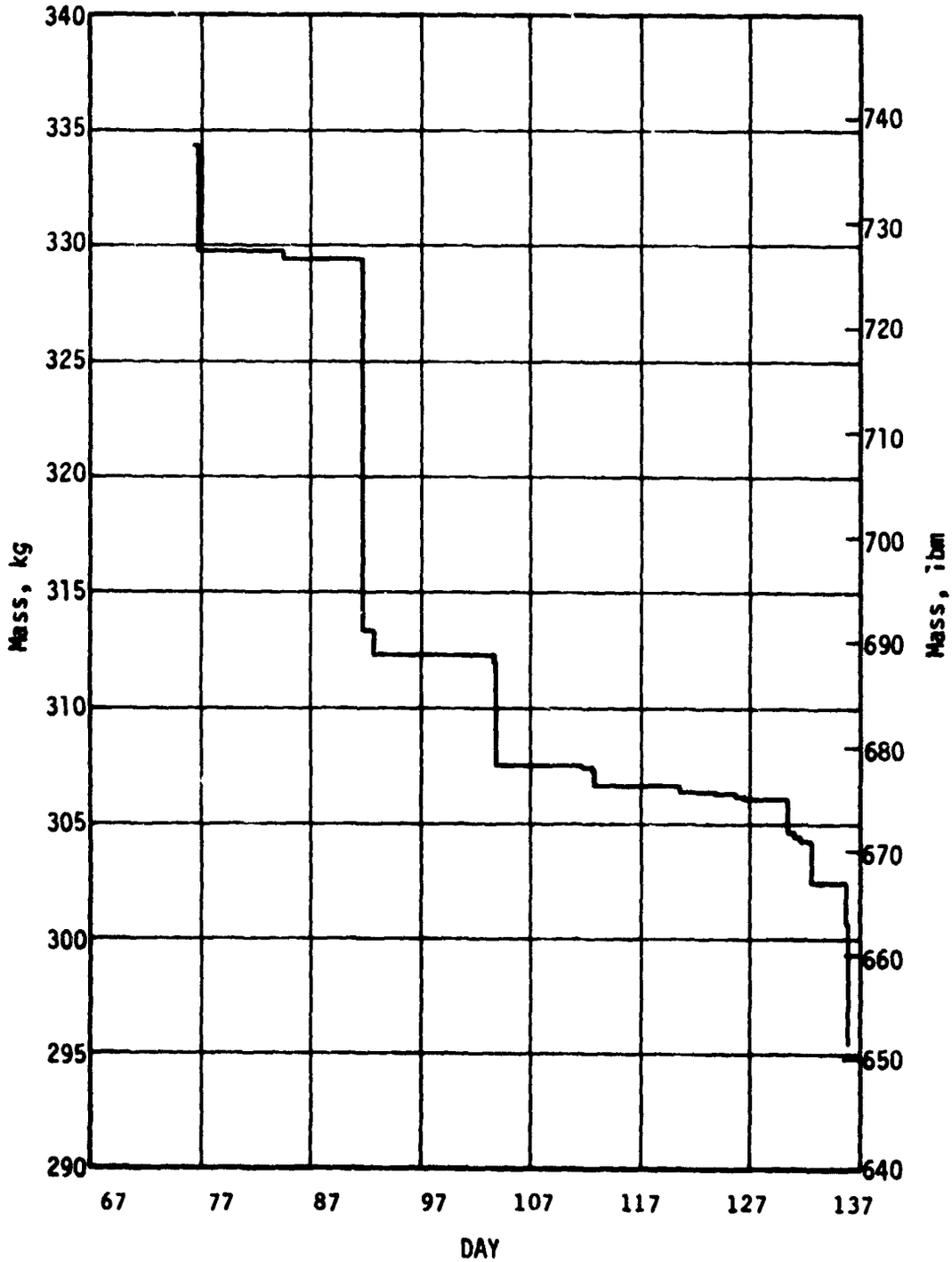

Figure 74. TACS GN_2 Mass Remaining, SL-3

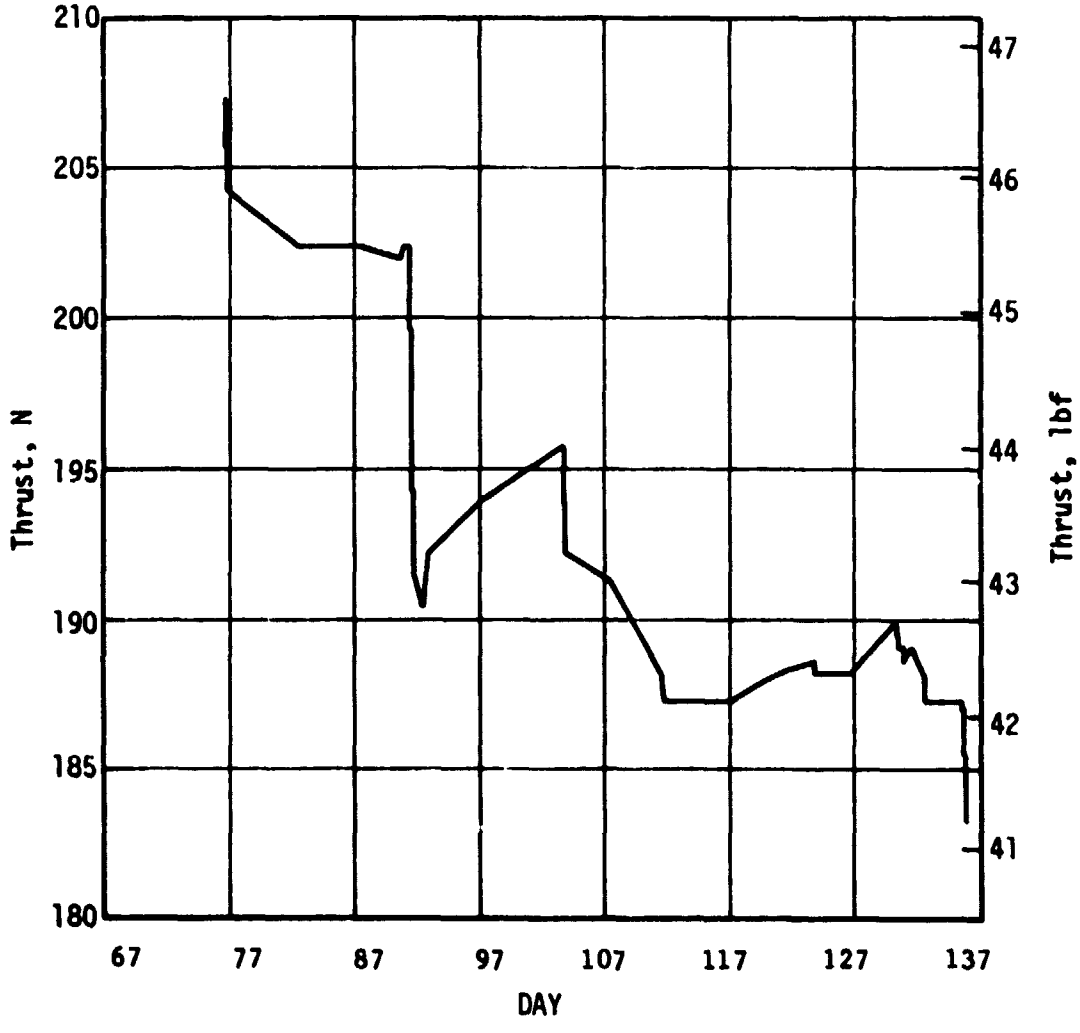

Figure 75. Thrust Levels, SL-3

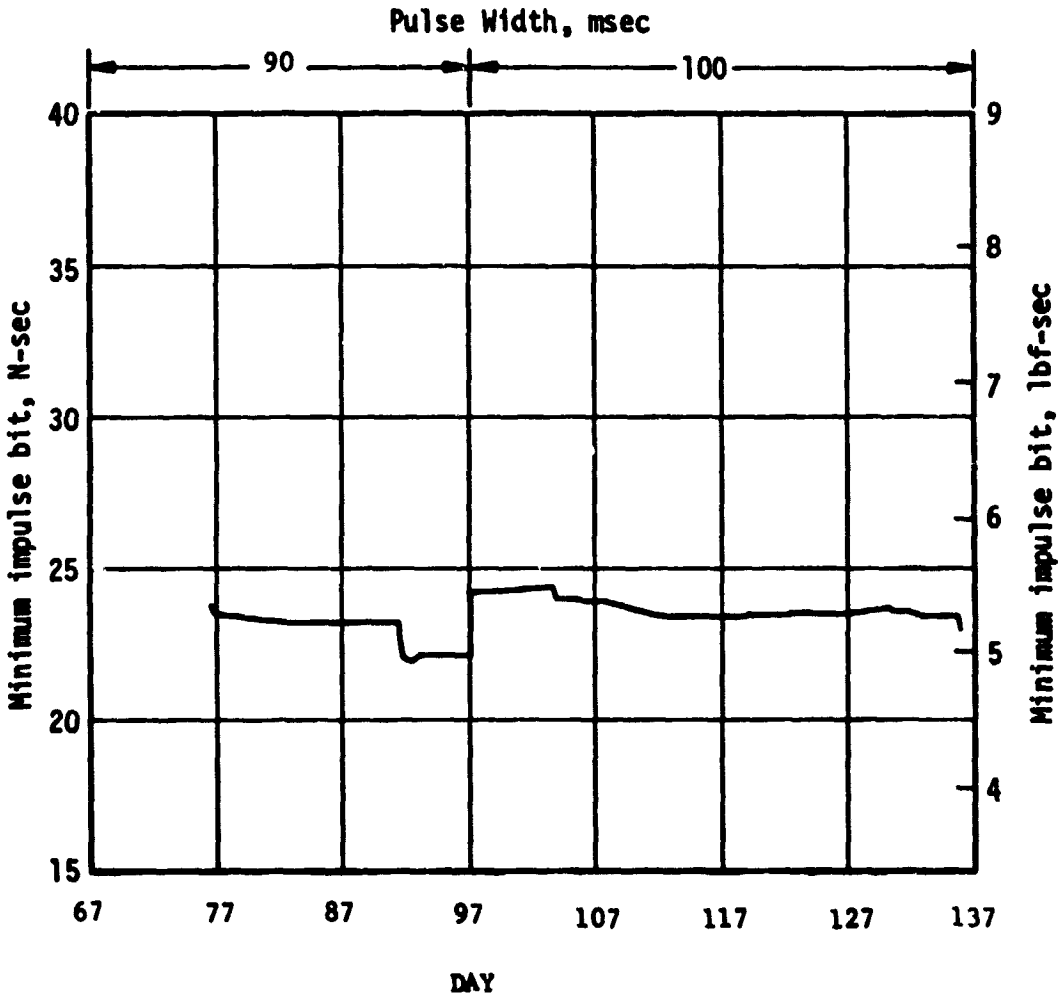

Figure 76. Nominal Minimum Impulse Bit, SL-3

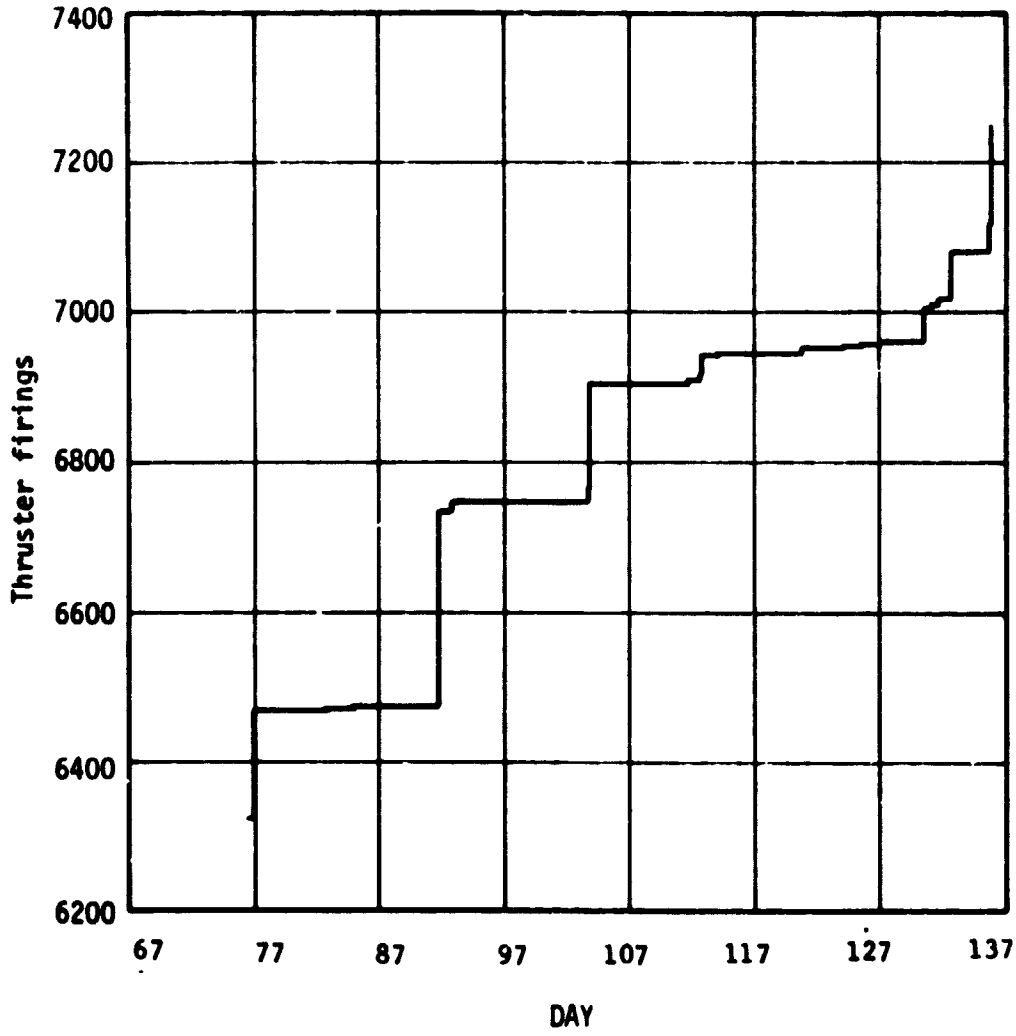

Figure 77. Accumulated MIB Firings, SL-3

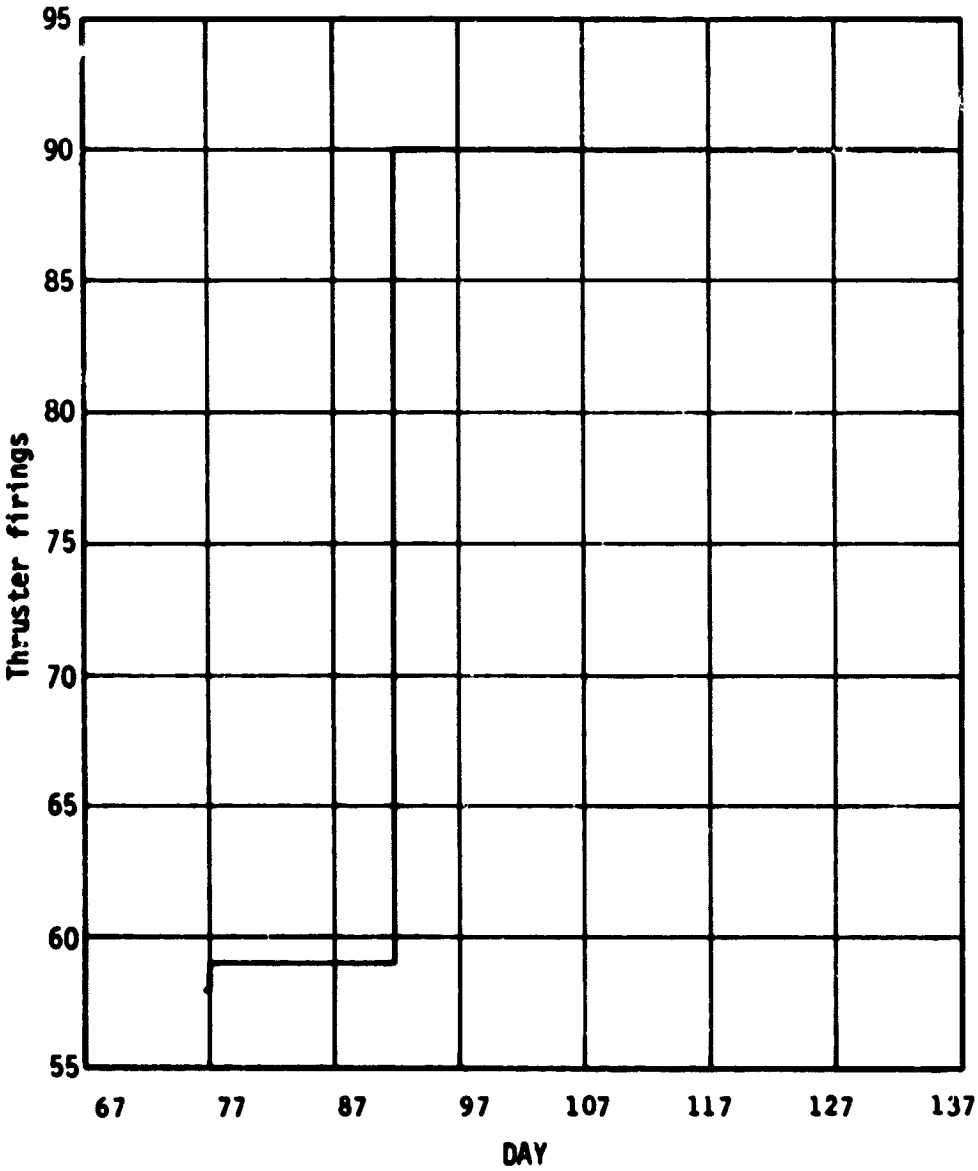

Figure 78. Accumulated Full-On Firings, SL-3

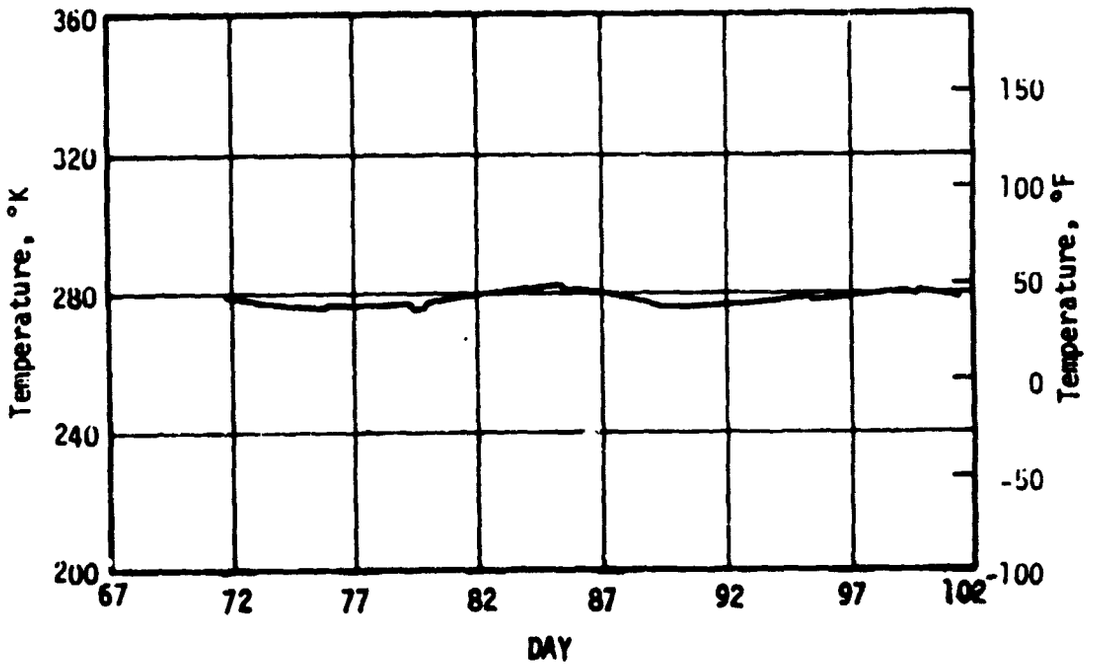

Figure 79. Average GN_2 Bulk Temperature, SL-3

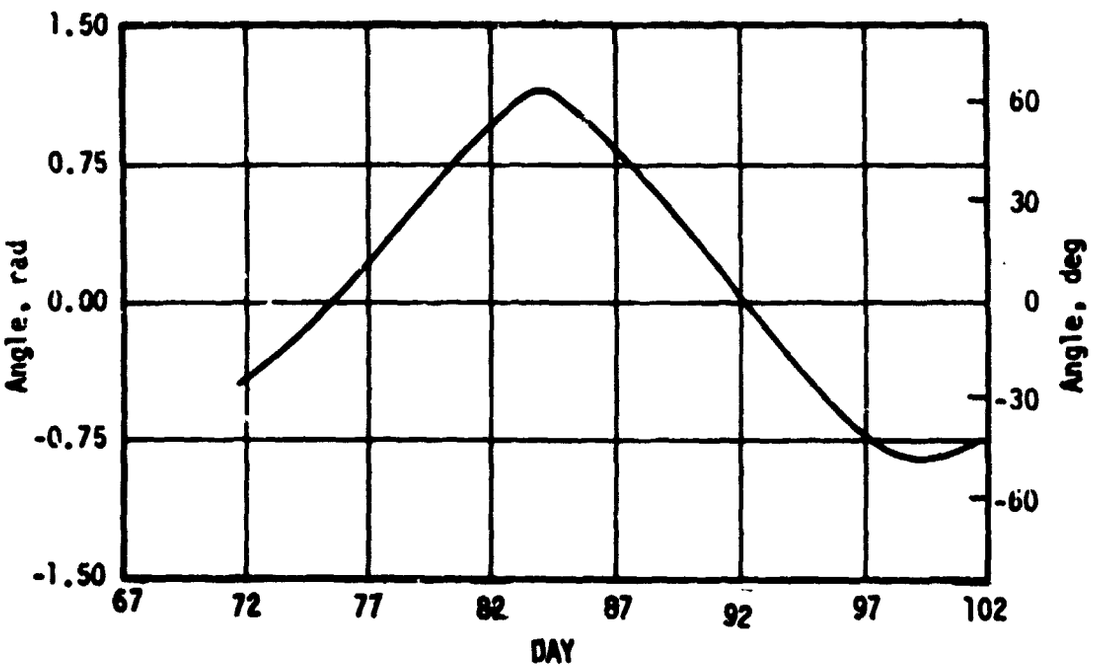

Figure 80. Solar Elevation Angle, SL-3

The module inlet gas temperatures and the average module inlet temperature are presented in figures 81 and 82.

e. Third Unmanned Orbital Storage Period. The Thruster Attitude Control System was inactive throughout the orbital storage period from approximately DAY 135 to DAY 187. The total impulse remaining, the gaseous nitrogen mass, the MIB firings and the Full-On firings were constant. The variation in system pressure, thrust, and Minimum Impulse Bit reflected changes in system pressure due to changes in bulk gas temperature.

f. Third Manned Mission, SL-4 (85 Days). The total impulse remaining for this third manned mission is presented in figure 83.

The system pressure decay and gaseous nitrogen mass are shown in figures 84 and 85. The thrust level variation for this phase of the mission is shown in figure 86 and is compared to the thrust level stored in the ATMDC. The variation in the MIB, figure 87, also shows the times at which the ATMDC command pulse width was updated. The Minimum Impulse Bit was maintained at approximately 22 N.s

The MIB and Full-On firing histories are shown in figures 88 and 89. The average GN_2 temperatures and solar elevation angles are shown in figures 90 and 91. The module inlet gas temperatures and the average module inlet temperature are presented in figures 92 and 93.

5. Anomalies.

a. Thruster Attitude Control System Thermal Anomaly. TACS hardware was designed and qualified for a maximum temperature of 347 degrees K. Since the operation of the solenoid control valves was critical to system operation, valve performance or anything that might affect performance was closely monitored. Analysis of flight data obtained during the SL-2 indicated that the valves at Position Plane I had reached their maximum qualification test levels during a high solar elevation angle period. The pre-mission thermal analysis had not predicted such an occurrence and, therefore, an investigation was initiated to determine the cause of the difference between the analytical and the actual temperature values. Correlation between the flight data and the analytical prediction was obtained by assuming that the aft skirt white paint solar absorptivity, alpha, was degraded by retro-rocket plume contamination. By varying alpha from a design value of 0.31 maximum to 0.34 and using an actual waste tank temperature value of 322 degrees K rather than the original prediction of 300 degrees K the thermal model predictions agreed closely with

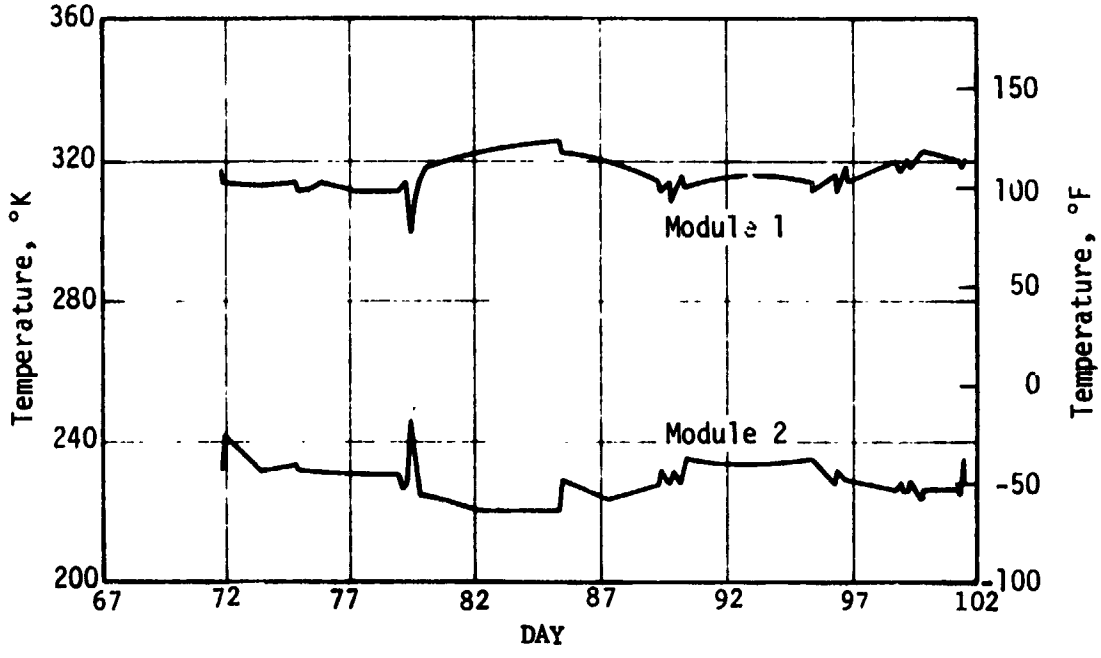

Figure 81. Thruster Module Inlet Temperatures, SL-3

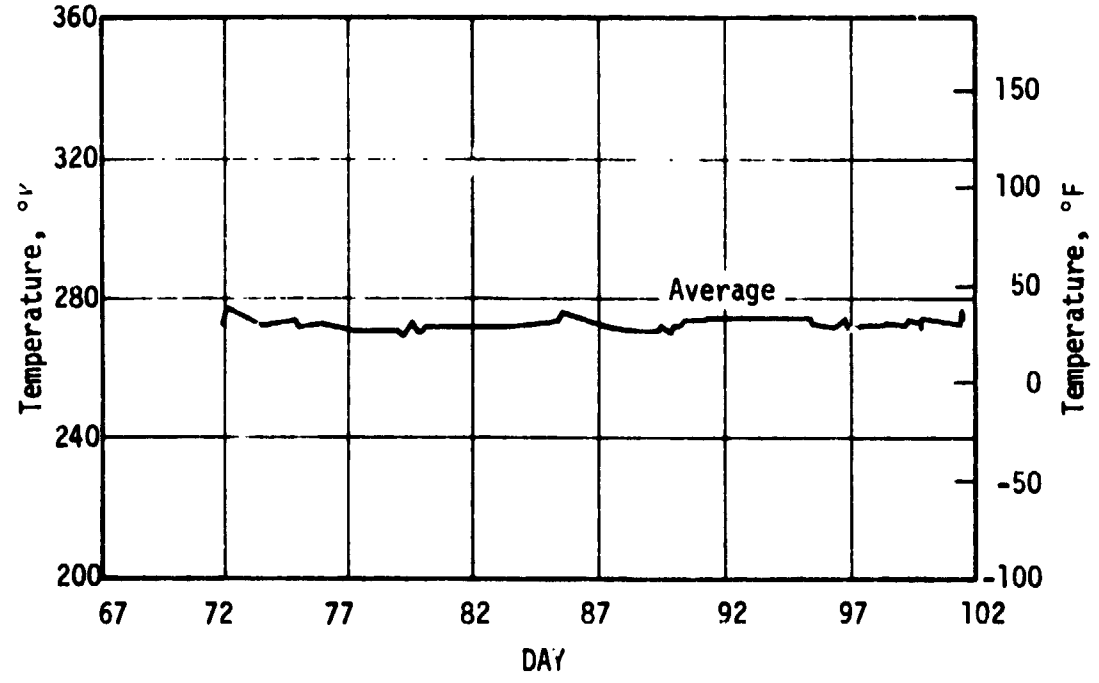

Figure 82. Average Thruster Module Inlet Temperature, SL-3

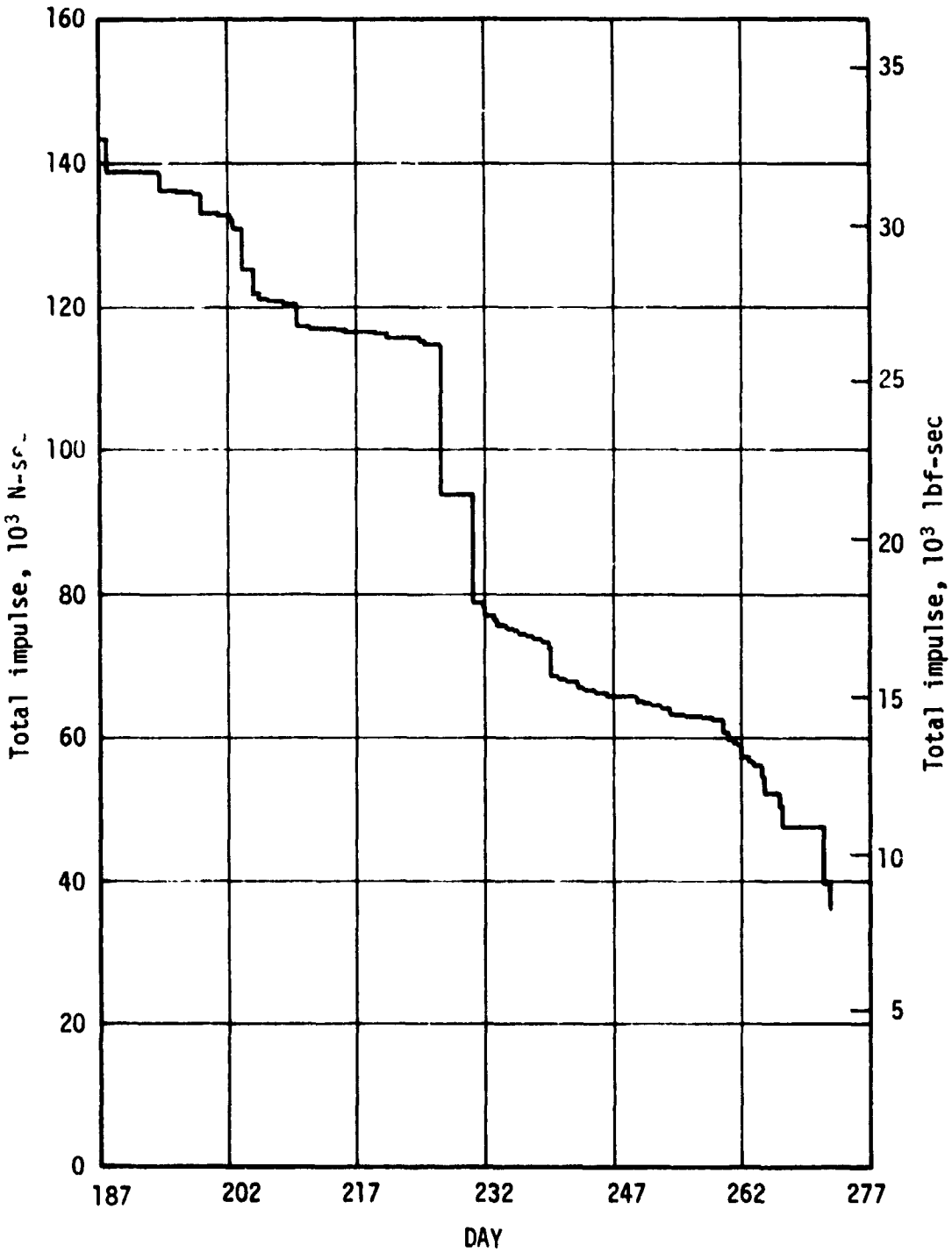

Figure 83. Usable Total Impulse Remaining, SL-4

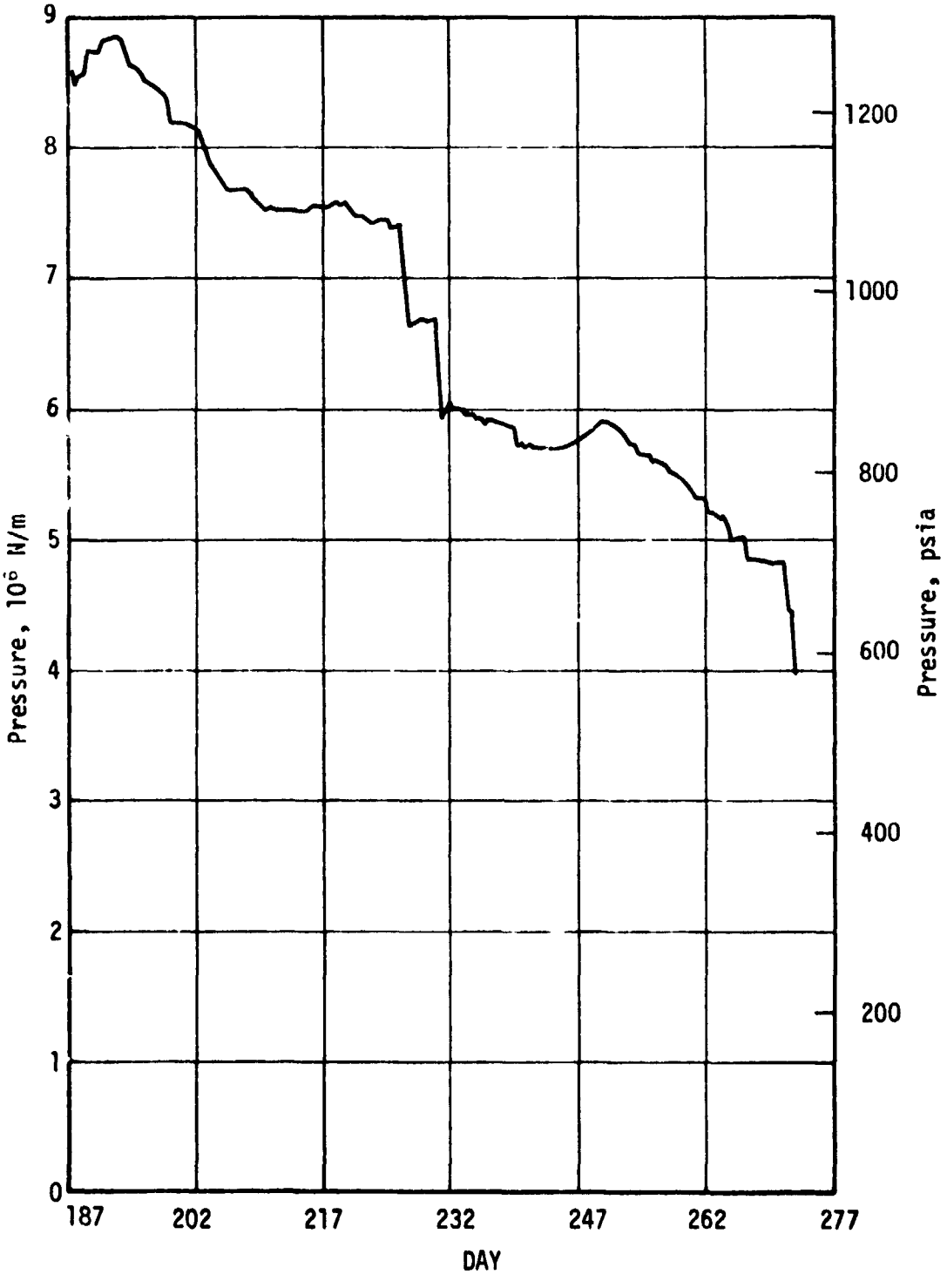

Figure 84. TACS GN_2 Pressure, SL-4

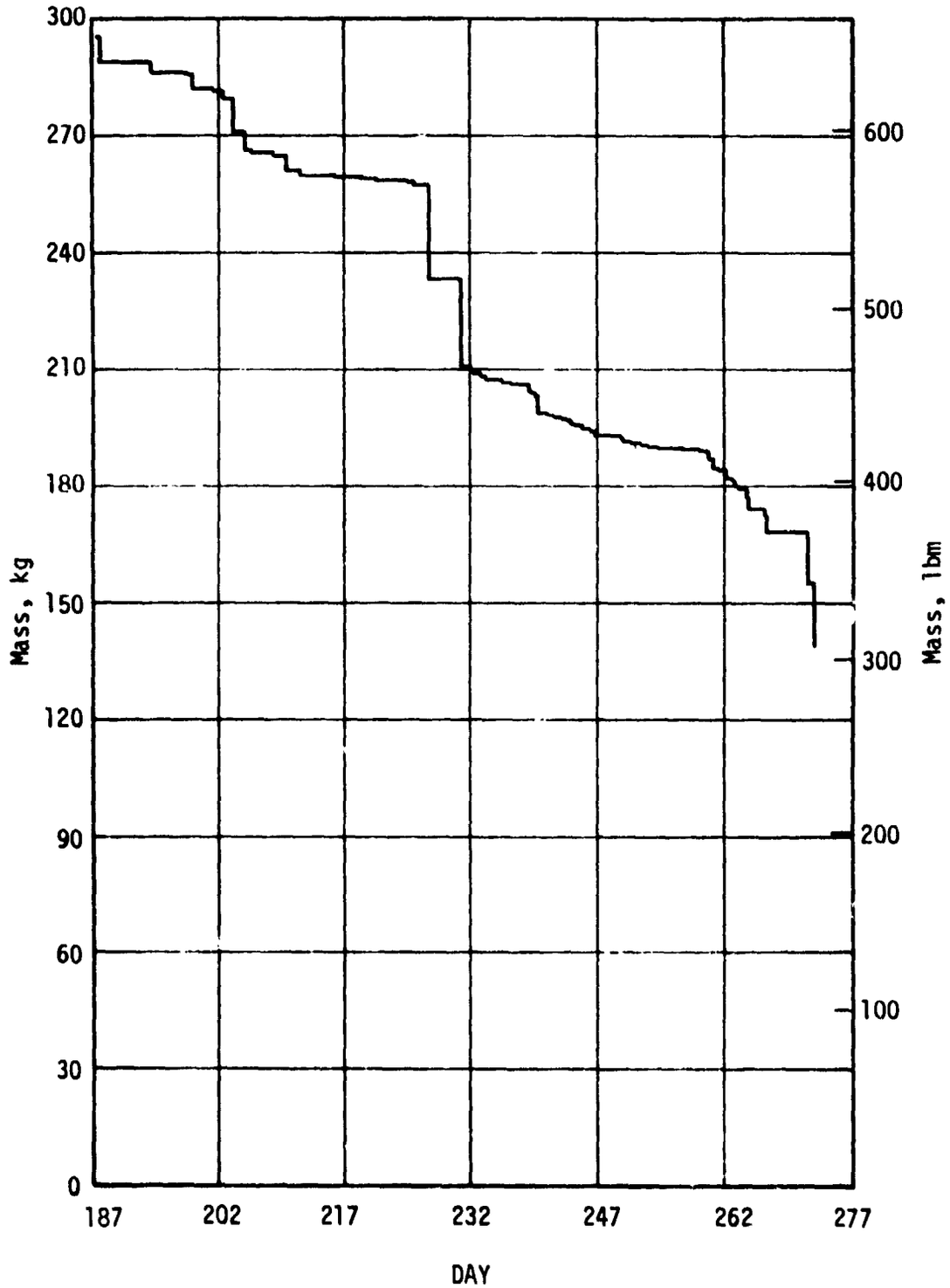

Figure 85. TACS GN_2 Mass, SL-4

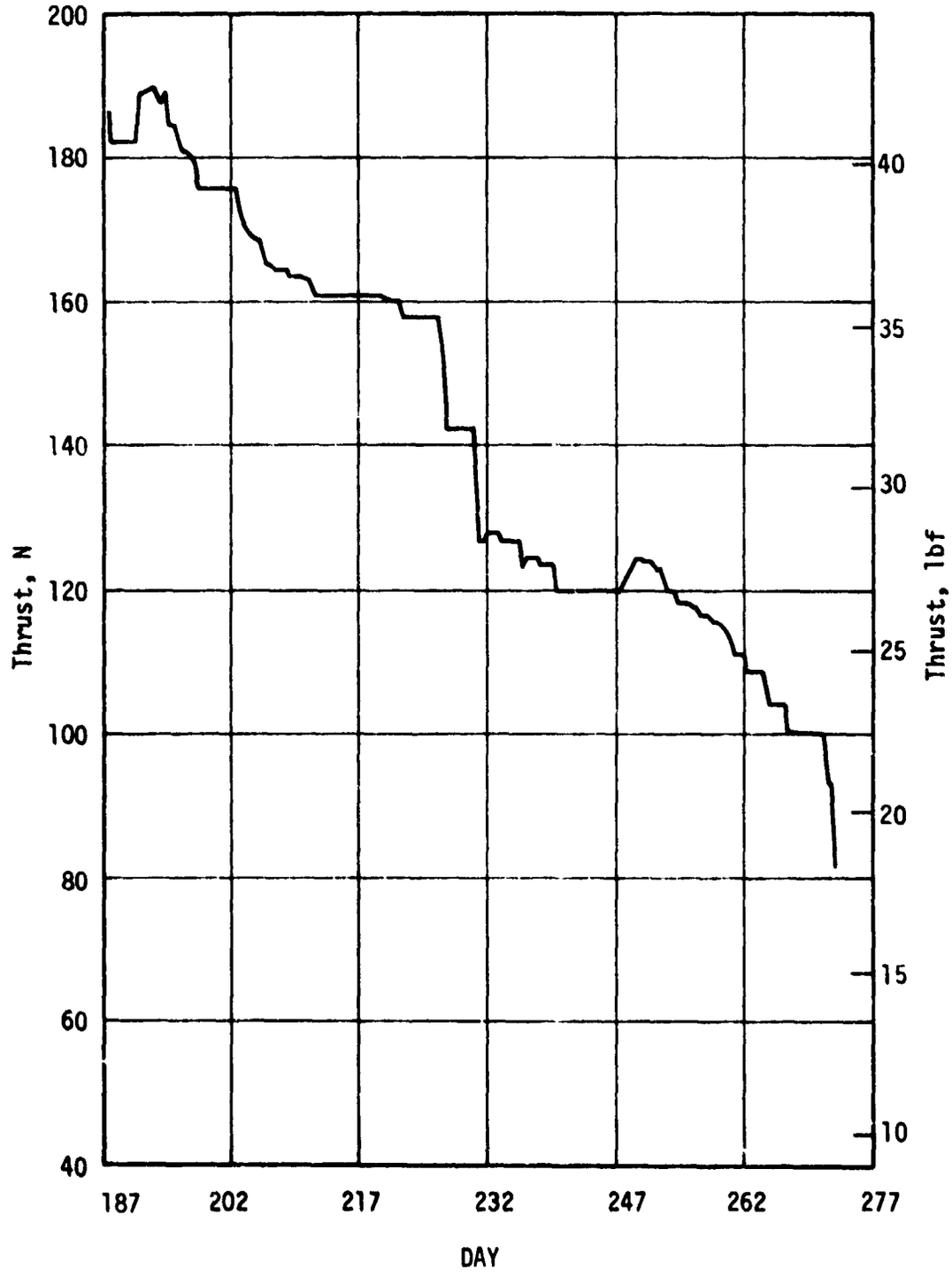

Figure 86. Thrust Levels, SL-4

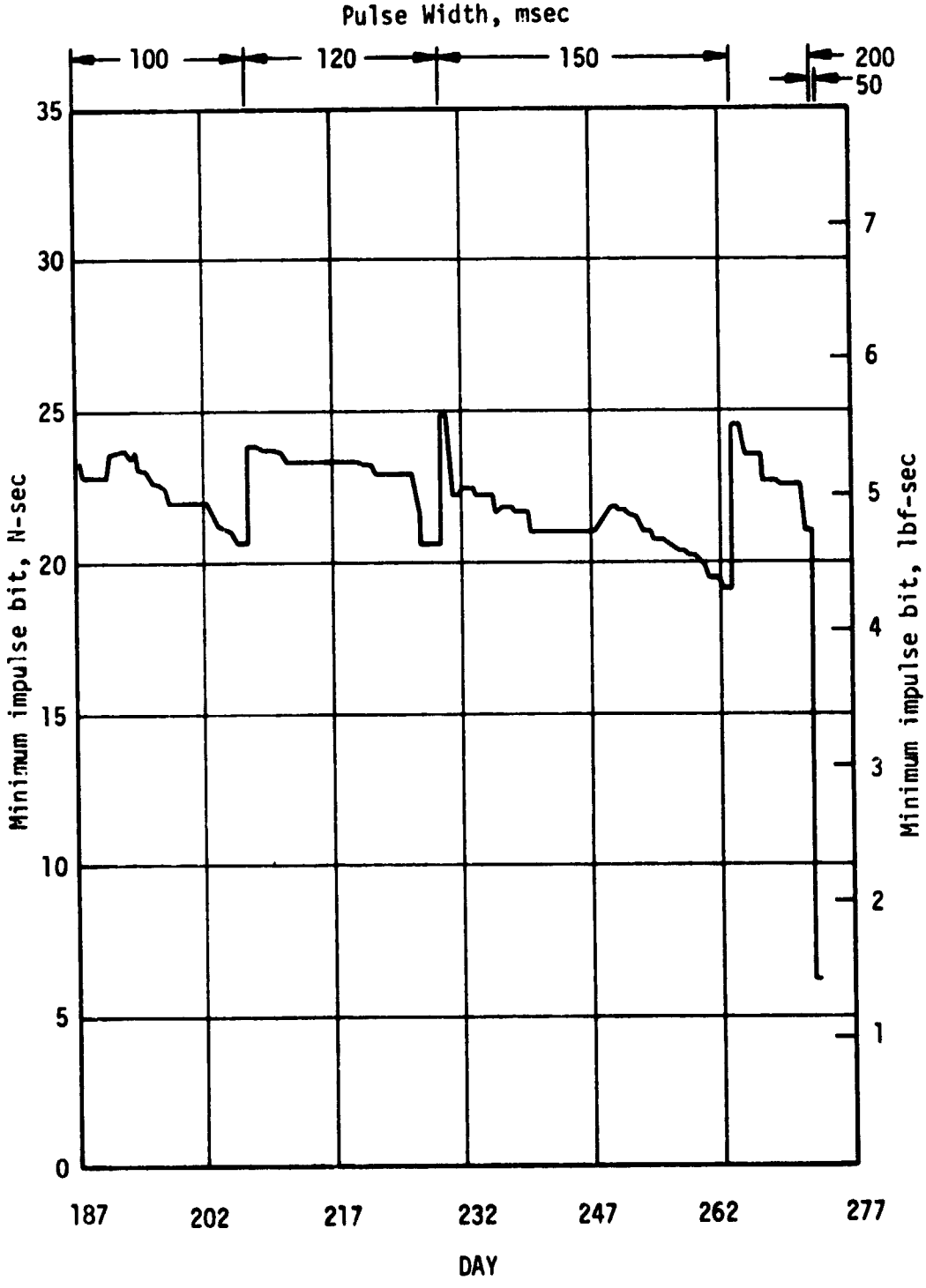

Figure 87. Nominal Minimum Impulse Bit, SL-4

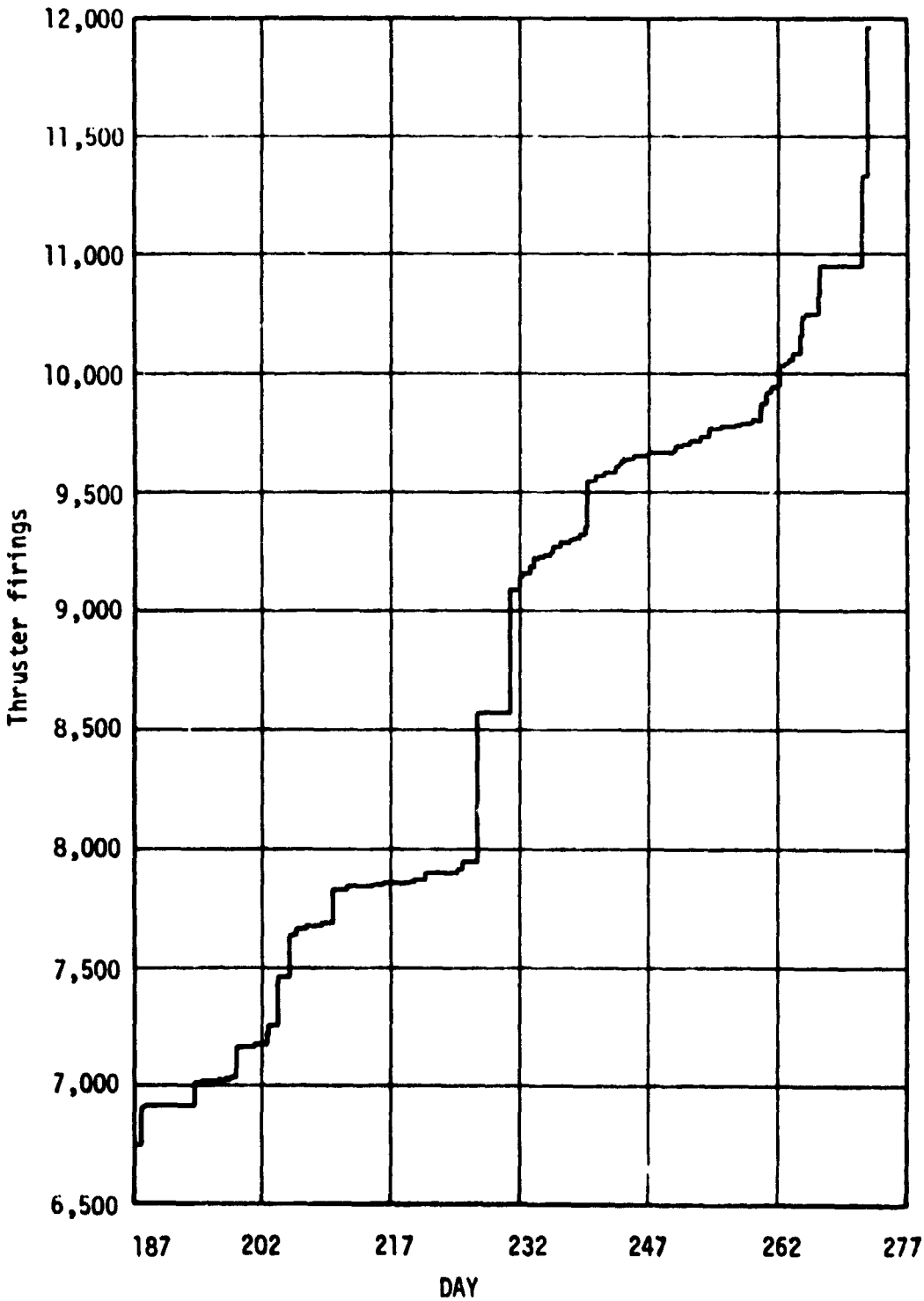

Figure 88. Accumulated MIB Firings, SL-4

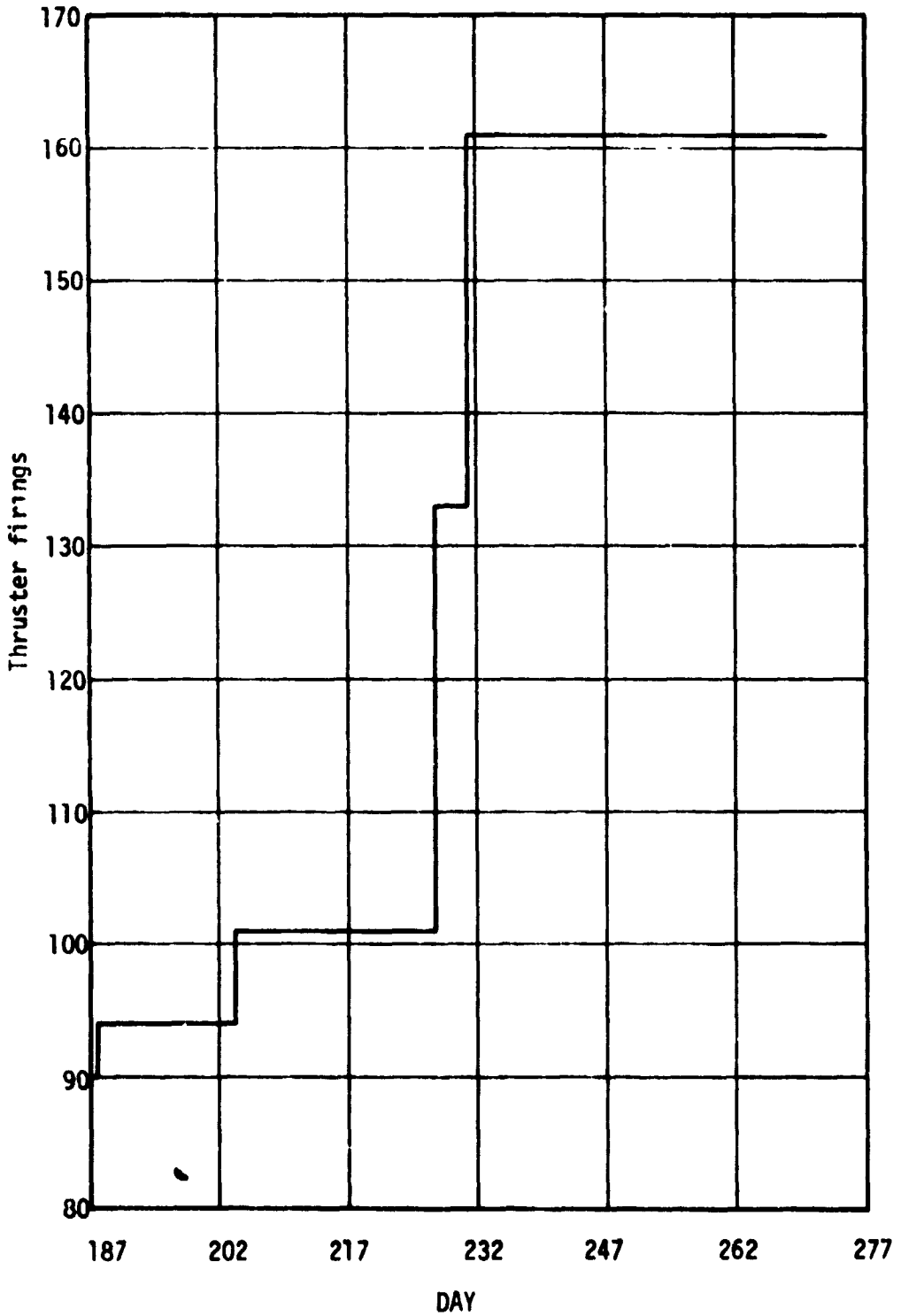

Figure 89. Accumulated Full-On Firings, SL-4

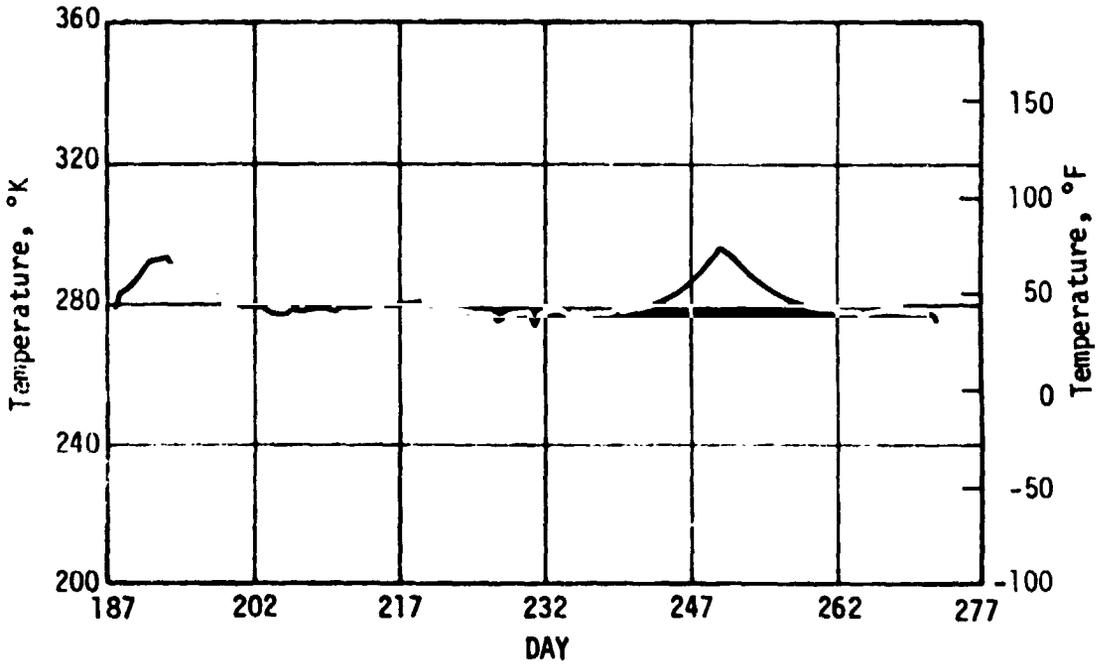

Figure 90. Average GN_2 Bulk Temperature, SL-4

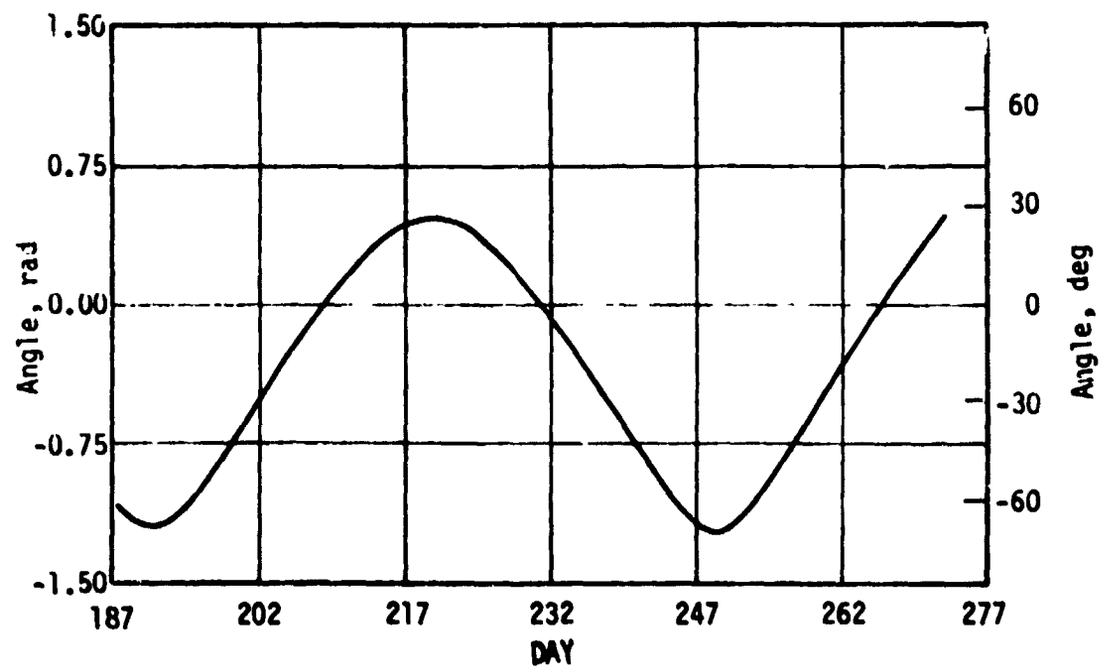

Figure 91. Solar Elevation Angle, SL-4

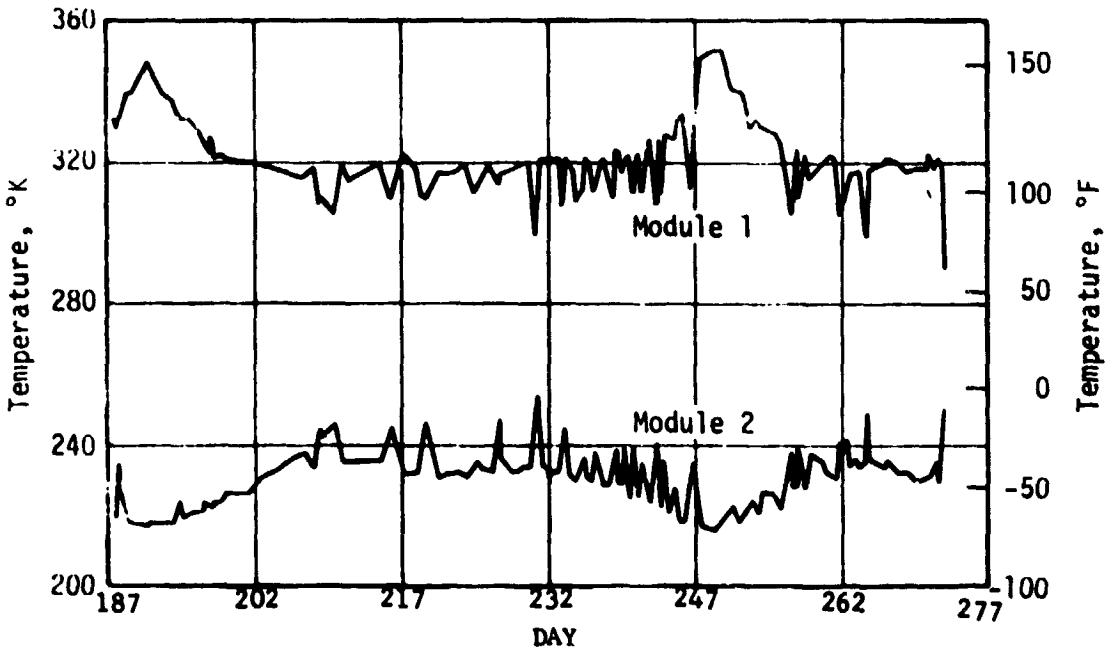

Figure 92. Thruster Module Inlet Temperatures, SL-4

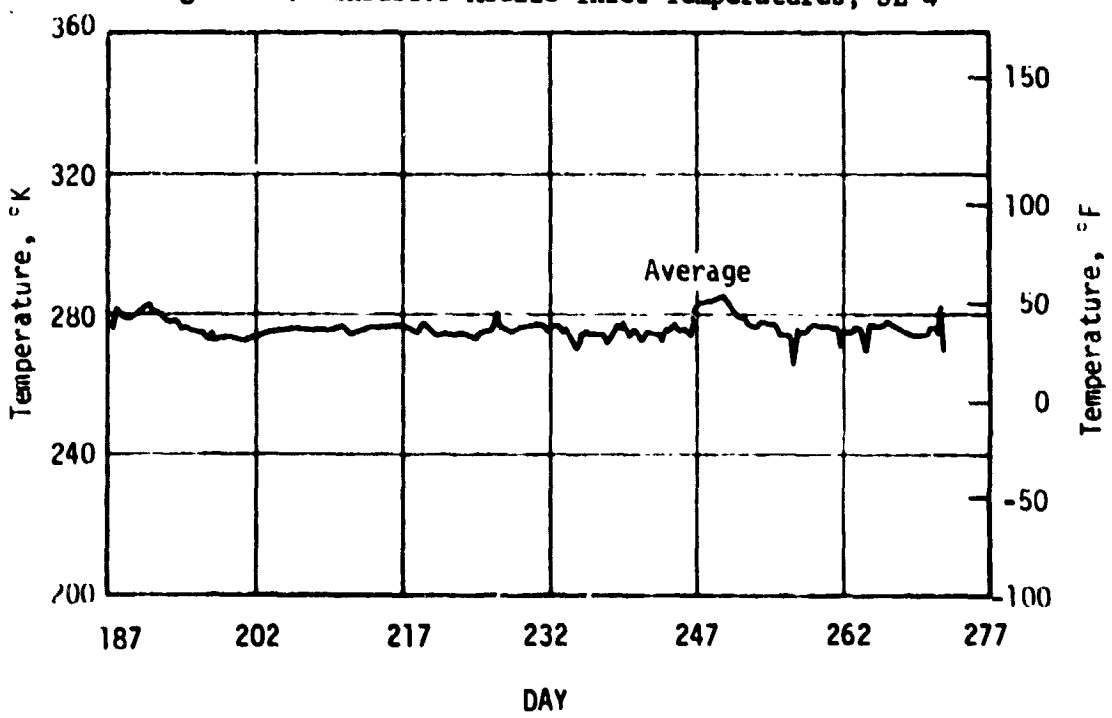

Figure 93. Average Thruster Module Inlet Temperatures, SL-4

the actual valve module temperatures. Photographs of the aft skirt area obtained by the first crew further verified the optical degradation of these surfaces. The increased alpha had resulted in higher temperatures than originally predicted.

Based on the above flight data correlations, predictions for the third and final manned mission indicated that the qualification maximum temperatures would be exceeded during the orbits where the vehicle was continuously exposed to the sun during the periods of minimum solar elevation angle. This would be caused by the increased solar intensity(s) in the November-January period as the earth approached and receded from perihelion, and also assumption of further degradation of the solar absorptivity, alpha, as the sun exposure time increased. A worst case temperature of 369 degrees K was predicted for the high solar elevation angle periods. Maximum, minimum and nominal thermal predictions for the third manned mission time period are shown in figure 94. Actual flight temperature data are also plotted for the Position Plane I module inlet. The maximum temperature actually observed was approximately 353 degrees K, indicating that the paint did not degrade as much as assumed in the worst case prediction.

b. TACS Pressure Transducer Noise. The telemetry system pressure measurements were observed to be fluctuating by as much as .4137 N/mm^2 just after the SL-3 CSM docking on DAY 76. The fluctuations were not noted during the previous orbital stowage phase of the mission. Although the measurements remained within system tolerances, an investigation was made to determine the probable cause of the noise.

Review of data from DAY 75 through DAY 83 indicated that the data on two different multiplexers and their respective reference channels were stable until the manned phase. When the Skylab was manned there was a noticeable increase in noise for the subject pressure measurements and their respective multiplexer reference channels. Three other reference channels were evaluated and they also showed increased noise content. Since the configuration of the Radio Frequency field may have changed following docking due to the pressure of the CSM, the most probable cause for the fluctuations was that the signal lines were experiencing radio frequency interference.

The fluctuations of both pressure measurements continued throughout the manned phases of the mission. However, accurate mass calculations could still be made by averaging many data points to remove the random fluctuations caused by the noise. No further investigation or troubleshooting of the instrumentation system was necessary.

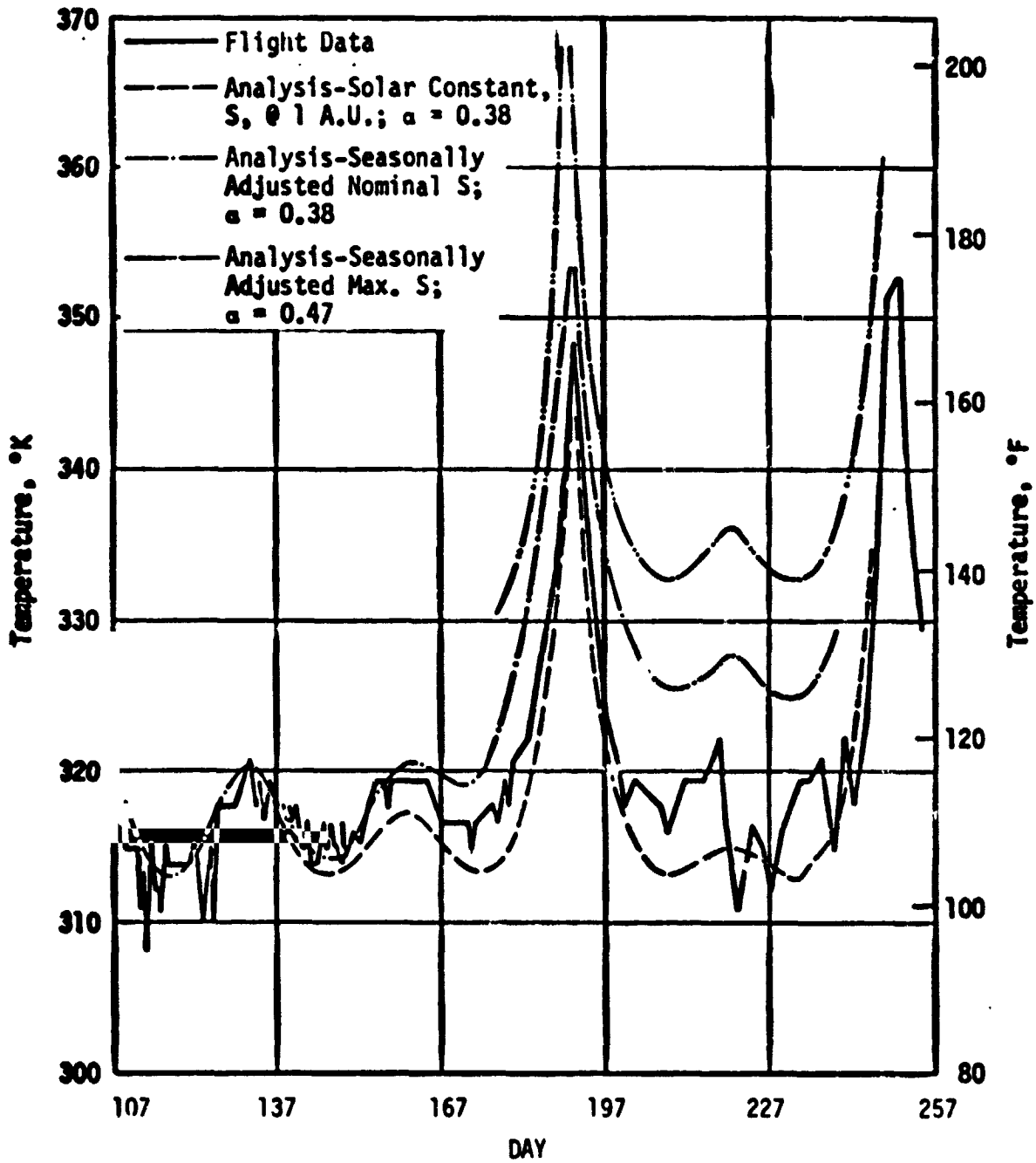

Figure 94. Position Plane I Thruster Module Inlet Temperature

c. Sphere Temperature Anomalies. During the mission support effort it was noted that mass calculations did not stabilize until some period of time after large gas usages. After equilibrium conditions were restored the mass calculations yielded consistent results. In order to evaluate the effect and to determine possible means of eliminating this phenomena from future missions an analysis of flight data was performed.

Calculations indicated conduction to be the dominant heat transfer mode in the storage sphere since body forces acting on the gas were small except for brief periods when gas was being withdrawn. In most instances the rate of withdrawal of gas from the spheres and the rate of change of the radiation environment were small enough that heat transfer by conduction could maintain a state of near equilibrium between the gas and the metal sphere. However, during periods of large usage, the gas tended to cool faster than the sphere due to gas expansion with the result that a non-equilibrium condition existed for some time after the usage. During this transient period, large temperature gradients could have existed within the gas.

The sphere temperature transducer installation was designed to minimize the effect of temperature gradients within the sphere by placing the sensing element at a point where it would read close to the mean gas temperature in the sphere during the transient period. Since this mean temperature point could shift during the transient and methods for analyzing its location are not very accurate, it was to be expected that there would be some error inherent in the temperature data during the transient periods. Figure 95 shows the approximate magnitude of this error for a representative gas usage period. The temperature during the transient period read higher than it should have based on calculations of mass from subsequent equilibrium data. This trend was observed during most periods of high gas usage. Mass calculations using pressure and temperature telemetry data performed during this transient period yielding erroneous results. These tended to indicate a greater mass usage than that calculated from equilibrium data.

The analysis indicated that the transducer sensing elements should have been located slightly farther from the wall in order to give a better estimate of the mean temperature during the transient period.

F. ATMDC, WCIU AND MLU

1. Description. The Skylab Attitude and Pointing Control System (APCS) Computer Subsystem consists of two Apollo Telescope Mount Digital Computers (ATMDCs), one Workshop Computer Interface Unit (WCIU), and one Memory Load Unit (MLU) and its associated tape recorder. Some of the more significant box characteristics and a simplified block diagram are shown in figure 96.

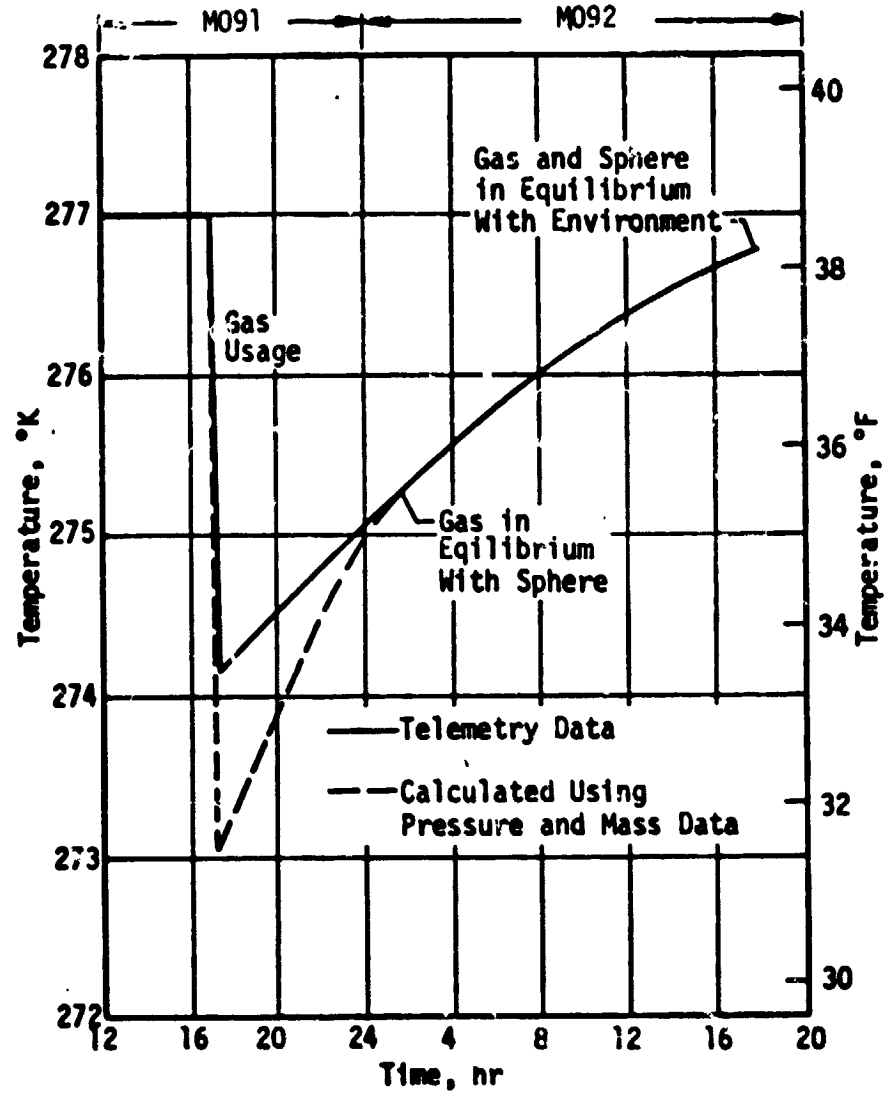

Average gaseous nitrogen temperature

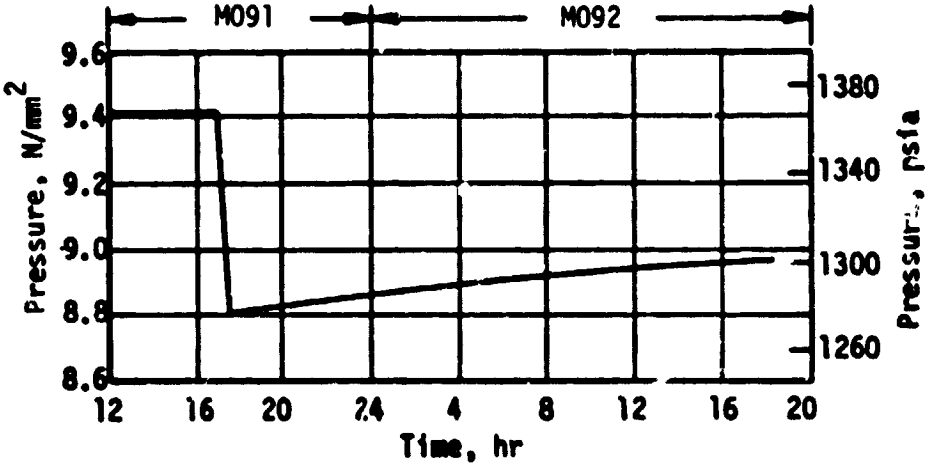

Average system pressure

Figure 95. Typical Nitrogen Temperature Error

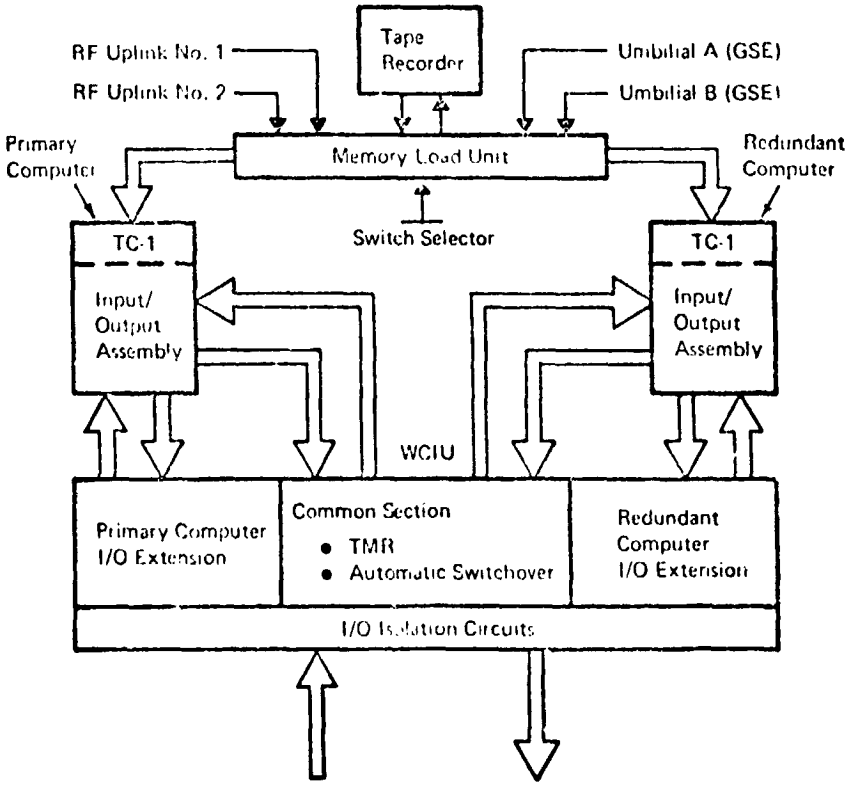

Figure 96. Skylab Computer System

The ATMDCs and WCIU constitute the heart of the first fully digital control system to be utilized on a manned space vehicle. Under control of the ATMDC Flight Program this hardware received inputs from the nine APCS Rate Gyros, three Control Moment Gyros (CMGs), two Acquisition Sun Sensors, and System Discrete Status Indicators. The Flight Program processed this input data and provided output commands necessary to maneuver the vehicle to any desired attitude. Similarly, analog and discrete signals were received and generated in support of the operation of the Apollo Telescope experiments. Software and hardware operations also controlled the redundancy of the onboard critical control system components. This Redundancy Management was accomplished automatically without crew or ground intervention.

The ATMDCs were basically IBM 4 Pi, TC-1 computers with additional I/O capability for interfacing with the Skylab experiment pointing system and the WCIU. Each computer contained two 8K word 16 bit memory modules.

The WCIU was an I/O extension for the ATMDC. The WCIU was divided into three sections; a section dedicated to each ATMDC and a common section. The dedicated WCIU sections contained the critical Skylab attitude control system inputs and outputs, as well as the isolation circuits to disconnect the "off" I/O (WCIU and ATMDC) output circuits from the external system and connect the active I/O to the external system.

The two ATMDCs operated in a one-on (primary), one-off (backup), configuration. The WCIU common section Triple Modular Redundant (TMR) 64-bit transfer register and TMR timer were updated under control of the ATMDC self-test program. Failure to update the timer would result in the WCIU generating a pulse to switch to the backup computer. The information contained within the transfer register was used to initialize the backup computer when it came on line.

The MLU provided the capability to re-load either ATMDC from the Onboard Tape Recorder or from the ground in a maximum of 11 seconds. The MLU also provided the capability to reload either 8K memory module with a modified program in the event a single memory module failure occurred, which greatly improved the overall ATMDC reliability. This was an important design consideration since the computer subsystem had to operate continuously for the entire 8-month Skylab mission.

2. Design History. The design evolution of Skylab's Attitude Control System started in 1966 with a mission called the Orbital Workshop (or Wet Workshop) and ended with the in-flight modifications made in 1973.

The computer hardware used in the final design performed flawlessly during Skylab's successful 271 day mission.

A brief discussion of the design development of the ATMDC, WCIU, and MLU follows:

a. Apollo Telescope Mount Digital Computer (ATMDC). The ATMDC provided high-speed general purpose computing capability and incorporated a versatile operation code set, a large capacity random access storage, and a multipurpose, flexible input/output capability. The ATMDC controlled data flow to and from its system interfaces and performed arithmetic and logical manipulation, routing, conversion, storage, timing, and formatting of data as required.

In addition, the ATMDC provided a Mission-Elapsed-Time clock that could be set to some initial time under program control. The timer was monitored by the ATM system for experiment film reference.

The ATMDC's schedule and constraints to using proven hardware limited the mechanical development of new technologies. Other significant design items were:

Developing and proving component mounting techniques for the planar I/O and analog circuits

Developing and proving the wiring harness and interconnection system in such a way to allow adequate maintainability and future change activity

Extensive design and process work in the multilayer interconnection boards to insure a high quality, reliable electronic circuits, without single point failures

Power supply development.

The ATMDC was functionally divided into four major sections as follows:

TC-1 Computer plus expansion storage assembly

Interface Control

Input/Output Assembly (IOA)

Power Supply Assembly (PSA).

Inputs accepted and processed by the ATMDC were the following types:

AC analog signals

DC analog signals

Continuous discrete signals

Momentary discrete signals

Interrupt discrete signals

Serial digital data

Parallel 8 bit digital data

Parallel 12 bit digital data

Parallel 16 bit digital data

Digital data from test equipment.

The following outputs were provided by the ATMDC:

DC analog signals

Continuous discrete signals

Momentary discrete signals

Control discretes and timing

Parallel 6 bit addresses

Parallel 13 bit digital data

Parallel 16 bit digital data

Parallel 29 bit digital clock data

Parallel 42 bit digital data

Parallel 50 bit digital data.

(1) ATMDC Design Problems. During the course of the Skylab Program various design problems were encountered. These problems were caused by worst case situations in piece parts over operating conditions, incompatibility of software processing with hardware design, and interface incompatibility within the APCS.

These problems were addressed from various disciplines such as Electrical and Mechanical Design, Flight Programming, and System Engineering.

Solutions to the individual problems were the results of this coordinated approach.

The following specific problems are indicative of the conditions that were encountered:

(a) Interrupts. Interrupt Processing problems in the ATMDC persisted during manufacturing and delivery of the units. The problems ranged from electrical design deficiencies, system software application, and system environment. The solutions to the problems required synchronization of interrupts to internal timing to prevent loss of interrupt and occurrence of double interrupts, expanding registers to insure entrapment of interrupts during register read instructions, providing design modifications to insure proper processing of interrupts during various instruction and data combinations that were encountered during system software processing.

(b) Memory Problems. The ATMDCs experienced memory problems during thermal and vibration environments. These problems were addressed both in Huntsville and Oswego. The solution was to re-design sense amplifier input circuitry, timing control, and vibration damping to insure that the core output would be detected over the environment to which the ATMDC was subjected.

These modifications were implemented in all flight units during a recycle phase.

(c) Analog Conversion. Analog conversion problems within the ATMDC manifested themselves during delivery and system testing. The main cause of these problems was in the detection of the signal after crossover, i.e., zero volts. This situation presented the problem of determining the polarity of the signal due to instability and noise. Various design modifications were implemented to eliminate the combinations of faults that were exposed during the different phases of the program. These changes improved the control logic ability to detect the fault conditions and provide correct processing of the signals.

(d) Temperature Problems. The NRL experiment input isolation circuits failed to function at cold temperature during the later phase of the manufacturing cycle. It was determined that a worst case situation existed in the circuit that prevented the processing of this signal. The circuit was modified to prevent this situation from occurring.

(e) Logic. Reset problems within various circuits of the ATMDC were detected during testing of the units. These problems generally fell into the category of race or silver conditions caused by combinations of the delays internal to the ATMDC. The approach to correcting the problems was to modify the logic to insure positive resetting or strobing of these circuits.

(f) Temperature Sensor Circuit. A problem was encountered when the temperature sensor element failed causing the operational amplifier to saturate. This condition forward biased the analog multiplexer providing an offset bias on the external analog signals. This condition was corrected by replacing the amplifier with another device that had short circuit protection.

(g) Interconnection Failures in Harness. The wiring harness was complex in that it allowed the three sections of the unit to be folded for maintenance. Space for terminating and strain relief was very limited. The unit design employed foam rubber bonded to the cover, but it clamped the upper harness runs when the cover was bolted in place. A great deal of development effort went into devising ways to terminate and support the wires at the page connectors and to eliminate chaffing when folded for maintenance. After qualification, a problem of shorts to ground developed.

Tolerance analysis of each stack was conducted. No mechanical interferences or problems were found. Analysis and testing indicated broad variation of loads created by the compressed foam due to tolerances affecting percent of deflection, variation in contact area, variation in foam density and vendor data. In addition, vertical drops of harnesses were quite rigid and if loaded, would carry load to page connector. Real time presentations and discussions were held with MSFC engineers.

The design was modified to limit foam pad to specific areas and to clear vertical drops of harness. The upper tray was reinforced to limit deflection toward the upper multiple interface board. This design modification was requalified as part of a planned requalification test. The schedule was not impacted. Few harness problems developed after this modification.

(h) Feed-Through Pin - Solder Joint Failure. A rework technique was developed to "save" existing inventory. An improved technique was developed for future build. Sample pages were built and tested to evaluate several soldering techniques. An analytical analysis of failures and projected merits of proposed redesign was conducted. Communications were opened with MSFC engineers.

The schedule was maintained. Analytical data and test data gave understanding of the failure and confidence that the modified design would not fail.

(i) Feed-Through Pin - Solder Joint Failure - Type 1300 Page Only Non-Flight Hardware. Investigation found that the arrangement of feed-through pins was unusual on Type 1300 pages and presented a failure mechanism not incurred in initial worst-case testing. Conservative decisions had previously modified Type 1300-page flight hardware to a best-possible design, but allowed non-flight hardware to be a lesser modification. Flight hardware was reproven by testing of samples. A new rework technique was developed.

Non-flight Type 1300 pages were reworked. Schedule and inventory was maintained.

(j) Capacitor Assembly Short. A situation developed whereupon under a combination of worst-case temperature, tolerance conditions and assembly clamping force, exposed pins of a large capacitor assembly could short against the ATMDC backpanel support plate. Analytical work addressed the decrease in clearance due to the cold and clamping conditions. An experimental analysis provided deflection contour maps of the critical areas under the same clamping and temperature conditions. This investigation showed that while this shorting condition was unlikely, it could occur again. As a result, in order for the ATMDC to be a completely reliable product, design changes were implemented into all capacitor assemblies such that no deflection, and thereby no shorting possibility, would occur under any conditions. This problem, therefore, did not recur.

(k) Memory Vibration Problems. Under long term vibration, the three memory connectors would experience excessive pin wear. A computer failure had been traced to this situation. An experimental analysis was initiated by creating a test plan to vibrate a memory under instrumented, controlled conditions. This test showed that there was relative movement between connector halves, thereby explaining the cause of wear. The addition of memory stiffeners and connector clamps alleviated this problem as demonstrated by additional vibration tests at the memory, and then at the ATMDC level. This analysis thoroughness created a solution which prevented recurrence of this problem.

Another ATMDC memory problem was breakage of sense wires of certain memory planes after long term vibration. A long, detailed study, including performance of several vibration tests on individual and certain combinations of pages, showed that the problem could only exist on an earlier design plane, and that it was caused by excessive crosstalk in a page fixture used in page vibration screen tests. Further tests showed that the new plane design was immune to this excessive vibration level. Those memories which had experienced this particular screen vibration test (some had not) had the suspect planes replaced for flight usage.

(l) Design Contract Changes. Load Enable - System testing of the ATM Control System at MSFC, produced a condition in which the ATMDC would enter a wait state or have altered memory locations. Investigation of this problem revealed that system noise was present at the ATMDC GSE test interface. The noise was above the threshold level of the input circuits, causing the ATMDC to produce the conditions described.

The source of the noise and subsequent elimination became a significant system problem. A change was proposed to MSFC to modify the GSE interface of the ATMDC, by providing a network controlled gate through a spare discrete input. This modification allowed system control of the interface preventing the spurious noise from effecting the ATMDC during normal operation.

(m) High Core Restart. The enhancement of the overall reliability of the computer subsystem was deemed desirable. A study was made to determine if a flight program could be developed that would require only half of the core capacity of an ATMDC.

It was determined that this was feasible. A change was proposed to modify the ATMDC in which network control of the memory modules through a spare discrete input would provide the option of operating the computer in a full memory mode or in a half or degraded memory mode. Thus flexibility was added to the computer subsystem providing fault isolation of a memory module through network control.

(n) Tape Timing Pulse. The GSE input to the ATMDC contained a tape recorder interface to load memory from the ground test equipment through 300 feet of cable. Problems were encountered during testing. Investigation revealed that the tape timing pulse was distorted due to the cable characteristics. To insure that this condition would not occur at KSC, a change was developed for the computer. This modification provided internal regeneration of this distorted signal to the computer circuitry, insuring positive clocking of the internal counter. Implementation of this change eliminated the problem.

(o) Momentary Discrete Change. The momentary discrete inputs to the computer system did not function as specified. A condition existed on which the input was not detected. The ATMDC circuits were modified to prevent the loss of the signal. This change was made within the ATMDC by removing a latch circuit function.

b. Workshop Computer Interface Unit (WCIU). The WCIU provided the capability to interface the one-ON/one-OFF (1+1 OFF) ATMDCs with the APCS. The WCIU provided the necessary buffering of ATMDC input/output (I/O) lines to accomplish this function. The WCIU, in conjunction with an active ATMDC, provided a means of sensing a failure of an ATMDC and the committed WCIU I/O pages.

WCIU mechanical design followed the same approach as ATMDC, but design requirements allowed use of the standard 4 Pi pages for logic and I/O. Plugable power supplies were developed. The harness complications were greatly simplified by the page on backpanel design with flat flexible printed circuit cable interconnection.

The cable and interconnection system was developed and proven for WCIU. The wiring harness from external I/O connectors to backpanel was simplified. Signals were sorted to make straight wire drops to the backpanel. This technique developed into mounting the external connectors directly to the multilayer backpanel and is used in ATS and currently proposed for future space applications.

The WCIU was made up of four main functional sections, as follows:

IOA extension section A

IOA extension section B

WCIU common section

Power supply section.

Only one of the two IOA Extension Sections was powered on at any time. The common section has power applied at all times when the system is functional. The power supply section furnished power to the active IOA Extension Section and to the common section.

Six separate power systems were required; Section A, Section B, Common Section, and three TMR Power systems.

The WCIU was composed of four backpanel assemblies interconnected with forty tape cables. The unit contained 37 4 Pi pages composed of 18 unique types.

(1) WCIU Design Changes

(a) Temperature Sensor Circuit. Since a problem was encountered in the ATMDC temperature circuit (previously addressed), the same change was implemented in the WCIU.

(b) MET B Reset. During vehicle switchover testing the software indicated a failure in the low order bit. It was determined that the tolerance of power-on reset signals between the ATMDC and WCIU would cause transients on the address and data lines which were decoded as write commands. The condition was corrected by providing a positive control at the MET B Interface Control Circuits during switchover.

(c) A/D Conversion Time. A logic change was made to eliminate a 208 microsecond delay in generating an analog interrupt upon completion of an analog conversion.

(d) Momentary Discrete Change. Previously mentioned in the ATMDC section. The same action was taken in the WCIU.

c. Memory Load Unit (MLU). The Memory Load Unit (MLU) provided the in-flight capability of loading Flight Programs into the ATMDC Memory from either an on-board magnetic tape unit or one of two Command Receiver uplink channels while maintaining the preflight interface capabilities. The MLU provided multiplexing of 39 data, address, and control lines to each ATMDC.

The MLU generated a load enable command to each ATMDC when either of the operating modes were commanded. A reproduce command would be sent to the on-board Magnetic Tape Unit when a memory load from magnetic tape would be commanded.

The MLU was functionally divided into four major sections as follows:

Control and Timing

Multiplexer

Command Receiver Interface

Power Supply

Inputs accepted and processed by the MLU were the following types:

One Manchester Type 2 biphase data input from the Magnetic Tape Unit

One digital serial clock from the Magnetic Tape Unit

One Manchester Type 2 biphase data input from each RF Command Receiver input (two total)

Four momentary discrete inputs from the ATM Switch Selector (SS)

Four high-level discrite from the test point panel or umbilical for each ATMDC

Thirty-nine data, address and control signals from the test point panel (including those from the umbilical plate) for each ATMDC.

The MLU generated the following types of output signals to be sent to external sources:

Parallel 8-bit digital data to each ATMDC

Parallel 15-bit digital address to each ATMDC

One high-level discrete to each ATMDC to enable the test connectors

Fifteen control signals to each ATMDC

One high-level discrete to the Tape Unit to command it to pull tape (reproduce command).

A dual RF Command Uplink capability was added to the MLU. This change provided in-flight loading of either ATMDC via ground uplink, thus expanding the flexibility of the Computer subsystem to receive changes of the Flight Program beyond the level of the stored programs in the Tape Recorder.

d. ATM/MLU Tape Recorder. The 50M17010 Telemetry Tape Recorder manufactured by Borg-Warner Controls, Santa Ana, California was selected as the MLU mass storage device.

The recorder was modified for the new application and manufacturing controls changed in the following areas:

Increased the screening requirements for piece-parts

Imposed piece-part screening where it did not exist before

Corrected a power supply design deficiency to allow more stable operation

Incorporated a design change to preclude errors being recorded on the tape as the recorder was being powered down

Imposed total box reliability screening.

The above resulted in a unit that would meet criticality 2 requirements and would satisfy the MLU operational requirements. Serial number 1 Tape Recorder was installed on Skylab 1 and launched on May 14, 1973. After 270 days in orbit, the MLU was commanded to load the memory. The Tape Recorder started and performed its required function.

3. Design Verification. A very thorough test program was implemented to insure that reliability objectives were met. Any failures which occurred during these tests were analyzed to determine corrective action. The more significant tests are listed below:

Rigorous environmental acceptance testing on each unit

Qualification testing on each unit type

Delta qualification testing when required

System compatibility testing at the subsystem level (i.e., two ATMDCs and WCIU)

Error detection and switchover testing at the subsystem level (i.e., two ATMDCs and WCIU)

Tape recorder, MLU, and ATMDC compatibility testing.

MSFC then conducted detailed prototype and KSC testing of the system. Each of the above tests will be discussed briefly.

a. Acceptance Test. The ATMDC Acceptance Test was divided into two steps. The preacceptance Test and the Formal Acceptance Test descriptions follow:

(1) Preacceptance Testing. The ATMDC Preacceptance Test was performed on various levels of page and system testing. The TC1 assembly was pretested in thermal operation for 200 hours. It was then subjected to a total of 9 minutes of error-free operational vibration.

The power supply assembly was bench-tested under both loaded and unloaded conditions. The I/O pages, power supply and computer were then integrated in a test fixture for functional verification of the system. Upon completion of this testing, the system was installed in the ATMDC electrical/mechanical assembly. The unit underwent various assurance tests to ascetain its integrity. These

included 75 hours of thermal cycling.

The unit was then loaded into its housing. An additional 24 hours of thermal cycling and 3 minutes of vibration testing in the flight axis was conducted.

(2) Formal Acceptance Test.

(a) The unit was removed from the temperature chamber and worst-case detailed measurements conducted on all inputs and outputs.

(b) The unit was then subjected to one complete temperature cycle while the functional test program was being run.

(c) Vibration profiles were run on all three axes with a special vibration test program being run in the ATMDC.

(d) Post-vibration detailed measurements were performed.

(e) A twelve-hour life test was run with the semi-automatic checkout equipment and the functional test program.

(f) The Acceptance Test Team met and reviewed all relevant documentation (i.e., MRB, UCR, failure analysis report and test history). If no open problems existed, the unit was accepted.

The requirement for entering formal acceptance test was that the last two preacceptance test temperature cycles be error free. If an error or part failure occurred during the last two preacceptance cycles, the problem had to be resolved and two additional error-free preacceptance temperature cycles run. This sequence would continue until two error-free temperature cycles had been completed.

If an error or part failure occurred during formal acceptance test, the problem was corrected and the Acceptance Team met to review the nature of the problem and its resolution. This meeting also determined the amount of retest required as a result of the failure. The amount of retest depended on the nature of the specific problem, and might result in going back into preacceptance testing. All formal testing was witnessed by DCAS.

ATMDC Acceptance Test Sequence - The test sequence is shown in figure 97.

WCIU Acceptance Test Sequence - The test sequence is shown in figure 98.

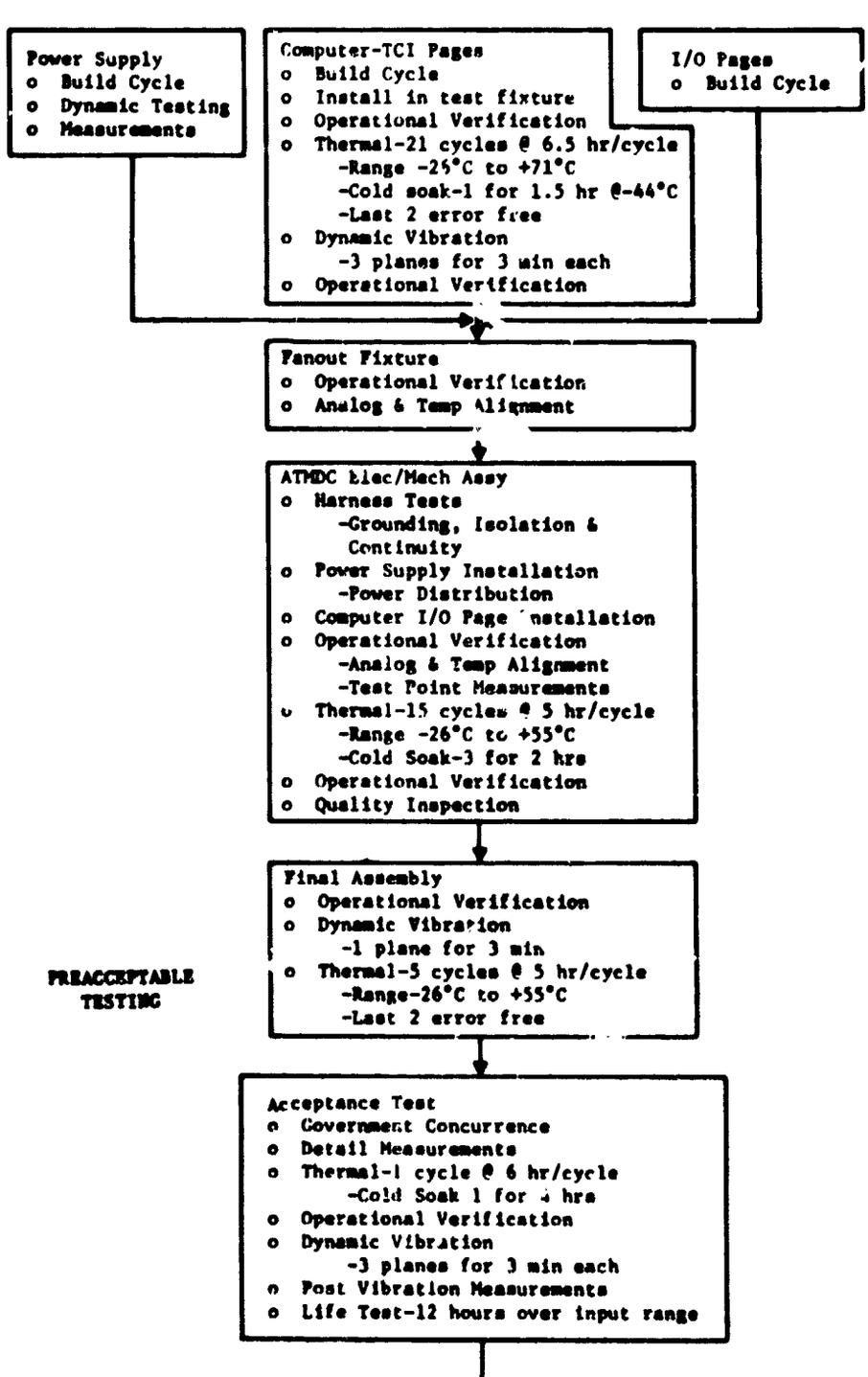

Figure 97. ATMDC Acceptance Test Sequence

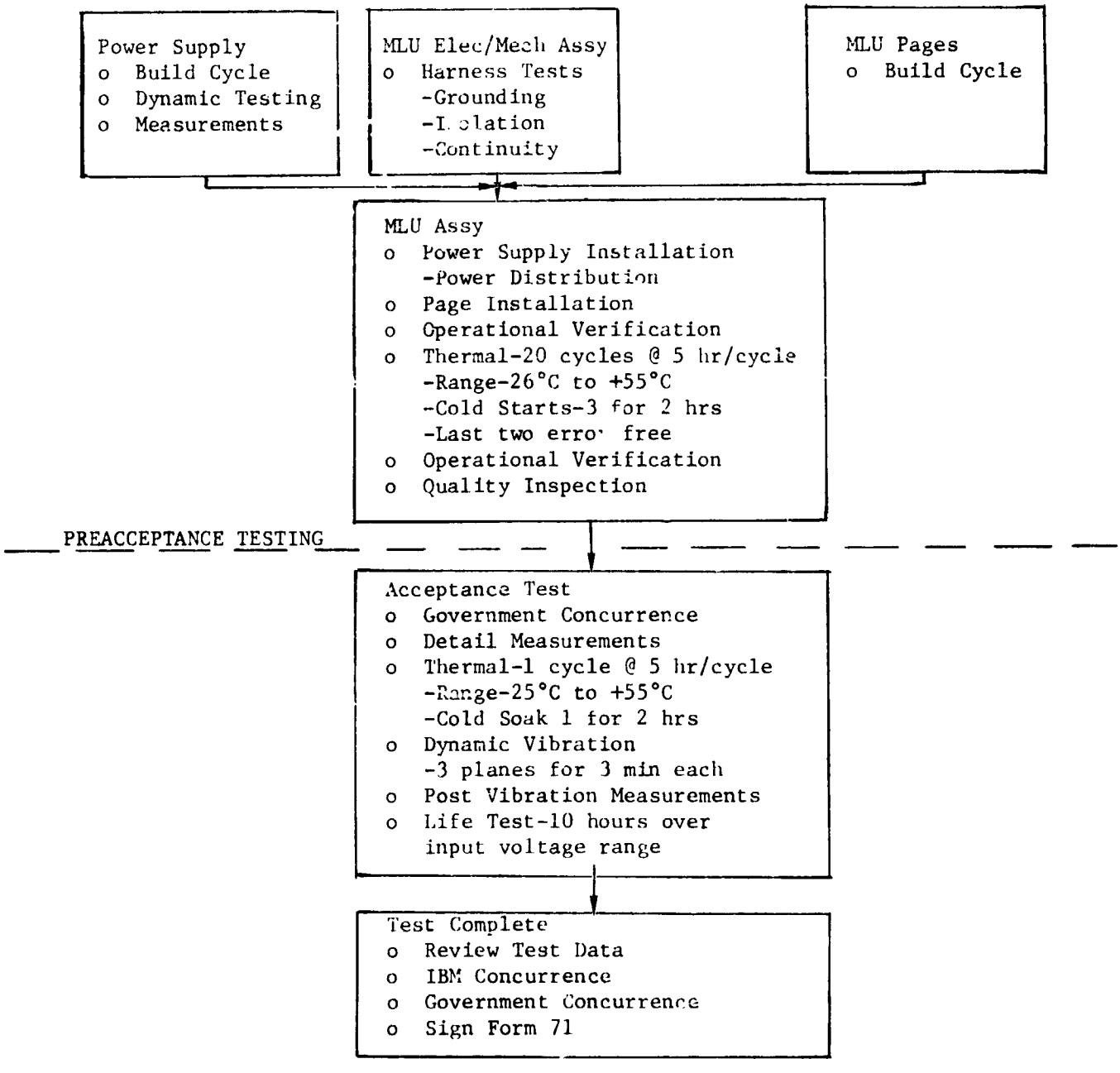

Figure 98. WCIU Testing Sequence

MLU Test Sequence - The test sequence is shown in figure 99.

b. Qualification Testing. The ATMDC Qualification Test results were documented in report IBM No. 70-K39-0001, ATM 275-036TM-0001, dated 12/10/70.

Apollo Telescope Mount Digital Computer S/N 003 successfully passed all the specified qualification test requirements with exception of the discrepancies noted during Detail Measurements, Thermal Vacuum Test, RFI, and Transient Test. Corrective action was initiated for discrepancies experienced during Detail Measurements and Transient Test.

The discrepancy experienced during Thermal Vacuum was considered a one time failure and not attributed to Qualification Test. The ATMDC passed all the RFI susceptibility tests, indicating that it was capable of tolerating RFI generated by other devices. The ATMDC failed the conducted and radiated interference tests. A Deviation Action Request (DAR) was submitted for those portions of MIL-I-61810 that were not passed.

The WCIU Qualification Test results were documented in report IBM No. 72W-00007, IBM-DRL-585-1 line item 036, dated 2/14/72.

No desigr changes were required as a result of Qualification Test.

The Workshop Computer Interface Unit S/N 003 successfully passed all the specified qualification test requirements with exception of the discrepancies noted during thermal shock testing, post vibration detail measurements, thermal vacuum, and RFI. Discrepancies noted during thermal shock, detail measurements, and thermal vacuum were attributed to defective piece parts and were not considered design qualification failures.

The MLU Qualification Test results are documented in report IBM No. 72W-00264, IBM-DRL-585-1 line item 036, dated 7/31/72.

No design changes were required as a result of Qualification Testing. The Memory Load Unit S/N 001 successfully passed all the specified qualification test requirements with the exception of the discrepancies noted during RFI and transient testing. Although the MLU failed portions of the conducted and radiated interference and transient generation tests, it did not fail any of the susceptibility tests. Thus, the MLU demonstrated that it was capable of tolerating both RFI and transients generated by other devices.

c. ATMDC Re-Qualification Test. Structural changes and additional structural supports on the memory assemblies dictated partial re-qualification. The test results obtained during the performance

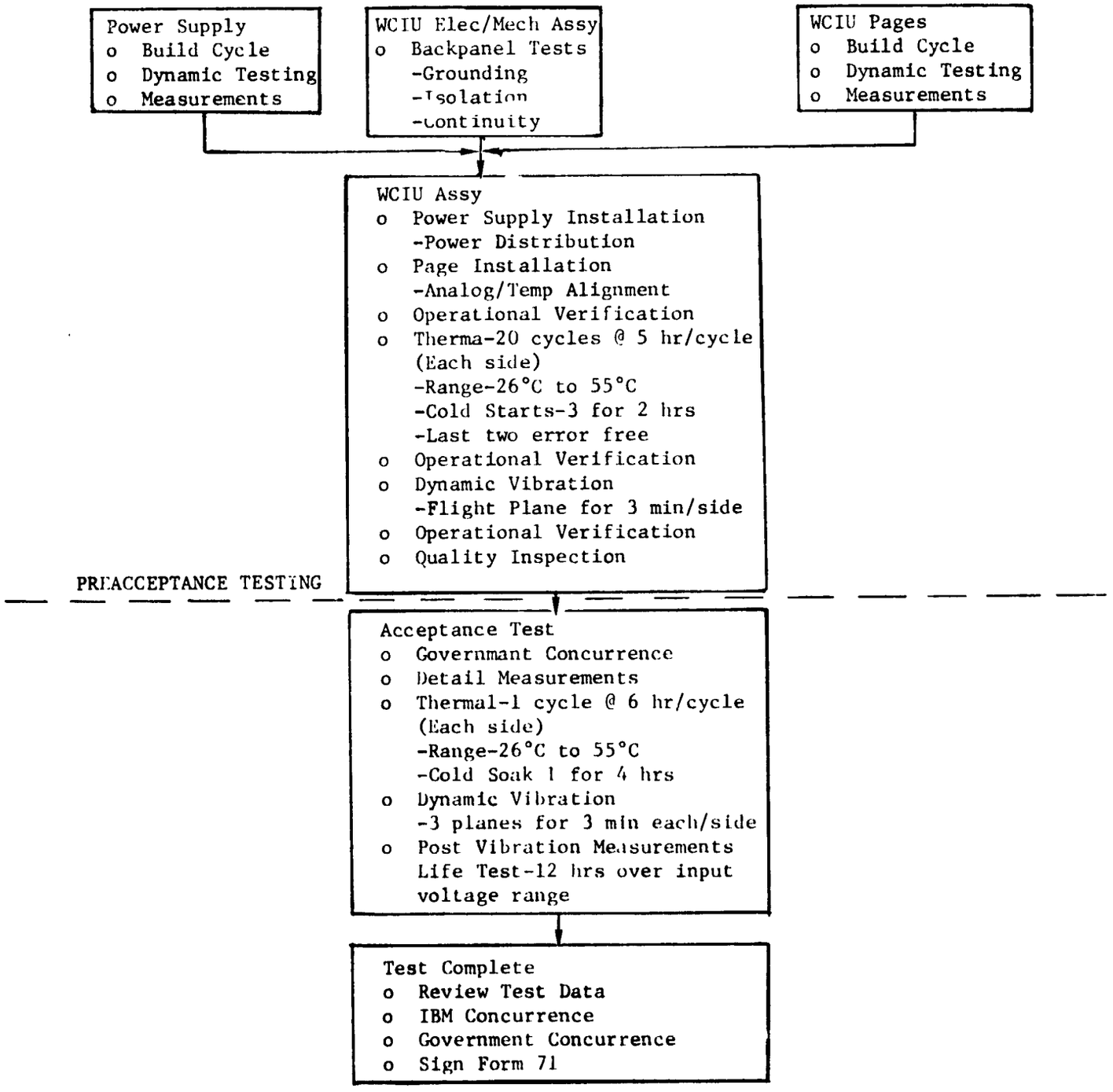

Figure 99. MLU Test Sequence

of a re-qualification test program determined the acceptability of the Apollo Telescope Mount Digital Computer, P/M 7196600, S/N 003.

Re-qualification testing consisted of vibration, teardown inspection, four-hour functional test and post-vibration detail measurements test. All testing was conducted at the IBM Corporation (Huntsville Facility), Huntsville, Alabama 35805 and the results are documented in report IBM No. 71W-00254, ATM No. 871-13, dated 7/30/71.

The ATMDC showed no sign of physical or functional degradation as a result of the vibration test. The ATMDC was functionally tested after each vibration run in each vibration axis and functionally tested during low level random vibration test. There were no functional discrepancies.

d. System Compatibility Tests. The primary objective of the Skylab System Compatibility Tests was to demonstrate that the ATMDC and WCIU would perform as designed in a simulated flight configuration, i.e., one ATMDC plus one section of the WCIU "ON" and one ATMDC plus the second section of the WCIU "OFF". Specifically, these engineering development tests were designed to show:

That the ATMDC could read and write through the ATMDC Control Connectors J-10 and J-18 all valid addresses associated with the WCIU, and also that this communication could be accomplished at operational speeds.

That the paralleling of inputs and outputs concept of two ATMDCs and one WCIU was valid, and that the specific buffering concepts used also had design margins.

That the power UP/DOWN sequencing specified in the CEI could be achieved. Spurious outputs during switchover, if any, would also be detected in these tests.

That a switchover and data transfer through the 64-bit WCIU Transfer Register could be accomplished.

That the common section functions such as Mission Timer B (MTB) perform correctly, i.e., be independent of Bus 1 or Bus 2, and that the MTB time data is available to both computers on demand.

The tests were performed using ATMDC S/N 2 and S/N 3 and WCIU S/N 2. ATMDC S/N 3 was designated the Prime computer and S/N 2 was designated the Backup Computer.

The ATMDC/WCIU computer system compatibility tests established the compatibility of the two unit designs (ATMDC and WCIU) while operating in a simulated system configuration. Switchovers were accomplished, thus establishing the basic one "ON", one "OFF concept of

the system. In addition, the buffering concepts were proved to be valid and all results predictable during switchover except as noted below:

During switchover, four to six ms pulses appeared on all TACS control lines. IBM released Engineering Order (EO) number 271 to correct this condition, since spurious TACS Thruster firings might occur during switchover.

Whenever +28 Vdc power was initially applied to the WCIU Common Section, a 3 to 4 millisecond pulse appeared which could conceivably initiate switchover. IBM released EO numbers 294 and 295 to prevent this spurious output.

Two ATMDC circuit anomalies were highlighted during compatibility tests, although they had no bearing on ATMDC/WCIU compatibility tests themselves. These collectively were labeled the ATMDC Serial Data problem and were both concerned with transmitting successive ones across a logic isolation circuit. The symptoms were: When a write command was issued to either ATMDC Mission Timer A (MTA) or one of the Experiment Output Registers with bit 15 of the data word a logic one and the preceding IOC instruction had left a logic one in the bit 15 position of the computer 1/O serial register, all data up to the first write zero was lost, i.e., all significant bits before the zero were written as zeros. EO number 277 was released to correct this problem.

e. ATMDC/WCIU Demonstration Test. The purpose of this test is to demonstrate that an Apollo Telescope Mount Digital Computer (ATMDC) system would perform properly when failures are injected into the system. In general, failure modes which were identified in Failure Mode, Effect, and Criticality Analysis for Skylab I Digital Computer Subsystem, IBM Document Number 70-383-0024, were utilized to demonstrate:

That a variety of critical failures to the on-line computer subsystem (i.e., the prime ATMDC and Section A and Common Section of the WCIU) could be detected and a system recovery from these failures could be implemented.

That non-critical failures did not affect critical system performance.

A system recovery from the critical failures was demonstrated as follows:

Power-down of failed on-line ATMDC subsystem.

Power-up of the backup ATMDC subsystem.

Initialization of the backup subsystem by the transfer of data from the WCIU 64-bit Transfer Storage Register.

Proper system operation after the initialization is completed.

The following guidelines were used in establishing the Demonstration Test planning and operation:

All hardware used in this test was required to pass a functional test as a unit level prior to integration into the system test configuration.

Prior to the start of this test, a system compatibility test was performed to assure proper system operation.

Failure cases were selected such that wide variety of critical functional failure was exercised during this test. Examples of functional failures were WCIU Analog-to-Digital Converter, TACS Output, and Memory Addressing.

Some failures were simulated by software techniques. In general, these were limited to critical failures in the computer memory which could not be properly injected into the hardware or which would cause excessive damage to the hardware.

Several non-critical failures were injected into the system to verify critical system performance would not be effected and forcing a non-required switchover.

Each failure was injected by the activation of a switch and removed by the deactivation of the same switch.

Each failure was injected into the hardware one at a time. Multiple failures were not inserted.

The basic failure mode was grounding a signal line. This reduced the probability of damaging the prime hardware.

The July 1, 1970 version of the Self Test routine was used in the demonstration program. In addition, other error detection routines were implemented to detect critical errors in WCIU inputs and outputs. An interval timer test was also provided to detect failures in the ATMDC since the present Self Test Routine checks interval timer operation.

The component test equipment used for ATMDC and WCIU acceptance testing was used to simulate the external system interfaces.

The Demonstration Test injected a total of sixty-seven failures to successfully demonstrate that critical failures could be detected by the software test routines similar to those implemented in the ATMDC Flight Program Self Test Routine. The critical failures which were not detected by the test routines induced erratic program operation and caused uncontrolled switchovers. The majority of ATMDC memory and CPU failure cases forced uncontrolled switchovers for which no test error codes were issued.

f. MLU Compatibility Test. This test was conducted to demonstrate MLU operation in the system configuration. Proper MLU operation was demonstrated at nominal and the low and high specified supply voltage levels, and nominal and low specified tape recorder and RF uplink MLU input signal levels.

At each supply voltage level, MLU tape recorder and RF uplink loads were performed and verified. During these loads the MLU to ATMDC, MLU to tape recorder, and MLU command receiver interface lines were monitored and photographed. The resulting signal characteristics were than verified to be within specified limits for the system configuration.

The tape recorder output and RF uplink signals were tested at their nominal and low specified values. Proper memory loads were performed and verified for all signal levels; nominal and off-nominal. The transmitter deviation effects on the RF uplink were evaluated and the results used to establish the ground transmitter deviations to be used for an RF uplink.

Overall, this test verified MLU system operation as designed and specified; no hardware changes were required as a consequence of this test. The test also provided useful data on system operation that influenced the load procedures and system setup configuration used during the post-Skylab mission MLU memory load test.

4. Hardware Integration. The ATMDC/WCIU was first integrated into the closed loop Attitude and Pointing Control System during testing in the Hardward Simulation Laboratory at MSFC in the summer and fall of 1971. ATMDC/WCIU performance was examined in closed loop operation with the CMG/TACS System and the Experiment Pointing Control System. Additional testing was performed during the winter of 1973 to investigate the effects of hardware input signal variations on ATMDC WCIU performance. Tests were also performed using the MLU to verify the capability of loading the 8K program and performing computer switchover.

Several problems were encountered during the above tests. These included:

The ATMDC was found to be sensitive to noise on the memory load lines. The ATMDC was modified to provide gating on the load line.

The ATMDC exhibited random incorrect processing of the 1 PPS and 24 PPS interrupts. This was corrected by an ATMDC modification.

A low temperature problem was found in the ATMDC 1 PPS interrupt circuit. The circuit was modified.

The WCIU MET B control logic was not reset during computer switchover. The WCIU was modified to correct the problem.

5. Hardware Verification. System-level tests were performed on the prototype and flight ATMs to verify system design and flight readiness. These tests included post-manufacturing checkout, vibration testing, thermal-vacuum testing and pre-launch checkout.

No significant ATMDC/WCIU problems were encountered during this testing.

6. Major Part Problems. There were several major part problems encountered during the Skylab program. Two of these are expanded in the following paragraphs:

Integrated Circuit Eutectic Particle Problem.

Vamistor Resistance Drift Problem.

a. Integrated Circuit Eutectic Particle Problem Assessment. On January 17, 1971, Workshop Computer Interface Unit (WCIU) S/N 3 failed after 13.5 minutes of random vibration acceptance testing. After the full 40 minutes of scheduled acceptance test random vibration, and during detailed electrical measurements, another failure was observed in WCIU S/N 3. This failure could have occurred during vibration and would not have been identified until post-vibration detailed measurements.

On January 18, 1971, WCIU S/N 4 failed after 2.0 minutes of random vibration pre-acceptance testing. On January 19, 1971, the Apollo Telescope Mount Digital Computer (ATMDC) S/N 5 failed after 3.5 minutes of random vibration acceptance testing.

All of the above were permanent failures and were isolated to TTL hermetically sealed Integrated Circuits (IC). After replacement of failed parts, the systems were subsequently vibrated for an additional 140 minutes with no further failures. The four failures yielded a total incident rate of 0.1 percent. The individual incident rate for the WCIU was 0.16 percent, and 0.05 percent for the ATMDC.

External visual inspection and radiographic examination of the failed ICs revealed no anomalies. All four failures were electrically verified as having open internal circuits.

Internal visual inspection of the devices showed the failure mechanism to be opened metallization and opened flying leads between Vcc and ground. It was determined that all failures were caused by metallic material shorting the Vcc-to-ground metallizations on the chip surface. This caused excessive current flow, resulting in an open lead or metallization. Particles ranged from 0.008 inch to 0.0013 inch, and were generally spherical in shape. Minimum spacing between critical metallization is 0.003 inch.

A scanning electro-microscope microprobe analysis was utilized in determining composition of the particle. In all cases the composition was identified as gold/tin alloy. This combination of metals is found only in the pre-form used in sealing the device during manufacture. No other foreign material was noted inside the device. It was, therefore, concluded that the particles were introduced during final sealing of the device, and shorted during vibration.

As part of the support to ATM equipment, static and dynamic analysis efforts were applied to a variety of problem types as they were identified. A first example of this support occurred during

fabrication and testing of the first several ATMDCs and WCIUs, when failures were traced to particles in certain types of flatpacks.

Support of this program consisted of furnishing vibration levels that pages and questionable flatpacks would experience, so that the ensuing vibration test program could evaluate the effectiveness of a vibration screen in detecting flatpacks with such particles. Analytical activity also examined forces associated with static electricity and other attractive forces which the vibration level would have to overcome to free the particles.

As assessment of the overall vibration capability of the ATMDCs and WCIUs was undertaken for potential application of higher vibration levels as a better screen device. The final conclusion, however, was that no effective screen existed for detecting flatpacks with particles, such that all suspect type flatpacks in the flight hardware were replaced with those of a type without a particle problem. This problem did not reoccur.

The conclusions of the analysis were:

Failures were caused by 0.0008" to 0.0013" gold/tin (Au Sn) eutectic particles shorting the Vdc-to-ground and metallizations on the surface of the IC chip.

Source of particles was the Au Sn Pre-form used in the final package sealing process.

Problem was process oriented; no correlation with the date of manufacture was found.

No known screens were effective in identifying suspected devices in completed hardware.

Established conclusively that the triboelectric charge immobilizes the particles, rendering vibration ineffective as a screen.

The measured incident rate of Au Sn particles in ICs was 8.8 percent.

At the time these ICs were procured in 1969 - 1970, the process for applying a glass passivation on the chip was not qualified. In February, 1971, the process for passivating ICs was qualified by MSFC. Therefore, to avoid the failure risk associated with the fold particles in existing unpassivated Sylvania ICs, they were replaced with passivated ICs in flight and prototype Skylab Digital Computer Subsystem hardware.

b. Vamistor Resistor Drift Problem. The Vamistor Resistor Drift Assessment was initiated by an Alert, (F8-A-72-01 and GSFC-72-10), from RCA Central Engineering in September 1972. RCA had experienced a failure in an ERTS Recorder after only 200 hours of operation. This fault was isolated to an RNR55C Resistor. The resistor had increased 50% in value during the 200 hours of Recorder operation.

RCA had taken corrective action with the vendor and had identified all products manufactured prior to 7226 as suspect and a low voltage screen was recommended. Subsequent testing by MSFC found the problem in date codes later than 7226. Also, the majority of the Skylab hardware was already built and resistors from this vendor's product had been used extensively.

The assessment objectives were to:

Validate, understand true failure mechanism causing problem.

Identify manufacturing process(es) which caused drift noted resistor value.

Identify environmental, application parameters which induce, aggravate problem.

Establish true failure rate of resistors built in this configuration.

Determine impact of problem on Skylab mission.

Four Main Thrust areas were identified for concentrated effort to meet the assessment objectives. These were as follows:

Survey vendor's facility and review processes to pinpoint cause of drift discrepancies.

Perform metallurgical laboratory analysis to identify factors during resistor manufacture and post manufacture utilization and handling that might have aggravated the mechanism of failure.

Determine where Vamistors were installed in flight designated Digital Computer Subsystem components and possible effect on mission. Perform Engineering analysis of circuitry to determine location of Vamistors used and power dissipation and expected mission operating temperature for each. Identify allowable percent drift for each application for circuit failure. Determine effect of failure on subsystem.

Remove Vamistors from non-flight hardware which accumulated considerable operating time to determine effects of system operation on Vamistors. Further rest removed Vamistors to observe performance. Use those that drift in the laboratory analysis to confirm failure mechanism.

Initiate test program to expose representative sample of resistors to varying degrees of temperature and voltage to define conditions which activate failure mechanism. Establish true failure rate of Vamistors under varying environmental and rated voltage conditions.

The conclusions reached as the result of the study were that plating solution residues and moisture existed inside the resistor, which supported electrolytic action that depleted the resistive film. In turn, this phenomenon accounted for opens and increase in resistance from their nominal values.

The lack of adequate manufacturing process control resulted in contaminant residues and moisture being left inside the resistors. These contaminants supported an electrolytic degradation under certain temperature/voltage conditions. It was also noted during hermeticity tests that the hermetically sealed resistors did not meet the requirements of MIL-R-55182 (C&E designations).

Operating temperature and applied voltage were the only conditions which aggravated the failure mechanism. This was determined by a test program utilizing 4300 parts.

The varied applications of the Vamistor resistors in Skylab hardware necessitated test simulation over a wide range of temperature and applied voltage. Tests were set up in a temperature/voltage matrix with temperature ranging from -20 degrees C to +125 degrees C and an applied voltage ranging from 0.0% to 110% of the rated voltage of the resistor. The matrix included the quantity of resistors tested in each of the temperature/voltage cells. Special test cases were included under matrix test cell no. 71 which was operated at 25 degrees C and rated voltages of 125%, 150%, 175%, and 200%. Also in matrix test cell no. 77 a test was conducted at 40 degrees C and applied voltage of 20-30% of rated voltage.

Reliability analysis of data from test programs established failure rates for the drift and for open circuit faults. The cause of drifting to a higher value and eventually to an open circuit was found to be the same (i.e., electrolytic degradation).

Failure rates were well within predicted values utilized in the initial Skylab reliability predictions, and the Digital Computer Subsystem was judged to be flight worthy as configured (WCIU-7, ATMDC-9, ATMDC-10 and MLU-2). One thousand (1000) hours of prelaunch operation was an effective screen for resistors which will exhibit gross drift.

7. System Operation. This section describes those mission events which affected or were affected by the operation of the computer subsystem hardware. This hardware includes the two ATMDCs, WCIU, MLU and tape recorder.

a. Thermal Characteristics. The temperatures experienced by the ATMDC and WCIU during the mission were, on the average, relatively mild. Figure 100 shows the average temperatures for the on-line ATMDC and WCIU for the entire mission. The temperature of the powered-off ATMDC was not telemetered.

The first temperatures read for the ATMDC and WCIU were 25.9 degrees C and 18.3 degrees C, respectively. During the first twelve days of the mission, the vehicle was maneuvered to various thermal attitudes most of which placed the sunline on the opposite side of the ATM from the ATMDC and WCIU. These components were therefore shaded and faced deep space, resulting in the lowest temperatures expericned by the two components during the entire mission. On DAY 5, the ATMDC reached a minimum of 21.7 degrees C and the WCIU reached -16.7 degrees C.

Following return to Solar Inertial attitude, the two component temperatures increased to more nominal levels. On DAY 27, a switchover to the secondary system was performed. The secondary system temperatures tended to be about one to two degrees higher than the primary system. After this time, the average day to day temperature was influenced, primarily, by the percent of sunlight experienced during each orbit. Each time the percentage of sunlight approached and/or exceeded the 65% value, the component temperature would increase. Figure 100 shows this temperature cycling during the entire mission.

The orbit-by-orbit fluccuation averaged about 1.5 degrees C for the ATMDC and about 2 degrees C for the WCIU during the low sun angle periods (low percent sunlight orbits). The orbit-by-orbit fluctuation tended to cease during periods when the percentage of sunlight was above 75 percent.

Prior to the loss of CMG No. 1, the Z-Local Vertical (Z-LV) maneuvers, at times, caused the temperature fluctuations to increase in magnitude. This increase depended on the position in the orbit

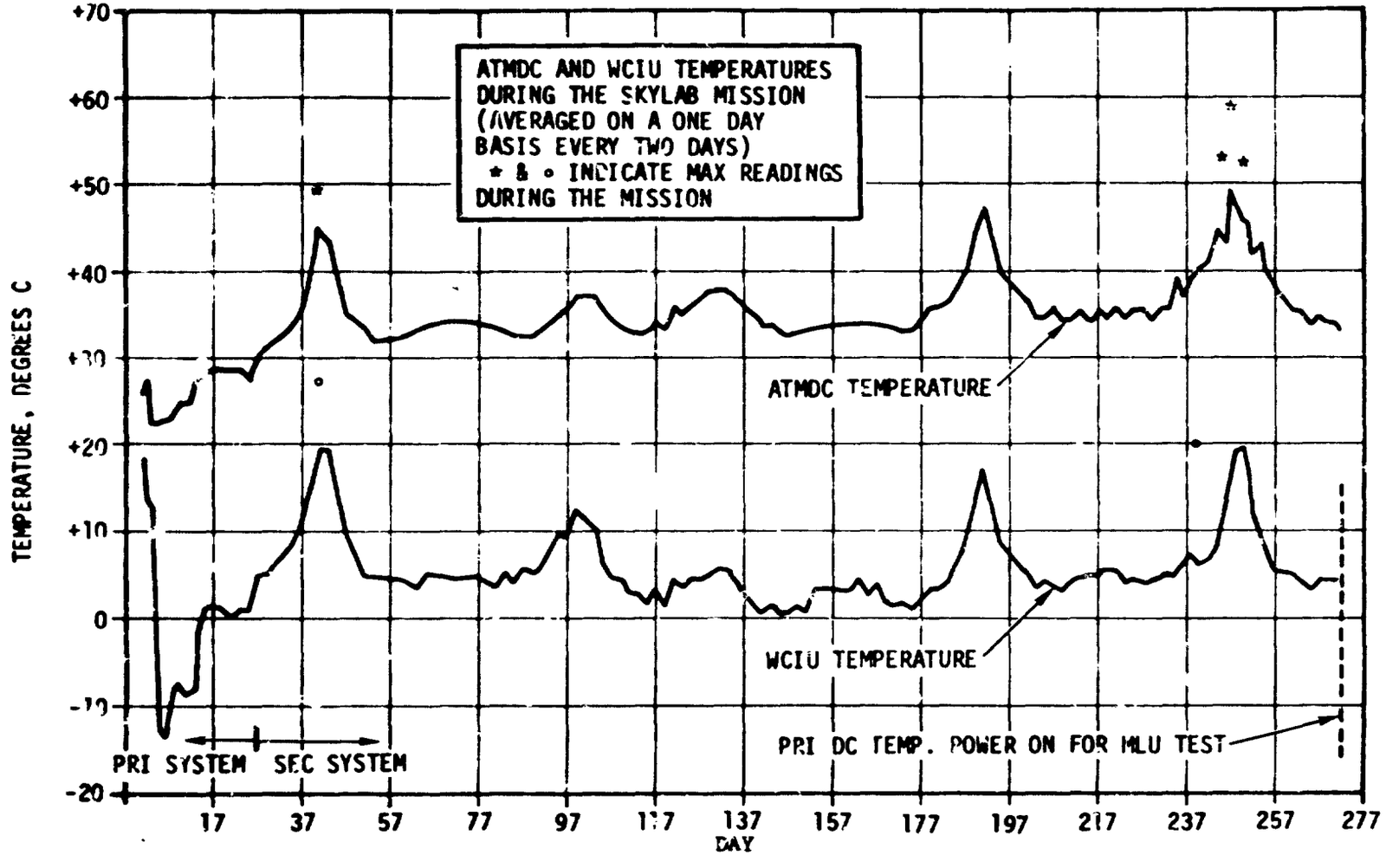

Figure 100. ATMDC and WCIU Average Temperatures

where the maneuver occurred. For example, Z-LV maneuvers at times caused ATMDC fluctuations of up to 6 degrees C and WCIU fluctuations of up to 5.5 degrees C. This higher ATMDC temperature fluctuation resulted from the location of the computer on the side panel nearer the sun line. The WCIU was located in a position such that the Z-LV maneuvers did not result in direct sunlight impingement.

Following the CMG No. 1 failure on DAY 194, many of the Z-LV maneuvers terminated in an attitude which could be held until a point in orbit was reached that would allow a minimum maneuver to the Solar Inertial attitude. This placed the computer in the sun for long periods of time. During the time from DAY 242 through DAY 248, the percent of sunlight increased from 75 to 100 percent. The two maneuvers during this time that caused significant temperature changes for the ATMDC are as shown in Table 43.

Table 43. ATMDC Temperature

DAY	Hrs	Low	High	Temp
12	4	39.6°C	53.0°C	13.4°C
14	5	41.7°C	58.9°C	17.0°C

These two maneuvers resulted in the computer temperatures exceeding 50 degrees C for the first time during the mission. The WCIU was essentially unaffected by these maneuvers because of its physical location on the ATM. No Z-LV maneuvers were performed during the DAY 247 to DAY 250 time frame to reduce the heating effect of such maneuvers which placed the unshielded portion of the workshop in direct sunlight for two or three hours. A Z-LV on DAY 251 caused the computer to peak at 53 degrees C which was the last temperature experience above 49 degrees C. As the sun angle decreased, the Z-LV maneuver temperature effects decreased in a similar fashion.

During the time from DAY 221 to DAY 244, special maneuvers (utilized to point cameras at the Comet Kohoutek) began to cause spikes in the ATMDC temperature. During the time from DAY 224 to DAY 227, these spikes averaged about 7 degrees C. The comet was then occulted by the sun until DAY 235 when the observations were begun again and continued on a more frequent basis. This caused temperature spikes of from 4 degrees to 10 degrees in the ATMDC temperature. The WCIU temperatures were affected by three of these maneuvers causing temperature spikes of 5 degrees C and 7 degrees C and one of 14.5 degrees C. This was the maximum rate of temperature change experienced by the WCIU during the mission.

Following the end of the last high sun angle period, the temperatures had decreased to the nominal values of about 33 degrees C for the ATMDC and 5.5 degrees C for the WCIU.

On DAY 222, an MLU test was conducted using the primary computer. Prior to switchover, the secondary ATMDC was at 33.1 degrees C and the WCIU was at 5.5 degrees C. The primary computer temperature was -15.4 degrees C at turn-on.

The MLU tape recorder load occurred at an ATMDC temperature of -12.7 degrees C, and the MLU RF uplink load occurred at an ATMDC temperature of +12.06 degrees C. When the APCS system was powered off, the primary ATMDC was 14.8 degrees C and the WCIU was 6.1 degrees C.

b. Commanded Switchovers/Computer Operational Times. As a result of the early mission problems and the thermal extremes experienced by the vehicle, it was decided to perform a manual switchover to the secondary computer system on DAY 27. This was a test to verify that the redundant capability of the computer subsystem was functional. At 16:38 on DAY 27, the crew selected the secondary computer and enabled auto switchover using the C&D Panel computer select switch. The secondary computer system powered on, initialized, and began operating properly. During the next two days, the program was updated to the FF70 level (same as the primary) by uplinking three program patches necessary to compensate for the continuing Rate Gyro anomalies and vehicle inertia changes due to loss of SAS wing 2 and meteoroid shield.

The primary computer had operated since APCS power-up on DAY 1, 19:07 (inflight elapsed time of approximately 622.5 hours).

The secondary computer then operated until DAY 272 14:29 when a switchover to the primary computer was commanded from the ground in support of the MLU load tests. The secondary computer system thus operated continuously for 5902 hours.

The switchover on DAY 272 was commanded from the ground by DCS. The switchover was nominal with proper telemetry and no self test errors. The primary computer then remained operational until the APCS power buses were powered down on DAY 272, 16:18:22.

The total time on the flight computer and WCIU common TMR section is shown in Table 44.

Table 44. Computer Subsystem Hours

	Hours at Launch	Inflight Hours	Total Accum. Hours
Primary ATMDC	1620	626	2246
Secondary ATMDC	1147	5902	7049
WCIU Common	2335	6527	8862

c. Memory Load Unit Engineering Test. No computer failures occurred during the mission; therefore, the memory load unit (MLU) was never used during the primary mission. It was decided to perform a test at the end of the mission to determine how well the MLU, tape recorder, and tape had withstood remaining idle in space for nine months and to demonstrate the RF uplink capability.

(1) MLU Tape Recorder Load. The flight programs FF 50 (16K) and F820 (8K) were recorded on the MLU Tape recorder at IBM Huntsville on February 14, 1973. The tape recorder was recorded and verified using the IBM System/360-44 computer system to generate the program data and sequence numbers.

The procedures for the MLU test called for a switchover to the primary computer and a load of the 16K program ID4, sequence 000C from the onboard recorder over Goldstone on DAY 272 at approximately 14:30:00. The actual sequence of events is summarized in Table 45. The primary computer powered up and initialized properly with no self test errors. The MLU and tape recorder were then powered up. Since no telemetry was available to indicate whether the MLU was "ON" or "OFF", the next command issued to the MLU was the"Stop". Issuance of this command caused the computer telemetry to stop being updated, thus verifying the MLU was on and operating properly.

The next command issued to the MLU was the command to load ID no. 4. It was predicted that the tape search time would be approximately 24 seconds after which time the mission timer A would stop updating. The timer stopped 25 seconds after the ID no. 4 execute command was issued, indicating a memory load was taking place. A 16K load nominally required 10.983 seconds to complete. Upon completion of the load, the timer restarted and the computer telemetry output resumed upon completion of the initialization. The time required for the actual load was 11 seconds. Within 3 seconds of the timer restart, the telemetry table appeared nominal and indicated no self test errors had occurred. Furthermore, memory location 0330 read 000C indicating the desired program had been loaded from the tape.

Table 45. MLU Tape Recorder Load Sequence Of Events

TIME	STA.	COMMAND/OPERATION
14:29:29	GDS	Primary ATMDC Power on
14:29:32	GDS	Primary Telemetry Valid - No Self Test Errors
14:30:03	GDS	MLU and TR Power On
14:31:51	GDS	Execute MLU Stop
14:31:52	GDS	Computer Telemetry Stops Updating
14:32:34	GDS	Execute Load Tape ID No. 4
-	GDS	Tape Being Searched for ID No. 4 (Nom. = 24 Sec.)
14:32:59	GDS	Mission Timer A Stops Updating
-	GDS	Computer Memory Being Loaded (Nom. = 11 Sec.)
14:33:10	GDS	Mission Timer A Starts Updating
14:33:11	GDS	Computer Telemetry Starts - No Self Test Errors - Location 0330 - 0C0C

(2) MLU 72 kbps RF Load. The RF uplink load via the MLU originated from a ground station tape recorder. The tape used was generated and verified at IBM Huntsville using the IBM 1800 computer system and a Bell and Howell VR3700B instrumentation recorder. There were two tapes generated for each ground station in the STDN network, plus several spares. Thirty tapes were delivered to GSFC for network distribution on February 17, 1973.

The post-mission test of this capability utilized two passes over Hawaii on DAY 272 to complete the process. The same ground transmitter was used to send DCS commands to the vehicle and transmit the 72 kbps uplink. Normally, two different transmitter deviations are used for these two operations. The Houston Networks group did not feel the ground station would be able to switch from DCS to 72 kbps uplinking during one pass. It was decided to send the DCS commands to select the command receiver No. 2 mode (ID 5) over Hawaii during the 16:08 pass and perform the actual RF uplink over Hawaii during the next pass (17:40:00).

Table 46 shows the sequence of events associated with this test. The command execute ID 5 was issued over Hawaii at 16:08:47. The computer continued cycling until Hawaii LOS. No stop command occurred prior to LOS since the RF uplink carrier remained enabled until LOS, thus quieting the command receiver output. It was predicted that once the uplink carrier was removed (LOS period for example) that the command receiver white noise output would be sufficient to run the MLU internal clock and result in a computer stop being issued. This was verified at the Vanguard pass at 15:00:00 when AOS showed the computer had stopped cycling. The mission timer, however, was still running and had not lost any time indicating that no extraneous sync messages had been detected.

Following Hawaii AOS and at approximately 17:00:54, the ground tape was started. It had been positioned about 40 seconds before the start of the first program on track 4. At 17:41:55, mission timer A stopped, indicating a load was taking place. Elever seconds later (indicating a 16K load) at 17:41:06, the timer re-started and within two seconds telemetry tables were being updated. Telemetry location 0330 indicated tape sequence number FF01 had been loaded. The telemetry was valid and no self test errors were experienced.

This marked the first time an inflight computer had been loaded using an RF uplink.

The MLU remained powered until the APCS buses were powered off at 11:16:22.

Table 46. MLU 72 KBPS RF Uplink Load Sequence Of Events

TIME	STA.	COMMAND/OPERATION
16:08:47	HAW	Execute Command Receiver ID No. 5
15:00:00	VAN	Computer Telemetry Stopped Updating
17:41:15	HAW	Start Uplink Tape Playback
-	HAW	Tape Being Searched for ID No. 5 (40 sec.)
17:41:55	HAW	Mission Timer A Stops Updating
-	HAW	Computer Memory Being Loaded (Nom. = 11 sec.)
17:42:06	HAW	Mission Timer A Starts Updating
17:42:08	HAW	Computer Telemetry Being Updated - No Self Test Errors - Location 0330 = FF01

d. S082B/ATMDC Interface Discrepancy. During the analysis of the S082B experiment data taken during the SL-2 mission, some difficulty was experienced in reducing the pitch and yaw data.

The S082B contains a Light Emitting Diode (LED) array that was exposed to the film each time an exposure was made. The LED array was driven from the mission timer and the experiment output register. The experiment output register (EOR) was a 42-bit output register containing 15 roll reference bits, 12 FSS pitch angle bits, 12 FSS yaw angle bits, and 3 special purpose bits. The problem experienced concerned the pitch, yaw, and special purpose bit outputs; the mission timer and roll reference outputs were correct. The validity (special purpose bit) bit is assumed correct but is not used by the S082B experiment.

The problem was apparently introduced into system between revisions D and E (dated 12/15/70) of the ATMDC/WCIU Contract End Item (CEI) Specification. A change was directed to be made to revision D that reversed the specified function of each output pin for the 41 bits (excluding the validity bit, which was a hardware function). This was an attempt to make the hardware compatible with the manner in which the software loads the experiment registers from the accumulator.

In the ATMDC hardware, the roll, pitch, yaw, and two special purpose bits were loaded into three separate registers under command of three separate IOCs. The reversal of the functions of the roll and pitch was properly accomplished, however, the yaw was complicated by the presence of the bias and data good bits (two remaining special purpose bits loaded with the yaw bits). The entire contents of the third register were directed to be reversed, whereas only the yaw data bits should have been reversed.

In addition to the above, a discrepancy existed between the identification of the pitch and yaw outputs in the CEI and the PDD. Register number 3 was called yaw and number 2 was called pitch in the CEI Specification. The PDD and, hence, the program referred to register number 3 as pitch and number 2 as yaw.

Table 47 shows the specified (CEI) output and the actual output as the experimenter was receiving.

Since all the data in these registers was displayed via the experiment LEDs (except the unused validity bit), the information presented in Table 47 enabled the experimenter to update his data reduction programs to unscramble the bits and obtain the proper information.

8. Conclusion. The ATMDC/WCIU and the MLU performed their designed function during the Skylab mission.

Table 47. Specified (CEI) Output And Actual Output To Experiment

CEI Specification		Actual Data to Experiment	
WCIU J18 Pin:	Title	Title	S082B J4 Pin:
S	FSS Pitch Angle Bit 1 (LSB)	FSS Yaw Angle Bit 1 (LSB)	AA
T	2	2	z
U	3	3	y
V	4	4	g
W	5	5	i
X	6	6	j
Y	7	7	L
Z	8	8	k
a	9	9	J
b	10	10	H
c	11 (MSB)	11 (MSB)	G
d	12 (Sign)	12 (Sign)	KK
e	FSS Yaw Angle Bit 1 (LSB)	Data Good	DD
f	2	NRL Bias	CC
g	3	FSS Pitch Angle Bit 1 (LSB)	BB
h	4	2	k
i	5	3	n
j	6	4	p
k	7	5	S
m	8	6	R
n	9	7	p
p	10	8	N
q	11 (MSB)	9	M
r	12 (Sign)	10	LL
s	NRL Bias	11 (MSB)	PP
t	Data Good	FSS 12 (Sign)	MM
u	Validity	Validity (not used)	NN

SECTION VIII. EXPERIMENT POINTING CONTROL SYSTEM

A. Pointing Control Subsystem

1. Design. The general requirements for Experiment Pointing accuracy and stability (see Table 48) could not be met by the CMG/TACS system in an environment of crew motion and vehicle disturbances. Consequently, the EPCS was designed to isolate the ATM experiments from the vehicle in two axes, as well as perform other experiment support functions.

Dynamic control was provided for the experiment canister UP/DN and L/R axes. The control loops were identical for both axes. The subsystem was active only during the Experiment Pointing Mode-Day. A block diagram of a single axis is shown in Figure 101. The FSS provided experiment package position information and the Spar-mounted Rate Gyros provided rate information. The position and rate signals were summed after passing through Bending Mode Filters (BMF) and then amplified by current amplifiers to drive two DC torquers. Each current amplifier output was limited to 3.75 amps to provide a maximum of 9.5 N.m torque. The two amplifiers and torquers operated in parallel for redundancy and power reduction purposes. They provided a total torque output of 19 N.m. In the event of a single amplifier or torquer failure, the loop could operate with the other amplifier or single torquer, without significant performance degradation.

Table 48. Experiment Pointing Control Design Requirements

Pointing Accuracy	$\pm$ 2.5 arc-sec
Stability	$\pm$ 2.5 arc-sec - 15 minutes
Jitter	1 arc-sec/sec

The EPC Bending Mode Filters were designed to maintain the rigid body phase and gain margins and control system bandwidth while attenuating the dominant flexible body modes. The flexible body modes associated with the EPCS were generally higher than those associated with the CMG system. The BMFs were designed for the range from 7 - 15 Hz. The BMFs consisted of a 5 Hz first order position filter and an 8 Hz second order rate filter with a 0.5 damping ratio.

2. Design Verification. Numerous studies, analyses and simulations of the EPC system were conducted in order to verify the design and functioning of the system.

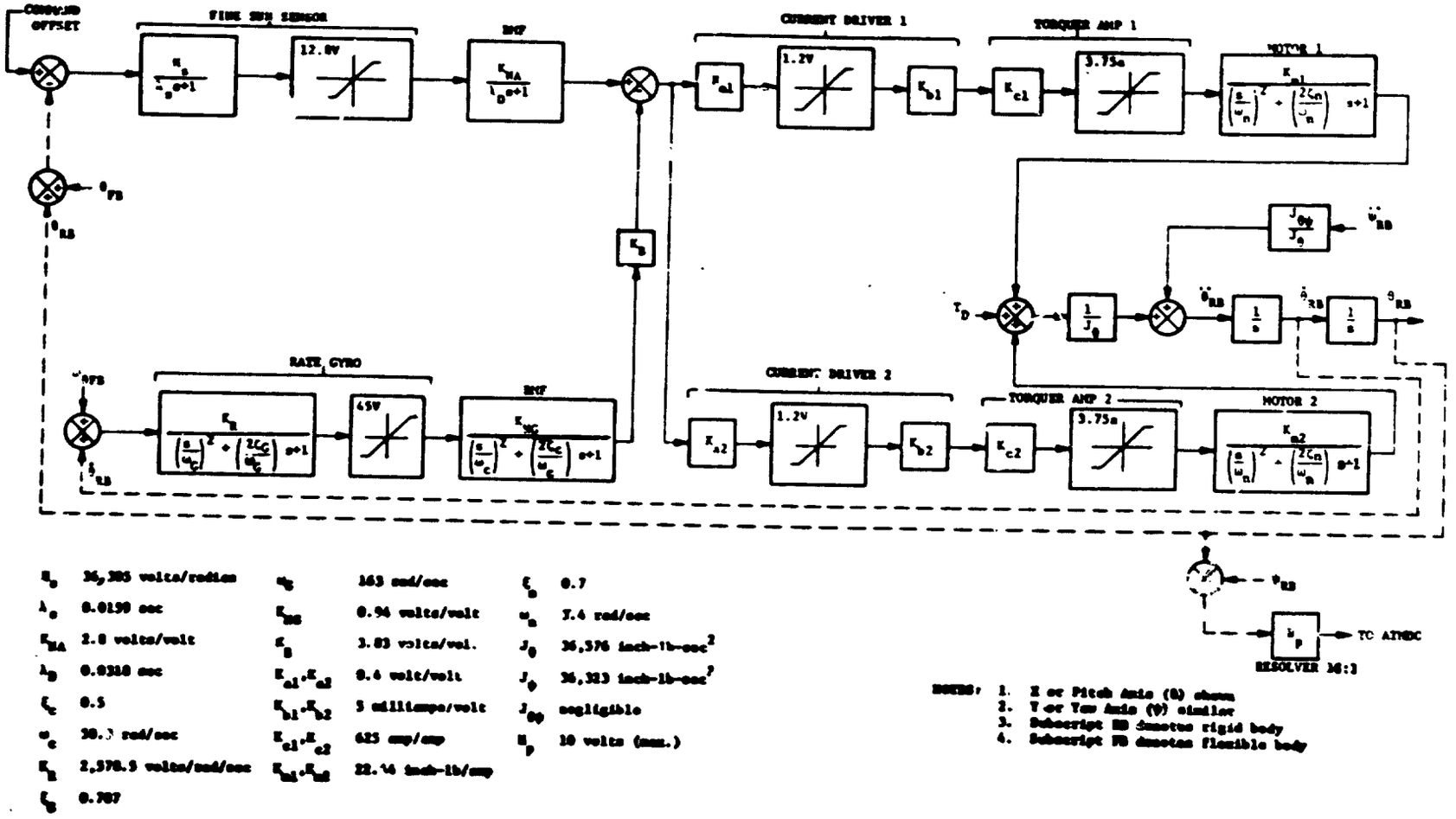

K_s	36,385 volts/radian	ω_s	163 rad/sec	ζ_s	0.7
λ_s	0.0150 sec	K_{RG}	0.94 volts/volt	ω_n	7.4 rad/sec
K_{HA}	2.8 volts/volt	K_R	3.83 volts/rad.	J_θ	36,376 inch-lb-sec^2
λ_D	0.0318 sec	K_{a1}-K_{a2}	0.4 volt/volt	J_ψ	36,323 inch-lb-sec^2
ζ_c	0.5	K_{b1}-K_{b2}	5 milliamps/volt	$J_{\theta\psi}$	negligible
ω_c	20.3 rad/sec	K_{c1}-K_{c2}	625 amp/amp	K_p	10 volts (nom.)
K_I	2,578.5 volts/rad/sec	K_{m1}-K_{m2}	22.14 inch-lb/amp		
ζ_D	0.707				

Figure 101. EPC UP/DN Or L/R Axis Control Loop

These studies indicated the system had sufficient phase and gain margins to meet all requirements. Some significant interaction was found between the EPCS and TACS during thruster firings, but this was not considered serious since TACS would not be utilized during normal EPS operation.

Design verification of the hardware system was conducted in the Hardware Simulation Laboratory. Interfaces, phasings and gains were found to be correct and the functional operation of the EPC system was verified. However, the pointing accuracy requirements were not demonstrated.

The HSL was equipped to measure motion of the EPC dynamic simulator to an accuracy of ± 1 arc-sec, the certified accuracy of a laser autocollimator used for position measurements. The autocollimator was believed to be accurate to ± 0.1 arc-sec, but this was virtually impossible to verify. Measured accuracy of the EPC system in the HSL was ± 20 arc-sec, and pointing stability was found to be ± 7 arc-sec for 15 minutes.

The two prime causes of the degraded accuracy were noise and collimation errors introduced by the fine sun source. The noise was observed as a 20 Hz signal on the FSS output. The signal was the beat frequency between the 80 Hz chopper in the FSS and a 60 Hz flicker from the sun source Xenon arc. The level of the signal was ± 2.8 volts RMS or ± 17.5 arc-sec RMS. Introduced into the EPC closed loop, it was seen as jitter of ± 7 arc-sec.

Offset pointing errors arose from poor collimation of the sun source light beam. Performance data for operation of the sun simulator gave the collimation half angle as 30 arc-min. There could be no means to differentiate between errors inherent in the EPCS and errors introduced by poor collimation.

Several studies were made of this situation. The studies increased confidence that the system would operate as designed, but no means of demonstrating the desired operation of a flight-type EPCS with the available facilities could be found.

The design requirements could have been verified by installation of a double mirror heliostat system. Use of a heliostat system would have permitted more accurate measurement of the system performance, but operation of the simulation would have been severely limited by weather. Installation of a heliostat was determined not to be feasible for the Skylab effort, but recommendations were made to consider such a device for future projects.

3. Subsystems Verification. The EPCS flight hardware was checked out during Post Manufacturing Checkout, Therman-Vacuum and Pre-launch Tests. No significant problems were encountered with the control system, although several hardware component changes and minor modifications were made.

4. Mission Operations. The EPCS performed as required during flight. Final evaluation of the level of pointing accuracy and stability achieved will be drawn from analysis of experiment photography. The crews reported that stability and control was excellent and, apparently, well within specifications.

Dynamic coupling between the vehicle ACS and the EPCS was a major source of transient disturbances to the ACS. An EPCS spar roll caused X and Z-axes Rate Gyro peak amplitudes of approximately 0.02 degrees per second at the start of the roll and 0.06 degrees per second when the roll command is terminated. Two predominant bending modes were excited with frequencies of approximately 0.81 Hz on the X and Z-axes and 1.48 Hz on the Y-axis.

On Day 64, during the second unmanned phase, the primary UP/DN Rate Gyro Processor became very noisy and eventually failed to zero output. The cause of the RGP failure was loosening of a fiber washer on a power switching transistor mounting. This allowed the transistor to saturate and eventually cause the RGP to overheat and fail. See Section VII. A., for details of the RGP failure mode.

In the absence of sensor information for rate damping, the EPCS became unstable. Large amplitude oscillations were set up on the UP/DN axis which kept the actuator currents very high. The actuators eventually overheated and seized.

Because the vehicle was in a period of minimal coverage by tracking stations at the time of the RGP Failure, an entire orbital day phase passed before the problem was fully evident. Solar Inertial mode was selected by ground command at 03:20, caging the canister and allowing the actuators to cool down. The secondary UP/DN Rate Gyro Processor was powered up and an Experiment Pointing mode was selected again at 17:26. No problems were encountered.

As a result of the EPC RPG failure and the RGP failures which had occurred in the ACS, the Derived Rate Conditioner Assembly (DRC) was designed, built and carried to orbit aboard SL-3. The DRC was designed to modify the TSS output to provide the EVA with rate information. If two RGP failures had occurred on a single EPC axis the DRC would have been installed by EVA, allowing ATM experiments to continue. However, no further EPC Rate Gyro Failures occurred,

and the DRC was never used. See Section IX.F., for a complete description of the DRC.

Also, as a result of the EPC RGP failure, the criteria for operation of the actuators was reviewed. A rule was established to limit continuous, unattended (either by crew or ground controllers) EPCS operation to fifty minutes. Studies indicated that the actuators could draw saturated current commands for fifty minutes without damage. Mission rules were changed to provide that Experiment Pointing mode be exited whenever the steady state actuator currents exceeded $\pm$ 1 amp.

Anomalies and failures experienced in the EPC system produced only temporary degradation to the control loops. EPCS components are discussed further in their respective sections.

5. Conclusions and Recommendations. The stability and pointing control loops of the Experiment Pointing Control System operated as designed. Increased telemetry capability for measurements of system operation would have been helpful in assessment of inflight stability.

B. Offset Pointing Control.

1. Design. The capability was required to point the ATM Experiment Package at targets offset from the heliocenter. This was accomplished by means of the FSS optical wedge mechanism (see Section VIII.C.1.) Rotation of the wedges produced a deviation of the incident light as seen at the FSS detection cell. This deviation produced a FSS error signal which the control loop would null by repositioning (offset pointing) the Experiment Canister. The capability was required to offset $\pm$ arc-min. on both the UP/DN and L/R axes. Radius of the solar disk is approximately 16 arc-min.

Another requirement was to position the Star Tracker Telescope to any point within its field of view.

Both of these tasks were processed by the EPEA positioning control loop. Command signals were processed and routed to either the FSS Control Electronics Assembly (CE) or to the Star Tracker Electronics Assembly (STE), depending on the operational mode.

Pointing commands were issued either by the Manual Pointing Controller (MPC), located on the Control and Display Panel, or from the ATMDC. The EPEA gave priority to inputs from the MPC, which

was selected by the MPC Enable Switch on the C&D Panel. If the Star Tracker Manual Mode was selected, the EPEA routed the MPC UP/DN output to the inner gimbal circuitry of the Star Tracker, and L/R MPC output to the outer gimbal circuitry. Positioning of the Tracker gimbals by the ATMDC was not a mission requirement.

If the MPC was not enabled, the FSS wedges could be driven via DAS/DCS through the ATMDC. Using this mode, the desired wedge positions were stored in the ATMDC and analog commands were computed and issued until the actual wedge positions, as indicated to the ATMDC by serial binary data from the FSS Signal Conditioner, were driven to within ± 20 arc-sec of the desired values. The ATMDC also utilized the MPC substitute function to provide roll about line-of-sight, described in Section VIII.D.

The FSS received wedge position hold/release commands from the ATMDC. These commands were issued each time the EPEA was enabled or inhibited.

2. Design Verification. Design analyses of the EPC offset pointing functions were conducted in conjunction with the control loop studies. No significant problems were found.

Design verification, conducted in the Hardware Simulation Laboratory determined that the system design was operational and functionally correct. Measurement of the offset pointing accuracy was limited by the system noise due to the facility sun source.

3. Subsystem Verification. The offset pointing subsystem performed satisfactorily during all systems level tests. No significant system problems were found.

4. Mission Operation. Manual pointing of the Star Tracker worked as designed, prior to the Tracker failure on DAY 228 (see Section VII.B.). The operational procedure developed for the Star Tracker during SL-3 required manual pointing of the Tracker each time a roll attitude update was desired. Thus, the Star Tracker manual pointing feature was utilized far more than originally anticipated.

The canister offset pointing function was utilized throughout the mission and its overall performance was as designed. Certain problems and difficulties were encountered, however.

Frequently, the FSS wedge count changed due to releasing the wedges before the FSS door was fully open. The FSS Wedge Encoder would interpret the change from dark to light as a change in the encoder wheel position. The counter would then change,

usually by a single count. If the wedges were not zeroed during the orbital day, the discrepancy between the actual wedge position and the position count would remain, and could be increased at the next orbital sunrise. Under most circumstances, the error could go unnoticed. During ATMDC controlled pointing, however, driving the wedges through the zero position could result in erratic behavior by the spar.

As an example, if the wedge position on an axis was at some positive location while the wedge readout indicated some smaller positive value, incorrect wedge drive commands would be issued if the ATMDC were to drive the wedge through zero. As the wedge reading decreased, it would overflow at the zero count. In the absence of an encoder zero pulse, the counter would reset to the maximum positive value. The ATMDC would then issue a full scale (5 Vdc, or 200 arc-sec per sec) wedge rate command. When the zero pulse was encountered the readout reset to zero. At this point, an overshoot may have occurred, and the ATMDC would issue a large command of the opposite polarity.

The effect of the error was particularly evident if the situation described above occurred during line-of-sight (LOS) roll (see Section IX.D.). This problem was the cause of several LOS roll anomalies.

Two different sets of circumstances led to releasing the wedges prior to the FSS door being fully open. In the first, when the Experiment Pointing mode was selected during the orbital day the FSS wedges were released and the door commanded open simulataneously (the door required 11-15 seconds to open). In the other case, during normal experiment pointing mode operation, the FSS wedges would be released at the beginning of orbital day, as computed by the ATMDC. The aperture door could be released as much as 40 seconds earlier (see Section VIII.E.) if the Acq. SS had detected sun presence. However, navigation and timing errors often resulted in sun presence being acquired within 2-3 seconds of computed day phase.

A related problem was that the wedges could be driven a full 360 degrees, but no positive indication of wedge position was provided on the back side of the wedges. On several occasions, the astronaut inadvertantly drove to the back sides of the wedges. The wedge counter does not track the wedges over the entire range and meaningless readouts could be encountered. In addition, operation on the back side of the wedges resulted in spar motions opposite in direction from the commands. On DAY 19, this problem arose and the astronauts did not recognize the cause. After consultation with ground support, the situation was corrected by re-zeroing the wedges.

5. Conclusions and Recommendations. Overall performance of the system was adequate and satisfactory. Based on problems encountered, certain recommendations for improvements can be made.

A means was needed to provide accurate and continuous correlation between the wedge position and the wedge position readout. The problem described above could have been avoided by any of several approaches. A crew procedure to re-zero the wedges each time Experiment Pointing Mode-Day was entered would have been a minimum safeguard. Due to the time required for this procedure, an automatic re-zero feature would have been desirable. Another approach would have been interlock logic which would not release the wedges until the FSS Aperture Door was completely open.

Modification of the FSS design could allow an internal light source to be used for operation of the Wedge Position Encoder. Also, a direct position encoder device for the full 360 degrees of wedge rotation would have eliminated the problem associated with operation on the backside of the wedges.

The astronauts have stated that an MPC Gain Switch would have been helpful to allow changes in canister position by small increments on the order of 1 arc-sec. The minimum rate command from the MPC was 4 arc-sec per second (from the ATMDC, the minimum command was 16 arc-sec per second).

C. Roll Positioning

1. Design. In addition to the dynamic control and offset pointing capability provided for the experiment package UP/DN and L/R axes, the Roll Position Mechanism (RPM), described in Section IX.D., was designed to rotate the spar about the EPC Z-axis over a range of ± 120 degrees. The mechanism was commanded by the astronaut via Rate Switches of the Manual Pointing Control Panel located on the Control and Display Console. Spar roll rates of + 7, ± 3.5,, ± 0.7 and ± 0.35 degrees per second could be commanded. Once the spar was positioned, the RPM would hold the location until a repositioning command was received. The astronaut repositioned the spar in accordance with experiment demand requirements. The astronaut could also utilize the ATM EVA Rotation Control Panel (during extravehicular activity) to command rate of + 7/3.5 or ± 0.7/0.35 degrees per second to reposition the spar. The rates were dependent on the setting of the Manual Pointing Roll Gain Switch on the ATM C&D Console. The spar roll position is displayed on the Control and Display Console. The roll positioning control loop is shown in Figure 102.

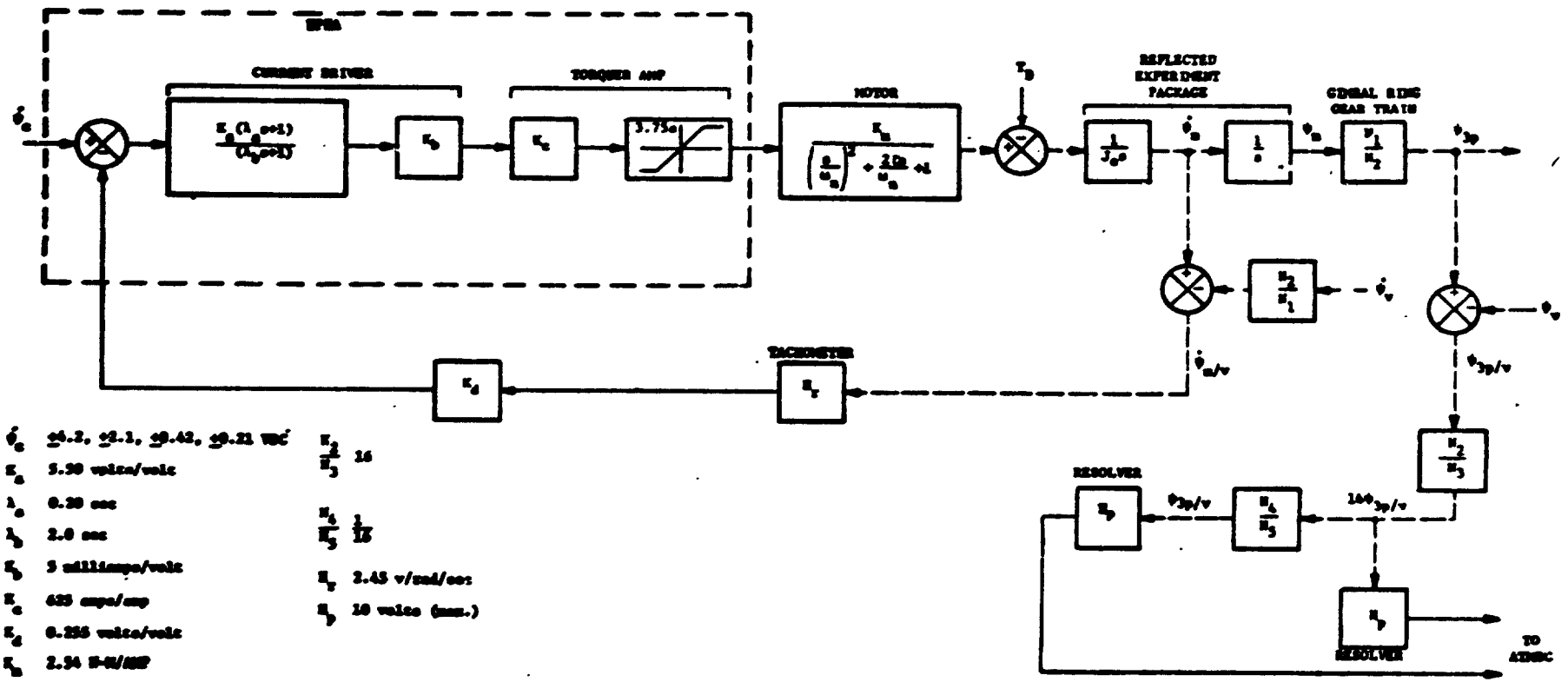

ϕ_c ±6.2, ±2.1, ±0.42, ±0.21 VDC
K_a 5.50 volts/volt
τ_a 0.20 sec
τ_b 2.0 sec
K_b 3 milliamps/volt
K_c 625 amps/amp
K_d 0.256 volts/volt
K_m 2.54 ft-lb/amp
ζ 0.7
ω_n 314 rad/sec
J_o 0.706 ft-lb-sec^2
$\frac{K_1}{K_2}$ $\frac{1}{35}$
$\frac{K_2}{K_3}$ 16
$\frac{K_4}{K_5}$ $\frac{1}{15}$
K_t 2.45 v/rad/sec
K_p 10 volts (max.)

Figure 102. EPC Roll Positioning Mechanism Control Loop

2. Design Verification. The roll loop design was verified in the Hardware Simulation Laboratory. The HSL test fixture limited roll movement to + 22.5 degrees. During Verification Testing, it was found that the high rate roll generated enough back emf from the roll motor to damage the EPEA electronics. The EPEA Torque Amplifiers were modified with zener diodes to protect the circuits.

3. Subsystem Verification. The roll positioning functions were checked during systems level tests and performed satisfactorily. No significant problems were found.

4. Mission Operations. The roll positioning function was used extensively during the mission. Most canister roll maneuvers were performed as line-of-sight (LOS) roll maneuvers (see Section VIII.D.), and most problems encountered were associated with the LOS roll system. The roll control loop functioned as designed throughout the mission. However, during SL-2 it was found that the 7 degrees per second roll rate could induce large Rate Gyro oscillations, and the crews were requested not to use that rate.

5. Conclusions and Recommendations. The roll positioning function operated as designed. It was found that the highest roll rate, 7 degrees per second, produced undesirable transients.

The discrete rate command switches made accurate roll positioning an involved process, often requiring many rate and direction changes. A continously variable rate command source would have been desirable. This could have been accomplished by an option to select one channel of the MPC for roll rate commands.

D. Line-of-Sight (LOS) Roll.

1. Design. Since the roll ring is the outermost of the EPC gimbals, roll operations would cause the EPC line-of-sight to transcribe a cone about the sun center. Due to the time required to reposition the spar to the original line-of-sight for experiment set up, a relatively late input was an astronaut request for LOS roll capability. This was implemented by programming the ATMDC to drive the FSS wedges during roll operations to maintain the original line-of-sight.

At any time when experiment pointing was active and the Star Tracker was not in the Manual Mode, all canister roll operations were automatically performed about the Experiment Package line-of-sight. If the EPEA was not enabled or if the Star Tracker was in Manual Mode, LOS pointing would not be processed.

The desired wedge positions were computed as the original positions resolved through the change in the canister roll position, whenever the change in roll position exceeded 0.174 degrees over the period of one computer slow loop. Wedge rate commands were generated from the desired wedge positions. The rate commands were limited to slightly less than 200 arc-sec per second. The computer would generate wedge rate commands until the difference between the desired and actual wedge position was less than or equal to 0.5 arc-sec or until three slow loops (approximately three seconds) after the last new set of desired wedge positions were computed.

2. Design Verification. The LOS roll function was studied for implementation and recommendations for a one Hz computation cycle, digital filter design and a three second LOS mode cutoff delay were made.

During design verification testing conducted in the HSL and during tests at MSC it was observed that the EPC did not exhibit stable fixed pointing. The problem was found to be that noise in the roll resolver feedback to the ATMDC was activating the LOS roll. The Pre-Flight and Phase II ATMDC Programs would activate LOS roll whenever the difference between the current and past roll positions was non-zero. The Final Flight Program incorporated the requirement for a roll position change of $\pm$ 0.175 degrees.

3. Subsystem Verification. LOS Roll operations were tested in systems level tests and performed satisfactorily. No significant problems were found.

4. Mission Operations. The LOS roll function was exercised extensively during the Skylab manned operations. Overall, the function performed as designed. Pointing stability was degraded during roll, but this was to be expected.

Anomalous spar behavior occurred several times during LOS roll. Three separate causes were identified.

On DAY 28, the canister pointing jumped about one-half solar radius during LOS roll. Attempts were made to duplicate the problem in the HSL, but without success. Later analyses showed that the situation was not anomalous, but was transient and canister pointing would recover.

On DAY 90, similar spar behavior was observed. In this case, however, the cause was determined to be a disparity between the FSS wedge position and the wedge position readout. In this situation, the counter reset prior to encountering the wedge zero pulse. The

ATMDC interpreted the readout as the maximum possible wedge position, and issued saturated wedge rate commands to compensate. (The problem is discussed at length in Section IX.B.). A procedure of re-zeroing the wedges prior to ATM operations was initiated to prevent recurrence.

A third pointing transient occurred as the result of erroneous canister roll position readouts. The roll resolver outputs were demodulated and converted to digital readings in the WCIU. If the actual canister roll position was zero, potentially one in every 100,000 readings would be converted to the binary maximum negative value. Whenever this event occurred, the erroneous position reading was interpreted by the Flight Program to be a large error, and a maximum wedge drive command was issued. After approximately four seconds, a correct position reading was received, and a true command was issued. Subsequent correct readings of the roll position would return the wedge positions approximately to their original position.

The anomaly was corrected by establishing the constraints of positioning the canister at the zero roll angle position only when required by the needs of the mission. The canister would otherwise be positioned at about one degree from zero.

5. Conclusions and Recommendations. The line-of-sight roll function performed as designed except for the impact of the FSS wedge encoder problem and the zero roll reading problem.

E. Fine Sun Sensor Aperture Door Control.

1. Design. The Fine Sun Sensor Assembly was equipped with an aperture door for protection of the sensor from optical contamination and from undesirable temperature gradients which could arise from thermal radiation during orbital night. The aperture door could be opened or closed by DAS/DCS, C&D Panel switches or through automatic control by the ATMDC. The door required 11 to 15 seconds to open or close.

If ATMDC control was enabled, the FSS door open command would be issued if the APCS was in Experiment Pointing mode and the vehicle was in the ATMDC computed day portion of the orbit.

2. Subsystem Verification. The door control functions were checked during systems level tests and no significant problems were found.

3. Mission Operations. The FSS Aperture Door operation performed as designed, throughout the mission. However, problems with other related systems did impact usage of the FSS door control.

On DAY 21, C&D Panel Status Flags indicated that the S054 experiment door had failed to open. The door was finally opened and a procedure adopted to prevent the door from being closed: the EVA Auto Door Control switch was placed in the inhibit position to prevent the ATMDC OPEN/CLOSE commands from reaching the FSS and experiment doors. Although the FSS door could still be commanded manually, it was left open to minimize crew and ground door procedures, and to preclude the inadvertent activation of the EPC system while the door was closed. An EVA was performed on DAY 21 and the S054 experiment aperture door was pinned open. Normal ATMDC control of the FSS door was resumed.

At a later date, it was found that the FSS wedges were being released by the ATMDC prior to the FSS door being fully open. (Section VIII.B.). A suggested solution was to lock the FSS door in the open position. The plan was not accepted, however, because the protection provided by the door was felt to be more significant than the wedge count problem.

4. Concludions and Recommendations. The FSS Aperture Door Control operated as designed. A improvement in FSS door operation could have been realized if the FSS door logic were completely isolated from the experiment door logic.

F. EPC Caging Control

1. Design. The EPC Experiment Canister was provided with locking mechanisms to protect the canister and gimbal components from damage during launch, docking and vehicle maneuvers. Two hardware systems were utilized: a launch lock mechanism was present to protect the structure from stress at launch only, and orbital locks were used in orbit to cage the spar at any time the experiment package was not in use. An early concept called for both lock systems to be engaged at launch, but testing showed that the orbital lock rails would be deformed when this occurred, so the vehicle was launched with the orbital locks uncaged.

The launch locks were designed to be pyrotechnically released after orbit was achieved.

Caging logic for control of the orbital locks was contained in the EPEA. The ATMDC, in turn, determined when the EPEA was to be enabled or inhibited, thereby indirectly controlling the CAGE/UNCAGE operation. When the APCS was in Experiment Pointing Mode (EPM), the ATMDC made the following checks to determine what the EPEA status should be.

If the APCS was in EPM, an SI acquisition maneuver was not in progress, the vehicle was in orbital day phase and the sum of the squares of the Acquisition Sun Sensor errors was less than or equal to $(1.3 \text{ deg})^2$, the EPEA would be enabled. If the EPEA was enabled, the sum of the squares of the Acquisition Sun Sensor errors would have to exceed $(1.4 \text{ deg})^2$, or any of the other conditions change in order to inhibit the EPEA.

When the EPEA received an enable command, it would energize the orbital lock motors to uncage the spar. Current would be supplied to each motor until an uncage verify discrete was received from the lock motor. The uncage verify discrete activated logic to remove power from the motor.

Conversely, when the EPEA was inhibited, power would be applied to the orbital lock motors to cage the spar. When locks achieved the cage position, a cage verify discrete was sent to the EPEA and power was removed from the motors.

Orbital lock motor redundancy status was slaved to the status of the UP/DN control loop. Failure in the primary orbital lock control for instance, would require switching to the secondary UP/DN channel.

The lock system concept remained basically the same throughout development. One notable change came when hardware tests demonstrated that the orbital lock rails would be damaged by launch and docking stresses. The rails were reinforced, but instead of launching with the orbital locks engaged, the spar was to remain uncaged until after orbit was achieved.

2. Subsystem Verification. The EPC caging control was checked during systems level tests and no significant problems were found.

3. Mission Operations. The EPC Caging Control functioned nominally until DAY 185 when the UP/DN orbital lock failed to uncage. The EPEA was switched to secondary, and the spar successfully uncaged when tested a few hours later. Using the secondary lock motors, the CAGE/UNCAGE function was tested again on DAY 189 and 190. Unrestricted operations resumed on DAY 191. However, on DAY 201, the UP/DN lock again failed to release.

Without any configuration changes, the lock successfully uncaged when tested about an hour after the second anomaly. This anomaly gave credance to the theory that intermittent mechanical binding was occurring possibly due to contamination from wiring insulation in the vicinity of the lock. The conclusion of investigations of the second anomaly was that there was no need to limit or inhibit EPC operation.

The uncage failure was not observed again, and the secondary orbital lock motor was used for the remainder of the Skylab mission.

4. Conclusions and Recommendations. The launch lock system performed as designed. No changes were recommended. The orbital lock system functioned as designed throughout most of the mission. The two orbital lock anomalies caused loss of some experiment operating time. Further design and hardware studies are indicated to resolve the cause of the lock anomalies.

SECTION IX. EXPERIMENT POINTING CONTROL HARDWARE

A. Fine Sun Sensor (FSS)

1. Description. The Fine Sun Sensor (FSS) provided the highly accurate attitude information for the UP/DN and L/R axes of the Experiment Pointing Control System. The FSS comprised four separate packages: an Optical-Mechanical Assembly (OM), Preamplifier Electronics Assembly (PE), Control Electronics Assembly (CE), and the FSS Signal Conditioner (SC), interconnected as shown in figure 103. The sensor was redundant in both axes and all four channels were identical. A functional description of a signal channel follows:

Sunlight passed through an alignment wedge which provided a spectral filter and a means for the adjustment of a null axis relative to the external reference mirror. The rays then passed through a deviation wedge which refracted the sunlight at a fixed angle in a controllable direction. Sunlight from the deviation wedge was then passed through the Critical Angle Prism (CAP). When light entered perpendicular to the base of the CAP, it was partially reflected internally. Of the remaining light, an equal amount passed through each face of the CAP and was focused on a silicon detector. A chopper, at an 80 Hz rate, caused the detector to look alternately at the light from each face. If the angle of light incidence changed, e.g., during offset pointing, more light passed through one face than the other. The output of the detector became a square wave with a peak-to-peak value proportional to the angular deviation of the incident light. This signal was amplified, demodulated, and sent to the Experiment Pointing Electronics Assembly (EPEA). A sun presence signal was also generated for display and telemetry. See figures 104 and 105.

Direction control for offset pointing originated from either the Manual Pointing Controller (MPC) or the ATMDC MPC Substitute function which could be activated via DAS/DCS. The command signal was amplified by the EPEA to drive a DC wedge torque motor. A tachometer feedback loop was included for rate control. The deviation wedge was rotated by the motor through a gear train, giving an apparent rotation of the line-of-sight of the sun.

Gimbal readout of the wedge rotation was accomplished by means of an optical encoder system. A three channel optical encoder pattern was attached to each deviation wedge so that as the wedge rotated, the encoder pattern turned with it. Sunlight passed through the code wheel and was detected by three silicon photodiode detectors whose output was proportional to the amount of light impinging on them. The detectors produced low-level incremental sine-cosine signals which were amplified and sent to the SC. Total angular motion was tracked in the SC by

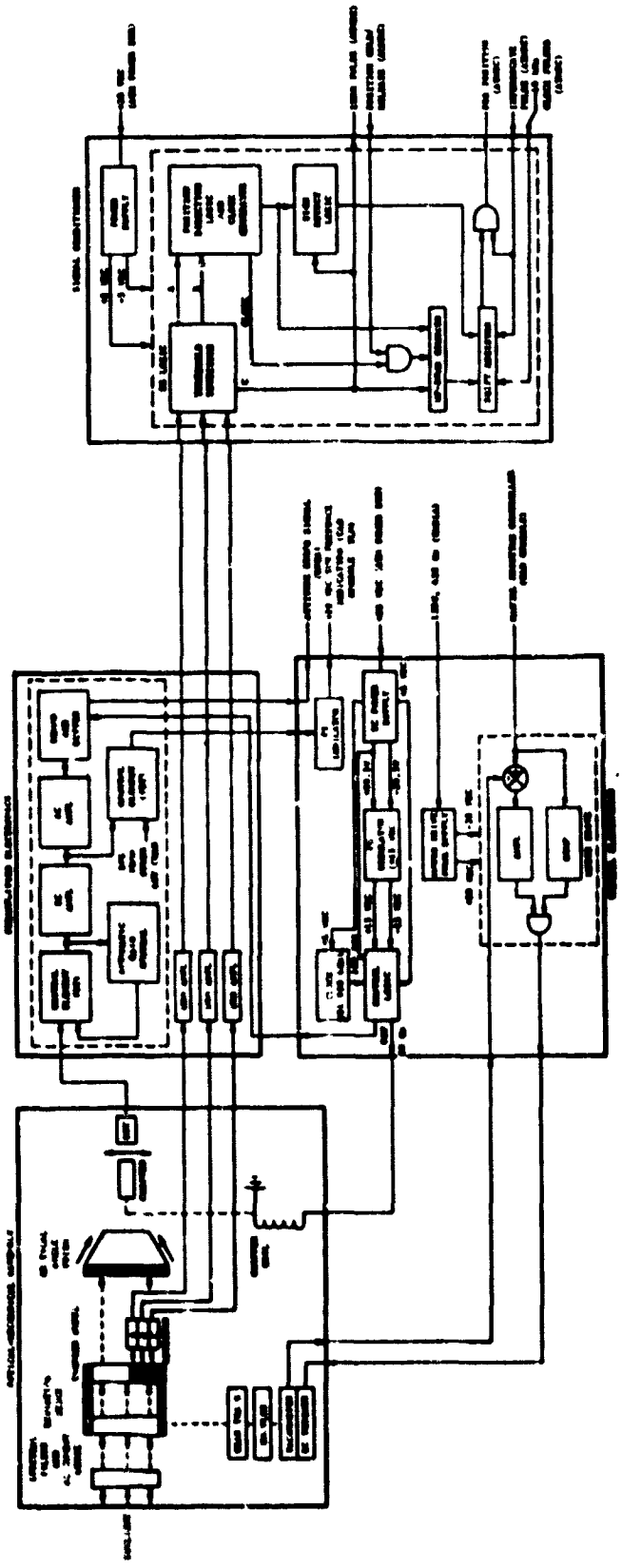

Figure 105. FSS Single Channel Block Diagram

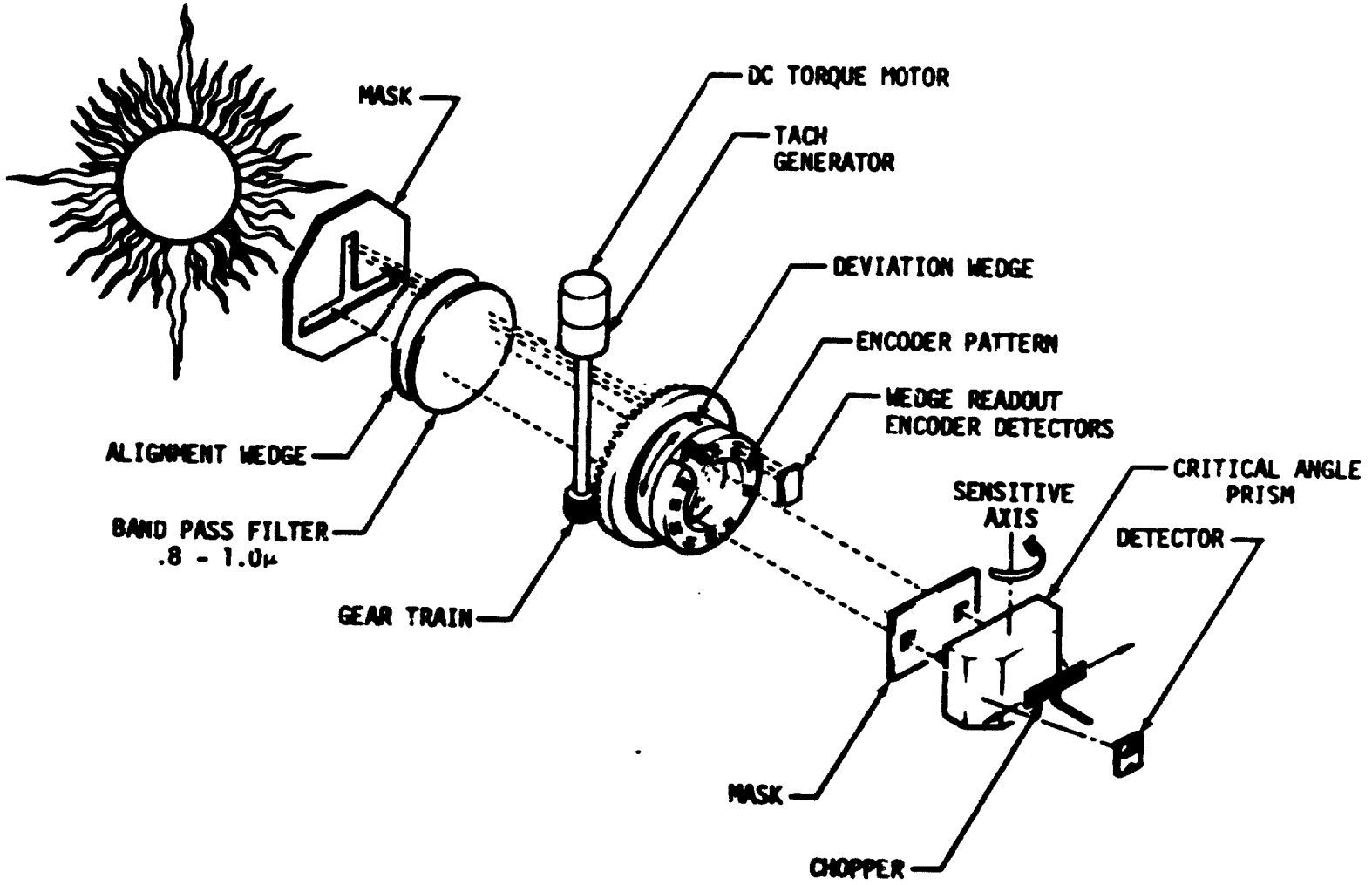

Figure 104. FSS Optical Mechanical Assembly (OMA)

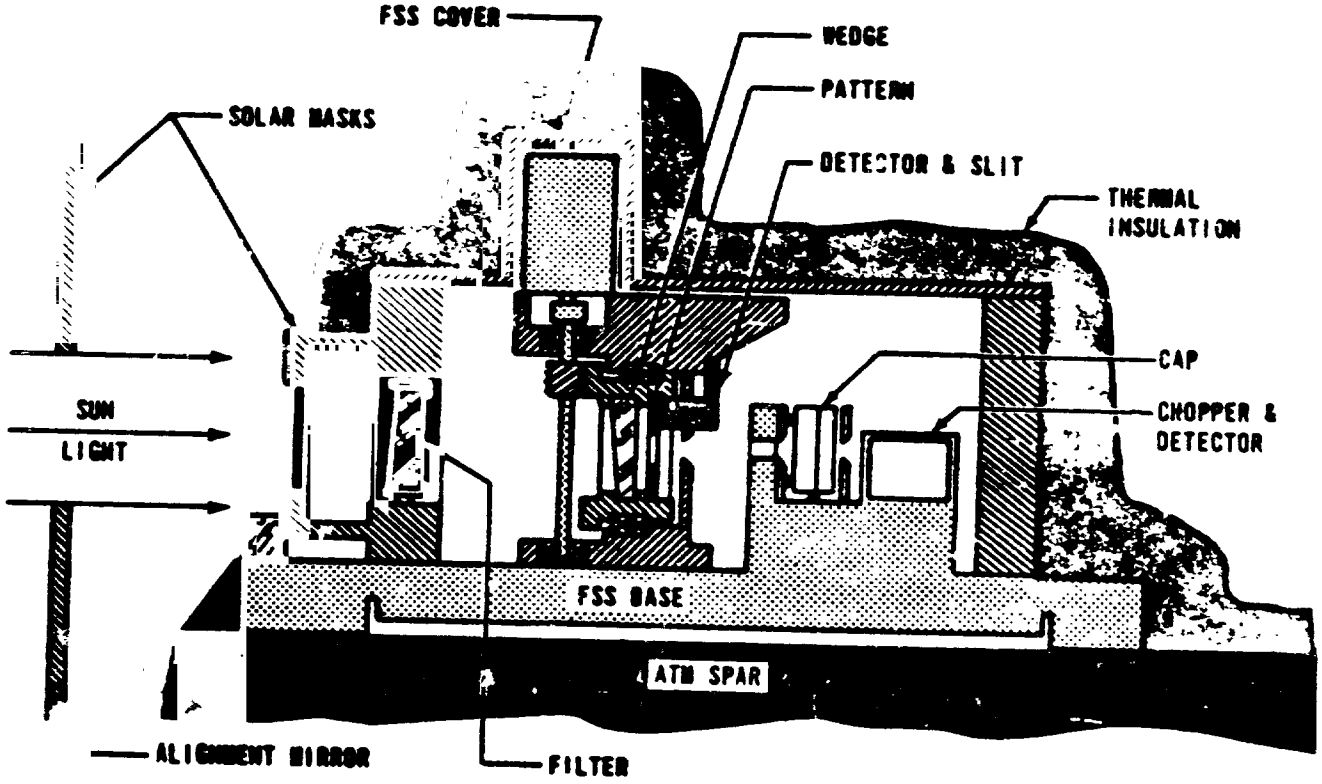

Figure 105. Cross Section Of FSS Optical Mechanical Assembly

counting the transitions from light to dark with direction determined by observing that the channel A signal led channel B, or channel B led channel A. The encoder output is shown in figure 106. The third (C) channel of the encoder pattern contained a single reference mark to indicate the zero wedge position. When the SC detected the zero pulse, it automatically reset the count to zero. The wedge positions were converted to serial-binary words in the SC and were sent to the ATMIC for processing and display. Table 49 lists the FSS performance specifications.

Table 49. FSS Specifications (Excluding the Signal Conditioner)

Sensitivity	172 ± 32 millivolts/arc-sec
Output Voltage Range	± 12.5 ± 2.5 Vdc
Pointing Accuracy	2.25 arc-sec (3 sigma)
Pointing Resolution	± 0.625 arc-sec (nominal)
Pointing Stability, Short Term	± 0.1 arc-sec (nominal)
Pointing Stability, Long Term	± 0.5 arc-sec (goal)
Temperature Stability	± 0.1 arc-sec/deg C (nominal)
Field of View:	
Sensor	± 5.5 ± 0.5 deg
Sun Presence Signal	± 110 arc-min of null
Spectral Response	0.8 microns to 1.0 microns
Frequency Response	≥ 10 Hz
Offset Pointing Capability	± 24.21 arc-min (each axis)
Offset Pointing Drive Rate:	2 arc-sec/sec (min)
	80 arc-sec/sec (avg)
Weight (without Signal Conditioner)	21.2 Kg
Power (peak)	20.5 watts
Power (average)	9.0 watts

2. Design History. The design concept for the Fine Sun Sensor was derived from the high accuracy Sun Sensor which was being developed for the Advanced Orbiting Solar Observatory (AOSO) prior to that program

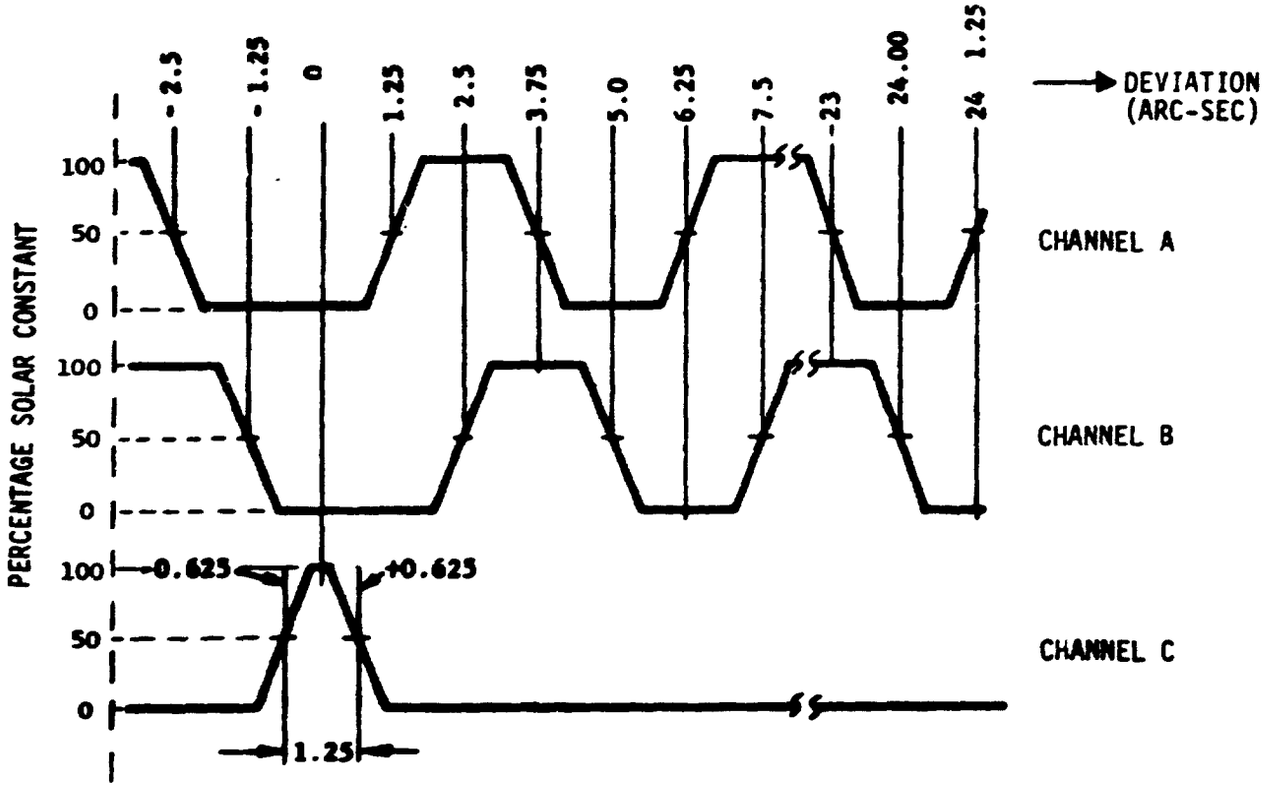

Figure 106. FSS Wedge Encoder Characteristics

being cancelled. With various modifications to the AOSO design, the system was selected for use on the ATM mission. The modification included such things as the alignment reference, physical configuration, wedge encoder patterns, and wedge drive motors. The stepping motors used in the AOSO design were replaced with a 400 Hz drive motor for the early ATM concept. However, due to what proved to be an undesirable gear train arrangement, the 400 Hz wedge drive system was replaced with a DC motor and direct pinion gear wedge drive and associated electronics. This modification to the design took place in early 1969 and only two other modifications were made to the system. The alignment wedges were skewed slightly to avoid internal light reflections that created erroneous wedge angle information.

Late in the program, a design change was implemented which separated the primary and secondary DC power input leads. Originally, the DC input leads were commoned on a latching relay used for redundancy switching. Separation eliminated a potential single point failure.

3. Design Verification. EPC subsystem integration and verification in the Hardware Simulation Laboratory included observation of the functional characteristics of the FSS. The interfaces, phasings and gains were found to be correct. Accuracy requirements were not observable in the HSL due to the system noise problem discussed in the pointing control section, VIII.A.

4. Hardware Verification. The FSS was initially qualified at the manufacturer's facility, Honeywell Radiation Center (HRC).

One of the most difficult tasks associated with testing and qualifying the FSS design was duplicating the solar image for intensity, solar spectrum, collimation, and stability while maintaining a stable thermal environment.

While testing in the lab, HRC used a small solar simulator of about 3% of one solar constant when determining and performing the system's alignment. Further testing was performed using the actual sun; however, due to limited, or poor, "seeing" conditions HRC could do little more than verify scale factor and functional operation parameters. With HRC's support, MSFC carried the Qual-FSS to Sac-Peak at Sun Spot, New Mexico to perform actual solar tests of the system. Sac-Peak is normally one of the nation's better locations for good "seeing" conditions. The results obtained at Sac-Peak compared very favorably with HRC's lab test.

All of the FSS systems built were later tested at MSFC utilizing the Astrionics Laboratory precision heliostat located in the Celestial Facility (Bldg. 4467).

The mechanical concept was proved first by testing a single channel and wedge drive mechanism and lubrication at variable speeds for 100 days in a hard vacuum and later the Qual-FSS was life tested in hard vacuum for 291 days for approximately 7000 hours.

For the 291 days, the system was tested in a sequence for a number of days operating with the wedges being driven at top speed, followed by a number of days in a storage mode. This was repeated several times at various temperature levels until the system had accumulated 4000 hours in operation and 3000 hours in storage.

This system also successfully underwent all ATM reliability analysis, thermal, vibration and outgassing tests necessary to qualify the system for flight.

5. Mission Operations. Operation of the FSS was first verified on DAY 15 when Experiment Pointing Mode was entered by ground command, and the ATMDC was used to command FSS wedge positions. The following day, the crew operated the experiments for the first time. A procedural problem resulted in selection of the secondary FSS. The primary FSS was reselected on DAY 22.

The system operated in the primary mode for approximately the first 4600 hours in orbit. Due to a suspected drift in alignment of the yaw primary channel, the system was switched to the secondary mode on DAY 213, where it remained for the last 1600 hours of the mission.

One anomaly occurred in the Electrical Power System which impacted the FSS. On DAY 177 a short developed on TV Bus 2. This caused a transient on the APCS power busses which caused the FSS wedge counter to be zeroed. On DAY 258 the FSS wedges were erroneously zeroed without being commanded by either astronaut or ground command. Only a signal or a noise pulse on the encoder "C" channel leads, connecting FSS to the FSS signal conditioner could have caused the erroneous zeroing on both pitch and yaw wedge angle readings. Since the wedge angle had not changed, as was confirmed by various solar experiments, that meant the erroneous zero information was the result of a noise transient on the encoder "C" track leads, going to the Fine Sun Sensor Signal Conditioner.

The thermal environment and power source supplying the system were maintained at an ideal level for the most accurate results; however, due to noise in the CAP's telemetry channel the error signals could never be fully appreciated or demonstrated by telemetry. The final analysis will depend on the evaluation of the experiment pictures and data.

During the course of the mission, the bias between the FSS null and the S082B Extreme Ultraviolet (XUV) spectrograph was observed to drift. On DAY 213 a four-limb coalignment was run to attempt to determine

if a changing null output could be causing the bias drift. The four-limb coalignment measures the limits of the east-west and north-south solar limb using the S082B, S055 (Ultraviolet Scanning Polychromator Spectroheliometers) and the FSS. The effort demonstrated very close (± 2 arc-sec) agreement between the primary and secondary FSS, but did not isolate the source of the experiment/FSS bias change. A warming trend had been noted in the ATM and thermally induced structural warpage was identified as another possible cause of the drift.

Under certain conditions, disparities between the actual FSS wedge position and the wedge position readout were generated. This occurred when the wedges were released (enabled) before the FSS aperture door was fully open. Transit of the door shadow terminator across the face of the FSS was observed at slightly different times by the A and B channel encoder detectors. The FSS Signal Conditioner interpreted this condition as rotation of the wedges. Consequently, the encoder wedge count increased, or decreased, creating an error between the actual wedge position and the wedge readout.

The flight FSS was operated over 600 hours during testing and ground checkout and another 6200 hours during the Skylab mission for a total of 6800 hours.

6. Conclusions and Recommendations. Performance of the Fine Sun Sensor was excellent. Based on laboratory and operational usage of the FSS, certain modifications can be recommended which would improve the operation and accuracy of the sensors.

The wedge encoder system should be modified to operate with an internal light source, as well as with the sun, and to give direct indication of the wedge position.

The Base Reference Mirror should be modified to allow more ease in initial alignment and the base should be constructed of a more stable material such as Cervit to provide for greater thermal stability.

The need for a mechanical chopper might be eliminated by changing the single photodetector to a twin photodetector. This would reduce the threshold noise allowing for a more sensitive and accurate system. State-of-the-art advances in detector design would allow greatly improved long-term stability and drift characteristics for twin photodetectors over what was available when the FSS design was finalized.

Add a second wedge to each channel to allow for greater precision in pointing. The wedges and encoder pattern would be modified to provide even arc-sec increments on the coarse wedge with a greater offset pointing capability and the fine wedge and encoder pattern would provide pointing information in 0.01 arc-sec increments.

B. Rate Gyro Processor (RGP)

The EPC Rate Gyro Processors were of the same type as used for APCS control. A complete discussion of the RGP hardware and the problems and failures experienced during the mission, including the EPC RGP failure, is presented in Section VII, A.

Four RGPs were mounted on the ATM experiment package, two per axis. The RGPs provided feedback to the EPC control loop for rate damping. The gains of the control loop were designed for the RGPs to be used only in the coarse mode. Automatic redundancy management was not provided for the EPC Rate Gyro Processors, although switching could be accomplished through both the Control and Display panel switches and via switch selector commands. Since automatic redundancy management was not provided, the secondary Rate Gyros were normally completely powered down, with the result that the units could not be used without a warmpup period. This was demonstrated on DAY 16 when cold Gyro Processors were selected for EPC control and the canister went unstable. The backup ACS Rate Gyros were always powered up with the gyro wheel inhibited, so that operating temperature would always be maintained.

The UP/DN primary gyro processor exhibited overheat conditions after 82 hours of operation. It later developed rate output oscillations and, ultimately, failed on DAY 64. The problems and failure were traced to faulty mounting of a power switching transistor.

Due to the early loss of redundancy, the EPC Derived Rate Control (DRC) Assembly was developed as a backup means for providing rate information to the control loop. The unit is described in Section IX.E.

C. Experiment Pointing Electronics Assembly (EPEA)

1. Description. The EPEA was a multipurpose analog assembly used for signal processing in the EPC subsystem. The electronics in the EPEA were divided into 12 channels. The six primary channels according to their functions are (see figure 107):

Canister UP/DN control

Canister L/R control

UP/DN Fine Sun Sensor (FSS) wedge or Star Tracker (ST) outer gimbal positioning

L/R FSS wedge or ST inner gimbal positioning

Canister Roll Drive

Orbital Locks operation.

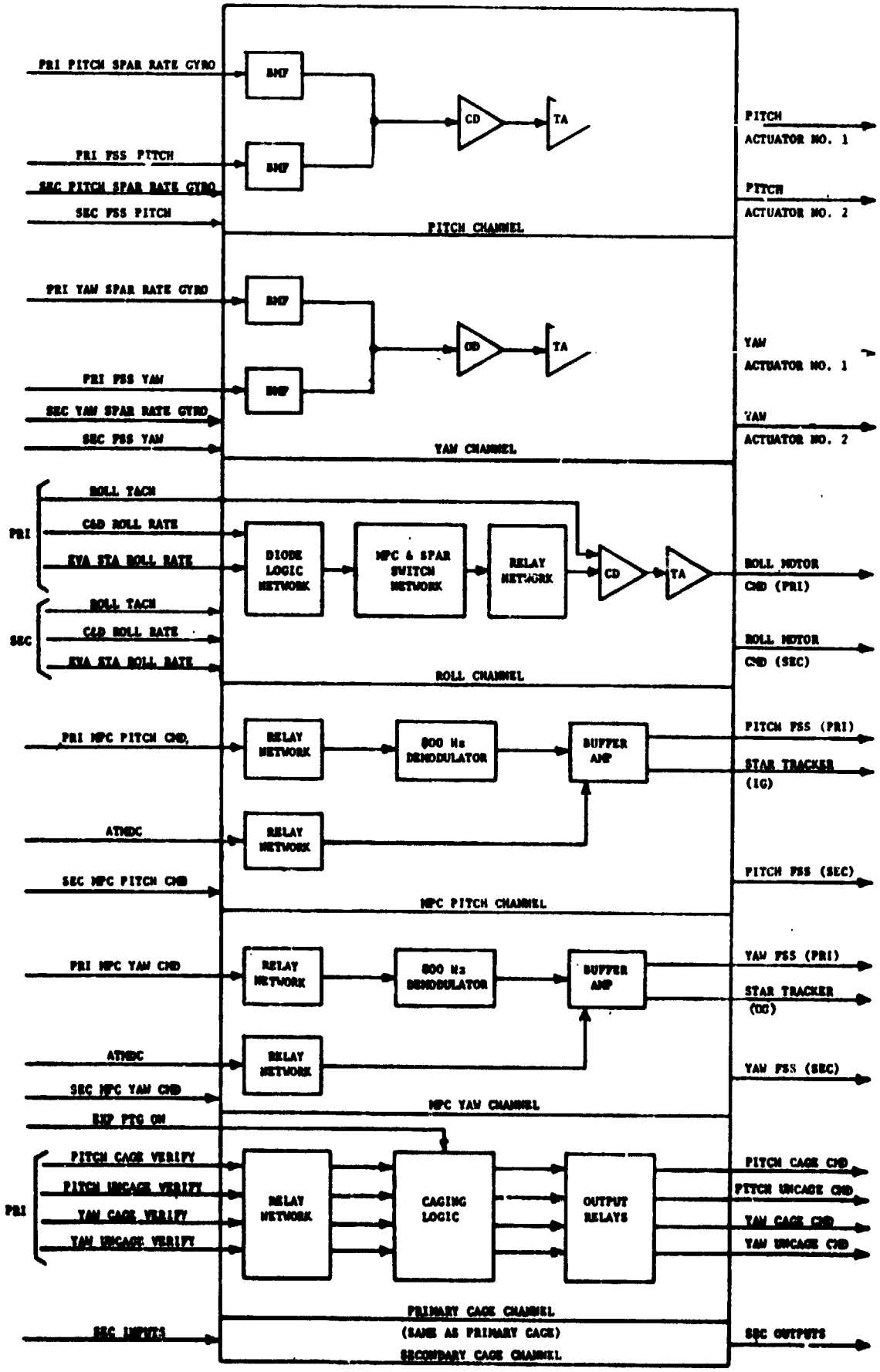

Figure 107. EPEA Single Channel Block Diagram

All six channels could be switched to six identical secondary channels and returned to primary channels by Switch Selector commands or by actuating a Control and Display (C&D) Console switch. All of the channels could also be individually commanded back to primary with the exception of the Orbital Locks operation which was slaved to the canister UP/DN control channel mode.

The UP/DN and L/R control channels accepted position error signals from the FSS and accepted rate signals from the EPC Rate Gyros. These signals were amplified and shaped to supply output currents to drive two actuators in each of the UP/DN or L/R axes. Inputs from the sensors were switched internally as the primary or secondary sensors were selected.

Canister offset pointing, while in the experiment pointing mode, was accomplished by setting the positions of the FSS wedges. The UP/DN and L/R angles of the canister depended on the positions of the respective UP/DN and L/R FSS wedges. The EPEA accepted signals from the Manual Pointing Control (MPC) Panel on the Control and Display (C&D) Console or from the ATM Digital Computer (ATMDC) to drive the FSS wedges. By selection on the C&D Console, the MPC derived outputs could be switched to position the ST by driving its outer and inner gimbals.

The Canister Roll channel of the EPEA accepted any one of four fixed rate commands from either the MPC panel or the external EVA Rotation Control Panel to drive the Roll Position Mechanism (RPM).

The UP/DN and L/R Cage/Uncage channels were provided for locking or unlocking of the canister. Locking signals were provided to cage the canister approximately in the zero positions in both axes during all APCS modes except the Experiment Pointing Mode-Day (EPM-Day). In EPM-Day, the canister was unlocked during the day portions of the orbits to allow solar experiments to be performed. The ATMDC determined these experiment periods and provided signals to the EPEA. Cage/Uncage verify signals, fed back to the EPEA from orbital locks, provided positive indication of the caging state and were incorporated into the caging loop logic.

2. Design History. During development of the "Wet" Workshop concept, control of the Experiment Pointing System was maintained by the ATM Control Computer (ATMCC). The ATMCC incorporated other functions such as (1) CMG control for vehicle attitude control, and (2) control logic to accept, decipher and implement a ten-bit digital word. The digital words were to implement the ATMCC operating modes, command control loop relay switching, and to communicate with other parts of the system, including the ATM Digital Computer.

When the "Wet" Workshop concept changed to the "Dry" Workshop, the ATM control system requirements also changed. The ATMCC function

was reduced to control the Experiment Pointing System only, and the name was changed to Experiment Pointing Electronics Assembly. Except for a few component changes, the basic design concept of the EPEA was not changed again.

3. Design Verification. As the central point of the EPC system, the EPEA was studied to assure that it could provide the desired control of the experiment canister. Analysis of spar bending modes and the EPEA Bending Mode Filters (BMF) was an ongoing project to insure that the flight EPEA would have optimum control capability.

Integration of the EPEA into the EPC system was done in the Hardware Simulation Laboratory (HSL). The HSL was also used for verification and checkout of the flight, flight-spare and prototype EPEAs.

During the HSL testing, it was found that sufficient back emf could be generated by the spar roll drive motor at the 7 degrees per second rate to damage the EPEA roll motor current amplifiers. The amplifier circuitry was modified with zener diodes to provide protection from the back emf.

4. Hardware Verification. The EPEA performed satisfactorily during systems level testing and no significant problems were found.

5. Mission Operations. The EPEA was first powered up five hours after launch to activate the spar caging logic. The EPEA was kept powered down to conserve power, except for brief periods on DAY 13 and DAY 14, until DAY 16, when the first manned ATM operations took place. Power remained on for the duration of the mission.

At the time of the SL-1 launch, the EPEA had 1,893 hours of operation divided between the primary and secondary electronics. During the Skylab mission, an additional 4,388 hours of operation were added to the primary EPEA and 2,086 hours to the secondary EPEA electronics for a total of 6,474 hours. The total lifetime operation of S/N 004 EPEA was 8,367.

No problems were encountered with the EPEA. Some EPEA redundancy switching was required to accommodate interfacing hardware problems. Secondary inputs were selected for the UP/DN Rate Gyro on DAY 64 and for the FSS on DAY 213. The secondary EPEA was selected on DAY 185 following the orbital lock problem. On DAY 254, the primary MPC loop was reselected.

During the ten-day period while the vehicle was in thermal attitude, the EPEA dropped to -32°C, well above the minimum storage temperature of -55°C. The maximum temperature recorded was +17°C during a period of continuous daylight over a number of orbits. The operational range was -40 to +74°C.

6. Conclusions and Recommendations. The Experiment Pointing Electronics Assembly (EPEA), operated as designed throughout the Skylab mission. In view of the performance of the EPEA during the mission, no changes were recommended.

D. Experiment Pointing Control and Roll Position Mechanism (EPC/RPM)

1. Description. The solar experiment canister was mounted to the ATM Rack through a three-degree-of-freedom gimbal mechanism - actuator assembly. The electromechanical system was composed of several integrally assembled components which performed a number of functions within the EPC system.

The supporting structure for the EPC/RPM system consisted of two large concentric rings. The outer, or Roll Ring, was attached to the ATM Rack by four symetrically placed roller bearings. The Roll Position Mechanism consisted principally of a drive and brake assembly, a Roll Position Indicator Assembly, the Roll Ring/Gear Assembly, roll bearings and a roll stop. The inner, or UP/DN-L/R gimbal ring contained four actuator assembly packages, UP/DN and L/R Orbital Locks and mechanical stops. In addition, Launch Locks were provided to constrain both rings under launch conditions.

Figure 7 shows the arrangement of the various components of the EPC/RPM system and Table 50 lists performance specifications for the components. The components are discussed below.

a. Actuators. Each of the four actuator assemblies comprised a brushless DC torque motor, a multispeed resolver, and a mechanical flexure bearing assembly. The packages provided a frictionless bearing along the UP/DN or L/R axis and also provided accurate, concentric mountings for the torque motors and resolvers. A self-aligning feature precluded straining the gimbal ring alignment when rotating the gimbal system in UP/DN and/or L/R. A self-aligning device was incorporated into the actuator package so that the required torque specifications could be met.

The drive source for the DC torque motors was from the EPEA (see Section IX.C). The multispeed (16:1) resolvers provided the UP/DN and L/R positions of the canister relative to the ATM Rack. Because of the limited motion involved (± 2 degrees), only the fine winding (16-speed) output of the appropriate resolver was utilized in the ATMDC. Only one UP/DN resolver output and one L/R resolver output were routed to the ATMDC. Each fine winding was rotor excited with 10 VRMS, 800 Hz and had an allowable error of one arc-minute (maximum).

Table 50. EPC/RPM Performance Characteristics

EPC Actuator	
Mechanical	
Angular rotation:	0° to 2° +5% (either direction)
Torsional spring rate:	6.01 N.m/rad
Breakaway torque:	0.136 N.m
Electrical	
Motor	
Maximum torque output:	9.5 ± 10% N.m (at 3.75 amp)
Nominal input voltage:	36.7 Vdc
Current:	3.75 amp
Breakaway torque:	0.1 n-m (maximum)
Resolver:	
Nominal input voltage:	10 Vac
Nominal frequency:	800 Hz
Output:	sinθ, cosθ (not used) sin 16θ, cos 16θ
Error:	1-Speed: 30.0 arc-min 16-Speed: 1.0 arc-min
Orbital Lock	
Mechanical	
Range:	Functional at any point from 0 to +2 degree gimbal deflection
Power:	Required only during locking and unlocking. Operating time is 5 seconds (maximum).
Capacity:	Capable of operating with maximum torque output from one pitch or yaw actuator with a reserve factor of two.

Table 50. (continued)

Electrical	
Maximum torque output (per motor):	1.5 ± 10% N.m (at 4.64 amp)
Nominal input voltage:	24.2 Vdc
Current	4.64 amp
Roll Brake and Drive Assembly	
Mechanical	
Maximum torque at output shaft:	8.4 ± 10% N.m
Maximum shaft speed:	65 ± 10% RPM (either direction)
Rating:	Continuous operation (either direction:
Brake Capacity:	De-energized torque: 20.4 N.m 10.9 N.m
Electrical	
Motor nominal input voltage:	36.7 Vdc
Motor current:	3.75 amp
Tachometer sensitivity:	2.7 volts/rad/sec
Brake solenoid nominal input voltage:	28 Vdc
Brake solenoid input current:	1.50 amp
Roll Position Indicator Assembly	
Accuracy	
Fine resolution:	± arc-min
Coarse resolution:	± 30 arc-min

Table 50. (continued)

Mechanical

Input shaft speed:	56 RPM (maximum)
Limit of rotation:	± 5.6 revolutions

Electrical

Resolvers:	Coarse	Fine
Nominal escitation frequency frequency:	800 Hz	800 Hz
Nominal excitation voltage:	10 Vac	10 Vac
Maximum input current:	0.03 amp	0.06 amp
Output impedance:	75 ohm	75 ohm
Transformation ratio:	1.0 ±3%	1.0 ±3%
Nominal output voltage:	10 Vac	10 Vac
Output phase angle:	5 deg. (max)	5 deg. (max)
Accuracy:	± 6 arc-min	± 6 arc-min
Harmonic distortion	0.2%	0.2%

Mechanical limits of the flexure bearing constrained gimbal ring motion to ± 2 degrees in UP/DN and L/R. Th e UP/DN actuator packages were located between the roll ring and the UP/DN-L/R gimbal ring; and L/R actuator packages were located between the latter ring and the canister girth ring.

Thermally, the actuator motors could withstand temperatures up to 125°C without damage. Temperatures above 168°C would result in permanent damage to the motor from fouling due to outgassing the epoxy encapsulant material. Motor seizure would occur at about 57°C. These temperatures apply to the actuator rotor. The temperature transducer, located on the motor housing, would reflect lower temperatures. EPC system constraints were developed to minimize the possibility of actuator overheating due to excessive currents. (See Pointing Control Subsystem, Section VIII.A.)

b. Orbital Locks. The purpose of the two Orbital Locks (see figure 108) was to cage the experiment package girth (spar) ring with respect to the UP/DN-L/R gimbal ring and cage the latter gimbal with respect to the roll ring. Each Orbital Lock consisted basically of a roller mechanism and four limit switches which were driven by one of two redundant brush-type DC torque motors. Two sets of rollers, one for each axis, were mounted on the UP/DN-L/R gimbal. These rollers engaged a set of rails that were located radially opposite the Orbital Lock motors. The rails for the UP/DN Orbital Lock were fixed to the roll ring and were located 20 degrees from the UP/DN axis. The rails for the yaw Orbital Lock were fixed to the girth ring and were located 23 degrees from the L/R axis. These locations resulted in an equal moment arm between each Orbital Lock and its corresponding axis of rotation. See figure 109.

In a caging cycle, the rails were contacted by the rollers and the Orbital Lock motors generated sufficient torques to cage the UP/DN-L/R gimbal to zero degrees from up to ± 2 degrees. In the caged position, the rollers were slightly over "top dead center" with respect to the rails and were firmly compressed (preloaded) between the two rails. The preload in the rails not only assisted in containing the rollers but it also eliminated backlash between the ATM canister and gimbal, or the gimbal and roll ring.

In the two end positions, Caged or Uncaged, two limit switches were activated. In the Caged position, the rollers were clamped between rails and accurately positioned by rail stops. In the Uncaged position, a pin which was attached to the motor rotor hub impacted another pin attached to the stationary hub to act as a stop and position the rollers. A spring also snapped against the motor rotor pins and held the Orbital Lock in the Uncaged position.

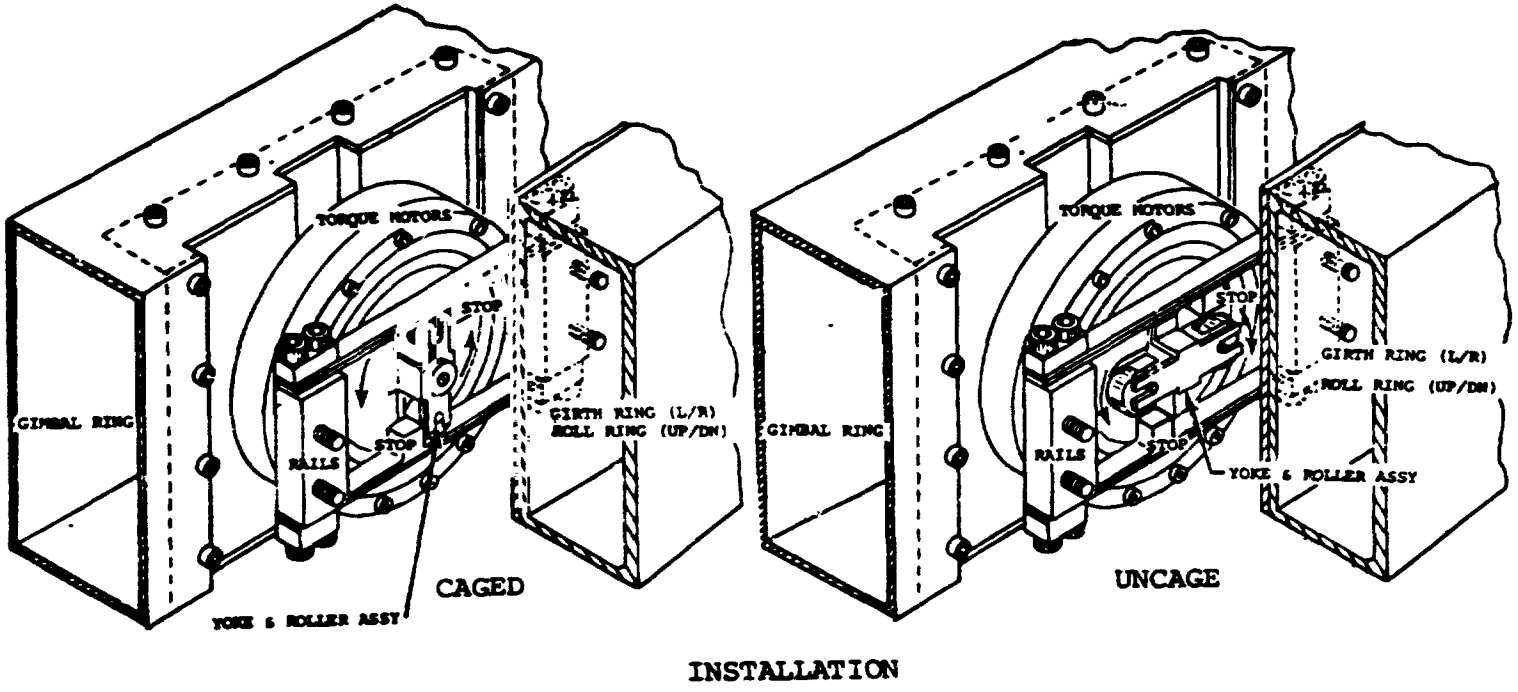

Figure 108. Orbital Lock Assembly

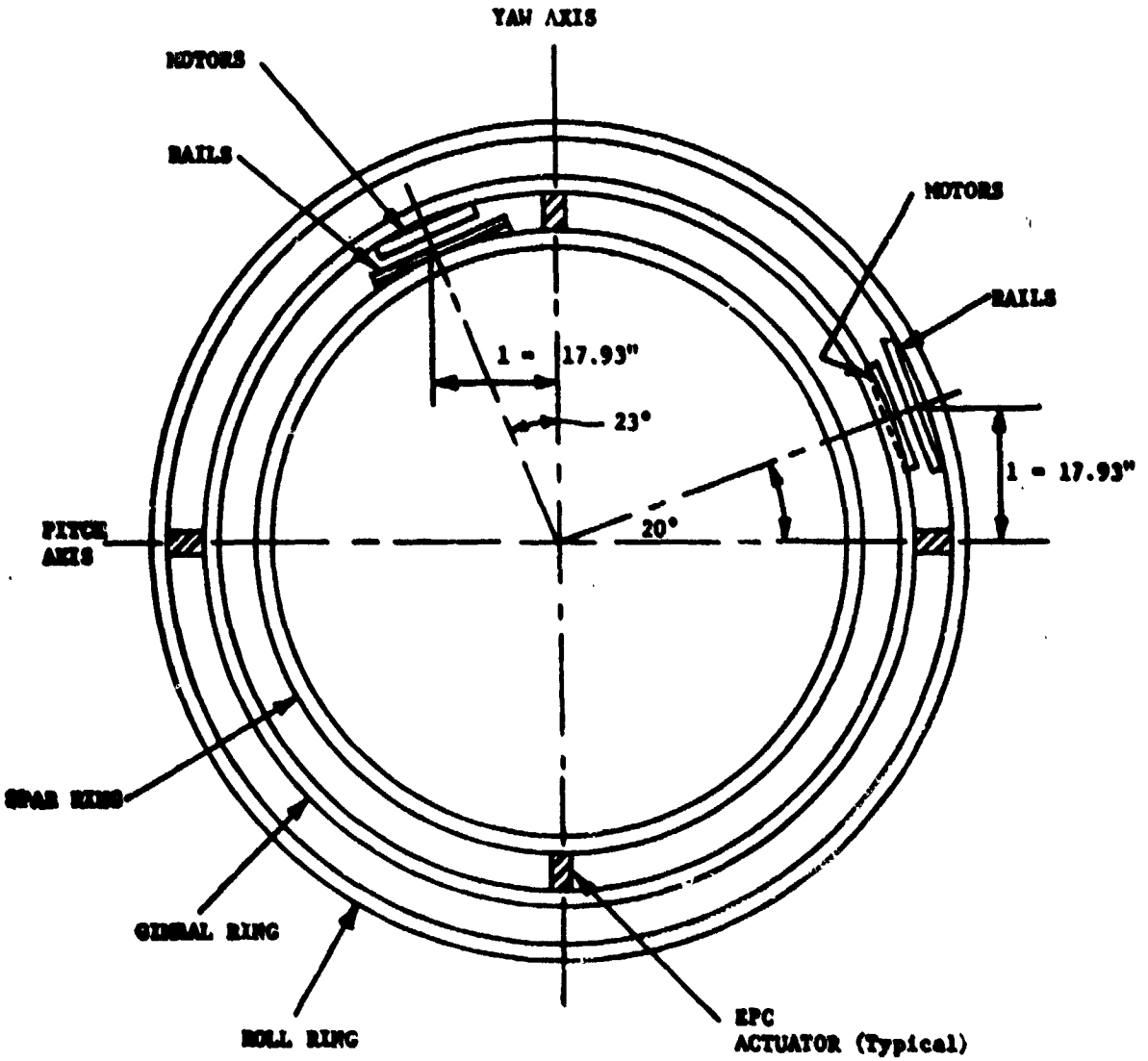

Figure 109. Orbital Lock Orientation

Each DC torque motor was capable of generating a peak torque of 1.5 ± 10% N.m at 4.64 amperes. The torque capability of the motor and its corresponding moment arm developed sufficient torque (± 10 N.m) to allow the Orbital Lock to override the EPC actuators and cage the experiment package in the event of a malfunction.

c. Roll Positioning Mechanism (RPM). The RPM roll drive and brake assembly consisted of two brush-type DC torque motors and two DC tachometers mounted on a common shaft which was geared to the roll ring, and a magnetically actuated disc type brake assembly. One motor and one tachometer were redundant; the brake coil had dual windings. The drive pinion and both tachometers were driven by either torque motor, allowing rotation of the roll ring gear. The tachometer rate output information was used in the roll control loop. With the brake coils deenergized, the armature was positioned up against the brake shoes, effectively locking the shaft and braking the roll ring.

The RPM was capable of rotating the canister with rates of ± 7, ± 3.5, ± 0.7, and ± 0.35 degrees per second depending on the commanded rates from the astronaut via the ATM C&D console.

The roll position indicator assembly consisted of a shaft that was driven at 16 times roll ring gear speed and another shaft that was driven at ring gear speed; four single-speed resolvers; and an associated precision gear train, bearings, and housing. The four identical resolvers provided a fine and a coarse resolution indication of the roll axis angle. The two fine resolution resolvers were driven at 16 times roll axis speed while the two coarse resolution resolvers were driven at roll axis speed. Two of the resolvers (coarse and fine) were redundant. The coarse and fine resolvers outputs were combined with additional data in the ATMDC/WCIU to obtain the roll reference angle and the roll angle of the canister with respect to the ATM Rack.

d. Launch Lock Assembly. The Launch Lock Assembly consisted of four lateral lock systems and one torsional lock system. Each lateral lock system consisted of two spring-loaded struts which were pyro-technically released once orbit was achieved. These struts were pivoted at the canister girth ring and symmetrically connected to the ATM Rack in four places. The struts restrained the canister assembly with respect to the Rack, and resisted the lateral and radial forces generated during the launch phase. The torsional Launch Lock consisted of a single spring-loaded strut which was also pyrotechnically released once orbit was achieved. This strut was attached to the Rack and the roll gimbal, restraining the gimbal and canister with respect to the Rack and resisting torsional forces generated during launch.

2. Design History. During design, development and construction of the EPC/RPM system, some fifty Engineering Change Proposals and Contract Modifications were processed. The more significant are listed below.

a. Redesign of the RPM. This change was introduced to enable both drive motors to be used together to overcome the operating friction of the brake assembly in the event of a brake failure in the "on" position and the resultant loss of canister roll capability.

b. Dry-Workshop Launch Configuration. When the Skylab concept changed from a Wet to Dry Workshop, the ATM launch vehicle was changed from a Saturn IV B to a Saturn V and inverted the ATM launch vector from that for which it was originally designed. The major impact of this change was to the Launch Lock System which had been designed to react to major launch loads in tension. In the new configuration the launch lock structure was required to withstand compressive loads and components were therefore required to be redesigned and manufactured.

c. Motor Retrofit. Due to cracking of the motor encapsulent and debonding of brush pads, a new procurement of brush and brushless type DC torque motors was implemented. These new motors were manufactured with improved potting compounds, to prevent cracking, and a modified brush bonding technique. All ATM assemblies containing the old motors were retrofitted with new units.

d. Orbital Lock Redesign. This change was required to improve the performance, reliability and service life of the assembly as a result of information obtained during development testing of the prototype unit. The modification consisted of minor changes to a number of detail parts within the assembly.

e. Deletion of the EVA Lock. The requirement for an EVA Lock, to prevent inadvertant roll, UP/DN or L/R motion of the Roll and Gimbal rings during astronaut EVA, was included in the original ATM specification. This was subsequently deleted and all EVA Lock assembly related hardware removed from the ATM.

f. Modification to Roll Axis Bearing Assemblies. A 0.2g docking shock load case was introduced to the structural design specification after Roll Bearing hardware had been fabricated. Stress analysis indicated that an overload condition could occur with possible damage to the Roll Axis Bearing assemblies. These units were modified to account for the revised loading condition.

g. Introduction of Improved Sensor Switches. Status Sensor Switches with an improved hermetic glass header seal and installation procedures were introduced on all ATM assemblies to prevent a possible failure and subsequent erroneous equipment function signal.

h. Modification to Launch Lock Pin-Pullers. Cracks occurred in the mounting flanges of Hi-Shear Pyrotechnique Pin-Pullers subjected to qualification test. Results indicated an overload condition. The redesign included strenghtening the mounting flanges and an improved heat treatment procedure for aluminum alloy components.

i. Reinforced Orbital Lock Rails. Tests showed that the orbital lock rails would deform under launch and docking stresses. The flight ATM was retrofitted with reinforced rails which were capable of withstanding the docking transients. The original system concept called for the Orbital Locks to be engaged at lift-off, in addition to the launch locks. Due to the stress problem, this was changed to launch with the orbital locks disengaged. Caging was to be commanded after orbit was achieved.

3. Design Verification. The EPC gimbal and roll position mechanisms were tested in the Hardware Simulation Laboratory using the mercury bearing (zero-g) test fixture to simulate experiment canister inertias. Roll movement of the test fixture was limited to $\pm$ 22.5 degrees, and non-flight cable stresses were present. However, the gimbal, roll and caging mechanisms were found to perform as designed.

4. Hardware Verification. During ATM prototype PMC testing at the Quality and Reliability Assurance Laboratory, MSFC, L/R actuators would not drive the canister which was supported by the zero-g test fixtures. Investigation indicated that the actuators were binding against the ring. Modifications were accomplished on the flight unit to eliminate this binding by making some cuts on the ring and by changing the procedure for installing the actuators to insure they are not preloaded.

5. Mission Operations. After SL-1 achieved orbit, the launch locks released as planned. During the launch phase, the orbital locks were in the Uncaged configuration. Five hours after launch the EPEA was powered up to activate the spar caging logic, and engage the locks.

On DAY 64, the primary UP/DN Rate Gyro failed, followed by UP/DN actuator motor seizure. The Gyro became noisy, then failed to zero output while the vehicle was outside of station coverage. At the next station, the problem was not isolated prior to orbital sunset. The vehicle was again outside of station coverage at the time of the next orbital sunrise DAY 64 02:04. When the vehicle telemetry was acquired at 02:50, the actuator housing temperature had risen from 5.6°C to 44.1°C, and the FSS error signal was oscillating at 0.5 Hz. The FSS wedges were commanded at 02:53. No spar response was seen on the FSS error signal. At orbital sunset, 03:01, the EPEA was automatically inhibited, and Solar Inertial Mode was selected at 03:20.

In the absence of Rate Gyro information for rate damping, the pointing control loops were unstable, causing large spar oscillations and high actuator currents. This was verified by analysis and by testing in the Hardware Simulation Laboratory. Based on analysis of the housing temperature, the actuator motor was estimated to have been heated to the seizure temperature (57°C) at about 02:25. At that time, a rapid transfer of heat to the actuator housing would occur. Maximum rotor temperature was established to have been 83-113°C, well below the upper limit of 168°C. The oscillations observed at 02:50 can be attributed to structural ringing of the spar following the motor seizure. Similar spar behavior had been observed in the HSL after engaging the orbital locks.

At 17:20, on Day 67, Experiment Pointing mode was selected again to test the EPC system using the secondary UP/DN Gyro. No problems were experienced with the actuators.

As a consequence of the actuator seizure, a mission rule was instituted to exit Experiment Pointing Mode if continuous, unattended EPC operation would exceed fifty minutes without station coverage. Also, the mission rules were changed to require switching to Solar Inertial when the current levels exceeded $\pm$ 1.0 amp, except during transients. Original criteria for management of EPC actuator currents required that Solar Inertial mode be selected if the currents exceeded $\pm$0.5 amp. However, operating levels of $\pm$ 0.7 amps were observed. The changing bias levels were a consequence of cable torques developed between the ATM Rack and Experiment Canister during roll and offset pointing operations. It was felt that the continuous current levels could not be reduced without restricting operations and that the operating levels were not having a detrimental effect on the actuators. Furthermore, studies showed that as long as the effective (RMS) current did not exceed 1 amp for the period of one orbit, the actuators would not be damaged.

On Day 185, during the unmanned phase between SL-3 and SL-4, the UP/DN Orbital Lock failed to uncage at orbital sunrise. Sunrise occurred outside of tracking station coverage and next station acquisition was six minutes later. At that time, the UP/DN actuators were observed to be drawing maximum current (-3.75 amp, the torquer amplifier limit). Solar Inertial mode was selected two minutes later, caging the spar. The gimbal actuators and Orbital Lock motors drew full current for eight minutes. Temperatures of the actuator housing and the lock housing both increased by 3.7°C. About three hours later, secondary EPEA was selected and Experiment Pointing mode was commanded. The orbital locks functioned normally.

Analyses and tests of possible failure modes were conducted. Analysis of flight data indicated that a failure of the primary orbital lock motor, or electrical relay failures had not occurred. This was based on study of the transfer bus currents.

Tests run on a motor in thermal vacuum at stall current produced a temperature rise similar to that seen during the anomaly. The motor was subjected to stall currents for three hours in one test and two hours in another. In both cases, after the current was removed and the motor allowed to cool down, its performance was normal.

It was concluded that a mechanical problem, such as binding, had occurred but was relieved by returning to SI. It was suggested that the primary Orbital Lock be tested again to verify that the problem was no longer present. However, this was never done. With the EPEA in secondary, the Orbital Locks were tested once on Daly 185, twice per day on Day 189 and 190 (SL-4 crew docked on Day 187). Unrestricted operations resumed on Day 191. However, ten days later, the UP/DN lock again failed to disengage.

Without any configuration changes, the lock successfully uncaged when tested about an hour after the second anomaly. This anomaly gave credance to the theory that intermittent mechanical binding was occurring possibly due to contamination from wiring insulation in the vicinity of the lock. The conclusion of investigations of the second anomaly was that there was no need to limit or inhibit EPC operation.

The uncage failure was not observed again, and the secondary Orbital Lock motor was used for the remainder of the Skylab mission.

6. Conclusions and Recommendations. The Experiment Package Caging and Gimbal Assembly operated without failure or problem, except for the two orbital lock anomalies. Further design studies might reveal the actual cause of the anomalies and indicate corrective changes which could be made to the EPC/RPM hardware. Otherwise, no design changes were recommended.

E. Manual Pointing Controller (MPC)

1. Design. The Manual Pointing Controller (MPC) allowed the astronaut to inject command signals in pure pitch (UP/DN), or pure yaw (LEFT/RIGHT), or combinations thereof, into the EPCS or the ST. The MPC was used to either offset point the ATM Solar Instrument Package or to manually search for a desired star. In either case, the MPC signal outputs were conditioned in the Experiment Pointing Electronics Assembly (EPEA) and then routed to the Control Electronics Assembly (CE) of the Fine Sun Sensor (FSS) or to the Star Tracker Electronics Assembly (STE) depending on the operational mode. The CE provided the drive circuitry to position optical wedges (FSS Optical-Mechanical Assembly) for offset pointing operations. The MPC UP/DOWN output was routed to the inner gimbal circuitry of the Star Tracker, and the MPC LEFT/RIGHT output was routed to the outer gimbal circuitry whenever the Star Tracker was in the Manual mode.

The MPC (see figure 110) had an upright control handle which could be tilted from a center null position to a LEFT/RIGHT position

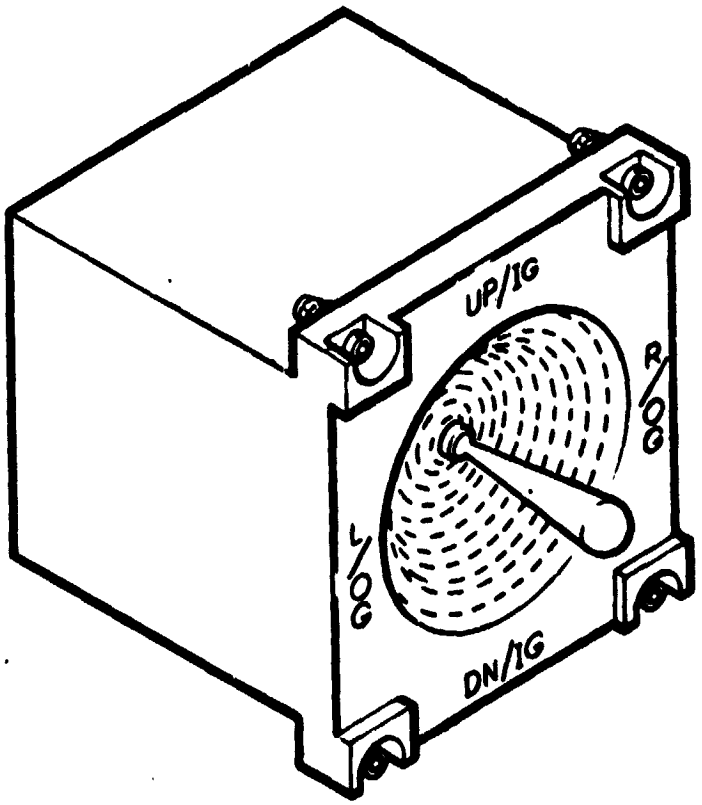

Figure 110. Manual Pointing Controller

for yaw, to an UP/DOWN position for pitch, or a combination of both positions. These positions were with respect to the MPC mounting configuration on the ATM Control and Display Console. The MPC consisted of a spring loaded two-axis gimbal control handle and mechanism, two linear transducers, and a housing with connectors for the INPUT/OUTPUT wiring. The pitch and yaw output signals were proportional to the handle deflection. Performance specifications for the MPC are listed in Table 51.

2. Design Verification. Checkout and integration of the MPC into the EPC system was performed in the HSL. The Unit was found to operate as designed.

Table 51. Manual Pointing Controller Performance Characteristics

ELECTRICAL INPUT	
Excitation:	28.0 ± 1.4 VRMS 800 ± 8 Hz sinusoidal
Impedance:	≥ 750 ohms 80 ± 10 degrees impedance angle
ELECTRICAL OUTPUT	
Amplitude:	4.2 to 5.5 VRMS at handle cardinal positions (limits)
Phase Shift:	≤ 7 degrees from full output, nominal
Linearity:	± 5 percent
Null:	≤ 5 100 millivolts RMS
Output Impedance:	16.7 K ohms, resistive
HANDLE PARAMETERS	
Tilt:	≥ 30 degrees at cardinal position
Force:	≥ 3.25 lbs, cardinal positions
Breakout Force:	0.40 lb., minimum either axis

3. Hardware Verification. The MPC performed satisfactorily during all system level testing.

4. Mission Operations. The MPC was first utilized during the initial manned ATM operations on DAY 16. No problems were encoundered with the MPC at any time during manned operation. Occasional procedural problems arose when the crew would leave the MPC Enable Switch activated, thereby preventing ground operation of the wedges.

5. Conclusions and Recommendations. The Manual Pointing Controller (MPC) functioned flawlessly throughout Skylab manned operations. No changes to the design of the unit is recommended, although the crews, during debriefing, expressed interest in system capability to drive the wedges at very low rates (threshold rate command was 16 arc-sec per sec).

F. Derived Rate Conditioner Assembly (DRC)

1. Design. Following the loss of the EPC Primary UP/DN Rate Gyro on DAY 64, and in view of the overall problems experienced with the Skylab Rate Gyro Processors, it was felt that there was a significant possibility that the secondary UP/DN Gyro would fail. The EPC was equipped with two Gyros per axis, so a second UP/DN Gyro failure would have terminated use of the EPC. Replacement or supplementing of the EPC Gyro System, such as had been done in the CMG/TACS system, was not considered feasible. Subsequently, a device, the EPC Derived Rate Conditioner Assembly, was designed to be inserted in series with the FSS output for the purpose of producing a pseudo rate signal to stabilize the EPC system in lieu of Spar Rate Gyros.

The EPC Derived Rate Conditioner Assembly contained a dc-dc converter, two linear signal conditioners, and two nonlinear signal conditioners in a single package. The system was to be installed by Tethering to the ATM, near the EPEA, and connecting the cable harness. An interconnecting diagram is shown in figure 111. UP/DN (and L/R) conditioner signals from the FSS were received by the EPC Derived Rate Conditioner electronics and conditioned by linear and nonlinear signal conditioners connected in parallel. The Linear Signal Conditioner produced a signal for stabilization when the Gyro signal was not available. The nonlinear Signal Conditioner produced an output to limit the error signal. These outputs were summed to produce the desired output. A block diagram of the EPC DRC system is shown in figure 112.

The system nominally required less than 1.8 watts (60 Ma @ 28 Vdc). The 28-volt input was converted to 15 Vdc by the dc-dc converter.

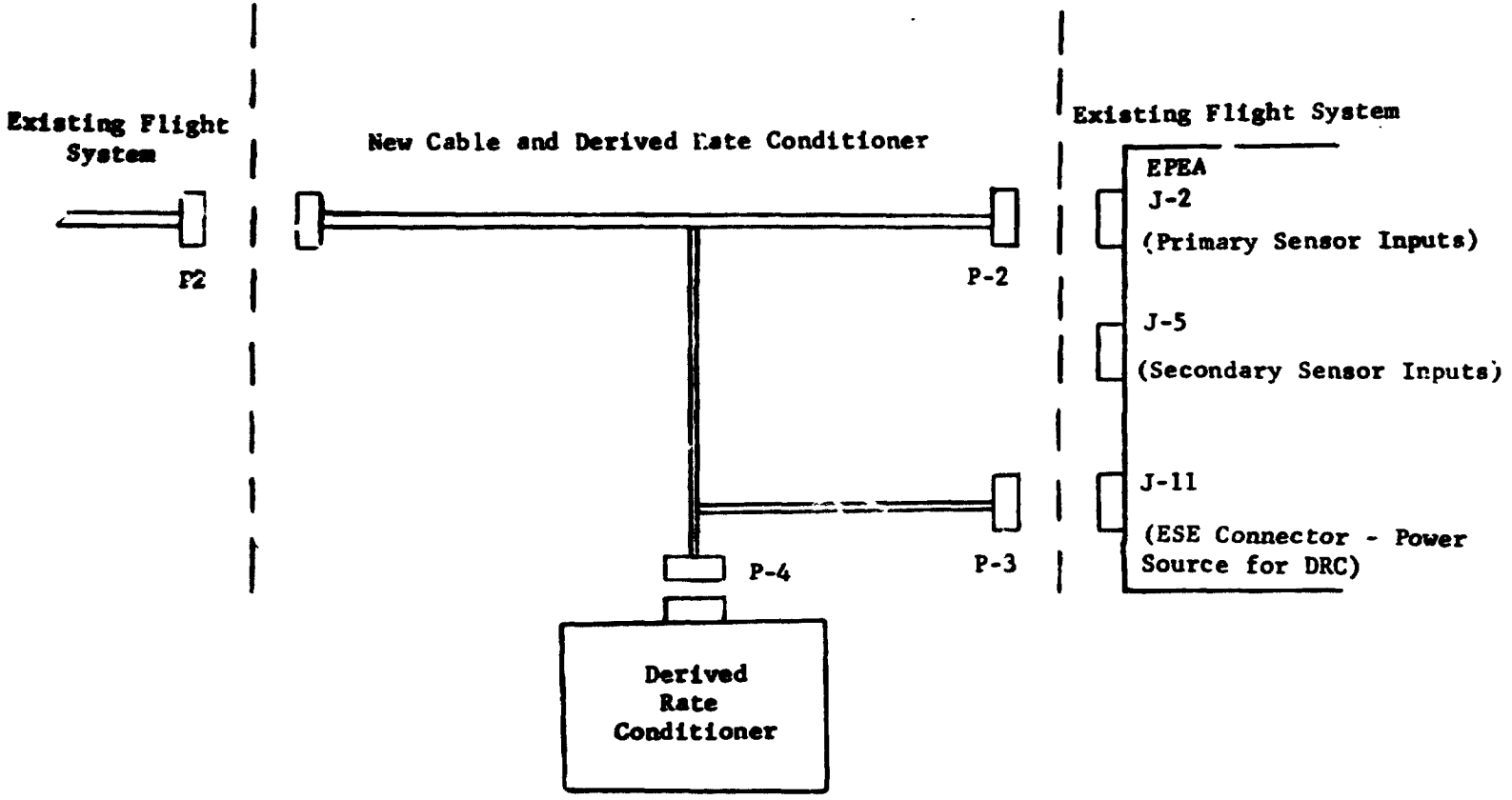

Figure 111. Derived Rate Conditioner Within the EPC Control Loop

The input signal ranged between -12.8 to +12.8 Vdc with the angular offset to the EPC Canister (see figure 113).

The output of the linear Signal Conditioner was proportional to position plus rate over a band of frequencies from 0.1 to 25 Hz. The output of the nonlinear Signal Conditioner is shown in figure 114. The saturated level output was set to limit the drive rate so that the system would not overshoot the linear range about null. The output of the EPC DRC system is the sum of the linear and nonlinear Signal Conditioners.

2. Design Vertification. Initial testing of the prototype DRC in the Hardware Simulation Laboratory revealed ground loop problems between the DRC and FSS. Both the FSS and DRC were common ground devices. Within theATM networks there was a reversal of the FSS UP/DN lines, so that direct connection of th e DRC shorted the L/R FSS output to ground. The problem was resolved by rewiring the cable harness to reverse the polarity of the L/R FSS signal going into the DRC and again before it was sent to the EPEA (see figure 115).

After this correction, the prototype and flight units were tested and found to function as designed, but with degradation to the EPC control loop bandwidth and pointing stability. Accurate determination of the pointing stability in flight could not be made in the HSL.

3. Hardware Verification. The DRC was subjected to verification testing under ambient and thermal-vacuum conditions as Astrionics Laboratory, MSFC, and to EPC Program integration tests at Quality and Reliability Assurance Laboratyr, MSFC, prior to shipment to KSC. Crew procedures for installation dur'ng EVA were verified in the Hardware Simulation Laboratory and the Neutral Buoyancy Simulator.

4. Mission Operations. One DRC unit with associated cabling was carried into orbit on SL-3. Additional cabling which would allow the unit to be used on either the UP/DN or L/R axis was carried to orbit on SL-4. The device was never installed, however, because no further EPC Rate Gyro failure occurred.

5. Conclusions and Recommendations. The EPC Derived Rate Conditioner Assembly was not required for use during Skylab. The unit provided assurance that ATM experiment operations could be continued in the event of the loss of the Secondary UpDN Rate Gyro.

The fact that it was necessary for theDRC to be designed, built and flown as an emergency system to provide EPC rate information in the event of complete loss of EPC Gyro hardware, indicates a need to locate mission critical hardware components, such as the Rate Gyro Processors, in areas where replacement and/or maintenance would be possible.

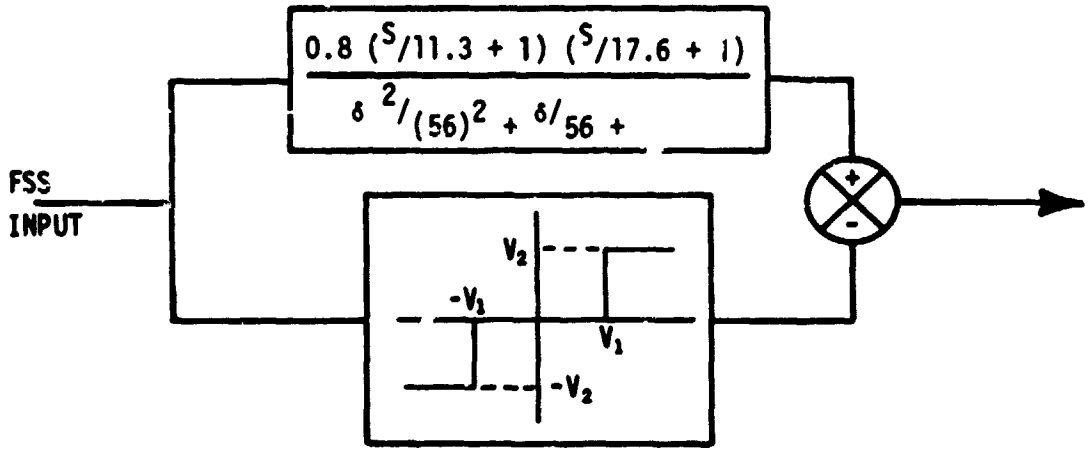

Figure 111. - Block Diagram Of Derived Rate Control System

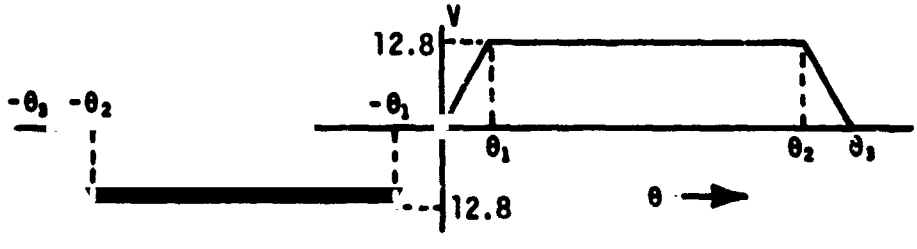

Figure 112. Input To Derived Rate Control System

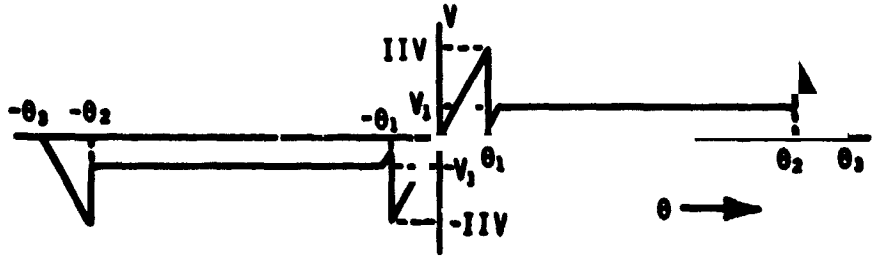

Figure 114. Output of Nonlinear Signal Conditioner

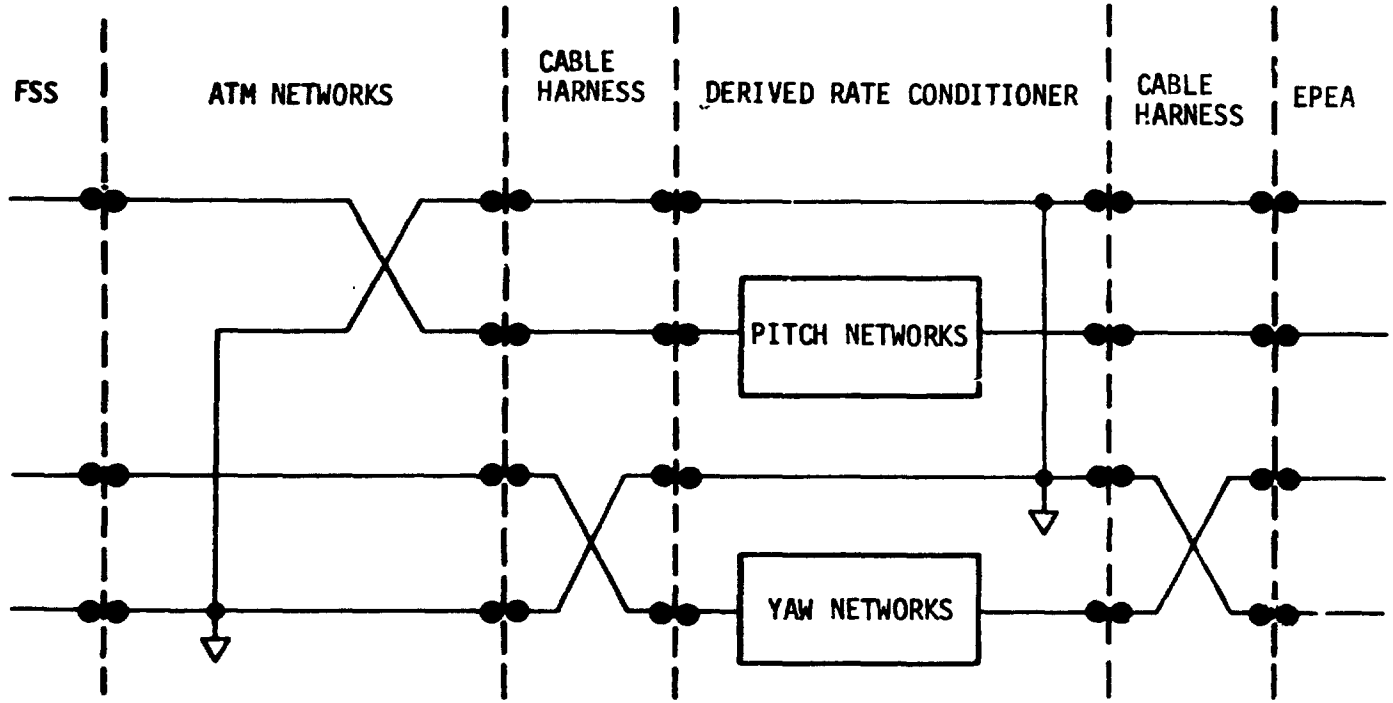

Figure 115. Cable Phasing Between the FSS and EPEA

SECTION X. REFERENCES

1. ATM Digital Computer Program Definition Document, (PDD) Part I, MSFC-DRL-585-1, Line Item 45, Contract NAS8-20899, IBM 70-207-000Z, George C. Marshall Space Flight Center, Huntsville, Alabama: Revision 22, 10 May 1973.

2. ATM Vehicle Flight Control Dynamics Verification with Phase I Flight Program, MCMO S&E-ASTR-SD-6-72, 26 January 1972

3. ATM Vehicle Flight Control Dynamics Verification with the Phase I-A Flight, Memo S&E-ASTR-SD-126-72, 26 December 1972

4. ATM Vehicle Flight Control Dynamics Verification with the Phase II Flight Program, Memo S&E-ASTR-SD-26-73, 19 April 1973

5. ATM Vehicle Control Dynamics Verification with the Final Flight Program, Memo S&E-ASTR-SD-44-73, 11 May 1973

6. Routine APCS Dynamics Analysis Report, MMC, ED-2002-1707-2, 31 December 1973

7. APCS Dynamics Anomaly Analysis Report, MMC, ED-2002-1707-3, 31 March 1974

8. APCS Dynamics Anomaly Analysis Report, MMC, ED-2002-1707-4, 31 March 1974

9. Routine APCS Dynamics Analysis Report, MMC, ED-2002-1707-5, 31 March 1974

10. Scofield, H. N., Final APCS Postflight Assessment, Memo S&E-ASTR-SD-50-74, 8 May 1974

11. Skylab SWS/OA APCS Postflight Performance Evaluation, NASA 80M19007, April 30, 1974

12. Design and Operation Assessment, ATMDC/WCIO and Related Software, IBM, 74W-00103, April 15, 1974

13. Attitude and Pointing Control System Summary Document, NASA 5078002

14. Apollo Telescope Mount Gyro Processor System Description NASA 50M37446, Rev. F. July 1, 1970

15. Performance Specification - ATM Rate Gyro, NASA 50M37705, Rev. F, September 21, 1972

16. Qualification Test Specification NASA 50M37742 Rev. A., February 27, 1970

17. Qualification Test Procedure NASA 50M37743 Rev. A, February 27, 1970

18. Report of Test on ATM/OWS Rate Gyro Processor P/N 50M37700, Flight Qualification Test Program Martin Marietta, 50M37740 April 14, 1970

19. Guidance, Control and Navigation System Test Report NASA 50M39070 Rev. A, June 8, 1972

20. Skylab Rate Gyro Processor Anomaly Report NASA 50M22139, December 1, 1973

21. Environmental Specification and Test Procedures for the CMG Subsystem of ATM, NASA 50M22162B

22. Environmental Qualification Test Report of the CMG Subsystem of ATM, NASA 50M22163

23. Skylab Thruster Attitude Control System, NASA TM X-64852

24. Analysis of Skylab Digital Computer Integrated Circuit Eutectic Particle Contamination Failures IBM Report No. 71W00224, June 9, 1971

25. Desired Rate Conditioner Testing in the Hardware Simulation Laboratory, Memo S&E - ASTR-SG 89-73, July 27, 1973

SECTION XI. BIBLIOGRAPHY

1. System Definition Document Workshop Attitude Control System. NASA 50M37935 February 28, 1969

2. Orbital Assembly Systems, APCS Design Certification Review, Phase I, Volume II, Section III, June 30, 1972

3. Gaines, B. J.: ATM Rate Gyro Processor Mission Evaluation Report, Memo S&E-ASTR-G-13-74, January 10, 1974

4. Lee, Charles E. and Rawls, F.C.: Skylab ATM Star Tracker Evaluation, Memo S&E-ASTR-G-1-74, January 4, 1974

5. Lee, Charles E. and Rawls, F. C.: ATM Star Tracker Mission Evaluation Report, Memo S&E-ASTR-G-57-74, February 20, 1974

6. Apollo Telescope Mount Star Tracker Operational Requirements and Descriptions, NASA 50M22143, July 8, 1969

7. Acceptance Test Procedure for the Apollo Telescope Mount Star Tracker System, Bendix Corporation, Navigation and Control Division, 21214427, June 2, 1970

8. Skylab A Guidance, Control and Navigation System Test Report NASA 50M39070, June 8, 1972

9. Cook, Lewis J.: Skylab ATM CMG Evaluation, Memo S&E-ASTR-G-17-74, January 14, 1974

10. Cook, Lewis J.: Skylab ATM CMG Mission Evaluation, Memo S&E ASTR-G-84-74, March 18, 1974

11. Design and Operation Assessment, ATMDC/WCIU and Related Software, IBM, 74W-00103, April 15, 1974

12. The Proceedings of "The Committee to Investigate the Skylab CMG No. 2 Orbital Anomalies" NASA 50M23157, January 18, 1974

13. Skylab Mission Events (SL-1/2, SL-3, SL-4) NASA 25M00700, February 1974

14. Kimmons, W. L. and Mastin, W. C.: Skylab ATM Acquisition Sun Sensor Evaluation, Memo S&E-ASTR-G-313-73, December 17, 1973

15. Kimmons, W. L. and Mastin, W. C.: Skylab ATM Acquisition Sun Sensor Mission Evaluation Report Memo, S&E-ASTR-G-47-74, February 14, 1974

16. Apollo Telescope Mount Acquisition Sun Sensor Operational Requirements and Description, NASA 50M23013, February 24, 1970

17. Design/Performance Specification SS-1090 Solar Sensor System, Ball Brothers Research Corporation, 30471, December 31, 1968

18. Apollo Telescope Mount Test and Checkout Requirements and Specification, Prototype and Flight Article, NASA 50M02425 Rev. A, January 10, 1972

19. EPC Line of Sight Roll, HOSC Action Request No. AR-639, August 21, 1973

20. Johnston, J. D.: Skylab Dump Tape 162-04, Time 1352-1402-13:51:50 SPT, NA Memo S&E-ASTR-G-145-73, June 15, 1973

21. Johnston, J. D.: ATM-FSS Mission Evaluation Report, Memo S&E-ASTR-G-80-74 March 13, 1974

22. Johnston, J. D. Fine Sun Sensor Mission Evaluation Report, Memo S&E-ASTR-G-9-74, January 9, 1974

23. ATM Experiment/FSS Alignment, Mission Action Request AX-2489 December 11, 1973

24. Johnston, J. D.: Response to AX-2489, Memo S&E-ASTR-G-304-73 December 12, 1973

25. Attitude and Pointing Control System (APCS) Definition Document, Volume II, APCS Hardware Complement, MMC, ED-2002-984 Rev. A March 23, 1973

26. FSS Wedge Readout Anomaly, HOSC Action Request AR-851, October 11, 1973

27. FSS (Sec) Wedge Angles, HOSC Action Request AR-1058, January 26, 1974

28. Bridges, J. K.: Skylab Mission Evaluation Report on EPEA, Memo S&E-ASTR-CFS-107-74 March 14, 1974

29. Bridges, J. D.: Skylab Mission Evaluation Report on EPEA Memo S&E-ASTR-CFS-100-74, January 14, 1974

30. Experiment Pointing Electronic Assembly (EPEA) Serial No. 002 Tests Report, Memo, S&E-ASTR-SG-154-71 November 30, 1971

31. Experiment Pointing Electronic Assembly (EPEA) Serial No. 004 Tests Report, Memo, S&E-ASTR-SG-189-71 January 17, 1972

32. Experiment Pointing Electronic Assembly (EPEA) Serial No. 006 Tests Report, Memo, S&E-ASTR-SG-209-72 December 22, 1972

33. Checkout of EPEA SN004, NASA 50M05180 May 1972

34. Checkout of EPEA SN002 NASA 50M05072 January 3, 1972

35. Final Test Specification and Procedure for the ATM Experiment Pointing Electronics Assembly (ATM/EPEA), Bendix Corporation, Navigation and Control Division, 2124418- (GTSP) July 14, 1970

36. Skylab APCS Simulation Laboratory Handbook NASA 50M04976 March 1971

37. Skylab APCS Functional Schematics, NASA 50M0496 June 30, 1971

38. Experimental Pointing Electronics Assembly System Control Drawings, Bendix Corporation, Navigation and Control Division 2124676, February 16, 1970

39. Skylab Program Operational Data Book, Vol. IV Skylab Performance Data NASA, MSC-0159 Rev. A, October, 1972

APPROVAL

MSFC SKYLAB ATTITUDE AND POINTING CONTROL SYSTEM
MISSION EVALUATION

By

W. B. Chubb

The information in this report has been reviewed for security classification. Review of any information concerning Department of Defense or Atomic Energy Commission programs has been made by the MSFC Security Classification Officer. This report, in its entirety, has been determined to be unclassified.

This document has also been reviewed and approved for technical accuracy.

M. Brooks
Chief,
Guidance and Control Branch

R. Ise
Manager,
Skylab Program Office

J. L. Mack
Chief,
Systems/Projects Office

F. B. Moore
Director,
Astrionics Laboratory